SEQUENCE STRATIGRAPHY OF THE PALEOCENE TO MIOCENE GAMBIER SUB-BASIN, SOUTHERN AUSTRALIA

Rosalie M. Pollock

(BSc Honours, University of Adelaide)

National Centre for Petroleum Geology and Geophysics

&

Department of Geology and Geophysics

Thesis submitted to the University of Adelaide in fulfillment of the requirement of the degree Doctor of Philosophy, November 2003.

ABSTRACT

The Gambier Sub-basin is part of the Australian Southern Rift System on the passive continental margin of Australia, which formed as a result of breakup and dispersal of Gondwana. Its fill comprises Cenozoic sediments overlying the western part of the Mesozoic Otway Basin. A four-part packaging of Cenozoic stratigraphy on the southern margin has been known of for some time. These packages span the (I) Late Paleocene-Early Eocene, (II) late Middle Eocene-Early Oligocene, (III) Late Oligocene-Middle Miocene and (IV) latest Miocene-Pleistocene. Within the first two of these second-order global packages (I and II), several third-order transgressive events have been identified using mainly foraminiferal biostratigraphy. Packages II and III are largely dominated by carbonate sediments and have been further sub-divided into seven unconformity-bounded packages based on biostratigraphy.

This study has extended knowledge of the packaging of southern margin Cenozoic stratigraphy into the seismic realm. Two megasequences were defined based on seismic interpretation. Megasequence 1 correlates to package I, and represents Late Paleocene to Early Eocene siliciclastic sediments deposited in a prograding deltaic environment. Four supersequences and nine sequences were interpreted on seismic data within Megasequence 1. Sedimentation rates were high and the sequences, dominated by highstand systems tracts, responded to rapidly fluctuating sea level, supported by biostratigraphic evidence of six rapid marine transgressions.

There is large gap of approximately nine million years in the Middle Eocene in the southern margin sedimentary record. The marine part of the record begins again in the late Middle Eocene with the Wilson Bluff (=Khirthar) Transgression. Deposition of the Nirranda Group in the eastern Otway Basin ensued, influenced by four more major marine transgressions occurring throughout the Late Eocene. However, in the Gambier Sub-basin a condensed section represents the late Middle Eocene to Late Eocene and the sedimentary record begins again with the Aldinga Transgression in the Early Oligocene, depositing the neritic cool-water carbonate Gambier Limestone. This package represents Megasequence 2. Two supersequences were identified on seismic data within Megasequence 2 – an Early Oligocene cool-water carbonate platform, unconformably overlain by a Late Oligocene to Middle Miocene package dominated by submarine canyon events.

Three palaeo-canyon systems striking perpendicular to the shelf break were identified on seismic data under the present day outer continental shelf and upper slope and were

subsequently named the Robe Canyon, Northumberland Canyon and Lakes Canyon Complex. The onset of submarine canyon incision was at the Early/Late Oligocene boundary (~28.5 Ma) and is correlated to a world-wide glacio-eustatic sea level fall. No less than 20 major successive canyon events were interpreted on seismic data in the Voluta Trough throughout the Late Oligocene to Middle Miocene. A eustatic sea level fall below the shelf edge caused minor fluvial incision across the outer shelf, which led to the development of "nick points" at the shelf edge at the beginning of the Late Oligocene. The following marine transgression inundated the shelf and the nick points were picked on by episodic mass wasting events and associated turbidity currents. The mass wasting events enlarged the canyons to the spectacular dimensions observed on seismic data and the resulting turbidity currents flowed down the sinuous canyon axes depositing dominantly fine-grained sediment in point bar-like deposits. Successive canyon events show lateral migration on seismic data and an analogy has been drawn between the evolution of the Gambier Sub-basin submarine canyons and migration of a fluvial meandering channel.

In addition to expanding the knowledge of the stratigraphic evolution of the Cenozoic southern Australian margin by correlation of seismically defined packages with tectono- and glacio-eustatic events, the hydrocarbon potential of the Gambier Sub-basin is also addressed. Analysis of faulting in the Gambier Sub-basin indicates that in the contemporary stress regime, the regional normal faults striking NW-SE are likely to have poor sealing potential. Therefore, reliance on fault traps for hydrocarbon plays in the Gambier Sub-basin is high risk.

Numerous stratigraphic plays exist on the outer shelf within the Early Eocene clastic succession where there is evidence on seismic data of sandy delta lobes, overlain by muddy coastal plain sediments. Incised meander channel belts were recognised on the outer shelf and the associated sandy lowstand shoreline and possible turbidites interpreted to occur further basinward form a potential play where sealed by a thick succession of fine-grained carbonate rocks. Other potential plays exist where coarse-grained carbonate sediments, sourced from the outer shelf and deposited within the submarine canyons, form reservoirs that are sealed by surrounding fine-grained carbonate sediments and charged by vertical migration of hydrocarbons from deeper Cretaceous sources.

STATEMENT OF AUTHENTICITY

This work contains no material which has been accepted for the award of any other degree or diploma in any university or other tertiary institution and, to the best of my knowledge and belief, contains no material previously published or written by another person, except where due reference has been made in the text.

I give consent to this copy of my thesis, when deposited in the University library, being available for loan and photocopying.

Rosalie M. Pollock

For Poppa, my greatest supporter.

ACKNOWLEDGEMENTS

In the course of a project as large as this, which runs over such a long period of time, there are many people to thank. I will begin by acknowledging the financial contributions to the larger Gambier project, of which this study was a key element. A SPIRT grant was awarded to Brian McGowran as Chief Investigator in the Department of Geology and Geophysics, Adelaide University, and Neville Alley as Industry Leader in Primary Industries and Resources, South Australia (PIRSA) to support an integrated basin history study of the Cenozoic Gambier Sub-basin. Marigold White (PIRSA) conducted a micropalaeontological analysis of petroleum wells in the Gambier Sub-basin and also raised funds and secured in-kind contributions to the project from PIRSA and industry, including Origin Energy (previously Boral Energy Resources). Qianyu Li (Adelaide University) conducted a study on the biofacies packaging in the marine limestones and Liliana Stoian and Andrew Rowett analysed the palynology, assisted by Lyn Broadbridge who carried out sample preparation.

Thanks goes to Cedric Griffiths (ex-NCPGG and co-supervisor when I first began my PhD) who secured further support from Origin Energy, which allowed access to their seismic database and scholarship funding. I would also like to thank Rob Willink, Richard Suttill, Rod Lovibond, Bronwyn Camac, James Donley and Andrew Davids from Origin Energy for their input and help during the project.

I am eternally grateful to my co-supervisors at the NCPGG and Department of Geology and Geophysics, without whose help I simply could not have gotten through this. Simon Lang (NCPGG), thankyou for all of the lively discussions and regular injections of infectious enthusiasm. Please keep teaching for many years to come. Brian McGowran and Qianyu Li, your advice, knowledge and help have proved invaluable, thankyou.

I sincerely thank my all of my family and friends for their support throughout my studies. And of course the NCPGG "family" were invaluable in their tutoring, friendship, guidance, support and help in my (many) years at the National Centre. More recently, while working at Geoscience Australia in the last few months, thankyou to Jane Blevin, Andrew Krassay, Kathe Trigg and Chris Nicholson, for your advice, support, accessing data, and allowing me to use GA's resources to get my thesis finished. Without your help, I'd still be going!!!

TABLE OF CONTENTS

LIST OF FIGURES AND TABLES

Chapter 1

Introduction

1 INTRODUCTION

1.1 PREVIOUS WORK

The southern Australian margin faced the developing Southern Ocean during Late Cretaceous and Cenozoic as the Australian and Antarctic continental plates separated. The development of this oceanic throughway between these two continents and the resulting periodic influences from different warm and cool oceanic currents was critical to the development of the Cenozoic neritic stratigraphic record in Southern Australia.

The Cenozoic stratigraphic record on the southern Australian margin sorts into four hiatus-bounded sequences, resembling global second-order cycles. They span the Late Paleocene to Early Eocene, late Middle Eocene to Early Oligocene, Late Oligocene to Middle Miocene and latest Miocene to Pleistocene. These packages have been defined mostly on micropalaeontology by authors including McGowran (1978, 1979a, b); Frakes et al. (1987); Quilty (1977, 1980, 1994) and McGowran et al. (1997).

Within the first two of these global second-order sequences, a series of rapid marine transgressive events were recognised during the Late Paleocene to Early Eocene and then in the Middle to Late Eocene, based mainly on planktonic foraminiferal assemblages (McGowran, 1986, 1987, 1989a, 1991; McGowran and Beecroft, 1985, 1986). There is a gap in the record of approximately nine million years between the early Palaeogene events and later Eocene transgressions, within which firm biostratigraphic dates are lacking (McGowran et al. 1997). McGowran (1991) terms the Late Paleocene to Early Eocene sea level events "ingressions", as they are "short lived thrusts by marine facies into an essentially marginal marine or paralic facies", as distinct from the later Eocene, continent-wide marine "transgressions". Six ingressions were identified in the Late Paleocene and Early Eocene; the Kings Park (lower part of Zone P4), Pebble Point (Zone P4/P5 boundary), Rivernook-A (Zone P6a), Rivernook (Zone P6b), Princetown (P7), and Burrungule (Zone P8) (Fig. 1.1).

Four continent-wide marine transgressions were noted in the Middle and Late Eocene and correlated with global plate tectonic reorganisations and climatic shifts that were based on isotopic data (McGowran, 1986; 1989a; 1991). Two of these transgressions occurred in the late Middle Eocene, with the first (Wilson Bluff) forming part of the Indo-Pacific Khirthar Transgression (high Zone P12), a response to seafloor spreading after India and Asia collided.

The second transgression (Tortachilla), also in the late Middle Eocene, occurred near the Zone P14/P15 boundary. The third transgression (Tuketja) occurred in the Late Eocene near the top of Zone P15 and the fourth (Aldinga) occurred low in Zone P17 (Fig. 1.1).

Sedimentation in the Gambier Sub-basin during the Late Paleocene to Early Eocene was rapid and dominated by marginal marine to marine, siliciclastic deltaic cycles (called the Wangerrip Group). Many sedimentological and biostratigraphic studies have been conducted on this package including Ludbrook (1971), Arditto (1995), Morton et al. (1995), Morgan et al. (1995) and White (1995). Holdgate (1981) conducted a high resolution sedimentary and facies analysis on this second-order sequence using well data from the central Otway Basin and considered these packages to be influenced more by local basinal process and did not define third-order packages that correlated to regional tectonic or eustatic cycles.

Since Middle Eocene times, neritic cool-water carbonates have been deposited along the southern Australian margin. This prograding carbonate platform has been studied by many authors in the last 50 years including Sprigg (1952), Ludbrook (1957, 1971), McGowran (1973), James et al. 1993, Bone et al. (1994), Morton et al. (1995), Morgan et al. (1995), White (1995, 1996), Gallagher and Holdgate (2000) and Li et al. (2000).

The second order unconformity-bounded packages identified on the southern margin spanning the late Middle Eocene to Early Oligocene and Late Oligocene to Middle Miocene have been further sub-divided, using foraminiferal biostratigraphy and stratigraphy, into unconformity-bounded third order packages, which can be correlated with glacio-eustacy. Feary and Loutit (1998) demonstrated that seismic packages in the offshore, deepwater Gippsland Basin are consistent with a global pattern and Holdgate and Gallagher (1997) and Gallagher et al. (1999) identified third-order sequences in the Gippsland and Otway Basin using stratigraphy and foraminiferal biostratigraphy. Seven third-order, unconformity-bounded packages were identified, also using foraminiferal biostratigraphy, in the Late Eocene to Middle Miocene Gambier Limestone in the Gambier Sub-basin, which were correlated to global glacio-eustatic patterns (Li et al. 2000) (Fig. 1.1).

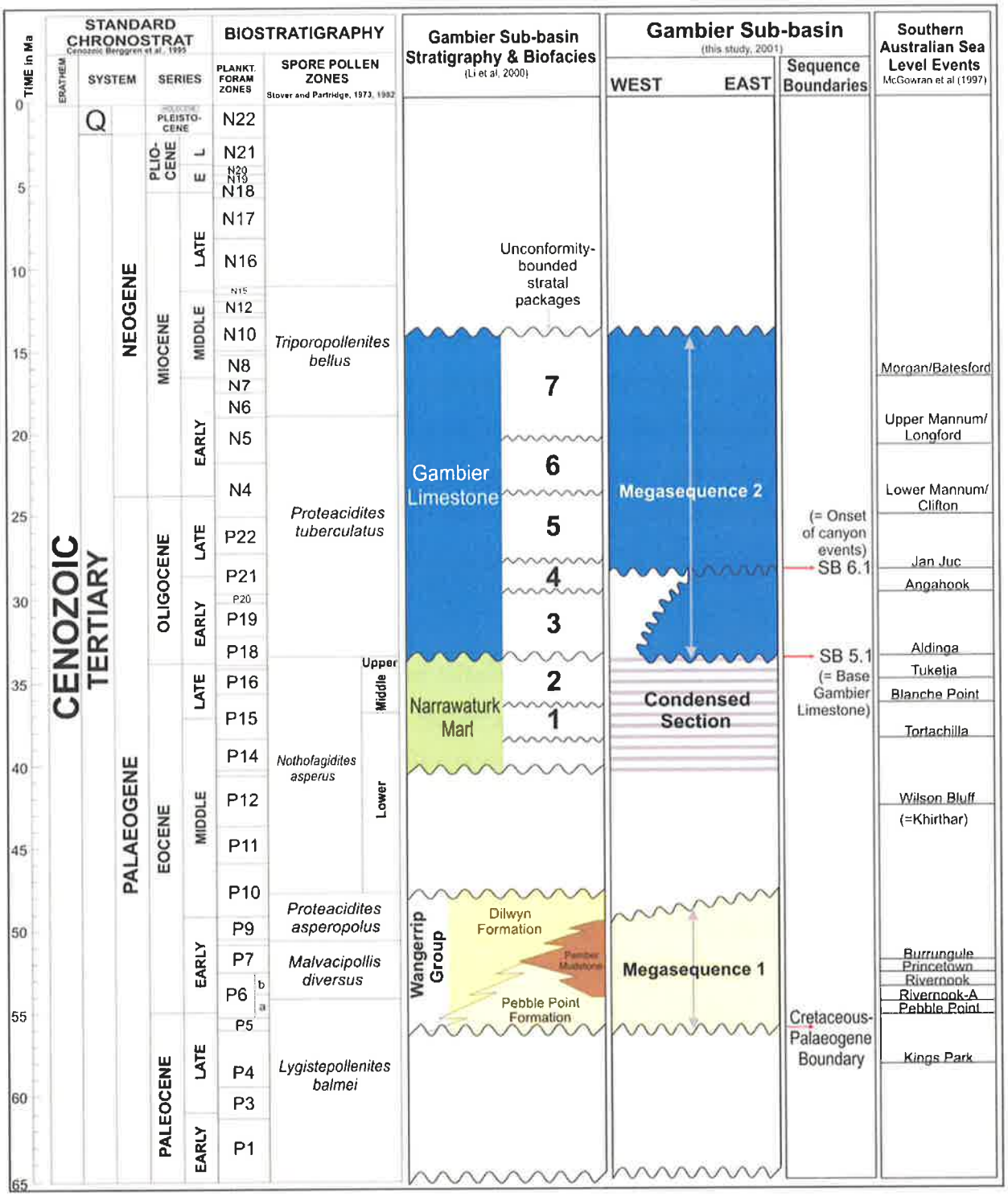

Figure 1.1 Summary stratigraphic column for the Gambier Sub-basin, southern Australia, illustrating the temporal distribution of the clastic (Megasequence 1) and carbonate (Megasequence 2) megasequences. These megasequences are compared with the Gambier Sub-basin lithostratigraphy, biofacies packages (Li et al. 2000) and southern Australian transgressive events (McGowran et al. 1997). This study concentrates on sediments deposited during the Cenozoic (i.e. since 65 Ma).

In addition to these previous studies that have analysed the stratigraphic evolution of the Cenozoic southern margin in terms of biostratigraphic species fluctuations and their relationship to global tectonics, glacio-eustacy and climate change, the southern Australian margin is an area that is actively explored for hydrocarbons. Petroleum exploration began in the Gambier Sub-basin in 1852 following the discovery of a black rubber-like substance called 'coorongite' that was recorded in and around the Coorong coastal lagoons (Wopfner and Douglas, 1971; McKirdy, 1985; Sprigg, 1985, Frears, 1995). The occurrence of coorongite and bitumen strandings aroused interest in petroleum prospecting and the first oil exploration well in Australia was drilled in 1866 at Alfred Flat, opposite the Coorong (Sprigg, 1985). 136 years later, the Gambier Sub-basin is still considered to be a frontier area with respect to petroleum exploration. There is currently very high demand on local energy markets and with the southeast of South Australia well supported by existing infrastructure, even relatively small gas discoveries could be economical to develop and ease the pressure on the market (Aust and Morton, 1995).

Exploration for oil and gas, especially within frontier basins, is a high-risk venture, generally due to the lack of detailed knowledge of basin history because of limited seismic and well control. Various methods are employed to reduce this risk, including application of predictive sequence stratigraphic studies integrated with biostratigraphy and seismic interpretation.

Sequence stratigraphy is an important technique that predicts the location of facies, allowing the position of potential sources of oil and gas to be identified (Kennard et al. 1999). The Gambier Sub-basin is an example of a frontier basin in southern Australia with only a few small developing gas fields. There is good seismic coverage and limited well coverage. Current exploration targets comprise Mesozoic plays, however a regional sequence stratigraphic study is needed to investigate the tectonic movements and sedimentation in the Cenozoic that have affected basin architecture and altered maturation and migration pathways of hydrocarbons into (and out of) Cretaceous petroleum systems and to predict the location of new Cenozoic plays.

1.2 Aims

The primary aim of this study is to develop a sequence stratigraphic framework for the Gambier Sub-basin which will extend knowledge of the four-part packaging of the Cenozoic southern

margin, already known from biostratigraphic and allostratigraphic studies, into the seismic realm. The study will also analyse the distribution of potential reservoir, source and seal facies and study the timing and degree of faulting within the established sequence stratigraphic and chronostratigraphic framework, integrating seismic data, wireline logs, biostratigraphy, outcrops, core and cuttings descriptions, to determine possible migration pathways from known source kitchens to potential stratigraphic and structural traps.

1.3 OBJECTIVES

To gain new insight into the development of the southern margin during the Cenozoic, analysis of the depositional sequence of packages on seismic data, integrated with outcrop and well data (including biostratigraphy), will be conducted. To this end, a significant component of this study will involve interpretation of 2D seismic data, integrated with all available well data, while employing sequence stratigraphic principles.

The distribution of the seismically defined sediment packages will be analysed spatially (by mapping) and temporally (by chronostratigraphic diagrams). This will allow interpretation of the progressively changing depositional environments in the sub-basin through time. This will potentially allow identification of hydrocarbon plays by defining the location and distribution of reservoir sands that are overlain by fine-grained sealing lithologies.

Further to understanding the development of petroleum systems in the sub-basin, the timing and magnitude of faulting affecting Cenozoic sediments will be analysed. Fault reactivation events will have influenced trap formation and integrity as well as potentially opening or closing vertical hydrocarbon migration pathways. This will be analysed through interpretation and mapping of faults on seismic data to determine if there is any pattern of fault movement at different times throughout the Cenozoic. This information will then be integrated with previous maturation and thermal history studies to define play concepts in the Gambier Sub-basin.

1.4 GEOLOGICAL SETTING

The southern Australian margin is a passive continental margin, shaped during the breakup and dispersal of eastern Gondwana and displaying a succession of phases—prerift, rift valley, oceanfloor emplacement, and progradation—during the Mesozoic and Cenozoic Eras (Veevers, 2000). The Gambier Sub-basin is located in the western part of the Otway Basin and forms part of the Australian Southern Rift System (Stagg et al. 1990). The Australian Southern Rift System (Fig. 1.2) is a divergent, passive continental margin that has experienced Jurassic-Palaeogene rifting and spreading, resulting in the separation of Australia and Antarctica.

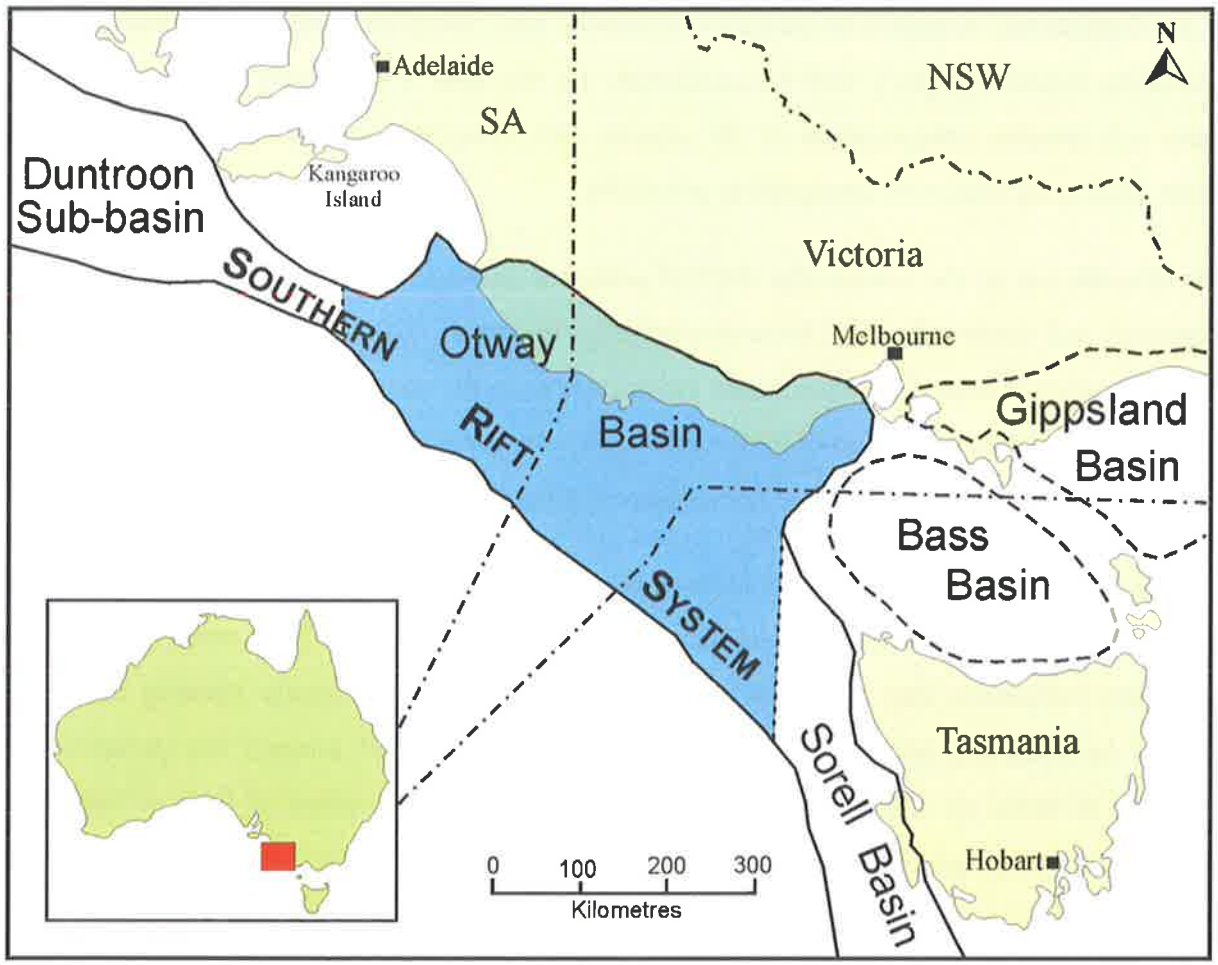

Figure 1.2 Location of the Otway Basin in the Australian Southern Rift System (Cockshell, 1995).

The Gambier Sub-basin (previously known as the Gambier Embayment of the Otway Basin—Wopfner and Douglas, 1971; White, 1995) consists of Cenozoic sediments overlying the Mesozoic wedge of the Otway Basin. Cenozoic sediments include two unconformity-bounded packages—the lower, early Palaeogene package comprising the Wangerrip Group siliciclastic sediments and the upper, late Palaeogene and Neogene package comprising the neritic, extra-tropical Gambier Limestone (Fig. 1.1).

The main study region is an area south of the Tartwaup Hinge Zone—the western Voluta Trough—on the south-eastern South Australian continental shelf and slope, and the Chama Terrace—an offshore structural high northwest of the Tartwaup Hinge Zone (Fig. 1.3). Increased subsidence south of the Tartwaup Hinge Zone during the latter part of the Mesozoic formed the Voluta Trough, which remained a topographic low into the early Cenozoic, thereby providing the main depocentre for Late Paleocene-Early Eocene Wangerrip Group sediments. Major marine transgressions submerged the Otway Basin in the later Eocene, encouraging progradation of the Gambier Limestone across the shelf during the Oligocene to Middle Miocene (Fig. 1.3).

The northern limit of the sub-basin is the E-W trending Padthaway Ridge (Sprigg, 1952; Cockshell, 1995), a submerged basement high that separates the Otway and Murray Basins (Fig. 1.3). The Merino Uplift marks the eastern limit, separating the Gambier Sub-basin and Port Campbell Embayment, while the south-western limit of the Sub-basin lies out on the abyssal plain in water depths of more than 4500 m (Figs. 1.3 & 1.4).

Onshore, surface expression is minimal with only a handful of outcrops. A large part of the Sub-basin is expressed as a coastal plain with extinct volcanoes and ridges of sub-parallel northwest trending dunes (Fig. 1.4). These dunes are 15-30 m high and are associated with regressive Pleistocene stranded shorelines (Wopfner and Douglas, 1971). Karst features, such as caves, dolines and sinkholes, within the Gambier Limestone dominate the sub-surface onshore. Offshore, the continental slope is incised by numerous large submarine canyons (Fig. 1.4; refer to Chapter 3 for a more detailed discussion).

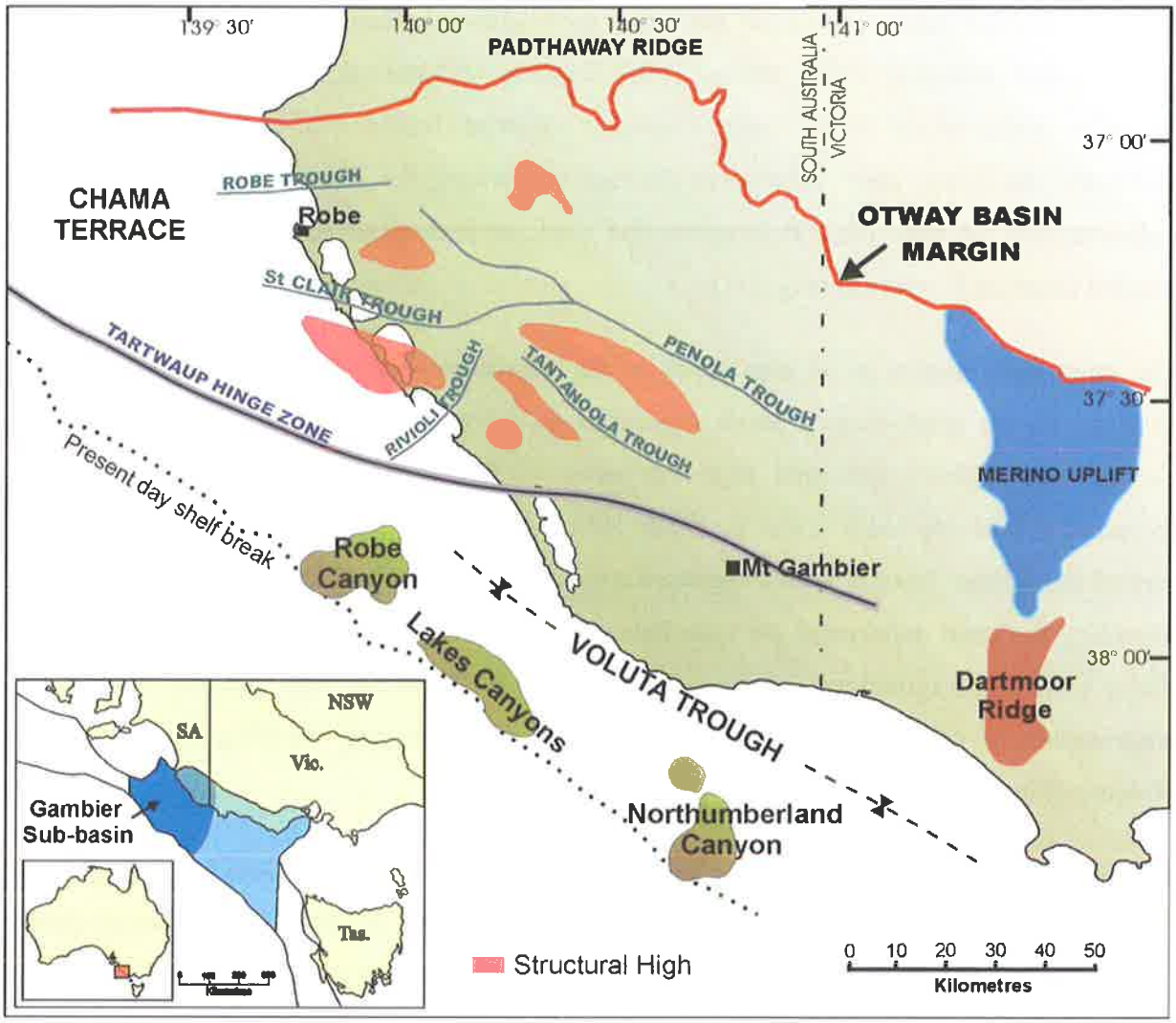

Figure 1.3 Location map of the Gambier Sub-basin illustrating the main structural elements, including the locations of the three major palaeo-submarine canyon systems (refer to Chapter 3; figure modified from White, 1995).

1.5 DATABASE AND DATA LIMITATIONS

The database for this sequence stratigraphic study includes 2D reflection seismic (Fig. 1.5), wireline log, well completion report, micropalaeontological, palynological, outcrop, sidewall core and cuttings data.

Origin Energy provided digital wireline logs from open file wells included in the study and a digital seismic data set consisting of 120 digital, un-interpreted, processed and migrated 2D seismic lines of vintages ranging from 1980-1997. The seismic grid consists of 55 onshore lines

and 65 offshore lines with a line spacing of 5-10 km (Fig. 1.5; line details in Appendix 1). The onshore seismic data initially acquired was not used due to very poor resolution in the shallow section, making interpretation impossible. The offshore seismic grid, integrated with available wells proved adequate for the initial sequence stratigraphic analysis however the grid was sparse in some areas which introduced griding artefacts during mapping and was orientated at such an angle that the full array of synthetic and antithetic faults could not be accurately analysed. Much more 2D seismic data exists than was used in this study so that quite a dense grid covers most of the offshore part of the Gambier Sub-basin, however due to the time constraint and scope of this study, interpretation of any more seismic data was not feasible.

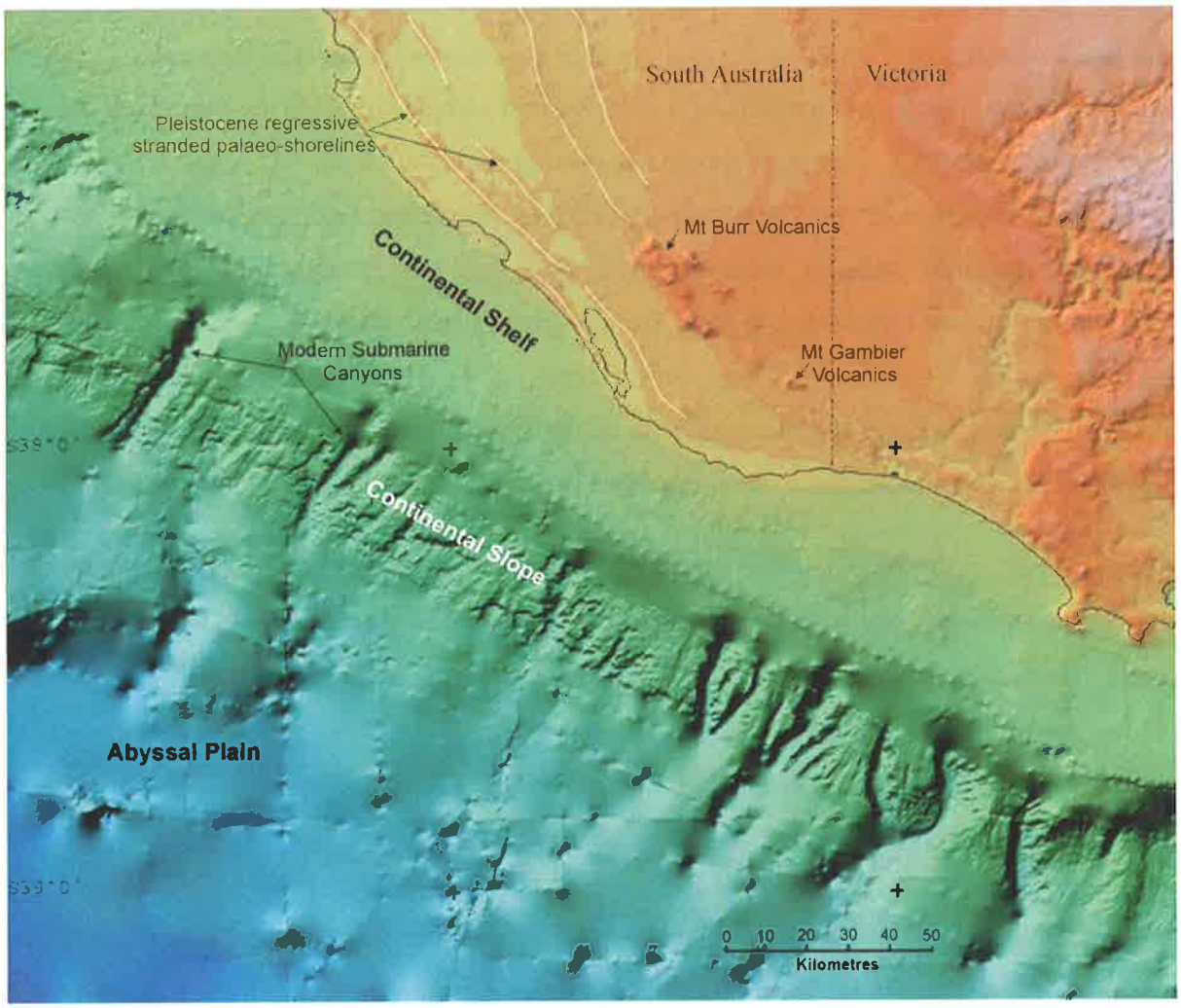

Figure 1.4 Topographic elevations and bathymetry, Otway Basin, South Australia (image supplied by Geoscience Australia).

Geoscience Australia (GA) provided four regional 2D deep-seismic lines (1994-95 vintage) that extend from the inner shelf to the abyssal plain (Fig. 1.5). This data had been reprocessed and was of good quality but was confidential and data licence agreements restricted publication of the seismic. This data was obtained to try to determine the basinward extent and character of the sediments and canyons on the slope, but upon interpretation of these lines, these features were not readily identifiable and did not add to the interpretations made in this study, therefore no seismic data from this survey has been presented in figures. Bathymetric maps were also supplied by GA. These grids include data from the GA ship-track database, swath bathymetry by National Oceans Office and GA along the continental slope, and digitised charts from the Australian Hydrographic Service on the shelf (Figs 1.4 & 1.5).

Primary Industries and Resources, South Australia (PIRSA) provided well completion report data for 26 open-file wells within the study area (Fig. 1.5—well details in Appendix 1). PIRSA also made conventional core available for analysis and samples of ditch cuttings from the zone of interest in most wells. Existing Cenozoic biostratigraphic data from wells was derived from a few samples, mostly near the Cretaceous-Palaeogene boundary, hence existing samples were re-analysed and new samples were obtained, processed and analysed for palynology and foraminifera in order to establish a more comprehensive biostratigraphic zonation through the Cenozoic section as required for this study (Appendix 1). However some of the wells were already over-sampled and the cuttings bags in the Government store contained less than the 100g to be retained as required by law, therefore preventing sampling for biostratigraphy.

The abundance of lithostratigraphic names defined over the last 50 years in the Gambier Sub-basin was very confusing with many names now superseded or redundant. Therefore, I have chosen to adopt the formation names and hierarchy defined by Morton et al. (1995).

1.6 Methods

A significant component of this study involved interpretation of an integrated dataset comprising 2D seismic data, wireline logs, biostratigraphy, core and cuttings data, employing sequence stratigraphic principles.

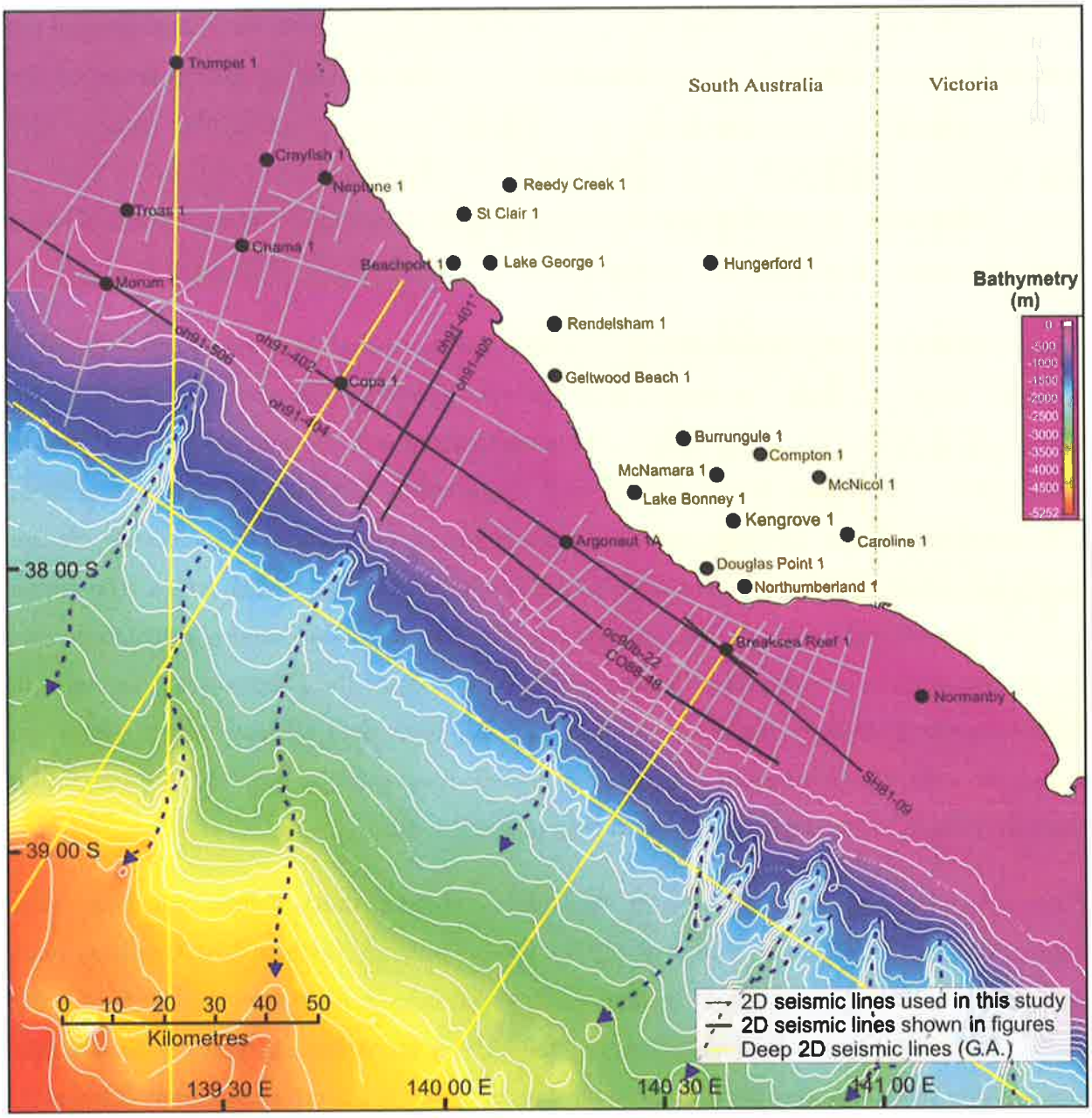

Figure 1.5 Map of the bathymetry in the Gambier Sub-basin. Also illustrated is the location of the offshore 2D reflection seismic grid and the well data. (Bathymetry is from a grid at 250 m cell size developed by Geoscience Australia.)

1.6.1 Seismic interpretation

Seismic data were interpreted using Geoframe's IESX 2D Interpretation module employing the standard methods covered in the Schlumberger User Manual. During interpretation of the Cenozoic succession, seismic packages were identified at smaller and smaller scales – with respect to time duration and aerial distribution. A naming scheme was defined in order to clearly communicate the results of the study by placing each package in its appropriate position in the hierarchy.

A megasequence was the largest package identified and represents the sedimentary response to a major phase of basin evolution (e.g. pre-rift, syn-rift, post-rift) (Hubbard, 1988). Megasequence boundaries in this study were regional unconformities that could be correlated to global tectonic or eustatic events. Within each megasequence, a number of supersequences were identified. These packages are bounded by locally extensive, conspicuously erosive sequence boundaries. Each supersequence comprised up to three sequences, which represented localised depositional events such a progradation of a delta lobe. The naming convention used for this hierarchy is, for example, "Sequence 2.3", which is the third depositional sequence in Supersequence 2. Where seismic resolution allowed, individual systems tracts within the sequences were also interpreted. These were named in accordance with the sequences; for example, HST 2.3 is the highstand systems tract in Sequence 2.3.

These sequences are not the same as the global second, third, fourth and fifth order sequences/cycles identified by Vail et al. (1977). Second order cycles span 10-100 million years and are controlled by glacio- and tectono-eustacy and consist of a grouping of third order cycles. Third order cycles have durations of 1-10 million years, but are typically shorter than three million years, however the control on third order cycles is a controversial topic (Plint et al. 1992). Fourth order (500,000-200,000 years) and fifth order (200,000-10,000 years) cycles are controlled by the Milankovitch cycles, astronomical perturbations in the Earth's orbit and axial tilt, which cause climatic fluctuations that result in sea level change (Plint et al. 1992).

Mapping of interpreted horizons and faults was carried out in the IESX Basemap Plus module and gridded surfaces were displayed in three dimensions (3D) in the Geoviz module. Time-structure and interval thickness maps were created for each major sequence and systems tract (Appendix 4).

1.6.2 Sequence stratigraphy

Sequence stratigraphy is a powerful tool for the stratigraphic analysis of sedimentary basins and is particularly applicable for hydrocarbon exploration (Kennard et al. 1999). It allows analysis of the sediment fill in basins in terms of sea level change, tectonism and sediment supply and enables a better understanding of the linkage between sedimentation patterns in different parts of a basin. Ultimately it can be used to predict the location of reservoir and seal-prone intervals and zones within a basin (Kennard et al. 1999).

Sequence stratigraphy is derived from seismic stratigraphy and with the integration of lithostratigraphy and facies analysis may be considered a special type of event stratigraphy (Miall, 1990). Much work has been done in the field of sequence stratigraphy in the last 40 years with Fisher and McGowen, 1967; Brown and Fisher, 1977; Posamentier et al., 1988; Kennard et al. 1999; Posamentier and Vail, 1988; Miall, 1990; Allen and Posamentier, 1993; Schlager, 1993; Wehr, 1993; and Emery and Myers, 1996—among others—being the main influence on the methodology used in this study. For a more comprehensive discussion on sequence stratigraphy and seismic stratigraphy please refer to Appendix 2.

1.6.3 Wireline logs

A suite of digital conventional wireline logs for wells included in this study were obtained from Origin Energy. The logs were converted from depth to two way time (TWT) for comparison with seismic by preparing synthetic seismograms in Geolog™. This was done using well checkshot data in accordance with the standard methods covered in the Geolog™ User Manual.

Interval velocities for each supersequence have been averaged from well checkshot data and are consistently used throughout the study for conversion of seismic picks in time to depth. These velocities are presented in Table 1.1.

1.6.4 Biostratigraphy

Results from a study conducted by White (1995), which analysed the biostratigraphy and sedimentology of Cenozoic sediments from petroleum wells in the Gambier Sub-basin, were integrated with additional palynological data analysed by Liliana Stoian and Andrew Rowett (PIRSA) (Appendix 1).

SUPERSEQUENCE	INTERVAL VELOCITY (M/SEC)
6	2300
5	2300
4	2300
3	2485
2	2620
1	2980

Table 1.1 Interval velocities used throughout this study for each supersequence.

In addition to analysis of previously prepared sample slides, new cuttings samples were obtained and prepared for palynological analysis according to standard practices (e.g. Traverse, 1988; Appendix 2). Dr. Qianyu Li of Adelaide University conducted micropalaeontological analysis on previously prepared slides containing washed, dried and sieved samples that were then dated (Appendix 1). This work supplemented a study of the foraminiferal biofacies in the Gambier Limestone that was conducted by Li et al. (2000) as part of the larger Gambier project.

1.6.5 Outcrop analysis

Outcrop analysis was completed during a field trip to the Mount Gambier region in South Australia and the Port Campbell Embayment in Victoria. The field trip guide is presented in Appendix 3.

1.6.6 Well correlation

Several stratigraphic cross-sections in both dip and strike directions were completed using all available data including wireline logs, seismic interpretation and biostratigraphy (Appendix 4). The biostratigraphic data used for the well correlations is often sparse or lacking completely in

onshore wells. In many onshore wells, the upper part of the clastic succession is lacking in biostratigraphic control and well correlation relied on wireline log signature alone with some interpolation from seismic data offshore. Some wells have only the gamma ray logs extending into the Cenozoic section, limiting the data required for reliable well correlation.

1.6.7 Palaeogeography

Seismic interpretation and stratigraphic cross-sections formed the basis of the palaeogeographic maps devised below to document transgression and regression of the shoreline throughout the Cenozoic and determine the potential distribution of reservoir and seal facies (Chapter 4). Table 1.2 illustrates the method used for determining the depositional environment of systems tracts and sequences from wireline log motifs (based on Allen, 1964; Coleman et al. 1969; Elliot, 1979; 1986; Battacharya and Walker, 1992; Van Wagoner et al. 1990; Galloway, 1998).

The percentage of sand for selected systems tracts and sequences was analysed and gridded in *Petroseis* using minimum curvature griding and bicubic interpolation with a 10% sample distance. These grids were then converted to geo-referenced tiff files via *ER Mapper*. The spreadsheet of raw values appears in Appendix 1. These maps were made using data from all available wells (as indicated on the maps) based on well correlations (Appendix 4), however due to onlap and erosion of sequences in the northern part of the Voluta Trough there are often not enough wells in which the sequences are represented. Hence there is a significant amount of uncertainty associated with these distribution maps and the finer detail of sandy fluvial channels and distributary mouth bars are largely lost.

The sedimentation rates and progradation to aggradation ratios were calculated on seismic lines UA82-31 and UA-82-35 (values in Appendix 1). Sedimentation rates were calculated by deriving the volume of each supersequence (2D area calculated from seismic data offshore plus average thickness in wells onshore, multiplied by the aerial extent of each sequence), divided by the approximate duration of each package, which gave the sedimentation rate in km^3/M.y. Where it was interpreted on seismic data that a supersequence had been partially eroded, the volume of the eroded portion was approximated and added to the preserved volumes to give an approximate original sedimentation rate. This value is just an approximation because the actual aerial extent of the supersequences cannot be determined accurately with the data available for this study (i.e. some sequences extend beyond this study area). Hence sedimentation rates are

most useful for comparisons within this study as a relative indication of changing rates in the Gambier Sub-basin.

In calculating the progradation to aggradation ratios the distance of progradation of each sequence, measured in metres (from shelf break to shelf break) on seismic data, was divided by the vertical thickness of each supersequence (measured in seconds TWT and converted to metres).

Table 1.2 Depositional environments identified in the Gambier Sub-basin during the Cenozoic with examples of the typical wireline log motifs for each environment and examples of modern analogues.

Depositional Environment	**WIRELINE LOG MOTIF**	**MODERN ANALOGUE**
Amalgamated Fluvial Channel Belt	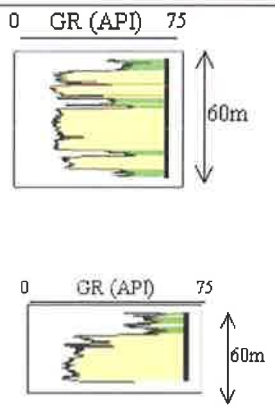	
Crevasse Splay	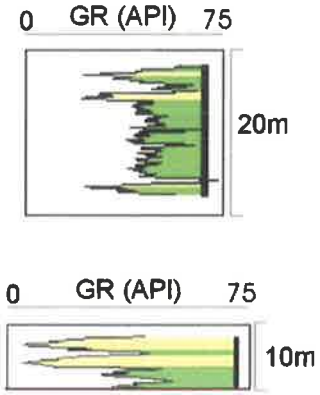	

Coastal Plain Lagoon/ Overbank Deposit	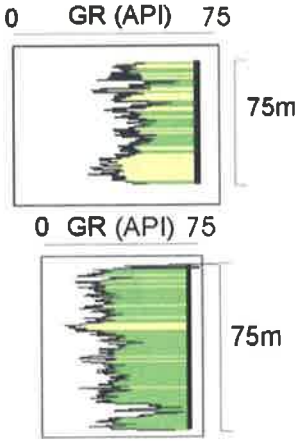	
Delta Lobe	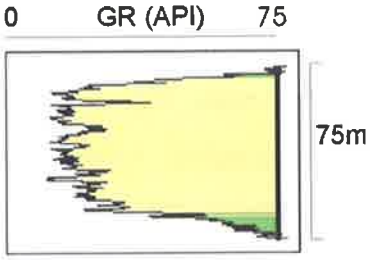	
Inter-Distributary Bay	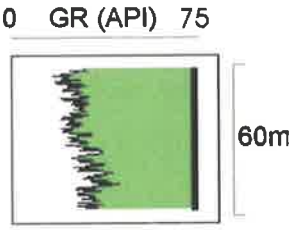	
Distributary Channel	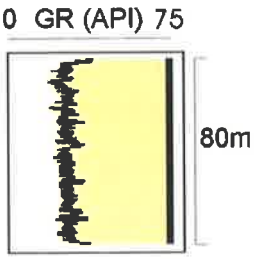	

Beach Barrier Bar	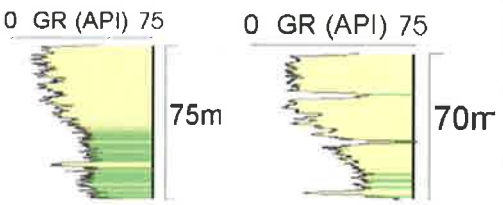	 Photo from http://www.photolib.noaa.gov/coastline

1.6.8 Chronostratigraphy

Interpretation and mapping of sediment packages from seismic data analysed the spatial distribution of sediment in the sub-basin, and once key surfaces were dated using biostratigraphy, construction of chronostratigraphic diagrams was facilitated. Chronostratigraphic diagrams are drawn to summarise the ordering of the deposition of sediment and are a means of showing the time relationships of these systems and their relationships to surfaces of non-deposition, condensation and erosion. These surfaces have little or no thickness in the rock record and their true significance can be better appreciated by considering them in their time dimension (Emery and Meyer, 1996) (Chapter 4). A chronostratigraphic chart has a vertical axis in time, with a spatial horizontal axis. On the chart are plotted the distribution of systems tracts, bounded by surfaces of onlap, toplap, downlap, etc.

1.6.9 Fault analysis

One of the aims of this study was to determine the timing and degree of faulting during the Cenozoic. Faults were interpreted on the 2D regional seismic grid (Fig. 1.5) using Geoframe's IESX 2D seismic interpretation module. The faults were then correlated, where appropriate, based on location relative to other interpreted faults on adjacent lines, magnitude of throw and dip direction. The regional normal-fault strike direction is in the northwest-southeast direction and the orientation of the seismic grid made these faults the easiest to correlate. However the 2D seismic grid was too coarse to allow accurate correlation of all identified faults. Faults were most dominant and therefore primarily interpreted on dip lines, which run perpendicular to the regional normal fault strike and to the present day shoreline. Normal faults with significant

throws and deep penetration into to Early Cretaceous sediments were correlated between adjacent seismic lines where possible.

Those faults with throws below seismic resolution could not be correlated to adjacent seismic lines and may represent synthetic or antithetic strike-slip faults. These faults with uncertain orientation are represented on the fault interpretation maps as dots. For fault interpretation maps at each Supersequence boundary please refer to Appendix 4.

The magnitude of throw for each correlated fault was calculated from seismic data at horizons SB 1.1, 2.1, 3.1, 4.1, 5.1, 6.1 and the sea floor, in milliseconds two way time (ms TWT) and converted to depth using the velocities in Table 1.1 (see Appendix 1 for data tables). Five types of faults were identified from seismic data based on the stratigraphic horizon to which they penetrated; K-P boundary faults (coloured coded red), Wangerrip faults (blue), carbonate faults (green), deep seafloor faults (orange) and recent seafloor faults (yellow).

"*Breakout*", a software program normally used to analyse the orientations of borehole breakouts, was adapted to analyse the orientation (strike of the faults measured from the fault interpretation maps), dip (calculated from seismic data), dip direction and throw of correlated faults in this study. Values were entered into a database that was queried by "*Breakout*" and plotted as throw-weighted rose diagrams (adapting the eccentricity-weighting used when analysing borehole breakouts), which image the orientation and total magnitude of throws, and tadpole plots, which image the dip and dip direction (Chapter 5).

The throw at a particular horizon represents the sum of all movement experienced by that fault in the time since that horizon formed. For example, total cumulative movement of faults during the Cenozoic is represented by throws at horizon SB 1.1. Therefore, by subtracting the throw of a particular fault at horizon SB 2.1 (which represents the total cumulative movement of that fault since SB 2.1 formed), the total throw that occurred at time SB 1.1 was derived. Hence, movement of faults at particular times during the Cenozoic were tabulated (see Appendix 1) and graphed (Chapter 5).

The faults were then divided into five categories and located on fault interpretation maps based on the shape of the graph of movement during the Cenozoic in an attempt to determine if different regions experienced active faulting at different times during the Cenozoic.

Hydrocarbon maturity data (Hill, 1995; Williamson et al. 1996), and fault analysis and timing were then combined with the results of the seismic sequence stratigraphic study to discuss potential plays in the Gambier Sub-basin.

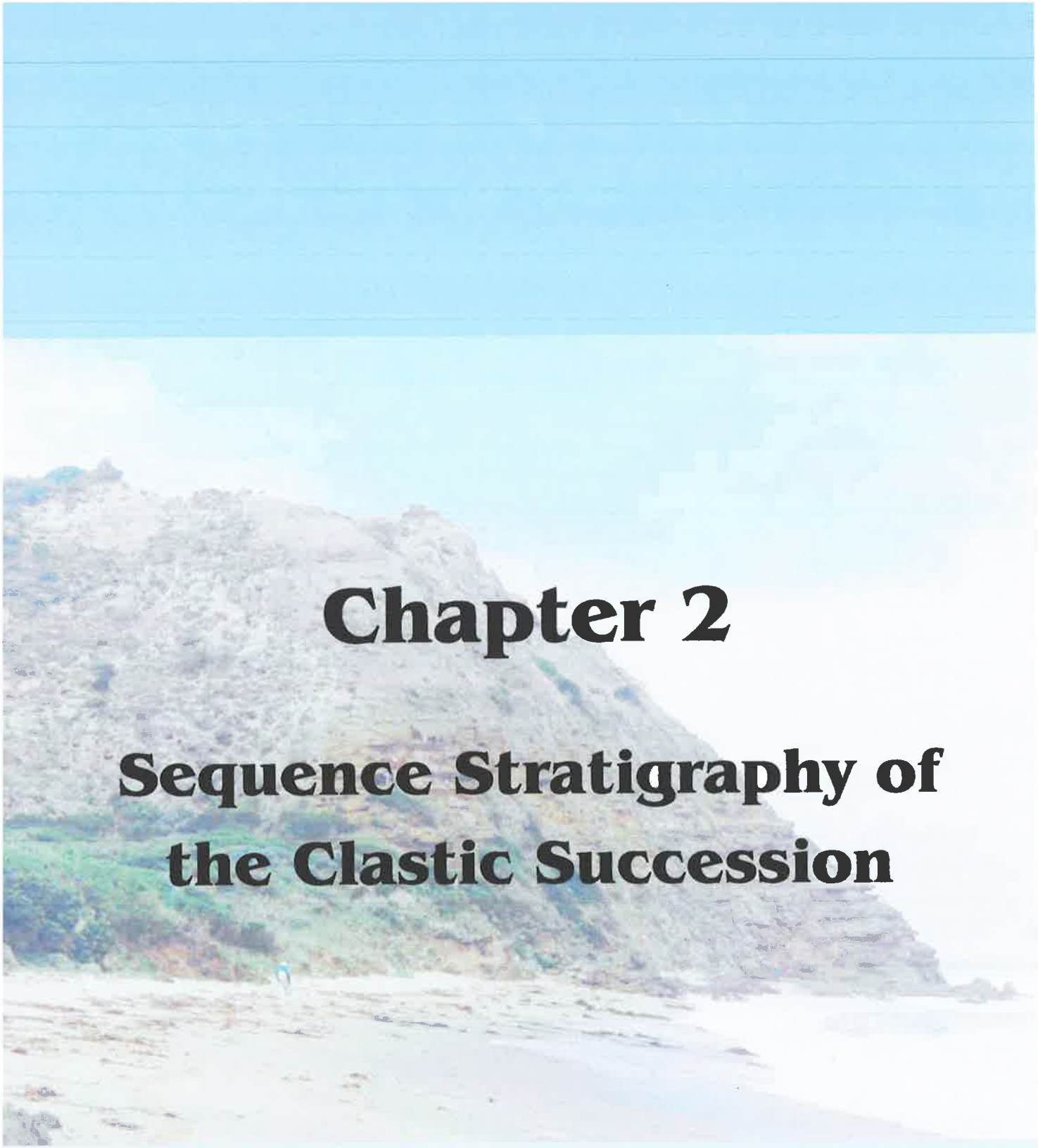

Chapter 2

Sequence Stratigraphy of the Clastic Succession

2 MEGASEQUENCE 1 – SEQUENCE STRATIGRAPHY OF THE CLASTIC SUCCESSION

The Otway Basin initially developed in the Jurassic and Early Cretaceous as an intra-continental rift basin prior to the breakup of Gondwana. During Middle Cretaceous times, a passive margin developed and the Australian and Antarctic continental plates started to drift apart, during which time, the Gambier Sub-basin was formed. A major marine transgression at the beginning of the Palaeogene led to the development of marginal marine and deltaic depositional environments in the Voluta Trough, south of the Tartwaup Hinge Zone. This chapter discusses the seismic, wireline log and outcrop expression of the Late Paleocene to Early Eocene Wangerrip Group sediments.

2.1 PREVIOUS WORK

Thermal doming, signifying the onset of an intra-continental extensional regime, began in the Late Jurassic to Early Cretaceous (Tithonian to Barremian) and later led to the separation of Australia and Antarctica (Middleton and Falvey, 1983; Yu, 1988; Pettifer et al. 1991; Cockshell, 1995; Finlayson et al. 1998; Norvick and Smith, 2001) (Fig. 2.1). Rifting was progressive from west to east and extension formed east-west trending grabens. The continent/ocean boundary formed during the Cenomanian, which marked the changeover from the intercontinental rift system to the phase of oceanfloor spreading (McGowran et al. 1997; Fig. 2.1). Oceanic spreading began in the Santonian in the southern Tasman Sea and slow extension caused thinning of the continental crust and subsidence into deeper water in the Otway Basin (Norvick and Smith, 2001; Fig. 2.1).

The magnitude of latest Jurassic to Early Cretaceous continental extension has been estimated to be in the order of 300 km (Powell et al. 1988; Willcox & Stagg 1990), in a NW-SE to NNE-SSW direction (the precise direction remains a point of contention eg. Boeuf & Doust 1975; Powell et al. 1988; Etheridge et al. 1985; Willcox & Stagg, 1990; Willcox et al. 1992; O'Brien et al. 1994; Hill et al. 1994; Perincek & Cockshell, 1995). The various interpretations of early extension direction, ranging from NW-SE to NE-SW, are probably partly the result of local variations in pre-rift basement structural grain, changes in intra-plate stress along the 4000 km

long plate boundary, and the effects of subsequent structural overprinting, as well as lack of deep seismic data (Hill et al. 1997).

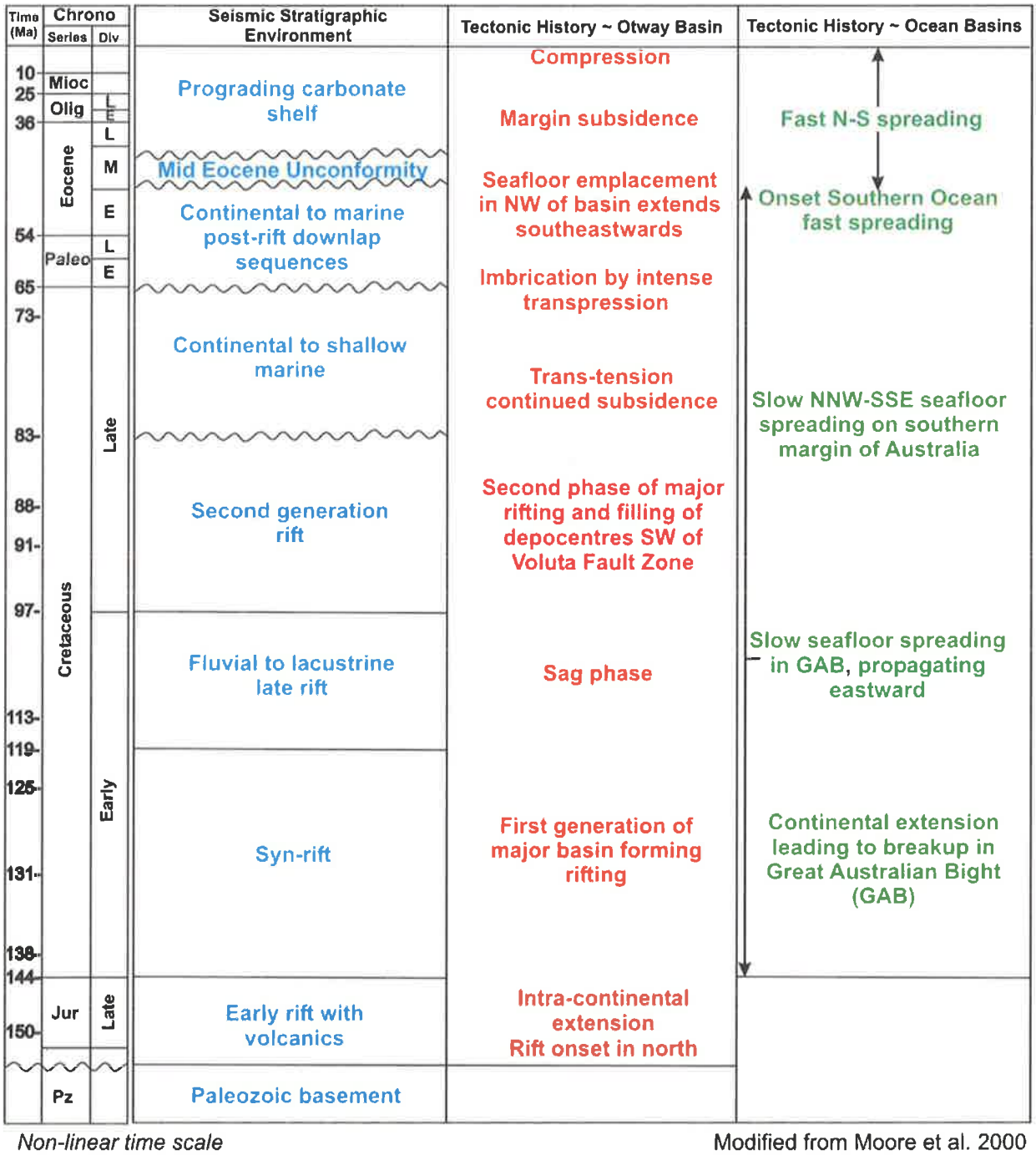

Figure 2.1 Summary of the tectonic history of the Otway Basin and southern margin.

Lowry (1987) suggests that during the middle Cretaceous, in addition to the slow spreading between Australia and Antarctica, the picture is complicated by the opening of the Tasman Sea, which resulted in the eventual separation of the New Zealand and Australian plates and the formation of the Gippsland Basin. Yu (1988) states that this east-west stress would have progressively uplifted the Otway Basin and formed the Gambier Sub-basin and Port Campbell Embayment and structural highs such as the Otway Ranges.

The subject of breakup off the southern margin of Australia is controversial. Early analysis of seafloor spreading anomalies by Weissel & Hayes (1972), put the onset of seafloor spreading at 55 Ma, then based on this, Falvey (1974) placed the breakup unconformity in the Otway Basin between the Late Cretaceous Sherbrook Group and the Paleocene/Eocene Wangerrip Group. Reinterpretation by Cande & Mutter (1982) revised the time of breakup as mid Cretaceous, which was further refined to 95±5 Ma by Veevers (1986). Subsidence curves and micropalaeontological studies derived from well data indicate a west to east propagation of breakup along the southern margin, with breakup off the Otway and Sorell Basins at ~60 Ma (Mutter et al. 1985; Shafik, 1990). Recent work on plate reconstructions by Norvick and Smith (2001) led them to admit that the breakup history of the southern margin is quite complex with the result being that the traditional concept of the "breakup unconformity" is somewhat irrelevant to southern Australia.

Seafloor spreading started in the Late Cretaceous and drifting occurred at the relatively slow rate of 4.3 mm half rate/year (i.e. rate of spreading on one side of the Mid Ocean Ridge only) for the next 40 to 50 M.y. (Cande and Mutter, 1982; Cockshell, 1995; Fig. 2.1). As drifting continued, a transgression occurred from the east in the early Palaeogene over the subsiding margin producing deltaic and marginal marine environments (Deighton et al. 1976; Yu, 1988). These deltaic sediments are known as the Wangerrip Group (Morton et al. 1995).

Spreading in the Tasman Sea finished at about 52-54 Ma, but slow spreading continued in the Southern Ocean (Norvick and Smith, 2001). In the Middle Eocene (~44 Ma) the spreading rate between Australia and Antarctica significantly increased and changed direction from NW-SE to N-S (Deighton et al. 1976; Yu, 1988; Cockshell, 1995; Hill et al. 1997; Norvick and Smith, 2001; Fig. 2.1). The Tasman Sea rift arm failed and aborted its spreading activity and the Southern Ocean spreading centre formed the more dominant arm of the rift system and continued spreading at an increased rate (Yu, 1988).

The increase in spreading rate resulted in thermal subsidence of the southern margin and a rise in relative sea level as well as the establishment of a proto-Circum-Antarctic Current. This led to the starvation of clastic sediments on the shelf and allowed progradation of cool water carbonates across the shelf from the latest Eocene (Deighton et al. 1976; Cockshell, 1995; Fig. 2.1). The Circum-Antarctic Current became fully established in the mid Oligocene and there were major increases in Antarctic sea level, glaciation and sediment progradation on the shelf (Norvick and Smith, 2001).

Two megasequences can be recognised in the Cenozoic Gambier Sub-basin based on seismic interpretation and supported by limited well data, which can be correlated to the global second-order packages identified by McGowran (1978, 1979a, b); Frakes et al. (1987); Quilty (1977, 1980, 1994) and McGowran et al. (1997) (refer to Chapter 1). Megasequence 1 comprises Late Paleocene to Early Eocene clastics of the Wangerrip Group and Megasequence 2 consists of up to 540 m of Oligocene to Middle Miocene carbonates of the Gambier Limestone. Six third order supersequences and 31 fourth-order sequences have been identified on seismic data within the Megasequences 1 and 2 (Fig. 2.2). Outcrop data has been used to support interpretations from seismic and well data (Fig. 2.3)

Sediments of late Middle Eocene to Late Eocene age (Mepunga Formation and Narrawaturk Marl) are only present in the northern Gambier Sub-basin and eastern Otway Basin (Port Campbell Embayment) and are not recognised on seismic data in the offshore Gambier Sub-basin. These sediments were deposited during a series of marine transgressions and are probably represented by a condensed section in the offshore Gambier Sub-basin, with the package being so thin it is below seismic and biostratigraphic resolution (Fig. 2.2).

2.2 SEISMIC AND WIRELINE LOG EXPRESSION

The distribution of Cenozoic sediments in the Gambier Sub-basin can be seen from an interval-thickness map (ms TWT) constructed between the seafloor and the basal Cenozoic surface. Figure 2.4 clearly identifies the two major structural provinces in the Cenozoic Gambier Sub-basin—the Chama Terrace in the west, which was a sediment by-pass margin during the Paleocene and Eocene; and the deep Voluta Trough to the east, which was the main depocentre for sediments of Megasequence 1 (Fig. 2.2).

Megasequence 1 comprises four supersequences, each bounded by regional unconformities resulting from relative sea level falls. Each supersequence contains discrete sequences and systems tracts (LST, TST, HST), although some are below seismic resolution.

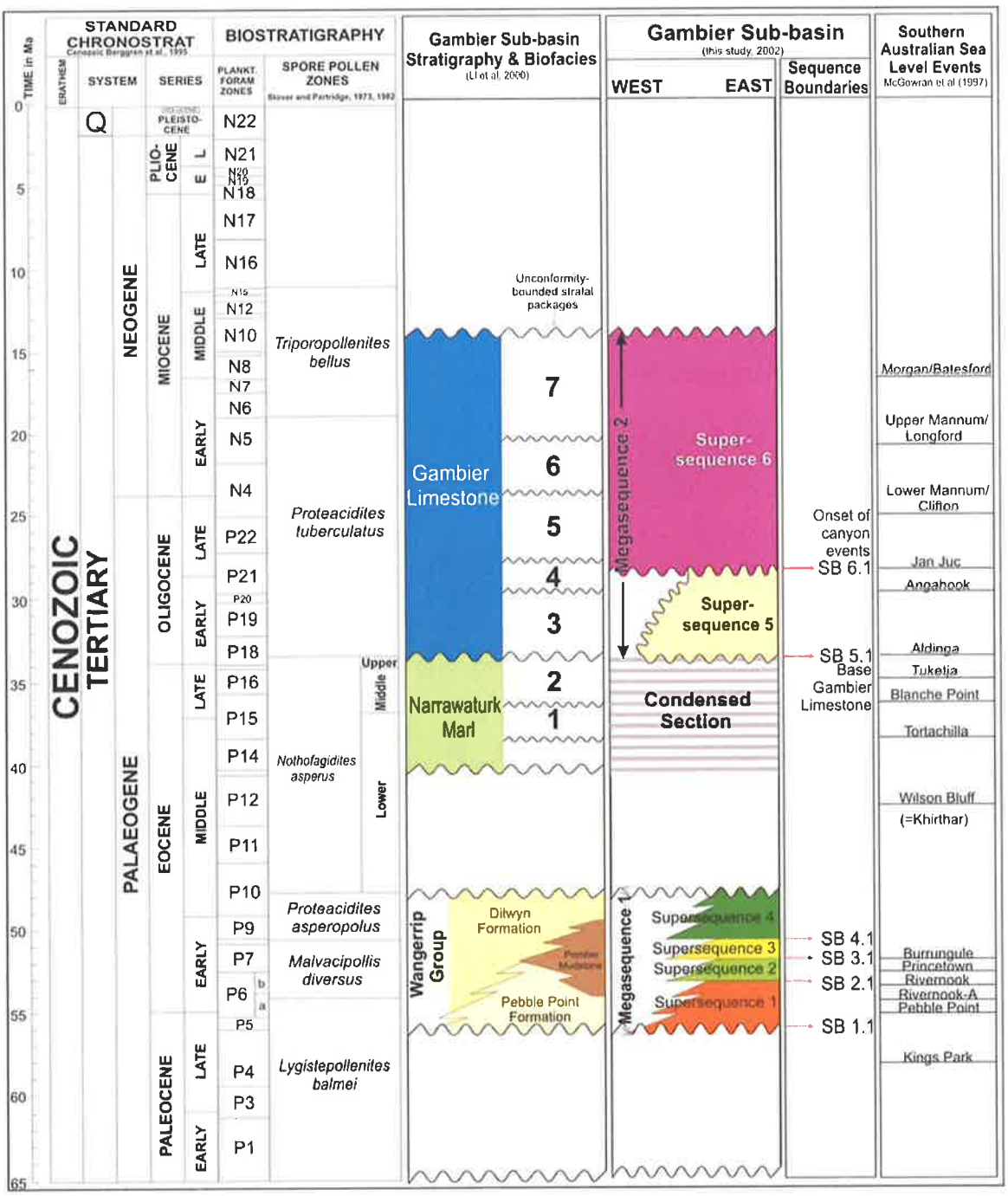

Figure 2.2 Summary of the temporal distribution of supersequences interpreted from seismic data in the Gambier Sub-basin. Also represented is the stratigraphy for the Gambier Sub-basin, the seven unconformity-bounded packages identified by Li et al. (2000) and Southern Australian Cenozoic sea level events (McGowran et al. 1997).

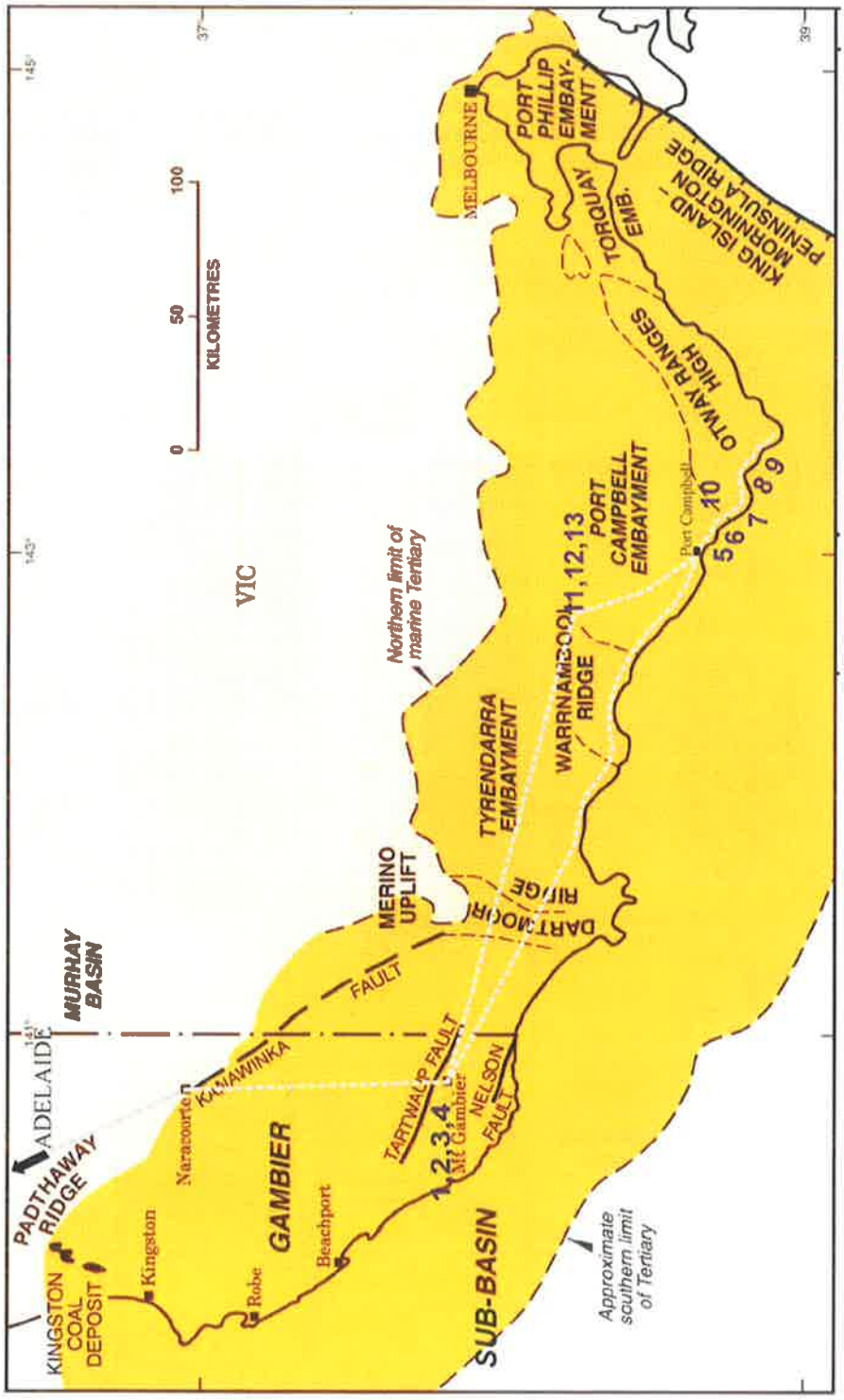

Figure 2.3 Location of outcrops studied in the Gambier Sub-basin and Port Campbell Embayment. Refer to Appendix 3 for more detail.

2.2.1 Supersequence 1

Supersequence 1 comprises just one sequence made up of a combined LST/TST and overlying HST deposited in the Voluta Trough. The LST/TST is interpreted to partially represent the Pebble Point Formation and the HST may, in part, constitute the Pember Mudstone and lower part of the Dilwyn Formation (Fig. 2.2). Supersequence 1 was deposited in the Voluta Trough, south of the Tartwaup Hinge Zone but is absent from the Chama Terrace, which was a structural high and sediment by-pass zone during the Paleocene and Early Eocene. This package records a major marine transgression in the western Otway Basin during *L.balmei* and *M.diversus* palynozones, resulting in marginal marine and deltaic environments.

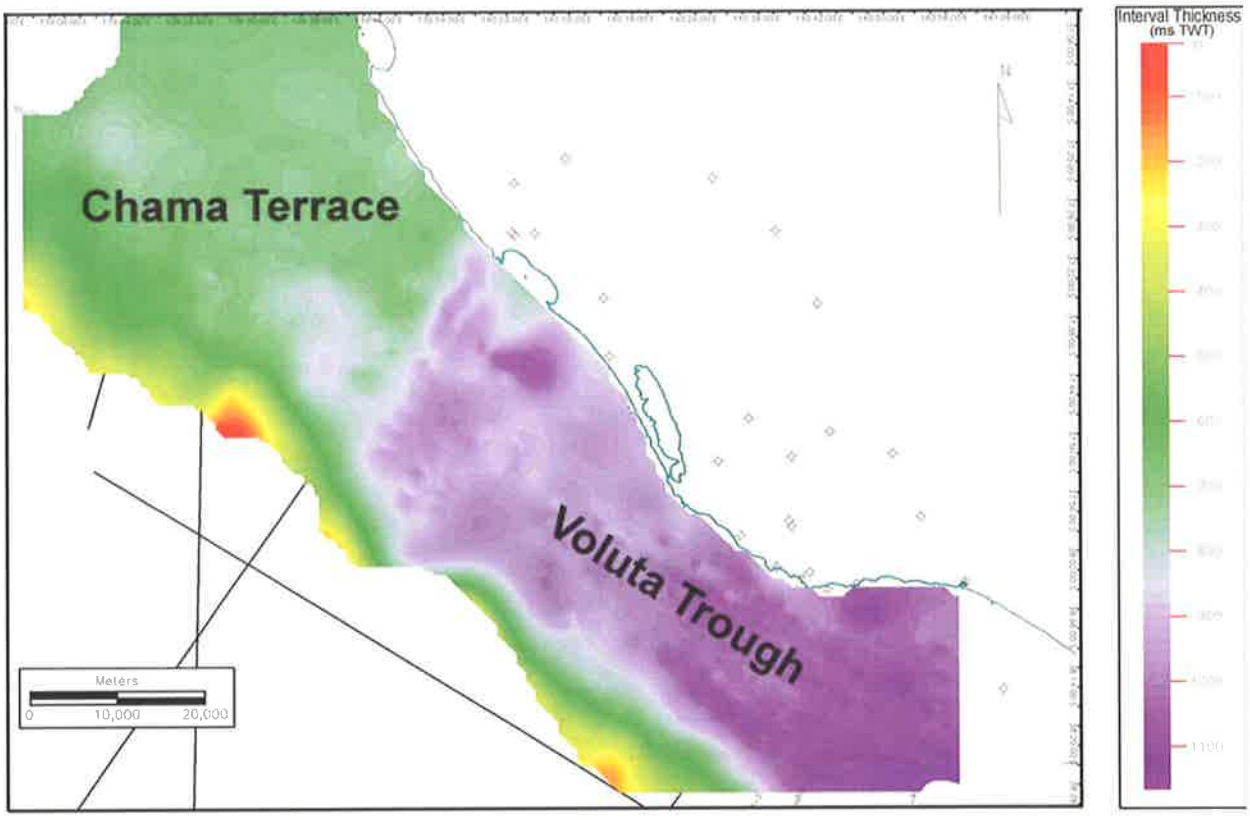

Figure 2.4 Thickness (ms TWT) of Cenozoic sediments in the offshore part of the Gambier Sub-basin. The two major structural provinces influencing sedimentation in the sub-basin are clearly illustrated: the thick section within the Voluta Trough (purple) that was the depocentre for clastic sediments of Megasequence 1, and the Chama Terrace (green), which was a shallow platform throughout the early Palaeogene that was a bypass margin for sediments until widespread carbonate deposition from the Late Eocene.

2.2.1.1 Seismic expression

SB 1.1 represents the Cretaceous-Palaeogene boundary, an unconformity which has been placed at the top of the Upper F. longus zone. Partridge (2001) identified a new unit which he called the "Massacre Shale" that straddles the Cretaceous-Palaeogene boundary – the thin shale unit contains both latest Maastrichtian and basal Paleocene biozones. Partridge (2001) identified this unit as a widespread transgressive event in the Otway Basin which overlies the Timboon Sandstone and underlies the Pebble Point Formation. It is included within the Pebble Point Formation in this study and SB 1.1 generally lies at the base of the shale unit, but is not mappable as a distinct unit on seismic data because it is too thin to resolve.

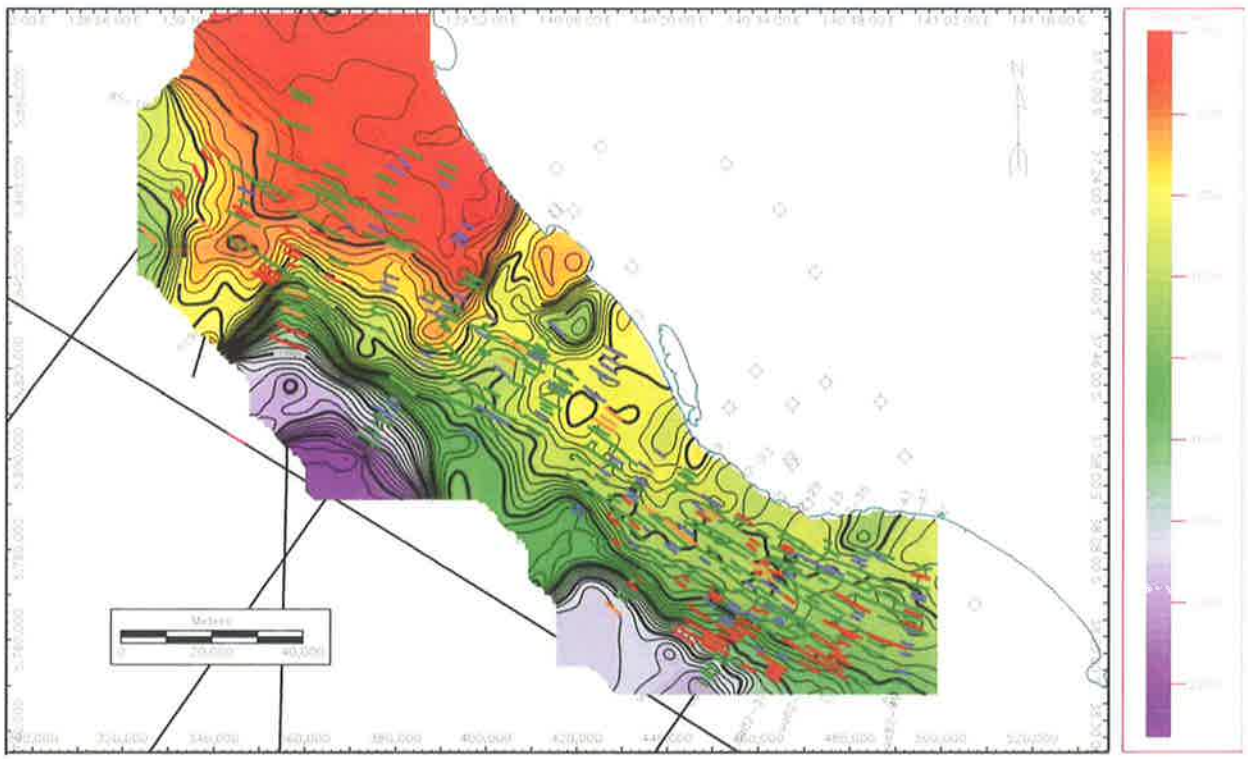

Figure 2.5 Time-structure map of SB 1.1, the Cretaceous-Palaeogene boundary. The listric faults strike in a northwest-southeast direction and dominate structure in the Voluta Trough, while the Chama Terrace experienced less faulting during the Cenozoic.

SB 1.1 is picked in Breaksea Reef 1 at a depth of 0.911 seconds TWT. The depth of this surface ranges from 300 ms TWT on the Chama Terrace in the west of the Sub-basin, to 1900 ms TWT

in the Voluta Trough to the east (Fig. 2.5). SB 1.1 has experienced severe normal, down-to-basin listric faulting with a dominant strike of ~300°, a result of the developing passive margin between the Antarctic and Australian plates during the Late Cretaceous and early Cenozoic. 3D visualisation of SB 1.1 (Fig. 2.6) illustrates the deep Voluta Trough, which was the depocentre during the Paleocene to Eocene, and the shallower Chama Terrace that was affected by erosion during the early part of the Cenozoic until carbonate deposition commenced in the Oligocene.

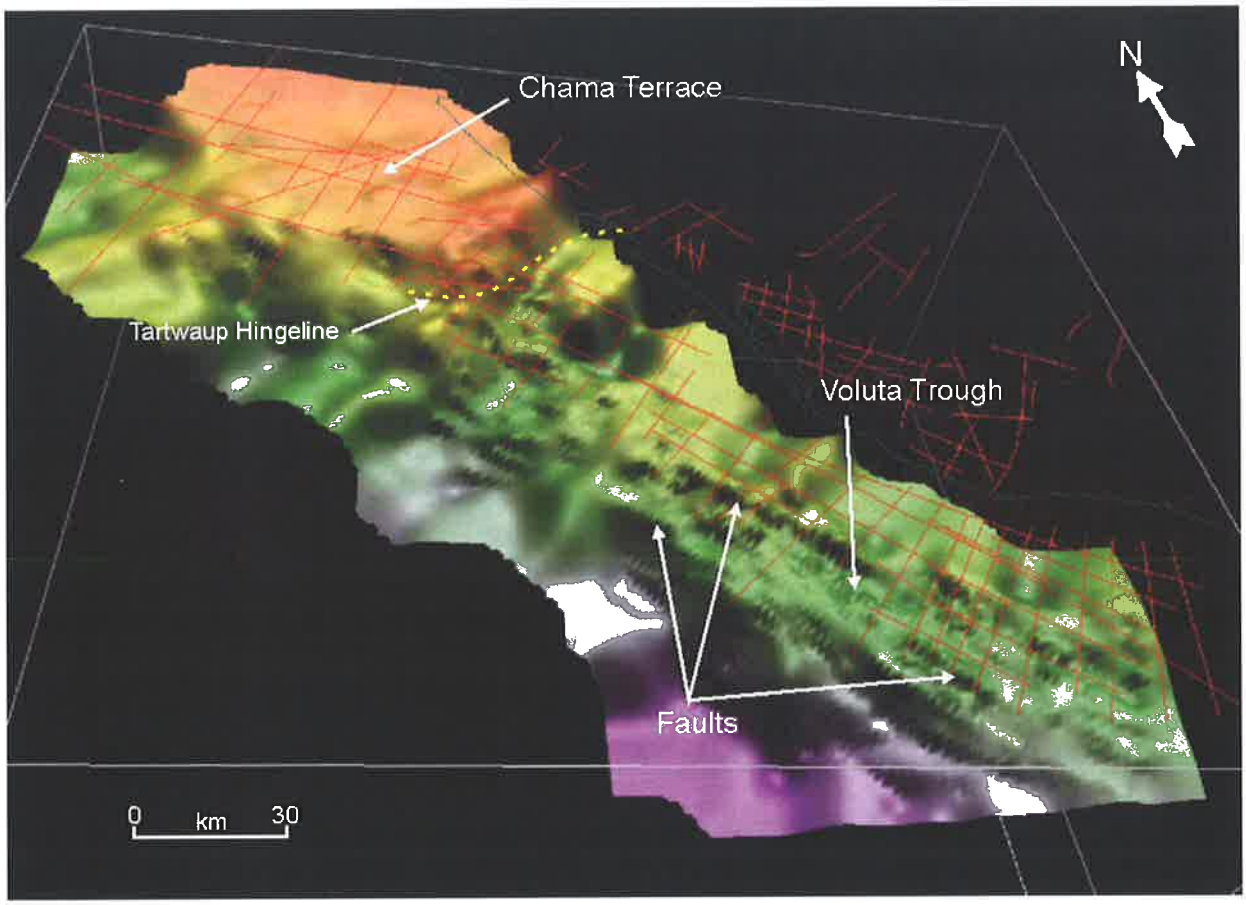

Figure 2.6 3D visualisation of the offshore part of the Gambier Sub-basin illustrating the Voluta Trough and the Chama Terrace [Vertical Exaggeration=10.35].

Downlapping onto SB 1.1 is the combined LST/TST package (since no transgressive surface was resolvable at seismic scale). This package is very thin (less than 200 ms) and displays parallel to sub-parallel internal reflectors thought to partially represent the transgressive Pebble Point Formation. Where this package becomes very thin, it is present only in the deep micro-

basins of the tilted fault blocks and onlaps onto the highs suggesting syn-depositional faulting (Fig. 2.7).

The overlying flooding surface (MFS 1.1) is a maximum flooding surface that was interpreted in the Voluta Trough and up to the base of the Chama Terrace. MFS 1.1 merges with SB 1.1 at its southern extent and onlaps onto the highs of the tilted fault blocks at the base of the Chama Terrace to the west.

HST 1.1 has a limited distribution on the inner to middle shelf in the eastern part of the Voluta Trough in the Gambier Sub-basin. Small sigmoidal clinoforms are seen prograding off the high sides of the tilted fault blocks into the micro-basins, with larger scale clinoforms prograding over the top, downlapping onto MFS 1.1 (Fig. 2.7). The highstand package has large-scale mound geometry approximately 3.5 km wide, observed when the seismic section was flattened on MFS 1.1 to remove post-depositional structuring effects (Fig. 2.8). Internal reflectors observed on seismic sections in the strike direction demonstrate bi-directional downlap onto MFS 1.1, with the HST sediments thinning dramatically and eventually pinching out at the flanks of the mound. The erosive nature of the overlying unconformity (SB 2.1) has removed the topsets of HST 1.1, producing an apparent angular unconformity with the high angle clinoform foresets terminating against SB 2.1.

2.2.1.2 Wireline log expression

Wireline logs show a distinct change in character at SB 1.1. In most wells the gamma ray log changes from blocky, interbedded high and low gamma beds characteristic of Late Cretaceous fluvial sediments, to a sharp-based sand that "fines upward" from the sequence boundary. The sonic and density logs show a baseline shift, indicating a change in compaction and lithological character above the boundary (Fig. 2.9).

The LST/TST package is represented in the gamma ray log as a "bell-shaped" package, with low gamma sands at the base gradually increasing in gamma value towards a gamma ray maxima (expressed as a spike in values) at MFS 1.1. Within this package the sonic log often displays an erratic, "ratty" signature, however, above LST/TST 1.1 the sonic log changes character to a smoother signature with less range in gamma values in the overlying HST. The wireline log expression of HST 1.1 initially demonstrates high gamma values, overlain by a

thick, blocky, low gamma bed. The sonic log demonstrates a baseline shift to slower values above MFS 1.1.

2.2.2 Supersequence 2

Supersequence 2 was deposited on the shelf in the Voluta Trough and comprises three fourth order sequences thought to partially represent the Dilwyn Formation with a biostratigraphic age equivalent to the *M.diversus* palynozone.

2.2.2.1 Seismic expression

SB 2.1, present on the inner to middle shelf in the Voluta Trough, merges with MFS 1.1 at its seaward extent and is truncated by SB 2.2 at the edge of the Chama Terrace in the west. The LST/TST package is very thin with internal reflections below seismic resolution, while the overlying HST has a large-scale mounded geometry with internal reflectors comprising sigmoid to oblique clinoforms that exhibit bi-directional downlap onto MFS 2.1 and SB 2.1 (Fig. 2.7). The internal reflectors on the flanks of the mound in a landward direction are sub-parallel, with some apparent truncation by SB 2.2 and SB 2.4.

SB 2.2 is the top-bounding surface to Sequence 2.1 and is present on the inner to middle shelf in the Voluta Trough. LST/TST 2.2 is a thin package less than 100 ms TWT thick and is present at the eastern edge of the study area. This sequence set comprises low to medium amplitude, sub-parallel topset reflectors that onlap SB 2.2 in a landward direction and hummocky to oblique prograding clinoforms that downlap onto SB 2.2 in a basinward direction. The topsets of this sequence set are apparently truncated by SB 2.3 at its landward extent (Fig. 2.7).

HST 2.2 is restricted to the eastern part of the study area due to erosion represented by the overlying sequence boundary, SB 2.3, which has removed highstand sediments from much of the western part of the Trough. Internal reflectors of the HST demonstrate oblique to hummocky clinoforms which downlap onto MFS 2.2. The top surface of this HST is interpreted to be SB 2.3 and SB 2.4, which merge at a landward direction (Fig. 2.7).

Figure 2.7 Seismic expression of sequences and systems tracts in Supersequences 1 and 2 in the Voluta Trough (Line UA82-31). Also shown are topsets of Supersequences 3 and 4 as they are represented on the palaeo-shelf. Faults are grouped and coloured according to the youngest sequence they penetrate which indicates when they were last active (see Chapter 5 for discussion on fault movement). Note that Breaksea Reef 1 is located off to the right of this section.

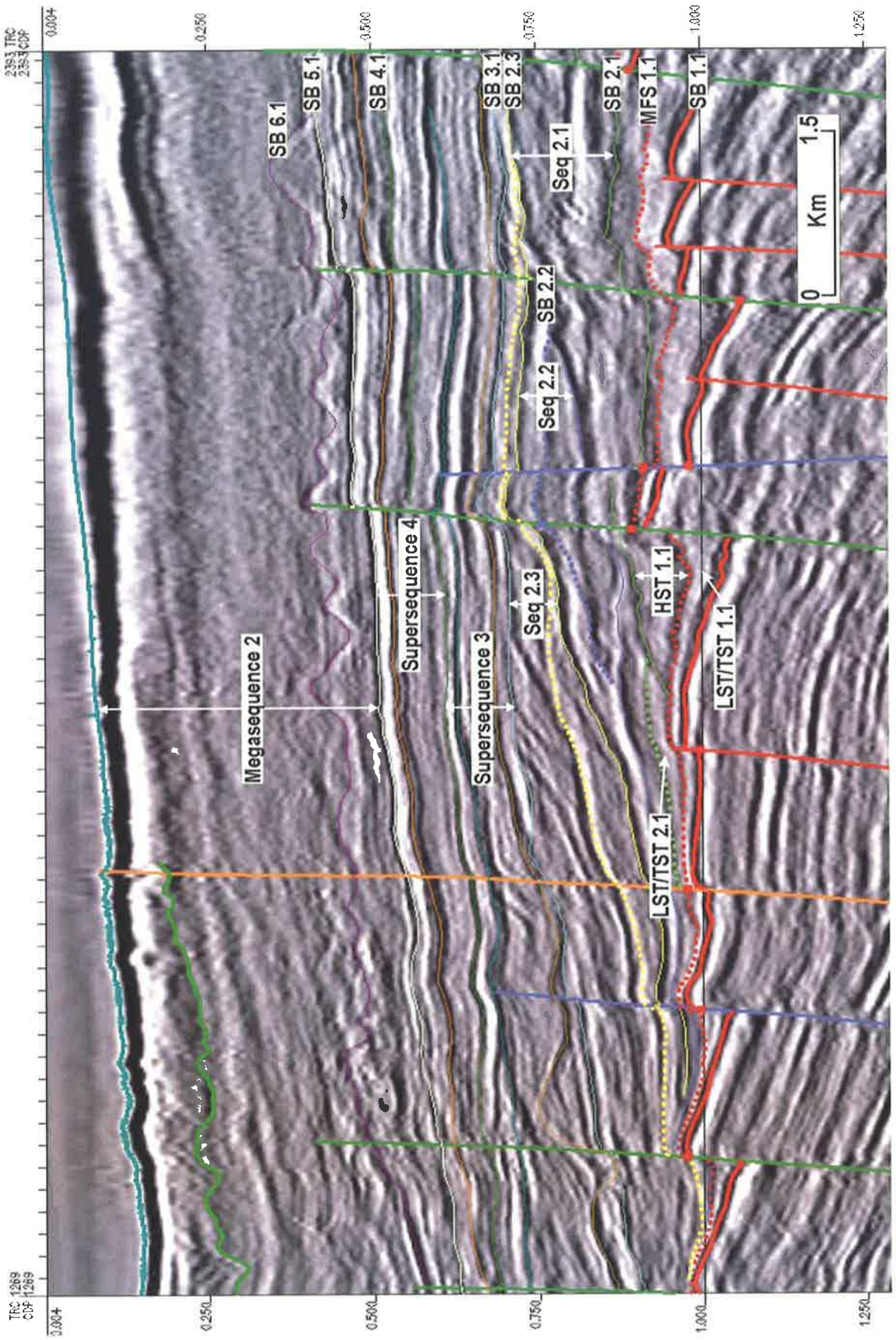
SB 6.1
SB 5.1
SB 4.1
SB 3.1
SB 2.3
SB 2.2
SB 2.1
SB 1.1
MFS 1.1
Seq 2.1
Seq 2.2
Seq 2.3
Megasequence 2
Supersequence 4
Supersequence 3
HST 1.1
LST/TST 1.1
LST/TST 2.1
0
1.5
Km

Figure 2.8 Seismic section flattened on horizon MFS 1.1 at 1.00 sec TWT. The large-scale mound geometry of HST 1.1 becomes obvious with bi-directional downlap of HST sediments onto MFS 1.1 (highlighted by white arrows) (Line oh91-402).

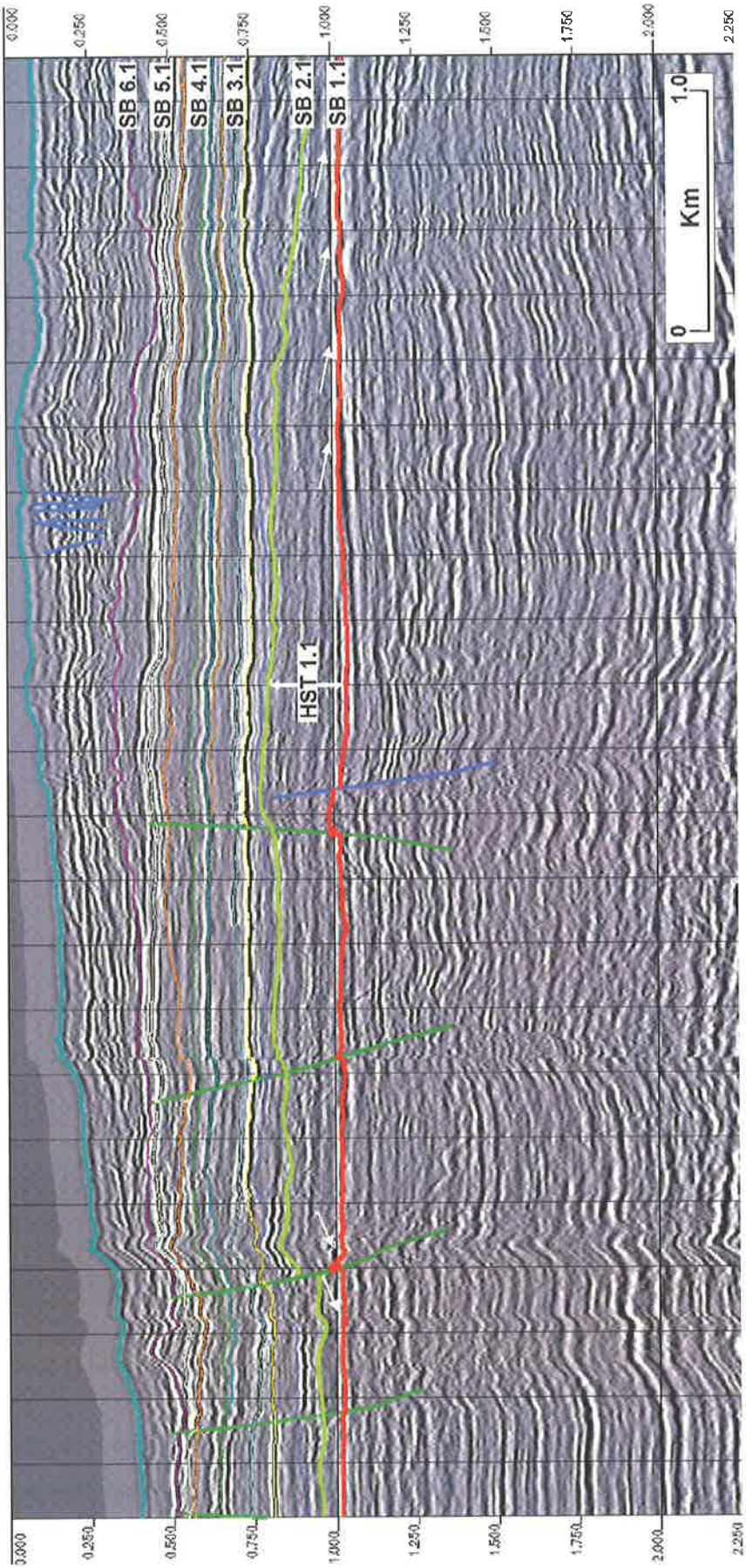
SB 6.1
SB 5.1
SB 4.1
SB 3.1
SB 2.1
SB 1.1
HST 1.1
0
1.0
Km

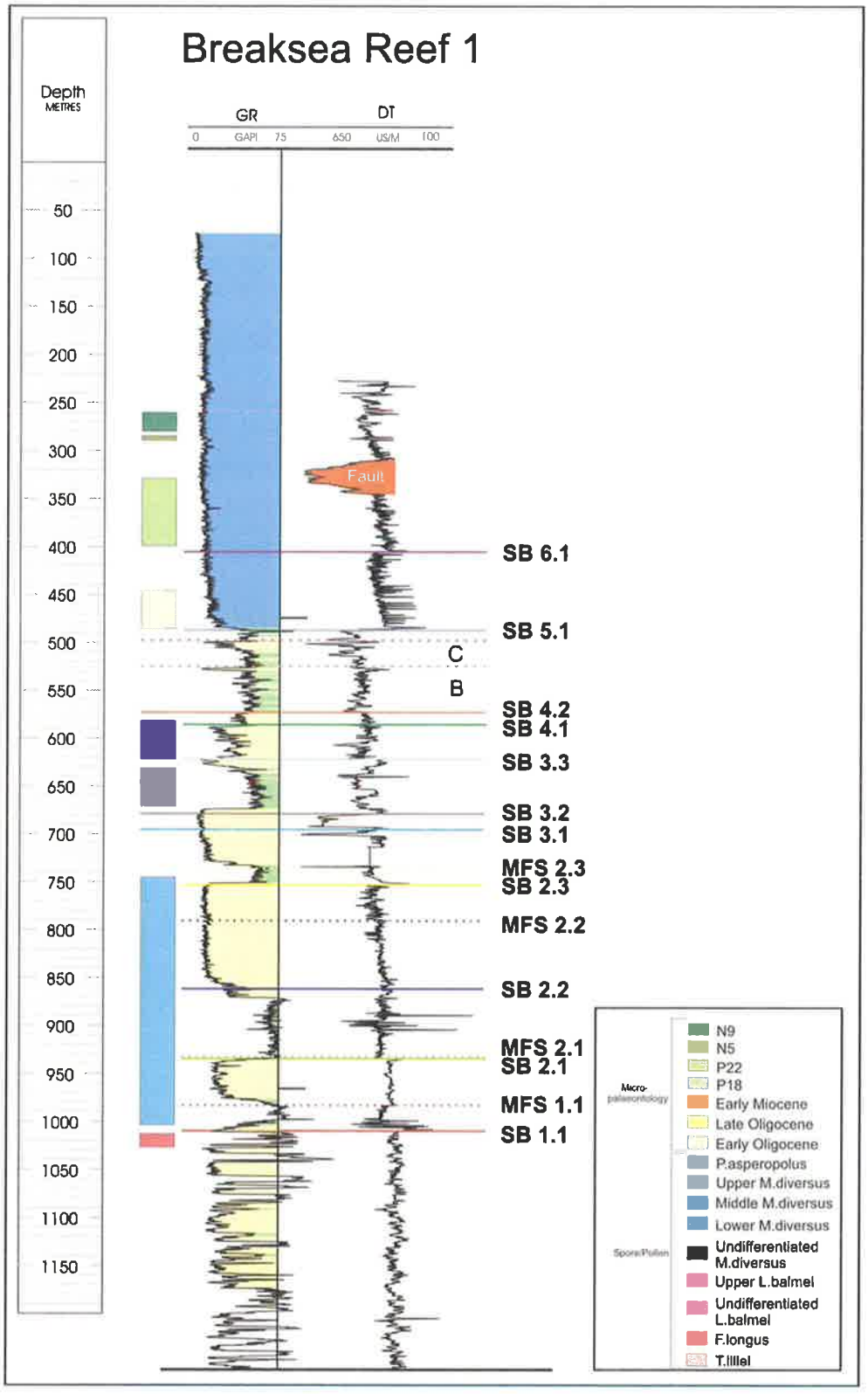

Figure 2.9 Gamma ray and sonic wireline logs from Breaksea Reef 1 illustrating the typical wireline log character and ages from biostratigraphy for sequences interpreted on seismic data. The yellow fill in the gamma ray log represents sand, the green represents silt/shale and the blue represents carbonate.

SB 2.3 is a regional unconformity, its erosional nature indicated by numerous small channels up to 700 m in width observed on seismic data on the shelf in the Voluta Trough (Fig. 2.10). The clustering of channels on this sequence boundary is interpreted to be an incised channel belt approximately 4 km wide. This sequence boundary merges with MFS 1.1 and SB 2.2 at its basinward extent and SB 2.2 at its landward extent and is truncated by SB 6.1 at its western limit on the edge of the Chama Terrace. Sigmoid prograding clinoforms of the LST/TST package downlap and onlap onto underlying SB 2.3. The channel-fill sediments also belong to the LST/TST sequence set. This package is quite thin across the central and western part of the study area where it onlaps onto the structural high, but thickens to the east, towards the centre of the Voluta Trough. HST 2.3 comprises parallel to sigmoid prograding clinoforms that downlap onto MFS 2.3 (Fig. 2.7).

2.2.2.2 Wireline log expression

The gamma ray signature representing Supersequence 2 displays a series of relatively thin intervals of high gamma value, shaly beds, which rapidly grade into very low gamma, amalgamated sand beds up 220 m thick. The sonic log is often erratic within the shaly beds and more consistent in the sandy beds (Fig. 2.9).

2.2.3 Supersequence 3

Supersequence 3 is interpreted across the shelf in the Voluta Trough in the Gambier Sub-basin and comprises marginal marine deltaic sediments of the Dilwyn Formation. Supersequence 3 has been seismic stratigraphically sub-divided into three fourth order sequences within the *M.diversus* palynozone.

2.2.3.1 Seismic expression

SB 3.1 is a regional unconformity, the erosional nature of this surface apparent by channels observed on strike lines. These channels are between 1500 and 1600 m wide and 249-323 m (100-130 ms TWT) deep. SB 4.1 truncates SB 3.1 near the base of the Chama Terrace in the western part of the sub-basin (Fig. 2.11).

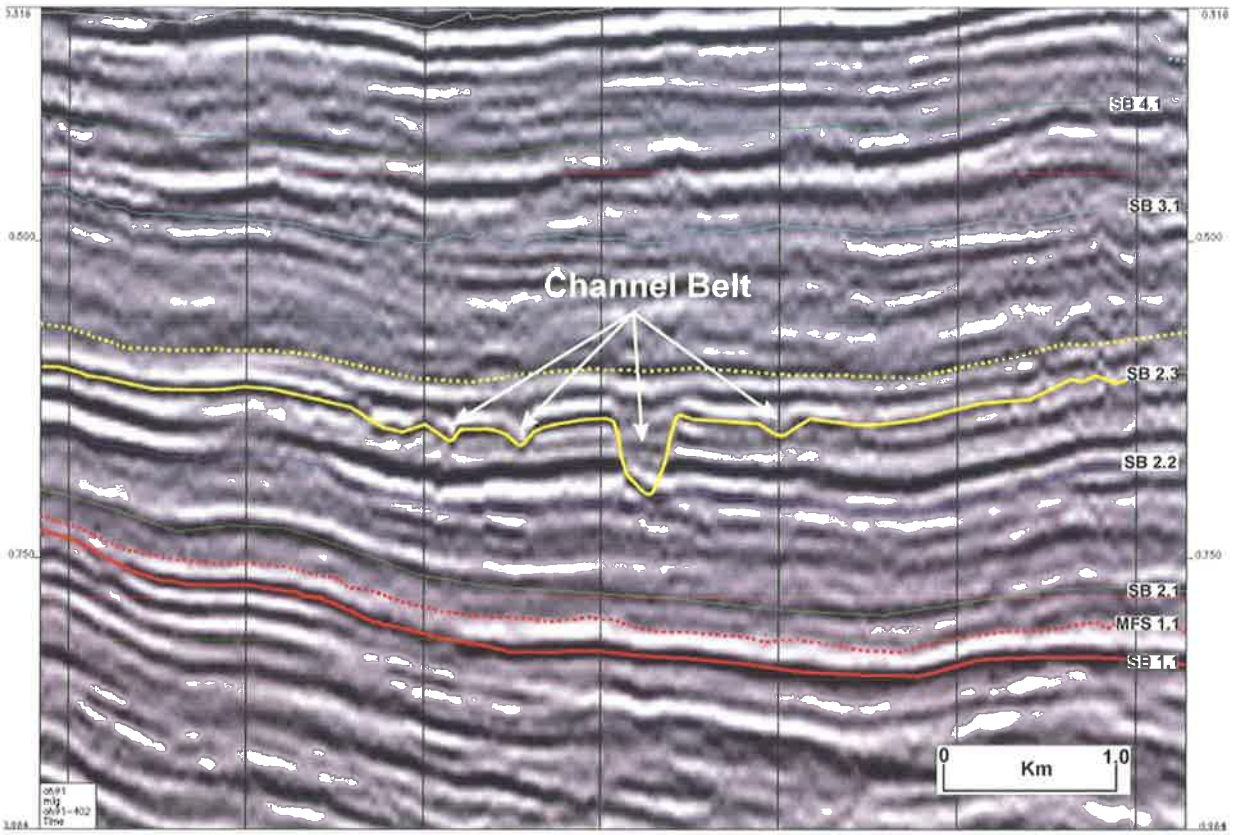

Figure 2.10 Seismic expression of erosional channels of a meandering incised channel belt at SB 2.3 on the shelf in the Voluta Trough (Line oh91-402).

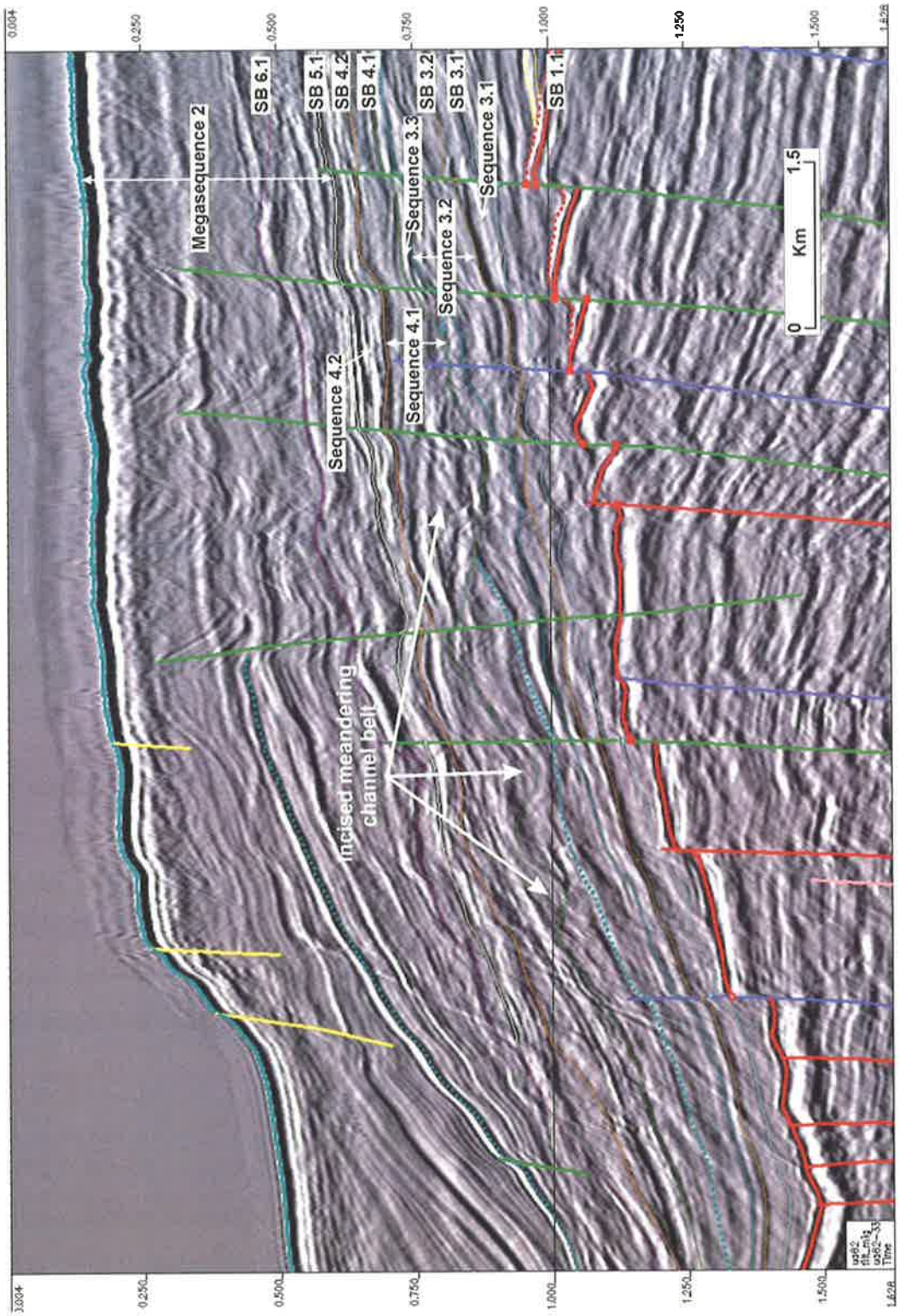

Figure 2.11 Seismic expression of Supersequences 3 and 4 on the outer shelf in the Voluta Trough (Line UA82-31). A large channel belt located under the present day outer shelf, basinward of Breaksea Reef 1, formed at SB 4.1 and incised into underlying sequences. Faults are grouped and coloured according to the youngest sequence they penetrate which indicates when they were last active (refer to Chapter 5 for discussion on fault movement).

Individual systems tracts in Sequence 3.1 are below seismic resolution. The LST/TST package may be present as channel-fill, but elsewhere, internal reflectors comprising the sequence set have a parallel to sub-parallel geometry with a seismically unresolvable MFS. Towards the edge of the Chama Terrace reflectors onlap SB 3.1, resulting in a thinning package which is eventually truncated by SB 4.1. In the eastern part of the Voluta Trough, the top bounding surfaces are SB 3.2 and 3.3, however, these two surfaces have a limited distribution in the eastern Voluta Trough, so towards the west, Sequence 3.1 is truncated at the top by SB 4.1.

SB 3.2 has a limited distribution in the eastern Voluta Trough and is truncated in the western part of the trough by SB 4.1. Due to poor data quality it could not be correlated beyond the Northumberland Canyon where it is truncated in the east. Again, individual systems tracts were not resolvable on the seismic data. This sequence is very thin with sub-parallel to parallel internal reflectors present in a landward direction. In a basinward direction the internal reflectors have tangential to parallel oblique prograding clinoforms with some evidence of contorted beds at the base of the sequence directly overlying the sequence boundary. The top bounding surfaces of this sequence set are SB 3.3 and SB 4.1 (Fig. 2.11).

SB 3.3 is present in the eastern part of the Voluta Trough and displays no evidence of erosive channels. The LST/TST package was deposited basinward of the palaeo-shelf break with sigmoid prograding clinoforms that onlap and downlap onto SB 3.3. HST 3.3 comprises sigmoid prograding clinoforms that downlap onto MFS 3.3 in a basinward direction and sub-parallel reflectors that are concordant with underlying sediments in a landward direction. The top of HST 3.3 is truncated by SB 4.1 giving rise to clinoforms that have a shingled appearance (Fig. 2.11).

2.2.3.2 Wireline log expression

The gamma ray log at the base of Supersequence 3 shows an interval of high gamma value, shaly sediments overlying the sequence boundary. The shaly sediments rapidly grade into a thick, low gamma value, sandy interval. On seismic section this is seen to represent a prograding delta lobe during a highstand in relative sea level. The sonic log spikes at the sequence boundary and the sonic signature becomes more erratic within overlying sandy sediments (Fig. 2.9). The sand is abruptly overlain by a low gamma, shaly bed, with the sonic log showing a change in character at this transition.

2.2.4 Supersequence 4

Supersequence 4 is interpreted across the entire Voluta Trough in the Gambier Sub-basin and comprises marginal marine deltaic sediments belonging to the Dilwyn Formation spanning the *M.diversus* and *P.asperopolus* palynozones. Supersequence 4 was sub-divided into two fourth order sequences based on seismic interpretation. However four additional sequences were identified in onshore wells and correlated to Supersequence 4 based on biostratigraphic age.

2.2.4.1 Seismic expression

SB 4.1 is present across the Voluta Trough in the study area up to the edge of the Chama Terrace where SB 5.1 truncates it. The presence of channels and truncation of underlying sediments indicates SB 4.1 is an erosive surface. These channels are up to 70 ms TWT deep and 800 m wide and are present in a belt 6 km wide on the edge of the present-day shelf (Fig. 2.11).

Systems tracts of Sequence 4.1 are below seismic resolution, however sediments in this sequence may largely consist of channel-fill sediments deposited during late lowstand and transgression. The channel-fill sediments display hummocky geometries that show apparent downlap onto SB 4.1, with sub-parallel to parallel topset reflectors present in a landward direction. Sediments possibly belonging to the HST downlap onto SB 4.1 and display low-angle prograding clinoforms observed on seismic lines oriented in the strike direction. The top of the sequence is eroded by SB 4.2 resulting in an angular unconformity that is most pronounced in a landward direction.

SB 4.2 is truncated by SB 5.1 at its western extent near the base of the Chama Terrace and has quite an erosive nature resulting in an apparent angular unconformity with underlying sediments of Sequence 4.1. Individual systems tracts in Sequence 4.2 are not resolvable on seismic data. This sequence is up to 572 ms TWT thick and comprises sub-parallel to parallel topset reflectors in a landward direction and sigmoid to oblique prograding clinoforms that onlap and downlap onto SB 4.2 on the palaeo-slope in a basinward direction (Fig. 2.11). The Northumberland Canyon and Lakes Canyon Complex truncate sediments of this sequence in the eastern part of the South Australian Voluta Trough.

2.2.4.2 Wireline log expression

The gamma ray log representing Supersequence 4 shows a variable character throughout the Gambier Sub-basin. Sequence 4.1 is relatively thin offshore, but appears to thicken in onshore wells as indicated by well correlations (Appendix 4). However, biostratigraphic control on well correlations in this interval is sparse and correlations have been made based on wireline log character alone resulting in high uncertainty. Sequence 4.2 appears to thicken dramatically in onshore wells where a thick *P.asperpolus* interval is present in some onshore wells but absent from offshore wells (cf. Figs. 2.9 & 2.12). These *P.asperopolus* cycles (A-E) are interpreted in Northumberland 1 (Fig. 2.12) as coarsening up deltaic cycles within the Dilwyn Formation that are not visible on seismic data offshore. Cycles B, C and the basal part of D are tentatively correlated to Breaksea Reef 1 in the interval 500-590 m where there is a lack of biostratigraphic data to constrain the age of these sediments. Mapping of the *P.asperopolus* cycles in the Gambier Sub-basin was not possible due to the lack of seismic and biostratigraphic data to constrain the well correlations and provide more confidence in them. Where the sonic log is present through the supersequence it shows a large base-line shift at the top of Supersequence 4 where there is an abrupt transition into the carbonates of Megasequence 2 (Fig. 2.9).

2.3 OUTCROP EXPRESSION

A field trip was conducted as part of this study to analyse the facies relationships of the sequences identified in outcrop. Outcrops near Mount Gambier and Dartmoor in the Gambier Sub-basin, and Port Campbell and Apollo Bay in the Port Campbell Embayment were visited. A summary of the lithofacies observed in outcrop is presented in Table 2.1, the locations of the outcrops are presented in Fig. 2.3, and a full description of the field trip is in Appendix 3.

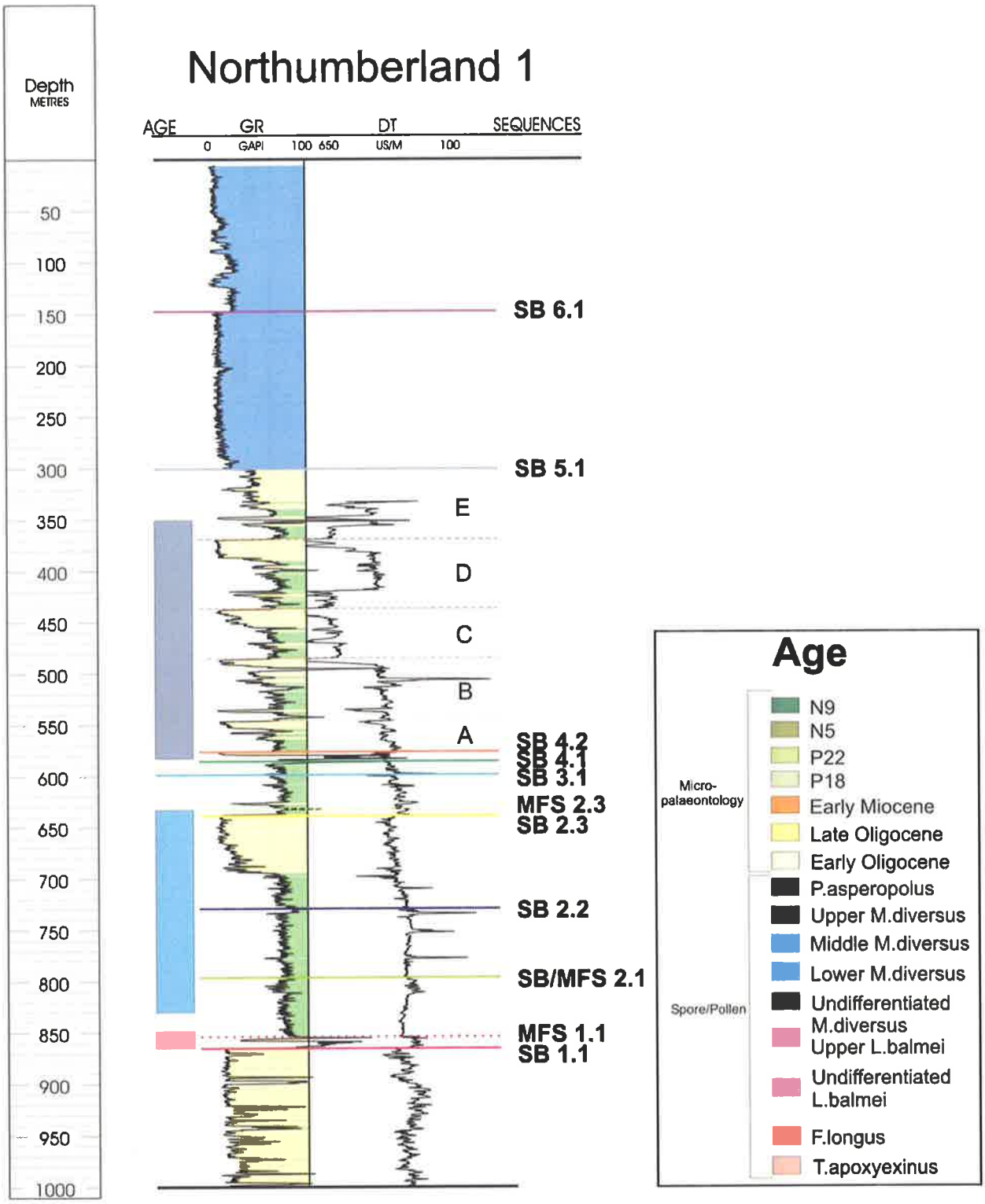

Figure 2.12 Wireline logs and biostratigraphic age of sequences in Northumberland 1. The yellow fill in the gamma ray log represents sand, green represents silt/shale and blue represents carbonate.

Lithofacies	Group	Formation/ Member	Location of outcrop	Description	Systems Tract	Depositional Environment
W1	Wangerrip Group	Pebble Point	PCE	Sandstone and pebbly conglomerate	Late LST - early TST	Transgressive Lag
W2		Pebble Point	PCE	Bioturbated, medium-grained sandstones and thinly interbedded mudstones	Late LST - early TST	Coastal plain channel complex
W3		Pember Mudstone	PCE	Interbedded brown mudstone, silty mudstone and argillaceous mudstone	Late LST - early TST	Shallow marine
W4		Dilwyn	GSB	White-cream, medium to coarse-grained sandstone	? Late LST - early TST	Channel
W5		Dilwyn	GSB	Cream and maroon firable shale	? Late LST - early TST	Overbank / interdistributary bay
W6		Dilwyn	PCE	Black carbonaceous clay	MFS - early HST	Anoxic waters, coastal plain/ back barrier lagoon
W7		Dilwyn	PCE	Interbedded mudstone and HCS sandy siltstone	HST	Interdistributary bay/ lagoon

Table 2.1 Summary of the lithofacies identified from outcrops of the Wangerrip Group (*Note*: PCE = Port Campbell Embayment; GSB = Gambier Sub-basin), refer to Fig. 2.3 for location map.

2.3.1 Supersequence 1

2.3.1.1 Lithofacies W1 – sandstone and pebbly conglomerate

The Pebble Point Formation (represented by LST/TST 1.1) outcrops in the Port Campbell Embayment where it dips seaward at ~5° and transgressively overlies the eroded surface of the Early Cretaceous Otway group. Generally, the Pebble Point Formation in the Port Campbell Embayment consists of quartz sandstone and fine conglomerate, commonly ferruginous, but in part glauconitic, calcareous and fossiliferous (Abele et al. 1976) (Table 2.1, Plate 1).

2.3.1.2 Lithofacies W2 – bioturbated sandstone and thinly interbedded mudstone

Lithofacies W1 rapidly grades into a thick package (10m) of fining upward very heavily bioturbated, medium-grained sandstones and thin, less bioturbated mudstones (Plate 1). The sandstone units, which were originally grey, have weathered to an orange colour and contain pebbly interbeds and shelly fauna that become more frequent towards the top of the package. There were grey mud rip-up clasts and mud drapes present throughout the sandstone. Sandstone beds were heavily bioturbated with branching dwelling burrows caused by *Thalassinoides* (Plate 1). The thin, fine-grained interbeds comprise purple to brown shale that are sparsely burrowed and dip shallowly seawards (Table 2.1, Plate 2).

2.3.1.3 Lithofacies W3 – interbedded mudstone and silty mudstone

The Pember Mudstone (represented at Buckley's Point by lithofacies W3) rests conformably and often transitionally on the Pebble Point Formation (Lithofacies W2) (Abele et al. 1976). The Pember Mudstone observed in outcrop at Buckley's Point comprises interbedded brown mudstone, silty mudstone and argillaceous mudstone and includes shell fragments, bivalves, bryozoa, gastropods and carbonaceous material (Table 2.1, Plate 2).

2.3.2 Supersequences 2, 3 & 4

Four lithofacies were identified in outcrop within the Dilwyn Formation that is represented by Supersequences 2, 3 and 4 (Table 2.1). These lithofacies characterize fluvial, estuarine,

interdistributary bay and deltaic depositional environments. Due to the lack of biostratigraphic data from the outcrops it is not possible to correlate each facies to a specific supersequence or sequence, however the depositional environments represented by these outcrops are likely to have occurred throughout the Sub-basin during the Early Eocene.

2.3.2.1 Lithofacies W4 - white to cream, medium-coarse grained sandstone

Medium to coarse grained, quartz-rich sand representing the Dilwyn Formation was observed in outcrop at two locations in the Gambier Sub-basin. In Allen's Sand Quarry there was a small "gravel pit" exposing a clean, cross-bedded, medium to coarse pebbly gravel (Table 2.1, Plate 3). The gravel contained sub-rounded quartz pebbles up to one centimetre in diameter, within a matrix of medium to coarse, sub-angular quartz (94%), with minor rock fragments (2%), and possible dolomite grains (4%). The quartz pebbles were imbricated along the bedding planes and cross bedding direction suggests flow was in a south-westerly direction at this location.

At the Crawford River Bridge, the Dilwyn Formation was exposed as a white, cross-bedded, medium grained quartz sand (95%), with minor mica (muscovite) (3%) and rock fragments (2%). Mud drapes were observed on the foresets of the cross-beds (Plate 3).

2.3.2.2 Lithofacies W5 - cream and maroon, friable shale

In Allen's Sand Quarry, a second outcrop of the Dilwyn Formation exposed a fine-grained friable unit that had undergone extensive weathering, resulting in buff coloured, soft shale. There were two oxidised, red/maroon horizons within this shaly interval thought to represent local flooding events (Table 2.1, Plate 3).

2.3.2.3 Lithofacies W6 - black carbonaceous clay

Near Buckley's Point in the Port Campbell Embayment, a sediment-starved surface was observed within the Dilwyn Formation, containing shark's teeth and solitary corals and was interpreted as a maximum flooding surface. This surface was overlain by fine-grained, aggradational sand units, which graded into an interbedded sand and carbonaceous clay (Table 2.1, Plate 4). The carbonaceous clay contains horizons of nodular pyrite indicative of an anoxic environment.

2.3.2.4 *Lithofacies W7 - interbedded mudstone and HCS sandy siltstone*

A road-cutting outcrop on the Great Ocean Road near Princetown exposed thin, bioturbated (*Chondrites*), mudstone intervals alternating with HCS sandy siltstone that contain *Ophiomorpha* burrows (Table 2.1, Plate 4). There is an absence of shelly material and the lower clay interbeds exposed in the road cutting are black in colour.

The gross wavelength of the HCS forming the large-scale bedding is 1-2m with amplitude of 5cm. Smaller scale HCS has wavelengths of 40-60cm and amplitudes of ~5cm. The HCS lamina geometries indicate both oscillatory flow and combined flow (with unidirectional downlap indicating palaeoslope dip direction) (Arditto, 1999).

2.4 OUTCROP INTERPRETATION

At the base of the outcrops at Buckley's Point and Point Margaret, the contact between sediments of the Early Cretaceous Otway Group and the Paleocene Wangerrip Group is exposed. The Otway Group sediments comprise grey/green medium-grained, well-sorted, clean sands deposited in a fluvial channel environment. The sandstone displays trough cross-bedding at the decimetre scale and the top of this unit is a sequence boundary and unconformity. Small scale scours (~30cm wide) on the unconformity surface are filled with green and red shales at Buckley's Point, while at Point Margaret, a channel (~3m wide) is cut into the top of the Otway Group and filled with a pebbly lag deposited during late lowstand and early transgression (Lithofacies W1). Wangerrip Group sediments, comprising a channel fill lag, overlain by sandstone and mudstone, onlap onto the unconformity.

Overlying the Cretaceous Otway Group and Paleocene transgressive lag is a series of parasequences approximately 10m thick comprising very heavily bioturbated, medium-grained sandstone, that fine up to less bioturbated, thinly bedded mudstones (Lithofacies W2). This package is thought to have been deposited during a series of channelling and channel abandonment episodes, followed by biological reworking and represents a late LST and early TST. These sediments have been assigned to the Early-Late Paleocene Pebble Point Formation (Arditto, 1999).

The sandstone representing the Pebble Point Formation (Lithofacies W2) was originally grey in colour, but has weathered to orange and has pebbly interbeds and shelly fauna that become more common towards the top of the package. Biological reworking of the sandstone is represented by the branching dwelling burrows of *Thalassinoides*. There are grey mud rip-up clasts and mud drapes present throughout the sandstone, indicating times of channel abandonment. The thin mudstone interbeds comprise purple to brown shale that is sparsely burrowed.

This unit is abruptly overlain by a flatly laminated grey-brown mudstone that is thought to represent the Pember Mudstone (Lithofacies W3). This mudstone contains *Chondrites* burrows and may have been deposited in a distal bay to offshore marine environment and represents a late TST and early HST.

The overlying Dilwyn Formation has been interpreted as a series of stacked deltaic cycles (Holdgate, 1981) and seismic interpretation has supported this general depositional environment, however outcrop analysis has revealed a number of varying depositional environments within the deltaic system.

The close proximity of the two outcrops of Lithofacies W4 and W5 at Allen's Quarry and also the location of Allen's Quarry near the northern edge of the Voluta Trough, suggests a proximal fluvial/channelised delta plain environment during the Paleocene-Eocene. The clean, quartz-rich, cross-bedded sand of Lithofacies W4 is interpreted as distributary channel-fill, while Lithofacies W5 is interpreted as the fine-grained overbank or interdistributary bay equivalent.

The sediment-starved surface at the base of Lithofacies W6 is interpreted as a maximum flooding surface. The fossils and shark's teeth found on the MFS indicate it is a condensed surface representing a long period of non-deposition. The overlying carbonaceous clay with nodular pyrite is interpreted as having been deposited in a coastal plain back barrier lagoonal environment during a highstand where there was a high input of organic material and perhaps restricted circulation, resulting in a reducing depositional environment.

The interbedded HCS sandy siltstone and shale of Lithofacies W7 is interpreted as having been deposited during a HST in an interdistributary bay and lagoonal environment where the HCS sandy siltstone is a result of short periods of high energy, flooding events and the shale was deposited during intervening times of quiescence. The distinct lack of shelly material and the

organic rich lower clay interbeds indicates deposition was in a sheltered marine environment rather than open shelf conditions.

2.5 DISCUSSION

Palynological analysis has identified a hiatus between Cretaceous and Palaeogene sediments that ranges from approximately 7.5 M.y. where the Maastrichtian biozone *F.longus* is overlain by the Late Paleocene *L.balmei* biozone in the south-eastern part of the Sub-basin; to as much as 40 M.y. in Troas 1 where the Santonian biozone *T.apoxyexinus* is overlain by Early Oligocene carbonates. The magnitude of this hiatus is a result of differential subsidence rates across the Sub-basin with the Tartwaup Hinge Zone acting as the pivot. Subsidence was thermally induced, a consequence of seafloor spreading in the Southern Ocean that resulted in increased subsidence south of the Tartwaup Hinge Zone, which in turn led to an increased amount of erosion in the western part of the Sub-basin. Evidence for this is observed on seismic sections from the Chama Terrace that display a high-angle angular unconformity between Late Cretaceous and Cenozoic sediments (Fig. 2.13).

The presence of Late Eocene pollen grains (*N.asperus*) in Troas 1 suggests a period of condensation following extensive erosion of Mesozoic sediments during the early Palaeogene and prior to carbonate deposition on the Chama Terrace.

Supersequence 1 marks a major marine transgression and transition from dominantly fluvial to marine conditions. Palynology indicates this supersequence was deposited during the Late Paleocene to earliest Eocene (Upper *L.balmei* to Lower *M.diversus*) The transgressive wireline log expressions indicate a deepening and landward movement of the shoreline during deposition of LST/TST 1.1 up to a maximum flooding event, MFS 1.1, marked by maximum gamma ray values (Fig. 2.9). The sometimes-erratic sonic log signature of LST/TST 1.1 suggests the presence of conglomerates within this package, a suspicion supported by outcrop analysis (Fig. 2.9). In outcrop this package represents a transgressive lag, deepening into marginal marine interbedded sandstone and mudstone beds interpreted as channelling and channel abandonment episodes on an embryonic delta plain.

HST 1.1 is interpreted on wireline logs as initially very muddy, overlain by thick, blocky sand. Seismic interpretation of offshore data indicates this package is a prograding delta lobe deposited during a highstand in relative sea level.

Supersequences 2, 3 and 4 are interpreted to comprise fluvial to marginal marine deltaic sediments, deposited during a time of slow seafloor spreading in the Early Eocene (*M.diversus* to *P.asperopolus* biozones). The supersequences are defined on the basis of their bounding surfaces, which are regional sequence boundaries that display evidence of erosion (i.e. unconformities) resulting from periods of low relative sea level. Sedimentation rates of these supersequences were quite rapid (up to 18 cm/K.y., while margin progradation rates were equally as rapid (approximately 5 m/K.y.) (refer to Chapter 4 for a more detailed discussion).

These supersequences are dominated by highstand systems tracts that are interpreted to be delta lobes, which prograde across the shelf during times of still-stand and slow relative sea level fall. When relative sea level reaches its lowest point, a sequence boundary forms and if sea level happens to fall below the shelf edge, erosion and fluvial incision into underlying sediments occurs. This is followed by periods of rapid rise during which time thin lowstand and transgressive systems tracts are deposited.

Near the base of Supersequence 4, fluvial and marginal marine environments prevailed as far basinward as the present day outer shelf, supported by the presence of incised meandering channel belt identified on seismic data (Fig. 2.11). A series of channels in the eastern part of the Voluta Trough was mapped in detail and when this erosion surface was viewed in 3D, the geometry revealed a potential incised meandering channel belt (Fig. 2.14). These incised channel belts have significant implications for potential hydrocarbon plays further down dip. The channel belt is located under the present day shelf edge, which implies that a sand-rich lowstand shoreline and turbidites may be present down dip, providing potential reservoir targets. The sealing potential of the overlying carbonates for this play is touched on in Chapter 3. Other channels are visible on seismic, however these are unable to be correlated to other lines and mapped in detail on the seismic grid in order to gain an understanding of their geometry.

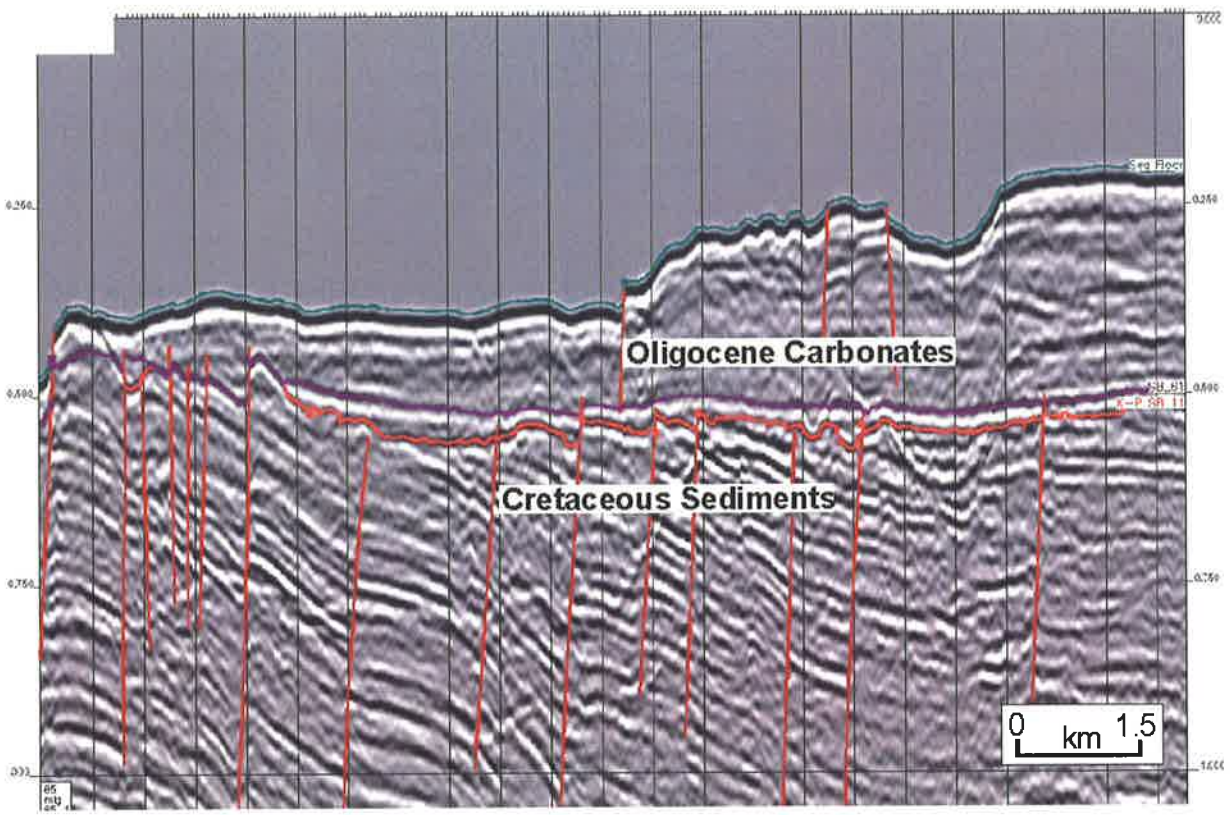

Figure 2.13 Seismic data from the Chama Terrace in the western part of the Gambier Sub-basin (Line oh91-506). Oligocene-Middle Miocene carbonates unconformably overlie heavily faulted Late Cretaceous sediments, forming an angular unconformity.

PLATE 1 (*Top*) Pebble Point Formation at Buckley's Point comprising quartz sandstone and fine-grained conglomerate (Lithofacies W1). The Pebble Point Formation overlies the Early Cretaceous Otway Group. The Otway Group sediments comprise grey/green medium-grained, well-sorted, clean sands. The sandstone displays trough cross-bedding at the decimetre scale and the top of this unit is a sequence boundary and unconformity. Small scale scours (~30cm wide) on the unconformity surface are filled with green and red shales at Buckley's Point, while at Point Margaret, a channel (~3m wide) is cut into the top of the Otway Group.

(*Middle*) Overlying the Early Cretaceous Otway Group at Buckley's Point is the Pebble Point Formation, present as a series of fining upward parasequences comprising heavily bioturbated, medium-grained sandstones with interbedded, less bioturbated mudstones (Lithofacies W2).

(*Bottom*) The sandstone beds in the Pebble Point Formation at Buckley's Point are highly bioturbated and comprise branching dwelling burrows caused by *Thalassinoides* (Lithofacies W1).

Note: Buckley's Point is marked as outcrop location 7 in Figure 2.3 and Appendix 3.

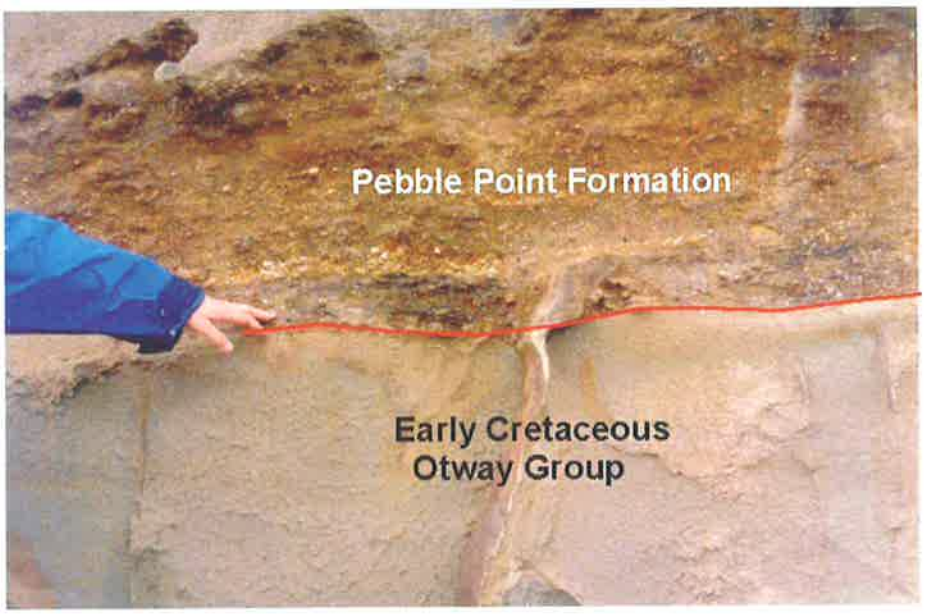
Pebble Point Formation
Early Cretaceous
Otway Group

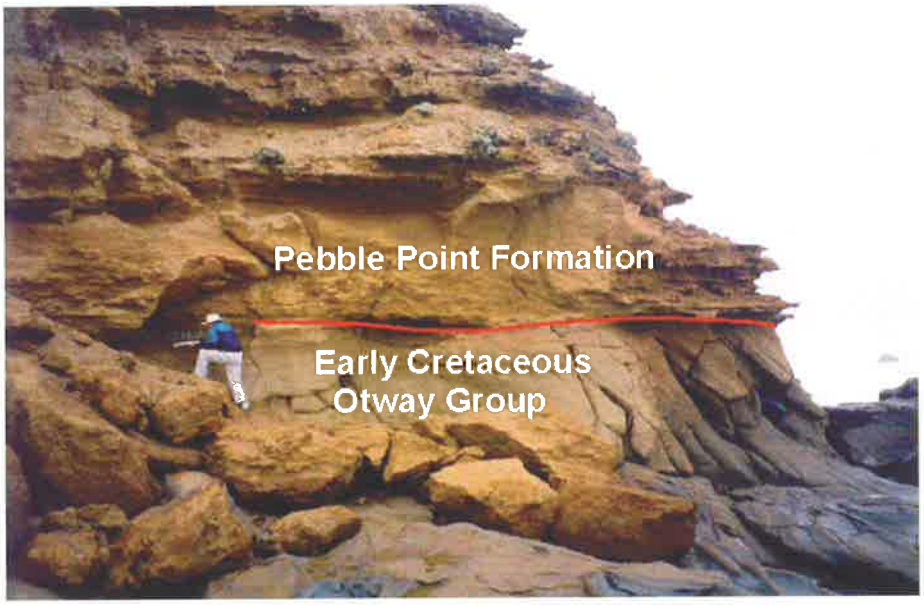
Pebble Point Formation
Early Cretaceous
Otway Group

PLATE 2 (*Top*) Thin, fine-grained purple to brown, shaly interbeds in the Pebble Point Formation at Buckley's Point (Lithofacies W2). *Thalassinoides* burrows can be seen near the top of the photo.

(*Bottom*) Pember Mudstone at Buckley's Point comprising interbedded brown mudstone, sandy mudstone and argillaceous mudstone that includes shell fragments and carbonaceous material (Lithofacies W3).

Note: Buckley's Point is marked as outcrop location 7 in Figure 2.3 and Appendix 3.


1

PLATE 3 (*Top*) Dilwyn Formation in Allen's Quarry (UTM position 0474625, 5820170) comprising cross-bedded, sub-rounded quartz gravel in a matrix of medium to coarse, sub-angular quartz (Lithofacies W4). *Note*: Allen's Quarry is marked as outcrop location 1 in Figure 2.3 and Appendix 3.

(*Middle*) Dilwyn Formation at the Crawford River Bridge (UTM position 0525513, 5802315) that comprises white, cross-bedded, medium-grained, quartz sand with minor muscovite (Lithofacies W4). *Note*: Crawford River Bridge is marked as outcrop location 12 in Figure 2.3 and Appendix 3.

(*Bottom*) Dilwyn Formation at Allen's Quarry (UTM position 0474625, 5820170) comprising a buff coloured, soft, fine-grained shale. The oxidised red/maroon horizons may represent local flooding surfaces (Lithofacies W5). *Note:* Allen's Quarry is marked as outcrop location 1 in Figure 2.3 and Appendix 3.

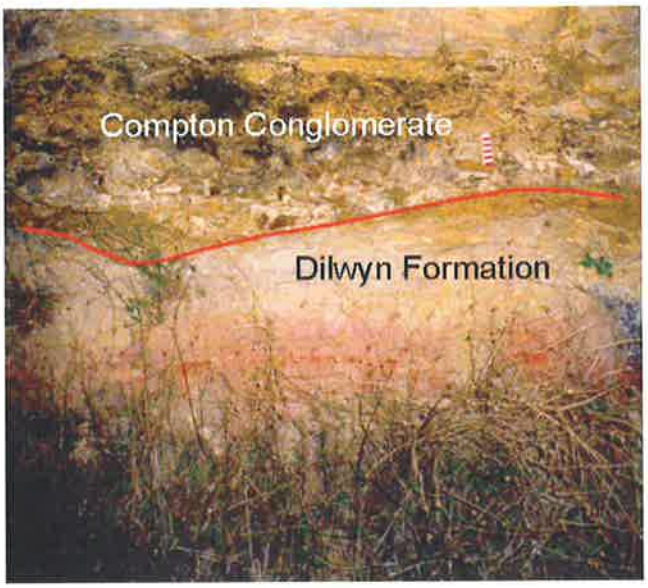
Compton Conglomerate
Dilwyn Formation

PLATE 4 (*Top*) Sediment starved, maximum flooding surface at the base of the Dilwyn Formation on which sharks teeth and solitary coral fossils were found. Overlying this surface is interbedded sand and carbonaceous clay (Lithofacies W6). *Note*: This outcrop is marked as location 7, Buckley's Point, in Figure 2.3 and Appendix 3.

(*Middle*) Dilwyn Formation near Buckley's Point comprising interbedded sand and carbonaceous clay (Lithofacies W6). *Note*: Buckley's Point is marked as outcrop location 7 in Figure 2.3 and Appendix 3.

(*Bottom*) Thin bioturbated mudstones alternating with HCS sandy siltstone intervals that contain *Ophiomorpha* burrows (Lithofacies W7). *Note*: This outcrop is marked as location 10, Road Cutting, in Figure 2.3 and Appendix 3.

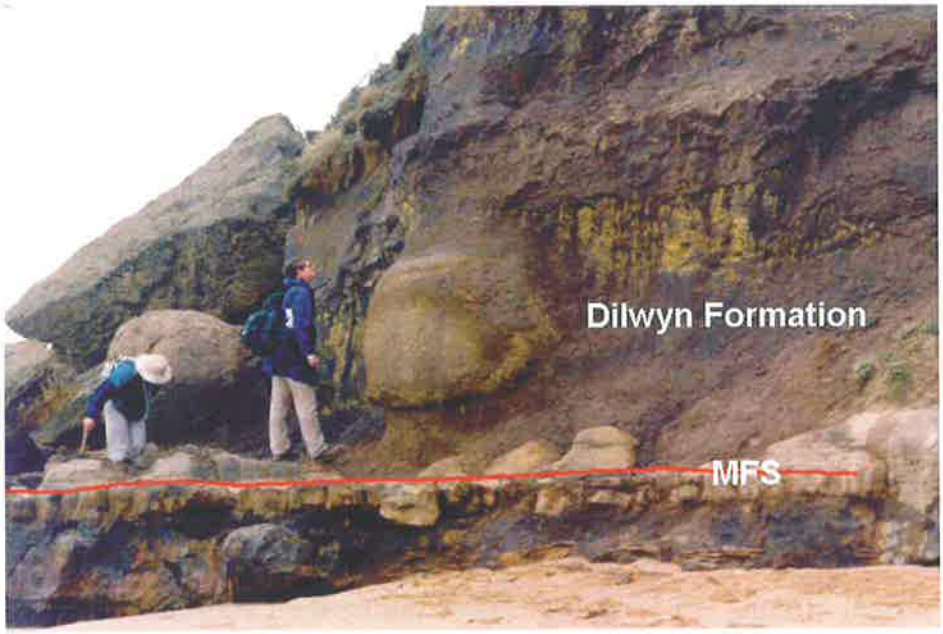
Dilwyn Formation
MFS

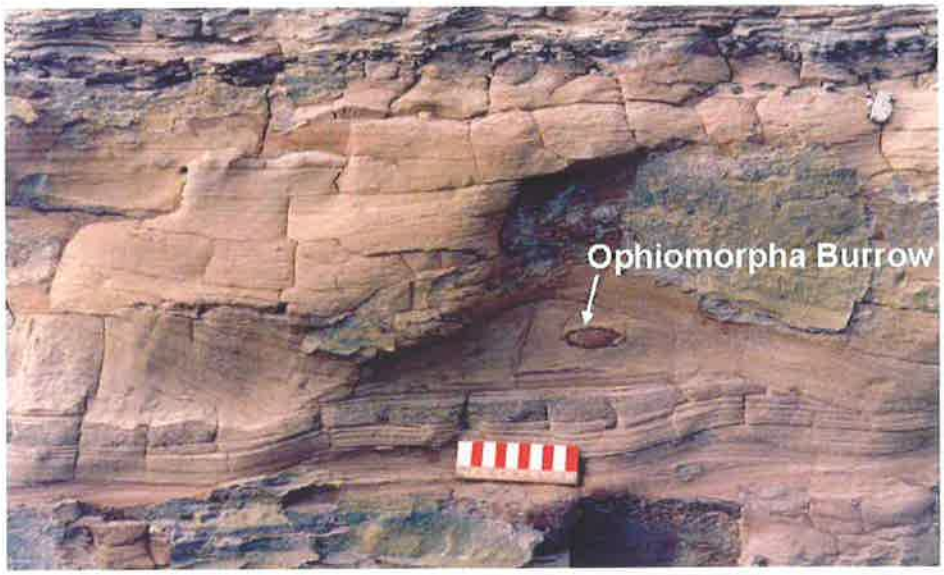
Ophiomorpha Burrow

The first of four global second-order packages identified on the southern margin by McGowran (1978) (among others, refer to Chapter 1) is equivalent to the Late Paleocene-Early Eocene Megasequence 1 that was seismically defined in this study. Sediments comprise the Wangerrip Group, an unconformity-bounded siliciclastic package that was rapidly deposited into the Voluta Trough. It overlies Late Cretaceous fluvial sediments and is overlain by the carbonate Gambier Limestone.

Six marine ingressions onto the southern Australian margin were identified during this time based on biostratigraphy (McGowran et al. 1997, among others). Resolution of biostratigraphic dating of Megasequence 1 does not allow for correlation of seismically identified maximum flooding horizons with individual biostratigraphically defined regional transgressive events. However, the pattern of rapid sea level fluctuations during the Late Paleocene-Early Eocene, both on seismic and biostratigraphic data, is obvious (Figure 2.15).

The Dilwyn Formation (represented by Supersequences 2, 3 and 4 in the Gambier Sub-basin) has previously been interpreted as a series of stacked deltaic cycles. Holdgate (1981) identified up to seven delta cycles based on wireline log motif correlation from 16 wells in the Tyrendarra Embayment and Victorian part of the Gambier Sub-basin. The dataset analysed by Holdgate (1981) involved sedimentological and wireline log analysis of a suite of wells that differs from the wells used in this study, however, recognition of rapid deposition of Late Paleocene to Early Eocene clastic sediments in successive, coarsening upward delta cycles was supported by this seismic stratigraphic study.

Holdgate (1981) concluded that these delta cycles were the result of local processes rather than being a consequence of any regional tectonic or eustatic cycle. However, McGowran (1991) provides evidence for correlation of the Late Paleocene-Early Eocene transgressive events to third-order regional tectono- and glacio-eustatic events that were also recognised in the Great Australian Bight, St. Vincent Basin, eastern Otway and Gippsland Basin. This suggests that the cause of the rapid relative sea level fluctuations influencing progradation and switching of the Wangerrip Group delta lobes was both local and regional.

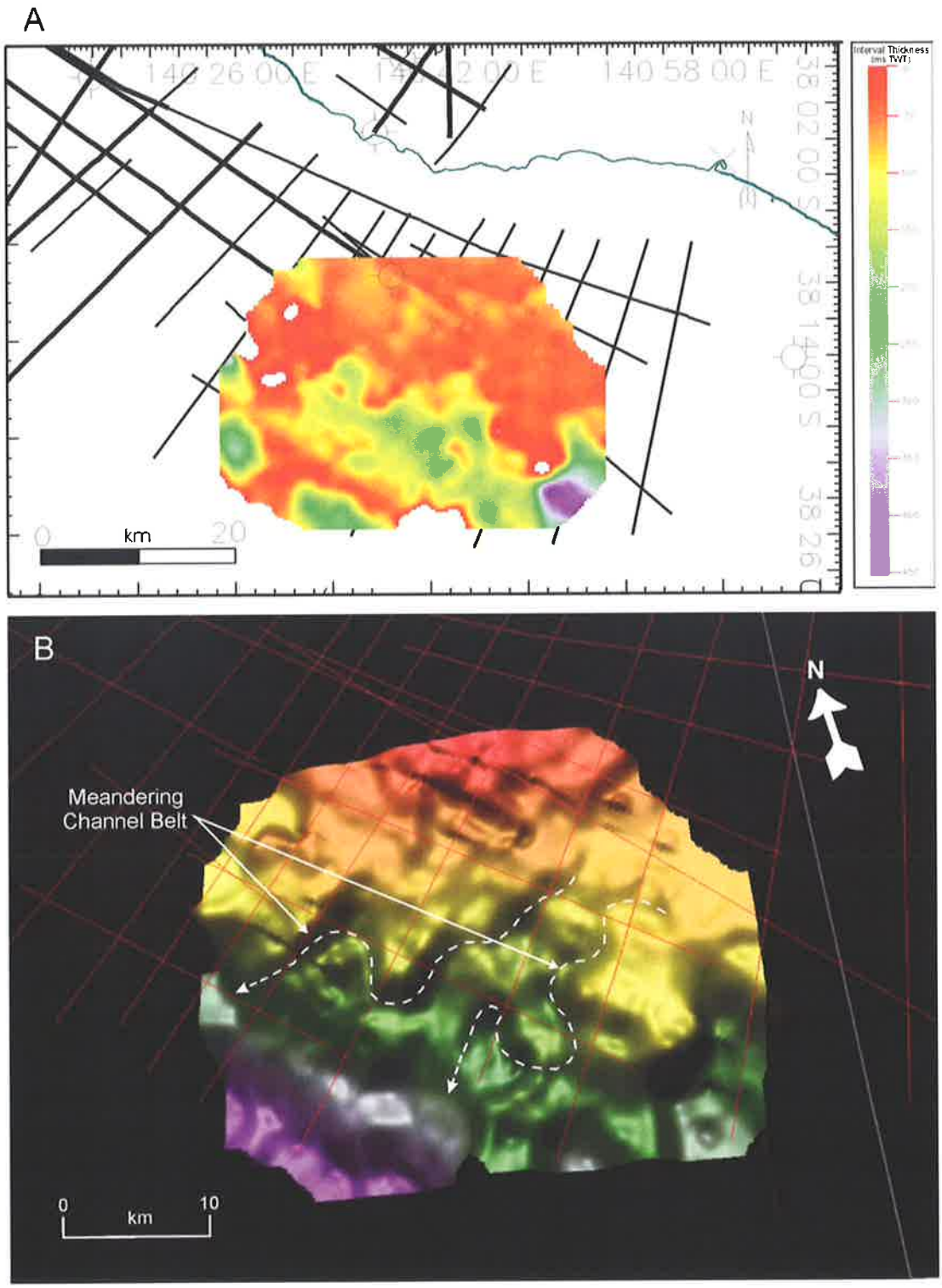

Figure 2.14 (A) Interval-thickness map (ms TWT) of Supersequence 4 around the vicinity of the meandering incised channel belt identified on seismic (Figure 2.11). The thickened area (green) represents the channel fill. (B) Geoviz 3D map of SB 4.1 showing the meandering incised channel belt under the present day outer shelf. There is possibly a sandy lowstand shoreline and turbidite deposits associated with this channel belt that would be potential reservoir targets further downdip.

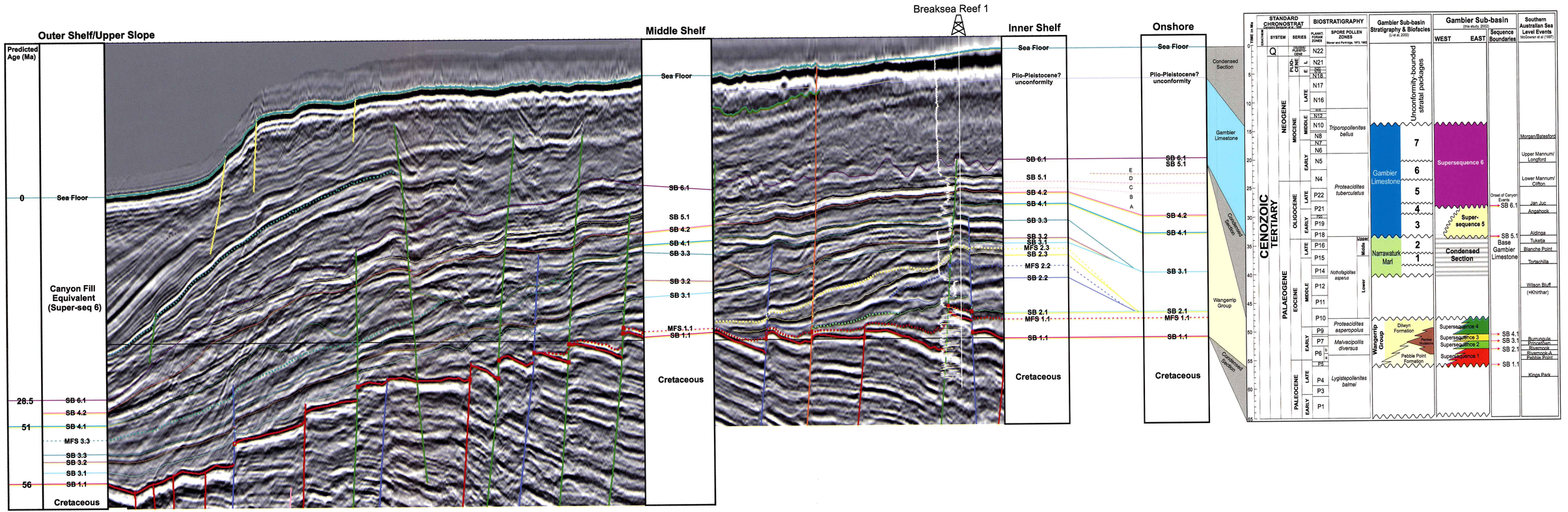

Figure 2.15 Summary of the distribution of Cenozoic sequences across the Gambier Sub-basin from the upper slope to onshore (southwest-northeast). Sequences interpreted on seismic data are correlated to onshore wells using biostratigraphy and wireline log correlations (see Appendix 4). Also illustrated is the relationship between the seismic sequences, their age and known regional southern margin transgressive sea level events that occurred in the early Paleogene (McGowran et al. 1997), and unconformity-bounded packages in the Gambier Limestone (Li et al. 2000) (Seismic Line UA82-31).

Chapter 3

Sequence Stratigraphy of the Carbonate Succession

3 MEGASEQUENCE 2 - SEQUENCE STRATIGRAPHY OF THE CARBONATE SUCCESSION

3.1 PREVIOUS WORK

The Gambier Limestone is a neritic, bioclastic carbonate deposited on the cool-water platform of the southern Australian margin and forms part of the Heytsbury Group (Morton et al. 1995). Of Oligocene to Miocene age, it is a major component of the prograding, extratropical ("cool-water") carbonates (i.e. carbonates accumulating in sea water colder than 20°C; James, 1997) draping the southern continental margin from the late Middle Eocene onwards. Several large palaeo-submarine canyons within the Gambier Limestone have been identified and mapped on seismic data in the Gambier Sub-basin. This chapter discusses the seismic expression of the carbonate succession and reports the discovery of three large canyon systems buried in the carbonates of the Gambier Sub-basin, which were initiated during the Oligocene (compared to the Early Miocene canyons identified in the eastern Otway Basin by Leach and Wallace, 2001). The canyons are new as to both their locale and their time of formation.

We have known for several decades that the modern southern margin is incised by several submarine canyons arrayed from the Perth to the Gippsland and Sorell Basins (von der Borch, 1968; von der Borch et al. 1970) and formed by some combination of tectonically generated morphology and late Neogene glacio-eustacy. Also known for some time is the existence of palaeo-canyons in the Gippsland Basin (James and Evans, 1971; Hocking et al. 1976), which seemed to be strongly clustered chronologically within the Eocene siliciclastics and Middle Miocene carbonates, as also emphasized by McGowran (1979a). The morphology and history of the Miocene canyons have continued to challenge seismic stratigraphers and explorationists (Feary and Loutit; 1998; Holdgate et al. 2000; Leach and Wallace, 2001). McGowran et al (1997) pointed out the chronological correlations of the Gippsland cutting events with "major" (actually North Atlantic) cutting events in the Eocene and Miocene (Haq, 1993)—thus enhancing the sense of both clustering in time and some more-than-regional control, such as eustacy.

Spreading in the Tasman and Coral Seas was aborted in the Middle Eocene and from 44 Ma the spreading rate between Australia and Antarctica significantly increased—a changeover that McGowran (1989) integrated into the global intra-Eocene pause in tectonism and seafloor spreading stemming from India-Asia collision that resulted in thermal subsidence and a rise in

relative sea level (Deighton et al. 1976; Yu, 1988; Cockshell, 1995). There is large gap of approximately nine million years in the Middle Eocene in the southern margin sedimentary record (McGowran et al. 1997). The marine record begins again in the late Middle Eocene with the Wilson Bluff (=Khirthar) Transgression (Fig. 2.2). Deposition of the Nirranda Group in the eastern Otway Basin ensued, influenced by four more major marine transgressions occurring throughout the Late Eocene. However, in the Gambier Sub-basin a condensed section represents the late Middle Eocene to Late Eocene and the sedimentary record begins again with the Aldinga Transgression in the Early Oligocene, depositing the neritic cool-water carbonate Gambier Limestone.

The sedimentary basins on the southern margin were reinvigorated by thermal subsidence, and the sedimentary environments of these basins were strongly influenced by the Circum-Antarctic Current, newly formed in the Oligocene when an oceanic throughway was completed by separation between Antarctica and the South Tasman Rise, then between Antarctica and South America. Favourable location, subsidence and upwelling by fertile waters washing across the Gambier Sub-basin combined to generate the impressive sheet of prograding carbonate known as the Gambier Limestone. Scenarios for the development of the southern margin during the Oligocene and Miocene were developed by Deighton et al. (1976), Cockshell (1995), and McGowran et al. (1997), among others. Li et al. (2000) used foraminiferal biostratigraphy to package the Gambier Limestone allostratigraphically into seven unconformity-bounded units (Fig. 2.2).

Along the southern Australian continental shelf, modern production of carbonate sediments is dominated by bryozoans growing in a ramp-style, open shelf environment (Bone and James, 1993). The Gambier Limestone terminated within the Middle Miocene and was eroded during the Late Miocene and late Pliocene-Pleistocene. The present day sea floor on the continental shelf is relatively featureless, apart from a few faults that are expressed at the surface as scarps, however the upper slope is incised by numerous modern submarine canyons (Figs. 1.4 & 1.5).

3.2 MEPUNGA FORMATION AND NARRAWATURK MARL

The Gambier Limestone represents Megasequence 2 and unconformably overlies the Paleocene to Early Eocene siliciclastic succession. In the eastern Otway Basin, and elsewhere on the southern margin, sedimentation re-commenced with the late Middle Eocene-Late Eocene Nirranda Group and equivalents, however in the Gambier Sub-basin this period is represented by a condensed section. Sediments of the Nirranda Group (Mepunga Formation and Narrawaturk Marl) were observed in outcrop in the Victorian Port Campbell Embayment, but were not recognised on seismic or well data in the Gambier Sub-basin.

Megasequence 2 was sub-divided into two supersequences, based on seismic interpretation and seven packages based on biostratigraphy (Li et al. 2000) (Fig. 2.2). Supersequence 5 comprises marls and prograding carbonates that were severely eroded by SB 6.1. SB 6.1 is the initial canyon incision event and sediments of Supersequence 6 comprise canyon fill. Supersequence 6 is bounded at the top by another regional, probably Pleistocene unconformity and the present-day sea floor.

The Mepunga Formation and Narrawaturk Marl represent a series of major marine transgressions that occurred in the later Middle to Late Eocene on the southern margin, beginning with the Wilson Bluff (=Khirthar) Transgression (McGowran et al. 1997). These units are not represented in offshore seismic data or wells within the study area, but the Mepunga Formation and Narrawaturk Marl is recorded in wells in the northern part of the study area (White, 1995), and both units were observed in outcrop in the adjacent Port Campbell Embayment.

3.2.1 Wireline log expression

The wireline log signature of the Mepunga Formation comprises interbedded low and high gamma (sand/shale) sediments and is probably best distinguished from the underlying Dilwyn Formation by the sonic log which displays a baseline shift to faster values.

3.2.2 Outcrop expression

Lithofacies	Group	Formation/ Member	Location of outcrop	Description	Systems Tract	Depositional Environment
N1	Nirranda Group	Mepunga Formation ("Turritella Clay")	PCE	Fossiliferous, dark grey clay	TST - early HST	Inner shelf, low oxygen waters
N2		Notostrea Greensand	PCE	Greensand	MFS	Condensed interval
N3		Mepunga Formation	PCE	Interbedded, fine-grained sands and marls	HST	Inner shelf
N4		Narrawaturk Marl	PCE	Grey, fossiliferous clays with interbedded skeletal grainstone	HST	Middle shelf

Table 3.1 Summary of lithofacies identified in outcrops of the Nirranda Group.

3.2.2.1 *Lithofacies N1 - fossiliferous, dark grey clay*

The Mepunga Formation in outcrop in the Port Campbell Embayment is predominantly dark grey and weathered orange-brown clay with common *Turritella* spp., *Spirocolpus aldingae* and the bivalve *Limopsis chapmani*, and is known as the "*Turritella* clays" (Shafik, 1983). This unit was bioturbated with some mud drapes visible and possible scattered pyrite (Table 3.1, Plate 5).

3.2.2.2 *Lithofacies N2 - greensand*

The *Turritella* Clay became less shelly towards the top of the unit until the abrupt transition into the 1m thick "*Notostrea* Greensand", which represents a condensed interval during a maximum flooding event (Table 3.1, Plate 5). The base of the greensand was sparsely shelly and gastropods, *Turritella* shells and bivalves became more common towards the top of the greensand.

3.2.2.3 *Lithofacies N3 - interbedded fine-grained sands and marls*

Approximately 200m northwest of Brown Creek is an outcrop of interbedded light grey to white marl and light grey, fine-grained sand package that overlies the *Notostrea* Greensand. At the base of the outcrop the marl beds are thin (up to 20 cm) and the sandy beds are quite thick (up to 1 m). Towards the top of this unit the marly interbeds become thicker (up to 1 m) and, correspondingly, the sandy beds become thinner (up to 40 cm) (Table 3.1, Plate 6).

3.2.2.4 *Lithofacies N4 - grey fossiliferous clays and interbedded skeletal grainstones*

The Narrawaturk Marl is exposed in outcrop at Castle Cove in the Port Campbell Embayment, but is recognised only in well cuttings in the northern and central Gambier Sub-basin. At Castle Cove, the Narrawaturk Marl comprises dark grey to grey, burrowed and bioturbated fossiliferous clays with thin, interbedded bryozoan skeletal grainstones (Table 3.1).

PLATE 5 (*Top*) The "*Turritella* Clay" (Lithofacies 8) at Brown Creek (UTM position 0708044, 5705923), which is equivalent to the Mepunga Formation, comprises weathered grey clay with abundant fossils dominated by *Turritella* spp. gastropods.

(*Middle*) Fossils present in the "*Turritella* Clay" (from left to right); fragment of mussel shell, solitary coral, schaphopod, articulated brachiopod.

(*Bottom*) "*Notostrea* Greensand" at Brown Creek consists of a 1-2 m thick bed of grey-green, glauconitic sand and represents a condensed section during a maximum flooding event.

Note: Brown Creek is marked as outcrop location 8 in Figure 2.3 and Appendix 3.

PLATE 6 Interbedded marl and sand units of the Mepunga Formation (Lithofacies N3) near Brown Creek (UTM position 0707942, 5706034). The sand beds near the base of the outcrop are very thick while the marl interbeds are thin. Towards the top of the outcrop, the sand beds decrease in thickness and the marl interbeds become quite thick (person is visible as scale). *Note*: Brown Creek is marked as outcrop location 8 in Figure 2.3 and Appendix 3.

3.2.3 Outcrop interpretation

The Mepunga Formation marks a major marine transgression (correlated to the Wilson Bluff Transgression; McGowran et al. 1997) that was apparently synchronous across the Otway Basin and was recorded in the eastern Gambier Sub-basin and the Brown Creek section in the Port Campbell Embayment (Shafik, 1983). The Mepunga Formation is interpreted to be a transgressive and early highstand unit deposited during the late Middle Eocene transgression. The *Turritella* clays (Lithofacies N1) were deposited in inner shelf conditions and the infauna appeared to be associated with a low oxygen, transgressive phase (Li, *pers comm.*, 2000). The *Notostrea* Greensand (Lithofacies N2) is a condensed section representing a maximum flooding event and on nearby offshore seismic data this unit is represented as a seismic downlap surface (Arditto, 1995).

Thickening of the marly beds and concurrent thinning of the sandy beds in Lithofacies N3 suggests a gradual shutdown of the clastic system and the emergence of a carbonate dominated system. This package is thought to represent a HST deposited in inner shelf conditions. The Mepunga Formation is Middle Eocene in age and lies within the *P.pachypolus* palynozone (Morton et al. 1995).

The Narrawaturk Marl (Lithofacies N4) was deposited in middle shelf conditions and conformably overlies the Mepunga Formation and unconformably overlies the Dilwyn Formation. It grades laterally and vertically into the Gambier Limestone (Morton et al. 1995). It is Late Eocene in age and lies within the Middle *N.asperus* palynozone (Wood, 1981).

3.3 SUPERSEQUENCE 5

3.3.1 Seismic expression

SB 5.1 was interpreted to be present in the Voluta Trough and on the edge of the Chama Terrace where SB 6.1 truncates it at its western extent (Fig. 3.1). A transgressive and maximum flooding surface was not resolvable on seismic data in Sequence 5.1, therefore this unconformity-bounded unit is treated as a sequence set for seismic interpretation purposes. At the base of this package, internal reflectors are sub-parallel to hummocky but towards the top of the sequence set in places where the overlying SB 6.1 demonstrates large amounts of erosion,

seismic reflections are contorted to chaotic. At its basinward extent, Sequence 5.1 is truncated by erosive canyon cut and fill episodes that have resulted in a palaeo-scarp underlying the present day shelf edge.

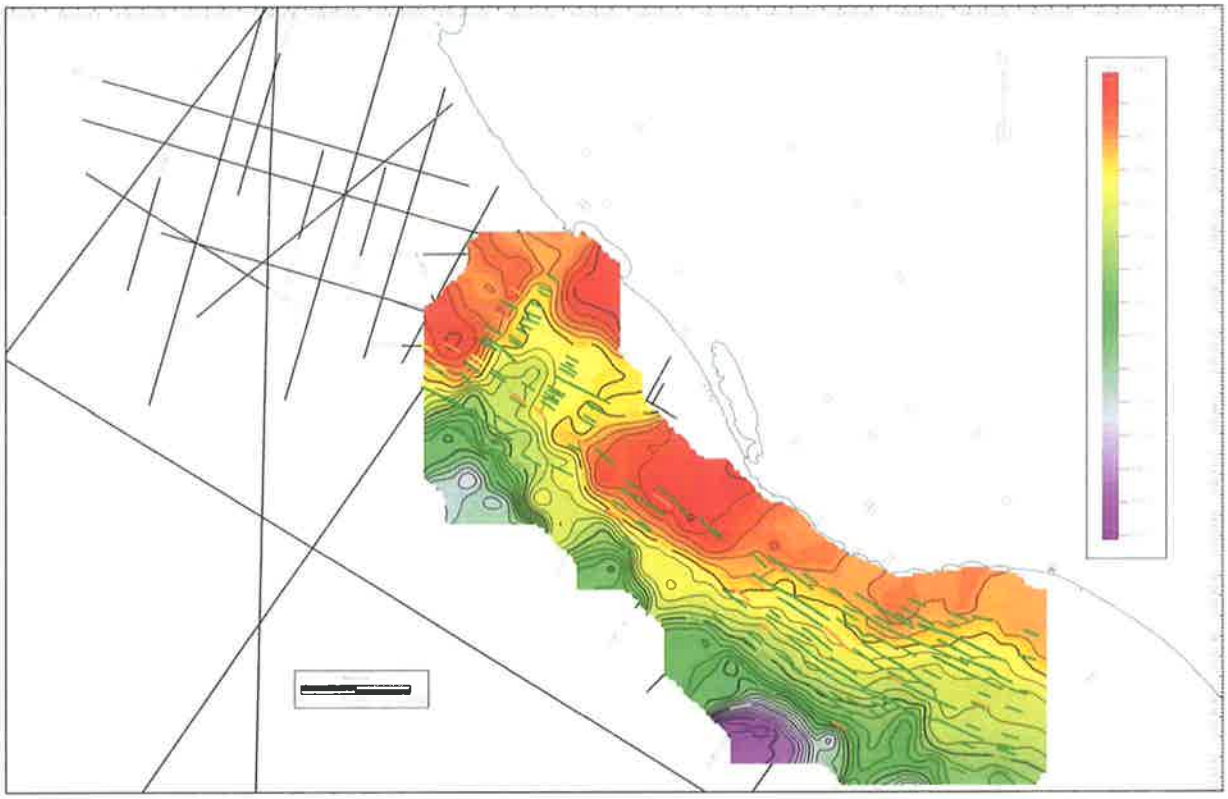

Figure 3.1 Time-structure map of SB 5.1 in the Gambier Sub-basin.

A canyon incising into Sequence 5.1 was identified on line OH91-404 and the surface was labelled as SB 5.2 due to the obvious erosive nature of the surface, however it could not be correlated to other lines in the seismic grid. The canyon is 1500 m wide and 120 ms TWT deep (~140 m) and it is likely that this surface has a limited distribution due to the erosive nature of SB 6.1 near the edge of the Chama Terrace (Fig. 3.2).

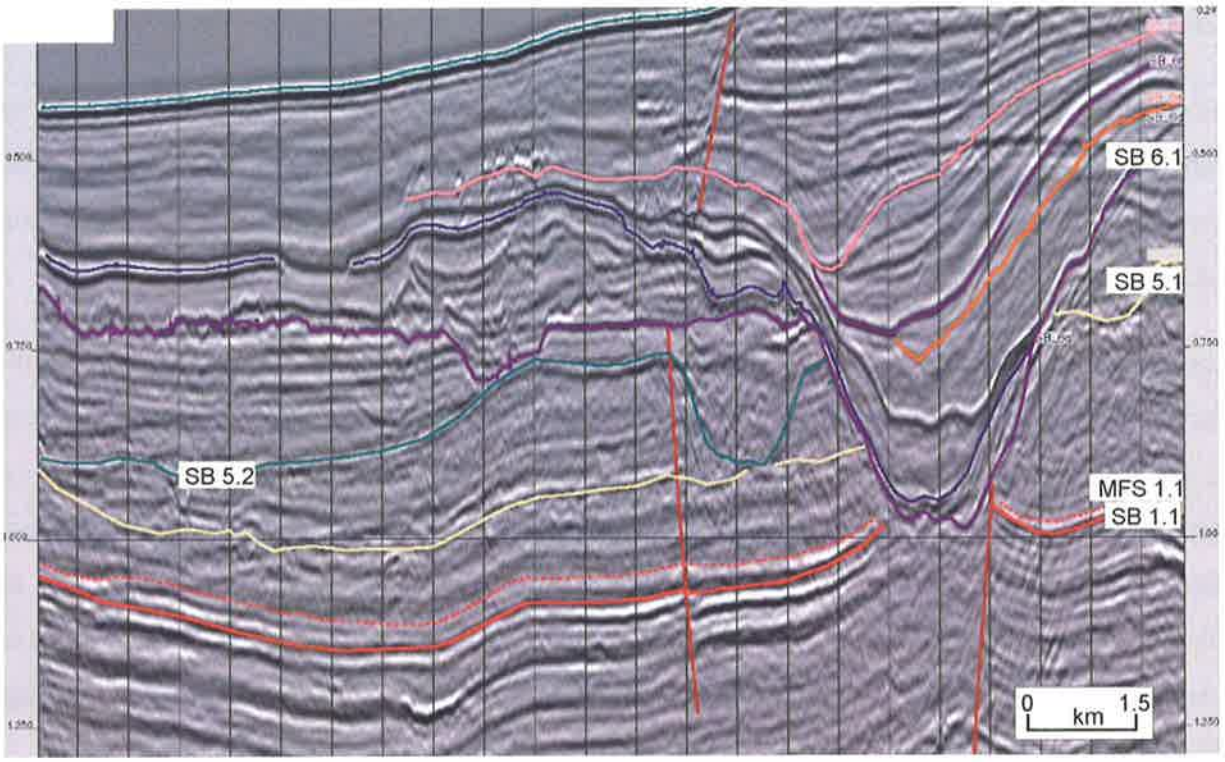

Figure 3.2 Seismic expression of Supersequence 5 (Line oh91-404).

3.3.2 Wireline log expression

The gamma ray and sonic signature (when present) for the Gambier Limestone in all wells in the Gambier Sub-basin is very featureless, making it difficult to identify packages on log motif alone. The gamma ray log comprises consistently low values and the sonic log, also with consistent values may only display a baseline shift at SB 6.1 (Fig. 2.9). For this reason, White (1995) devised a three-fold sub-division of the Gambier Limestone by analysis of the cuttings and micropalaeontology. However, this study had adopted the sequence stratigraphic nomenclature defined as a result of seismic interpretation and only briefly refers to the three-fold lithostratigraphic divisions defined by White (1995) in the lithofacies descriptions (Section 3.4.3).

In Breaksea Reef 1, the log signatures are typical for the Gambier Limestone with low gamma values and featureless log characters. At 405 m there is a slight sonic baseline shift to the right (decreasing speed) over the transition from Supersequence 5 to 6, which was correlated to SB 6.1, a highly erosive palaeosurface (Fig. 2.9).

3.3.3 Discussion

Biostratigraphic analysis from offshore wells in the Voluta Trough suggests the base of Supersequence 5 is close to the Eocene-Oligocene boundary (between P15 and top P20 foraminiferal zones) and ranges up to the Early/Late Oligocene boundary (refer to Section 3.4.4).

Supersequence 5 marks the onset of fully marine carbonate deposition in the Gambier Sub-basin. SB 5.1 forms the basal surface of the Gambier Limestone in the eastern and middle parts of the Sub-basin, however differential subsidence across the Sub-basin after deposition of Supersequence 5 resulted in erosion of these sediments and their complete removal in the west. Basin tilting after deposition of Supersequence 5 is inferred because there is little onlap of Supersequence 5 sediments onto SB 5.1 near the Chama Terrace, suggesting these sediments were deposited horizontally and have been eroded by the event producing SB 6.1 after tilting (Fig. 3.3).

3.4 SUPERSEQUENCE 6

The greater part of the carbonate section in the Voluta Trough comprises canyon cut and fill episodes, beginning with SB 6.1 near the Early/Late Oligocene boundary (28.5 Ma). No less than 20 major canyon cutting events have been interpreted across the Sub-basin in the Voluta Trough but due to the poor seismic data quality so near the surface, it was not possible to correlate all major unconformities across the entire study area or to tie the surfaces to nearby wells. For this reason it was not viable to date the canyon events that occurred after SB 6.1, so they have been assessed as being between Late Oligocene to Middle Miocene in age. Some of the events interpreted in the east and west Voluta Trough that could not be tied may be equivalent in age.

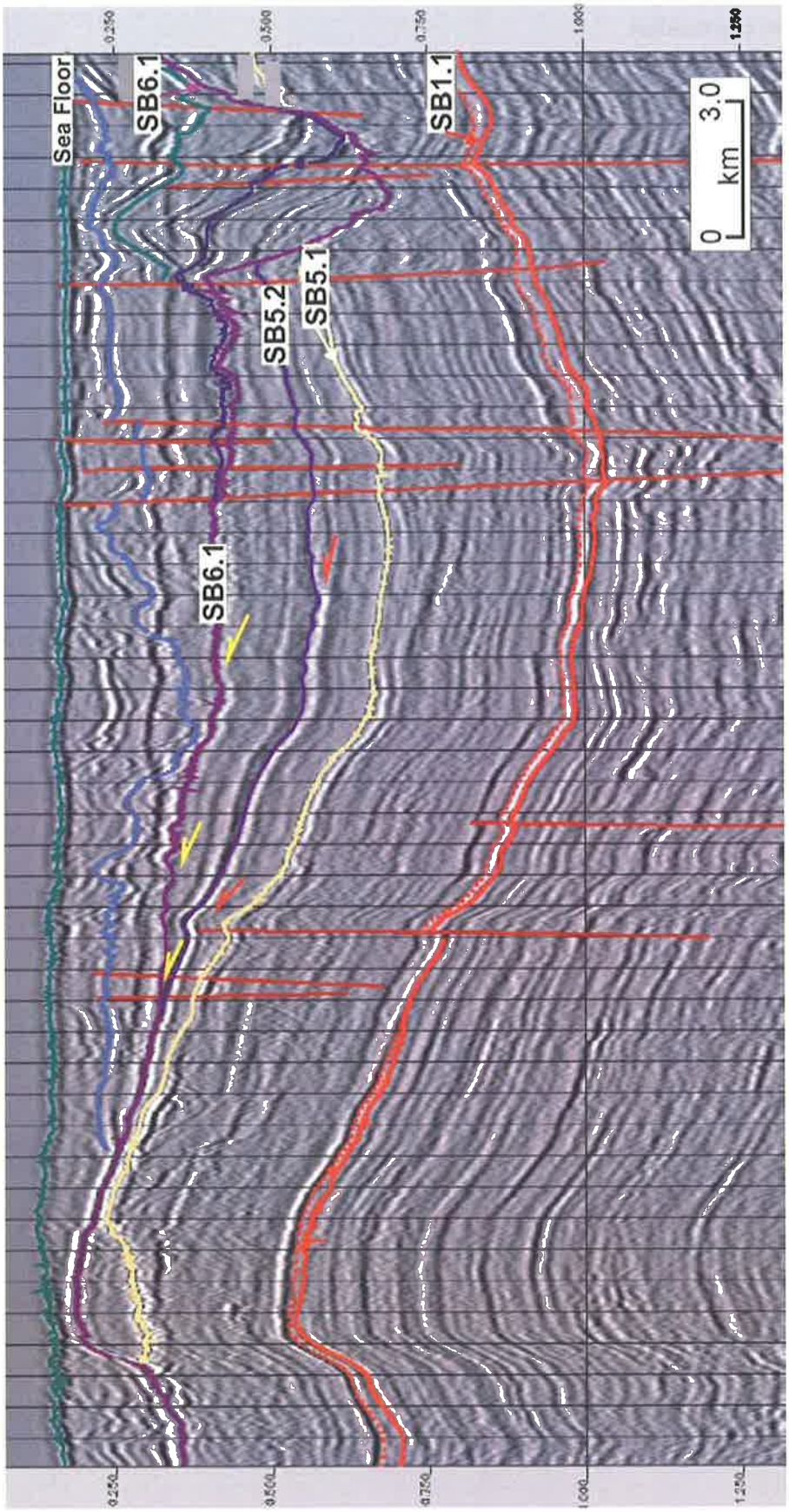

Figure 3.3 Seismic section showing erosion of Supersequence 5 by SB 6.1 (Line oh91-402).

3.4.1 Seismic expression

SB 6.1 is extremely erosive in nature and forms the basal surface of erosion for the three major palaeo-canyon systems identified in the Gambier Sub-basin (Fig. 3.4; Section 3.5). These canyon systems incise into the underlying clastic succession of the Wangerrip Group. SB 6.1 truncates SB 5.1 near the edge of the Chama Terrace and therefore forms the base of the Gambier Limestone in the western part of the basin (Fig. 3.5). Sediments of Supersequence 6 comprise canyon fill.

3.4.2 Wireline log expression

Gamma ray log expression for Supersequence 6 is the same as Supersequence 5 and is only distinguished by a baseline shift in the sonic log (e.g. at 405 m in Breaksea Reef 1). The gamma ray log comprises low values and a featureless signature. No density logs penetrate Supersequence 6 in the Gambier Sub-basin. The erratic sonic signature between 330-368 m in Breaksea Reef 1 has been attributed to a fault that was identified on seismic and is apparently intersected by the well (Fig. 2.9).

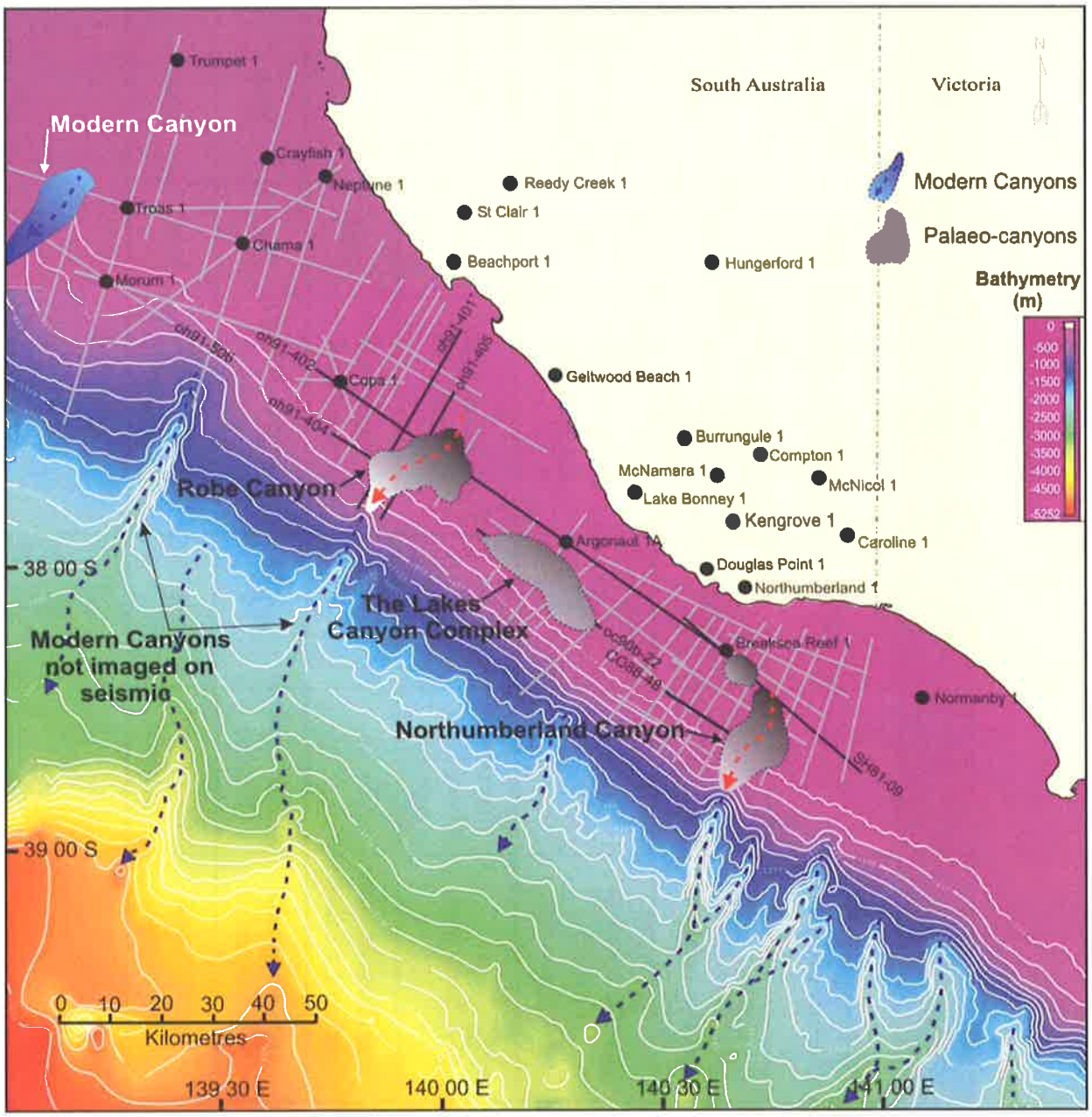

Figure 3.4 Location map and bathymetry of the Gambier Sub-basin showing the location of palaeo- and modern canyons on the continental shelf and slope.

3.4.3 Outcrop expression

The lithofacies defined in the Heytsbury Group are summarised in Table 3.2.

Lithofacies	Group	Formation/Member	Equivalent unit in GSB	Location of outcrop	Description	Systems Tract	Depositional Environment
H1	Heytsbury Group	Greenways Member (Gambier Limestone)		GSB	Grey, marly limestone	HST	Inner - mid shelf
H2		Camelback Member (Gambier Limestone)		GSB	White, off-white and fawn bryozoal limestone	HST	Inner - outer shelf
H3		Camelback Member "Compton Conglomerate"		GSB	Poorly sorted conglomerate	?	? Shoreline beach platform
H4		Gellibrand Marl	Camelback-Green Point Members	PCE	Grey, bioturbated marl	HST	Inner Shelf
H5		Green Point Member (Gambier Limestone)		GSB	Grey limestone with abundant chert	HST	Inner - mid shelf
H6		Port Campbell Limestone	Green Point Member	PCE	Fine-grained, orange - brown packstone	HST	Shelf
H7		Port Campbell Limestone	Green Point Member	PCE	Cream - brown wakestone	HST	Shelf

Table 3.2 Summary of lithofacies observed in the Gambier Limestone, Gellibrand Marl and Port Campbell Limestone.

3.4.3.1 *Lithofacies H1 - grey marly limestone*

The Greenways Member typically comprises a lower lithology of grey limestone, marly limestone and marl with glauconite, passing into an upper lithology of grey limestone (White, 1996). In addition to glauconite, the lower lithology contains abundant bioclasts (gastropods, echinoderms, bryozoa, foraminifera, and sponge spicules) as well as chert, quartz and goethite. Typically, the foraminifera are either all or mostly benthonic rotaliines, sometimes with planktonics and rarely with milioliines (White, 1996). The depositional environment of the Greenways Member was inner and middle shelf, based mainly on the relative proportions of planktonic to benthonic foraminifera (White, 1995).

3.4.3.2 *Lithofacies H2 - white, off-white and fawn limestone*

The Camelback Member is generally composed of off-white, white or fawn limestone with abundant bryozoa in the Gambier Sub-basin. Other components include bivalves, gastropods, echinoderms, coral, foraminifera, ostracods, sponge spicules, wood, quartz, chert, glauconite, calcite rhombs and rock fragments. This limestone may be at least partially recrystallised (e.g. Caroline 1) (White, 1996). At some localities the base of the Camelback comprises a unit varying from conglomerate to very coarse-grained calcarenite (White, 1996). This includes the type section of the 'Compton Conglomerate' (see below, Lithofacies H3).

3.4.3.3 *Lithofacies H3 - poorly sorted conglomerate*

This unit is known as the Compton Conglomerate and is recognised only in one outcrop in the Gambier Sub-basin, as it cannot be identified with any certainty in wells. It is up to 0.7m thick and is a sequence-bounded unit, representing a long period of time (Plate 7). The upper and lower contacts of the conglomerate are unconformable and discrete, caused by denudation and erosion, resulting in a conglomerate that contains clasts from many sources and of varying ages.

It had a multi-event history and includes quartz pebbles, clasts from the Greenways Member of the Gambier Limestone (early Oligocene grey/green marl), Camelback Member (early-mid Oligocene pink dolomite), ironstone "buckshot" clasts, and ferruginised calcarenite (Plate 7). There was some apparent imbrication of the large clasts within the conglomerate, but there appeared to be no preferred orientation. Brachiopods were observed in the matrix and a solitary coral and a cast of a brachiopod shell was seen in a clast within the conglomerate. This facies of

the Camelback Member is only present in outcrop where the Greenways Member is absent and the Camelback Member rests unconformably on older strata (White, 1996).

Unconformably overlying the conglomerate was a thin (1-2cm), continuous ironstone layer that is possibly a palaeo-hardground formed as a result of subaerial exposure (Plate 7). This conglomerate may have originated from "beach rock" deposited at the shoreface.

3.4.3.4 Lithofacies H4 - grey bioturbated marl

The Gellibrand Marl outcrops along much of the Victorian Great Ocean Road in the Port Campbell Embayment. Foraminifera indicate the marl was deposited from the Late Oligocene to Middle Miocene (Abele et al. 1976) and is, therefore, equivalent in age to the Camelback and Green Point Members of the Gambier Limestone.

At Loch Ard Gorge, near Port Campbell, the Gellibrand Marl is a dark to medium grey, highly bioturbated/churned, skeletal wackestone/packstone that was dominated by red algal tubular fragments (Plate 8). Gross bedding up to 0.5 m is marked by nodular horizons, but there are no primary sedimentary structures present due to the high degree of bioturbation.

The nodules within the marl are a result of bioturbation. Bifurcating burrows, mud-lined burrows (Plate 8) and spreite (dwelling burrows) (Plate 8) are visible. The marl appears to be 100% carbonate, hence differential erosion can explain the positive relief of the burrows where larger crystals replacing the burrows has resulted in slower erosion of the burrows compared to fine-grained surrounding sediment (Plate 7). Fossils observed in the marl included red algae stalks, shell debris and forams (globigerina planktonics and small *Cibicides* benthonics).

Due to the highly bioturbated nature of the marl, it is thought that this initially soft sediment was deposited either in deep water on the shelf or in a shallow protected embayment, the latter perhaps being more applicable, based on interpreted palaeogeography during the Late Oligocene to Middle Miocene. The presence of red algae suggests a cool paleo-water temperature.

3.4.3.5 *Lithofacies H5 - grey limestone with abundant chert*

This unit comprises grey limestone with abundant chert as well as bivalves, echinoderms, bryozoa, foraminifera, ostracods, quartz, glauconite and pyrite and is known as the Green Point Member of the Gambier Limestone (White, 1996). This member was found by White (1995) to occur in the offshore wells in the Gambier Sub-basin.

3.4.3.6 *Lithofacies H6 - fine-grained, orange-brown packstone*

Overlying the Gellibrand Marl at Loch Ard Gorge was a 4m thick pale orange/brown fine-grained calcarenite packstone that is part of the Port Campbell Limestone. The Port Campbell Limestone grades laterally into the Gambier Limestone and foraminifera indicate an age of Early to Late Miocene (Abele et al. 1976), equivalent to the Green Point Member of the Gambier Limestone. The packstone beds comprise significant shell debris and are well bedded at the decimetre scale. There is some hint of convex up bedding structure towards the top of the unit indicating hummocky cross stratification (HCS), which suggests these beds were deposited between storm and fair weather zones. The approximate wavelength of the HCS was 1.0-1.3m with amplitude of 5-10cm. The packstone beds contained very shelly, nodular horizons, overlain by a thin muddy horizon, which is consistent with storm lag. The intervening wackestone was also well bedded at the decimetre scale.

3.4.3.7 *Lithofacies H7 - cream-brown wackestone*

This unit is a massively bedded pale creamy brown wackestone within the Port Campbell Limestone at Loch Ard Gorge. It contained several nodular horizons around shell debris and there was some suggestion of bedding (possibly cross bedding). Scattered red algae fragments were common along with some shells. When viewed from a distance, the wackestone appeared to downlap onto the underlying packstone unit.

PLATE 7. (Top) Compton Conglomerate at Allen's Quarry (Lithofacies 12) (UTM position 0474670, 5820067) comprising clasts up to 30 cm diameter from the Greenways and Camelback Members of the Gambier Limestone as well as ironstone "buckshot" clasts, fossils and ferruginised calcarenite. *Note*: Allen s uarr is marked as outcrop location in Figure 2.3 and Appendix 3.

(Middle) Thin, continuous ironstone layer directly overlying the Compton Conglomerate that possibly formed as a result of sub aerial exposure.

(Bottom) Differential erosion of coarse-grained burrows from surrounding fine-grained carbonate sediment in the Gellibrand Marl at Loch Ard Gorge (UTM position 0680290, 5720818). *Note:* Loch Ard Gorge is marked as outcrop location 5 in Figure 2.3 and Appendix 3.


A

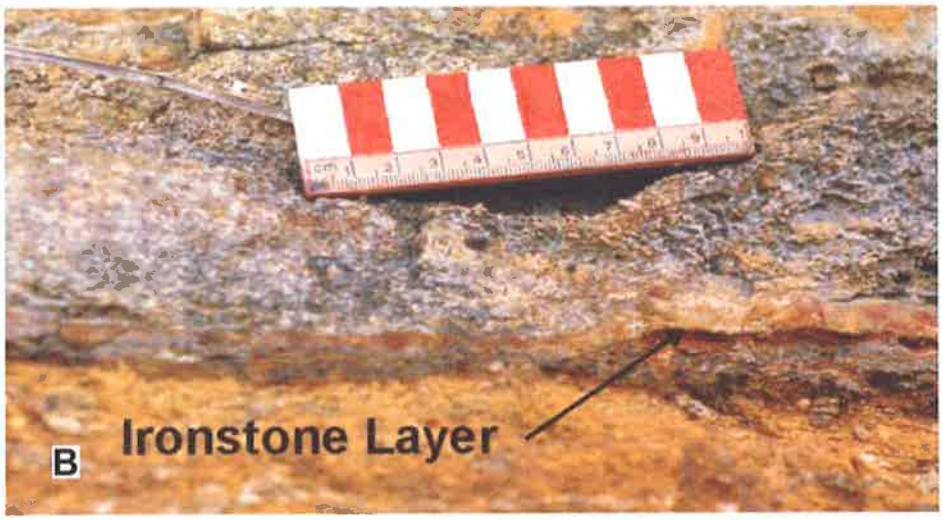
Ironstone Layer
B

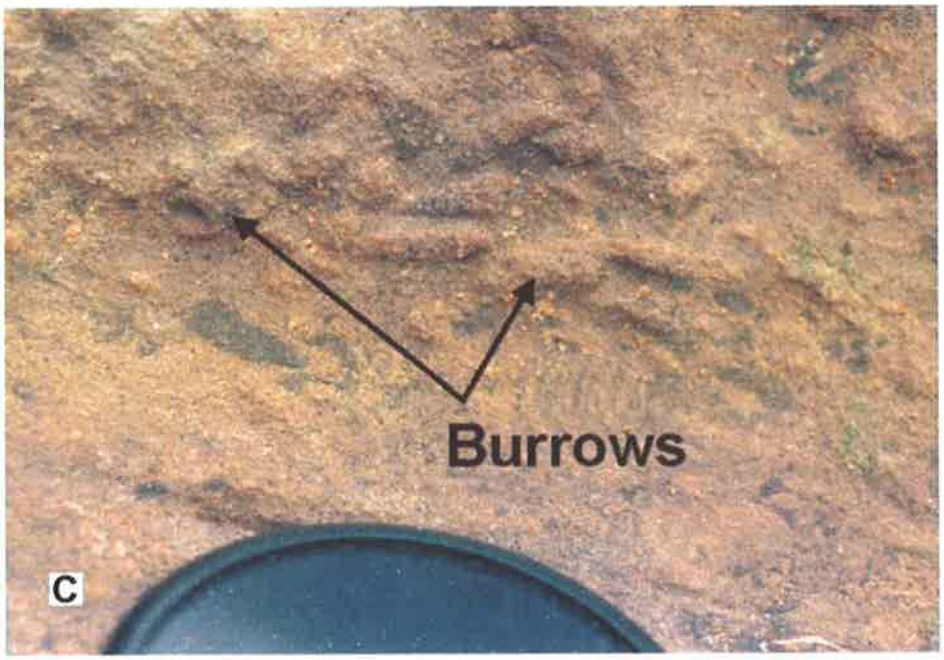
Burrows
C

PLATE 8. (Top) Tubular red algae fragments in the highly bioturbated Gellibrand Marl (Lithofacies 11) at Loch Ard Gorge (UTM position 0680290, 5720818). The Gellibrand Marl in the Port Campbell Embayment is equivalent to the Camelback Member of the Gambier Limestone in the Gambier Sub-basin.

(Middle) Mud-lined burrows in the Gellibrand Marl at Loch Ard Gorge.

(Bottom) Dwelling burrows (spreite) in the Gellibrand Marl at Loch Ard Gorge.

Note: Loch Ard Gorge is marked as outcrop location 5 in Figure 2.3 and Appendix 3.

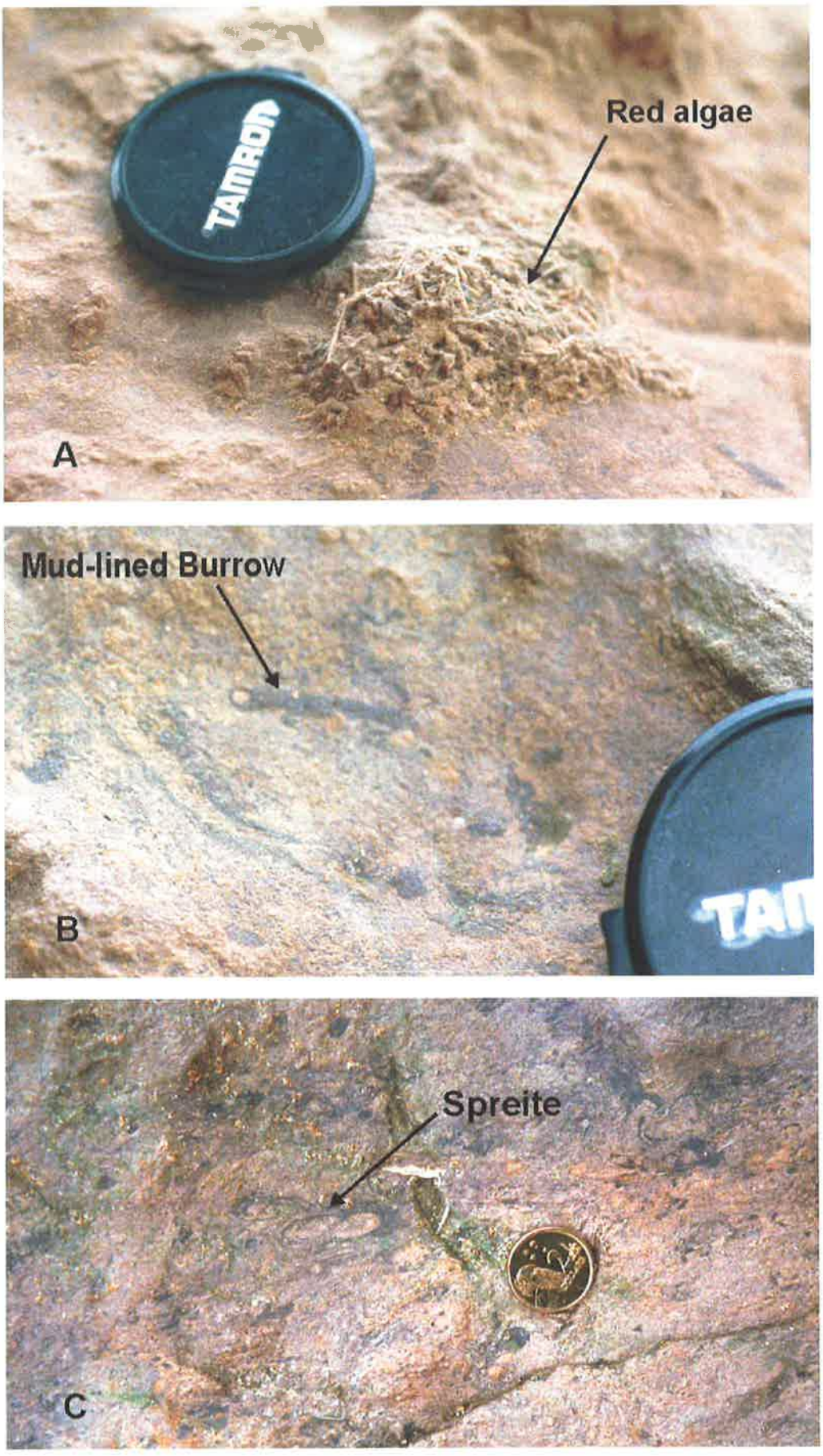
Red algae
A
Mud-lined Burrow
B
Spreite
C

3.4.4 Outcrop Interpretation

White (1995, 1996) defined inner, middle and outer shelf environments of deposition for the Gambier Limestone and Gellibrand Marl based on the ratio of planktonic to benthonic foraminifera. The carbonates of the Gambier and Port Campbell Limestone rapidly prograded south on the subsiding southern continental margin, producing prograding, clinoformal seismic character (Arditto, 1999).

3.5 PALAEO-SUBMARINE CANYONS

Two large submarine canyons or canyon complexes have been identified on seismic data and named the Robe Canyon and the Northumberland Canyon. A third group of slightly smaller canyons have been identified on seismic data and named the Lakes Canyon Complex. The location and aerial extent of these canyons in relation to seismic and well data has been mapped and appears in Figures 3.4 and 3.5. SB 6.1 forms the basal surface of erosion for the three major palaeo-canyon systems. It ranges in depth from 200 to 1600 ms TWT and is extremely erosive in nature, incising into Supersequence 5 and the underlying clastic succession of the Paleocene to Early Eocene Wangerrip Group (Fig. 3.5).

3.5.1 Robe Canyon

3.5.1.1 Dimensions

The Robe Canyon is located near the western limits of the Voluta Trough on the outer continental shelf. The main canyon axis strikes NNE-SSW and is approximately 30 km long, 4-5 km wide, and runs perpendicular to the present day shelf break with a slightly sinuous path (Fig. 3.6). A smaller tributary is observed on the eastern side of the main canyon and strikes NE-SW and is approximately 12 km long and 3 km wide. The original canyon (identified as interpreted horizon SB 6.1) at this position is approximately 410 m deep (0.358 sec TWT) and 5.4 km wide (Fig. 3.7). Towards the southwest near the toe of the complex, the original canyon (SB 6.1) narrows to 4.3 km and deepens to approximately 615 m (0.534 sec TWT) (Fig. 3.8).

3.5.1.2 Seismic expression

SB 6.1 is a high-amplitude, highly correlative reflector that was interpreted across the entire study region. The erosive nature of this unconformity is evident across the sub-basin by the truncation of underlying sediments and the undulose nature of the reflector. In a proximal location the initial canyon has a U-shaped cross-section with small-mounded features on each bank. The western bank of the canyon has been eroded down to a lower level than the eastern bank (Fig. 3.7). Distally, the canyon becomes more V-shaped in cross-section and the mounded features are no longer apparent on the banks of the canyon (Fig. 3.8).

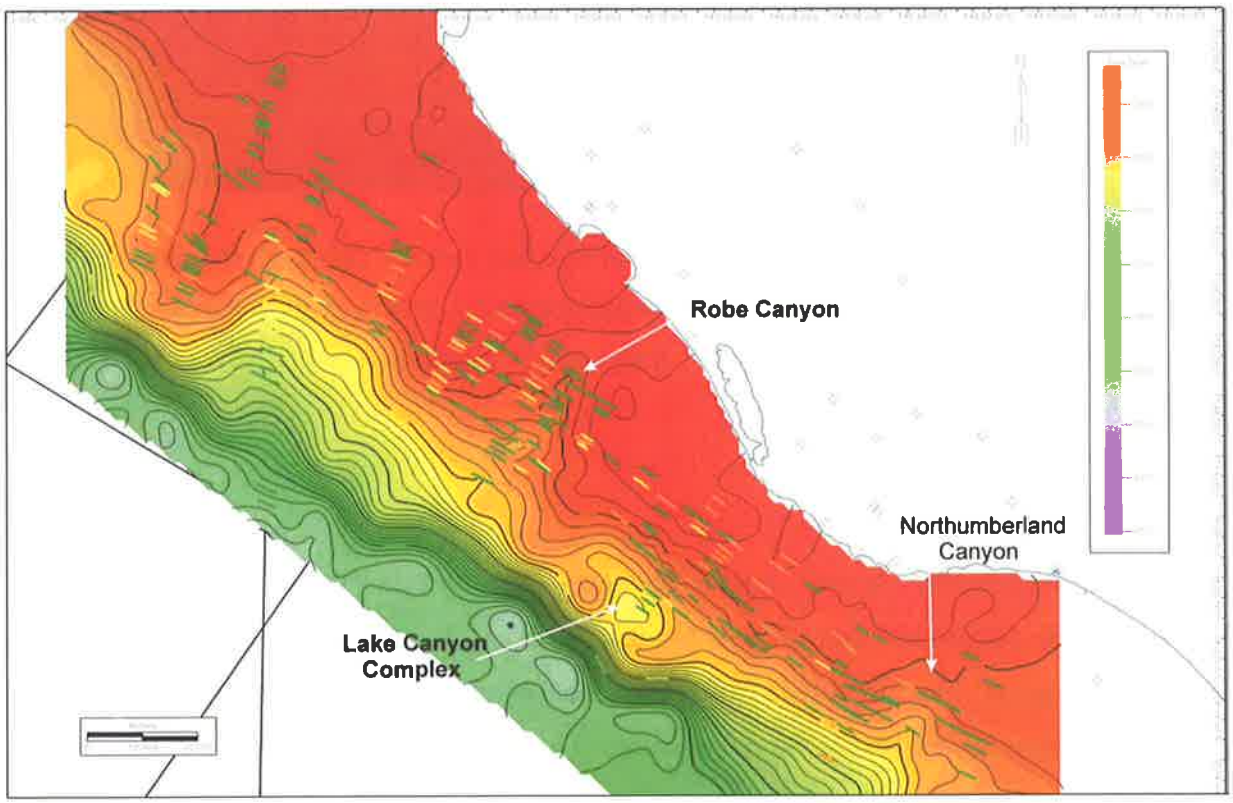

Figure 3.5 Time-structure map of SB 6.1 showing the locations of the three palaeo-submarine canyons identified on seismic data in the Gambier Sub-basin.

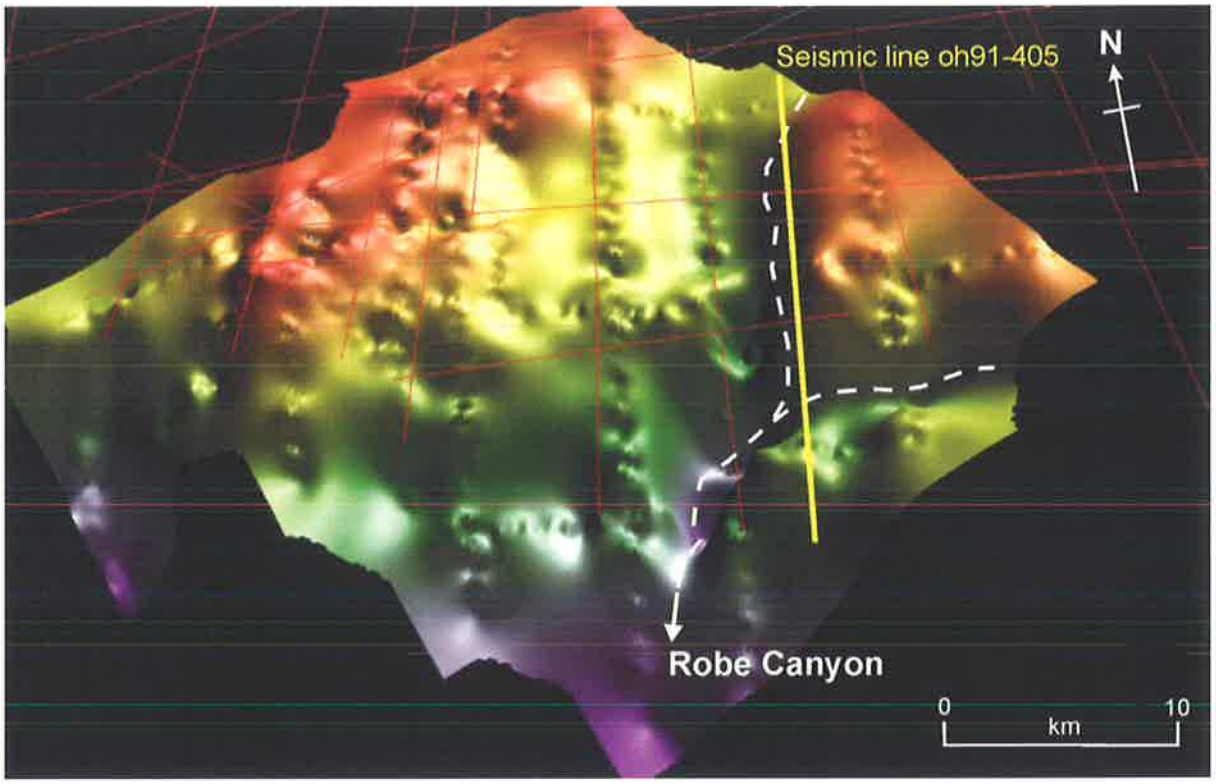

Figure 3.6 3D visualisation of the initial canyon incision surface (SB 6.1) showing the Robe Canyon. The main canyon axis strikes northeast-southwest and is slightly curved. There is a smaller tributary canyon that joins the main canyon from the east (Vertical Exaggeration=10.35).

Eight major successive canyon cuts have been identified in the Robe Canyon (A-H). Proximally, the canyon cut and fill events laterally migrate to the southeast. The canyon-fill packages comprise low amplitude reflectors that display apparent sigmoidal prograding clinoforms, bounded by high amplitude reflectors (Fig. 3.7).

In a distal position the succession of later canyon fill events demonstrates the same seismic character (i.e. high amplitude reflectors bounding low amplitude canyon-fill packages). However, the canyon fill packages display sub-parallel to divergent reflector patterns and successive events laterally migrate to the southwest. Seismic "pull-up", indicating a velocity anomaly in overlying sediments, is observed directly below the canyon complex at a distal location (Fig. 3.8).

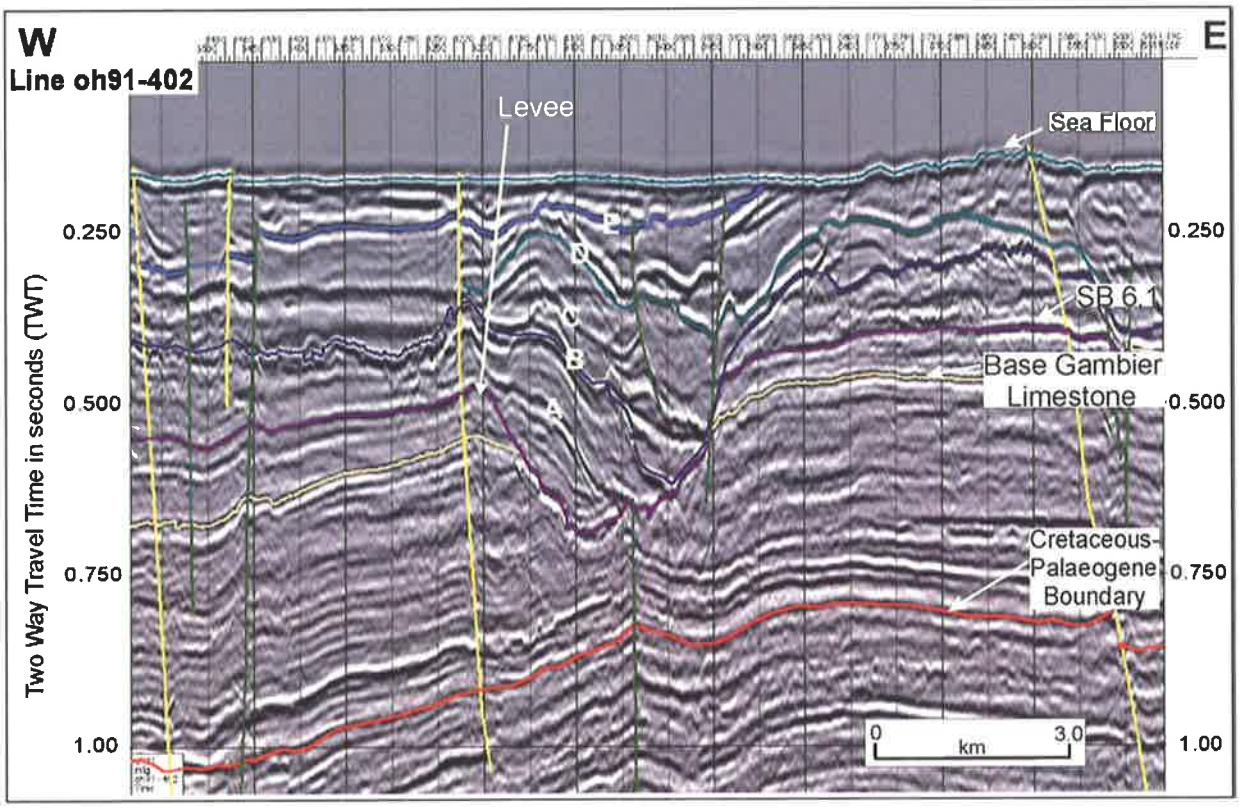

Figure 3.7 Seismic expression of the Robe Canyon (line oh91-402) across its axis at a landward position near the head of the canyon. SB 6.1 is the initial canyon incision event and is followed by five successive canyon cut and fill events (A-E). At this location the successive canyon events migrate laterally to the east.

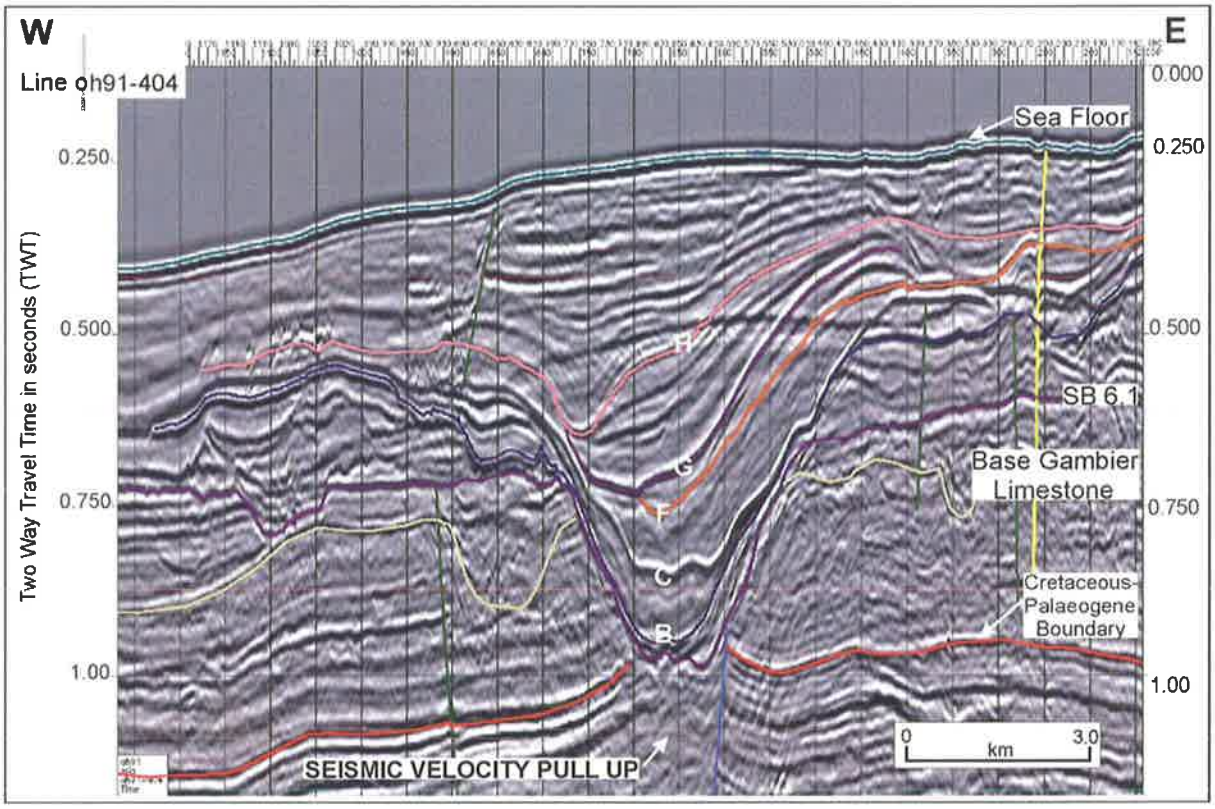

Figure 3.8 Seismic expression of the Robe Canyon (line oh91-404) across its axis at a more distal location near the toe of the canyon. SB 6.1 was the initial canyon incision event, followed by five successive cut and fill events (B, E, F, G, H). Events B and E were correlated from further up dip in the canyon, but events F-H were truncated by overlying unconformities and do not extend along the canyon axis to be imaged in the up dip seismic line.

Seismic examples from an oblique section along the axis of the canyon show the down-dip geometry of the canyon fill. Hummocky to mounded reflectors resting on SB 6.1 were observed at the base of the original canyon and the canyon fill packages prograde down the axis of the canyon from the northeast and downlap onto the underlying canyon cut (Fig. 3.9).

Although normal faults intersect the canyon and can be seen to extend into underlying sediments, these faults do not have any influence on the formation of the canyon.

3.5.2 Lakes Canyon Complex

3.5.2.1 Dimensions

The initial canyon cutting event (SB 6.1) that produced the Lakes Canyon Complex resulted in the formation of three canyons approximately 2-2.5 km apart (A, B, C). These canyons extend approximately 10 km along their axes and are orientated in a north-south direction, perpendicular to the present day shelf break.

Canyon A is located in the western-most part of the complex and is 177 m deep (0.154 sec TWT) and 2.9 km wide. Approximately 2 km to the east lies Canyon B, which is a slightly larger canyon, being 267 m deep (0.232 sec TWT) and 3.5 km wide. Canyon C is located approximately 2.7 km east of Canyon B and is 246 m deep (0.214 sec TWT) and 2.3 km wide (Fig. 3.10).

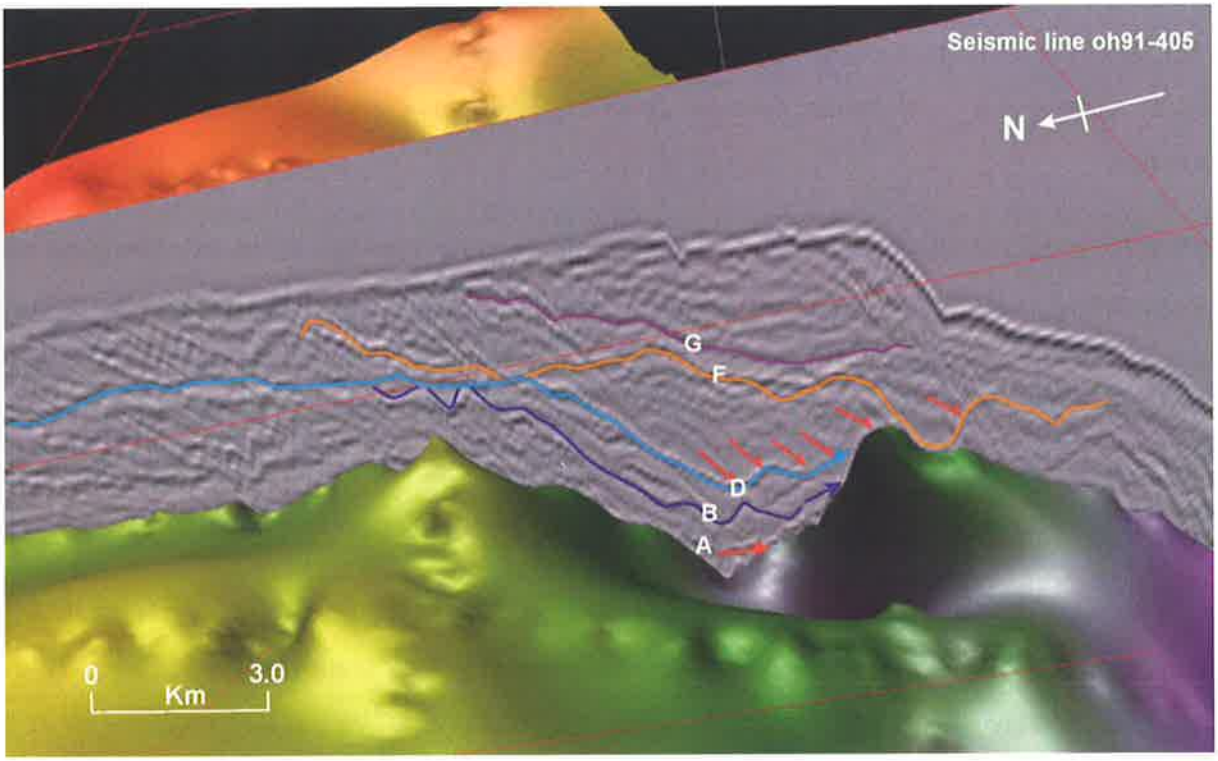

Figure 3.9 Seismic dip line (Line oh91-405) intersecting SB 6.1 approximately parallel to the axis of the Robe Canyon. Canyon fill packages prograde down dip and onlap onto the underlying canyon cut. Events F and G have been truncated by an unconformity just below the present day sea floor.

3.5.2.2 Seismic expression

SB 6.1 is a high amplitude, continuous reflector and the three canyons that comprise the Lakes Canyon Complex are U-shaped in cross-section. Six major successive canyon cutting events were identified in the Lakes Canyon Complex (C2b, C2c, C3, C3b, C4 and C6), three of which were correlated to the Northumberland Canyon (C3, C4 and C6).

In the Lakes Canyon Complex, Canyon A initially has a relatively flat base and successive cut and fill events display a similar seismic reflection character to that observed in the Robe Canyon with high amplitude reflectors bounding low amplitude packages. Canyon fill packages display divergent to sub-parallel internal geometries and younger events migrate in a southwest direction.

Canyon B is the result of the merger of two canyons as suggested by the double chute observed on seismic. The next two incision events also produced a canyon with a double chute (C2b and C2c), however successive events have only a single chute. Low amplitude canyon fill packages display divergent to sub-parallel internal geometry and younger events migrate towards the southeast.

Canyon C is also U-shaped in cross-section and the seismic character of the overlying cut and fill succession is similar to that observed in Canyon B and younger incision events also migrate laterally towards the southeast. There is a slight suggestion of a seismic "pull up" below each of these canyons indicating a velocity anomaly in the overlying sediments. Further to the east of Canyon C is a younger canyon (Canyon D) formed during event C3 (Fig. 3.10). The canyon fill is sub-parallel to hummocky and successive canyon episodes laterally migrate to the southeast.

In dip section, the canyons appear as a series of scarps close to the present day shelf break. The sediment filling the canyons comprises sigmoidal prograding clinoforms of medium to low amplitude bounded by high amplitude reflectors, while the large-scale, medium to high amplitude progradational clinoforms at the shelf edge have a very smooth texture.

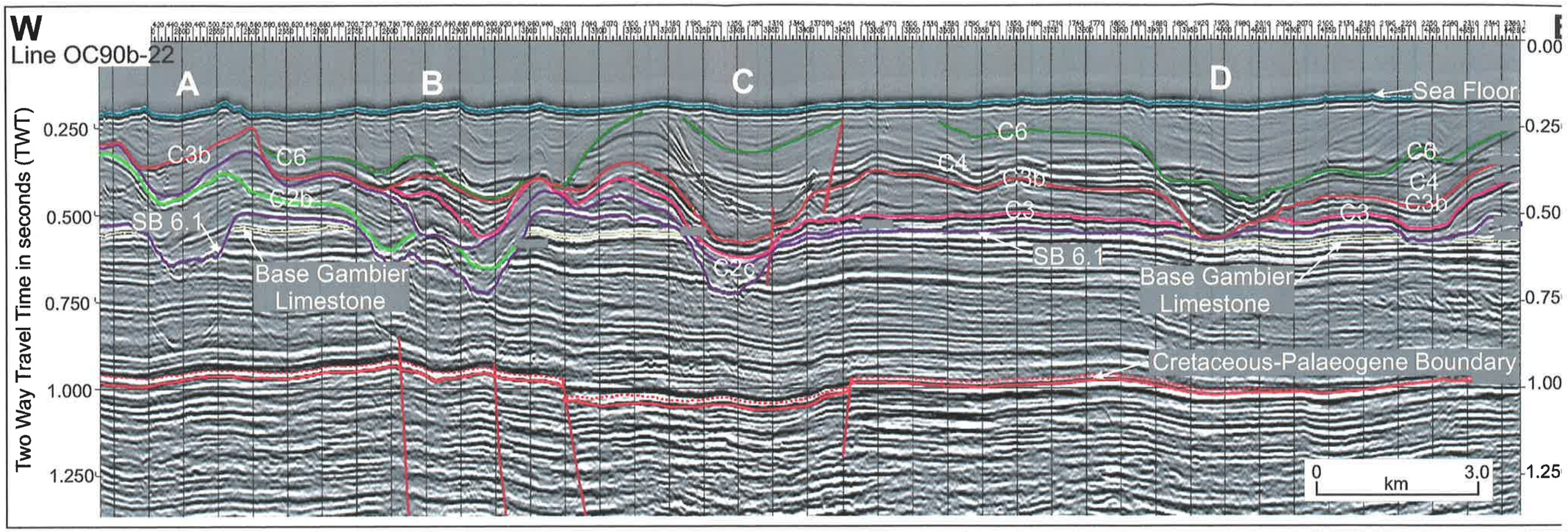

Figure 3.10 Seismic expression of the Lakes Canyon Complex (Line OC90b-22). During event SB 6.1 three canyons were incised into the upper slope and shelf (A, B and C). Six major successi canyon events occurred after the initial incision, with events C3, C4 and C6 correlated with events in the Northumberland Canyon to the east. These successive incision events also show late migration. During incision event C3 another canyon was formed to the east of the existing canyons (D).

3.5.3 Northumberland Canyon

3.5.3.1 Dimensions

Near the head of the Northumberland Canyon the complex comprises a single large channel 4.8 km wide and approximately 340 m deep (0.296 sec TWT) and a smaller channel to the north that is 1.5 km wide and approximately 200 m deep (0.176 sec TWT) (Fig. 3.11). Further basinward the main canyon widens to 6.7 km, but remains approximately the same depth at 336 m (0.292 sec TWT) and the smaller tributary canyon visible in a proximal position has probably joined the main canyon and is therefore not imaged in the distal position (Fig. 3.12). The Northumberland Canyon has a straight axis that is approximately 14.8 km long and 6.7 km at its widest point and is orientated perpendicular to the present shelf edge (Fig. 3.13).

3.5.3.2 Seismic expression

At a proximal location, this canyon has a very smooth U-shape in cross-section with a flat canyon floor. The initial incision surface is marked by high amplitude reflectors, however the canyon fill and successive canyon cutting events are largely obscured by a seafloor multiple and diffuse reflectors. The small tributary canyon to the west of the main canyon displays the same seismic character but has a sharper base (Fig. 3.11).

At a more distal location, the canyon profile becomes rough and the canyon floor is no longer flat. Nine successive canyon cutting events were identified in the Northumberland Canyon (C1-C9), three of which were correlated to the Lakes Canyon Complex (C3, C4 and C6). The successive canyon cut and fill events comprise high amplitude reflectors bounding medium to low amplitude reflectors as observed in the other canyons, and the fill packages have a divergent to sub-parallel internal geometry. Seismic "pull-up" below the canyon indicates a velocity anomaly in the overlying sediments. However, in the Northumberland Canyon, the younger incision events show no lateral migration and are positioned vertically on top of one another (Fig. 3.12).

In a down-dip direction along the axis of the canyons, seismic reflectors have medium to strong amplitude and parallel to hummocky prograding character which downlap onto underlying unconformities.

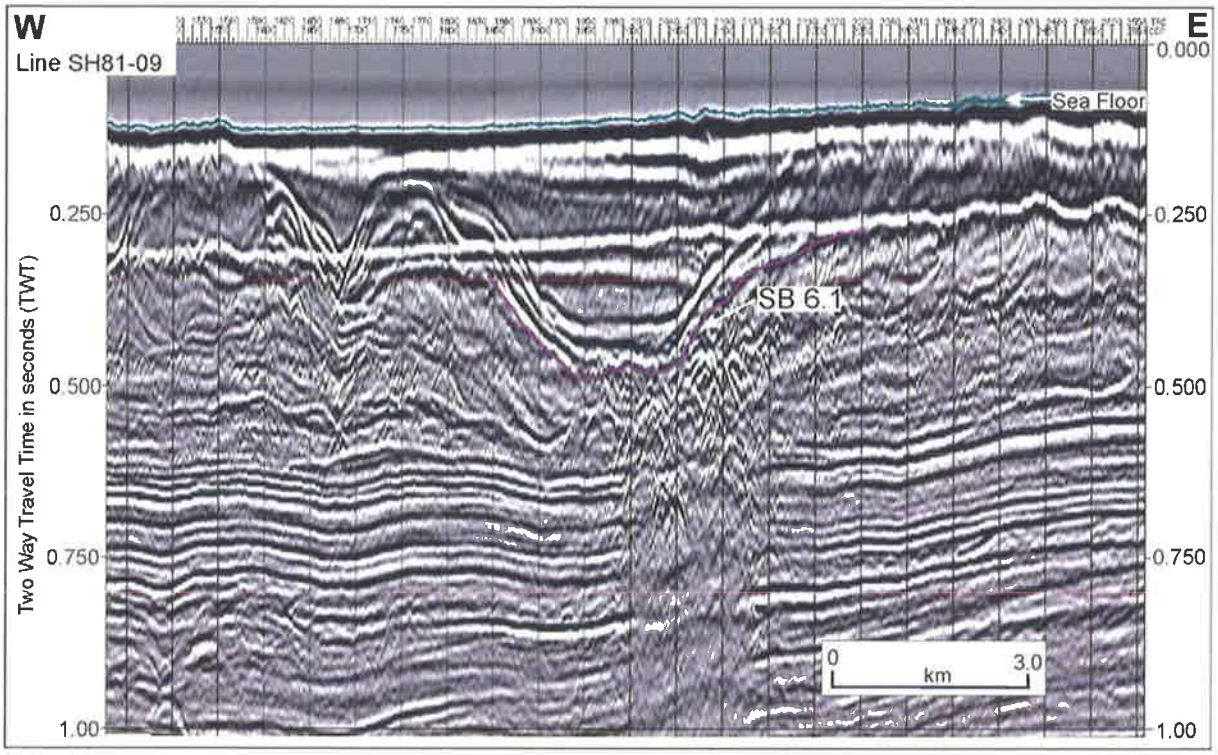

Figure 3.11 Seismic expression of the Northumberland Canyon at a proximal location near the head of the canyon (uninterpreted Line SH81-09). The initial canyon incision (SB 6.1) has a U-shaped geometry and is represented by high amplitude reflectors, however the canyon fill is obscured by sea floor multiple reflections.

3.5.4 Discussion

The seismic data indicate a complex series of canyon cutting events in the Gambier Sub-basin since the end of the Early Oligocene. Figure 3.14 is a cross-section through the Sub-basin from NW to SE showing the age of SB 6.1. Sediment dating was mainly based on planktonic foraminifera in cuttings samples from several industrial wells. Below SB 6.1, planktonic foraminifera are characterised by *Subbotina angiporoides, Globorotaloides suteri* and *Chiloguembelina cubensis*, indicating an age older than 30-31 Ma. Samples from above SB 6.1 contain *Globorotalia euapertura, Globigerina ciperoensis, G. angulisuturalis, Paragloborotalia nana*, and (benthic) *Victoriella conoidea*. The absence of Zone P21 marker species such as *Paragloborotalia opima* suggests an assemblage likely within upper Oligocene Zone P22, between about 24-27 Ma. In areas affected by canyons, missing sections are common. The lower Oligocene was either missing (in Troas 1) or partially eroded (in Morum 1

and Copa 1). Lower and middle Miocene sediments contain a slightly higher proportion of planktonic foraminifera (20-40%), indicating deepening water depths, with such species as *Globoturborotalita woodi, G. connecta, Globoquadrina dehiscens, Globigerinoides trilobus*, and (in the middle Miocene) *Orbulina universa*.

The Early Oligocene saw a change from a temperate neritic environment where the Gambier Sub-basin was influenced by a warm, saline proto-Leeuwin Current, to emergence of the cold and very fertile Antarctic Circumpolar Current (Li et al. 2000). This shift stimulated prolific carbonate production on the southern Australian margin and a large prograding carbonate wedge accumulated on the continental shelf. This bryozoa-dominated facies was calcitic, lacking the abundant skeletons of aragonite from which tropical limestones draw their cement for rapid diagenesis. Accordingly, the prograding wedge is interpreted to have remained significantly unlithified (below hardgrounds at unconformities representing brief hiatuses) and therefore susceptible to mass wasting if or when perturbed.

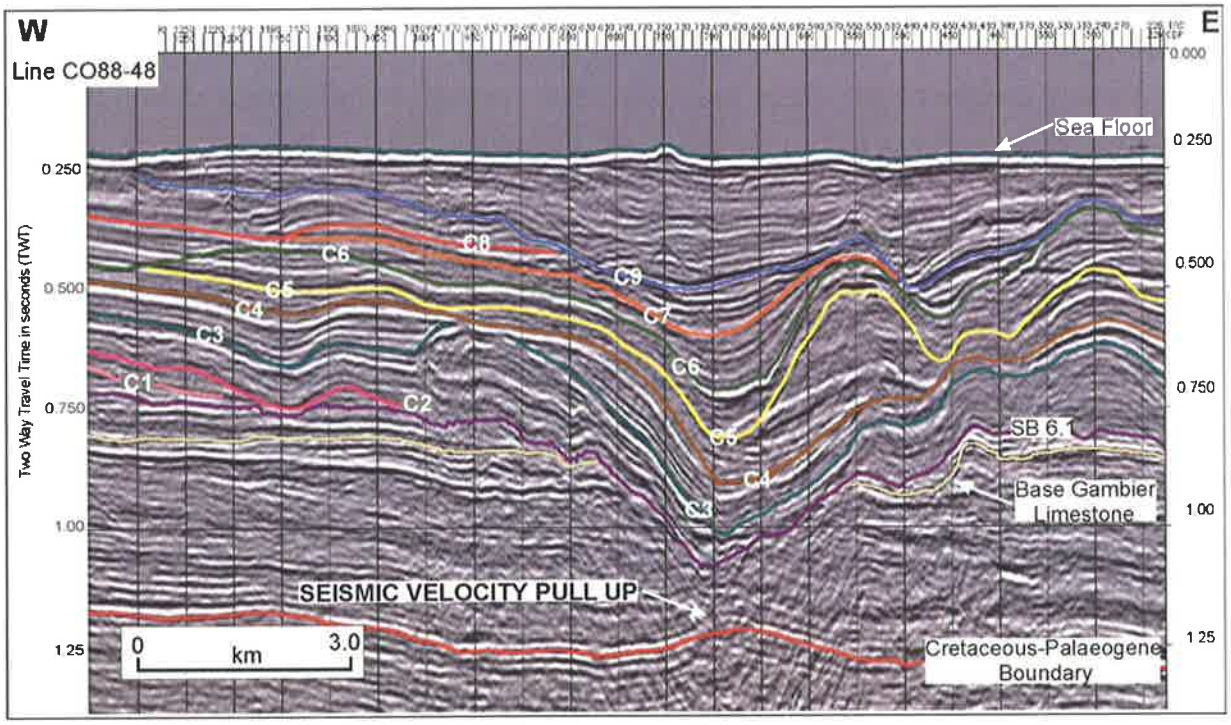

Figure 3.12 Seismic expression of the Northumberland Canyon at a more distal location near the toe of the canyon (Line CO88-48). Nine successive events were identified, three of which were correlated to events in the Lakes Canyon Complex. The initial event, SB 6.1 created a canyon with a V-shaped base and successive cut and fill events vertically aggrade. The incision events are represented by high amplitude reflectors that bound low amplitude canyon fill packages.

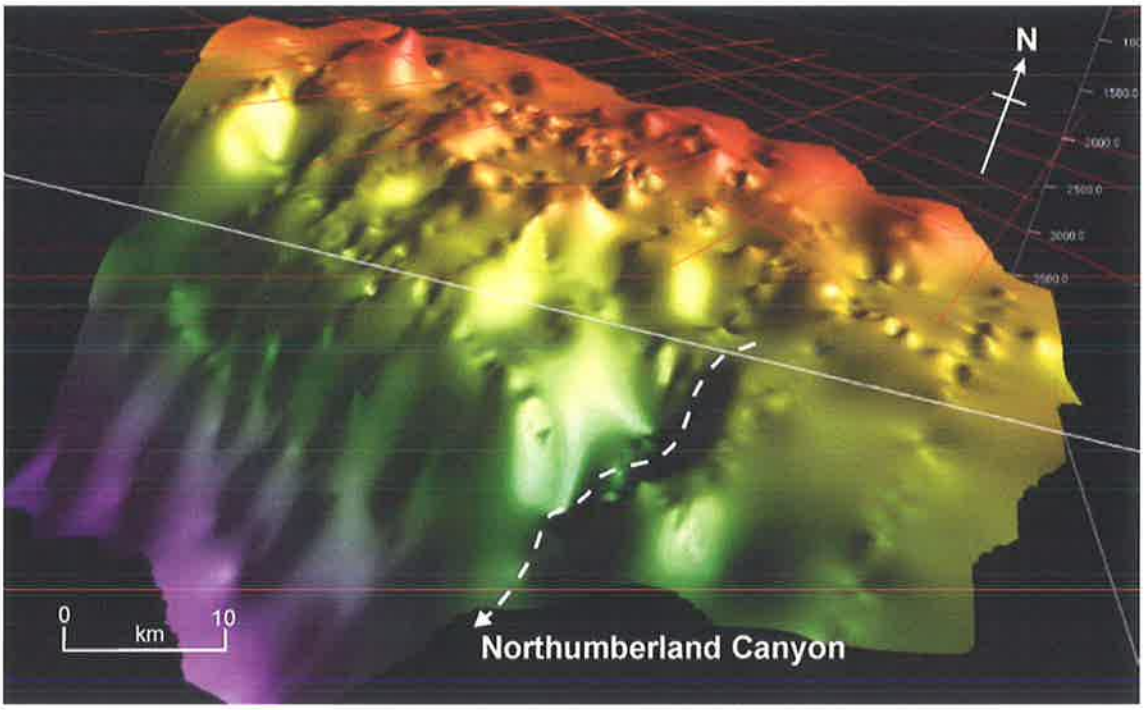

Figure 3.13 3D visualisation of the initial canyon incision surface (SB 6.1) showing the Northumberland Canyon. The axis of the canyon is straight and strikes northeast-southwest (Vertical Exaggeration=10.35). (Note: the rough linear features on the surface striking N-S and E-W are artefacts of griding and do not represent real data.)

During the middle Oligocene there was a glacio-eustatic sea level fall world-wide, probably coupled with a tectonic uplift in the region. The latter assertion was judged on a widespread mid-Oligocene unconformity and the absence of the lower Gambier Limestone (=Greenways Member) from many localities along the Tartwaup Hinge Zone, north of Mt Gambier (Li et al. 2000). This resulted in exposure of much of the shelf in the sub-basin, significant erosion and formation of SB 6.1.

During this sea level low it is suggested that the shoreline migrated basinward and fluvial incision occurred across the shelf. This is thought to have formed "nick points" at the shelf edge and possibly resulted in heightened deposition on the uppermost slope. These factors then combined to form favourable locations for initiation of submarine canyons by mass wasting and headward erosion during the ensuing transgression and highstand.

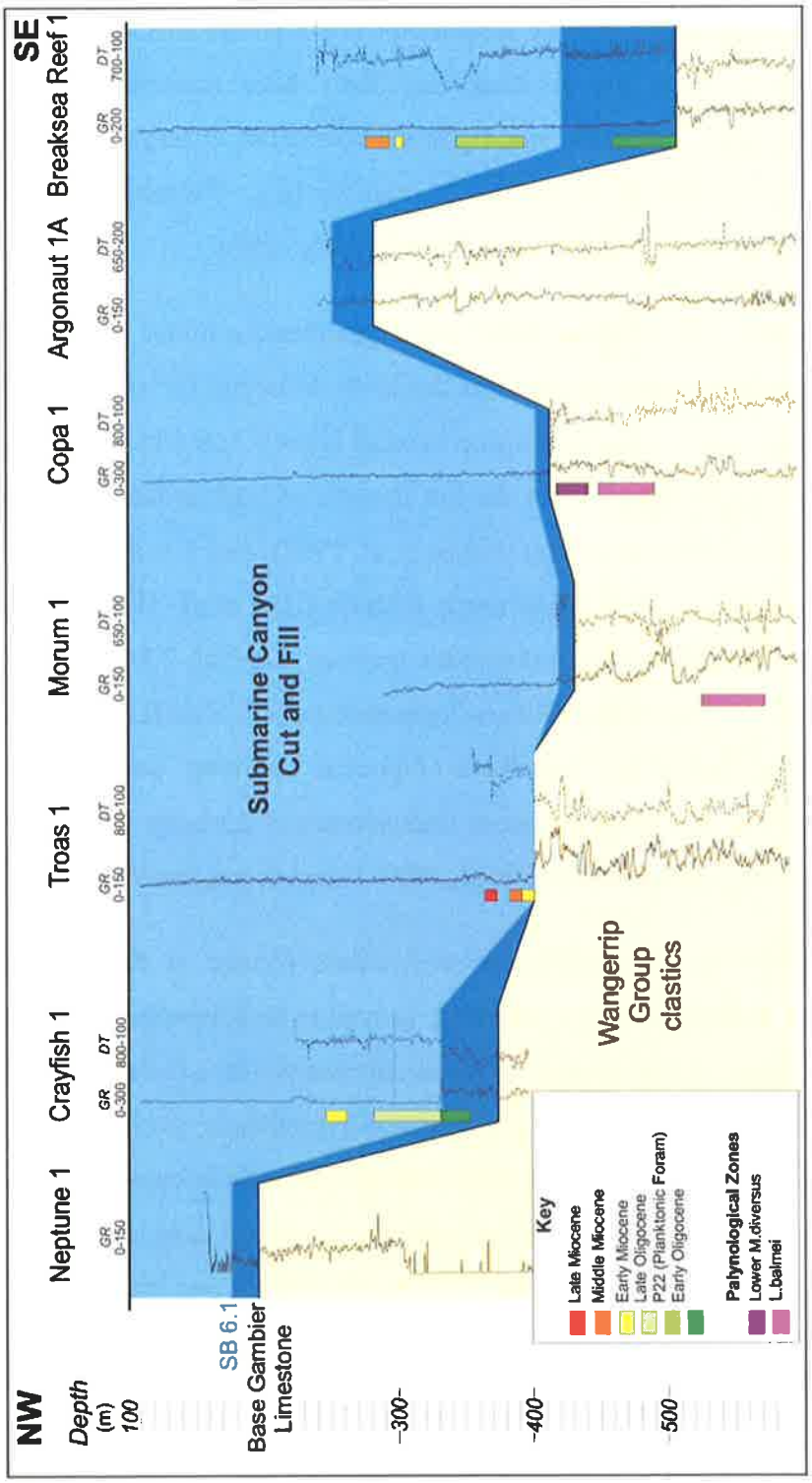

Figure 3.14 Cross-section in a strike direction through wells on the continental shelf from the Chama Terrace in the northwest to the Voluta Trough in the southeast. Illustrated are the gamma and sonic logs through the carbonate section and the available biostratigraphic data. Interpreted is the unconformity between the clastics and carbonates (base of the Gambier Limestone) and surface SB 6.1. Near the base of the Chama Terrace SB 6.1 erodes into the underlying clastic succession, thereby forming the base of the Gambier Limestone.

Evidence for fluvial processes and the formation of nick points was not visible on seismic data in this study and much of the evidence has likely been removed by subsequent canyon formation, however such processes leading to the formation of large submarine canyons have previously been suggested by a number of authors (e.g. Baclawski 1976; Shepard 1981; Cavazza and DeCelles 1993; Pratson et al. 1994; Talling 1998).

In the later Oligocene, the Gambier Sub-basin experienced a major marine transgression with high sea levels persisting episodically into the Early Miocene (Li et al. 2000). The early/late Oligocene boundary was a critical transition in earth history. It marks the low point between the Palaeogene and Neogene megacycles on the criteria of both putative global sea levels and temperature (oceanic oxygen isotopes) (Abreu et al. 1998); and it is also the time of the middle Oligocene canyon cutting event in the north Atlantic (Haq et al. 1993). In the Gambier Sub-basin it is the time of clustered unconformities onshore (Li et al. 2000); and in the eastern part of the Otway Basin the base of the Clifton Formation records a shift in biofacies that correlates to a major sea level fall at the Early/Late Oligocene boundary coincident with a major ice advance in Antarctica and mid-Oligocene unconformities globally (Kennett, 1977; Prothero, 1994; Poag and Ward, 1987; Gallagher et al. 1999, Norvick and Smith, 2001).

After the late Oligocene inundation, the nick-points formed at the shelf break by fluvial channels that were active during the lowstand, proved to be submarine conduits for down slope movement of turbidity currents, which provided an erosive force for enlarging the canyons. The turbidity currents were sourced from the shelf and periodically overfilled the canyon, spilling over the banks forming levee deposits. The model of submarine canyon formation by turbidity currents has been cited as the cause of canyons on the New Jersey passive continental margin by authors such as Farre et al. (1983) and Pratson et al. (1994) and Pratson and Coakley (1996).

Once the canyon had formed, some seafloor lithification took place. High-amplitude reflectors represent (multiple) canyon cuts contrasted with the low-amplitude reflectors of the fine-grained sediments of the canyon fill. Following diagenesis of carbonates at the canyon floor and formation of a hardground, turbidity currents became active once again depositing sediment in the canyon. This is demonstrated in Fig. 3.15 using the events in the Robe Canyon as an example. High amplitude incision events do not appear to cut into underlying fill, but instead are concordant with the sediments below. The geometry of the cut and fill events indicates a continuous process of erosion/non-deposition and fill rather than an episodic history of

sedimentation that completely fills the canyon and then an erosive period incising into that canyon fill. It also suggests there was not a great change in mechanism during sedimentation and erosion.

In the Robe and Lakes Canyons the successive cut and fill events migrated laterally. Near the head of the Robe Canyon successive sequences appear to laterally aggrade and migrate towards the east, but towards the toe of the canyon, the sequences laterally migrate towards the west. This suggests that the turbidity currents that acted as both the erosive force enlarging the canyon and the source of sediment had a sinuous thalweg, analogous to a meandering fluvial channel, depositing large-scale point bars and resulting in a canyon with a curved axis.

The mounded features observed on the banks of the initial Robe Canyon at a proximal location are interpreted as levee overbank deposits formed by overspill of turbidity currents in the early stages of canyon formation. The internal layering of these mounds indicates several episodes of breaching of the banks by sediment flows. This feature is also analogous to fluvial meandering channels. Similar cut and fill geometry in the Lakes Canyons indicates a comparable process.

Unlike the Robe and Lakes Canyons, The Northumberland Canyon has a straight axis and for this reason the successive cut and fill packages appear to vertically aggrade and show no lateral movement, suggesting the absence of a sinuous thalweg. The canyon fill packages lie almost symmetrically at the base of the canyons compared to the apparent lateral infilling observed in the Robe and Lakes Canyons.

Lithology in nearby wells shows that the interval affected by canyon incision is carbonate, and the seismic "pull-up" features affecting reflectors underlying the canyons suggest that the canyon fill is fine-grained. The smooth texture and convex-up curve of the clinoforms in the large prograding wedge on the shelf edge and upper slope in the Voluta Trough also suggests the sediment is fine-grained. This large fine-grained carbonate wedge is dominated by highstand systems tracts and may comprise re-sedimented carbonates, a product of highstand shedding on the shelf.

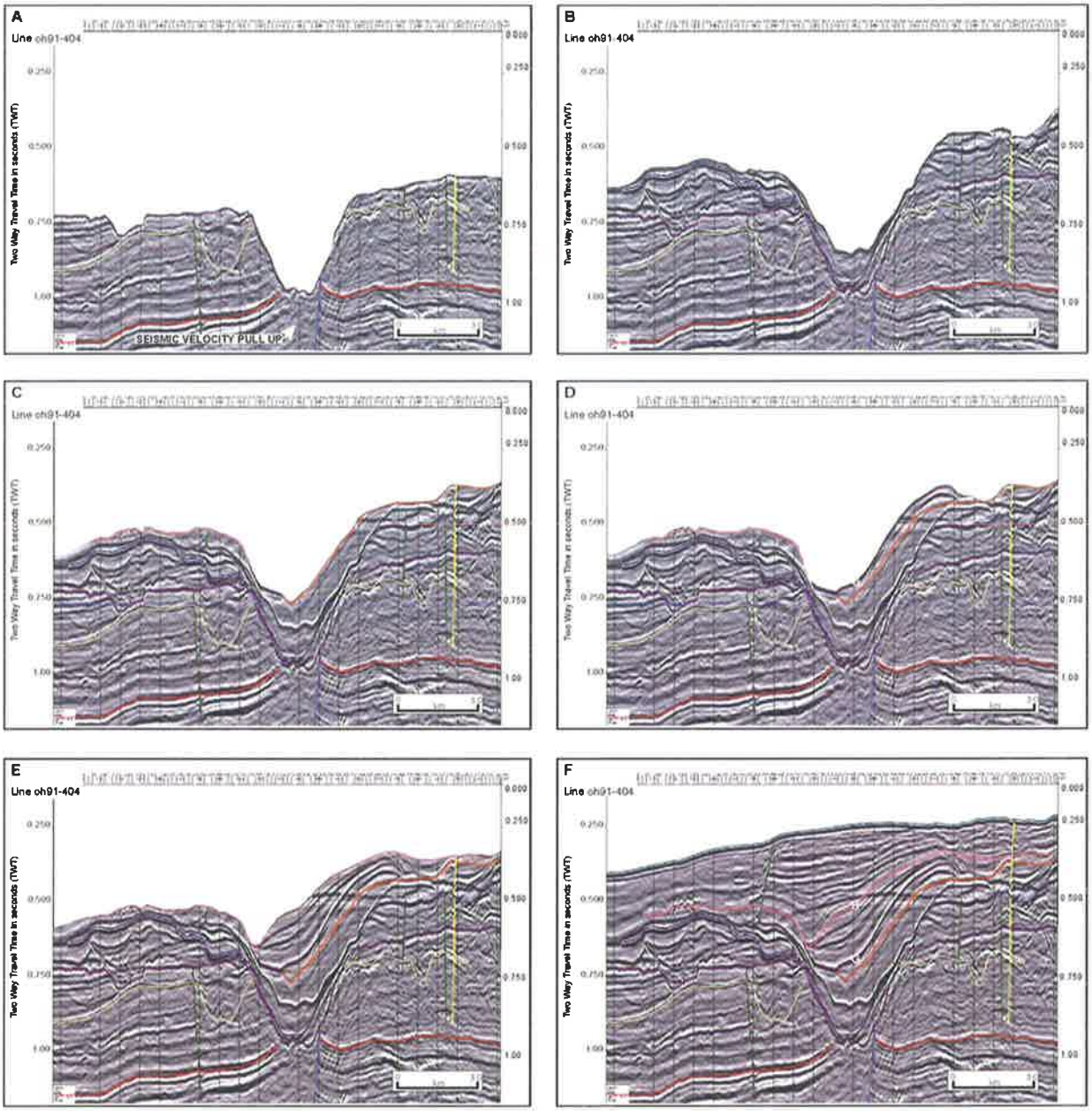

Figure 3.15 Stages of progressive filling and subsequent erosion of canyon events by turbidity currents in the Robe Canyon. (A) The initial canyon at time SB 6.1 incising into the underlying siliciclastic Wangerrip Group. (B-E) Successive canyon events occurring during the Late Oligocene-Middle Miocene resulting from the erosive and depositional nature of turbidity currents. The canyon incision surfaces were subjected to diagenetic alteration, forming hardgrounds and are represented by high amplitude reflectors. These incision surfaces bound unlithified canyon fill represented by low amplitude reflectors. (F) Present day Robe Canyon. Expression of the canyon at the sea floor has been removed by erosion during low sea level in the Plio-Pleistocene.

Similar palaeo-canyons have been identified on seismic data in the eastern Otway Basin by Leach and Wallace (2001). Although canyon incision is interpreted to have begun in the Early Miocene (slightly later than the canyons in the Gambier Sub-basin), their seismic expression is very similar to the canyons described in the Gambier Sub-basin, including the presence of velocity pull-ups and the interpretation that the canyon fill is carbonate-rich. However, the canyons in the eastern Otway Basin show consistent lateral migration and fill towards the west. Leach and Wallace (2001) attribute this to slope sediment influx into the canyons controlled by a shelf break parallel palaeocurrent.

3.6 BIOGENIC MOUNDS

The widespread development of broad low-relief, biogenic (bryozoan [?]-sponge), shelf and upper slope mounds in the Eucla Basin was reported by Feary and James (1995; 1998) and James et al. (2000). Similar structures are observed on the edge of shelf in the Voluta Trough in the Gambier Sub-basin (Fig. 3.16).

Feary and James (1995) suggest that these build-ups are biogenic mounds (*sensu* James and Bourque, 1992) constructed primarily by bryozoans and perhaps with supplementary sponge constituents. This interpretation was based on the absence of large reef building corals existing in cool-water carbonates on the southern margin; bottom profiles from the cool-water modern shelf show mound-like structures on the upper slope; and bottom samples and photographs indicate that the sea floor between 200-400 m water depth is rich in robust bryozoans. These biogenic mounds are also very similar to mounds that are known to typify carbonate ramps throughout the Phanerozoic.

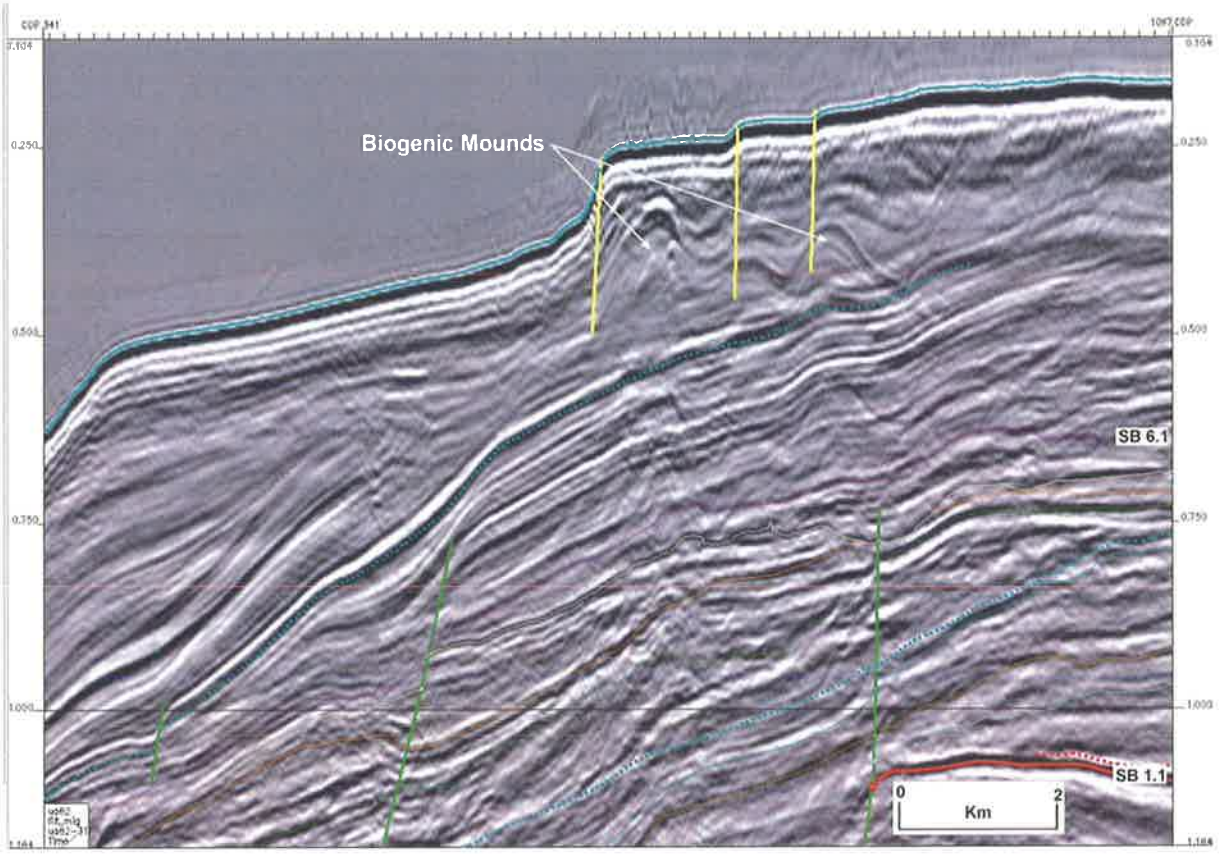

Figure 3.16 Seismic expression of carbonate biogenic mounds on the shelf edge in the Voluta Trough (Line UA82-31).

3.7 MODERN SUBMARINE CANYONS ON THE SOUTHERN MARGIN

Submarine canyon formation has continued into the Holocene with up to 25 large, well-developed modern submarine canyons mapped on seismic, magnetic and bathymetry data along the southern Australian continental slope from Perth in Western Australia to the western coast of Tasmania (Leach and Wallace, 2001; von der Borch, 1968). These modern canyons incise the shelf for up to 65 km from the shelf break and have widths and depths of up to 40 km and 2200 m, respectively.

Pliocene to Recent canyons were identified on seismic and magnetic data in the eastern Otway Basin by Leach and Wallace (2001). The canyons are widespread on the upper slope and have been partly attributed to a major uplift event near the Otway Ranges at the Miocene-Pliocene boundary (Dickinson et al. 2001). The Pliocene canyon fill is clastic and shows aggradational to slightly eastward lateral migration, which is attributed to a weak easterly palaeo-current (Leach

and Wallace, 2001). The modern canyons in the eastern Otway Basin were seen to occupy the same position on the shelf as the Pliocene canyons suggesting the canyons advance seaward as the shelf progrades (Leach and Wallace, 2001).

High-resolution bathymetry data has imaged seven submarine canyons incising the modern seafloor on the continental slope in the Gambier Sub-basin (Fig. 3.4). The heads of these canyons lie just below the shelf break at approximately -600 m and the curved axes of the canyons can be traced for more than 50 km down slope. These canyons do not lie offshore from any major fluvial source, however two modern canyons lie directly down-dip from the Oligo-Miocene Robe and Northumberland Canyons, suggesting they are the modern equivalents of the palaeo-canyons that are now located seaward as the continental shelf has prograded since the Miocene.

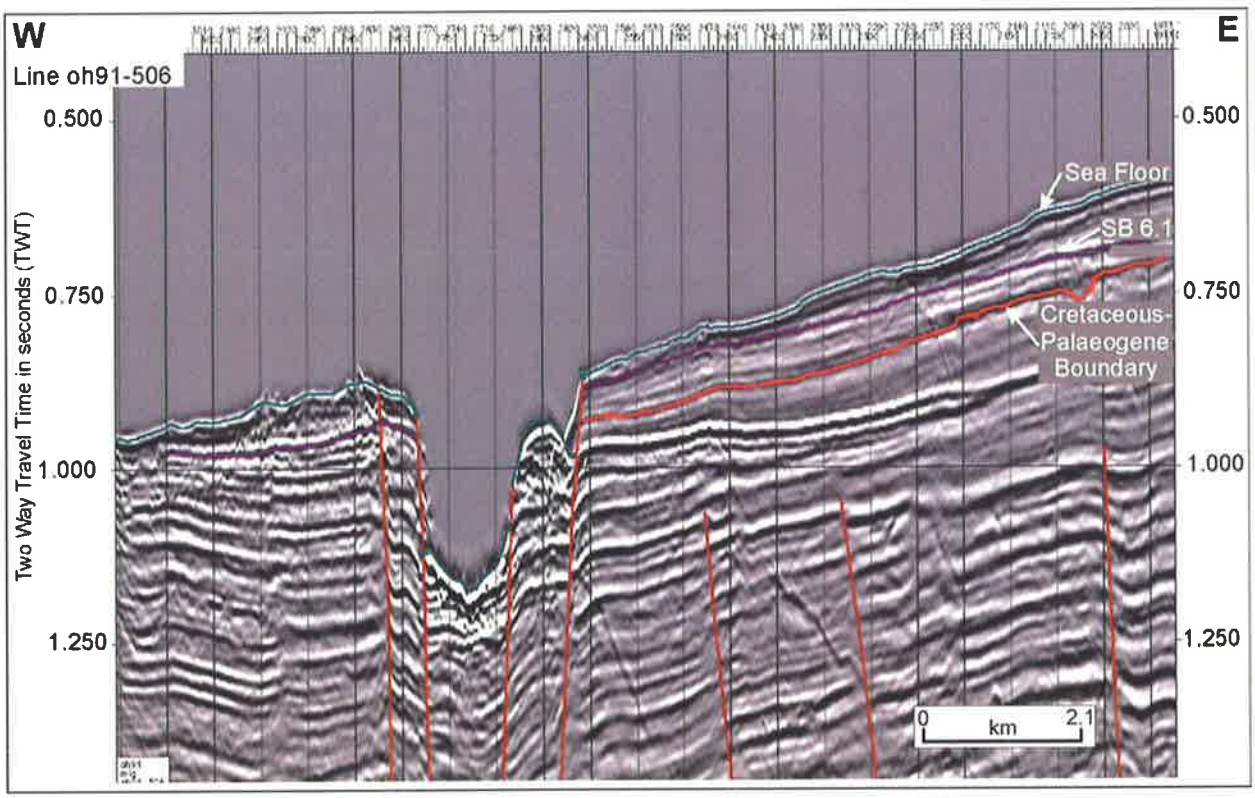

Figure 3.17 Seismic expression of the modern canyon located on the shelf edge on the Chama Terrace in the Gambier Sub-basin (Line oh91-506). This canyon differs from the palaeo-canyons in that the walls of the canyons are fault controlled and hence the axis of the canyon strikes northwest-southeast, parallel to the regional fault strike.

The head of a modern canyon on the edge of the continental shelf in the western part of the sub-basin has been identified on seismic data. This canyon differs from the observed palaeo-canyons as it is fault controlled and consequently lies almost parallel to the shelf edge and the fault strike direction. This canyon is 2.4 km wide and approximately 350 m (0.310 sec TWT) deep (Fig. 3.17). A seismic "push down" effect, caused by the rapid change in velocity at the water-sediment interface may be enhancing the steepness of the canyon wall and its apparent depth. However the faults can be interpreted at depth below this canyon, and this combined with the orientation of the canyon, supports the interpretation of fault-controlled canyon walls.

Sufficient data is not available to deduce the cause of initiation of this modern canyon. It is likely that during retrogressive headward erosion of this canyon a normal fault array was intersected and subsequence erosion was preferentially along these faults, resulting in the canyon head striking parallel to the shelf break and the regional structural grain.

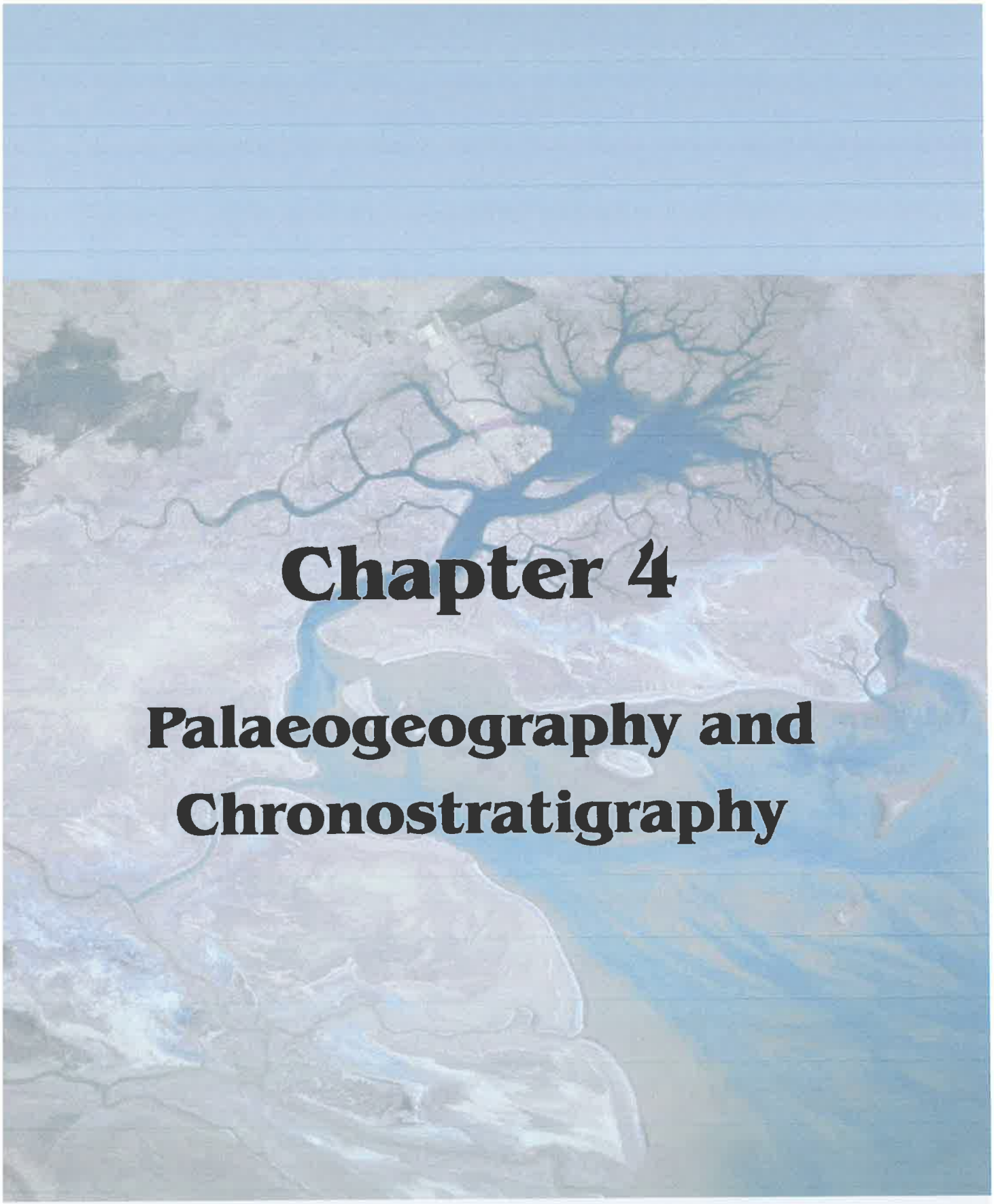

Chapter 4

Palaeogeography and Chronostratigraphy

4 PALAEOGEOGRAPHY AND CHRONOSTRATIGRAPHY

A deltaic depositional environment for the Late Paleocene-Early Eocene clastic Wangerrip Group was proposed by Holdgate (1981) based on wireline log and lithological character – a model that has been supported by seismic interpretation in this study. Cenozoic sedimentation began in the Gambier Sub-basin in the Late Paleocene with a major second order marine transgression that established marginal marine to fully marine conditions (McGowran, 1978; 1979; Quilty 1980; 1994). A series of rapid marine transgressions resulting from third order tectono- and glacio-eustatic sea level fluctuations during the Late Paleocene and Early Eocene (McGowran, 1986; 1989; 1991; McGowran and Beecroft, 1985; 1986) influenced deposition of the deltaic cycles by creating accommodation space into which the clastic sediments prograded.

Extension and seafloor spreading continued to propagate eastwards from the Great Australian Bight towards the Otway Basin during the Late Cretaceous and early Palaeogene (Norvick and Smith, 2001). From the Late Cretaceous the Voluta Trough subsided at more than 10 times the rate of the Chama Terrace (Williamson et al. 1996). This created a depocentre for the Paleocene to Eocene deltaic sediments in the western part of the Voluta Trough. Steady subsidence of the Voluta Trough during the Palaeogene and the large volume of sediment influx into the depocentre suggest that the main control on deposition of the Wangerrip Group sediments were the third order tectono-and glacio-eustatic transgressive events identified by McGowran (1991), which resulted in fluctuations in local accommodation space.

At the Paleocene/Eocene boundary seafloor spreading in the Tasman Sea finished but slow spreading continued in the Southern Ocean (Norvick and Smith, 2001). A nine million year gap in the stratigraphic record during the early part of the Middle Eocene is evident across the southern margin (McGowran et al. 1997). In the later part of the Middle Eocene at approximately 44 M.a. the rate of seafloor spreading in the Southern Ocean dramatically increased which led to rapid thermal subsidence and marine transgression on the southern Australian margin (Norvick and Smith, 2001). Also at this time, India and Australia became part of a single plate as India/Antarctica spreading joined with Australia/Antarctica spreading to form the present southeast Indian Ridge (McGowran, 1989). The mid Eocene has been cited as time for major global tectonic reorganisation.

Four global third order marine transgressions were identified in the late Middle Eocene to Oligocene stratigraphic record on the southern margin (McGowran, 1986; 1989). The first of

these, the Wilson Bluff Transgression, is the response to the global plate tectonic reorganisation that occurred in the Middle Eocene. In the eastern Otway Basin the Mepunga Formation and Narrawaturk Marl of the Nirranda Group were deposited during the Late Eocene. However, in the Gambier Sub-basin this period is represented by condensed sections. The marine stratigraphic record in the Gambier Sub-basin begins again in the Early Oligocene with the Gambier Limestone.

Deposition of neritic, cool-water carbonates on the southern Australian margin from the latest Eocene onwards was a response to the establishment of the Circum-Antarctic Current that formed when the Australian and Antarctic plates finally broke apart and the Indian and Pacific Oceans were connected (McGowran et al. 1997; Norvick and Smith, 2001).

A major glacio-eustatic sea level fall at the end of the Early Oligocene led to initiation of submarine canyons on the outer shelf and upper slope in the Gambier Sub-basin that further developed during the following transgression and highstand (Chapter 3). Another major sea level fall in the Plio-Pleistocene resulted in significant erosion of shelf sediments and removal of any expression of the submarine canyons from the shelf.

The modern sea floor in the Gambier Sub-basin is a cool-water, prograding carbonate shelf dominated by bryozoa (Boreen and James, 1995; James et al. 1993). Numerous submarine canyons, several of which are the modern equivalents of the Oligo-Miocene palaeo-canyons, incise the upper slope and probably actively transport carbonate sediment from the outer shelf to the abyssal plain (von der Borch, 1968; von der Borch et al. 1970; Leach and Wallace, 2001).

The aim of this chapter is to map (1) the evolution of the delta system that was active during the Late Paleocene and Early Eocene; and (2) the development of cool-water carbonates during the Oligocene to Middle Miocene, using interpretations from seismic and well data. The spatial distribution of sequences will then be plotted in time to analyse the chronostratigraphic evolution of the Cenozoic succession. These chronostratigraphic diagrams will illustrate periods of sedimentation in the sub-basin and identify times of significant erosion and non-deposition. An attempt will be made to compare these local events with regional and global tectonic and/or eustatic events, which will put the stratigraphic evolution of the Gambier Sub-basin into a wider context.

4.1 DELTAIC ENVIRONMENTS

A delta is a discrete shoreline protuberance formed at a point where a river enters an ocean and supplies sediment more rapidly than it can be redistributed by basinal processes (Elliot, 1979). Coleman and Wright (1975) developed a six-fold classification of deltas based on sand distribution patterns, however the most widely used classification scheme today is that of Galloway (1975) who subdivided deltas according to the dominant processes controlling their morphology; rivers, waves and tides.

Many deltas cover a large area, and have been influenced by a variety of fluvial and marine processes. These distinct sub-environments of deposition can be identified within a delta (Elliot, 1979, 1986): delta plain (where river processes dominate); delta front (where river and basinal processes are both important); and prodelta (where basinal processes dominate). Delta plains usually contain relatively straight, bifurcating distributary channels and a wide variety of non-marine to brackish environments including swamps, marshes, tidal flats, and interdistributary bays (Elliot, 1986).

The delta front is the site of much of the active deposition in deltaic environments, particularly at the mouths of distributaries where the coarsest sediment is deposited in distinct bars. In siltier or sandier systems deposited in shallower water, distributaries switch more rapidly and coalesce to form more lobate deltas (Elliot, 1986). The prodelta is the area where fine material settles quietly out of suspension. It is commonly extensively bioturbated, and merges seaward with fine-grained sediment of the basin floor (Elliot, 1986).

Coleman and Wright (1975) recognised that the sand body geometry of a delta should uniquely reflect the relative importance of fluvial and marine processes. With increasing wave influence, the sand fraction tends to be reworked alongshore and the finer fraction swept out to sea. Sand bodies trend parallel to the shoreline, and within the delta proper, fines only accumulate in lagoons behind the shore-parallel beaches and beach ridges.

In an attempt to determine the degree of wave influence on the Paleocene to Early Eocene delta in the Gambier Sub-basin the percentage of sand was analysed for some sequences. It was expected that if there was a low wave influence on the delta, sand percent would show shoreline-perpendicular trends as the fluvial source distributed the sand further out into the basin without much redistribution of sediment by waves. If there was a large influence from

waves then, as discussed previously, the sand would tend to be redistributed into shoreline-parallel bodies. However, due to the limited number of data points (i.e. wells) available to analyse the percentage of sand for many of the sequences, the resulting maps lack detail and provide ambiguous results.

4.2 PALAEOGEOGRAPHY

4.2.1 Supersequence 1

4.2.1.1 LST/TST 1.1

Supersequence 1 represents a major marine transgression that affected the southern Australian margin in the Late Paleocene. Sequence set LST/TST 1.1 is thin and widespread in the Gambier Sub-basin (Fig. 4.1) and was deposited during active faulting as seen on seismic data. This sequence set is interpreted to have been deposited in a shallow marine to embryonic deltaic environment in response to a regional third order transgressive event (McGowran, 1991) (Fig. 4.2).

Palynology suggests that sediments comprising LST 1.1 were marine (Appendix 1), however, there may have been an embryonic delta plain forming to the north of the Tartwaup Hinge Zone, resulting in fluvial environments in the far northeast of the study area. Elliot (1986) suggests that in immature drainage systems a number of closely spaced rivers can develop which induce uniform progradation of the entire coastal plain rather than point-centred progradation into depocentres. This is what is interpreted to have occurred during Supersequence 1 as no individual delta lobe indicating a single large depocentre was observed on seismic data. The percentage of sand in LST/TST 1.1 (Fig. 4.3) suggests a high sand content in the region of Caroline 1 and McNamara 1. The blocky nature of the gamma logs at these wells, coupled with the high sand content suggests these wells may have penetrated distributary channels. The very fine-grained sediments penetrated by Hungerford 1, Kalangadoo 1 and Rendelsham 1 in the northern part of the study area may represent the coastal plain. On the shelf the sequence set is dominantly silty represented by interbedded sands and silts of the embryonic delta system.

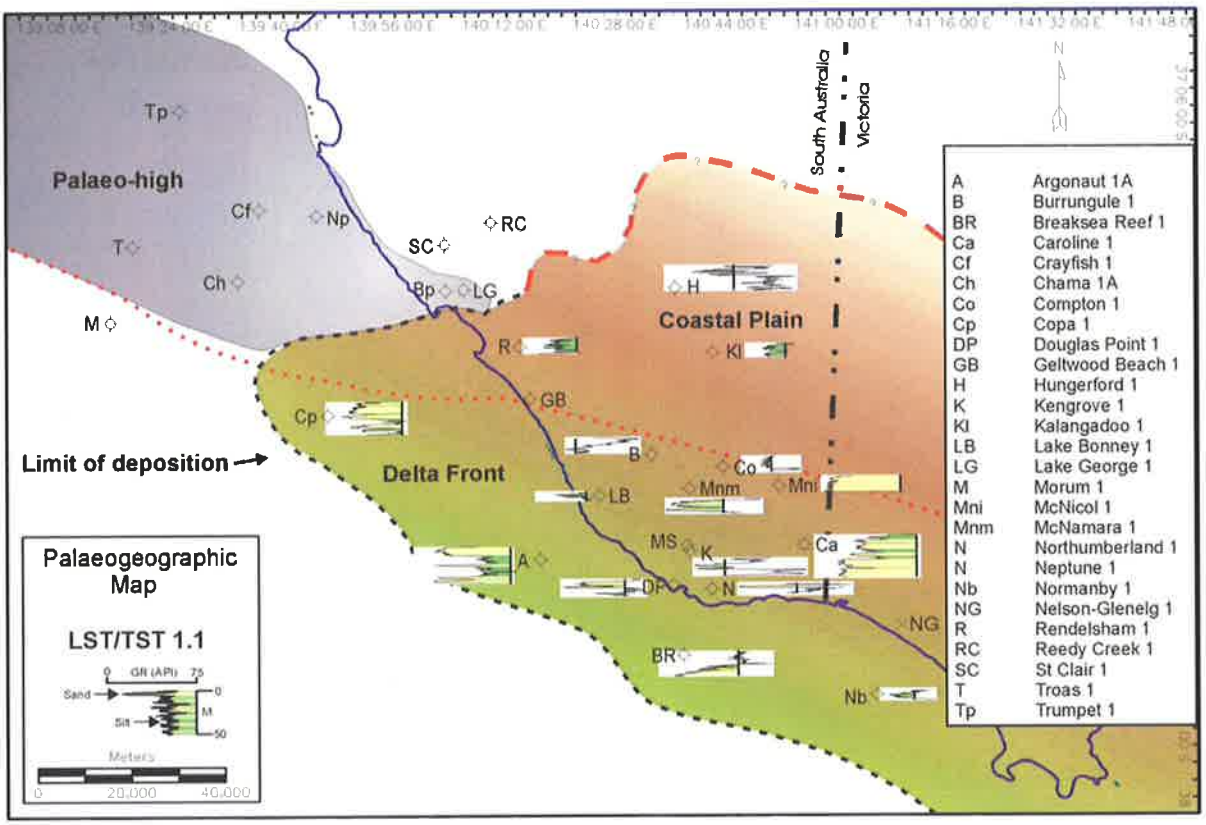

Figure 4.1 Palaeogeographic map of LST/TST 1.1 showing gamma ray log response and distribution of sediments.

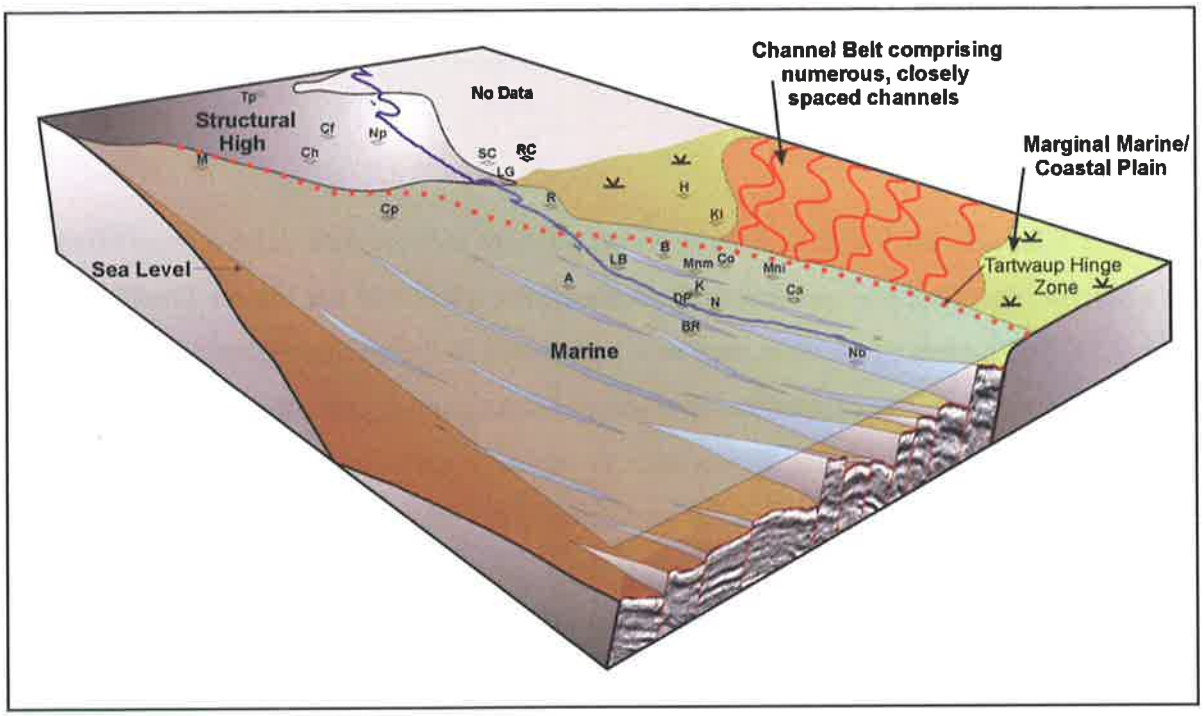

Figure 4.2 Concept block diagram illustrating the depositional environments existing in the Gambier Sub-basin during deposition of LST/TST 1.1.

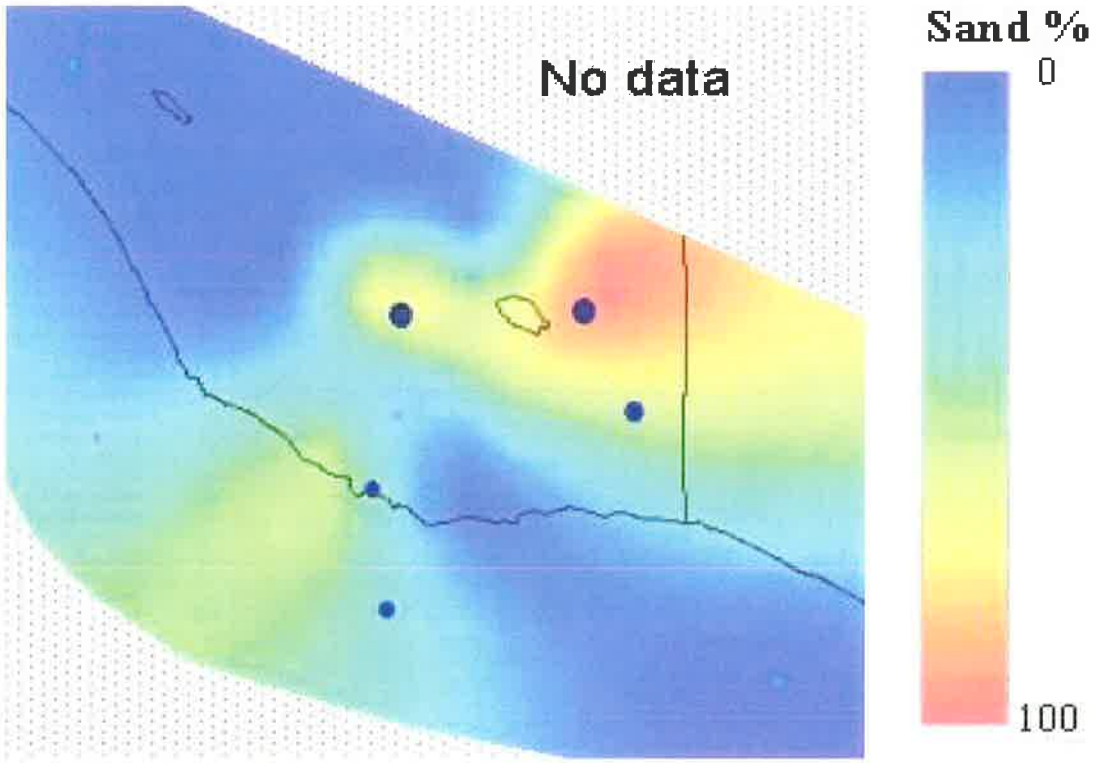

Figure 4.3 Map of the Gambier Sub-basin showing percentage of sand within LST 1.1. The blue dots represent sample points (i.e. wells) and the relative size of the dot indicates the percentage of sand, which correlates the shading of the grid represented by the colour bar.

4.2.1.2 HST 1.1

HST 1.1 is relatively thick and is interpreted on offshore seismic data to be a prograding delta lobe where sediment supply approximately matched subsidence in the Voluta Trough (Chapter 2, Fig. 2.5). The highstand systems tract was interpreted in the onshore Gambier Sub-basin by correlation of wireline logs (Appendix 4) where the delta plain is present north of the Tartwaup Hinge Zone. Wireline log motifs display typical lagoonal, crevasse splay, distributary channel and prograding delta front characteristics as discussed in Elliot (1979) and Van Wagoner et al. (1990) and represented in Table 4.1 (Fig. 4.4 & 4.5).

HST 1.1 in Hungerford 1, Reedy Creek 1 and St Clair 1 is relatively thin and very fine-grained as indicated by high values in the gamma log. These log signatures have been interpreted as representing coastal plain sediments deposited in overbank flooding events. The gamma log in Kalangadoo 1 shows coarsening upward signatures interpreted as thin crevasse splays, which

have breeched the main channel. HST 1.1 in Rendelsham 1 and Lake George 1 is thicker and dominantly fine-grained as indicated by the high gamma ray values. These two wells are interpreted to have intersected a coastal plain (back barrier) lagoon. A few kilometres basinward of these wells, Burrungule 1 shows a thick prograding, coarsening upward profile and is interpreted to have intersected the prograding sandy shoreface or barrier bar that separated the coastal plain from the open ocean. Other wells are interpreted to have penetrated the marine part of the delta plain where fluvial influence has given way to basinal processes. The seaward position of the sandy delta lobe intersected by Breaksea Reef 1 could alternatively interpreted as part of a falling-stage systems tract at the top of HST 1.1, however seismic data shows a prograding package that is onlapped by the following lowstand systems tract, hence its interpretation as part of the (probably late) highstand. Other wells may have penetrated sandy distributary channels or channel mouth bars, or muddy interdistributary bays located within the delta complex.

Mapping the shape of the delta lobe by seismic interpretation indicates that the delta is lobate and therefore wave dominated (Elliot, 1979; 1986). It is likely that the wave approach was from the southwest as the opening rift between Australia and Antarctica was widening from west-east and oceanic currents (e.g. proto-Leeuwin Current) flowed in an easterly direction along Australia's southern margin (McGowran et al. 1997). Oblique wave contact on the delta would have resulted in re-distribution of delta front sediments (via longshore drift) along the coast towards the east as shoreface sands and barriers in the Port Campbell Embayment.

Analysis of sand distribution in HST 1.1 (Fig. 4.6) reveals high proportions of sand at Kalangadoo 1, which was interpreted as representing crevasse splays; Burrungule 1, which is interpreted as a shoreface/barrier bar; Lake Bonney on the distal delta plain may represent a distributary mouth bar; and Breaksea Reef 1 penetrated the prograding delta lobe as seen on seismic data.

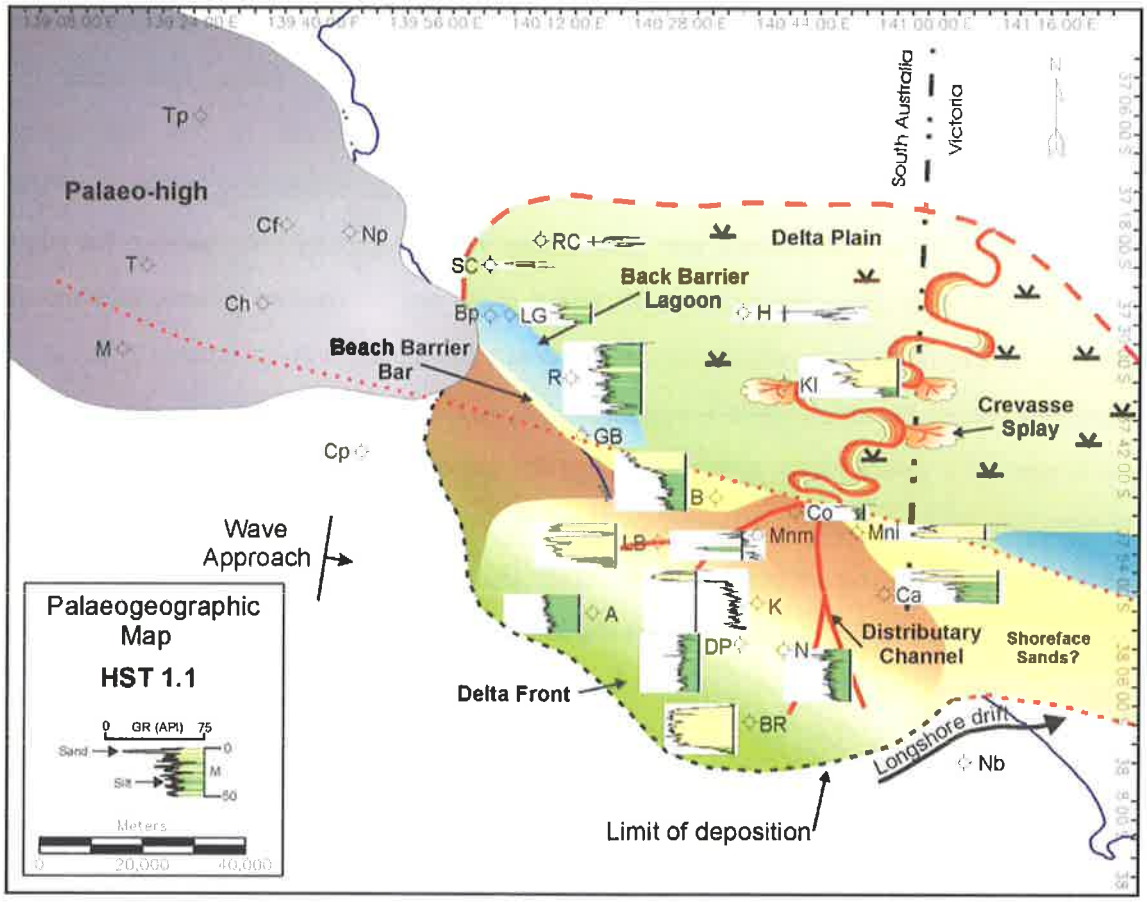

Figure 4.4 Palaeogeographic map of HST 1.1 showing gamma ray log response and distribution of sediments in the Late Paleocene and Earliest Eocene.

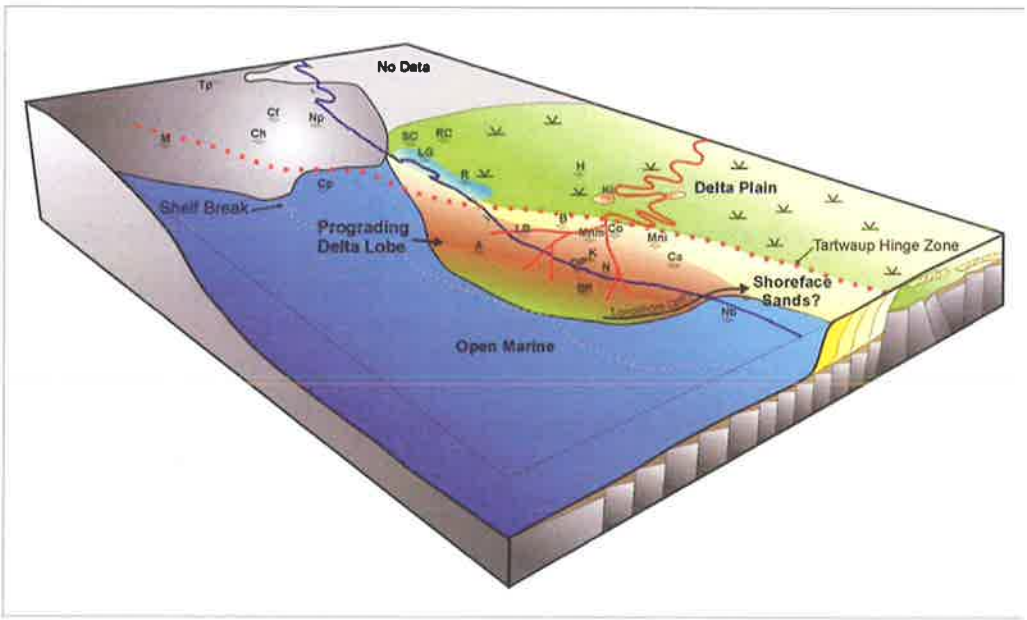

Figure 4.5 Concept block diagram illustrating the depositional environments existing in the Gambier Sub-basin during deposition of HST 1.1.

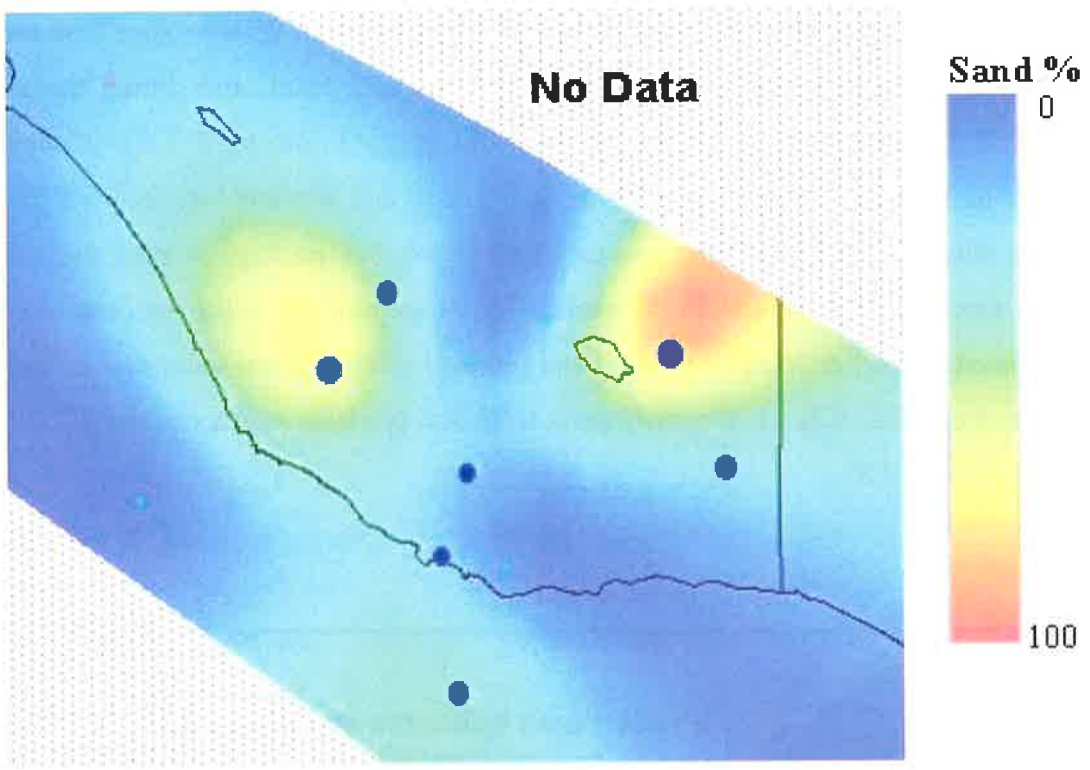

Figure 4.6 Analysis of the percentage of sand in HST 1.1 in the Gambier Sub-basin. The blue dots represent sample points (i.e. wells) and the relative size of the dot indicates the percentage of sand, which correlates the shading of the grid represented by the colour bar. High proportions of sand are located at Kalangadoo 1, which was interpreted as representing crevasse splays; Burrungule 1, which is interpreted as a shoreface/barrier bar; Lake Bonney on the distal delta plain may represent a distributary mouth bar; and Breaksea Reef 1 penetrated the prograding delta lobe as seen on seismic data.

4.2.2 Supersequence 2

4.2.2.1 Sequence 2.1

Deposition of HST 1.1 occurred as relative sea level reached stillstand and prior to the next relative fall in sea level. This fall in relative sea level is interpreted to have been quite quick as no forced regressive deposits were recognised on seismic data (Posamentier et al. 1992). When relative sea level reached its lowest point, deposition of LST 2.1 occurred basinward of Breaksea Reef 1 and Argonaut 1A, a result of fluvial incision across the shelf. This package is represented on seismic data (see Chapter 2, Fig. 2.5), but onlaps onto HST 1.1 and pinches out before being intersected by Breaksea Reef 1.

Relative sea level is interpreted to have risen quickly because no transgressive systems tract was recognised. When relative sea level reached its highest point, and during the ensuing stillstand, HST 2.1 prograded across the shelf and downlapped onto MFS 2.1 as a delta lobe. HST 2.1 can be seen on seismic data (Chapter 2, Fig. 2.5) and wireline logs indicate this delta lobe is very silty (Fig. 4.7). Seismic interpretation shows this package is truncated near the present day shoreline by the overlying Sequence 2.2 suggesting the following drop in relative sea level caused erosion on the palaeo-shelf and removal of delta plain sediments of Sequence 2.1 from the shelf (Fig. 4.7). Hence, only delta front and prodelta sediments of HST 2.1 have been preserved (Fig. 4.8).

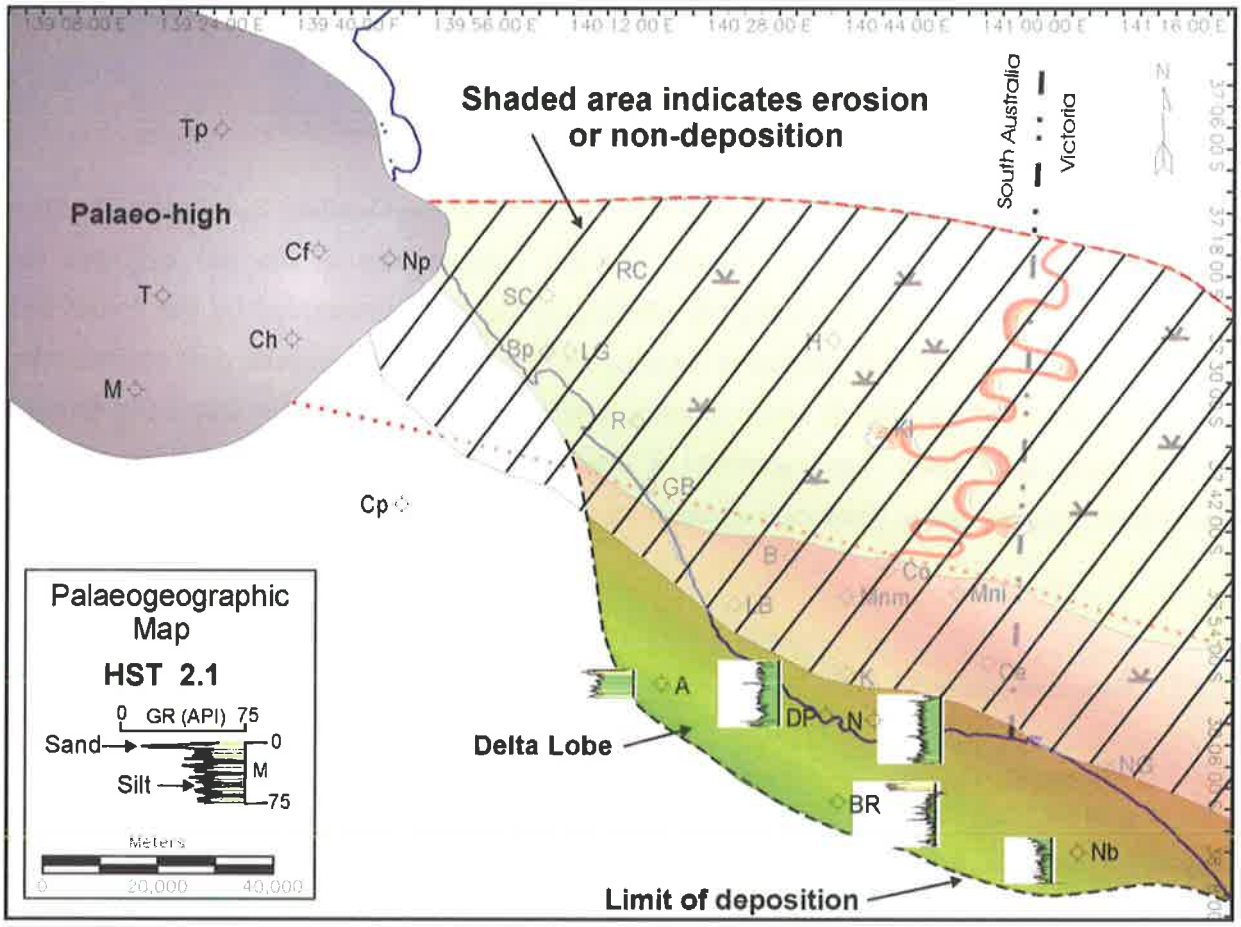

Figure 4.7 Palaeogeographic map of HST 2.1 showing gamma ray log response and distribution of sediments. The shaded area represents the region of the sub-basin where HST 2.1 sediments are either not preserved due to erosion, or were not deposited due to stratigraphic pinch out or onlap onto underlying sequences.

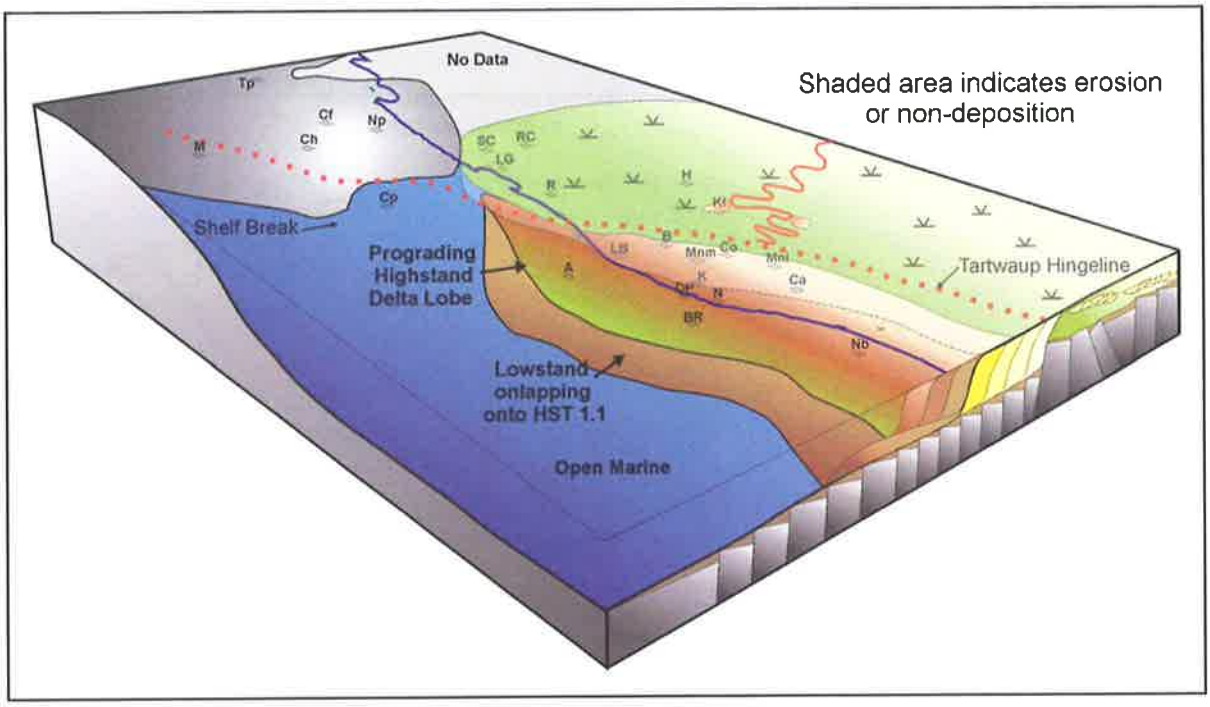

Figure 4.8 Concept diagram illustrating the depositional environments existing in the Gambier Sub-basin during deposition of HST 2.1.

4.2.2.2 Sequence 2.2

The following relative sea level fall again caused fluvial incision across the shelf, which resulted in deposition of LST 2.2 in the south-eastern part of the Voluta Trough in South Australia. This package is relatively thick and sandy in Breaksea Reef 1 and seismic data show LST 2.2 downlaps onto HST 1.1 and LST/TST 2.1 (Chapter 2, Fig. 2.5). The thinner edge of the systems tract is intersected by Normanby 1 further to the east as it pinches out laterally, and landward of Breaksea Reef 1 seismic data show the lowstand sediments onlapping onto HST 2.1 and pinching out (Fig. 4.9 and Chapter 2, Fig. 2.5). The limited distribution and dominantly sandy nature of LST 2.2 suggests it could be a small lowstand delta deposited on the outer shelf during low relative sea level.

The transgressive systems tract that would record the following relative sea level rise is not identified on seismic or well data suggesting relative sea level rise was rapid (Fig. 4.9). The maximum flooding surface that recorded this transgressive event was recognised as a seismic downlap surface (Chapter 2, Fig. 2.5).

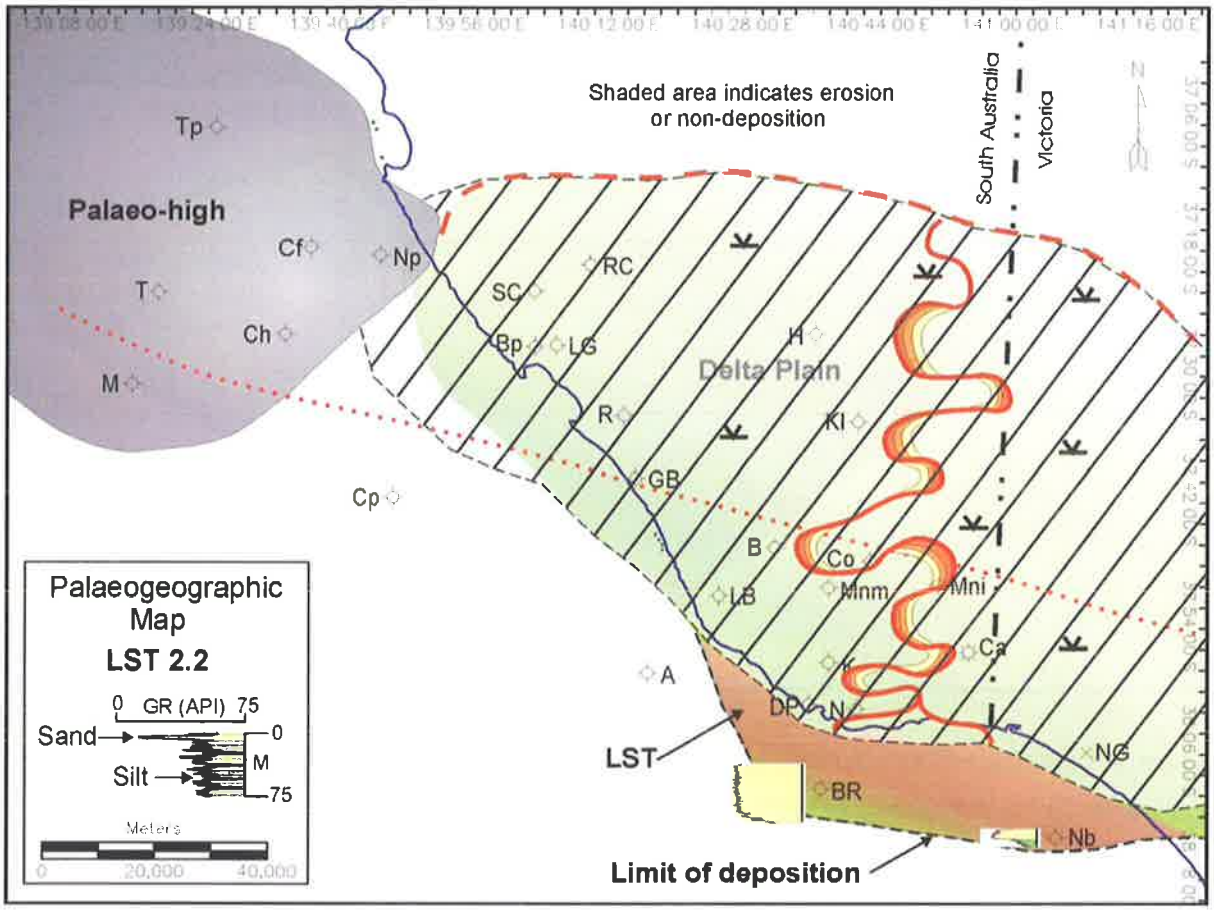

Figure 4.9 Palaeogeographic map of LST 2.2 showing gamma ray log response and distribution of sediments.

During the following highstand and ensuing sea level fall, sediments of HST 2.2 prograded across the shelf, downlapping onto MFS 2.2. The prograding geometry of the highstand delta lobe can be seen on seismic data (Chapter 2, Fig. 2.5) and wireline log signatures indicate dominantly silty sediments with prograding geometries (Fig. 4.10). The topsets of HST 2.2 were eroded during the event that formed SB 2.3 (Fig. 4.11).

The distribution of sand in HST 2.2 (Fig. 4.12) suggests a large sand-rich plume was distributed across the shelf from a point source near Northumberland 1. The sand-rich prograding delta lobe that Breaksea Reef 1, Douglas Point 1 and Northumberland 1 penetrate may have been affected by oblique wave contact from the southwest that re-distributed sediment towards the east into the Port Campbell Embayment.

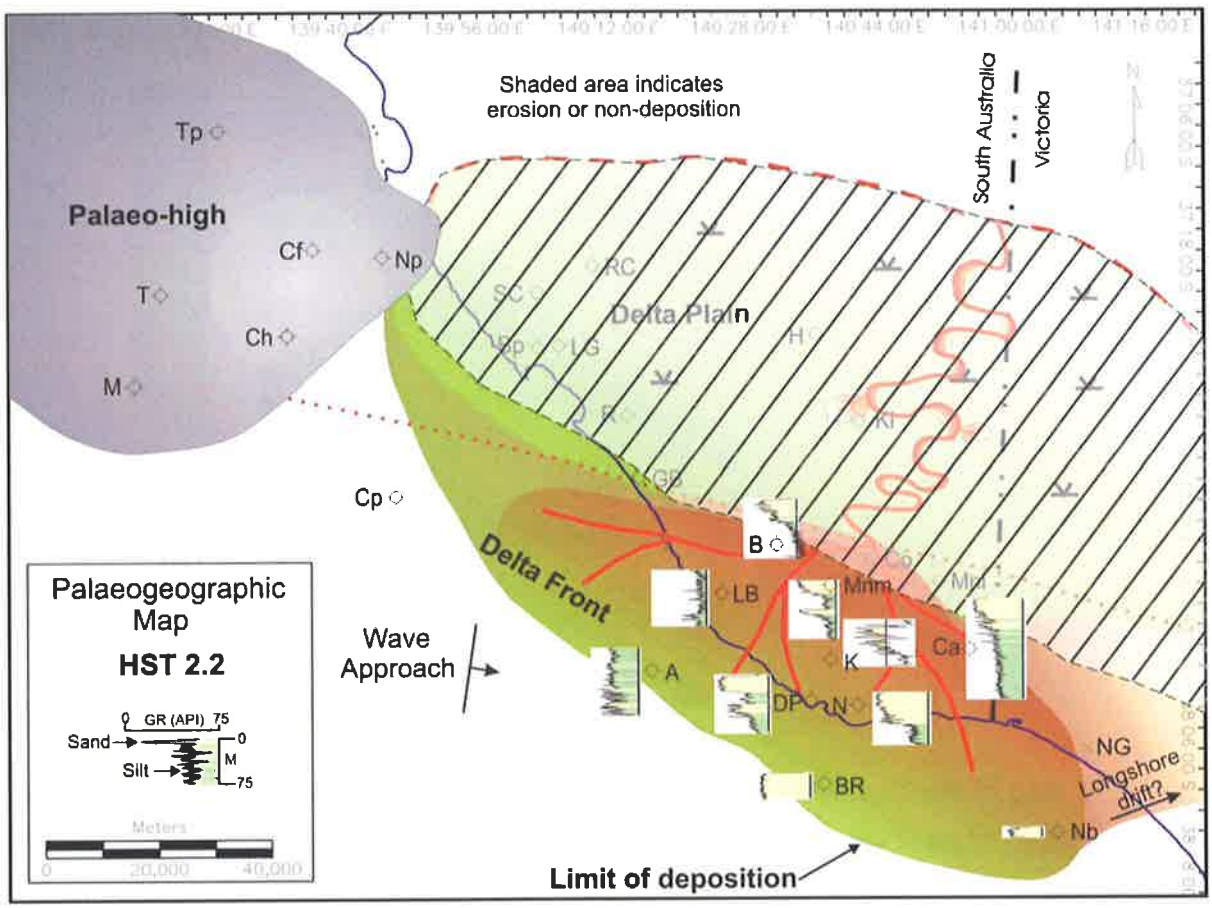

Figure 4.10 Palaeogeographic map of HST 2.2 showing gamma ray log response and distribution of sediments in the Gambier Sub-basin.

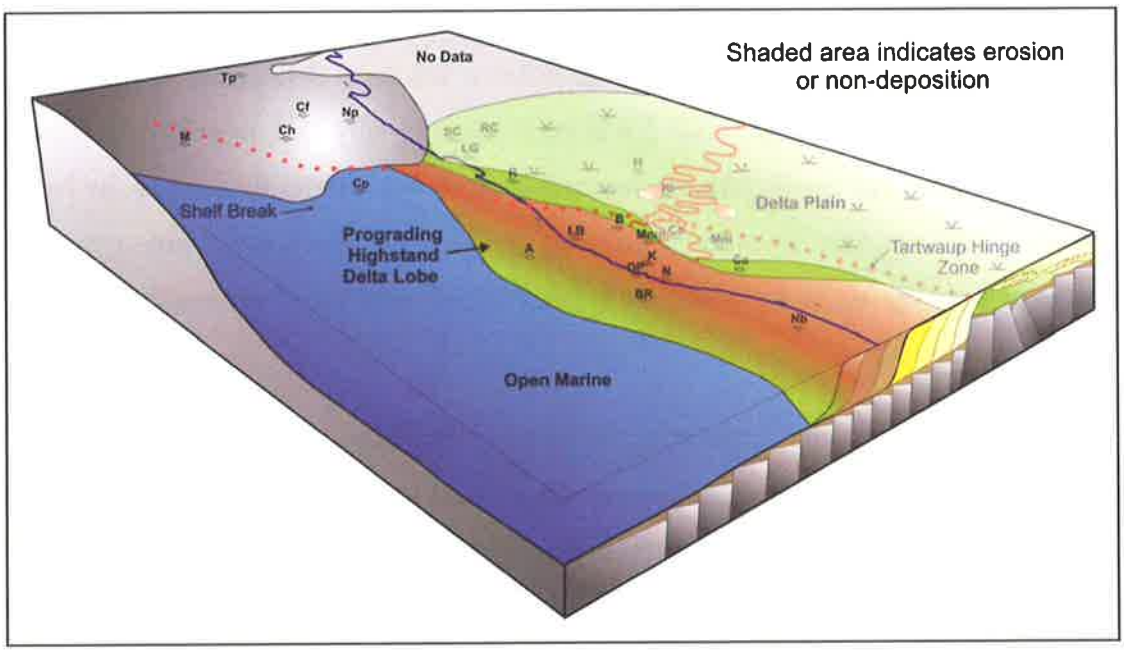

Figure 4.11 Concept block diagram illustrating the depositional environments existing in the Gambier Sub-basin during deposition of HST 2.2.

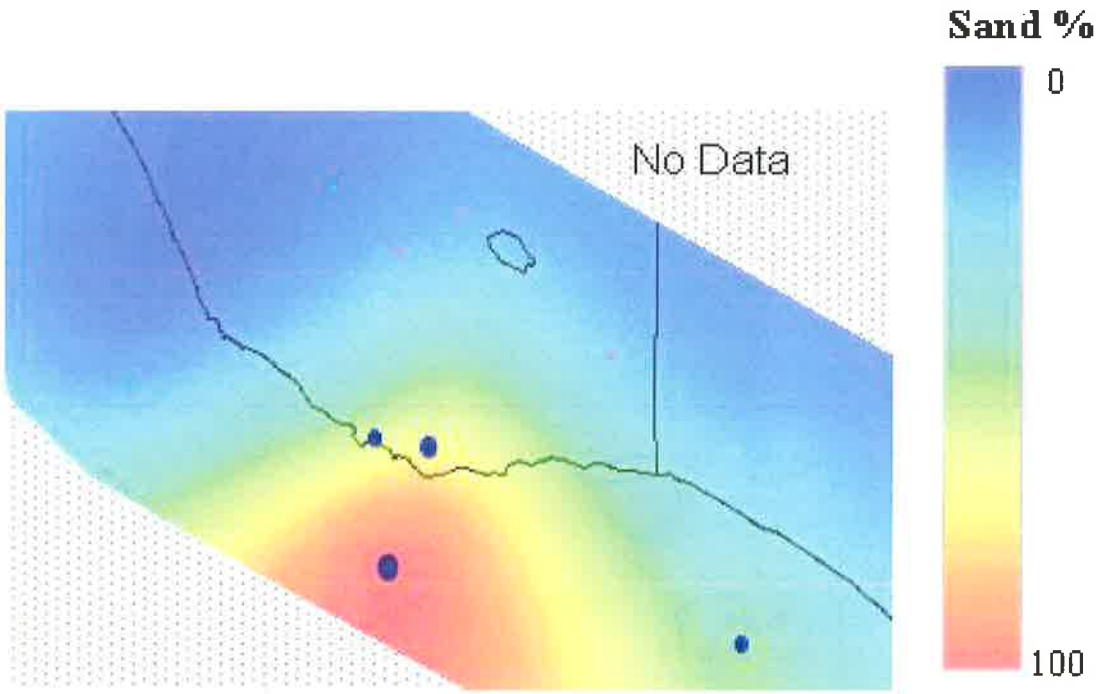

Figure 4.12 Map of the distribution of sand in HST 2.2 in the Gambier Sub-basin suggests a large sand-rich plume was distributed across the shelf from a point source near Northumberland 1.

4.2.2.3 Sequence 2.3

SB 2.3 is a regional unconformity formed as relative sea level fell again, despite continued subsidence of the Voluta Trough. LST 2.3 is very thin and silty and seismic data (Chapter 2, Fig. 2.7) show numerous small channels indicating there was fluvial incision as far basinward as the present day middle to outer shelf (Fig. 4.13). The dominantly silty nature of the sediments suggests the wells have intersected interdistributary bays and swamps between the distributary channels.

Sea level again rose rapidly, depositing a thin transgressive systems tract and HST 2.3 prograded across the shelf, downlapping onto MFS 2.3 (Fig. 4.14, 4.15). The prograding delta front is visible on seismic data, while the delta plain environment is present in the northern Voluta Trough, with wireline log motifs suggesting wells have penetrated back barrier lagoons, barrier bars, distributary channels, crevasse splays and interdistributary bays.

The distribution of sand in HST 2.3 (Fig. 4.16) suggests the delta system was more sand rich in the eastern part of the study area. The blocky gamma log motifs in Breaksea Reef 1, Normanby 1 and Caroline 1 suggest that these wells represent sandy distributary channel deposits.

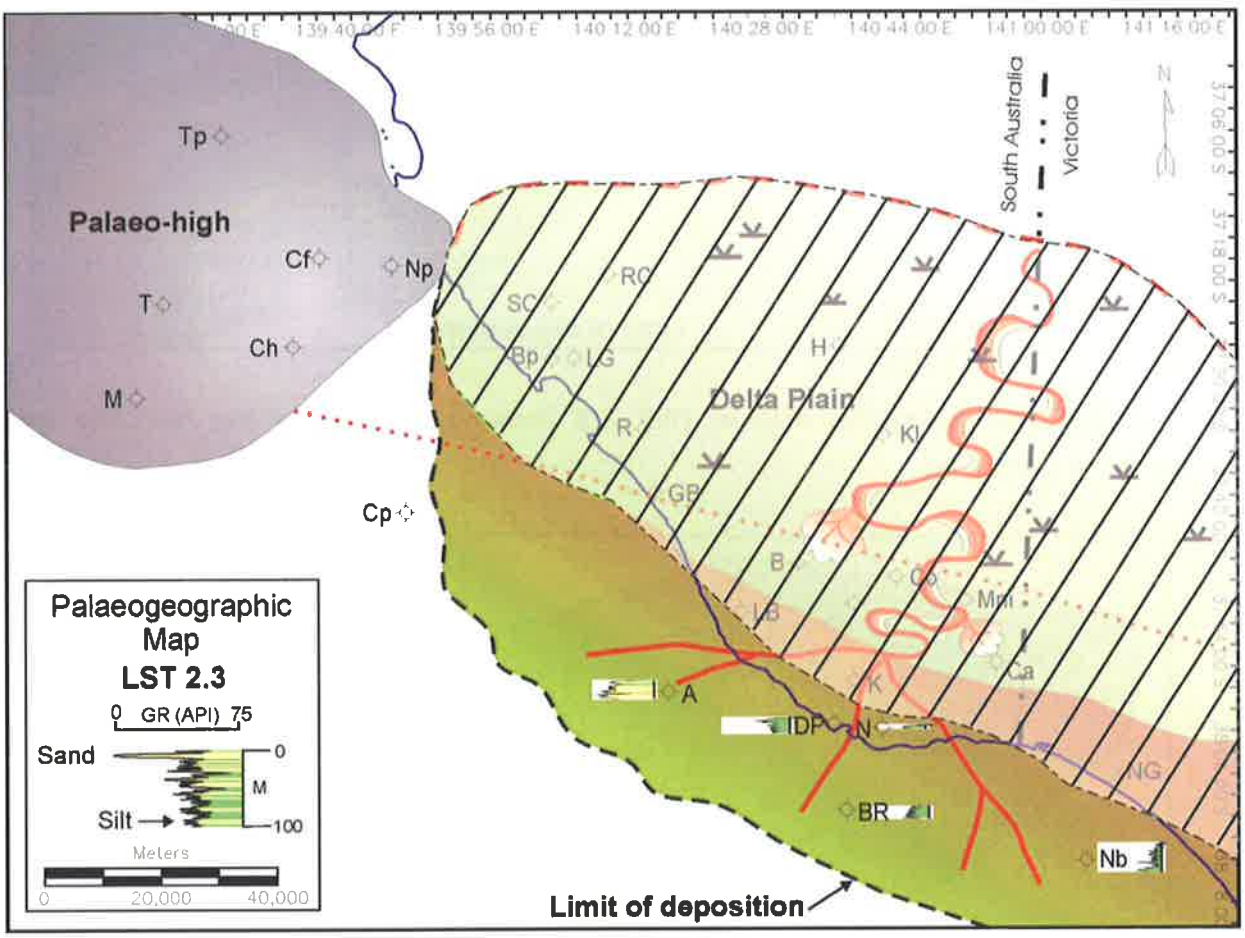

Figure 4.13 Palaeogeographic map of LST 2.3 showing gamma ray log signature.

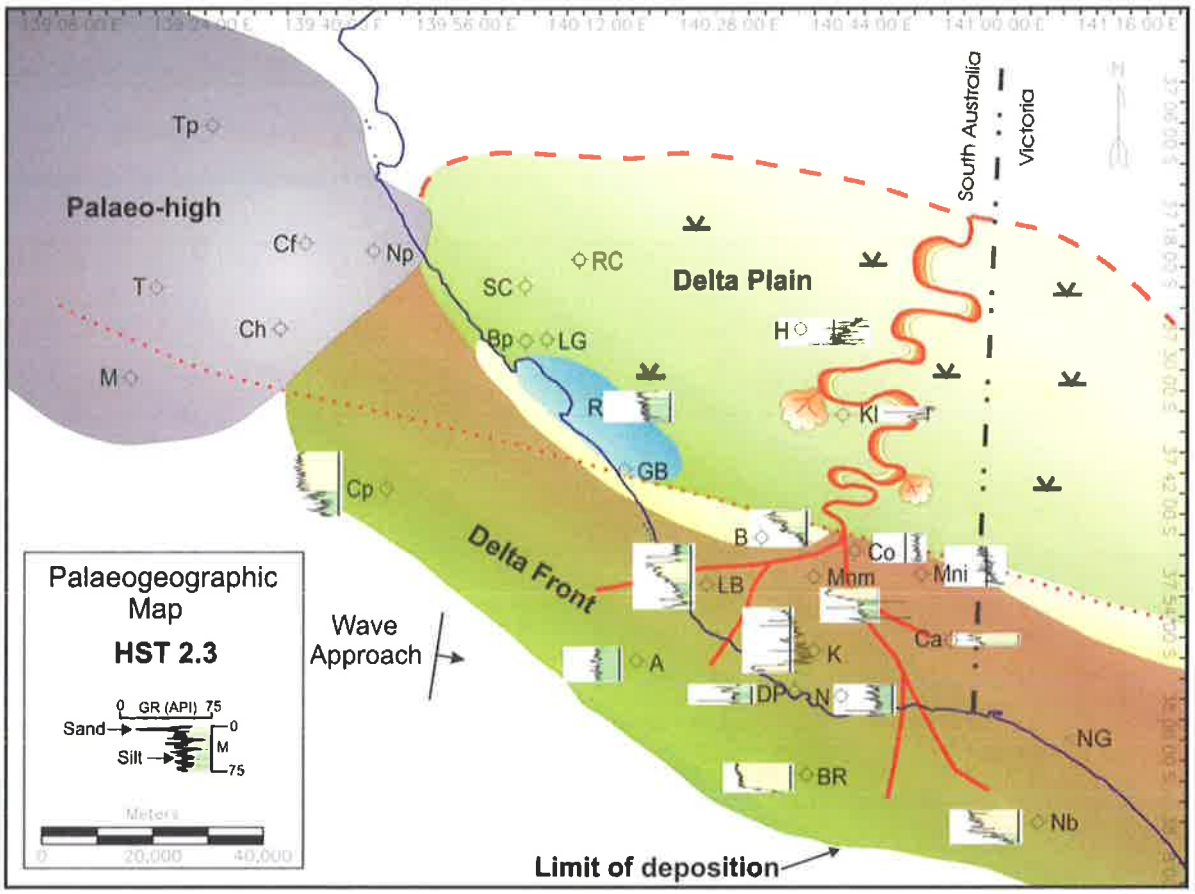

Figure 4.14 Palaeogeographic map of HST 2.3 showing gamma ray log response and distribution of sediments.

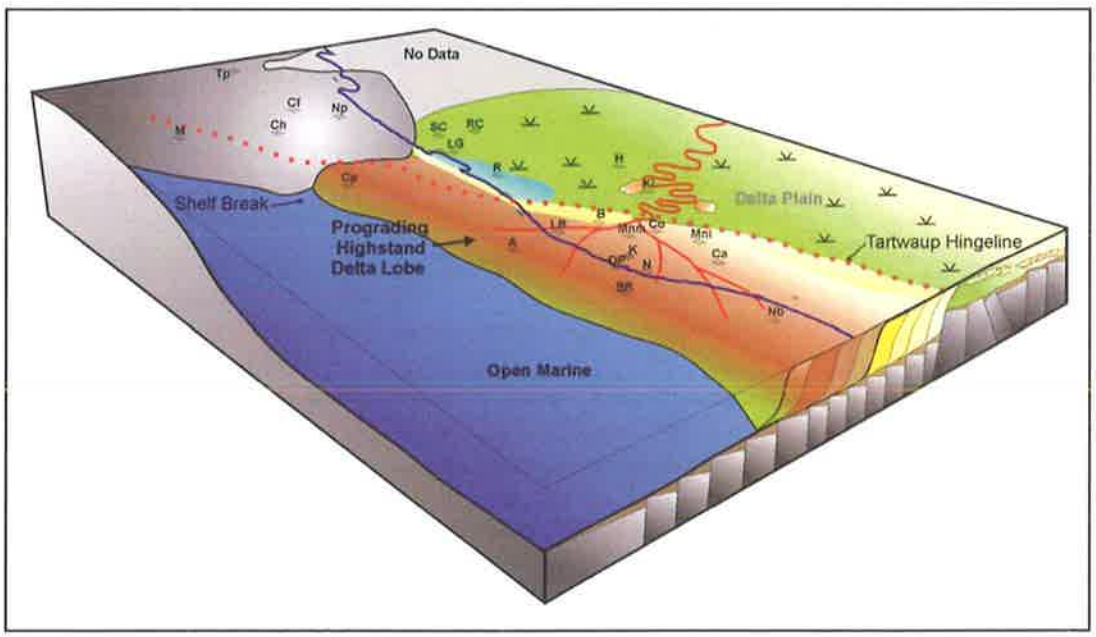

Figure 4.15 Concept block diagram illustrating the depositional environments existing in the Gambier Sub-basin during deposition of HST 2.3.

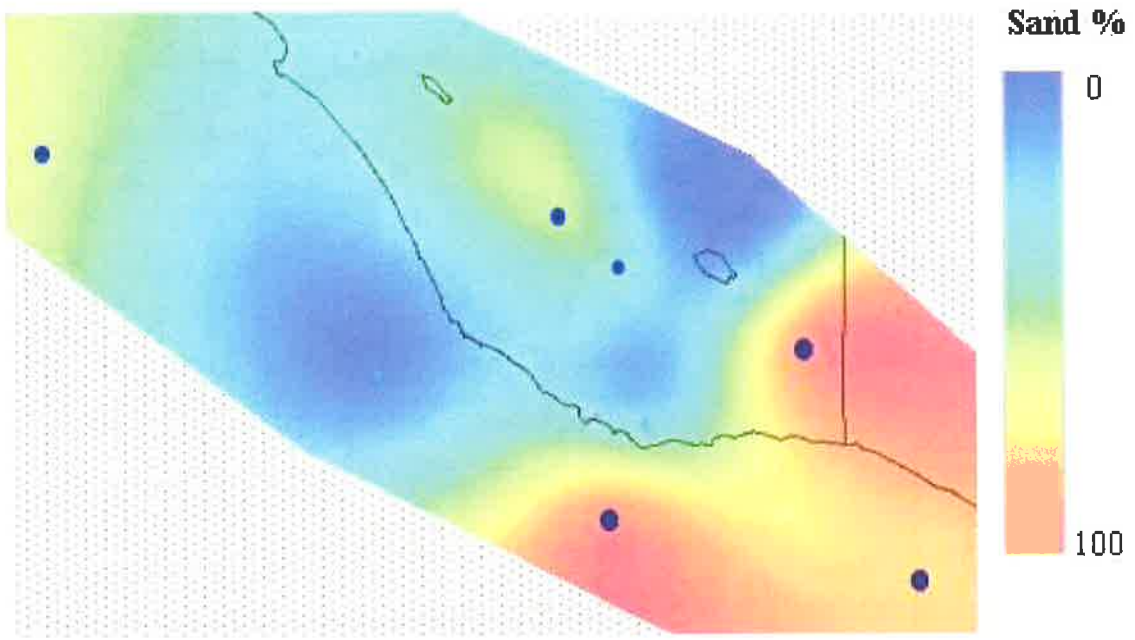

Figure 4.16 Distribution of sand in HST 2.3 in the Gambier Sub-basin suggests the delta system was more sand rich in the eastern part of the study area. The blocky gamma log motifs in Breaksea Reef 1, Normanby 1 and Caroline 1 suggest that these wells represent sandy distributary channel deposits.

4.2.3 Supersequence 3

SB 3.1 is a regional unconformity interpreted on seismic data across the Voluta Trough in South Australia. There are numerous channels observed on the seismic data at SB 3.1 indicating fluvial incision extended as far basinward as the present day outer shelf (Chapter 2). The lowstand systems tract (LST 3.1) is interpreted to be present as incised valley-fill packages, however these are not resolvable on seismic. The seismic topsets, representing the delta plain facies extend basinward of Breaksea Reef 1 and the prograding clinoforms observed on seismic data that downlap onto SB 3.1 are interpreted to largely represent highstand sediments. Gamma ray log motifs (Fig. 4.17) indicate the wells have intersected a range of delta plain environments.

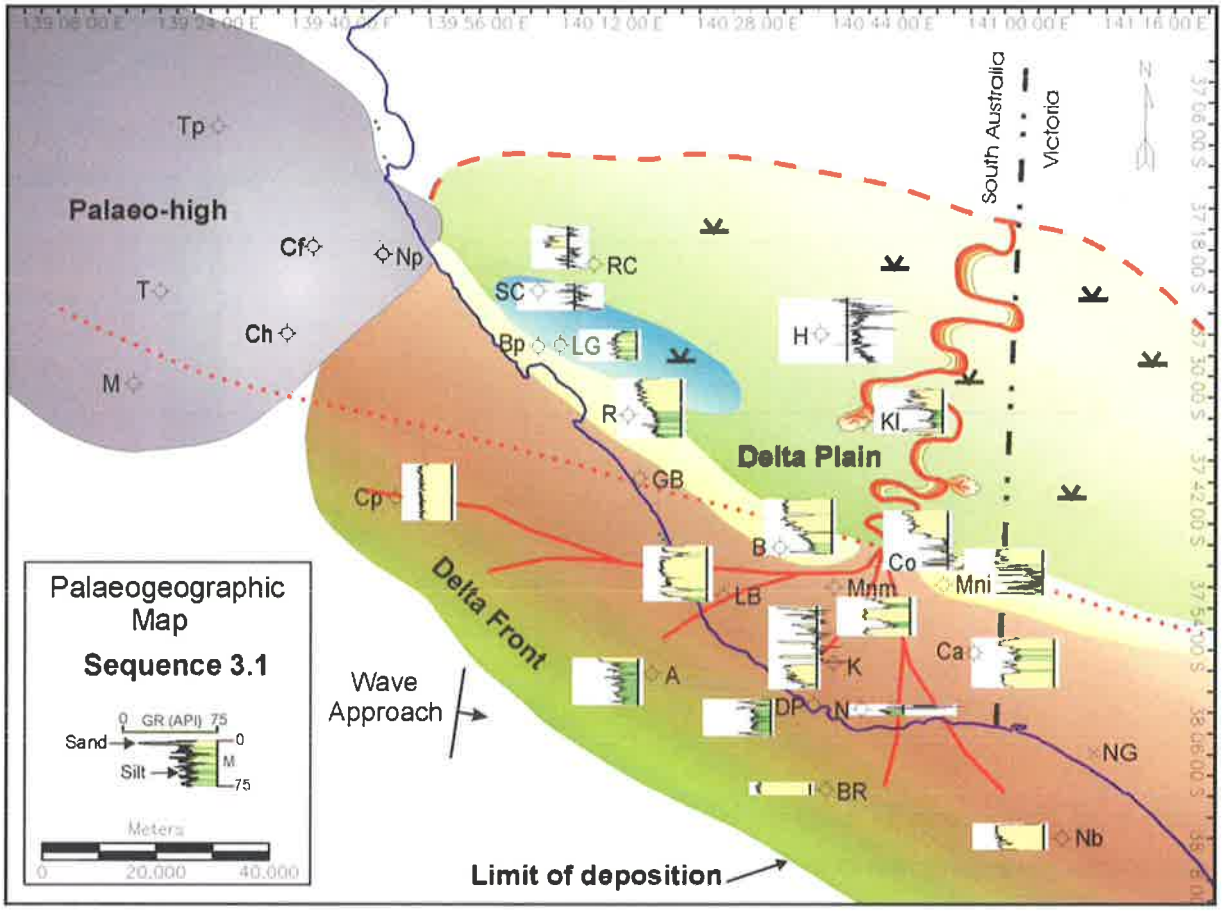

Figure 4.17 Palaeogeographic map of sequence set 3.1 showing gamma ray log response and distribution of sediments.

The dominantly fine-grained nature of sediments intersected in Reedy Creek 1 and Hungerford 1 suggests they may represent silty overbank deposits. St Clair 1 and Lake George 1 are interpreted to have intersected back barrier lagoonal facies, while Rendelsham 1, Burrungule 1 and McNicol 1 show coarsening upward gamma log motifs suggesting they penetrated the prograding sandy shoreface or barrier bar separating the coastal plain from the open ocean.

Wells located basinward of Burrungule 1 penetrated distributary channels, distributary mouth bars and interdistributary bays on the delta plain and delta front. The distribution of sand in sequence 3.1 and the blocky to prograding gamma log motifs suggests that, Breaksea Reef 1, Normanby 1, Caroline 1, McNamara 1, Lake Bonney 1 and Copa 1 may have penetrated sandy distributary channels or mouth bars (Fig. 4.17 and 4.18). Northumberland 1, Douglas Point 1 and Argonaut 1A show silty motifs and may have penetrated interdistributary bays.

4.2.3.1 Sequences 3.2 and 3.3

Sequences 3.2 and 3.3 are only preserved in a small area around Breaksea Reef 1. The reader is referred to the seismic character of these sequences in Chapter 2 (Fig. 2.9) and the stratigraphic cross-sections in Appendix 4 for the wireline log character. The erosional event forming SB 4.1 is interpreted to have eroded the delta plain facies of sequences 3.2 and 3.3 landward of Breaksea Reef. 1.

During deposition of Supersequences 1, 2 and 3, the delta systems prograded southward, an observation that is supported by high progradation to aggradation ratios and sedimentation rates calculated from seismic data on these supersequences (Fig. 4.18). Sedimentation rates of Supersequences 2, 3 and 4 were also high (approximately 18 cm/K.y.). Major marine transgressions during the later Early Eocene (identified by McGowran, 1991) may have resulted in significant relative sea level rise despite continued subsidence in the Voluta Trough creating large accommodation space in the Voluta Trough. This resulted in deposition of Supersequence 4 as a retrogradational package with a negative progradation to aggradation ratio (Fig. 4.18).

4.2.4 Supersequence 4

Seismic data show meandering incised channel belts at SB 4.1 located basinward of Breaksea Reef 1, suggesting delta plain facies and fluvial environments existed under the present day outer shelf and upper slope during this lowstand in relative sea level (Chapter 2, Fig. 2.9 and 2.12). Sediments of Sequence 4.1 around Breaksea Reef 1 and Argonaut 1A are interpreted on seismic data to fill the incised channels formed during the preceding lowstand. Wireline log motifs indicate this sediment is silty and may be the distal deposit of a distributary mouth bar (Fig. 4.19).

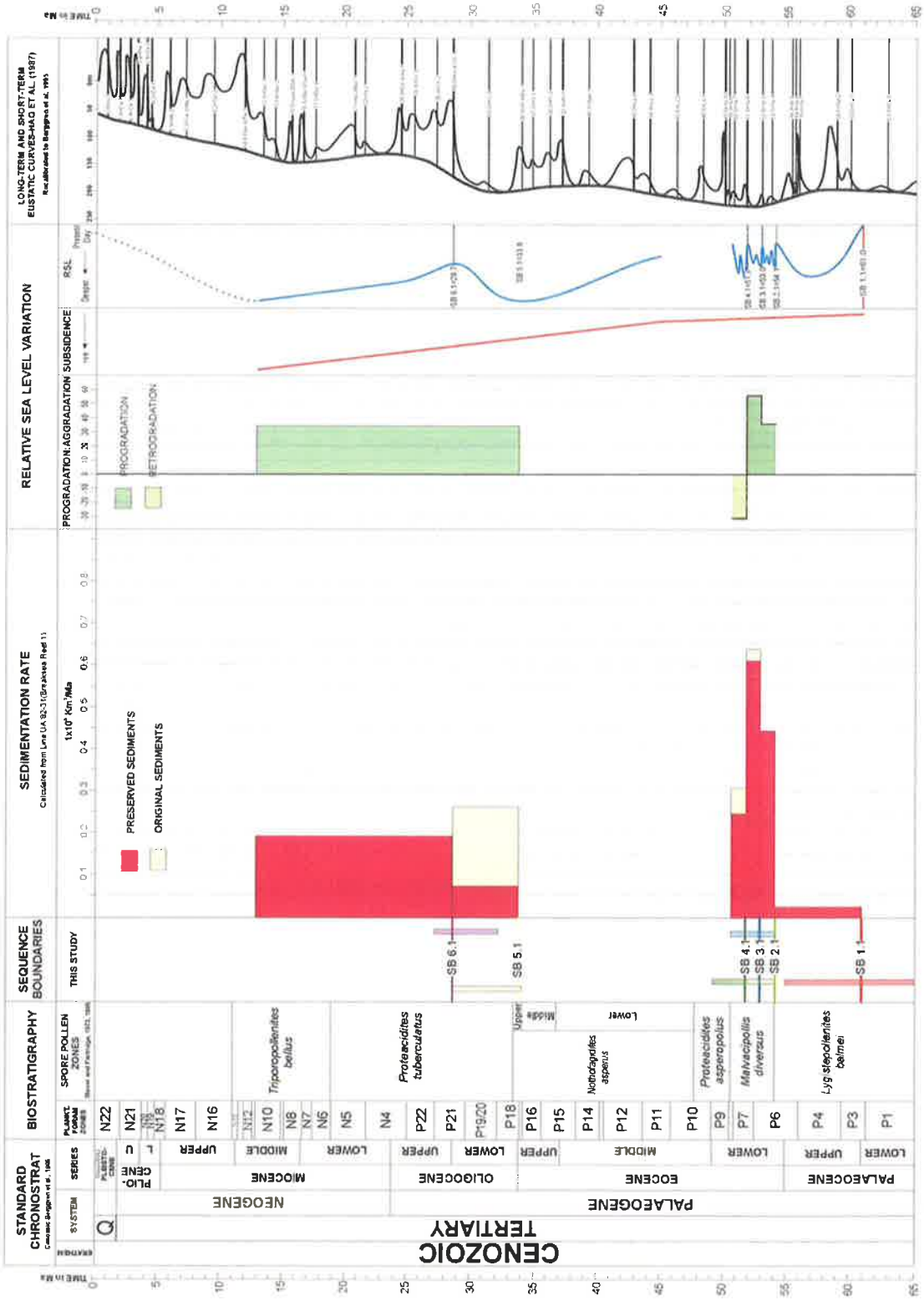

Figure 4.18 Composite diagram illustrating the temporal location of seismic supersequences and their approximate sedimentation rates as determined from 2D seismic. The progradation to aggradation ratios of the supersequences is also compared with interpreted local subsidence and sea level, and eustatic sea level.

The distribution of sand within sequence 4.1 suggests the delta system is very sandy around Compton 1, McNicol 1, Caroline 1, McNamara 1 and Burrungule 1. These wells show blocky to prograding log motifs and are interpreted to intersect distributary channels or mouth bars, and those will high gamma log values suggesting silty sediments are interpreted as interdistributary bay deposits (Fig. 4.19 and 4.20). McNicol 1 has a distinct prograding, coarsening upward log motif that has been interpreted as a barrier bar deposit. Wells in the north-western part of the study area are dominantly fine grained and have been interpreted as coastal plain overbank deposits.

Palaeogeography of Sequence 4.2 is very similar to that of sequence 4.1 and individual systems tracts are not seismically resolvable.

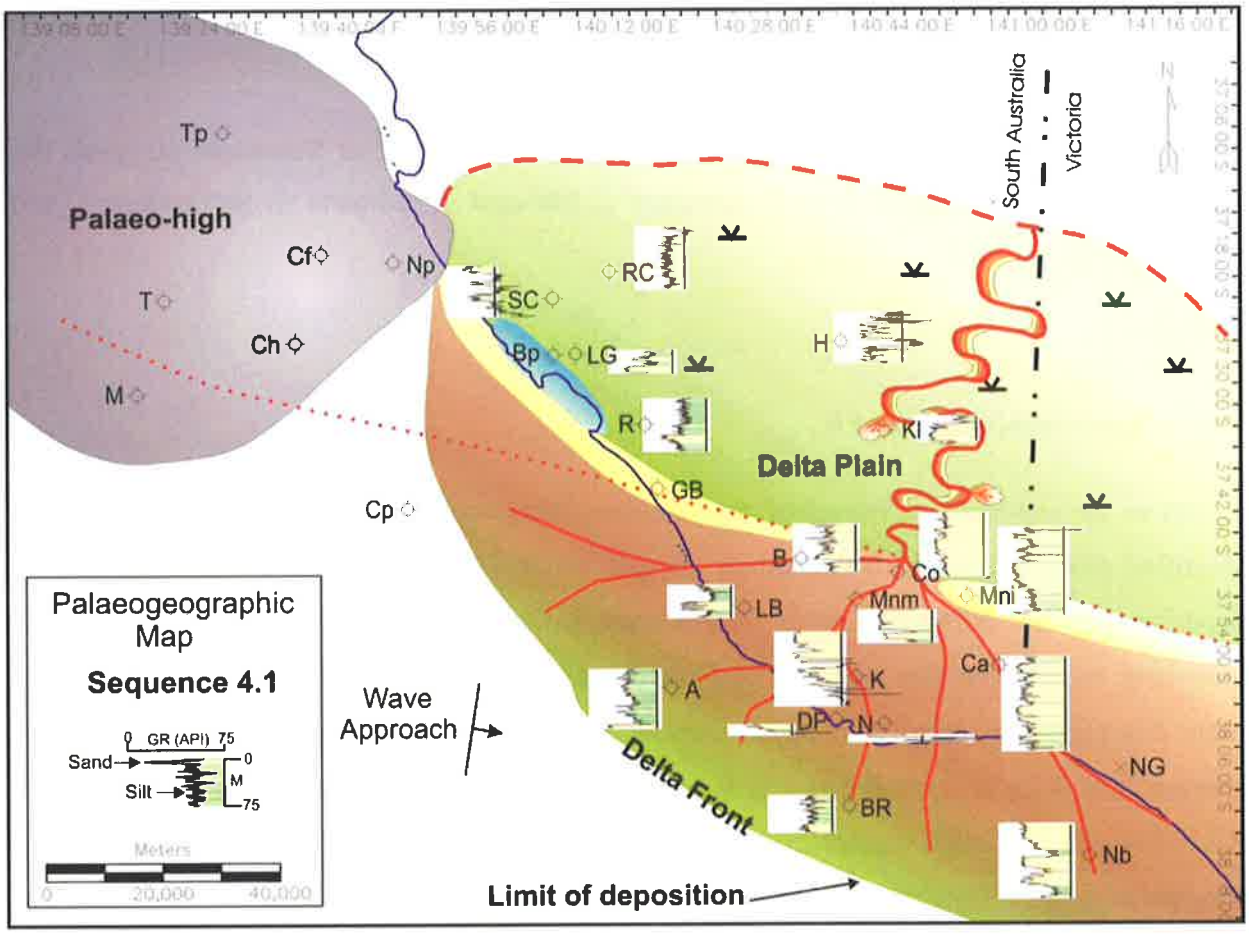

Figure 4.19 Palaeogeographic map of Sequence 4.1 showing gamma ray log response and distribution of sediments.

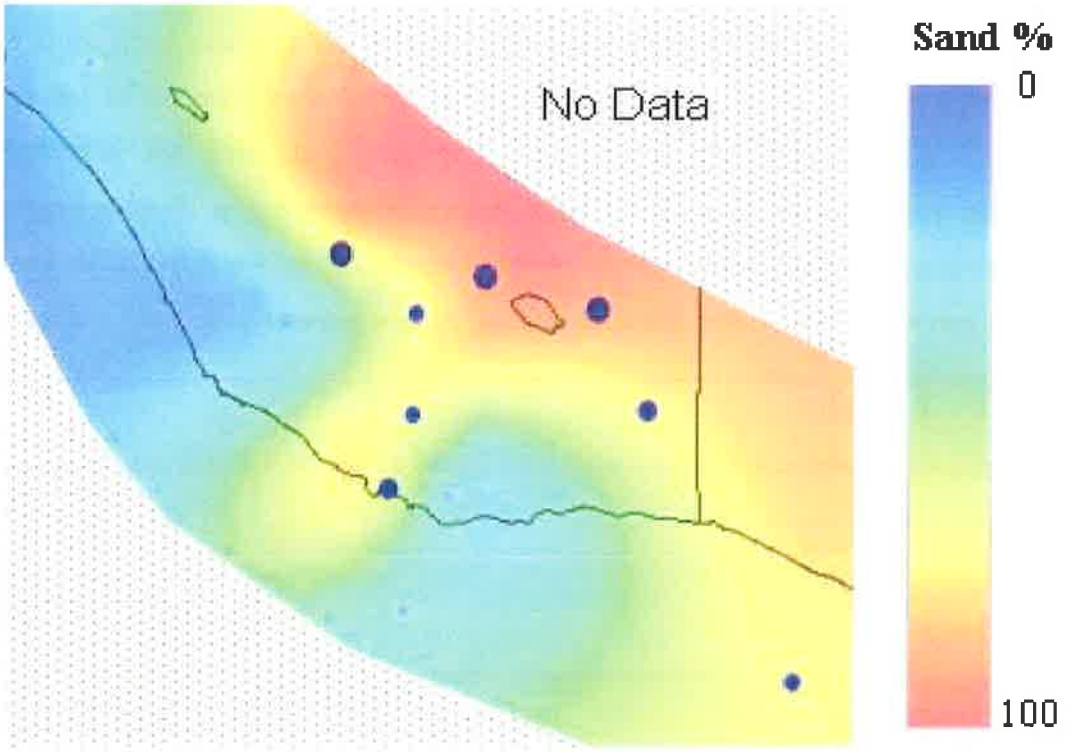

Figure 4.20 Distribution of sand within Sequence 4.1 in the Gambier Sub-basin suggests the delta system is very sandy around Compton 1, McNicol 1, Caroline 1, McNamara 1 and Burrungule 1.

4.2.5 Supersequences 5 and 6

A gap in the sedimentary record of nine million years during the Middle Eocene has been identified along the southern Australian margin, which was followed in the Late Eocene by deposition of the Nirranda Group in the eastern Otway Basin (and equivalent packages elsewhere on the southern margin) (McGowran et al. 1997). However, in the Gambier Sub-basin this period is represented by condensed sections and the presence of the Late Eocene spore-pollen, *N.asperus*, in Troas 1 is the only evidence of sedimentation during this period. According to the biostratigraphy, it is likely there was almost 15 M.y. of erosion and condensation in the Gambier Sub-basin during the late Middle and Late Eocene (Chapter 3, Fig. 3.14).

When the Australian and Antarctic continents finally broke away from each other in the Middle Eocene, the cold, fertile Circum-Antarctic Current became established, and at the beginning of

the Oligocene cool-water, bryozoa-rich carbonates prograded across the shelf in the Gambier Sub-basin (Chapter 3). The Gambier Limestone was deposited in fully marine, inner, middle and outer shelf environments (Morton et al. 1995; White, 1995) (Fig. 4.21 and 4.22).

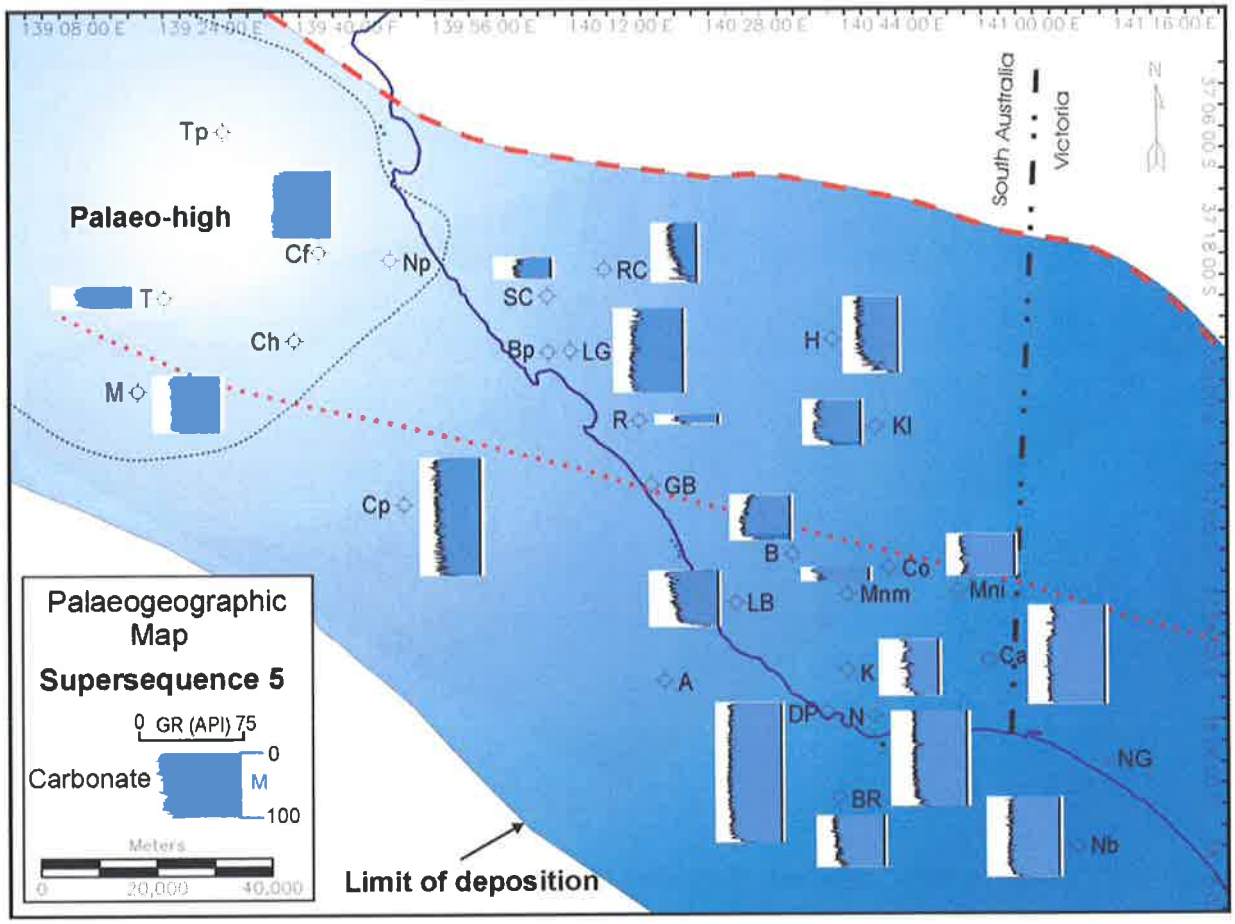

Figure 4.21 Palaeogeographic map of Supersequence 5 showing gamma ray log response and distribution of carbonate sediments of the Gambier Limestone.

At the end of the Early Oligocene a glacio-eustatic sea level fall exposed the Gambier Sub-basin and sea level fell below the shelf break. This led to minor fluvial incision across the outer shelf and created "nick points" at the shelf edge. When sea level rose again, these points were picked on by mass wasting events and turbidity currents, leading to formation of large submarine canyons (Chapter 3, Fig. 3.4). Sediments of Supersequence 6 comprises multiple episodes of canyon fill (Fig. 4.23) deposited in outer shelf environments (Fig. 4.24). The wireline log motifs representing Supersequence 6 in some onshore wells (e.g. Lake Bonney 1,

Burrungule 1 and Compton 1), are not representative of the true original thickness of this package as there has been significant uplift and erosion in the Gambier Sub-basin since the Middle Miocene (Dickinson et al. 2001). Sedimentation within the canyons throughout the Late Oligocene and Early-Mid Miocene was entirely submarine and episodic in nature.

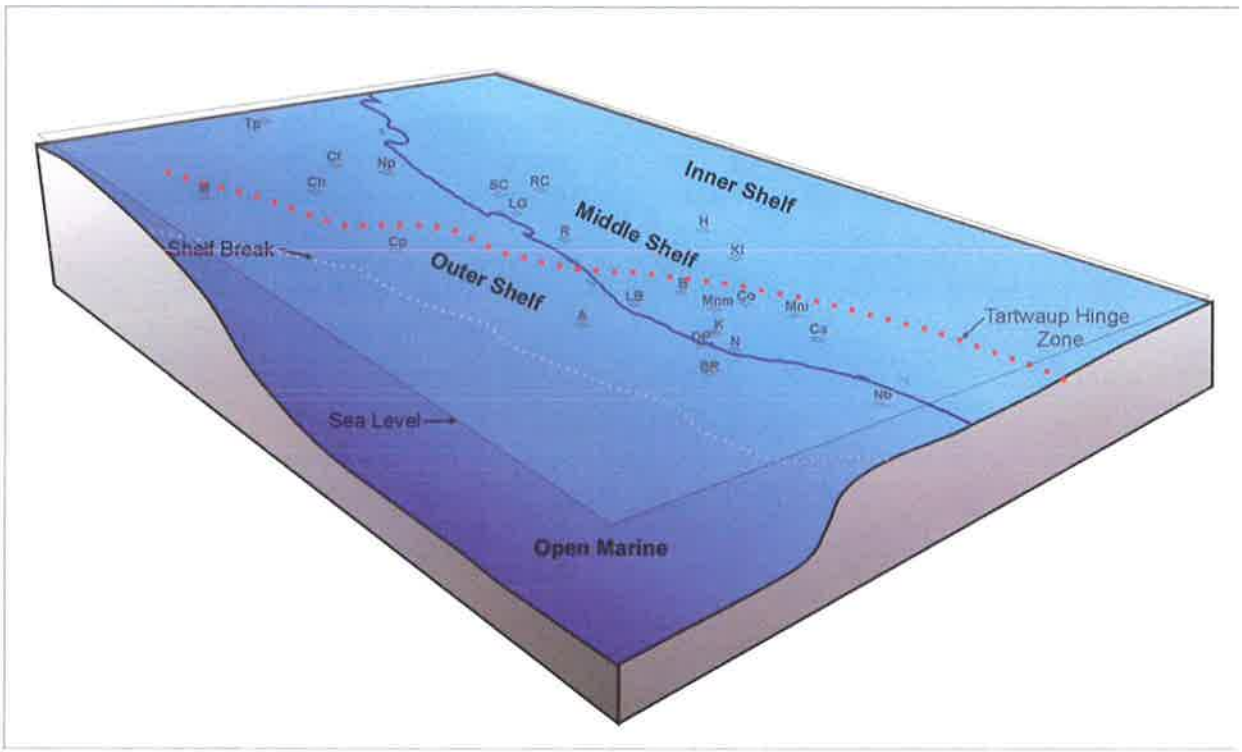

Figure 4.22 Concept block diagram illustrating the depositional environments existing in the Gambier Sub-basin during deposition of Supersequence 5.

Deposition of the Gambier Limestone is interpreted to have terminated in the Middle Miocene (Li et al. 2000). Sediments deposited on the shelf during the Late Miocene and Pliocene were subsequently eroded during the Plio-Pleistocene when a glacio-eustatic sea level fall caused sea level to fall below the shelf edge, eroding carbonate sediment from the shelf and removing expression of the submarine canyons from the present day shelf. A thick wedge of sediment on the upper slope and outermost shelf may be the remnant of deposition during the Late Miocene and Pliocene (Fig. 3.16).

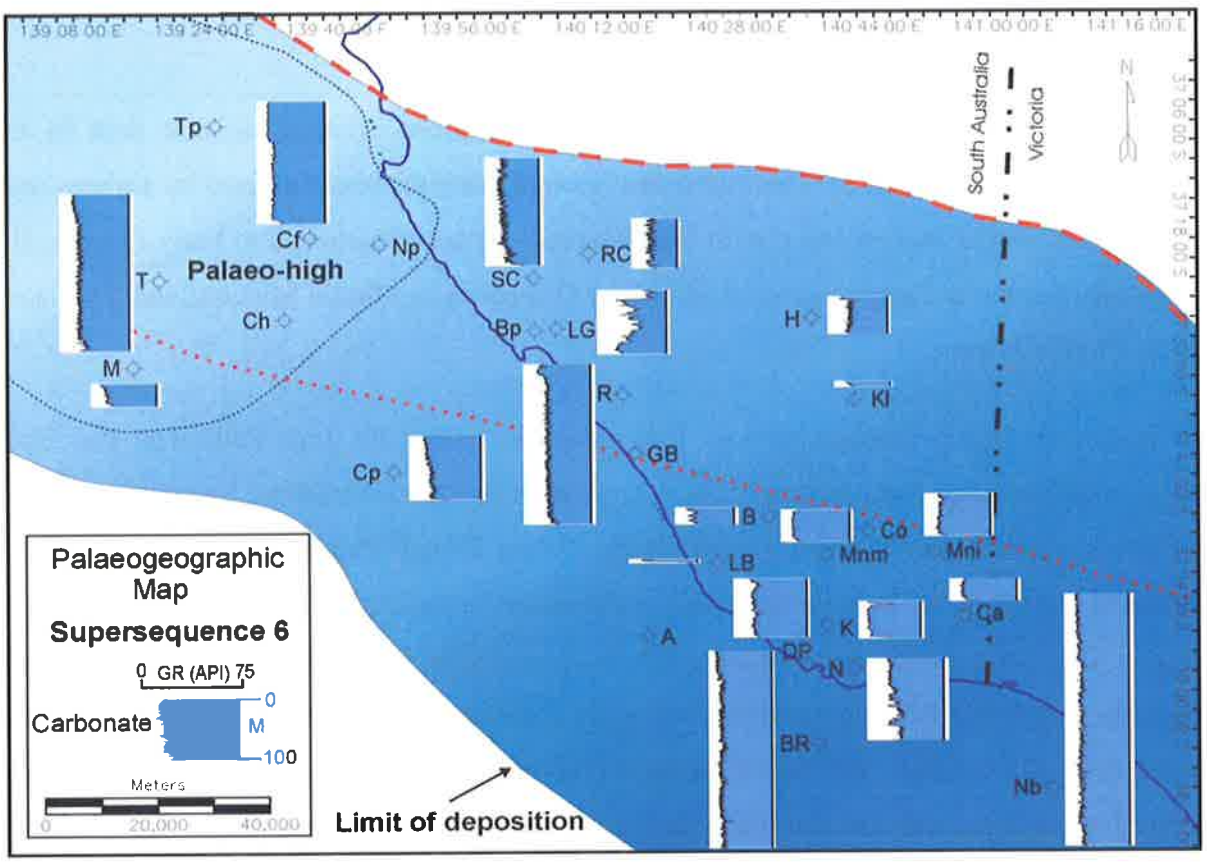

Figure 4.23 Palaeogeographic map of Supersequence 6 showing gamma ray log response and distribution of sediments.

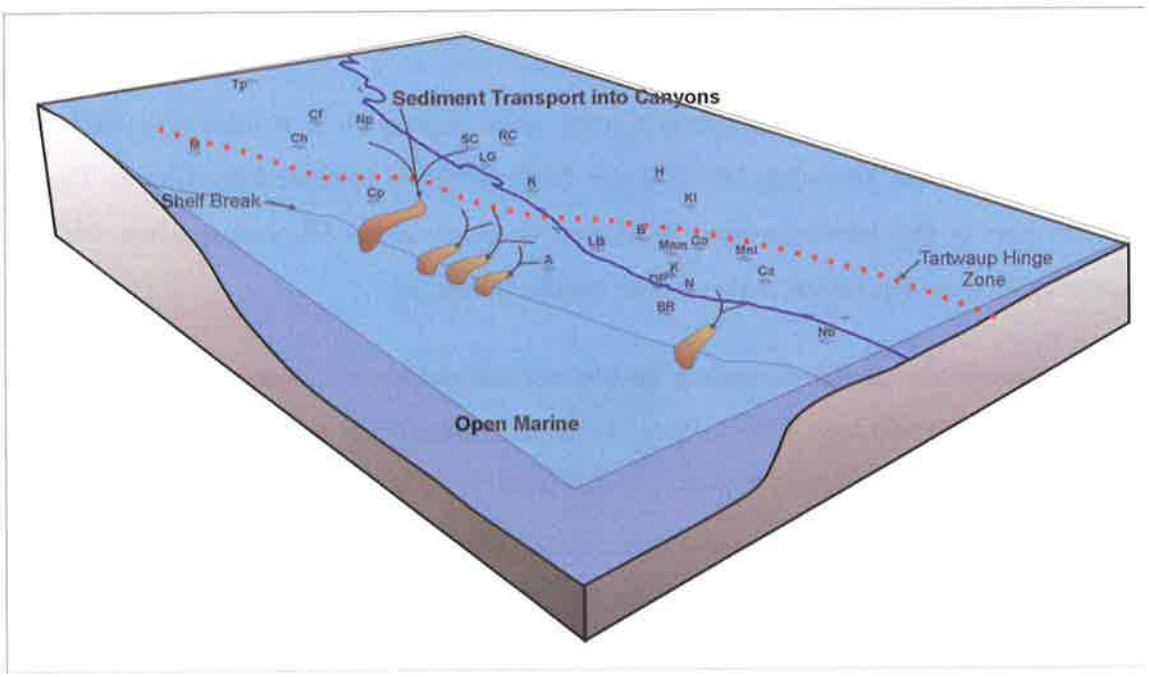

Figure 4.24 Concept block diagram illustrating the depositional environments existing in the Gambier Sub-basin during deposition of Supersequence 6.

4.3 CHRONOSTRATIGRAPHY

A summary chronostratigraphic chart was constructed from offshore seismic data in the Gambier Sub-basin (Fig. 4.25). The four global second order packages defined by authors such as Quilty (1977) and McGowran (1978) are observed: (I) Late Paleocene to Early Eocene, (II) late Middle Eocene to Early Oligocene, (III) Late Oligocene to Middle Miocene and (IV) latest Miocene to Pleistocene.

The Wangerrip Group (Supersequences 1-4) deposited during the Late Paleocene and Early Eocene correlates to global package I. These sequences are characterised by high sedimentation rates into a prograding deltaic environment in the Voluta Trough. Package II is represented by a condensed section in the Late Eocene and the carbonate Supersequence 5 in the Gambier Sub-basin in the Early Oligocene. Package III is represented by Supersequence 6, the Late Oligocene to Middle Miocene neritic cool-water carbonate that is dominated by submarine canyon cut and fill events. The fourth package (IV) of Late Miocene to Pleistocene age is not observed on seismic data or identified on well data in the study area, hence this period is represented by possible erosion or a condensed section on the chronostratigraphic chart.

4.4 DISCUSSION

The deltaic sediments of the Wangerrip Group were deposited in a relatively well defined depocentre south of the Tartwaup Hinge Zone. Sedimentation bypassed the Chama Terrace in the western part of the sub-basin until the Late Eocene to Early Oligocene when widespread cool-water carbonate deposition began on the southern margin.

In the Late Cretaceous, at approximately 96 Ma, subsidence slowed dramatically on the Chama Terrace from approximately 170 m/M.y. to approximately 5 m/M.y to the present day (Williamson et al. 1996). In the Voluta Trough from the Late Cretaceous to the present day, subsidence is estimated to be, on average, 70 m/M.y. This is caused by a combination of tectonically-driven subsidence during sea floor spreading, and high load-driven subsidence due to high rates of sediment input throughout the Late Cretaceous and early Cenozoic. From 96 Ma to present the load-driven subsidence is between 1.3 and 1.5 times the tectonically-driven subsidence (Williamson et al. 1996).

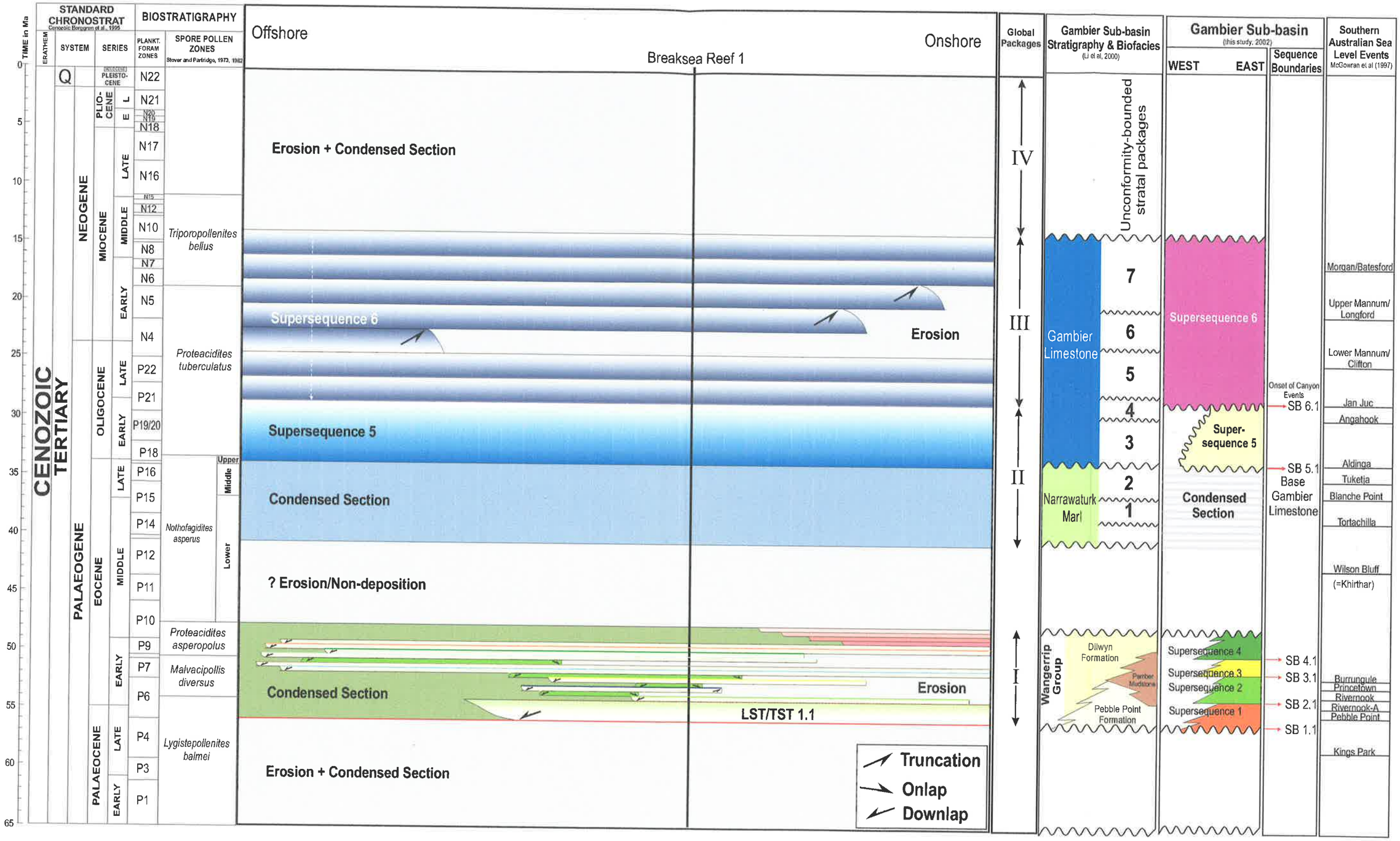

Figure 4.25 Chronostratigraphic chart of the Cenozoic sedimentary record in the Gambier Sub-basin.

These differential subsidence rates of the Chama Terrace and Voluta Trough supports observations from seismic data that the Voluta Trough was topographically lower and therefore captured the Late Paleocene to Early Eocene deltaic sediments. The Chama Terrace experienced significant erosion, observed on seismic data as an angular unconformity (Chapter 2, Fig. 2.11) between Late Cretaceous sediments and Oligocene carbonates.

Active faulting at the end of the Cretaceous and into the Late Paleocene caused rotation of "domino" fault blocks, the erosion of which would have created a sediment source for the Late Paleocene "Pebble Point Formation" sediments (Waltham et al. 1993). One suggested scenario for the source of the Late Paleocene to Early Eocene fluvial and marginal marine sediments is the presence of a proto-Murray River system, the mouth of which delivered sediment into the western Voluta Trough (Holdgate, 1981).

The sedimentation rates calculated for this study (Fig. 4.18, Appendix A1.6) are determined from distribution and thickness of sequences interpreted on seismic and well data in the study area (i.e. western Voluta Trough and Chama Terrace). Hence, the derived values cannot be directly compared with sedimentation rates in other delta systems on the southern margin, or indeed, the world, as the calculated rate is dependent on the aerial extent of the unit. So unless rates are calculated using data from the entire basin or drainage area, the results will not be comparable to other deltas in the world.

However, the relative rates of sedimentation between the clastic and carbonate supersequences can be seen in Fig. 4.18. Calculations for this study indicate that deposition of Supersequences 2-4 were up to 17 times faster than sedimentation rates for Supersequence 1. And average sedimentation rates for the clastic supersequences were over eight times faster than rates of carbonate deposition. One dimensional (1D) sedimentation rates can be calculated (i.e. thickness of a sequence derived from wells—disregarding the effect of post-depositional compaction—divided by the duration of that package) and compared with other delta systems in the world where rates are calculated using the same method.

When calculating the 1D sedimentation rates in the Gambier Sub-basin the following logic was used (values from Appendix A1.6 were used): Supersequence 1 was deposited over a 7 M.y. period and attains an average thickness of 67 m in the study area, which works out to be a sedimentation rate of 9.6 m/M.y. or 0.96 cm/K.y. If it is assumed that Supersequences 2-4 had an equal duration within the Early Eocene (since all sediments in the offshore part of the sub-

basin are *M. diversus* age and cannot be further sub-divided), then each supersequence was deposited over 1.167 M.y. Supersequence 2 has an average thickness of 176 m, which translates to a sedimentation rate of 15 cm/K.y. Supersequence 3 has an average thickness of 112 m, which results in a sedimentation rate of 9.6 cm/K.y., and Supersequence 4 has an average thickness of 208 m, resulting in a sedimentation rate of 18 cm/K.y.

Carbonate sedimentation rates are significantly slower (as indicated in Fig. 4.18) and 1D calculations indicate Supersequence 5 was deposited at 1.7 cm/K.y., and sediments of Supersequence 6 were deposited at a rate of approximately 0.6 cm. These values are approximate minimum rates, as the effects of post-depositional compaction and erosion are not taken into account. If these factors could be accounted for, they would effectively increase the calculated rates of deposition.

Holdgate (1981) indicates that deposition of the Dilwyn Formation in the Victorian Port Campbell Embayment of the Otway Basin occurred at a minimum rate of approximately 30 cm/K.y. However, it is not clear how this value was derived and since differing methods of calculation affects the result, direct comparison of rates is ill advised. A previously mentioned, sedimentation rates determined from this present study are most useful for internal comparison (eg. comparing the rate of clastic vs. carbonate sedimentation).

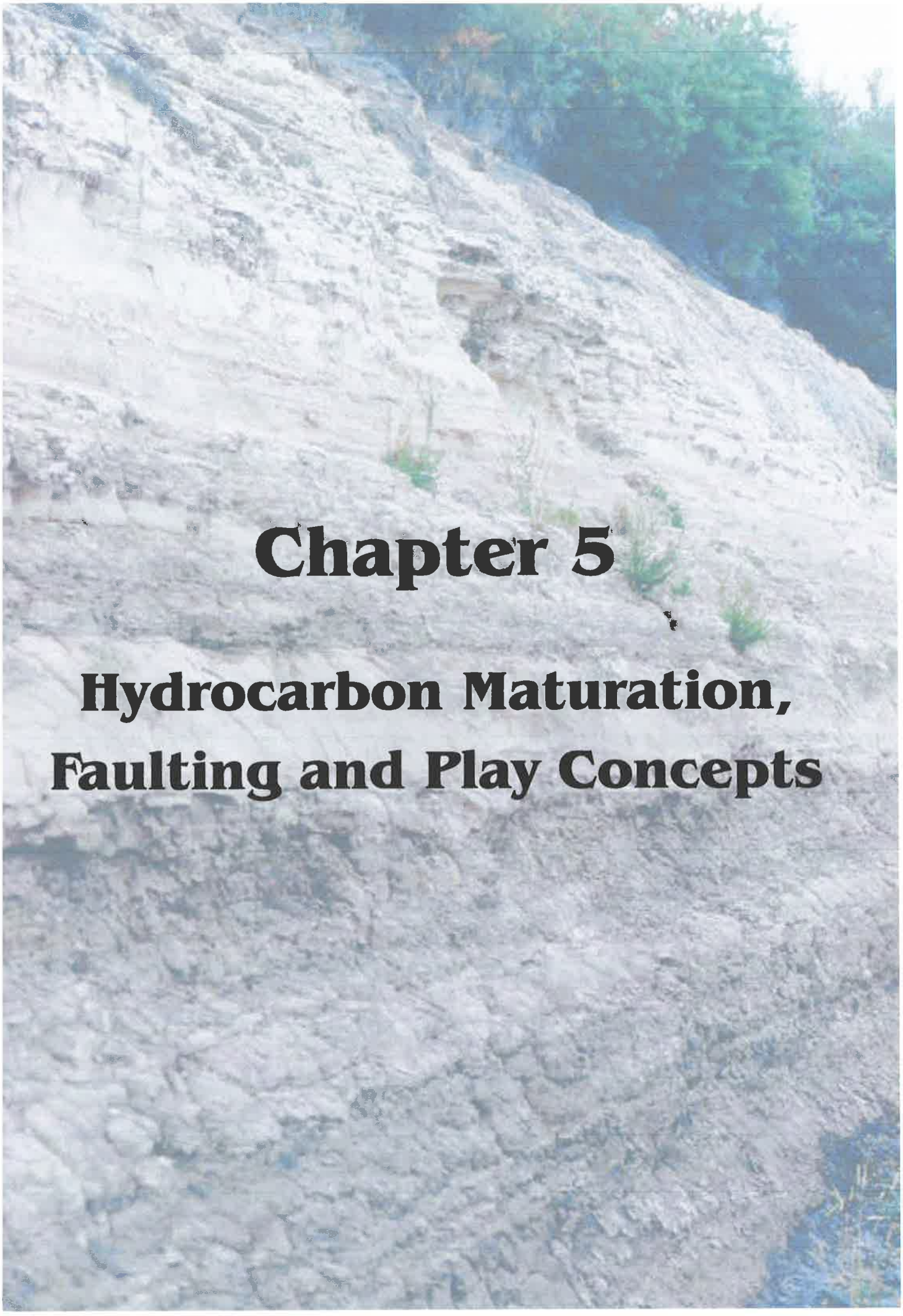

Chapter 5

Hydrocarbon Maturation, Faulting and Play Concepts

5 HYDROCARBON MATURATION, FAULTING AND PLAY CONCEPTS

The Otway Basin developed as one of a series of Late Jurassic to Recent rift to passive margin basins on the southern Australian margin. The Southern Ocean now occupies what was the Late Jurassic rift axis between the Australian and Antarctic continental plates. The formation of the Otway Basin during the numerous rifting and intervening sag phases in the Mesozoic, followed by later Cenozoic subsidence, compression and inversion allowed deposition of source, reservoir and seal rocks, formation of traps and generation of hydrocarbons. The contemporary stress regime now influences the migration pathways of hydrocarbons from generating source kitchens into reservoirs that are adequately sealed.

A three-phase breakup history for the southern margin has been proposed by Norvick and Smith (2001). The first phase began in the Middle to Late Jurassic with rifting in the western Bight Basin that progressively extended eastwards into the south-east margin basins, including the Otway Basin, by the early Tithonian (145 Ma). New half grabens were formed resulting from minor rearrangements of extension directions between Antarctica and eastern Australia (Norvick and Smith, 2001).

The magnitude of latest Jurassic to Early Cretaceous continental extension has been estimated to be in the order of 300 km (Powell et al. 1988; Willcox & Stagg 1990), in a NW-SE to NE-SW direction (the precise direction remains a point of contention eg. Boeuf & Doust 1975; Powell et al., 1988; Etheridge et al., 1985; Willcox & Stagg, 1990; Willcox et al. 1992; O'Brien et al. 1994; Hill et al. 1994; Perincek & Cockshell, 1995). The various interpretations of early extension direction, ranging from NW-SE to NE-SW, are probably partly the result of local variations in pre-rift basement structural grain, changes in intra-plate stress along the 4000 km long plate boundary, and the effects of subsequent structural overprinting (Hill et al. 1997)

Lakes formed in the deep half grabens of the developing rift have been suggested as source rocks in the Otway Basin (Edwards et al. 1999). Seismic data in the onshore Otway Basin (Finlayson et al. 1996) indicate that the Otway Basin experienced a sag phase in the Late Aptian and Albian (110-100 Ma) during which time the Eumeralla Formation was deposited (Norvick and Smith, 2001).

The second rift phase affecting the southern margin began during the Cenomanian (95 Ma) with a reorganisation of the eastern Australian basin framework, thought to have been caused by cessation of subduction east of New Caledonia (Norvick and Smith, 2001). The Otway Basin experienced folding and uplift and structures formed in the first rifting phase suffered inversion (Norvick and Smith, 2001). Oceanic spreading began in the southern Tasman Sea in the Santonian (85 Ma) and slow extension caused thinning of continental crust in the Bight and Otway Basins and fault block rotation in the offshore Otway Basin (Norvick and Smith, 2001). Seafloor spreading began in the Great Australian Bight in the Early Campanian (83 Ma) (Sayers et al. 2001), while fault block rotation continued in the offshore Otway Basin in a sinistral transtensional stress regime (Norvick and Smith, 2001).

In the Late Cretaceous, the structural development of the Otway Basin diverged from that of the Gippsland and Bass Basins. While continental expansion proceeded to final breakup of Australia and Antarctica in the axis of the Otway rift and west of Tasmania, the Gippsland and Bass Basins remained as failed rifts within the continental crust of Bass Strait (Palmowski et al. 2001; St John, 2001).

At the Cretaceous-Tertiary boundary (65 Ma) sedimentation in the Otway Basin gradually changed to sag geometries, with minor faulting and broad uplift (Norvick and Smith, 2001). Tasman Sea spreading finished at the end of the Palaeocene (52-54 Ma), but slow seafloor spreading continued in the Southern Ocean (Norvick and Smith, 2001). This event led to the initiation of fast spreading in the Southern Ocean from approximately 44 Ma (Mid Eocene), causing rapid thermal subsidence and marine transgression. First ocean crust formed off the Otway Basin, which propagated southwards along the western margin of Tasmania (Royer and Rollet, 1997). The Circum-Antarctic Current became fully established in the mid Oligocene and cool-water carbonate deposition became widespread on the south-eastern Australian margin (Norvick and Smith, 2001).

At the end of the Cretaceous, the south-eastern Australian margin came under the influence of an east-west oriented dextral shear through Bass Strait, with Tasmania moving relatively westward (Fig. 5.1) (St John, 2001; Palmowski et al. 2001). This stress regime, which has continued through the Cenozoic, resolves into northwest-southeast directed compression and northeast-southwest directed tension, and was recognised as being responsible for all the major

Tertiary compressive uplifts of the southeast margin, such as the Strzelecki and Otway Ranges and the Mornington Peninsula (Hill et al. 1995; Palmowski et al. 2001; St John, 2001).

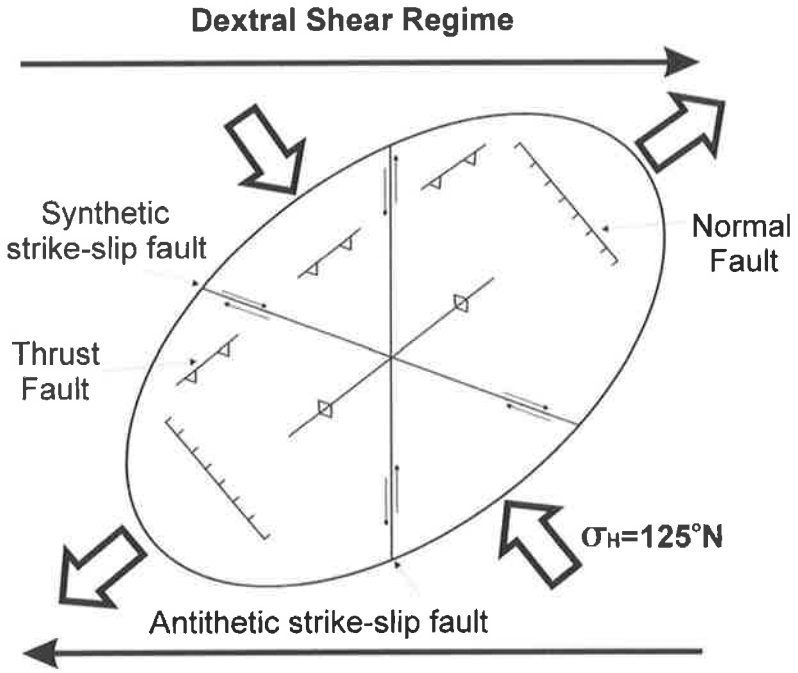

Figure 5.1. Model of the dextral shear tectonic regime that existed in the Otway Basin throughout the Tertiary. Normal faults are oriented sub-parallel to the maximum horizontal stress direction (σ_H), which, in the Gambier Sub-basin, is 125°N (Hillis et al, 1995). Synthetic and antithetic strike-slip faults are oriented at an angle of 30-45° to the normal faults.

5.1 HYDROCARBON MATURATION

Due to the lack of well data in the southern part of the Gambier Sub-basin, detailed maturity data is absent. Limitations of time and scope of this study has meant that the maturation history of the Gambier Sub-basin has been gleaned from previous studies (e.g. Hill, 1995; Williamson et al. 1996). Figure 5.2 illustrates the Mesozoic and Cenozoic stratigraphy of the Gambier Sub-basin, highlighting the source/seal and reservoir prone units recognised in the Otway Basin.

Previous hydrocarbon maturation studies (mentioned above) have been used to explain the mechanisms of basin development, the extent and timing of sedimentation, and the nature of the thermal and rift-related subsidence phases. In particular, the timing of the maturation of potential source rocks is studied in relation to the timing of faulting associated with both Cretaceous rifting and Tertiary reactivation (Williamson et al. 1996).

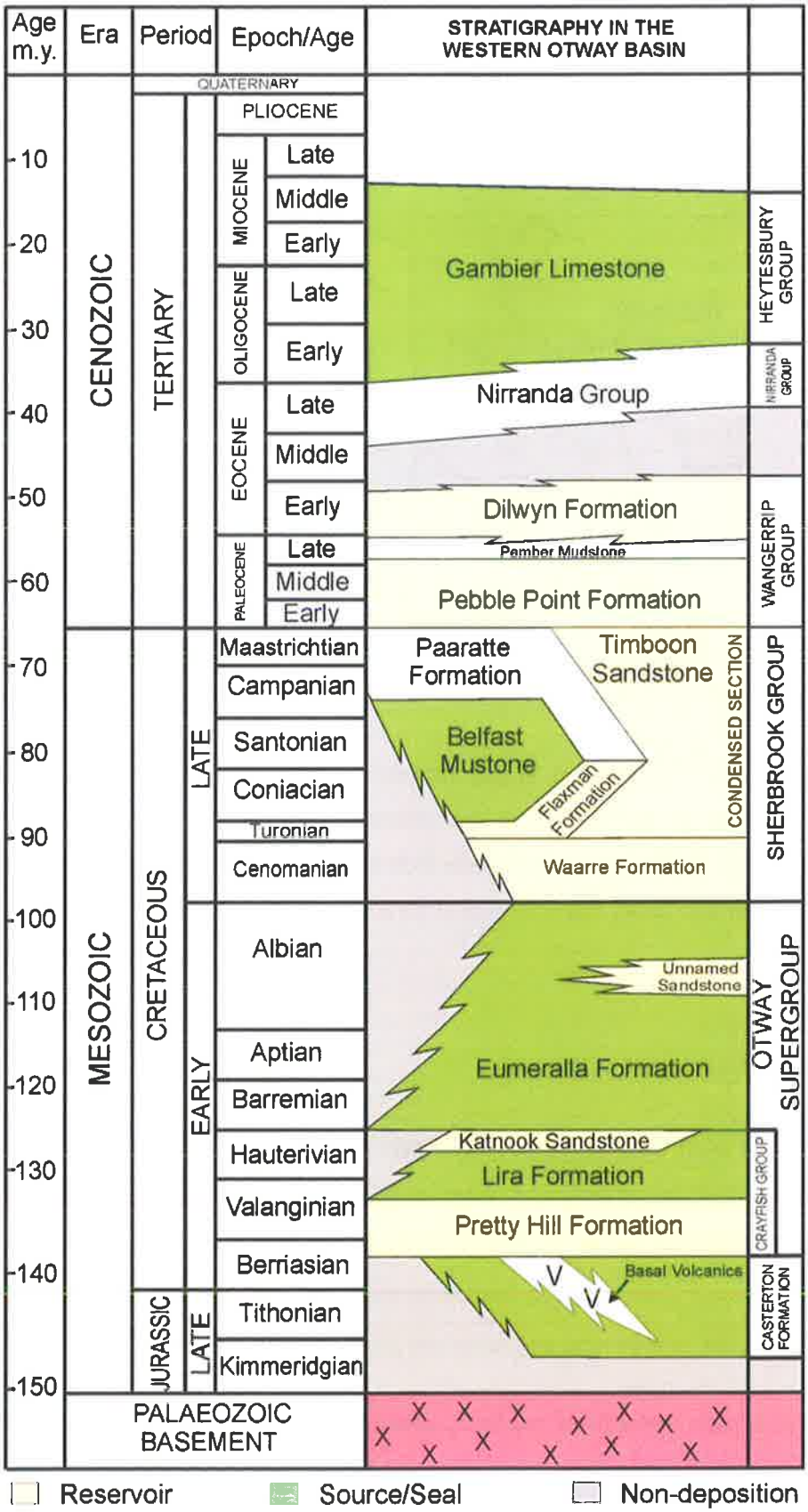

Figure 5.2 Mesozoic and Cenozoic stratigraphic chart of the Gambier Sub-basin showing source/seal and reservoir prone units (Modified from Morton et al. 1995).

5.1.1 Casterton Formation

Knowledge of the source potential of the Late Jurassic Casterton Formation is restricted to an area north of the Tartwaup Hinge Zone (Hill, 1995; Williamson et al. 1996). These sediments are Late Jurassic to Early Cretaceous interbedded non-marine siltstones, mudstones, minor coals and volcanics (Wopfner and Douglas, 1971; Morton et al. 1995). In general, the lacustrine Casterton Formation is gas to oil prone, with the richest source intervals occurring towards the base of the unit, possibly reflecting high concentrations of terrestrial detritus in localised rift lakes (Hill, 1995). Source rock analysis indicates oxidised and/or Type III kerogen in the upper part of the Casterton Formation. However, in the basal part of the formation, there is an increase in source potential and a terrestrial Type II-III kerogen is inferred (Hill, 1995).

5.1.2 Crayfish Group

Crayfish Group source rocks are non-marine Type III-IV kerogens derived from land plants with some Type II algal-rich shales present, especially in the early rift succession. Sediments of the Crayfish Group tend to be overmature for oil generation in the deeper portions of half graben and mature for gas (Fig. 5.3, Table 5.1). On the flanks of troughs they tend to be early mature to mature for oil generation whilst on basement highs they are immature to marginally mature (Hill, 1995) (Fig. 5.4, Table 5.2).

No widespread source rocks have been intersected within the Pretty Hill Formation offshore, though mature Type II-III organic matter with good source potential is locally developed within the upper part of the western Voluta Trough (McKirdy, 1987). The upper parts of the Pretty Hill Formation remain thermally immature at Crayfish 1A, and at Chama 1A and Neptune 1, parts of the Pretty Hill Formation are still within the oil window (Ro=0.7-1.3); the basal Pretty Hill Formation is overmature for oil (Ro=>1.3) (Williamson et al. 1996).

Algal-rich zones, which correspond to lake maxima, occur in mappable units and are best developed in the Early Cretaceous upper Laira Formation. They reflect a transition from the fluvial coastal plain depositional environment of the Pretty Hill Formation and lower Laira Formation to a shallow lacustrine environment in the upper Laira Formation (Hill, 1995).

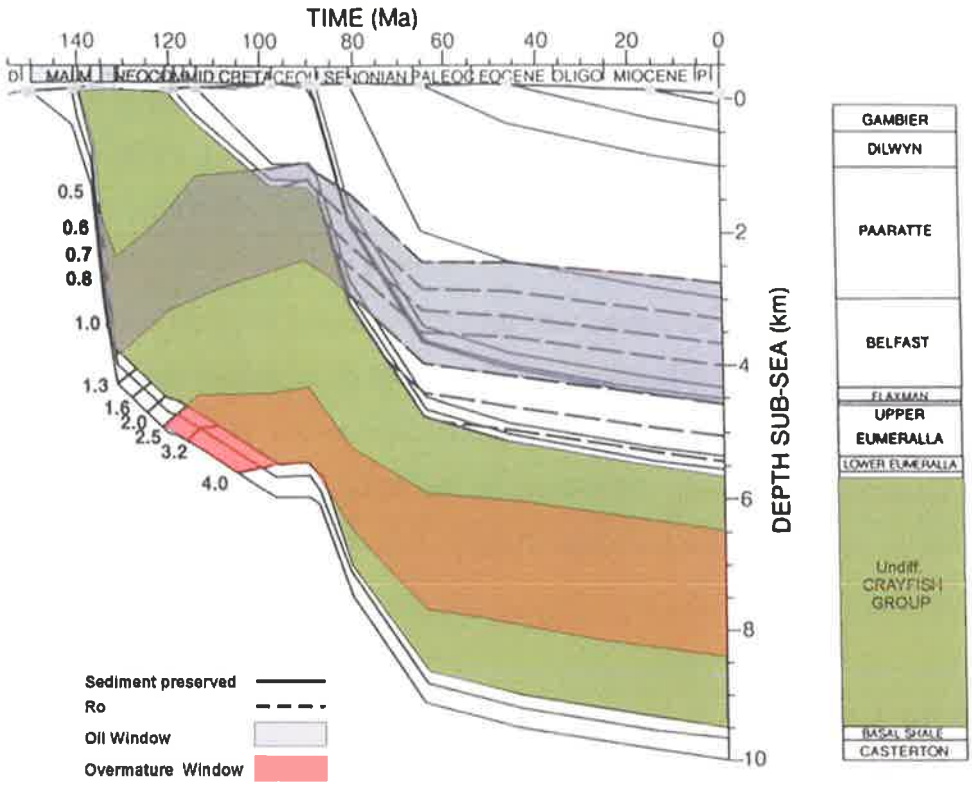

Figure 5.3 Geohistory plot based on Breaksea Reef 1 in the Voluta Trough, highlighting the maturity of the Crayfish Group in this part of the Gambier Sub-basin (modified from Hill, 1995; Kinetic Maturity Method used).

FORMATION	RV (%)	MATURITY WINDOW	DEPTH (M SUBSEA)
Paaratte Formation	0.5	Early Mature (oil)	2700
Paaratte Formation, Belfast Mudstone	0.7	Mid-mature (oil)	3500
Belfast Mudstone, Flaxman Formation, Waarre Sandstone, Upper Eumeralla Formation	1.0	Late Mature (oil)	4500
upper & lower Eumeralla Formation, Windermere Sst, undifferentiated Crayfish Group	1.3	Main Gas generation	4900
undifferentiated Crayfish Group	2.5	Overmature	6000

Table 5.1 Hydrocarbon maturity (modelled on Breaksea Reef 1) in the Voluta Trough (modified from Hill, 1995).

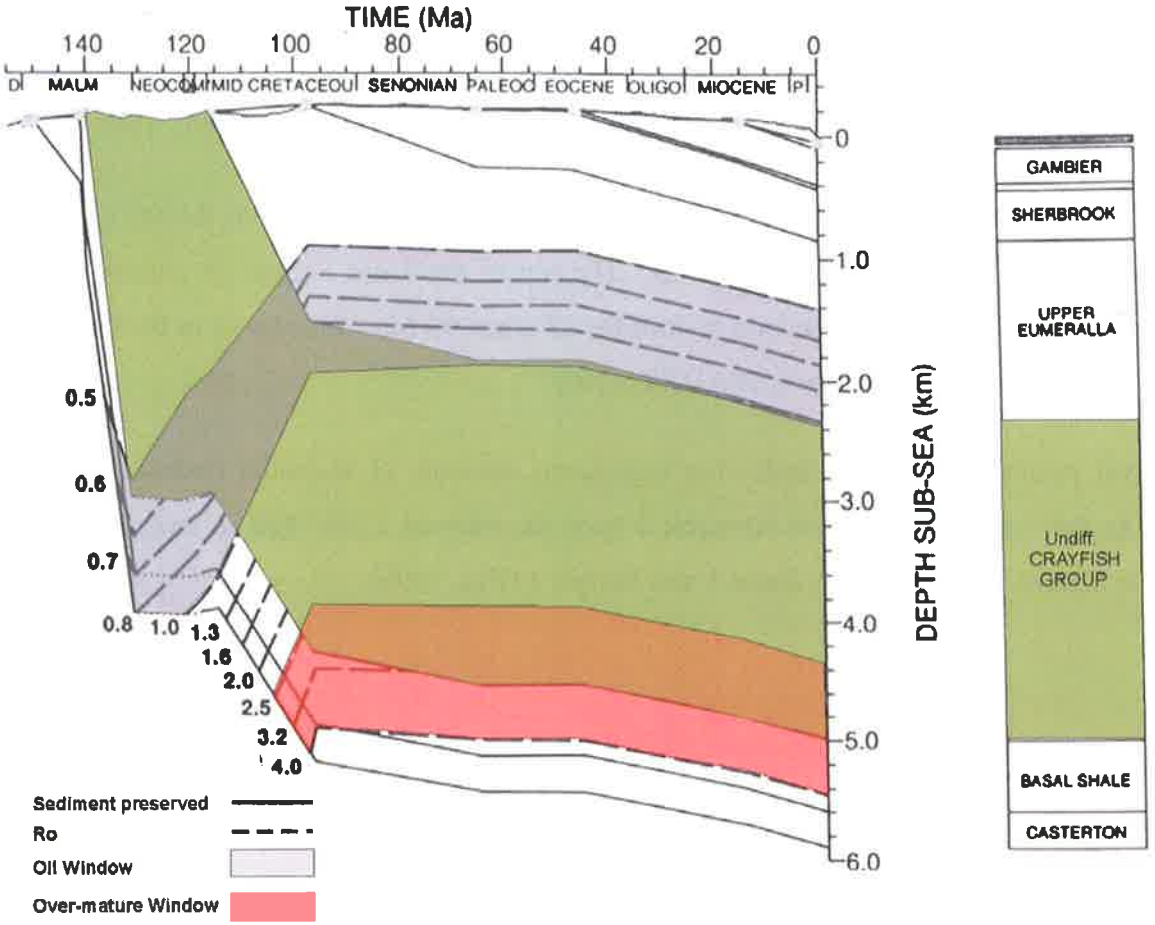

Figure 5.4 Geohistory plot based on Troas 1 in the Chama Terrace, highlighting the maturity of the Crayfish Group in this part of the Gambier Sub-basin (modified from Hill, 1995; Kinetic Maturity Method used).

FORMATION	RV (%)	MATURITY WINDOW	DEPTH (M SUBSEA)
upper Eumeralla Formation	0.5	Early Mature (oil)	1500
lower Eumeralla Formation, undifferentiated Crayfish Group	0.7	Mid-mature (oil)	2100
undifferentiated Crayfish Group	1.0	Late Mature (oil)	2650
undifferentiated Crayfish Group	1.3	Main Gas generation	3000
undifferentiated Crayfish Group	2.5	Overmature	4350

Table 5.2 Hydrocarbon maturity (modelled on Troas 1) on the Chama Terrace (Hill, 1995).

The Laira Formation predominantly comprises Type IV grading to at best Type III kerogen and is mainly gas prone. Mean TOC values vary from 0.25-2.02% (i.e. poor to good source richness) with the richest source rocks occurring along the axes of the trough (Hill, 1995).

In the Chama Terrace, the Laira Formation is mature for oil generation, with the top of the oil window occurring below depths of 2100 m. The top of the Laira Formation entered the oil window at ~105 Ma and has remained mature for oil since 95 Ma. Elsewhere in the basin, the Laira Formation is immature (Rv<0.5%) (Hill, 1995).

Rock-Eval pyrolysis results indicate that significant amounts of migrated hydrocarbons are present in the Laira Formation in Katnook 3 over the interval 2200-2800 m and, to a lesser extent, in Chama 1A, Katnook 2, Zema 1 and Sawpit 1 (Hill, 1995).

5.1.3 Eumeralla Formation

One third of the total Eumeralla Formation source interval is characterised by thin bituminous coal seams up to 1 m thick. Tupper et al. (1993) identified two broad source intervals on the Chama Terrace. The lower occurs within the *Pilosisporites notensis* palynological zone and has a maximum thickness of 140 m in Geltwood Beach 1 and Chama 1A. It is absent from wells drilled close to the basin margin. The upper interval is less well developed and occurs at the base of the *Crybelosporites striatus* zone (Hill, 1995). It has a maximum thickness of 120 m in Geltwood Beach 1.

TOC and Rock-Eval analyses consistently demonstrate marked differences in kerogen type between the lower Eumeralla source intervals and the siltstone and mudstone dominated upper Eumeralla Formation. In the Chama Terrace, coal is best developed in the *P. notensis* source interval (lower Eumeralla Formation) (Tupper et al. 1993) where TOC values and potential yield indicate excellent source richness (mean TOC=31%). In contrast, upper Eumeralla source rocks have low to moderate organic richness (mean TOC=1%) and poor to fair genetic potential (Hill, 1995).

The *P. notensis* interval comprises Type II-III kerogen and is potentially capable of generating oil and gas. Source quality in the upper Eumeralla Formation deteriorates indicating gas-prone Type IV kerogen (Hill, 1995).

The most basinward intersection of the Eumeralla Formation occurs at the southern margin of the Chama Terrace where the sedimentary package thickens and improves in source quality. The extent and likely direction of source quality improvement, however, is unknown although the observed thickening of the fluvio-lacustrine sequence to the south may provide a clue (Hill, 1995).

Tupper et al. (1993) concluded that mid-mature oil and/or wet gas generation from the lower Eumeralla Formation can be expected from 0.7-1.0% Rv, peak oil and wet gas generation from 1.0-1.3% Rv, and dry gas generation from 1.3% Rv onwards (Hill, 1995).

Thermal modelling of Troas 1(Fig. 5.5) indicates that the lower Eumeralla Formation source interval has not yet reached peak oil generation but has been early mature for oil since 96 Ma. Only in the Voluta Trough, where there is a substantial thickening of Sherbrook Group sediments, does the lower Eumeralla Formation source interval enter the zone of peak oil generation (Hill, 1995, Williamson et al. 1996). Thermal modelling in the inner Voluta Trough indicates that the lower Eumeralla Formation entered the oil window in the Late Albian (~100 Ma), reaching peak maturity for oil at the close of the Sherbrook Group deposition, and has increased only marginally in maturity from the Tertiary to the present day (Fig. 5.6). This highlights the importance of a thick Sherbrook Group as a mechanism for elevating and retaining heat flow (Hill, 1995).

5.1.4 Belfast Mudstone

TOC ranges from fair to very good with an observed increase in source richness in the southern part of the Gambier Sub-basin in the vicinity of Breaksea Reef 1. Source quality and richness improve to the south and more favourable source rocks could occur in the deeper offshore areas of the Voluta Trough.

Geochemical data indicate a Type IV grading at best to Type III kerogen (Figs. 5.6 and 5.7). The Belfast Mudstone is composed of terrigenous DOM rich in inertinite and lean in vitrinite. Gravestock et al. (1986) likened the Sherbrook Group to the Tertiary of the Niger Delta. Prodelta muds of the Niger Delta are commonly of Type III and to a lesser extent Type II kerogen. A key to the viability of the Belfast Mudstone as an oil source may be to delineate a more distal facies to the south of Breaksea Reef 1 (Hill, 1995).

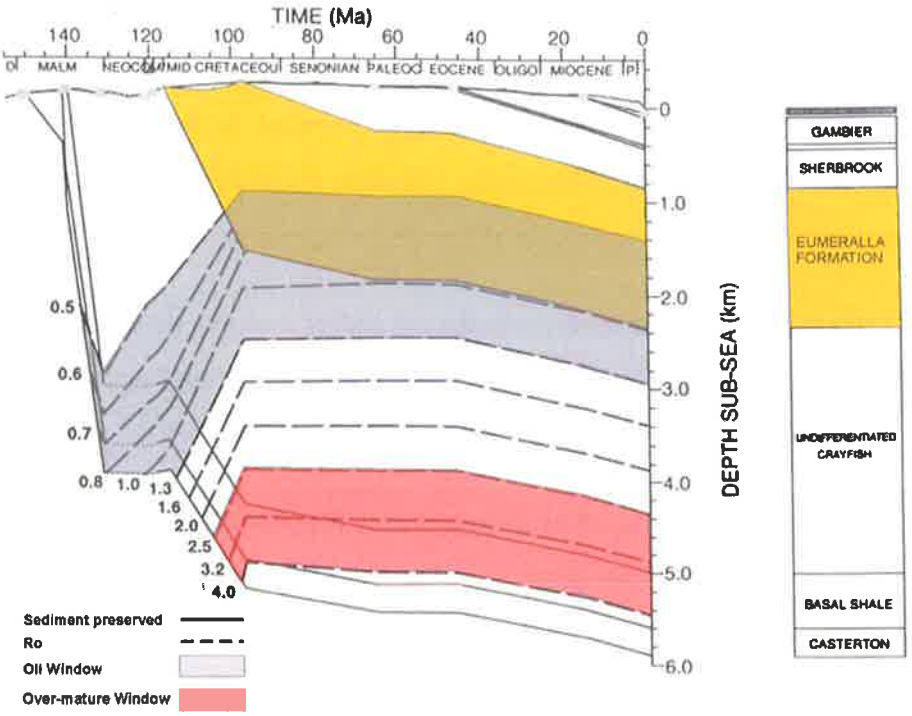

Figure 5.5 Geohistory plot based on Troas 1 in the Chama Terrace, highlighting the maturity of the Eumeralla Formation in this part of the Gambier Sub-basin (modified from Hill, 1995; Kinetic Maturity Method used).

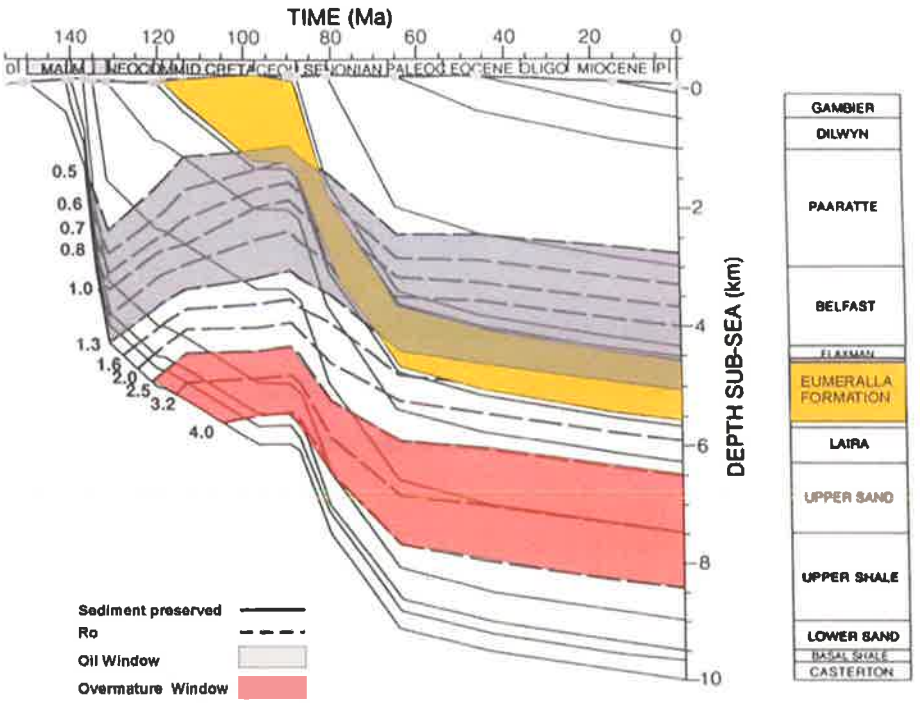

Figure 5.6 Geohistory plot based on Breaksea Reef 1 in the Voluta Trough, highlighting the maturity of the Eumeralla Formation in this part of the Gambier Sub-basin (modified from Hill, 1995; Kinetic Maturity Method used).

HI values are highly variable and indicate that the Belfast Mudstone is predominantly gas prone, although some potential to generate liquids is present (McKirdy, 1987; O'Brien and Heggie, 1989; Hill, 1995).

Maturity modelling indicates the Belfast Mudstone is mid-mature for oil generation only in the offshore Voluta Trough in the vicinity of Breaksea Reef 1 and Argonaut 1, whilst Copa 1 is immature (Fig. 5.7). The top of the oil window ranges between 3500 and 4500 m throughout the central Voluta Trough, with peak generation for oil occurring in the deeper parts of the trough. The Belfast Mudstone entered the base of the oil window at ~70 Ma and remained in that window until the present day (Fig. 5.8) (Hill, 1995).

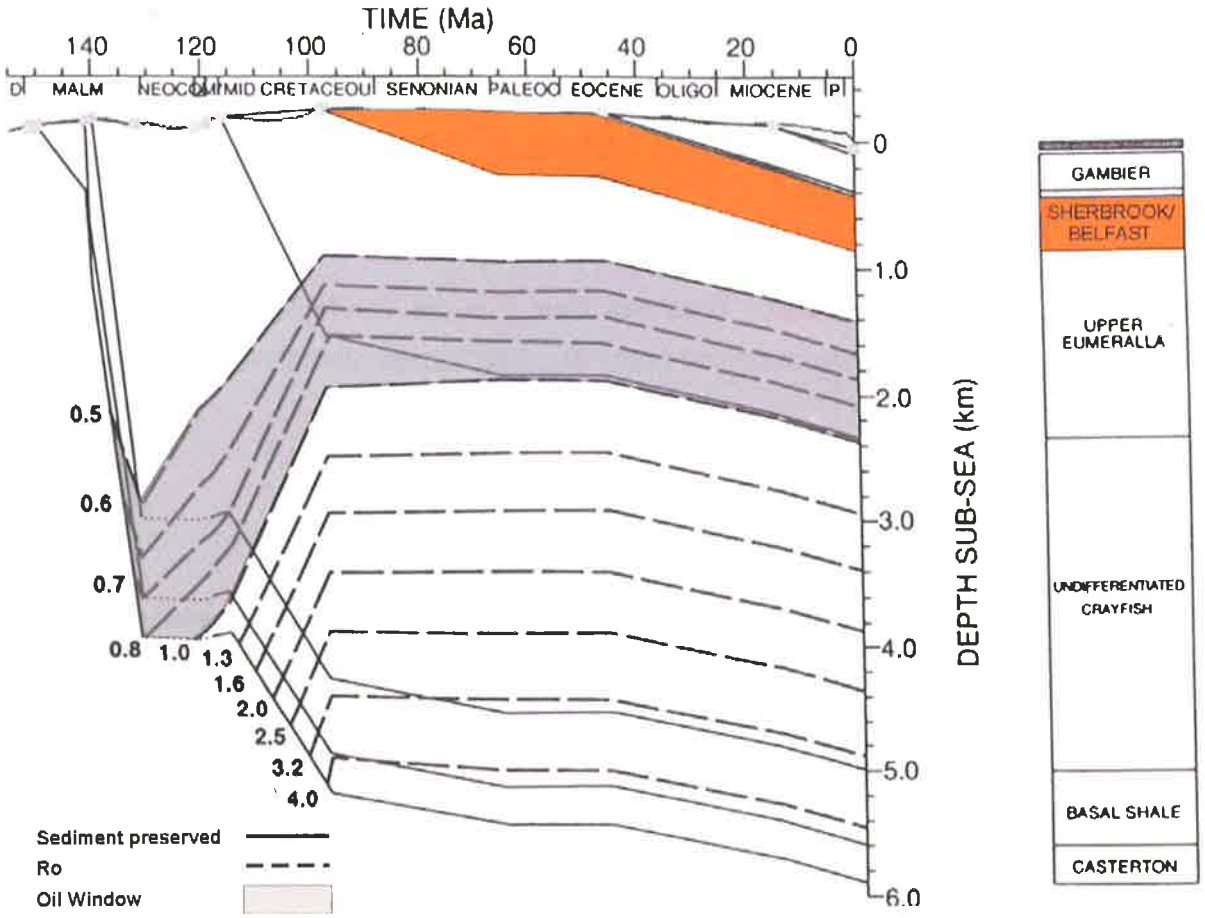

Figure 5.7 Geohistory plot based on Troas 1 in the Chama Terrace, highlighting the immaturity of the Belfast Mudstone in this part of the Gambier Sub-basin (modified from Hill, 1995; Kinetic Maturity Method used).

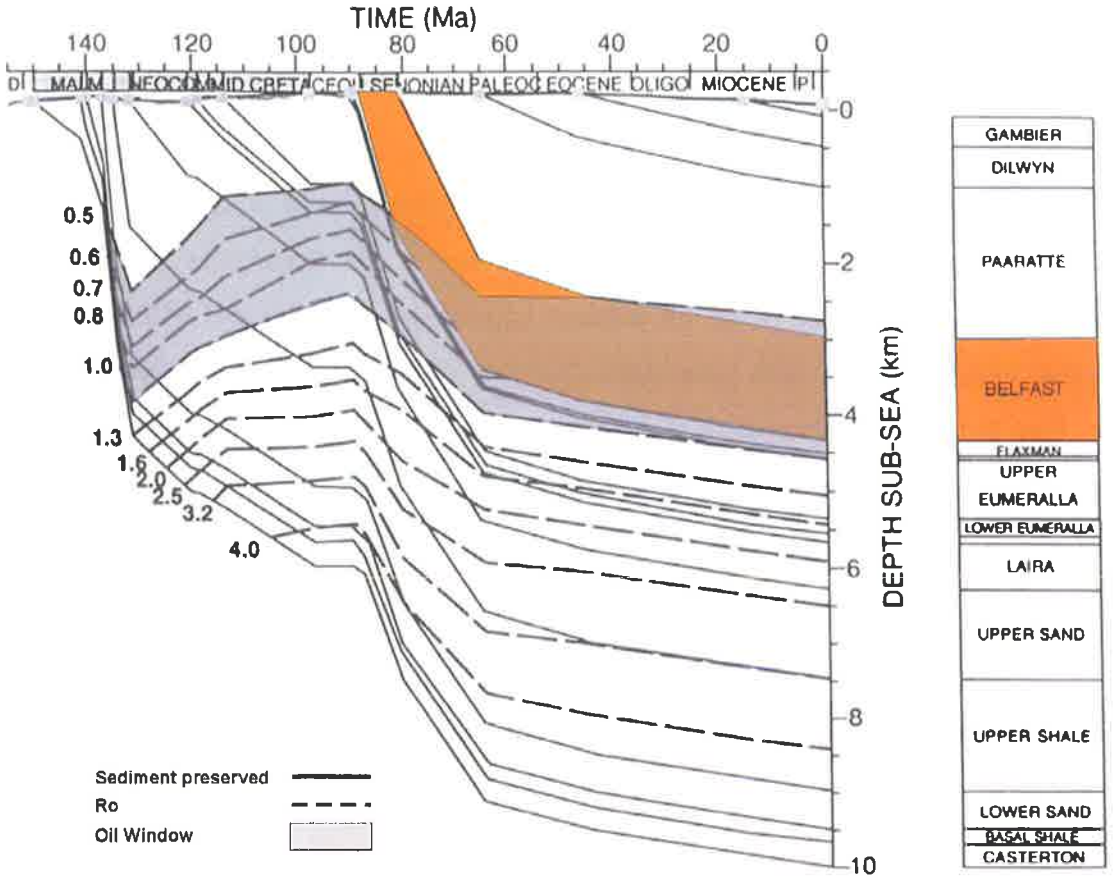

Figure 5.8 Geohistory plot based on Breaksea Reef 1 in the Voluta Trough highlighting the maturity of the Belfast Mudstone (modified from Hill, 1995; Kinetic Maturity Method used).

5.1.5 Cenozoic sediments

Cenozoic sediments in the Gambier Sub-basin are immature for hydrocarbon generation (Hill, 1995).

5.2 FAULTING

The seismic data suggest that the Voluta Trough had significantly developed by the end of the Late Cretaceous and acted as the depocentre for clastic Cenozoic sediments. From the end of the Late Cretaceous until the beginning of the Oligocene, the Chama Terrace was a bypass margin for sediments and experienced large amounts of erosion. This simultaneous sediment loading in the Voluta Trough and erosion on the Chama Terrace during the Late Palaeocene and

Early Eocene could very well have created a positive feedback system, further enhancing subsidence in the eastern part of the sub-basin and erosion in the west.

Seismic interpretation revealed the Late Palaeocene LST/TST 1.1 was deposited during active fault movement resulting in thickened sedimentary sections on the down-thrown side of the fault, adjacent to the normal fault plane. Late Cretaceous sediments immediately underlying the Cenozoic section show no suggestion of growth sedimentation, which suggests they have been affected by post-depositional faulting.

While there is evidence of syn-depositional fault movement during the Late Palaeocene and into the earliest Eocene, there is little indication of growth faulting during deposition of Supersequences 2.0-4.0 (*M. diversus*). These Early Eocene sediments appear to have been displaced by reactivation of the Cretaceous-Palaeogene fault system some time between the Middle Eocene and beginning of the Oligocene. The most likely time of fault reactivation is in the Middle Eocene when seafloor spreading was aborted in the Tasman Sea, resulting in an increase in spreading rate at the Otway rift axis, the stress of which probably caused reactivation of existing fault systems. This, in turn, led to thermally induced subsidence and establishment of cool-water carbonate deposition on the continental shelf.

Faults terminating within the carbonates show little displacement on seismic data. These faults may have been subject to strike-slip movement during the Oligocene and Early Miocene, the vertical displacement of which are not imaged on seismic data. This is likely the result of a dextral shear regime in the Sub-basin during the Tertiary (Fig. 5.1).

5.2.1 Magnitude of faulting during the Cenozoic

1) **K-P Boundary Faults** (red) displace the Cretaceous-Palaeogene Boundary but do not penetrate higher into the stratigraphic section. These faults dominate the mid to outer shelf in the Voluta Trough and the western Chama Terrace (Fig. 5.9, 5.10). Ten K-P Boundary faults were correlated between adjacent seismic lines in the Voluta Trough (R1-R10), however many more were identified on seismic data but were not correlated. These faults were active during the Late Cretaceous and Palaeocene during deposition of Supersequence 1 and have a mean throw of 94 m. Dips range from 35-77° and dominant dip direction is to the south (Fig. 5.11 & 5.12).

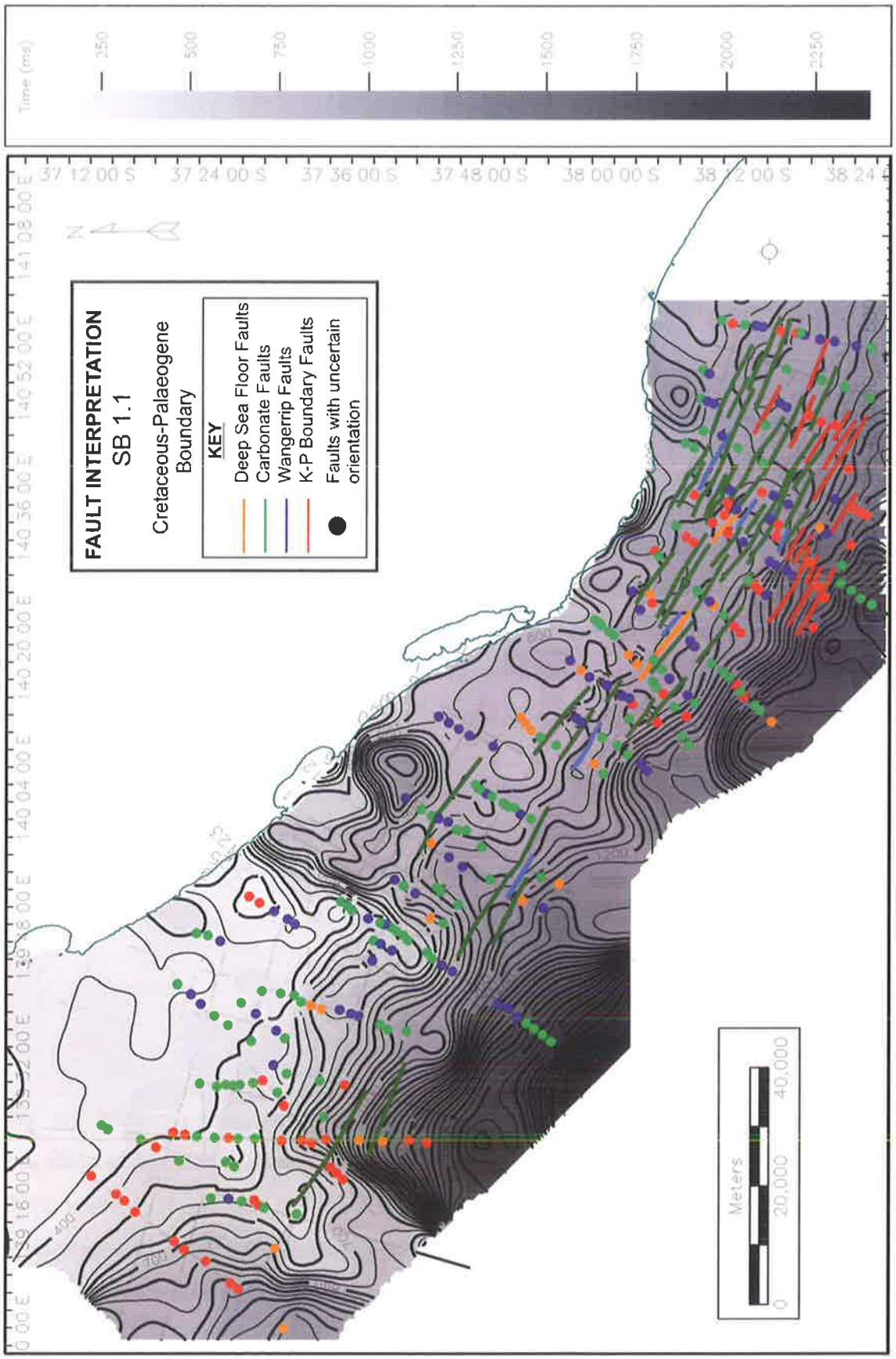

Figure 5.9 Fault interpretation map of the Cretaceous-Palaeogene boundary (SB 1.1).

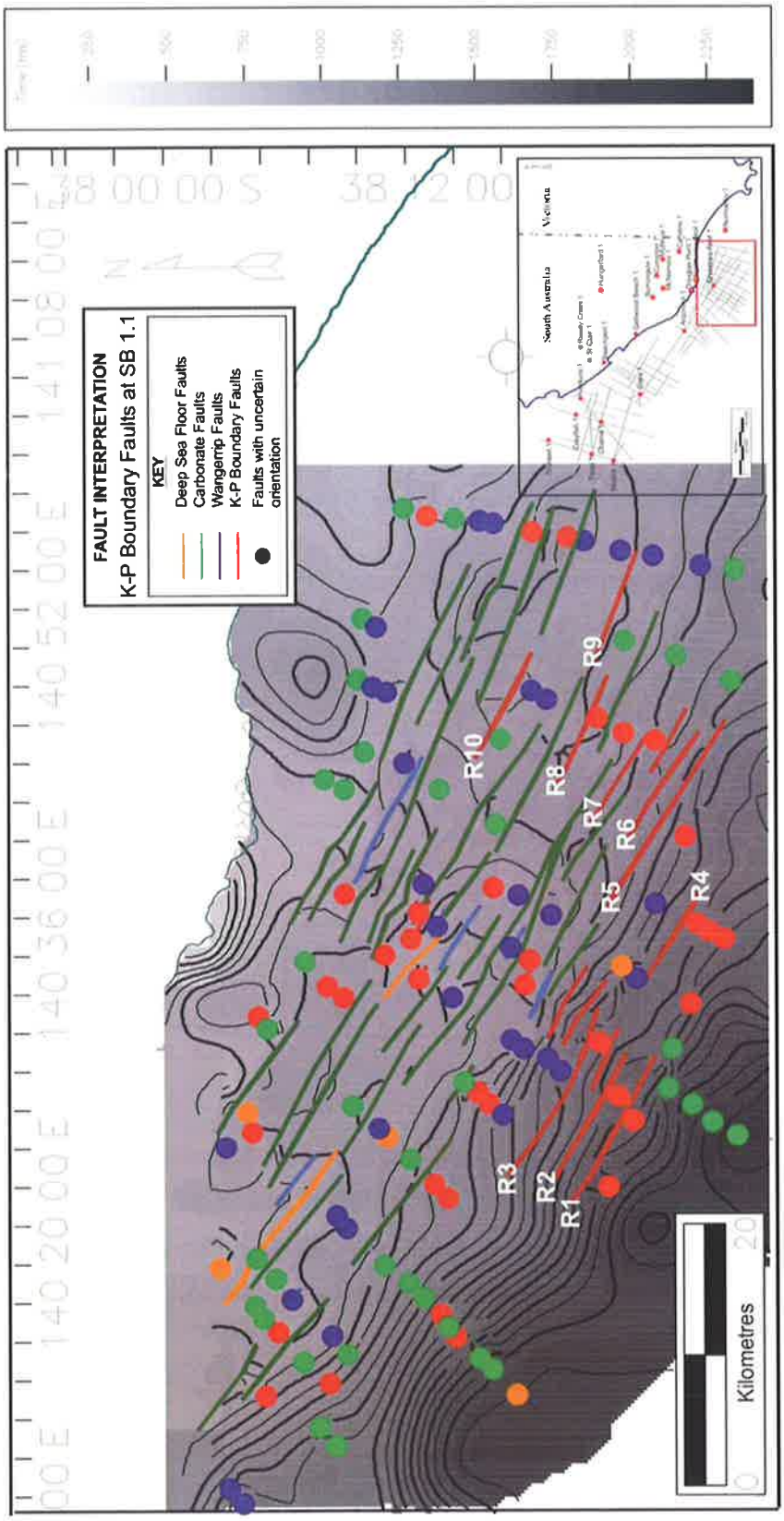

Figure 5.10 Cretaceous-Palaeogene boundary fault interpretation showing the location of K-P boundary faults (R1-R10). Those faults with uncertain orientation that were not correlated to adjacent lines are represented by dots.

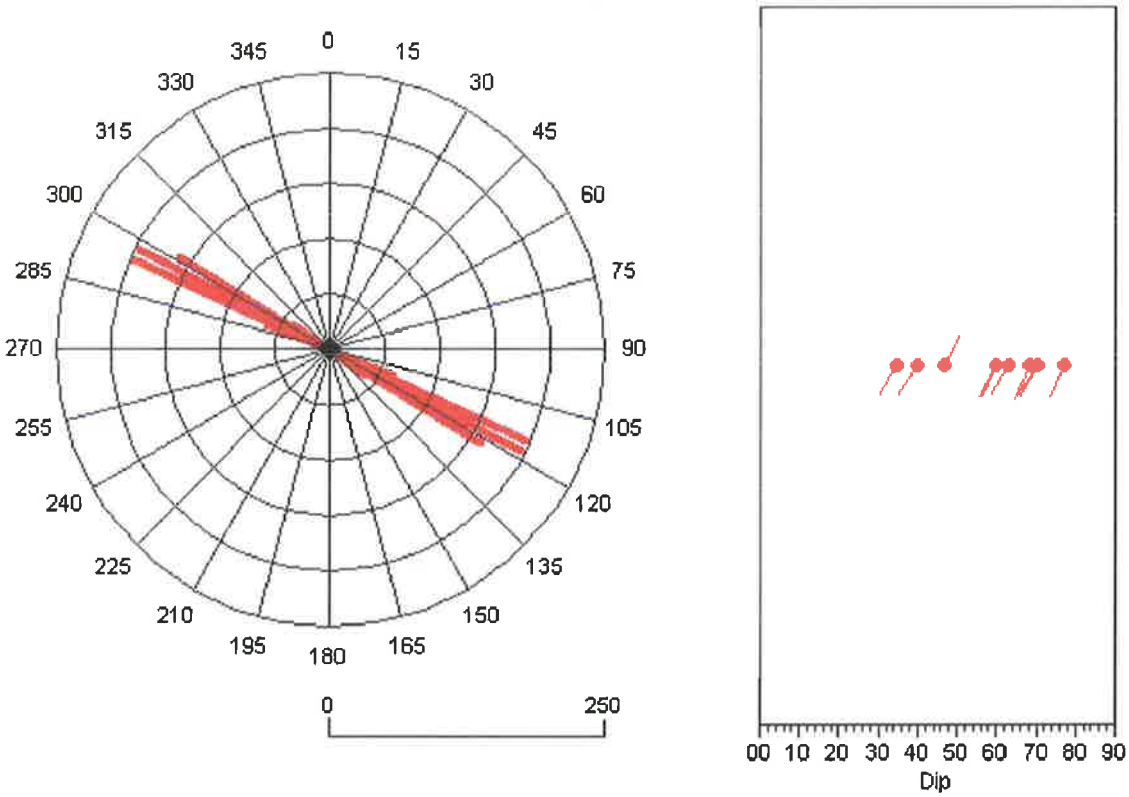

Figure 5.11 Throw-weighted rose plot and "tadpole" plot showing the strike and dips of K-P boundary faults. Petal lengths in the rose plot represent the frequency of faults with a particular strike orientation and the bin size (petal width) is 1°. Mean strike orientation = 298° (NW-SE); standard deviation = 3.45; Total cumulative throw = 744 m; n=10.

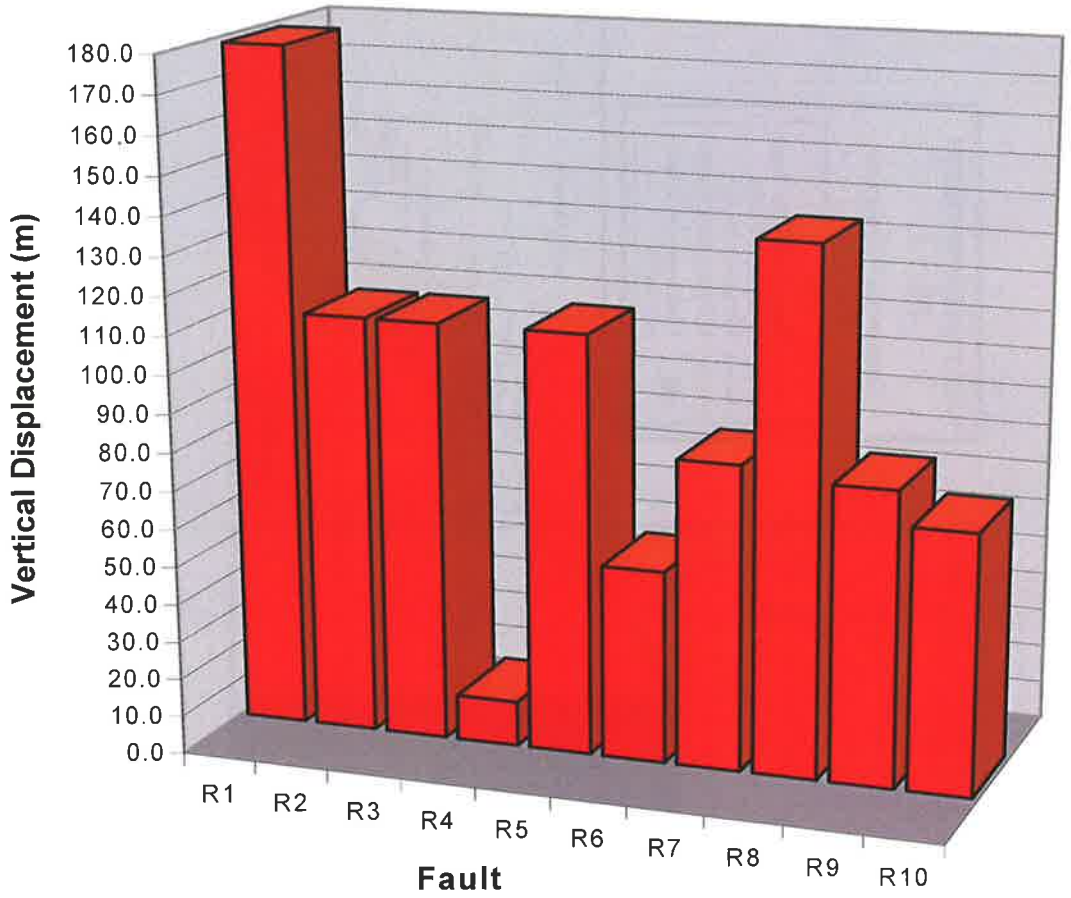

Figure 5.12 Vertical displacement of K-P boundary faults in the Voluta Trough. These values represent the total cumulative movement of faults since the end of the Cretaceous and up to the end of the Palaeocene.

2) **Wangerrip Faults** (blue) terminate within the clastic sediments of the Wangerrip Group. Only four faults were correlated with any certainty in the Voluta Trough because the Wangerrip faults are often shallow and have experienced little throw (B1-B4) (Fig. 5.13). These faults were most likely re-activated during the Middle to Late Eocene after deposition of Supersequences 2, 3 and 4, and have a mean throw of 77 m. These faults dip generally dip towards the south at angles between 43-63° (Fig. 5.14 & 5.15).

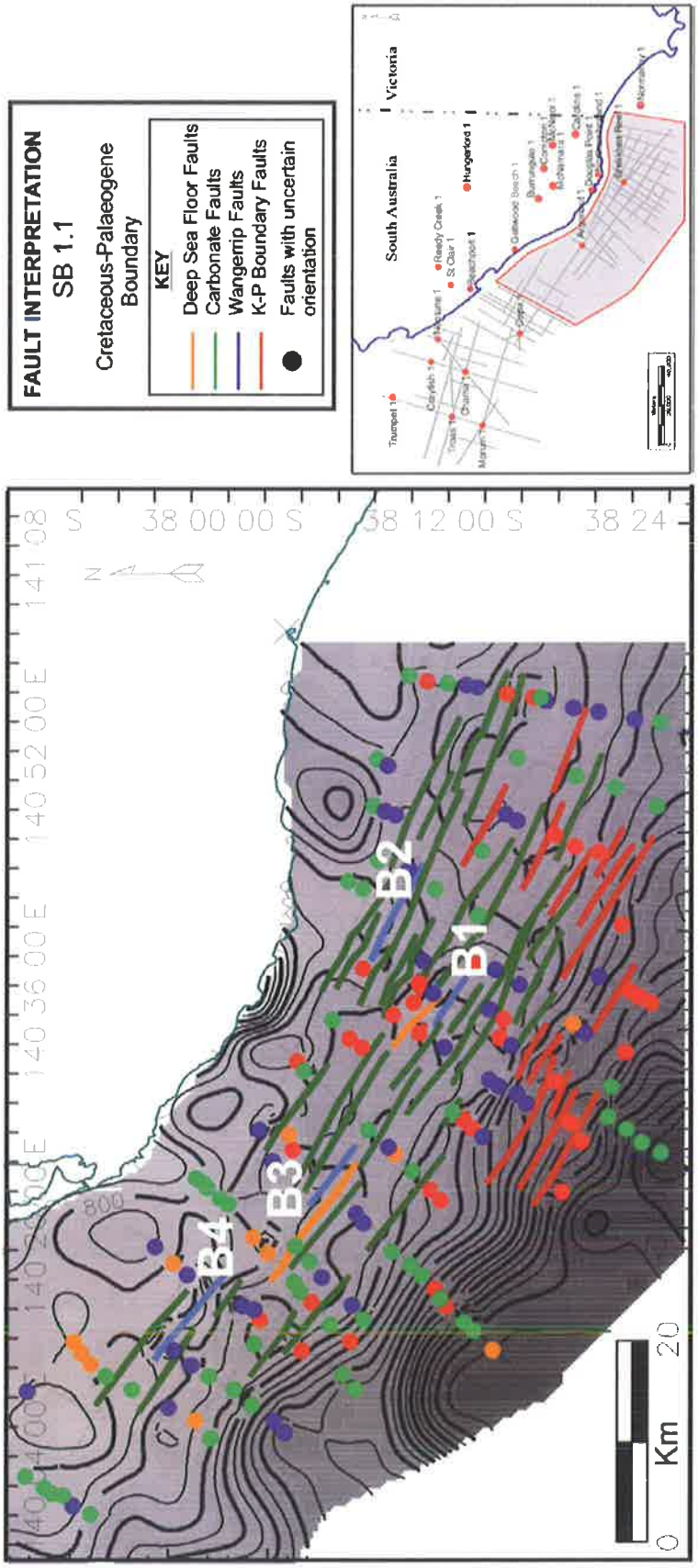

Figure 5.13 Cretaceous-Palaeogene boundary fault interpretation showing the location of Wangerrip faults (B1-B4).

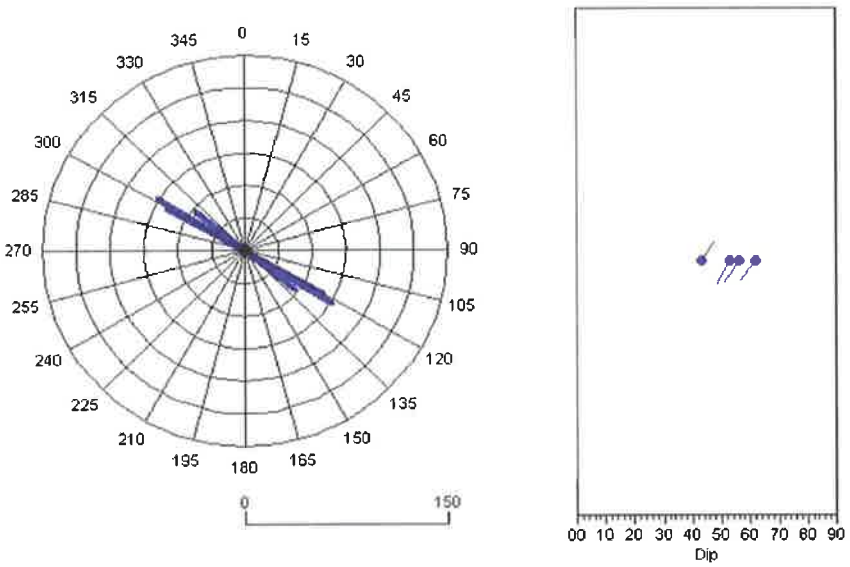

Figure 5.14 Throw-weighted rose plot and "tadpole" plot showing the strike and dips of Wangerrip faults. Petal lengths in the rose plot represent frequency and the bin size (petal width) is 1°. Mean strike orientation = 300° (NW-SE); standard deviation = 3.47; Total throw = 243 m; n=4.

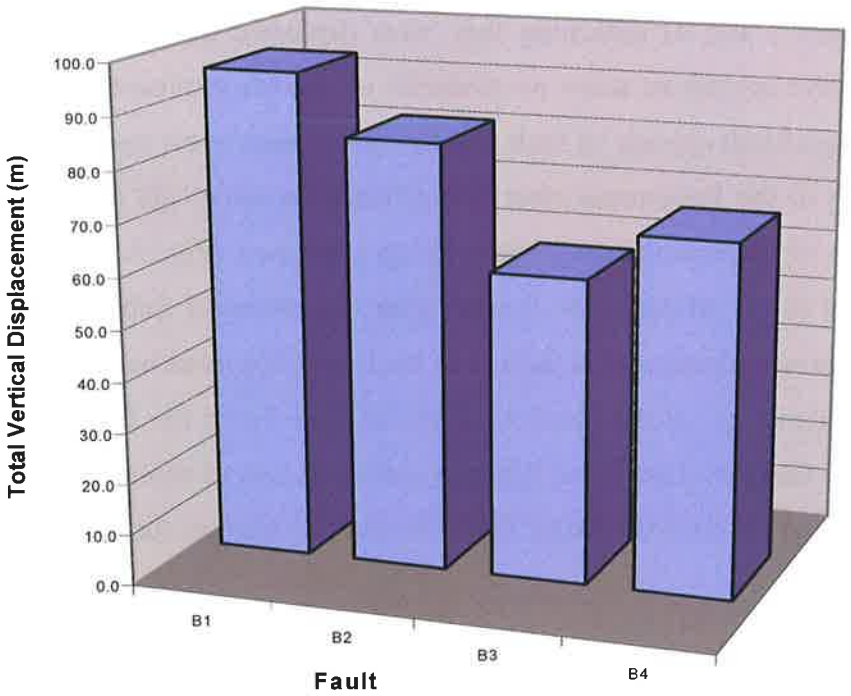

Figure 5.15 Total vertical displacements of Wangerrip faults in the Voluta Trough. These values represent the total cumulative movement experienced by these faults between the end of the Cretaceous and the Middle Eocene, however movement is likely to have been episodic rather than slow and continuous.

3) **Carbonate Faults** (green) terminate within the Gambier Limestone. These are the most prolific faults in the Gambier Sub-basin and have been correlated in the Voluta Trough and on the Chama Terrace, although the seismic line spacing on the Chama Terrace is too broad to correlate faults with any certainty. Analysis of this fault set can give the most comprehensive history of fault movement during the Cenozoic in the Gambier Sub-basin as these faults can be interpreted to near the seafloor and they often penetrate deeply into the basin, intersecting Early Cretaceous sediments near the decollemont surface at approximately 7 seconds TWT.

34 Carbonate faults (G1-G34) were correlated and are interpreted to strike in a northwest-southeast direction (Fig. 5.16). These are all normal faults that were last active during the Middle-Late Miocene and have experienced a mean cumulative throw of 162 m during the Cenozoic. Carbonate Faults dominantly dip towards the south at angles of 36-74° (Figs. 5.17 & 5.18).

Seismic data illustrate that Late Cretaceous sediments immediately underlying the K-P boundary are only affected by post-depositional faulting (i.e. no growth sedimentation is apparent). Sediments of Supersequence 1 show evidence of growth sedimentation on seismic data (see Chapters 2 and 4) indicating they were deposited during active fault movement, however successive sequences show no evidence of growth sedimentation. Hence it can be implied that a significant episode of fault movement occurred at the end of the Cretaceous and in the early part of the Palaeocene after Late Cretaceous sediments had been deposited and while sediments of Supersequence 1 were being deposited (Fig. 5.19). Other episodes of faulting occurred in the Middle-Late Eocene after deposition of Supersequences 2, 3 and 4 within the *M.diversus* palynozone; at the end of the Early Oligocene before the formation of SB 6.1, the initial submarine canyon incision event (Chapter 3); in the Early-Mid Miocene after deposition of the Gambier Limestone (Supersequence 6) had terminated in the Gambier Sub-basin; and recent movement recorded by faults that have penetrated the seafloor.

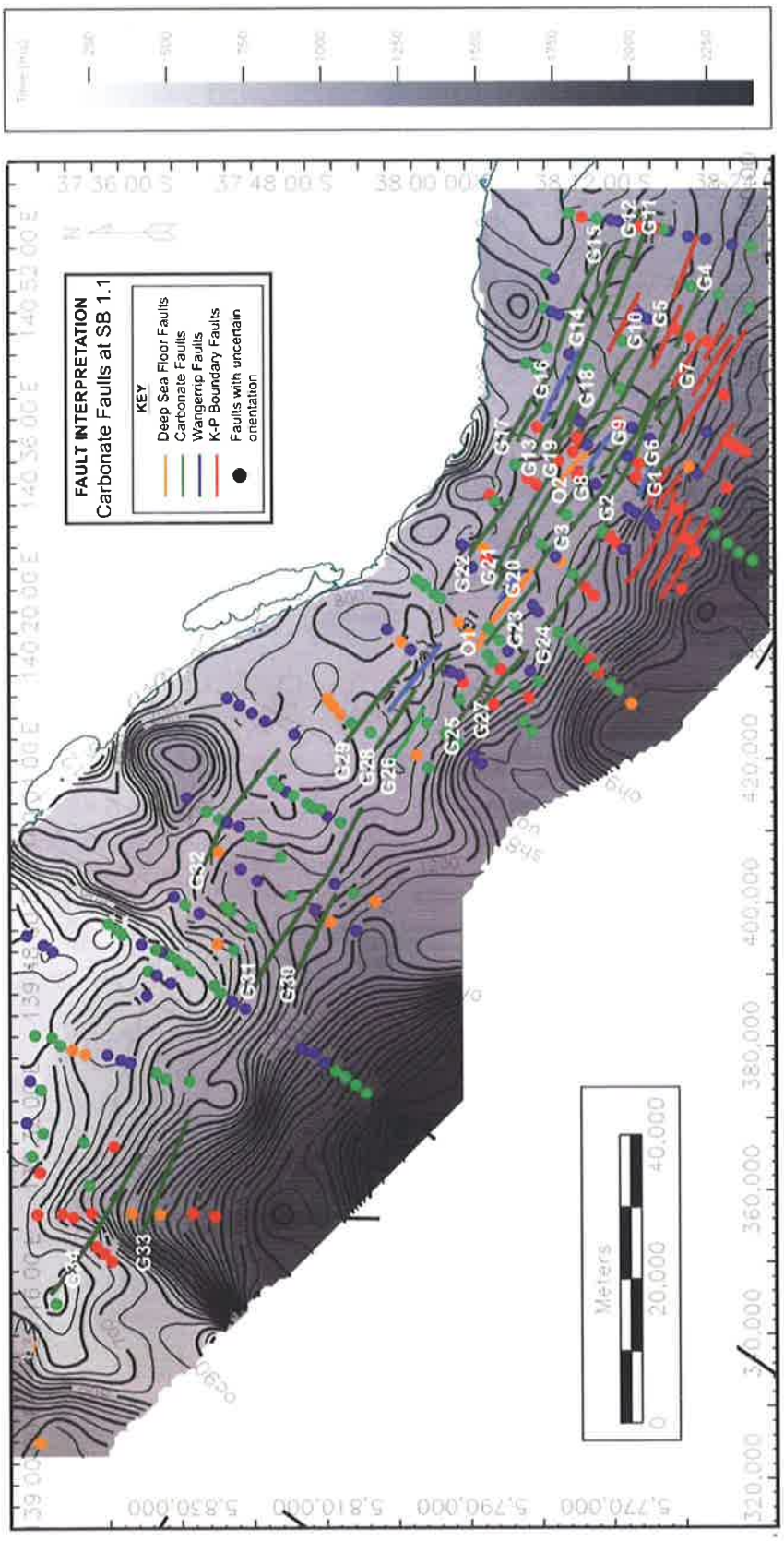

Figure 5.16 Cretaceous-Palaeogene boundary fault interpretation of Carbonate (G1-G34) and Deep Sea Floor Faults (O1-O2). Those faults with uncertain orientation that were not correlated to adjacent lines are represented by dots.

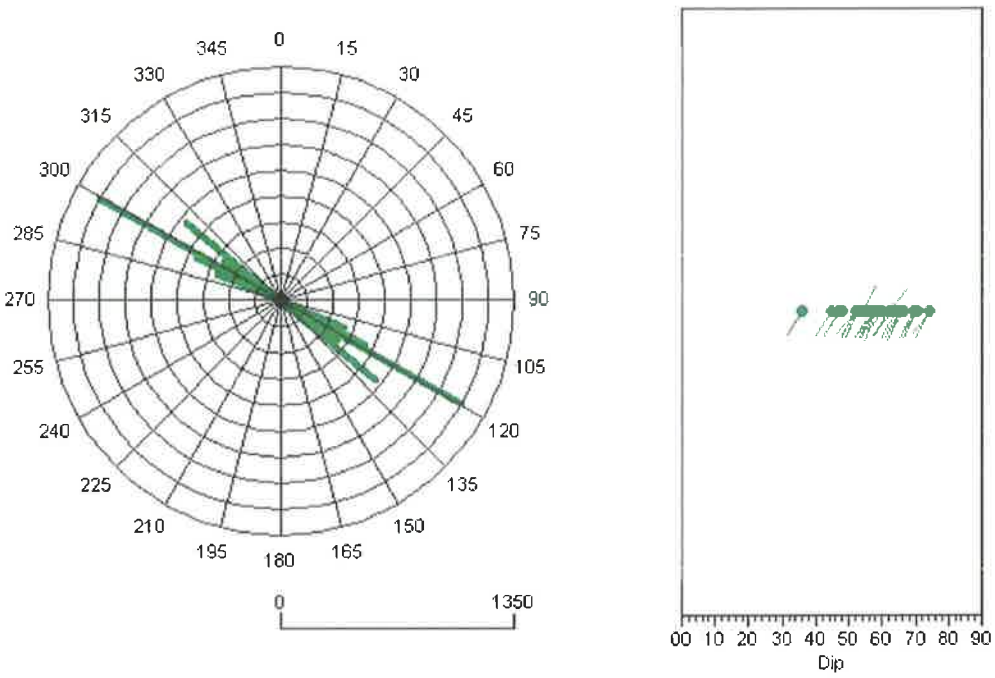

Figure 5.17 Throw-weighted rose plot and "tadpole" plot showing the strike and dips of the Carbonate faults. Petal lengths in the rose plot represent frequency and the bin size (petal width) is 1°. Mean orientation = 300° (NW-SE); standard deviation = 5.43; Total throw = 4403 m; n=34.

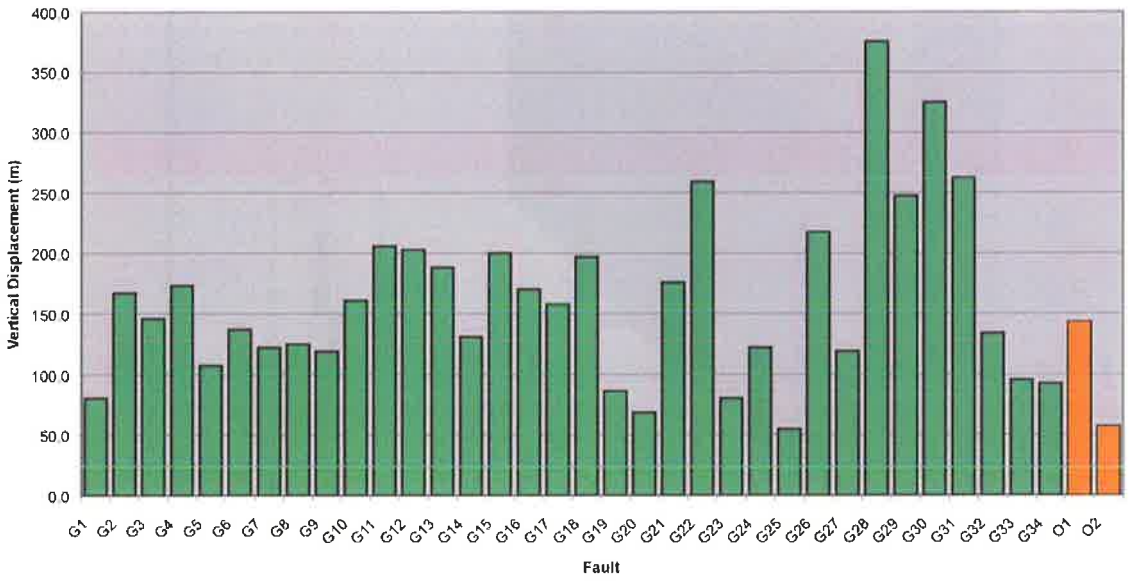

Figure 5.18 Total vertical displacement of Carbonate faults (green bars) and Deep Seafloor faults (orange bars). These values represent the total cumulative displacement experienced by the faults between the end of the Cretaceous and up to the Middle Miocene (carbonate faults) and recent movement (deep seafloor faults).

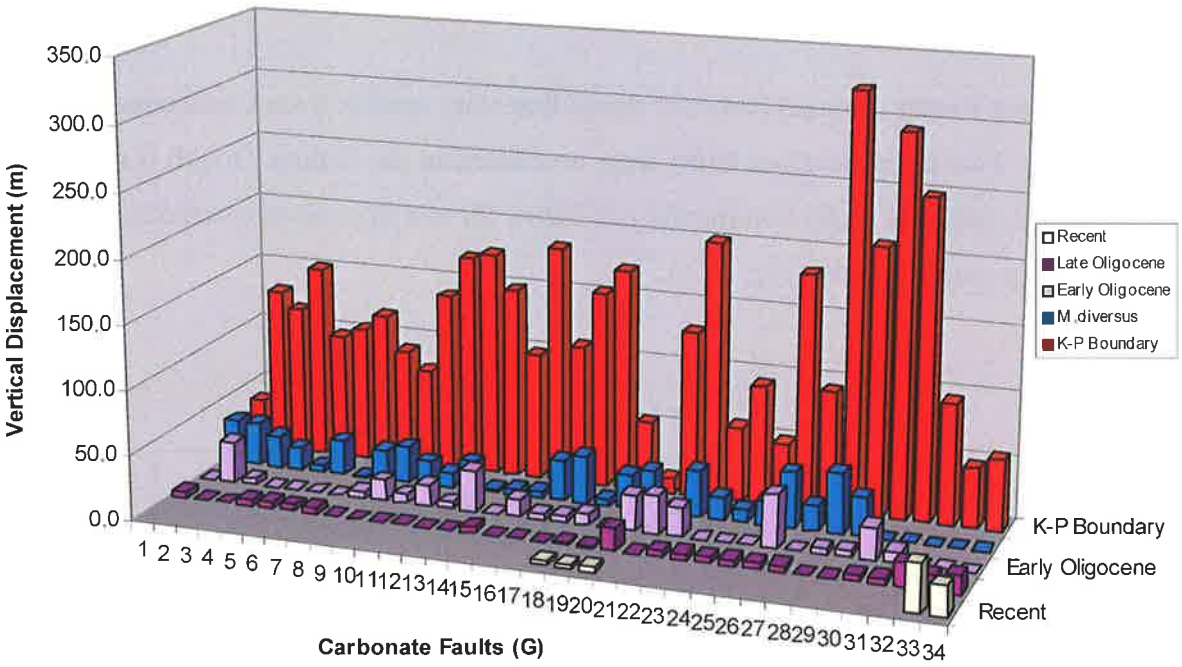

Figure 5.19 This graph represents the relative amount of vertical displacement experienced by the Carbonate faults through time: (1) at the K-P boundary (i.e. movement at the end of the Cretaceous and in the early Palaeocene: red bars); (2) during the Mid-Late Eocene (i.e. after deposition of Wangerrip Group sediments: blue bars); (3) at the end of the Early Oligocene (i.e. movement experience before formation of SB 6.1: light purple bars); (4) during the Late Oligocene and Middle Miocene (i.e. movement experience after formation of SB 6.1: dark purple bars); and (5) recent movement on faults as indicated by intersection of the sea floor (yellow bars).

The Carbonate Faults experienced the most movement during reactivation at the end of the Cretaceous and during the Early Palaeocene with the exception of G33 and G34, which are located on the outer shelf of the Chama Terrace (Fig. 5.19). In the Voluta Trough, fault movement at the end of the Cretaceous was the main contributor to the total throw experienced by the faults followed by movement in the Middle to Late Eocene and then in the Oligocene (Fig. 5.19).

The Cenozoic section on the Chama Terrace is very thin and faults G33 and G34 have penetrated the sea floor in places along their length indicating they have experienced significant recent reactivation.

4) **Deep Seafloor Faults** (orange) penetrate the sedimentary section from Cretaceous sediments to the seafloor. Two Deep Seafloor faults were correlated in the Voluta Trough (O1 and O2); however, a few carbonate faults terminating just below the sea floor were correlated along their length with deep seafloor faults (Fig. 5.16).

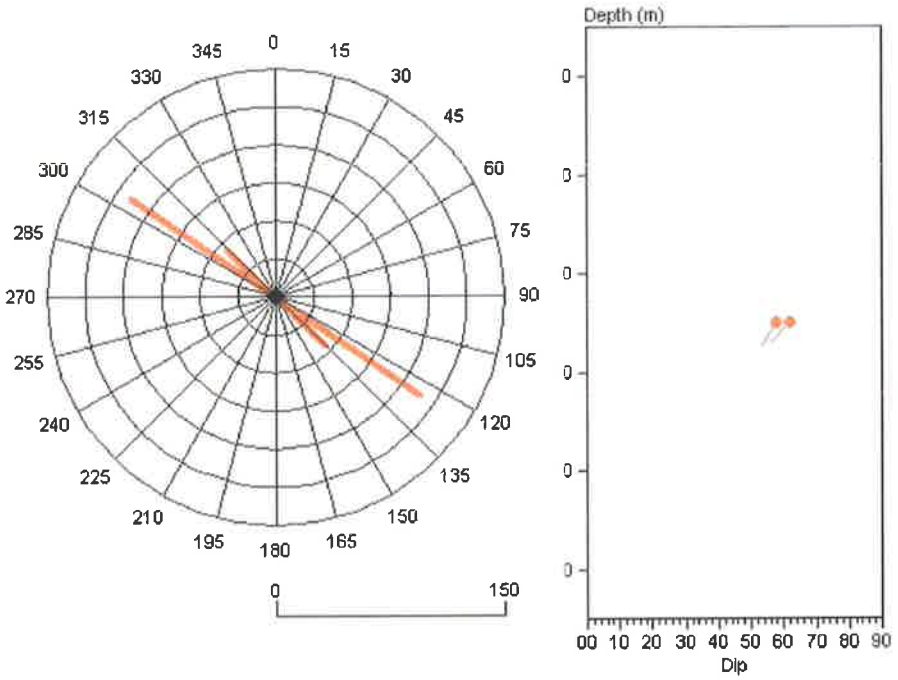

Figure 5.20 Throw-weighted rose plot and "tadpole" plot showing the strike and dips of the Carbonate faults. Petal lengths in the rose plot represent frequency and the bin size (petal width) is 1°. Mean strike orientation = 307° (NW-SE); standard deviation = 4.45; Total throw = 159 m; n=2.

5) **Seafloor Faults** (yellow) are shallow, recent faults that cut the sea floor but do not persist with depth into the underlying sedimentary section. They are rarely seen to penetrate below the base of the carbonates. Where the throw is above seismic resolution there is often a scarp at the seafloor. Due to the shallow nature of these faults they are not likely to be laterally persistent and were therefore not correlated between adjacent seismic lines in this study.

5.2.2 Timing of faulting during the Cenozoic

Cumulative vertical displacement (throw) was plotted against time to determine when the faults were most likely active. This technique is unable to account for the strike-slip movement that occurred perpendicular to the seismic line and therefore is not expressed as vertical displacement on seismic data. Five categories were defined based on the timing of fault movement during the Cenozoic.

Category 1: These faults were active at the end of the Cretaceous and during the Early Palaeocene but then did not become active again until the Oligocene when they experienced (probably episodic) movement through to recent times (Fig. 5.21). G33 and G34 are located on the Chama Terrace (Fig. 5.16), which was a sediment bypass margin during deposition of Megasequence 1 sediments, hence any movement that may have occurred during the Palaeocene and Eocene was not recorded on seismic data. Therefore, this fault analysis for G33 and G34 may be biased in interpreting a period of tectonic quiescence up to the Oligocene due to the lack of evidence of movement in the earlier part of the Cenozoic.

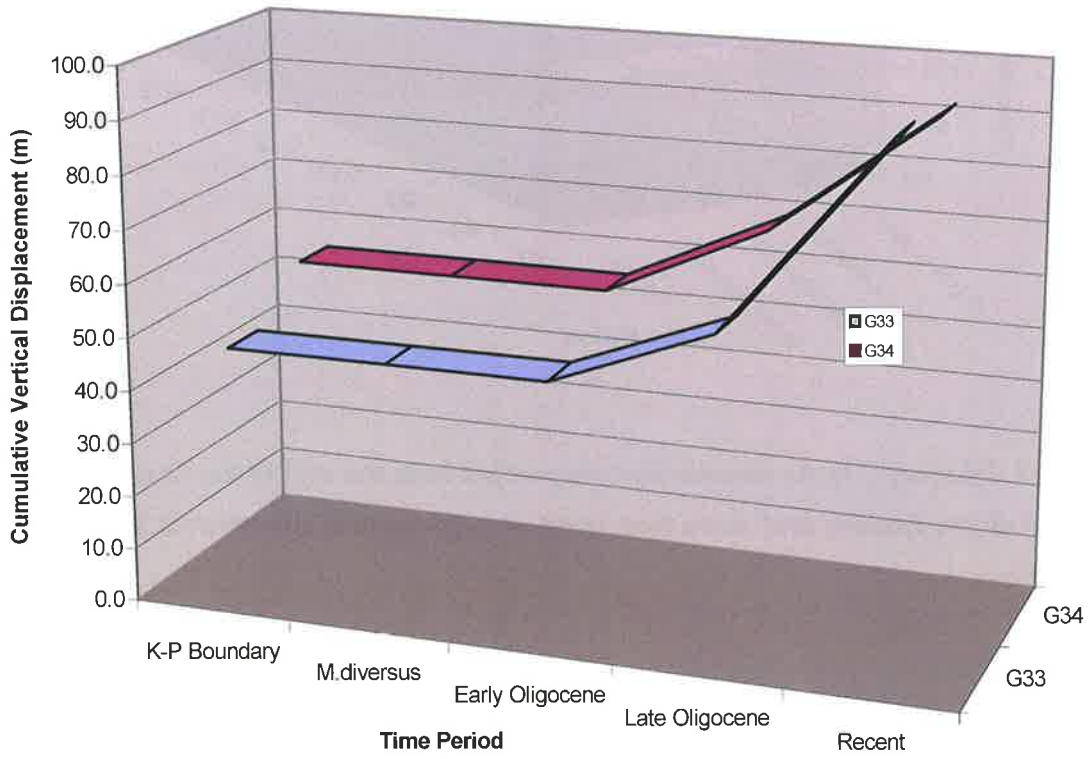

Figure 5.21 Category 1 faults showing initial movement at the end of the Cretaceous and Early Palaeocene. The faults then showed no seismically resolvable movement until the Oligocene when they became active again and have remained active until recent times.

Category 2: After reactivation at the end of the Cretaceous, category two faults experienced continued movement during the later part of the Eocene with sub-seismic scale movement during the Oligocene and Miocene (Fig. 5.22).

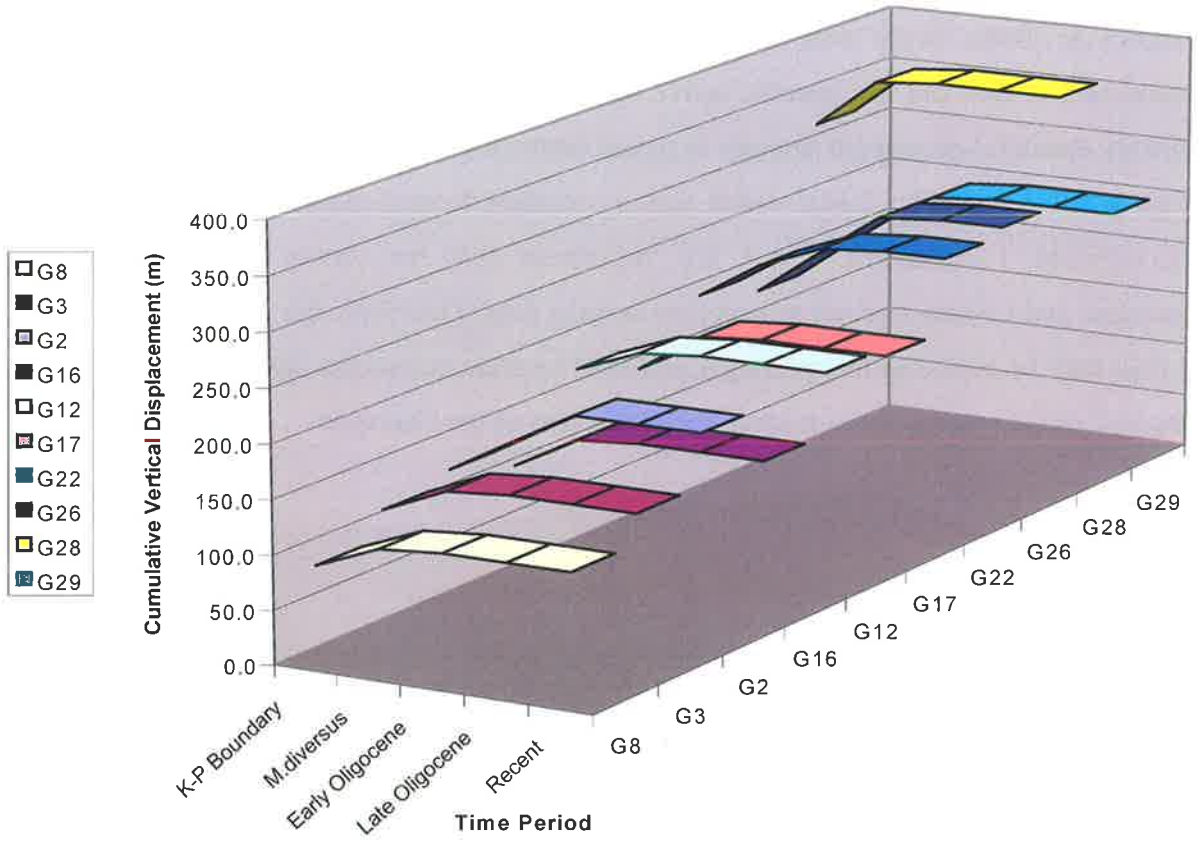

Figure 5.22 Category 2 faults experienced movement from the end of the Cretaceous through to the end of the Eocene and were then quiet or experienced sub-seismic scale movement since the Eocene.

Category 3: Category three faults were re-activated at the end of the Cretaceous and during the Early Palaeocene but then experienced little or no movement during the Eocene and Early Oligocene. They then experienced renewed activity in the Late Oligocene to Mid Miocene but have experience little movement in recent times (Fig. 5.23).

Category 4: After re-activation at the end of the Cretaceous, faults in this category show little or no movement during the Late Palaeocene through to the Oligocene, when the rate of movement significantly increases. During recent times there is little movement of the fault again (Fig. 5.22).

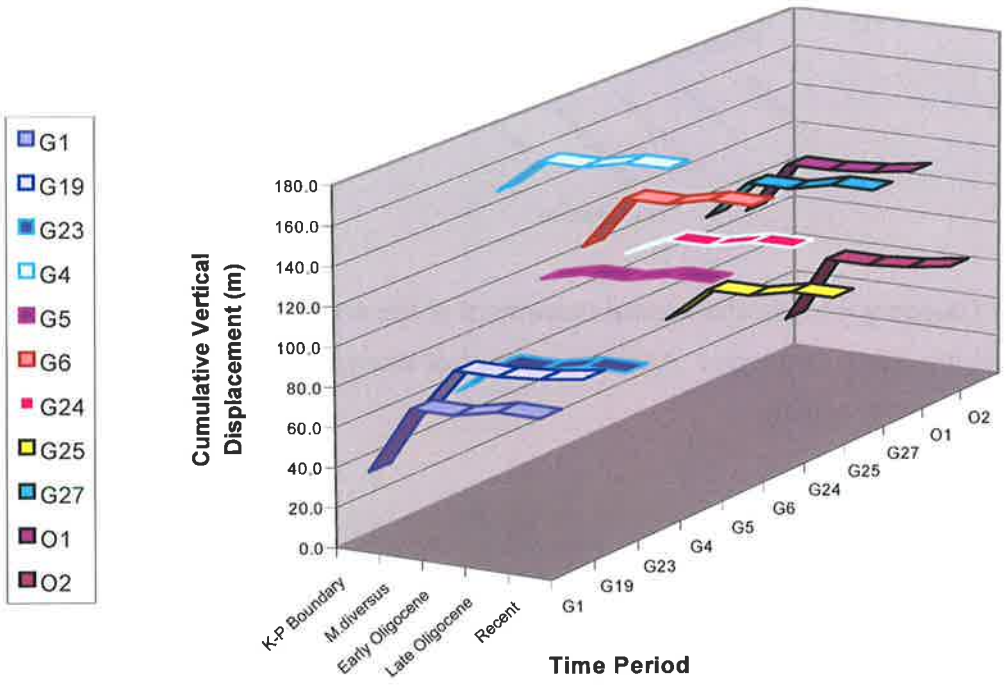

Figure 5.23 After initial movement at the end of the Cretaceous, Category 3 faults were tectonically quiet during the Mid-Late Eocene and Early Oligocene. The faults were reactivated again in the Early-Mid Miocene but have experienced little movement during recent times.

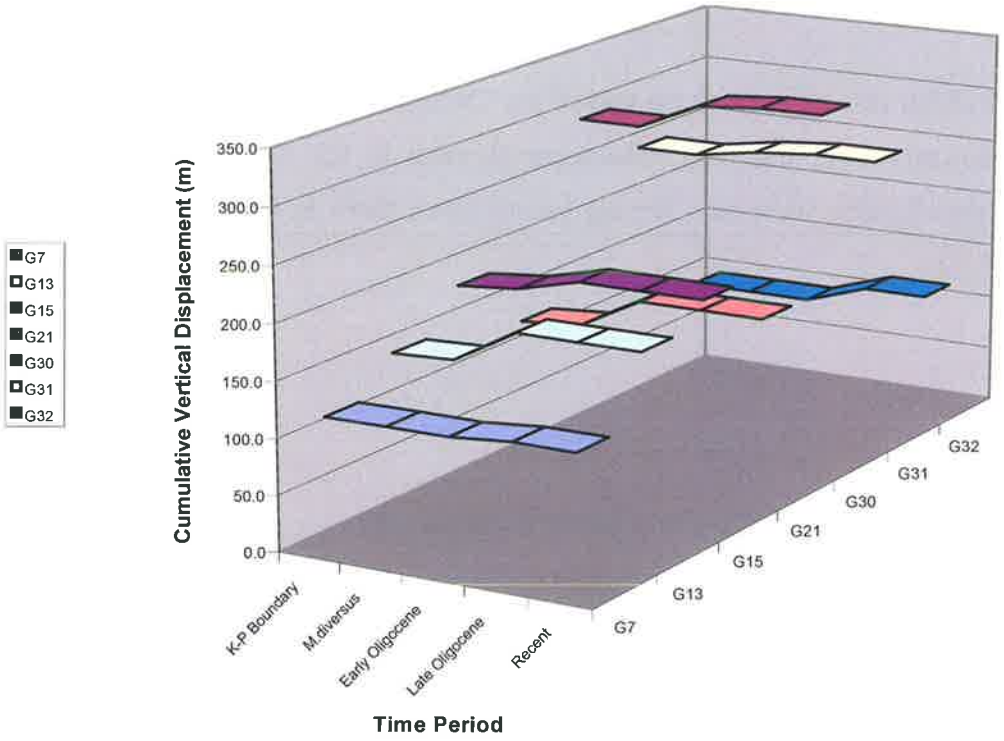

Figure 5.24 Category 4 faults show initial movement at the end of the Cretaceous, but are then inactive until the Early Oligocene. After this period of movement in the Early Oligocene, the faults show no further activity.

Category 5: Category five faults experienced tectonic activity from the end of the Cretaceous through to the Oligocene, but since the Mid-Late Miocene and in more recent times the rate of movement has decreased (Fig. 5.25).

Category 6: Category 6 faults experienced constant movement throughout the Cenozoic (Fig. 5.26). These faults are the deep seafloor faults that penetrate through the sedimentary section from the Cretaceous to Recent.

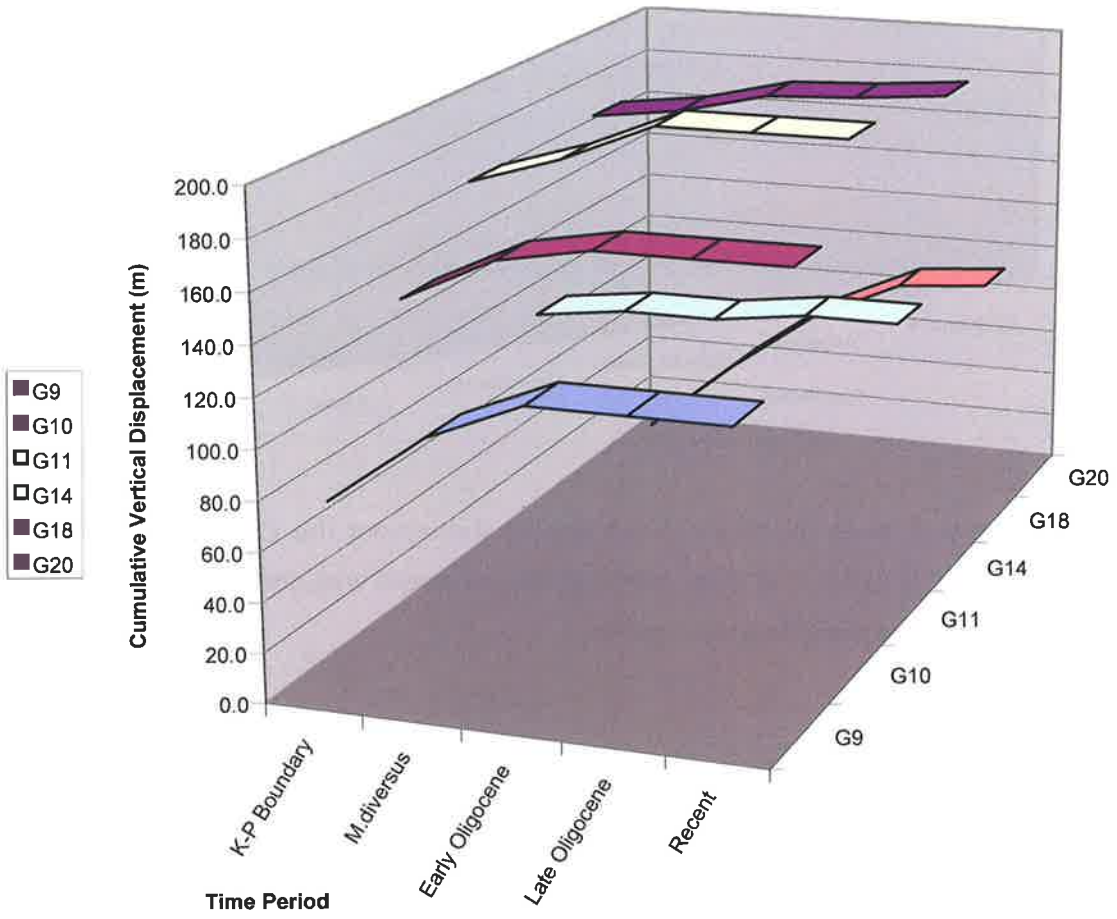

Figure 5.25 Category 5 faults were active in the early Cenozoic up until the end of the Oligocene to Miocene when they became tectonically quiet.

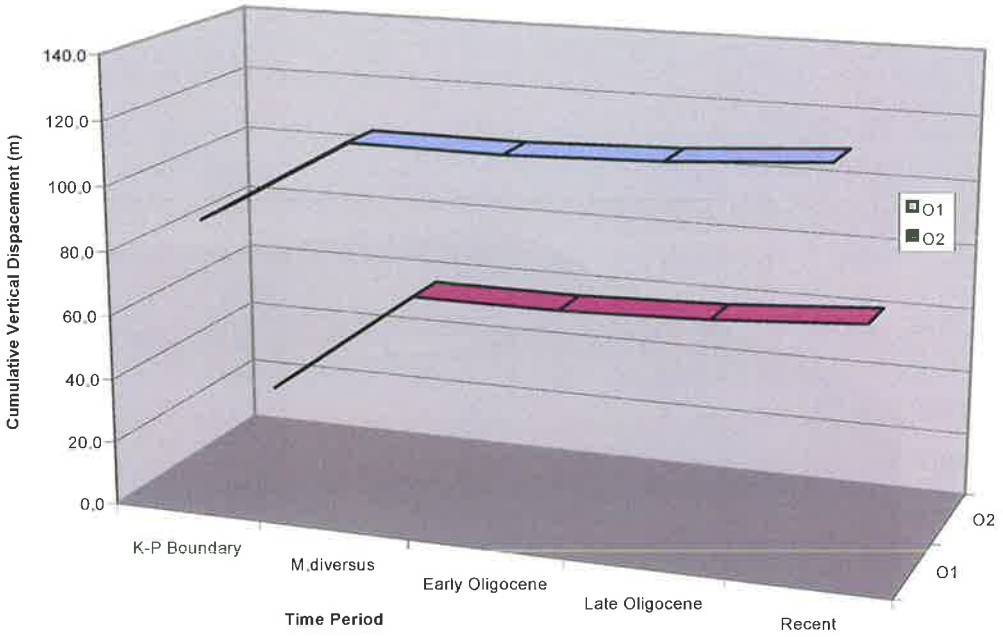

Figure 5.26 Category 6 faults experienced movement throughout the Cenozoic. Movement was rapid in the early Cenozoic, and then, although displacement was observed at later times, the magnitude of throw was considerably smaller.

5.2.3 Discussion

One of the aims of analysing the timing of fault movement throughout the Cenozoic was to determine if there was a pattern of distribution of faults in each category, which would indicate that different parts of the Sub-basin experienced tectonic activity at different times. However, no logical pattern was apparent when faults from each category were located on a map. Due to the severity of faulting in the Gambier Sub-basin, which resulted in closely spaced normal faults and implied transfer fault sets (i.e. strike-slip synthetic and antithetic faults) with overlapping fault tips, it is more likely that there was no pattern in the movement of faults in different parts of the Sub-basin. Instead, the stress and strain occurring in the Sub-basin during the Cenozoic due to evolving plate tectonics and stresses was accommodated by whichever fault or fault set happened to be closest to the origin of the stress. The resulting movement is likely to have passed onto adjacent faults by the accommodation zones between the tips of normal faults. This has resulted in the apparent random distribution of movement on faults at different times during the Cenozoic.

The dominant structural trend in the Gambier Sub-basin is NW-SE, close to the orientation of σ_H (i.e. maximum horizontal stress; σ_H =125°N; therefore the minimum horizontal stress σ_h=035°N) (Hillis et al, 1995). The normal faults that were correlated across the regional seismic grid in this study had a mean strike of 129°N, which is very close to the maximum horizontal stress direction identified by Hillis and others (1995) (Fig. 5.27). Faults oriented parallel to σ_H have the least potential for dynamic fault sealing – that is, they have a high risk of being "leaky faults" (Mildren et al. 1994). Hence, normal extensional faults following the dominant NW-SE structural trend of the offshore Gambier Sub-basin are relatively poorly oriented with respect to dynamic sealing potential (Hillis et al. 1995).

A study by Jones et al. (2000) in the Penola Trough in the onshore Gambier Sub-basin found the highest risk of regional seal breach due to the reactivation of faults and fractures occurs when faults are steep (>60°) and strike between 110°N and 200°N. Such features can provide a pathway for secondary hydrocarbon migration.

The orientation of the horizontal stresses can be used to predict the fault directions most prone to (a component of) strike-slip reactivation. Planes inclined at 45° to the maximum principal stress are subject to the maximum shear stress (Hillis et al, 1995). However, failure often occurs on planes at a somewhat lower angle to the principal stress, typically 30°. Pre-existing vertical faults striking at 30-45° to the σ_H direction are thus the most prone to at least a component of strike slip motion. Faults striking 080-095°N are prone to dextral movement, and those oriented 155-170°N are prone to sinistral movement. Vertical planes oriented parallel and perpendicular to the σ_H direction are subject to the least horizontal shear stress, and are the least prone to a component of strike slip.

Samples analysed in this study were plotted as poles to planes on a stereonet, overlying a grid of the relative risk that the faults will be non-sealing (Fig. 5.27). The faults striking in a NW-SE direction plotted exclusively in the red zones of Fig. 5.27, indicating that they have a very high risk of being non-sealing faults and are more likely to act as migration conduits for hydrocarbons. For this reason, stratigraphic traps not relying on fault seals may have better potential for trapping hydrocarbons in the offshore Gambier Sub-basin.

Due to the large seismic line spacing and orientation of this regional grid, synthetic and antithetic faults striking at an angle of 30-45° to the regional fault strike of 129°N that would be most prone to strike-slip reactivation were very difficult to identify on seismic data and to

correlate to adjacent lines. It is likely that these strike-slip synthetic/antithetic fault sets are also relatively poorly orientated in the contemporary stress regime to provide adequate seals for hydrocarbon traps.

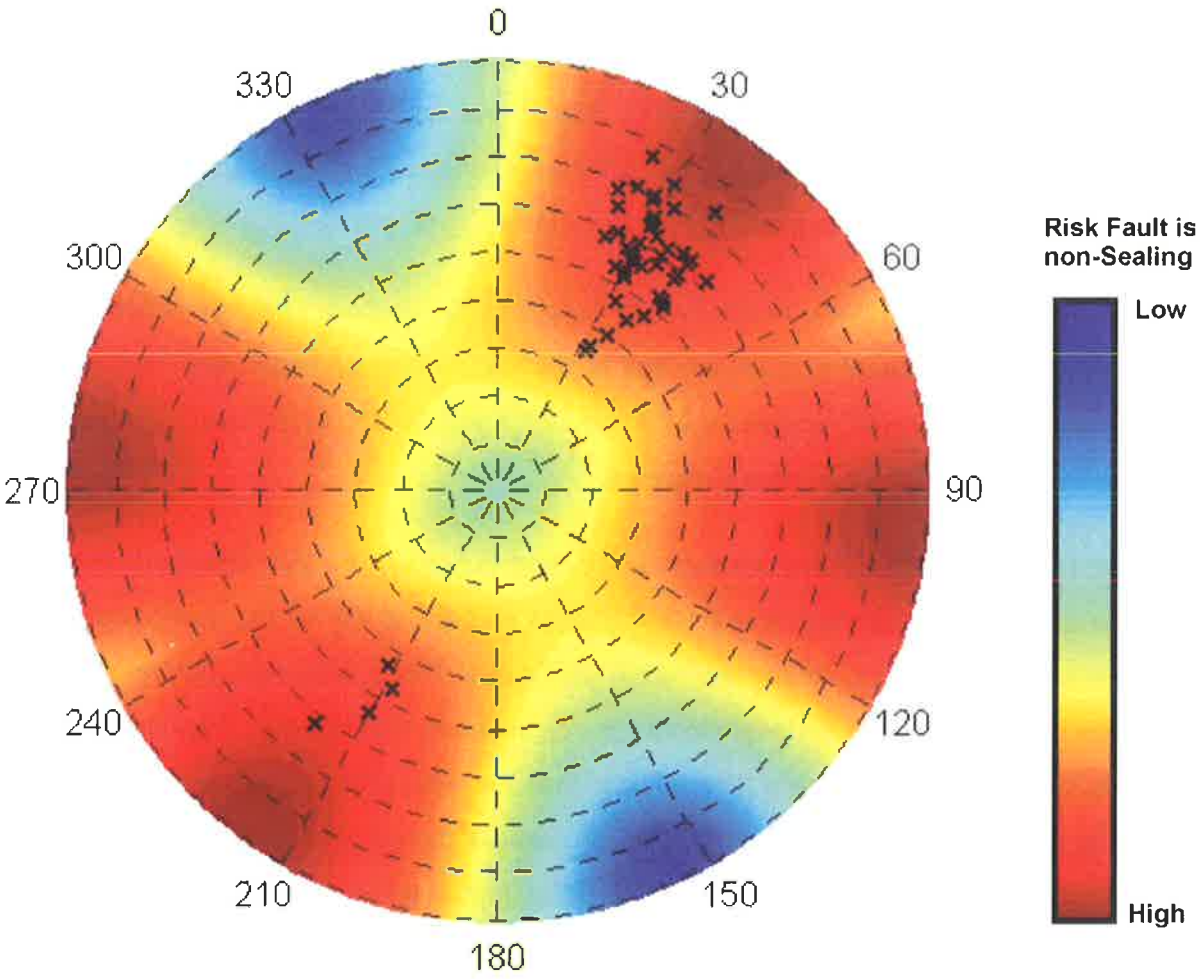

Figure 5.27 Fault sealing risk of normal faults analysed in this study. Samples (represented as crosses) were plotted as poles to planes on the stereonet, overlying fault sealing potential. The fault sealing potential is based on the contemporary stress field in the Otway Basin as determined by Hillis et al. (1995) and Jones et al. (2000). The colour spectrum indicates the relative sealing potential of faults for any particular orientation. If a fault plots in the red zone, there is a high risk that it will be non-sealing. If a fault plots in the blue zone, there is a low risk that it will be non-sealing. [Assumptions made when plotting the stereonet: Depth=1000 m; Po=9.7 Mpa; Shmin=16.2 Mpa; Sv=20 Mpa; Shmax=27 Mpa; σHmax=156°N; μ=0.6; assuming DITF (drilling induced tensile fractures) at this depth and no cohesive strength.]

5.3 TIMING OF GENERATION VERSUS TRAP FORMATION

Structural traps on the Chama Terrace formed during the initial rifting phase and consist of Pretty Hill Formation sands sealed by Eumeralla Formation shales. The basal parts of the Pretty Hill Formation entered the oil window between approximately 130 and 115 Ma in the Chama Terrace (Williamson et al. 1996). If lacustrine source rocks are present within the lower parts of the Pretty Hill Formation or the upper Casterton Formation, then maturity for the basal Cretaceous in the Chama Terrace either predates, or approximately coincides with, the timing of structuring at top Pretty Hill Formation level (~120 Ma) and deposition of the overlying Eumeralla Formation seal. It is therefore possible that some hydrocarbons generated from the basal Crayfish Group source rocks were not trapped, but migrated vertically through the porous Pretty Hill Formation until they were biodegraded at or near the surface (Williamson et al. 1996). The oil-prone lower Eumeralla Formation has been mature since the Late Cretaceous and hence post-dates the formation of the petroleum traps in the Chama Terrace. Therefore, the relative timing of liquid generation and trap formation could be ideal (Williamson et al. 1996).

In the western Voluta Trough the basal Late Cretaceous Waarre Formation reservoirs overlying Early Cretaceous (top Otway Supergroup) tilted fault blocks have been the principal exploration target. These tilted fault blocks formed between 100 and 96 Ma (Williamson et al. 1996). Prospective structures at the shallower top Late Cretaceous horizon (top Paaratte Formation) formed during the Late Cretaceous via the reactivation of the deeper rift faults. This reactivation may have been principally driven by rapid sediment loading as a large delta system prograded through the Voluta Trough (Williamson et al. 1996).

The basal Otway Supergroup in the Chama Terrace and Voluta Trough entered the oil window between ~110 and 120 Ma, and was over-mature for oil generation by the Late Cretaceous (Williamson et al. 1996). Therefore, it seems unlikely that oil generated from any basal Crayfish Group source rocks could have been trapped in Waarre Formation reservoirs overlying top Otway Supergroup structures. In Argonaut 1A, maturation appears to have been later, with the basal Crayfish group passing into the thermal gas regime by the Campanian (~80 Ma) and thus the relative timing of trap formation and maturation is more favourable (Williamson et al. 1996).

Results from the maturation study in the Voluta Trough by Williamson et al. (1996) suggest that oil charging of Waarre Formation traps requires the presence of an upper Otway

Supergroup source (i.e. upper Eumeralla Formation) or a Late Cretaceous Belfast Mudstone source. The top Eumeralla-base Waarre Formation horizon entered the oil window during the Campanian (~80 Ma) in the central Voluta Trough and during the Eocene (~40 Ma) at Argonaut 1A. The top Eumeralla-base Waarre Formation horizon has remained immature (Ro <0.6) to the present day at Morum 1A. In the central Voluta Trough, the Belfast Mudstone progressively entered the oil window from Campanian to the Quaternary, whereas for Argonaut 1A, this occurred from Eocene to Quaternary (Williamson et al. 1996).

Within the central Voluta Trough the Eumeralla Formation is over-mature, whereas the Belfast Mudstone is at present optimally mature and could charge Waarre Formation reservoirs. However, source rock (McKirdy, 1987) and sediment geochemical data (O'Brien and Heggie, 1989) indicate that the Belfast Mudstone is gas prone. Consequently, the potential for significant oil accumulations in the central Voluta Trough could be low (Williamson et al. 1996).

5.4 PLAY CONCEPTS

The dominant exploration play in the Voluta Trough has been the Late Cretaceous Waarre Formation sands, which overlie the upper Eumeralla Formation and are sealed by the regional Belfast Mudstone (Williamson et al. 1996). These sands may be charged from the underlying Eumeralla Formation or from the overlying Belfast Mudstone, both of which are apparently gas-prone. At the end of the Cretaceous the Eumeralla Formation was in the oil window over most of the Voluta Trough. However, some areas of the Voluta Trough on the outer continental shelf were already in the thermal gas window at that level (Williamson et al. 1996).

The top Belfast Mudstone, which could source the Late Cretaceous Paaratte sands in the western Voluta Trough via reactivated faulting, is usually thermally immature, except where the Eumeralla Formation is now in the thermal gas regime on the outer continental shelf of the Voluta Trough (Williamson et al. 1996).

The shallow water Paaratte Formation, which does contain coals with good source characteristics, is unfortunately immature throughout the western Voluta Trough. The Paaratte and Timboon sands and equivalents may not be prospective elsewhere due to lack of access to migration pathways (Williamson et al. 1996).

On the Chama Terrace, oil exploration relies upon a mid to lower (but not basal) Pretty Hill Formation source for present day generation (Williamson et al. 1996). Due to the very thin Cenozoic section in the western-most part of the Gambier Sub-basin, Cretaceous reservoirs must provide the primary targets. The dominantly fine-grained nature of the carbonate sequences in the Chama Terrace will potentially provide additional sealing properties for underlying reservoirs.

Structural restoration carried out by Palmowski et al. (2001) showed that large Santonian-Campanian listric faults allowed deposition of a thick Late Cretaceous sequence that led to hydrocarbon generation whilst the regional dip was strongly up towards the southwest, so that hydrocarbons would have migrated southwest. This suggests significant potential for structures currently in deep water (Palmowski et al. 2001).

Analysis of normal extensional faults striking NW-SE in the Gambier Sub-basin indicated that in the present day stress regime, these faults have a high risk of being non-sealing and therefore likely to act as migration conduits. Hence, stratigraphic traps and structural traps not relying on a fault seal will provide the best potential for trapping hydrocarbons in the Gambier Sub-basin.

5.4.1 Carbonate plays

Palaeo-submarine canyons in the Gambier Sub-basin (discussed in Chapter 3) offer insights into the scale, geometry and genesis of slope and deep water carbonate reservoirs and seals. Although in this basin it seems that the role of the carbonate is largely irrelevant to any active petroleum system (i.e. none of the carbonates are known to act as reservoirs or seals), there is potential for carbonate reservoirs to exist within the palaeo-canyons and upper slope, sealed by fine-grained marls. It is likely that in the present day stress regime, normal faults striking NW-SE will act as migration conduits, transporting hydrocarbons from underlying sources. This has occurred on the NW Shelf where the Maitland gas discovery was made in clastic sand that was charged with hydrocarbons that had migrated into the reservoir from a deeper source.

Hydrocarbon producing slope carbonate reservoirs are known to exist in many parts of the world. For example, hydrocarbons are produced from allochthonous carbonate slope debris flows and gravity flows (Cherry Canyon Formation) in the Delaware Basin, West Texas (Harris and Wiggins, 1985; Sarg, 1988); slope grainstones and basin floor turbidites (Mission Canyon

Formation) in the Williston Basin (Reid and Dorobek, 1993; Heck et al. 2001); and distal slope debris flows (Tamabra Formation) in the Poza Rica Field in Mexico (Jordan and Wilson, 1994). Platform, ramp and slope carbonate reservoirs of equivalent age to the Gambier Sub-basin carbonates (Oligo-Miocene) are prolific hydrocarbon producers in the Philippines, Java, Irian Jaya and Papua New Guinea (Jordan and Wilson, 1994).

The Gambier Sub-basin carbonate canyons provide a useful data source towards the potential scale and geometry of the canyon fill. The canyons range in width from 3-5 km and depths up to 615 m, with estimated sediment volumes within the canyons in the order of tens of cubic kilometres. It is also assumed that there are slope and basin floor deposits resulting from downslope debris and turbidity flows from the canyons that would also amount to significant volumes.

The seismic facies of the canyon-fill and slope deposits have been interpreted to represent predominantly fine-grained carbonate based on the presence of seismic "pull up" velocity anomalies under the canyons and the very smooth, convex-up nature of the seismic reflectors within the canyons and on the upper slope. However, well cuttings through the carbonates and shallow core and grab sampling from around the southern Australian margin (Passlow, 1997) shows sand-sized carbonate material can make its way onto the outer shelf and upper slope, therefore, potential does exist for carbonate reservoir rocks to be located within the canyons (Fig. 5.28).

A key issue for explorers in the Gambier Sub-basin is the presence of adequately sealed reservoirs. Fault leakage is a significant problem for Cretaceous petroleum systems in the Gambier Sub-basin and there is a high risk of breaching of the top seal by faults. The thick succession of dominantly fine-grained carbonates on the shelf and upper slope and within the palaeo-submarine canyons may provide an adequate regional seal should hydrocarbons migrate into underlying Palaeocene and Early Eocene clastic reservoirs from deeper failed Cretaceous plays (Fig. 5.28).

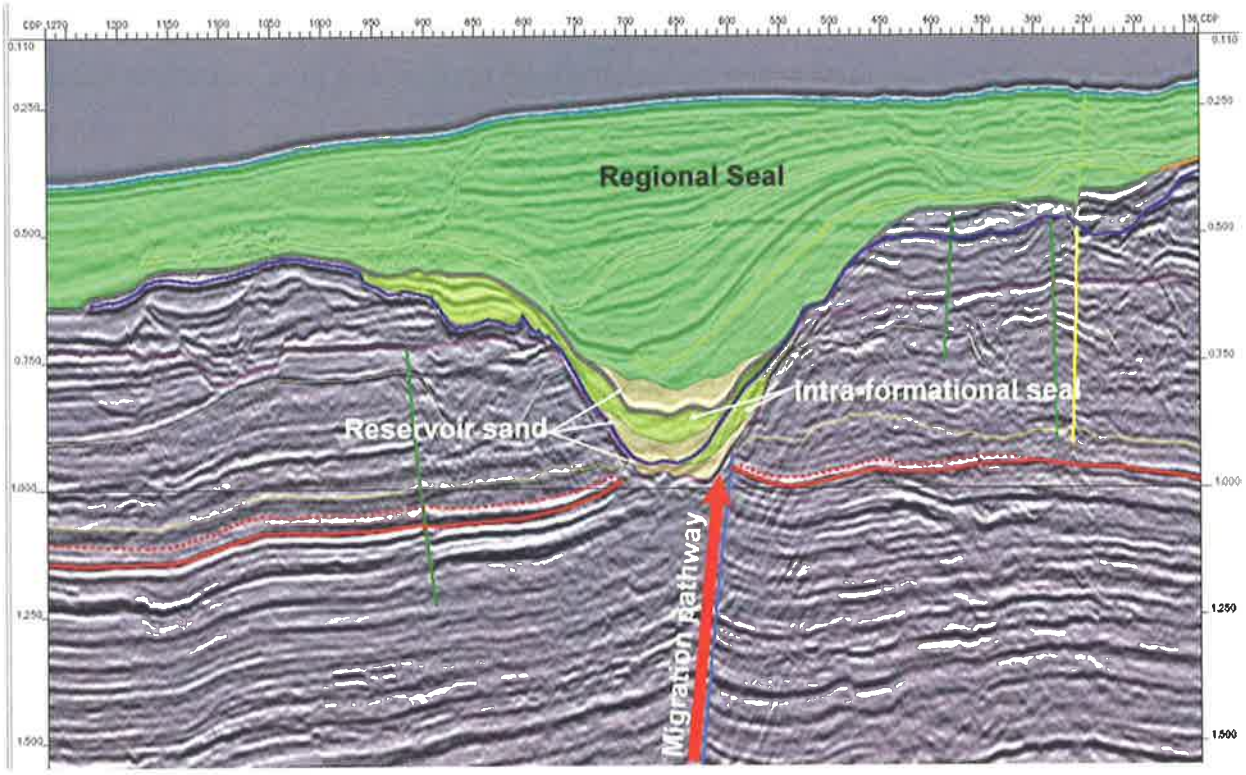

Figure 5.28 Example of a carbonate canyon play in the offshore Gambier Sub-basin. This play concept has potential where reservoir sands are transported down the canyons from the shelf edge and are deposited within the canyons. These reservoirs may be sealed by intra-formational, fine-grained carbonates within the canyons and by a regional blanket of carbonate marls overlying the canyon complex. Hydrocarbons are sourced into these reservoirs via vertical migration along normal NW-SE faults from deeper Cretaceous source kitchens comprising lower Eumeralla Formation or Belfast Mudstone.

5.4.2 Siliciclastic plays

Seismic interpretation and mapping of the clastic Wangerrip Group sequences in the Voluta Trough revealed a number of incised channel belts that are interpreted to be part of the delta plain. Incised valleys and channels associated with deltaic environments are traditionally good targets for oil and gas (Elliot, 1986) as the channels are often filled with coarse sand, with a lateral and top seal of floodplain and levee muds and silts.

The severity of faulting and later structural inversion in the Gambier Sub-basin has provided numerous structural traps such as normal fault traps and rollover anticlines. However, analysis of the contemporary stress field has revealed that the normal faults, which dominantly strike

NW-SE have a high risk of being non-sealing and may preferentially act as vertical migration pathways for hydrocarbons. Hence, relying on structural traps sealed by a normal fault has an extremely high risk in the Gambier Sub-basin and there may be lower risk in targeting stratigraphic traps. Figure 5.29 is a seismic example of potential structural plays present in the Gambier Sub-basin.

A meandering incised channel belt located on the outer shelf, basinward of Breaksea Reef 1 was identified in the Voluta Trough (Chapter 2; Fig. 2.12 and 2.13). This feature was interpreted in Supersequence 4, which was deposited during a lowstand in relative sea level and suggests that fluvial environments existed as far basinward as the present day shelf break. It is therefore assumed that further basinward of this meandering incised channel belt there was a sandy lowstand shoreline and coastal environment, perhaps a delta, and further basinward from the coastline, there may be turbidite deposits. These environments are potential reservoir targets that would be sealed by both intraformational mudstones and a thick regional succession of fine-grained carbonate sediments and charged by hydrocarbons that have migrated from deeper source kitchens where the Eumeralla Formation and Belfast Mudstone are present. The seismic grid does not extend beyond the present day shelf break and upper slope in the Voluta Trough, hence the existence of these associated environments is implied and more exploration work is required to delineate these features, however potential does exist for deep water targets.

Another stratigraphic play concept in the Gambier Sub-basin involves vertical migration up normal faults from deeper Cretaceous source kitchens, into Late Palaeocene and Early Eocene reservoirs, which are sealed by the fine-grained carbonates of the Gambier Limestone. Trapping mechanisms may involve a combination of stratigraphic and structural styles (Fig. 5.29).

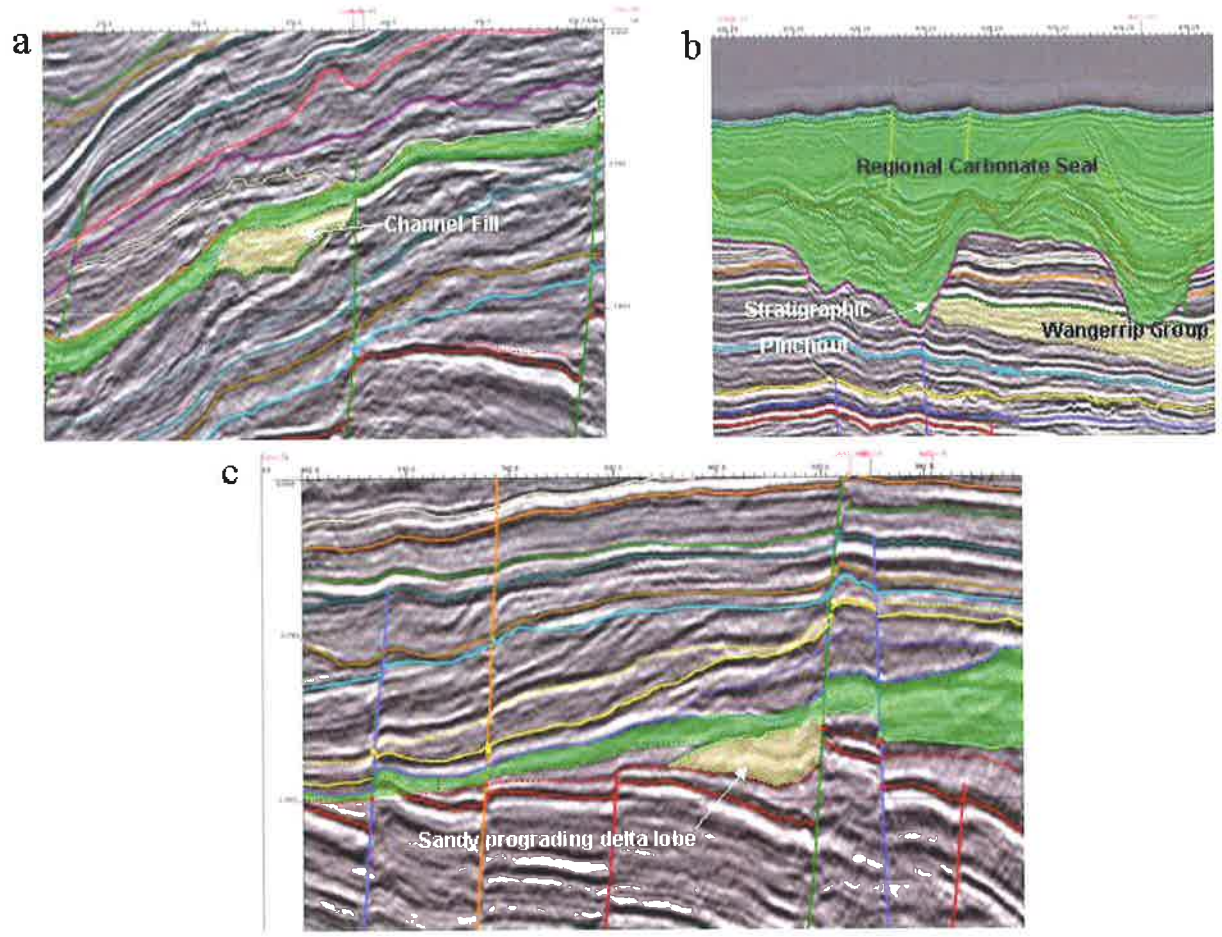

Figure 5.29. Siliciclastic play concepts in the Gambier Sub-basin. (a) sand-rich channel fill may provide a potential reservoir charged by migration up faults from deeper sources and sealed by overlying, laterally extensive fine-grained TST and distal HST sediments. (b) stratigraphic pinch out of potential clastic reservoir packages against fine-grained carbonate canyon fill sediments which provide a potential regional seal. (c) prograding sandy delta lobe observed on seismic and well data may prove to be a potential reservoir when charged by migration of hydrocarbons up the faults and sealed by an overlying, laterally extensive fine-grained package. This play relies on a component of fault seal. The thickness of the sealing facies means it is laterally continuous across the fault, however its integrity may still be compromised and allow hydrocarbons to migrate into shallower plays.

6 CONCLUSIONS

6.1 SUMMARY

The Cenozoic Gambier Sub-basin partially overlies the Mesozoic wedge of the western Otway Basin. The Gambier Sub-basin developed in the Late Cretaceous and Palaeogene on the southern passive continental margin of Australia, which formed as a result of breakup and dispersal of Gondwana. The evolution of Cenozoic stratigraphy on the southern Australian margin has long been recognised as forming four unconformity-bounded second order packages. These occur in the (I) Paleocene-Early Eocene, (II) later Middle Eocene-Early Oligocene, (III) Late Oligocene-Middle Miocene, and (IV) latest Miocene-Pleistocene.

Biostratigraphic studies of these second order packages revealed a clustering of third order transgressive sea level events in packages I and II within dominantly siliciclastic sediments. Packages II and III are dominated by cool-water neritic carbonate sediments and foraminiferal biostratigraphy defined seven third order unconformity-bounded packages within the carbonate succession.

This integrated sequence stratigraphic study supported the presence of these second- and third order packages on seismic data. Two megasequences, based on seismic interpretation, were defined in the Gambier Sub-basin; the Late Paleocene to Early Eocene Wangerrip Group siliciclastic succession, unconformably overlain by the Oligocene to Middle Miocene Gambier Limestone.

Interpretation was based on mapping 2D seismic data in a regional offshore grid, tied to onshore and offshore exploration well data including biostratigraphy. Seismic interpretation of Megasequence 1 resolved four supersequences deposited in marginal marine to marine deltaic environments. Supersequence 1 is represented, in part, by the Pebble Point Formation, a transgressive unit deposited in the Voluta Trough during a period of active fault movement in the Late Paleocene (*L.balmei* palynozone). Supersequences 2, 3 and 4 are partially represented by the Pember mudstone and Dilwyn Formation and are latest Paleocene to Early Eocene (*M.diversus- P.asperopolus* palynozones) in age. The higher order sequences making up the supersequences respond to rapidly fluctuating relative sea level, controlled by eustacy as the Gambier Sub-basin was steadily subsiding. These high frequency fluctuations can be correlated

to the biostratigraphically defined transgressive events within the global second order package I.

A gap of approximately nine million years has been identified in the stratigraphic record of the southern margin in the Middle Eocene between the second order packages I and II. Sedimentation began again in the late Middle Eocene with deposition of the Mepunga Formation and Narrawaturk Marl in the eastern Otway Basin, a response to a tectono-eustatic sea level rise (Wilson Bluff Transgression). These units are represented only by some highly condensed sections in the study area. The fully marine sedimentary record in the Gambier Sub-basin begins with the Aldinga Transgression in the earliest Oligocene, leading to progradation of the Gambier Limestone across the shelf. This cool-water carbonate package represents Megasequence 2.

The Gambier Limestone was sub-divided into two supersequences, based on seismic interpretation. Supersequence 5 is Early Oligocene in age and is a neritic, cool-water, bryozoa-rich platform carbonate that correlates to the later part of the global second order package II. Supersequence 5 is unconformably overlain by the Late Oligocene to Middle Miocene Supersequence 6, which comprises a series of submarine canyon cut and fill events and is correlated to the global second order package III.

The onset of canyon incision is marked by SB 6.1, a highly erosive sequence boundary/unconformity resulting from a glacio-eustatic sea level fall during the middle Oligocene. It lies near the Early/Late Oligocene boundary (~28.5 Ma) and no less than 20 major successive canyon cutting events were interpreted in the Voluta Trough. The canyon events that occurred after SB 6.1 are between Late Oligocene and Middle Miocene in age.

Three palaeo-submarine canyon systems, striking perpendicular to the shelf break, were identified on the outer continental shelf in the Gambier Sub-basin and were analysed within the newly established sequence stratigraphic framework. These canyon systems were subsequently named the Robe Canyon, Northumberland Canyon and the Lakes Canyon Complex.

The canyons were initiated during a lowstand when relative sea level dropped below the shelf edge resulting in minor fluvial incision across the shelf and the formation of "nick points" at the shelf break. A major transgression in the later Oligocene inundated the shelf and the nick-points formed focal points for down slope movement of mass wasting events, which provided an

erosive force for enlarging the canyons. The resulting turbidity currents flowed down the sinuous canyon axes and deposited dominantly fine-grained sediment on the canyon floors in laterally migrating deposits comparable to fluvial point bar deposits. An analogy has been drawn between the development of the Gambier Sub-basin submarine canyons and fluvial meandering channels.

Analysis of faulting in the Gambier Sub-basin, with respect to the contemporary stress regime, indicates that the regional NW-SE striking normal listric faults that dominate the Mesozoic and much of the Cenozoic section are likely to be non-sealing. Hence, reliance on un-faulted structural traps and stratigraphic traps within the Cenozoic sediments may prove to be less risky in the search for hydrocarbons.

Numerous plays exist within the Early Eocene clastic succession where there is evidence of incised meander belts on the outer shelf. The associated sandy lowstand shoreline and possible turbidites interpreted to occur further basinward form a potential play where the seal is outer shelf and upper slope, fine-grained carbonate rocks.

The presence of sand-sized carbonate sediment on the outer shelf in the Otway Basin has been demonstrated. Hence, a potential play exists where carbonate reservoir sands, sourced from the outer shelf, are present within the canyons and are sealed by surrounding fine-grained marls. Migration of hydrocarbons up fault planes from underlying Cretaceous sources into the carbonate sands would be required to charge these reservoirs.

The thick canyon-fill succession and platform carbonate in the Gambier Sub-basin is interpreted as dominantly fine-grained and may therefore act as a regional seal to underlying clastic reservoirs within Megasequence 1. These plays would also need to be charged by migration of hydrocarbons from Cretaceous sources as maturity modelling in the Gambier Sub-basin indicates potential Cenozoic source rocks are immature.

6.2 FUTURE WORK

Exploration within the Gambier Sub-basin, especially in the offshore part of the sub-basin where there has been recent acreage release (Part 2, APPEA Journal 2002), would benefit from an integrated sequence stratigraphic study of the Mesozoic succession of the underlying Otway

Basin. To date, exploration targets have been Cretaceous reservoirs charged by non-marine Cretaceous source rocks. A sequence stratigraphic study, similar to this one, establishing a sequence stratigraphic framework within which the basinal palaeogeography and then timing of generation, trap formation and migration could be analysed would lead to a better understanding of the rock relationships and distribution of likely source, reservoir and seal packages.

The major inhibitor in this study was the lack of detailed data. Majority of the wells available in the study area were drilled 20-30 years ago and lack full suites of wireline logs through the Cenozoic succession. The deeper Mesozoic section comprises comprehensive wireline log suites, potentially enabling more accurate analysis of lithologies at depth and correlation between wells where seismic data is lacking.

Due to the lack of biostratigraphic data in the Cenozoic section, wells had to be resampled and analysed, however some of the wells were already oversampled and the cuttings bags in the Government store contained less than the 100 g to be retained as required by law, therefore preventing sampling for biostratigraphy. The Mesozoic succession was initially better sampled for biostratigraphy at the time of drilling since the drilling targets were within Cretaceous sediments. It is likely though, that further analysis and sampling may improve stratigraphic understanding of the Mesozoic.

A regional 2D seismic dataset was employed in this study due to the large study area. The onshore seismic data initially acquired was not used due to very poor resolution in the shallow section, making interpretation impossible. The offshore seismic grid, integrated with available wells proved adequate for the initial sequence stratigraphic analysis however the grid was too sparse and orientated at such an angle that the full array of synthetic and antithetic faults could not be accurately analysed. Much more 2D seismic data exists than was used in this study so that quite a dense grid covers most of the offshore part of the Gambier Sub-basin. An analysis of the fault arrays using a dense 2D seismic grid would potentially provide more accurate data on the sealing potential of faults of different orientations.

The lack of understanding of how the Gambier Limestone affects seismic data and, consequently, depth conversion in the Gambier Sub-basin may lead to problems with identifying accurate depths of reservoir targets in proposed exploration wells. Therefore it is

imperative that current drilling programs in the Sub-basin conduct velocity surveys through the carbonate section so these problems can be addressed.

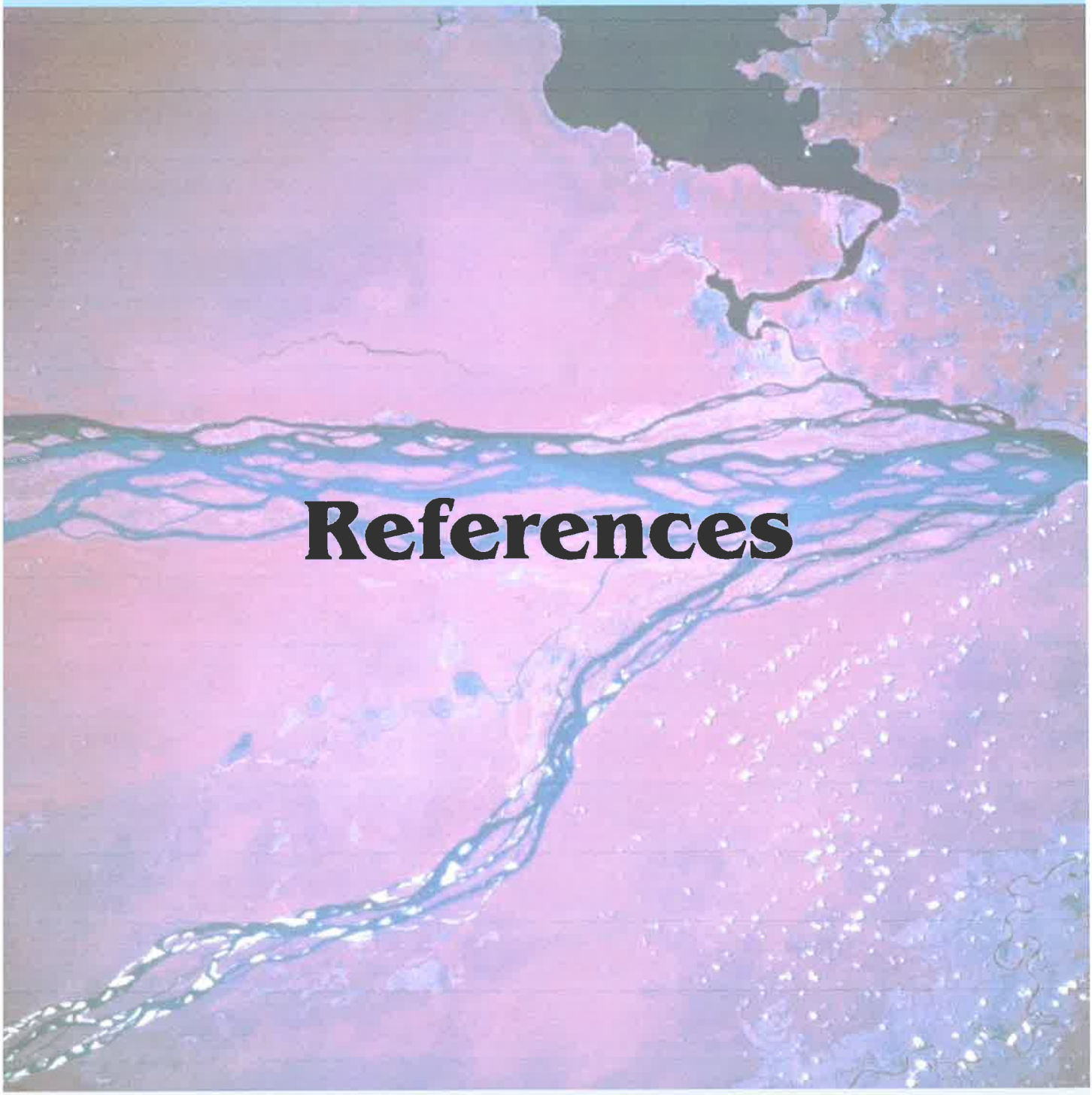

References

REFERENCES

Abele, C., Gloe, C. S., Hocking, J. B., Holdgate, G., Kenley, P. R., Lawrence, C. R., Ripper, D., and Threlfall, W. F., 1976. Tertiary. Special Publication - Geological Society of Australia 5, Geology of Victoria, p177-274.

Abreu, V.S. and Haddad, G.A., 1998. Glacioeustatic fluctuations: the mechanism linking stable isotope events and sequence stratigraphy from the Early Oligocene to Middle Miocene. *In:* P. Graciansky, J. Hardenbol, T. Jacquin, and P. Vail (eds). Mesozoic and Cenozoic Sequence Stratigraphy of European Basins. SEPM Special Publication 60, p245-260.

Ahr, W. M., 1973. Carbonate Ramp; alternative to Shelf Model. AAPG Bulletin 57(9), p1826.

Allen, P., 1964. Sedimentological models. Journal of Sedimentary Petrology 34(2), p289-293.

Allen, G., Lang, S., Musakti, O., and Chirinos, A., 1996. Application of sequence stratigraphy to continental successions: implications for Mesozoic cratonic interior basins of eastern Australia. Geological Society of Australia. Abstracts, v. no.43. p22-26.

Allen, G. P. and Posamentier, H. W., 1993. Sequence stratigraphy and facies model of an incised valley fill; the Gironde Estuary, France. Journal of Sedimentary Petrology 63(3), p378-391.

Alliance, O. D. A. N., 1966. Completion report Kalangadoo well No.1, OEL 22, South Australia. Petroleum Search Subsidy Acts Report, v. 65/4153.

Alliance, O. D. A. N., Laing, A. C. M., Le, B. M. C., and Stephens, G. J., 1968. Completion report Alliance Lake Bonney No.1 well, OEL 22, South Australia. Petroleum Search Subsidy Acts Report, v. 67/4261.

Alliance, O. D. A. N. and Le, B. M. C., 1967. Completion report Caroline well No.1, OEL 22, South Australia. Petroleum Search Subsidy Acts Report, v. 66/4222.

Arditto, P. A., 1995. The eastern Otway Basin Wangerrip Group revisited using an integrated sequence stratigraphic methodology. The APEA Journal 35, Part 1; p372-384. 1995.

Arditto, P. A., 1999. Sequence stratigraphic workshop on the Palaeocene-Eocene Wangerrip Group, eastern Otway Basin. Field Tutorial Guide Book. February 1999.

Aust, T. and Morton, J. G. G., 1995. Infrastructure and gas markets. *In*: J. G. Morton and J. F. Drexel (eds). Petroleum Geology of South Australia: Volume 1.Petroleum Division: SA Department of Mines and Energy Report Book 95/12, p1-6.

Ballantyne, R. S. and Willis, R., 1973. Genex Douglas Point 1, Otway Basin, South Australia, well completion report.: General Exploration Co Australia Pty Ltd, v. E2312.

Beach, P. N., Gas, a. F. E. N., Home, E. C. L., Poseidon, O. P. L., MIM, H. L., and Rayner, B. L., 1987. McNamara 1. Well completion report. South Australia. Department of Mines and Energy. Company Report, v. E7051/6.

Beach, P. N., Gas, a. F. E. N., Home, E. C. L., Poseidon, O. P. L., MIM, H. L., Towers, K., and Buffin, A., 1988. Compton 1, well completion report. South Australia. Department of Mines and Energy. Company Report, v. E7126/6.

Beach, P. N., Geosurveys, o. A. P. L., Laws, R. A., and Woolley, J. B., 1964. Well completion report, Geltwood Beach well No.1 OEL 22, SA. Petroleum Search Subsidy Acts Report, v. 62/1403.

Berggren, W. A., Kent, D. V., Swisher, C. C. and Aubry, M., 1995. A revised Cenozoic geochronology and chronostratigraphy. *In*: W. A. Berggren, D. V. Kent, M. Aubry, and J. Hardenbol (eds). Geochronology, time scales and global stratigraphic correlation. SEPM Special Publication 54, p129-212.

Bernecker, T., Partridge, A. D. and Webb, J. A., 1997. Mid-Late Tertiary deep-water temperate carbonate deposition, offshore Gippsland Basin, southeastern Australia. SEPM Special Publication 56, 221-236.

Bhattacharya, J. P. and Walker, R. G., 1992. Deltas. *In*: R. G. Walker and N. P. James (eds). Facies models: a response to sea level change. Gelological Association of Canada, p157-177.

BHP, P. P. L., SAGASCO, R. L., Ampol, E. L., Lakes, O. L., Command, P. H. N., and Cultus, P. N., 1993. Troas 1, well completion report (basic data portion). South Australia.

Department of Primary Industries and Resources. Open File Envelope, v. 7434/6 R 1.

Boeuf, M. G. and Doust, H., 1975. Structure and development of the southern margin of Australia. APEA Journal 15(1), p33-43.

Bone, Y. and James, N. P., 1993. Bryozoans as carbonate sediment producers on the cool-water Lacepede Shelf, southern Australia. Sedimentary Geology 86(3-4), p247-271.

Bone, Y., James, N. P., and Kyser, T. K., 1994. Shallow burial dolomitisation and dedolomitisation of the cool-water, calcitic Gambier Limestone, South Australia. Geological Society of Australia. Abstracts, v. no.37. p35.

Boreen, T. D. and James, N. P., 1995. Stratigraphic principles and patterns of cool-water carbonate deposition: Tertiary limestones, SE Australia. Geological Society of Australia. Abstracts, v. no.38. p12-14.

Brown, L. E. and W. L. Fisher, 1977. Seismic stratigraphic interpretation of depositional systems: examples from Brazil rift and pull-apart basins. *In*: C. E. Payton (ed). Seismic stratigraphy—applications to hydrocarbon exploration. AAPG Memoir 26, p213-248.

Cadart, M. L. P., 1975. Completion report Alliance Burrungule no.1 well. Alliance Oil Development Australia NL, v. E2646.

Calvet, F., Tucker, M. E., and Henton, J. M., 1990. Middle Triassic carbonate ramp systems in the Catalan Basin, Northeast Spain; facies, systems tracts, sequences and controls. Special Publication of the International Association of Sedimentologists 9, p79-108.

Cande, S. C. and Mutter, J. C., 1982. A revised identification of the oldest sea-floor spreading anomalies between Australia and Antarctica. Earth and Planetary Science Letters 58(2), p151-160.

Cavazza, W. and DeCelles, P.G., 1993. Geometry of a Miocene submarine canyon and associated sedimentary facies in southeastern Calabria, southern Italy. Geological Society of America Bulletin 105, p 1297-1309.

Cockshell, C. D., 1995. Structural and tectonic history. *In*: J. G. Morton and J. F. Drexel (eds). Petroleum Geology of South Australia: Volume 1.Petroleum Division: SA Department

of Mines and Energy Report Book 95/12, p15-45.

Coleman, J. M., Gagliano, S. M., and Ferm, J. C., 1969. Deltaic environments. AAPG Bulletin 53(3), p712.

Coleman, J. M. and Wright, L. D., 1975. Modern river deltas; variability of processes and sand bodies. Houston Geol. Soc. Houston, United States, p99-149.

Cultus, P. A. N., Hershey, O. C., Fay, R. A. L., Petrocorp, E. L., Priest, P., and Luxton, C., 1990. Copa 1, well completion report. South Australia. Department of Mines and Energy. Company Report, v. E8323.

Curray, J. R., 1964. Transgressions and regressions, [Chapter] 10. *In*: Papers in marine geology--Shepard Commemorative Volume, p175-203.

Deighton, I., Falvey, D. A., and Taylor, D. J., 1976. Depositional environments and geotectonic framework: southern Australian continental margin. APEA Journal 16(1), p25-36.

Dickinson, J. A., Wallace, M. W., Holdgate, G. R., Daniels, J., Gallagher, S. J., and Thomas, L., 2001, Neogene tectonics in SE Australia: Implications for petroleum systems. APPEA Journal 41(1), p37-52.

Droxler, A. W. and Schlager, W., 1985. Glacial versus interglacial sedimentation rates and turbidite frequency in the Bahamas. Geology (Boulder) 13(11), p799-802.

Edwards, D. S., Struckmeyer, H. I. M., Bradshaw, M. T., and Skinner, J. E., 1999. Geochemical characteristics of Australia's southern margin petroleum systems. APPEA Journal 39(1), p297-321.

Elliot, T., 1979. Deltas. Elsavier, New York, N. Y., United States, p97-142.

Elliot, T., 1986. Deltas. In: H. G. Reading (ed). Sedimentary Environments and Facies, 2nd Edition. Blackwell Scientific Publications, p113-154.

Emery, D. and Myers, K. (eds), 1996. Sequence stratigraphy. Oxford: Blackwell Science.

Esso, A. L., Esso, E. a. P. A. I., and Hematite, P. P. L., 1975. Morum 1 well completion report. South Australia. Department of Mines and Energy. Unpublished Report, v. E6524.

Esso, E. a. P. A. I. and James, E. A., 1968. Esso Argonaut A1, South Australia, Offshore well completion report. Petroleum Search Subsidy Acts Report, v. 68/2018.

Esso, E. a. P. A. I. and Whittle, A. P., 1970. Esso Lake George 1, well completion report, PEL 8, South Australia. Petroleum Search Subsidy Acts Report, v. 69/2030.

Etheridge, M. A., Branson, J. C., and Stuart, S. P. G., 1985. Extensional basin; forming structures in Bass Strait and their importance for hydrocarbon exploration. The APEA Journal 25(1), p344-361.

Eyles, D. R., Esso, E. a. P. A. I., and Hematite, P. P. L., 1974. Chama 1A well completion report. South Australia. Department of Mines and Energy. Unpublished Report, v. E6523.

Eyles, D. R., Esso, E. a. P. A. I., and Hematite, P. P. L., 1975. Neptune 1 well completion report. South Australia. Department of Mines and Energy. Unpublished Report, v. E6525.

Eyles, D. R., Esso, E. a. P. A. I., and Hematite, P. P. L., 1974. Trumpet 1 well completion report. South Australia. Department of Mines and Energy. Unpublished Report, v. E6526.

Falvey, D. A., 1974. The development of continental margins in plate tectonic theory. APEA Journal 14(1), p95-106.

Farre, J. A., Mcgregor, B. A., Ryan, W. B. F., and Robb, J. M., 1983. Breaching the shelfbreak: Passage from youthful to mature phase in submarine canyon evolution. *In*: D. J. Stanley, and G. T. Moore (eds.). The shelfbreak: Critical interface on continental margins. SEPM Special Publication 33, p25-39.

Feary, D. A. and James, N. P., 1995. Cenozoic biogenic mounds and buried Miocene(?) barrier reef on a predominantly cool-water carbonate continental margin - Eucla Basin, western Great Australian Bight. Geology 23(5), p427-430.

Feary, D. A. and James, N. P., 1998. Seismic stratigraphy and geological evolution of the Cenozoic, cool-water Eucla Platform, Great Australian Bight. AAPG Bulletin 82(5A), p792-816.

Feary, D. A. and Loutit, T. S., 1998. Cool-water carbonate facies patterns and diagenesis - the key to the Gippsland Basin 'velocity problem'. APPEA Journal 38(1), p137-146.

Finlayson, D. M., Collins, C. D. N., Lukaszyk, I., and Chudyk, E. C., 1998. A transect across Australia's southern margin in the Otway Basin region; crustal architecture and the nature of rifting from wide-angle seismic profiling. Tectonophysics 288(1-4), p177-189.

Finlayson, D. M., Johnstone, D. W., Owen, A. J., and Wake, D. K. D., 1996. Deep seismic images and the tectonic framework of early rifting in the Otway Basin, Australian southern margin. Tectonophysics 264(1-4), p137-152.

Fisher, W. L. and McGowen, J. H., 1967. Depositional systems in the Wilcox Group of Texas and their relationship to the occurrence of oil and gas. Transactions of the Gulf Coast Association of Geological Societies 17, p105-125.

Frakes, L. A., McGowran, B., and Bowler, J. M., 1987, Evolution of Australian Environment. In: Dyne, G. R. and Walton, D. W. (eds). Fauna of Australia: General Articles: Canberra Australian Government Public Service Volume 1A, p1-6.

Frears, R. A., 1995. History of Petroleum Exploration. *In*: J. G. G. Morton, and J. F. Drexel (eds). The petroleum geology of South Australia. Volume 1: Otway Basin, South Australia. Department of Mines and Energy. Report Book, v. 95/12.

Gallagher, S. J. and Holdgate, G., 2000. The palaeogeographic and palaeoenvironmental evolution of a Palaeogene mixed carbonate-siliciclastic cool-water succession in the Otway Basin, Southeast Australia. Palaeogeography, Palaeoclimatology, Palaeoecology 156(1-2), p19-50.

Gallagher, S. J., Jonasson, K., and Holdgate, G., 1999. Foraminiferal biofacies and palaeoenvironmental evolution of an Oligo-Miocene cool-water carbonate succession in the Otway Basin, southeast Australia. Journal of Micropalaeontology 18(2), p143-168.

Galloway, W. E., 1975. Process framework for describing the morphologic and stratigraphic evolution of deltaic depositional systems. Houston Geol. Soc. Houston, United States. p87-98.

Galloway, W. E., 1989. Genetic stratigraphic sequences in basin analysis; I, Architecture and

genesis of flooding-surface bounded depositional units. AAPG Bulletin 73(2), p125-142.

Galloway, W. E., 1998. Siliciclastic slope and base-of-slope depositional systems; component facies, stratigraphic architecture, and classification. AAPG Bulletin 82(4), p569-595.

Gas, a. F. E. N., Magellan, P. A. L., Cultus, P. A. N., TMOC, E. P. L., and Akbari, V., 1993. Saint Clair 1, well completion report. South Australia. Department of Mines and Energy. Company Report, v. E7448/6.

Gas, a. F. E. N., Magellan, P. A. P. L., Cultus, P. A. N., AGL, P. O. P. L., and Akbari, V., 1992. Reedy Creek 1, well completion report. South Australia. Department of Mines and Energy. Company Report, v. E7406/6.

Gravestock, D. I., Hill, A. J., and Morton, J. G. G., 1986. A review of the structure, geology and hydrocarbon potential of the Otway Basin in South Australia. South Australia. Department of Mines and Energy. Unpublished Report, v. RB 86/077.

Haq, B. U., 1993. Deep-sea response to eustatic change and significance of gas hydrates for continental margin stratigraphy. *In*: H. M. Posamentier, C. P. Summerhayes, B. U. Haq, and G. P. Allen, G.P. (eds). Sequence stratigraphy and facies associations, International Association of Sedimentologists, Special Publication 18, p93-106.

Harris, P. M. and Wiggins, W. D., 1985. Allochthonous carbonates of the Getaway Limestone, Upper Permian of the Delaware Basin. SEPM Core Workshop 6, p174-211.

Heck, T. J., Lefever, R. D., Fischer, D. W. and Lefever, J., 2001. Overview of the Petroleum Geology of the North Dakota Williston Basin www.state.nd.us/ndgs/Resources/WB%20Petroleum.htm.

Hill, K. A., Cooper, G. T., Richardson, M. J., and Lavin, C. J., 1994. Structural framework of the Eastern Otway Basin: inversion and interaction between two major structural provinces. Exploration Geophysics 25(2), p79-87.

Hill, A. J., 1995. Source rock distribution and maturity modelling. *In*: J. G. G. Morton, and J. F. Drexel (eds). The petroleum geology of South Australia. Volume 1: Otway Basin, South Australia. Department of Mines and Energy. Report Book, v. 95/12.

Hill, K. A., Finlayson, D. M., Hill, K. C., and Cooper, G. T., 1995. Mesozoic tectonics of the Otway Basin region; the legacy of Gondwana and the active Pacific margin; a review and ongoing research. The APEA Journal 35(1), p467-493.

Hill, P. J., Meixner, A. J., Moore, A. M. G., and Exon, N. F., 1997. Structure and development of the west Tasmanian offshore sedimentary basins: result of recent marine and aeromagnetic surveys.: Australian Journal of Earth Sciences 44(5), p579-596.

Hillis, R. R., Monte, S. A., Tan, C. P., and Willoughby, D. R., 1995. The contemporary stress field of the Otway Basin, South Australia; implications for hydrocarbon exploration and production. The APEA Journal 35(1), p494-506.

Hocking, J.B., 1976. Gippsland Basin. *In*: J. G. Douglas and J. A. Ferguson (eds). Geology of Victoria: Melbourne, Geological Society of Australia, Special Publication 5, p248-274.

Holdgate, G. R., 1981. Stratigraphy, sedimentology and hydrocarbon prospects of the Dilwyn Formation in the central Otway Basin of southeastern Australia. Proceedings of the Royal Society of Victoria 93(1-2), p129-148. Royal Society of Victoria. Melbourne, Victoria, Australia.

Holdgate, G. R. and Gallagher, S., 1997. Microfossil palaeoenvironments and sequence stratigraphy of Tertiary cool-water carbonates, onshore Gippsland Basin, southeastern Australia. *In*: James, N. P. and Clarke, J. A. (eds). Cool water carbonates. SEPM Special Publication 56, p205-220.

Holdgate, G. R., Wallace, M. W., Daniels, J., Gallager, S. J., Keene, J. B. and Smith, A. J., 2000. Controls on Seaspray Group sonic velocities in the Gippsland Basin-A multidisciplinary approach to the canyon seismic velocity problem. APPEA Journal 40, p295-313.

Hubbard, R. J., 1988. Age and significance of sequence boundaries on Jurassic and Early Cretaceous rifted continental margins. AAPG Bulletin 72(1), p49-72.

James, N. P., 1997. Cool-water carbonate depositional realm. *In*: N. P. James and J. A. D. Clarke (eds). Cool-water carbonates. SEPM Special Publication, v. no.56. p1-20.

James, N. P., Bone, Y., and Kyser, T. K., 1993. Shallow burial dolomitization and

dedolomitization of Mid-Cenozoic, cool-water, calcitic, deep-shelf limestones, southern Australia. Journal of Sedimentary Petrology 63(3), p528-538.

James, E. A. and Evans, P. R., 1971. The stratigraphy of the offshore Gippsland Basin. APPEA Journal 11(1), p71-4.

James, N. P., Feary, D. A., Surlyk, F., Simo, J. A. T., Betzler, C., Holbourn, A. E., Qianyu, L., Matsuda, H., Machiyama, H., Brooks, G. R., Andres, M. S., Hine, A. C., and Malone, M. J., 2000. Quaternary bryozoan reef mounds in cool-water, upper slope environments: Great Australian Bight. Geology 28(7), p647-650.

James, N. P. and Bourque, P. A., 1992. Reefs and mounds. Geological Association of Canada. St. Johns, NF, Canada. p323-347.

Jervey, M. T., 1988. Quantitative geological modeling of siliciclastic rock sequences and their seismic expression. SEPM Special Publication 42, p47-69. 1988.

Jones, B. and Desrochers, A., 1992. Shallow platform carbonates. *In*: R. G. Walker and N. P. James (eds). Facies models: a response to sea level change. Gelological Association of Canada, p277-301.

Jones, R. M., Boult, P., Hillis, R. R. and Mildren, S. D., 2000. Integrated hydrocarbon seal evaluation in the Penola Trough, Otway Basin. APPEA Journal 40(1), p194-214.

Jordan, C. F. and Wilson, J. L., 1994. Carbonate Reservoir Rocks. *In*: L. B. Magoon and W. G. Dow (eds). The petroleum system—from source to trap. AAPG Memoir 60, p141-158.

Kendall, C. G. S. C. and Schlager, W., 1981. Carbonates and relative changes in sea level. Marine Geology 44(1-2), p181-212.

Kennard, J. M., Allen, G. P. K., and Kirk, R. B., 1999. Sequence stratigraphy: a review of fundamental concepts and their application to petroleum exploration and development in Australia. AGSO Journal of Australian Geology and Geophysics 17(5-6), p77-104.

Kennett, J. P., 1977. Cenozoic evolution of Antarctic glaciation, the Circum-Antarctic Ocean and their impact on global palaeoceanography. Journal of Geophysical Research 82(27), p3843-3860.

Lakes, O. L., Cultus, P. A. L., Mirboo, R. P. L., Victoria, P. N., Petroleum, V. L., Mulready, C. S. P. L., Tabassi, a. A. P. L., Mulready, J., and Tabassi, A., 1994. Northumberland 1, well completion report. South Australia. Department of Mines and Energy. Company Report, v. E7455/6.

Lakes, O. N., Victoria, P. N., Mirboo, R. P. L., Cultus, P. A. N., Mulready, J. N., and Short, D. A., 1997. McNicol 1, well completion report. South Australia. Department of Primary Industries and Resources. Open File Envelope, v. E07581/006.

Leach, A. S. and Wallace, M. W., 2001. Cenozoic submarine canyon systems in cool water carbonates from the Otway Basin, Victoria, Australia. PESA Eastern Australasian Basin Symposium, Melbourne, Victoria, November, 2001, p465-473.

Li, A., McGowran, B., and White, M. R. 2000. Sequences and biofacies packages in the mid-Cenozoic Gambier Limestone, South Australia; reappraisal of foraminiferal evidence. Australian Journal of Earth Sciences 47(6), p955-970.

Loucks, R. G. and Sarg, J. F. (eds), 1993. Carbonate sequence stratigraphy: recent developments and applications. AAPG Memoir, v. 57.

Lowry, D. C., 1987. A new play in the Gippsland Basin. The APEA Journal 27(1), p164-172.

Ludbrook, N. H., 1957. A reference column for the Tertiary sediments of the South Australian portion of the Murray Basin. Journal of Proceedings for the Royal Society of N.S.W. 90, p174-180.

Ludbrook, N. H., 1971. Stratigraphy and correlation of marine sediments in the western part of the Gambier Embayment. *In:* H. Wopfner and J. G. Douglas (eds). The Otway Basin of Southeastern Australia. Special Bulletin No. 5. Adelaide, Geological Surveys of South Australia and Victoria, p47-67.

McGowran, B., 1973. Observation bore no.2, Gambier Embayment of the Otway Basin: Tertiary micropalaeontology and stratigraphy. Mineral Resources Review, South Australia, v. 135.

McGowran, B., 1978. Stratigraphic record of early Tertiary oceanic and continental events in the Indian Ocean region. Marine Geology 26(1-2), p1-39.

McGowran, B., 1979a The Tertiary of Australia; foraminiferal overview. Marine Micropaleontology 4(3), p235-264.

McGowran, B., 1979b, Comments on Early Tertiary tectonism and lateritization. Geological Magazine 116(3), p227-230.

McGowran, B., 1986. Cainozoic oceanic events: the Indo-Pacific biostratigraphic record. *In:* W. A. Berggren (ed). Global stratigraphic correlation of Mesozoic and Cenozoic sediments. Palaeogeography, Palaeoclimatology, Palaeoecology 55, p247-265.

McGowran, B., 1987, Late Eocene perturbations: foraminiferal biofacies and evolutionary overturn, southern Australia. Paleoceanography 2(6), p715-727.

McGowran, B., 1989a. The later Eocene transgressions in southern Australia. Alcheringa 13(1), p45-68.

McGowran, B., 1989b. Silica burp in the Eocene ocean. Geology 17, p857-860.

McGowran, B., 1991. Maastrichtian and Early Cainozoic, southern Australia: planktonic foraminiferal biostratigraphy. *In*: M.A.J. Williams, P. De Deckker and A.P. Kershaw (eds). The Cainozoic in Australia: a re-appraisal of the evidence. Geological Society of Australia Special Publication v. no.18, p79-98.

McGowran, B. and Beecroft, A., 1985. Guembelitria in the early Tertiary of southern Australia and its palaeoceanographic significance. Special Publication - South Australia, Department of Mines and Energy, 5, p247-261. South Australia, Department of Mines and Energy. Adelaide, South Aust., Australia.

McGowran, B. and Beecroft, A., 1986. Foraminiferal biofacies in a silica-rich neritic sediment, late Eocene, South Australia. Palaeogeography, Palaeoclimatology, Palaeoecology 52(3-4), p321-345.

McGowran, B., Qianyu, L., and Moss, G., 1997, The Cenozoic neritic record in southern Australia: the biogeohistorical framework. *In*: N. P. James and J. A. D. Clarke (eds). Cool-water carbonates. SEPM Special Publication 56, p185-203.

McKirdy, D. M., 1985. Coorongite, coastal bitumen, and their origins from the lacustrine alga

Botryococcus in the western Otway Basin. Otway 85: earth resources of the Otway Basin. Summary of papers and excursion guides of the symposium, Mount Gambier, South Australia, 7-10, February, 1985, by the Geological Society of Australia, South Australian and Victorian Divisions. p34-49.

McKirdy, D. M., 1987. Otway Basin source rocks: observation and inference. Bureau of Mineral Resources, Geology and Geophysics. Record 1987/9, p18-19.

Miall, A. D., 1990. Principles of sedimentary basin analysis. 2nd ed. New York: Springer-Verlag., v. xv, 668 pages.

Middleton, M. F. and Falvey, D. A., 1983. Maturation modeling in Otway Basin, Australia. AAPG Bulletin 67(2), p271-279.

Mildren, S. D., Hillis, R. R., Fett, T., and Robinson, P. H., 1994. Contemporary stresses in the Timor Sea: implications for fault-trap integrity. *In*: P.G. Purcell and R.R. Purcell. (eds). The sedimentary basins of Western Australia. Proceedings of the West Australian Basins Symposium. PESA, p291-300.

Mitchum, R. M., 1977. Seismic stratigraphy and global changes of sea level; Part 1, Glossary of terms used in sequence stratigraphy. *In*: C. E. Payton (ed). Seismic stratigraphy—applications to hydrocarbon exploration. AAPG Memoir 26, p205-212.

Morgan, P. A., Alley, N. F., Rowett, A. J. and White, M. R., 1995. Biostratigraphy. *In*: J. G. G. Morton, and J. F. Drexel (eds). The petroleum geology of South Australia. Volume 1: Otway Basin, South Australia. Department of Mines and Energy. Report Book, v. 95/12.

Morton, J. G. G., Alexander, E. M., Hill, A. J. and White, M. R., 1995. Lithostratigraphy and Environments of Deposition. *In*: J. G. G. Morton, and J. F. Drexel (eds). The petroleum geology of South Australia. Volume 1: Otway Basin, South Australia. Department of Mines and Energy. Report Book, v. 95/12.

Mutter, J. C., Hegarty, K. A., Cande, S. C., and Weissel, J. K., 1985. Breakup between Australia and Antarctica: a brief review in the light of new data. Tectonophysics 114(1-4), p255-279.

Norvick, M. S. and Smith, M. A., 2001. Mapping the plate tectonic reconstruction of southern

and southeastern Australia and implications for petroleum systems. APPEA Journal 41(1), p15-35.

O'Brien, G. W. and Heggie, D. T., 1989. Hydrocarbon gases in seafloor sediments, Otway and Gippsland Basins: implications for petroleum exploration. APEA Journal 29(1), p96-113.

O'Brien, G. W., Reeves, C. V., Milligan, P. R., Morse, M. P., Alexander, E. M., Willcox, J. B., Yunxuan, Z., Finlayson, D. M., and Brodie, R. C., 1994. New ideas on the rifting history and structural architecture of the Western Otway Basin: evidence from the integration of aeromagnetic, gravity and seismic data. APEA Journal, 34(1), p529-554.

Oil, D. N., 1962. Completion report Mount Salt well No.1 and Mount Schank Farm-out. Petroleum Search Subsidy Acts Report, v. 62/1100.

Palmowski, D., Hill, K. C., Hoffman, N., Bernecker, T., 2001. Otway Basin rifting to sea floor spreading—hydrocarbon implications. PESA Eastern Australasian Basins Symposium, Melbourne, November 2001, p499-505.

Partridge, A.D., 2001. Revised Stratigraphy of the Sherbrook Group, Otway Basin. PESA Eastern Australasian Basins Symposium 2001 (eds) K.C. Hill and T. Bernecker, p455-464.

Passlow, V., 1997. Slope sedimentation and shelf to basin sediment transfer; a cool-water carbonate example from the Otway margin, southeastern Australia. *In*: N. P. James and J. A. D. Clarke (eds). Cool-water carbonates. SEPM Special Publication, v. no.56. p107-125.

Payton, C. E. (ed). Seismic stratigraphy—applications to hydrocarbon exploration. AAPG Memoir 26.

Perincek, D. and Cockshell, C. D., 1995. The Otway Basin; Early Cretaceous rifting to Neogene inversion. The APEA Journal 35(1), p451-466.

Pettifer, G., Tabassi, A., and Simons, B., 1991. A new look at the structural trends in the onshore Otway Basin, Victoria, using image processing of geophysical data. The APEA Journal 31(1), p213-228.

Plint, A. G., Eyles, N., Eyles, C. H. and Walker, R. G., 1992. Control of sea level change. *In*: R. G. Walker and N. P. James (eds). Facies models: a response to sea level change. Gelological Association of Canada, p15-25.

Posamentier, H. W., Jervey, M. T., and Vail, P. R., 1988. Eustatic controls on clastic deposition; I, Conceptual framework. SEPM Special Publication 42, p109-124.

Posamentier, H. W. and Vail, P. R., 1988. Eustatic controls on clastic deposition; II, Sequence and systems tract models. SEPM Special Publication 42, p125-154.

Poag, C. W. and Ward, L. W., 1987. Cenozoic unconformities and depositional sequences of North Atlantic continental margins; testing the Vail model. Geology (Boulder) 15(2), p159-162.

Powell, C. M., Roots, S. R., and Veevers, J. J., 1988. Pre-breakup continental extension in East Gondwanaland and the early opening of the eastern Indian Ocean. Tectonophysics 155(1-4), p261-283.

Pratson, L. F. and Coakley, B. J., 1996. A model for the headward erosion of submarine canyons induced by down-slope eroding sediment flows. Geological Society of America Bulletin 108, p225-234.

Pratson, L. F., Ryan, W. B. F., Mountain, G. S. and Twichell, D. C., 1994. Submarine canyon initiation by downslope-eroding sediment flows: evidence in late Cenozoic strata on the New Jersey continental slope. Geological Society of America Bulletin 106, p395-412.

Pratson, L.F., William, B.F., Gregory, S.M. and Twichell, D.C., 1994. Submarine canyon initiation by downslope-eroding sediment flows: Evidence in late Cenozoic strata on the New Jersey continental slope. Geological Society of America Bulletin 106, p395-412.

Prothero, D. R., 1994. The late Eocene-Oligocene extinctions. Annual Review of Earth and Planetary Sciences 22, p145-165.

Quilty, P. G., 1977. Cenozoic sedimentation cycles in Western Australia. Geology (Boulder) 5(6), p336-340.

Quilty, P. G., 1980. Sedimentation cycles in the Cretaceous and Cenozoic of Western Australia.

Tectonophysics 63(1-4), p349-366.

Quilty, P. G., 1994. The background: 144 million years of Australian palaeoclimate and palaeogeography. *In:* R. S. Hill (ed). History of the Australian Vegetation: Cretaceous to Recent. Cambridge University Press, Cambridge, p14-43.

Read, J. F., 1982. Carbonate platforms of passive (extensional) continental margins; types, characteristics and evolution. Tectonophysics 81(3-4), p195-212.

Read, J. F., 1985. Carbonate platform facies models. AAPG Bulletin 69(1), p1-21.

Reid, S. K. and Dorobek, S. L., 1993. Sequence stratigraphy and evolution of a progradational, foreland carbonate ramp, Lower Mississippian Mission Canyon Formation and stratigraphic equivalents, Montana and Idaho. *In*: R. G. Loucks and J. F. Sarg (eds). Carbonate Sequence Stratigraphy: recent developments and applications. AAPG Memoir 57, p327-352.

Royer, J. Y. and Rollet, N., 1997. Plate-tectonic setting of the Tasmanian region. Australian Journal of Earth Sciences 44(5), p543-560.

SAGASCO, R. L., TMOC, E. P. L., Ampol, E. P. P. L., Reeve, J., and Skinner, J., 1994. Rendelsham 1, well completion report. South Australia. Department of Mines and Energy. Open File Envelope, v. 7479/006.

SAGASCO, S. E. I., Minora, R. N., SAGASCO, R. L., Basin, O. N., Cultus, P. A. N., GFE, R. N., and Donley, J. A., 1994. Hungerford 1, well completion report. South Australia. Department of Mines and Energy. Open File Envelope, v. 7478/6.

Sarg, J. F., 1988. Carbonate sequence stratigraphy. *In:* Wilgus, C. K., Hastings, B. S., Kendall, C. G. St. C., Posamentier, H. W., Ross, C. A., and Van, Wagoner J. C., (eds). Sea-level changes: an integrated approach. SEPM Special Publication 42, p 155-181.

Sayers, J., Symonds, P. A., Direen, N. G. and Bernardel, G., 2001. Nature of the continent-ocean transition on the non-volcanic rifted margin of the central Great Australian Bight. *In*: R. C. L. Wilson, R. B. Whitmarsh, B. Taylor and N. Froitzheim (eds). Non-volcanic rifting of continental margins: a comparison of evidence from land to sea. Geological Society, London, Special Publications 187, p51-77.

Schlager, W., 1981. The paradox of drowned reefs and carbonate platforms. Geological Society of America Bulletin 92(4), p197-211.

Schlager, W., 1993. Accommodation and supply; a dual control on stratigraphic sequences. *In*: S. Cloetingh, W. Sassi, F. Horvath, C. Puigdefabregas (eds). Basin analysis and dynamics of sedimentary basin evolution. Sedimentary Geology 86(1-2), p111-136.

Schlager, W., 1999. Sequence stratigraphy of carbonate rocks. The Leading Edge 18(8), p901-907.

Shafik, S., 1983. Calcareous nannofossil biostratigraphy: an assessment of foraminiferal and sedimentation events in the Eocene of the Otway Basin, southeastern Australia. BMR Journal of Australian Geology and Geophysics 8(1), p1-17.

Shafik, S., 1990. The Maastrichtian and early Tertiary record of the Great Australian Bight Basin and its onshore equivalents on the Australian southern margin: a nannofossil study. BMR Journal of Australian Geology and Geophysics 11(4), p473-497.

Shepard, F.P., 1981. Submarine canyons: multiple causes and long time persistence. AAPG Bulletin 65, p1062-1077.

Short, D. A., Harris, R. I., Hartogen, E. L., Beach, P. N., Western, M. C. L., Poseidon, O. P. L., Plateau, O. a. G. N., Alliance, O. D. A. N., Alliance, M. A. N., and Shoreline, E. C., 1987. Camelback 1. Well completion report. South Australia. Department of Mines and Energy. Company Report, v. E7053/6.

Sprigg, R. C., 1952. The geology of the southeast province, South Australia with special reference to Quaternary coastline migration and modern beach developments. South Australian Geological Survey Bulletin 29.

Sprigg, R. C., 1985. A history of the search for commercial hydrocarbons in the Otway Basin complex. In: R. C. Glenie (ed). 2nd South-eastern Australia Oil Exploration Symposium, Melbourne, 1985. Technical Papers. Petroleum Exploration Society of Australia (Vic. and Tasmanian Branches), p173-200.

Stagg, H. M. J., Cockshell, C. D., Willcox, J. B., Hill, A. J., Needham, D. J. L., Thomas, B., O'Brien, G. W. and Hough, L. P., 1990. Basins of the Great Australian Bight region:

geology and petroleum potential. Bureau of Mineral Resources, Geology and Geophysics, Australia. Continental Margins Program Folio, 5.

St John, V. P., 2001. The Petroleum Prospectivity of the Otway Basin. PESA Journal 55, p44-46.

Stover, L. E. and Partridge, A. D., 1973. Tertiary and Late Cretaceous spores and pollen from the Gippsland Basin, southeastern Australia. Royal Society of Victoria. Proceedings 85(2), p237-286.

Stover, L. E. and Partridge, A. D., 1982. Eocene spore-pollen from the Werillup Formation, Western Australia. Palynology 6, p69-96.

Talling, P.J., 1998. How and where do incised valleys form if sea level remains above the shelf edge? Geology 26(1), p87-90.

Traverse, 1988. Paleopalynology. Unwin Hyman, Boston.

Tupper, N. P., Padley, D., Lovibond, R., Duckett, A. K., and McKirdy, D. M., 1993. A key test of Otway Basin potential: the Eumeralla-sourced play on the Chama Terrace. APEA Journal 33(1), p77-93.

Ultramar, A. I. and Shoreline, E. C., 1984. Breaksea Reef 1. Well completion report. South Australia. Department of Mines and Energy. Company Report, v. E5631.

Vail, P. R., Mitchum, R. M., Todd, R. G., Widmier, J. M., Thompson, S., Sangree, J. B., Bubb, N. J. and Hatlelid, W. G., 1977. Seismic stratigraphy and global changes in sea level. *In*: C. E. Payton (ed). Seismic stratigraphy—applications to hydrocarbon exploration. AAPG Memoir 26, p49-212.

Van Wagoner, J. C., Mitchum, R. M., Campion, K. M. and Rahmanin, V. D., 1990. Siliciclastic sequence stratigraphy in well logs, core and outcrop. AAPG Methods in Exploration Series 7.

Van, Wagoner, J. C., Posamentier, H. W., Mitchum, R. M. Jr., Vail, P. R., Sarg, J. F., Loutit, T. S., and Hardenbol, J., 1988. An overview of the fundamentals of sequence stratigraphy and key definitions. SEPM Special Publication 42, p39-45.

Veevers, J. J., 1986. Breakup of Australia and Antarctica estimated as Mid-Cretaceous (95 + or - 5 Ma) from magnetic and seismic data at the continental margin. Earth and Planetary Science Letters 77(1), p91-99. 1986.

Veevers, J.J. (ed), 2000. Billion-year earth history of Australia and neighbours in Gondwanaland. GEMOC Press, Sydney.

Von der Borch C.,C., 1968. Southern Australia submarine canyons: their distribution and ages. Marine Geology 6, 267-279.

Von der Borch, C.C., Conolly, J.R. and Deitz, R.S., 1970. Sedimentation and structure of the continental margin in the vicinity of the Otway Basin, South Australia. Marine Geology 8, p59-83.

Waltham, D., Hardy, S., and Abousetta, A., 1993. Sediment geometries and domino faulting. Geological Society Special Publications 71, p67-85.

Weissel, J. K. and Hayes, D. E., 1972. Magnetic anomalies in the southeast Indian Ocean. Antarctic Research Series 19, p165-196.

Weher, F. L., 1993. Effects of variations in subsidence and sediment supply on parasequence stacking patterns. *In*: P. Weimer and H. W. Posamentier (eds). Siliciclastic sequence stratigraphy—recent developments and applications. AAPG Memoir 58, p369-379.

White, M. R., 1995. Micropalaeontological analysis of 26 petroleum wells in the Gambier Basin, South Australia. South Australia. Department of Mines and Energy. Unpublished Report, v. RB 95/6.

White, M. R., 1996. Subdivision of the Gambier Limestone. MESA Journal 1, p35-39.

Willcox, J. B., Colwell, J. B., and Constantine, A. E., 1992. New ideas on Gippsland Basin regional tectonics. Energy, economics and environment. Gippsland Basin Symposium, Melbourne, 22-23 June, 1992 Papers. AusIMM Publication Series 3/92, p93-110.

Willcox, J. B. and Stagg, H. M. J., 1990. Australia's southern margin: a product of oblique extension. Tectonophysics 173(1-4), p269-281.

Williamson, P. E., O'Brien, G. W., and Swift, M. G., 1996. Petroleum maturation and

subsidence history of the offshore Otway Basin, southeastern Australia - implications for exploration. PESA Journal 24, p77-103.

Willis, T. H. and Shoreline, E. C., 1977. Kentgrove 1. Well completion report. South Australia. Department of Mines and Energy. Company Report, v. E2936.

Wood, G., 1981. Palynological analysis of Eocene coals in the Gambier Embayment near Kingston. Adelaide University. Department of Geology and Mineralogy. Hons Thesis (unpublished).

Wopfner, H. and Douglas, J.G. (eds), 1971. The Otway Basin of Southeastern Australia. Special Bulletin No. 5. Adelaide, Geological Surveys of South Australia and Victoria.

Yu, S. M. Structure and development of the Otway Basin. The APEA Journal 28(1), p243-254.

Publications

PUBLISHED PAPERS AND ABSTRACTS

Pollock, R. M., 2000. Sequence stratigraphy, biostratigraphy and depositional systems in the Cainozoic Gambier Sub-basin, southern Australia. AAPG Bulletin 84(11), p1871.

Pollock R., Lang S. C., McGowran, B. and Li, Q., 2000. Sequence stratigraphy, biostratigraphy and depositional systems analysis—an integrated study in the Gambier Basin, southern Australia. Geological Society of Australia, Abstracts no. 59. 15th Australian Geological Convention, Sydney, July 2000, p394.

Pollock R., Lang S. C., McGowran, B. and Li, Q., 2000. Integration of carbonate sequence stratigraphy, biostratigraphy and depositional systems analysis in the Gambier Sub-basin, southern Australia. AAPG Bulletin 84(9), p1476.

Pollock, R. M., Li, Q., McGowran, B. and Lang, S. C., 2002. Oligo-Miocene canyons in the Gambier Sub-basin, southern Australia—deepwater analogues for petroleum exploration. APPEA Journal 42(1), p311-329.

Pollock, R.M., Li, Q., McGowran, B. and Lang, S. (2002) Oligo-miocene canyons in the gambier sub-basin, Southern Australia: deepwater analogues for petroleum exploration.
APPEA Journal, v. 42 (1), pp. 311-329, 2002

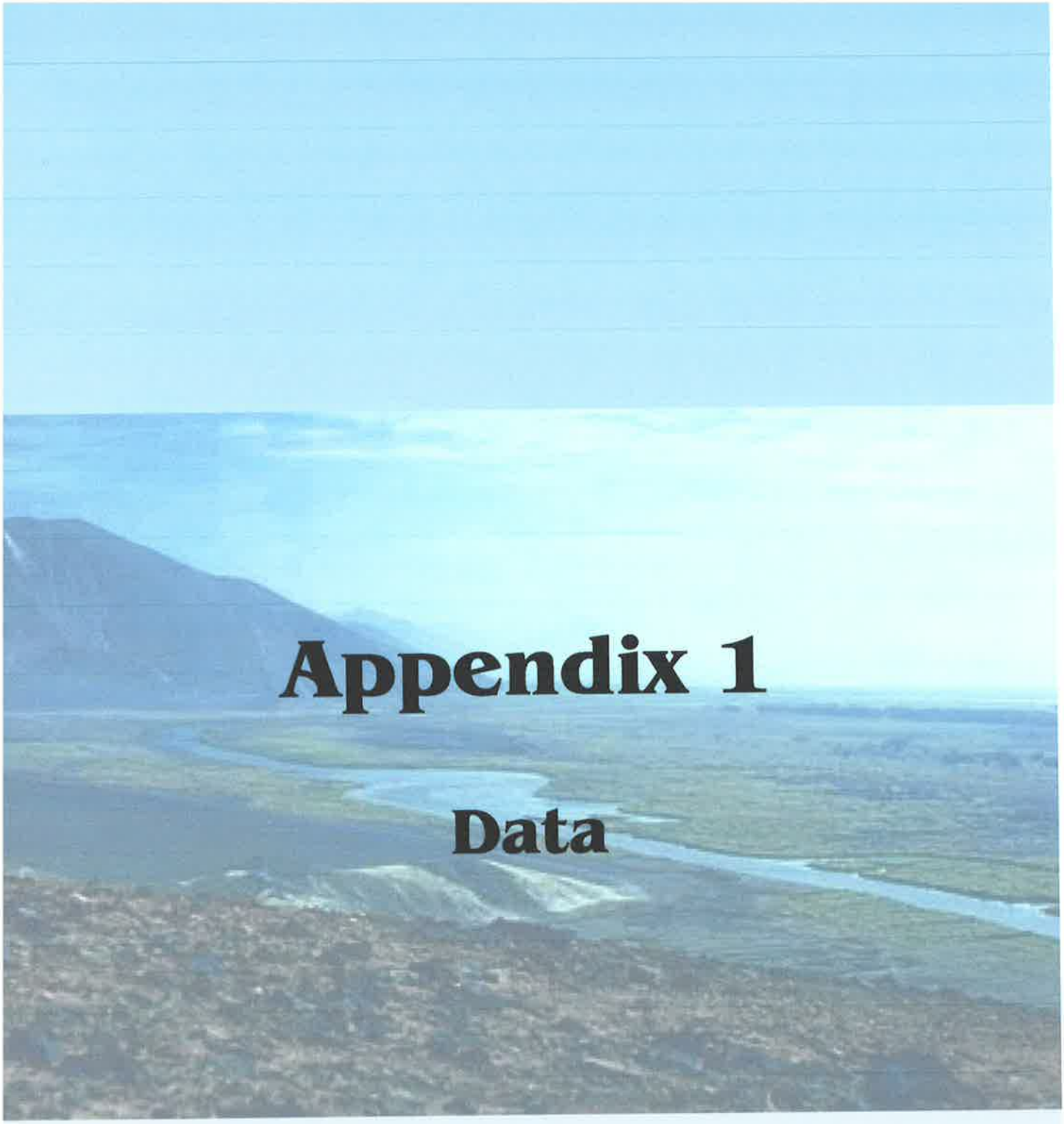

Appendix 1

Data

APPENDIX 1 DATA

APPENDIX	DESCRIPTION
1.1	Summary of well data in the Gambier Sub-basin used in this study.
1.2	Summary of seismic data used in this study (for a location map refer to Chapter 1, Fig. 1.5).
1.3	Biostratigraphic results analysed for this study.
1.4	Thickness of systems tracts and sequences and the percentage of sand within each package determined from well data.
1.5	Calculations for the progradation to aggradation ratio for each supersequence.
1.6	Calculations for sedimentation rates of each supersequence.
1.7	Summary of fault throw magnitudes at each supersequence boundary.
1.8	Analysis of fault movement of Gambier Sub-basin faults during the Cenozoic.

WELL	DATE	LATITUDE	LONGITUDE	LOGS	CHECK SHOT	BIOSTRAT QUALITY	CORE	CUTTINGS
Argonaut 1A	1968	37 58' 17.7"S	140 15' 52.9"E	cali, GR, DT, RHOB, DRHO	Yes	Poor	Yes	Yes
Beachport East 1	1973	37 26' 59.9"S	140 5' 9.43"E	GR	No	Poor	No	Yes
Breaksea Reef 1	1983	38 9' 30.9"S	140 36' 44.4"E	cali, GR, DT, RHOB, NPHI	Yes	Fair	No	Yes
Burrungule 1	1975	37 46' 16"S	140 32' 18"E	cali, GR, DT	No	Poor	Yes	Yes
Caroline 1	1967	37 56' 30"S	140 54' 30"E	cali, GR, DT, NEUT	Yes	Poor	Yes	Yes
Chama 1A	1970	37 25' 36.9"S	139 32' 36.7"E	cali, GR, DT, NEUT	Yes	Poor	No	Yes
Compton 1	1988	37 47' 42.3"S	140 42' 42.9"E	cali, GR, DT, RHOB, NPHI	Yes	Poor	No	Yes
Copa 1	1989	37 41' 18.3"S	139 45' 22.0"E	cali, GR, DT, RHOB, NPHI	Yes	None	No	No
Crayfish 1	1967	37 17' 22"S	139 35' 50"E	cali, GR, DT, RHOB	Yes	Poor	Yes	Yes
Douglas Point 1	1973	38 01' 33"S	140 35' 44"E	cali, GR, DT, RHOB	No	Poor	No	Yes
Geltwood Beach 1	1962	37 39' 44"S	140 14' 35"E	SP, LN, SN	No	Poor	No	Yes
Kentgrove 1	1976	37 56' 48"S	140 37' 25.2"E	cali, GR, DT	No	Poor	No	Yes
Lake Bonney 1	1967	37 50' 39"S	140 28' 21"E	cali, GR, DT	No	Poor	Yes	Yes
Lake George 1	1969	37 27' 9"S	140 2' 35"E	cali, GR, DT, RHOB, DRHO	No	Poor	No	Yes
McNamara 1	1987	37 50' 13.9"S	140 37' 46.0"E	cali, GR, DT, RHOB, NPHI	Yes	None	No	Yes
McNichol 1	1997	37 49' 58.0"S	140 50' 52.5"E	cali, GR, DT	Yes	Poor	No	Yes
Morum 1	1975	37 30' 9.0"S	139 14' 7.8"E	cali, GR, DT, RHOB, NPHI	Yes	Poor	No	Yes
Mount Salt 1	1962	37 57' 25"S	140 37' 43"E	cali, SP	No	Poor	No	Yes
Neptune 1	1974	37 18' 13.0"S	139 44' 8.5"E	cali, GR, DT, RHOB, NEUT	Yes	Poor	No	Yes
Normanby 1	1986	38 14' 11.6"S	141 5' 3.3"E	cali, GR, DT, CNL	No	Poor	No	Yes
Northumberland 1	1993	38 02' 9.4"S	140 39' 58.4"E	cali, GR, DT, RHOB, NPHI	No	Poor	No	Yes
Rendlesham 1	1994	37 33' 46.6"S	140 13' 55.0"E	cali, GR, DT, RHOB, NPHI	Yes	Poor	No	Yes
Troas 1	1993	37 22' 1.8"S	139 23' 22.3"E	cali, GR, DT, RHOB, NPHI	Yes	Poor	Yes	Yes
Trumpet 1	1973	37 05' 47.3"S	139 24' 0"E	cali, GR, DT, RHOB, NPHI	No	None	No	Yes

Summary of well data used in this study.

SURVEY	LINE	LENGTH (km)
85	85-02	46.90
	85-06	76.84
	85-13	83.71
	85-25	59.70
	85-25A	15.84
	85-31	51.70
BO 97	BO97A-01	27.45
	BO97A-02	18.53
BO 98	BO98A-01	16.72
	BO98-02	23.07
	BO98A-03	20.00
	BO98B-05	19.67
BU 85	BU85-07	10.16
	BU85-09	17.60
	BU85-11	16.15
	BU85-17	8.93
	BU85-40	8.00
	BU85-48	12.33
	BU85-50	24.65
	BU85-50A	16.66
BUD 86	BUD86-67	6.17
	BUD86-76	7.12
CO88	CO88-11	17.85
	CO88-16	22.33
	CO88-46	16.20
	CO88-48	27.00
GA 88	GA88-04	9.13
	GA88-05	15.00
KO 90	KO90-01	15.03
	KO90-02	17.70
	KO90-03	5.66
ME 93	ME93-01	7.57
	ME93-02	8.70
	ME93-03	11.30
	ME93-04	8.44
	ME93-05	7.73
	ME93-06	10.30
	ME93-07	18.83
	ME93-08	18.52
	ME93-09	14.90
	ME93-10	15.30
CO90	CO90-14 (EXT)	20.25
	CO90-32	35.57
SCD 91	SCD91-116	12.06
	SCD91-123	7.23
	SCD91-125	14.21
R93	R93-17	17.20
	R93-23	11.25
OP 80	OP80-22	63.45
90 HA	90HA-04	18.66

SURVEY	LINE	LENGTH (km)
OC 90	OC90B-21	18.00
	OC90B-22	27.37
	OC90B-27	14.20
	OC90C-02	61.13
	OC90C-31	16.10
	OC90C-37	16.50
	OC90C-506	39.15
	OC90C-523	21.15
OH 91	OH91-401	41.53
	OH91-402	106.00
	OH91-404	18.82
	OH91-405	30.33
	OH91-409	18.72
	OH91-411	27.18
	OH91-509	27.23
UA 82	UA82-05	41.64
	UA82-08	86.65
	UA82-13A	18.65
	UA82-16	31.38
	UA82-14	27.20
	UA82-18	48.05
	UA82-19	27.10
	UA82-20	31.90
	UA82-22	23.00
	UA82-23	38.40
	UA82-25	24.37
	UA82-27	33.95
	UA82-29	30.22
	UA82-31	30.00
	UA82-35	35.00
	UA82-33	30.77
	UA82-37	36.00
	UA82-41	32.00
	UA82-43	35.00
	UA82-47	33.30
	UA82-49	31.15
UA 85	UA85-01.5	34.00
	UA85-02.5	21.00
	UA85-03.5	37.40
	UA85-04.7	14.10
	UA85-5.5	27.00
	UA85-07.5	24.30
91 MH	91MH-08	14.60
	91MH-11	7.90
	91MH-12	16.75
137	137-01	300.00
	137-03	250.00
	137-04	235.00
	137-10	215.00
	137-12	215.00
TOTAL	**100 Lines**	**3676.43**

Summary of the seismic data used in this study.

WELL	SAMPLE	DEPTH (m)	SPORE/POLLEN	DINOFLAG.	FORAMINIFERA	AGE	PALAEOENV.
Argonaut 1A	cuttings	26.5			elphidina, poroides		IS
	cuttings	27.1			elphidina, parrellina		IS
	cuttings	274.3			elphidina, pararotalia		IS
	cuttings	289.6			bivalves only		
	cuttings	326.1			elphidina, parrellina, cibicides		
	cuttings	329.2			Notorotalia		IS/Mm
	cuttings	350.5			elphidina, parrellina		IS/Mm
	cuttings	365.8			elphidina, parrellina		IS
	cuttings	381.0					IS
	cuttings	457.2			microgastropodes		IS/Mm
	cuttings	472.4			parrallina, cerroazulelı, microgastropod		IS/Mm
	cuttings	487.7			cibicides, discorbid		IS/Mm
	cuttings	634.0	Upper Malvacipollis diversus-Lower Nothofagidites asperus			Early Eocene-Mid Eoc.	Mm
	cuttings	637.0	Upper Malvacipollis diversus-Lower Nothofagidites asperus			Early Eocene-Mid Eoc.	Nm
	cuttings	646.2	Upper Malvacipollis diversus-Lower Nothofagidites asperus			Early Eocene-Mid Eoc.	Nm
	cuttings	649.2	Upper Malvacipollis diversus			Early Eocene	Mm
	cuttings	658.4	Upper Malvacipollis diversus			Early Eocene	Nm
	cuttings	661.4	Upper Malvacipollis diversus			Early Eocene	Mm
	cuttings	664.5	Lower Malvacipollis diversus			Early Eocene	Nm
	cuttings	667.5	Lower Malvacipollis diversus			Early Eocene	Mm
	cuttings	673.6	Lower Malvacipollis diversus			Late Paleoc-Early Eoc.	Mm
	cuttings	670.6	Lower Malvacipollis diversus			Late Paleoc-Early Eoc.	Nm
	cuttings	679.7	Lower Malvacipollis diversus			Late Paleoc-Early Eoc.	Mm
	cuttings	688.8	Upper Lygistepollenites balmei			Late Paleocene	Mm
	cuttings	691.9	Upper Lygistepollenites balmei			Late Paleocene	Mm

Results of the biostratigraphic analysis conducted for this study.

WELL	SAMPLE	DEPTH (m)	SPORE/POLLEN	DINOFLAG.	FORAM.	AGE	PALAEOENV.
Breaksea Reef 1	cuttings	280			archeomenardii, dehiscens, G.woodi	> N9	OS
	cuttings	300			Globerosa suturalis, dehiscens	N9	OS
	cuttings	305			woodi, dehiscens, connecta	N5	MS
	cuttings	310			woodi, dehiscens, connecta	N4	MS
	cuttings	350			suterii, sellii tripartiva	P22	MS
	cuttings	400			suterii, sellii, euapertura	P22	MS
	cuttings	470			suterii, euapertura c.f. angiporoides	Early Oligocene	IS
	cuttings	475			tripartira group, saferi, aficrassata	Early Oligocene	IS
	cuttings	485			c.f. angiporoides, dissimilis	Early Oligocene	IS
	cuttings	490			suterii c.f. dissimilis	Early Oligocene	IS
	cuttings	500			angiporoides	Early Oligocene	IS
	cuttings	510			angiporoides	Early Oligocene	IS
	cuttings	515			Cyclamina and caved freah benthics		IS
	cuttings	520			Cyclamina and caved freah benthics		IS
	cuttings	670.6-673.6	? Forcipites longus zone			Maastrichtian	Mm
	cuttings	610.0	Upper Malvacipollis diversus			Early Eocene	Mm
	cuttings	620.0	Upper Malvacipollis diversus			Early Eocene	Mm
	cuttings	630.0	Upper Malvacipollis diversus			Early Eocene	Mm
	cuttings	635.0	Upper Malvacipollis diversus			Early Eocene	Mm
	cuttings	650.0	Upper Malvacipollis diversus			Early Eocene	Mm
Transition zone	cuttings	660.0	Malvacipollis diversus			Early Eocene	Mm
	cuttings	665.0	Malvacipollis diversus			Early Eocene	Mm
	cuttings	680.0	Lower-?Up. Malvacipollis diversus			Early Eocene	Mm
	cuttings	700.0	Lower-?Up. Malvacipollis diversus			Early Eocene	Mm
	cuttings	775.0	Lower Malvacipollis diversus			Early Eocene	Mm
	cuttings	780.0	Lower Malvacipollis diversus			Early Eocene	Mm
	cuttings	925.0	Lower Malvacipollis diversus			Early Eocene	Mm
	cuttings	950.0	Lower Malvacipollis diversus			Early Eocene	Mm
	cuttings	960.0	Lower Malvacipollis diversus			Early Eocene	Mm
	cuttings	965.0	Lower Malvacipollis diversus			Early Eocene	Mm
	cuttings	970.0	Lower Malvacipollis diversus			Early Eocene	Mm
	cuttings	975.0	Lower Malvacipollis diversus			Early Eocene	Mm
	cuttings	980.0	Lower Malvacipollis diversus			Early Eocene	Mm
	cuttings	985.0	Lower Malvacipollis diversus			Early Eocene	Mm
	cuttings	1000.0	Lower Malvacipollis diversus			Early Eocene	Mm
	cuttings	1005.0	Lower Malvacipollis diversus			Early Eocene	Mm
	cuttings	1010.0	Lower Malvacipollis diversus			Early Eocene	Mm
	cuttings	1020.0	Lower Malvacipollis diversus			Early Eocene	Mm
	cuttings	1025.0	Lower Malvacipollis diversus			Early Eocene	Nm
	cuttings	1030.0	Lower Malvacipollis diversus			Early Eocene	Mm
	cuttings	1035.0	Lower Malvacipollis diversus			Early Eocene	Mm
	cuttings	1040.0	Lower Malvacipollis diversus			Early Eocene	Mm
	cuttings	1050.0	Upper Forcipites longus			Upper Cret-?Early Paleo	Mm
	cuttings	1055.0	Upper Forcipites longus			Upper Cret-?Early Paleo	Mm

Results of the biostratigraphic analysis conducted for this study

WELL	SAMPLE	DEPTH (m)	SPORE/POLLEN	DINOFLAG.	FORAM.	AGE	PALAEOENV.
Burrungule 1	cuttings	100-110				N4	IS
	cuttings	634.0-637.0	Lygistepollenites balmei			Late Paleocene	Mm
	cuttings	640.1	Lygistepollenites balmei			Late Paleocene	M
	cuttings	643.1-646.2	Lygistepollenites balmei			Late Paleocene	Mm
	cuttings	649.2-652.4	Forcipites longus			Maastrichtian	Mm
	cuttings	655.3-658.4	Forcipites longus			Maastrichtian	M
	cuttings	661.4-664.5	Forcipites longus			Maastrichtian	Mm
	cuttings	667.5-670.6	? Forcipites longus			Maastrichtian	Mm

WELL	SAMPLE	DEPTH (m)	SPORE/POLLEN	DINOFLAG.	FORAM.	AGE	PALAEOENV.
Caroline 1	cuttings	6.0			Elphidina, cibi, H.	Plio-Pleistocene	IS
	cuttings	12.2			H.brevalis, C.pseudo? C.f. index, triloba, unicarns, woodii, suteri	Oligo-Miocene	IS
	cuttings	42.7			brevis group	P18	MS
	cuttings	64.0			brevis group, turborotalia, breseri	P18	MS
	cuttings	79.2			planktonic woodii, cibii Heterolepa	P18	MS
	cuttings	103.6			Victoriella conoidea, Notorotalia poroides	Oligocene	IS
	cuttings	112.8			Victoriella, ampliapertura	Oligocene	IS
	cuttings	115.8			planktonic undiff.	Oligocene	IS
	cuttings	121.9			benthic only	Oligocene	IS
	cuttings	134.1			globigerinid, T.c.f. increbescens	Oligocene	IS
	cuttings	213.4-214.9	Proteacidites asperopolus			Ealry-Middle Eocene	Mm
	cuttings	234.7	Malvacipollis diversus			Early Eocene	Mm
	cuttings	265.2	Malvacipollis diversus			Early Eocene	Fl
	cuttings	286.5	Malvacipollis diversus			Early Eocene	Fl
	cuttings	313.9	Malvacipollis diversus			Early Eocene	Fl
	cuttings	347.4	Malvacipollis diversus			Early Eocene	Fl
	cuttings	731.5	Malvacipollis diversus			Early Eocene	Fl
	cuttings	747.9	Malvacipollis diversus			Early Eocene	Fl
	cuttings	807.7	Malvacipollis diversus			Early Eocene	Fl
	cuttings	822.9	Malvacipollis diversus			Early Eocene	Fl
	cuttings	853.4	Malvacipollis diversus			Early Eocene	Fl
	cuttings	883.9	Malvacipollis diversus			Early Eocene	Mm
	cuttings	890	Malvacipollis diversus			Early Eocene	Mm
	cuttings	896	Malvacipollis diversus			Early Eocene	Mm
	cuttings	899.1	Malvacipollis diversus			Early Eocene	Mm
	cuttings	929.6	Lygistepollenites balmei			Late Palaeocene	Mm

Results of the biostratigraphic analysis conducted for this study.

WELL	SAMPLE	DEPTH (m)	SPORE/POLLEN	DINOFLAG.	FORAM.	AGE	PALAEOENV.
Chama 1	cuttings	286.5			bulloides, obesa	Pliocene if not caved	MS
	cuttings	289.5			c.f. crassaformis	Pliocene if not caved	MS
	cuttings	292.6			benthics, discammdina spinid form	Pliocene if not caved	MS
	cuttings	335.3			siphonina, orbulina, crassaformis	Miocene	MS
	cuttings	338.3			parvulus, trilobus, decoraperta, orbulina	Miocene	OS
	cuttings	350.5			Lenticulina, Gyridinoides	Oligocene	MS
	cuttings	365.7			benthics only	Oligocene	IS
	cuttings	368.8			Victoriella conoidea, globossa + other benthics	Oligocene	IS
	cuttings	371.8			agglutinated bi-uni serial	Oligocene	IS
	cuttings	374.9			Victoriella + Wadella	Oligocene	IS
	cuttings	381.0			Victoriella + Lenticulina	Oligocene	IS
	cuttings	384.0			Victoriella + Lenticulina + Wadella	Oligocene	IS
	cuttings	387.1			Victoriella + Lenticulina	Oligocene	IS
	cuttings	390.1			Victoriella + Lenticulina+polymorph	Oligocene	IS
	cuttings	393.2			Olagenid	Eocene - Oligocene	IS
	cuttings	396.2			Lenticulina, cibicidoides, Bulimina	Eocene - Oligocene	IS
	cuttings	405.4			fish tooth	Eocene - Oligocene	IS
	cuttings	408.4			Lenticulina	Eocene - Oligocene	IS
	cuttings	487.7			subglobosa	Eocene - Oligocene	IS
	cuttings	499.9			Gyroidinoides	Eocene - Oligocene	IS
Compton 1	cuttings	590-595	Lygistepollenites balmei			Paleocene	Mm
	cuttings	600-605	Lygistepollenites balmei			Paleocene	Mm
	cuttings	605-610	Malvacipollis diversus			Paleocene	Mm
	cuttings	610-615	Forcipites longus			Late Cretaceous	Mm
	cuttings	615-620	Forcipites longus			Late Cretaceous	Mm
	cuttings	620-625	? Forcipites longus			Late Cretaceous	Nm

WELL	SAMPLE	DEPTH (m)	SPORE/POLLEN	DINOFLAG.	FORAM.	AGE	PALAEOENV.
Copa 1	cuttings	430	Lower Malvacipollis diversus		caved suturalis, dehiscens	Early Eocene	M
	cuttings	440	Lower Malvacipollis diversus		globigerinid, Lenticulins	Early Eocene	Mm
	cuttings	450	Lower Malvacipollis diversus		Lenticulina	Early Eocene	M
	cuttings	460	Lower Malvacipollis diversus			Early Eocene	M
	cuttings	470	Lower Malvacipollis diversus		Lenticulina, subbotina sp.	Early Eocene	Mm
	cuttings	490-500	Lower Malvacipollis diversus			Early Eocene	Mm
	cuttings	500	Lower Malvacipollis diversus			Early Eocene	M
	cuttings	500-510	Upper Lygistepollenites balmei-?Lower Malvacipollis diversus			Late Paleoc-Early Eoc.	Mm
	cuttings	520-530	Upper Lygistepollenites balmei-Lower Malvacipollis diversus			Late Paleoc-Early Eoc.	Mm
	cuttings	530-540	Upper Forcipites longus-Lygistepollenites balmei			Late Cret-Late Paleoc.	Mm
	cuttings	540-550	Upper Forcipites longus			Upper Maastrichtian	Mm
	cuttings	550-560	BARREN				
	cuttings	560-570	Upper Forcipites longus			Upper Maastrichtian	Mm
	cuttings	570-580	BARREN				
	cuttings	580-590	Upper Forcipites longus			Upper Maastrichtian	Mm
	cuttings	680-690	Forcipites longus			Upper Maastrichtian	Mm
Crayfish 1	cuttings	249.9			Lenticulina	Early Miocene	IS
	cuttings	256.0			dehiscens, dissimilis, c.f. siahensis, connecta, bulloides	Early Miocene	IS
	cuttings	274.3					IS
	cuttings	286.5			Victoriella conoidea	Late Oligocene	IS
	cuttings	304.8				Late Oligocene	IS
	cuttings	323.0			Lenticulina	Late Oligocene	IS
	cuttings	326.1			Lenticulina, V.conoidea, W.globiformis	Late Oligocene	IS
	cuttings	329.2			V.conoidea	Late Oligocene	IS
	cuttings	332.2			abiaerassata, bulloides	Early Oligocene	IS
	cuttings	335.3			globigerinid, cibi, gyroi, globocassi	Early Oligocene	Mm
	cuttings	341.3			angiporoides, V.conoidea	Early Oligocene	Mm
	cuttings	350.5			angiporoides, Victoriella, praebulloidies	Early Oligocene	Mm
	cuttings	356.6			Centiculina, Tuborotalia c.f. ampliaperura, euapertura		Mm
	swc	363.3	Upper Lygistepollenites balmei			Palaeocene	Mm

Results of the biostratigraphic analysis conducted for this study.

WELL	SAMPLE	DEPTH (m)	SPORE/POLLEN	DINOFLAG.	FORAM.	AGE	PALAEOENV.
Douglas Point 1	swc	970.2	Lower Malvacipollis diversus			Early Eocene	Mm
	swc	979.0	Lower Malvacipollis diversus			Early Eocene	Mm
	swc	985.1	Lower Malvacipollis diversus			Early Eocene	Mm
	swc	991.5	Lower Malvacipollis diversus			Early Eocene	M
	swc	994.9	Lower Malvacipollis diversus			Early Eocene	Mm
	swc	1008.0	Lygistepollenites balmei			Late Paleocene	M
	swc	1010.1	Lygistepollenites balmei			Late Paleocene	Mm
Lake George 1	cuttings	246.9				P17-P20	IS
	cuttings	250.0				P17-P20	MS
	swc	249.9-252.7	Middle Nothofagidites asperus (P16)			Late Eocene	
	cuttings	253.0				P15-P18	
	cuttings	259.0				P15-P18	MS
	cuttings	262.0				P15-P18	MS
	cuttings	265.2					IS
	swc	267.3	Lower Nothofagidites asperus			Eocene	
	cuttings	274.3				Eocene	
	swc	279.0	Proteacidites asperopolus			Early-Middle Eocene	IS
	cuttings	280.4				Early-Middle Eocene	IS
	cuttings	320.0				Early-Middle Eocene	IS
	cuttings	344.4				Early-Middle Eocene	IS
	cuttings	387.0				Early Eocene (P6B-P9)	IS
	swc	389.2	Upper Malvacipollis diversus			Early Eocene	

WELL	SAMPLE	DEPTH (m)	SPORE/POLLEN	DINOFLAG.	FORAM.	AGE	PALAEOENV.
Kentgrove 1	cuttings	417.6-420.6	Upper Malvacipollis diversus - (Proteacidites asperopolus)			Early Eocene	
	cuttings	426.7-429.8	Upper Malvacipollis diversus - (Proteacidites asperopolus)			Early Eocene	
	cuttings	442.0-445.0	Upper Malvacipollis diversus			Early Eocene	
	cuttings	457.2-460.2	Upper Malvacipollis diversus			Early Eocene	
	cuttings	472.4-475.5	Upper Malvacipollis diversus			Early Eocene	
	cuttings	487.7-490.7	Lower Malvacipollis diversus			Early Eocene	
	cuttings	502.9-506.0	Upper Malvacipollis diversus			Early Eocene	
	cuttings	518.2-521.2	(Lygestipollenites balmei) - Lower Malvacipollis diversus			Early Eocene	
	cuttings	533.4-536.4	(Lygestipollenites balmei) - Lower Malvacipollis diversus			Early Eocene	
	cuttings	548.6-551.7	(Lygestipollenites balmei) - Lower Malvacipollis diversus			Early Eocene	
	cuttings	563.9-566.9	(Lygestipollenites balmei) - Lower Malvacipollis diversus			Early Eocene	
	cuttings	670.6-673.6	(Lygestipollenites balmei) - Lower Malvacipollis diversus			Early Eocene	
	cuttings	685.8-688.8	(Lygestipollenites balmei) - Lower Malvacipollis diversus			Early Eocene	
	cuttings	701.0-704.1	(Lygestipollenites balmei) - Lower Malvacipollis diversus			Early Eocene	
	cuttings	716.3-719.3	(Lygestipollenites balmei) - Lower Malvacipollis diversus			Early Eocene	
	cuttings	731.5-734.6	(Lygestipollenites balmei) - Lower Malvacipollis diversus			Early Eocene	
	cuttings	746.8-749.8	? (Lygestipollenites balmei) - Lower Malvacipollis diversus			Early Eocene	
	cuttings	762.0-765.0	(Lygestipollenites balmei) - Lower Malvacipollis diversus			Early Eocene	
	cuttings	792.5-795.5	(Lygestipollenites balmei) - Lower Malvacipollis diversus			Early Eocene	
	cuttings	838.2-841.2	Lygestipollenites balmei - (Lower Malvacipollis diversus)			Late Paleoc-Early Eoc.	
	cuttings	853.4-856.5	Lygestipollenites balmei - (Lower Malvacipollis diversus)			Late Paleoc-Early Eoc.	
	cuttings	862.6-865.6	Lygestipollenites balmei - (Lower Malvacipollis diversus)			Late Paleoc-Early Eoc.	
	cuttings	868.7-871.7	Lygistepollenites balmei			Middle - Late Palaeocene	
	cuttings	875.4-878.4	Lygistepollenites balmei			Middle - Late Palaeocene	
	cuttings	880.9-883.9	Lygistepollenites balmei			Middle - Late Palaeocene	
	cuttings	914.4-917.4	Lygistepollenites balmei			Middle - Late Palaeocene	
	cuttings	944.9-947.9	Lygistepollenites balmei			Middle - Late Palaeocene	

McNamara 1	cuttings	560-570	Malvacipollis diversus			Early Eocene	Mm
	cuttings	570-580	Malvacipollis diversus -Lygistepollenites balmei			Late Paleocene-Early E	Mm
	cuttings	590-600	? Forcipites longus-Lygistepollenites balmei			?Late Cretac-Paleocene	Mm
	cuttings	600-610		Isabelidinium korojonense zone		Campanian-Maastrichti	M
	cuttings	610-620	Tricolporites lilliei			Campanian-Maastrichti	Mm
	cuttings	620-630	Tricolporites lilliei			Campanian-Maastrichti	Mm
	cuttings	630-640	? Tricolporites lilliei (Late Paleocene microflora abundant)			Campanian-Maastrichti	Mm
	cuttings	640-650	? Tricolporites lilliei			Campanian-Maastrichti	Mm

Results of the biostratigraphic analysis conducted for this study.

WELL	SAMPLE	DEPTH (m)	SPORE/POLLEN	DINOFLAG.	FORAM.	AGE	PALAEOENV.
McNicol 1	cuttings	617	Upper Malvacipollis diversus - (Proteacidites asperopolus)			Early Eocene	
	cuttings	650	Upper Malvacipollis diversus			Early Eocene	
	cuttings	677	Lower Malvacipollis diversus			Early Eocene	
	cuttings	708	Lower Malvacipollis diversus			Early Eocene	
	cuttings	725	Lygistepollenites balmei			Middle - Late Paleocene	
	cuttings	756	Forcipites longus			Maastrichtian	
Morum 1	cuttings	436.7-445			agglutinated tri-bi serial	Middle Miocene	
	cuttings	527.3	Lygistepollenites balmei			Late Paleocene	Mm
	cuttings	536.4	Lygistepollenites balmei			Late Paleocene	Nm
	cuttings	545.6	Lygistepollenites balmei			Late Paleocene	Mm
	cuttings	554.7	Lygistepollenites balmei			Middle Paleocene	Mm
	cuttings	563.9	Lygistepollenites balmei			Middle Paleocene	Mm
	cuttings	573.0	Upper Forcipites longus			Upper Maastrichtian	M
	cuttings	582.2	Upper Forcipites longus			Upper Maastrichtian	Mm
	cuttings	591.3	Upper Forcipites longus			Upper Maastrichtian	Mm
	cuttings	600.5	Upper Forcipites longus			Upper Maastrichtian	Mm

Results of the biostratigraphic analysis conducted for this study

Mount Salt 1	cuttings	303.3	Upper Malvacipollis diversus			Early Eocene	
	cuttings	487.7	Upper Malvacipollis diversus			Early Eocene	
	cuttings	490.7	?Malvacipollis diversus*			Early Eocene	
	cuttings	585.2	Lower Malvacipollis diversus			Early Eocene	
	cuttings	588.3	?Malvacipollis diversus*			Early Eocene	
	cuttings	665.7	Lower Malvacipollis diversus			Early Eocene	
	cuttings	667.5	?Malvacipollis diversus*			Early Eocene	
	cuttings	883.9	Upper Lygistepollenites balmei			Early Eocene	
	cuttings	887.0	?Malvacipollis diversus*			Early Eocene	
	cuttings	957.7	Upper Lygistepollenites balmei			Early Eocene	
	cuttings	958.6					
	cuttings	1123.2	?Forcipites longus			Maastrichtian	
	cuttings	1220.7	?Forcipites longus - Tubulifloridites lilliei			Maastrichtian-Campanian	
	cuttings	1286.3					
	cuttings	1382.3	?Tubulifloridites lilliei	Xenikoon australis		Maastrichtian-Campanian	
	cuttings	1460.0					
	cuttings	1510.3					
	cuttings	1536.2		Nelsoniella aceras		Campanian - Santonian	
	cuttings	1764.8		Isabelidinium cretaceum		Santonian	
	cuttings	1830.3					
	cuttings	2129.0					
	cuttings	2185.4		Isabelidinium cretaceum			
	cuttings	2419.2					
	cuttings	2420.1					
	cuttings	2567.9	Phyllocladidites mawsonii			?Turonian	
	cuttings	2871.2	Phyllocladidites mawsonii			?Turonian	
	cuttings	3003.2					
	cuttings	3060.8				Albian - Cenomanian	

*Yarrow, 1981 Phillips Australian Oil Co. Perth

WELL	SAMPLE	DEPTH (m)	SPORE/POLLEN	DINOFLAG.	FORAM.	AGE	PALAEOENV.
Neptune 1	cuttings	182.9			benthics only, Lenticulina, Wodella, globocassi, euporoides	Oligo-Miocene	IS
	cuttings	192.0			Wodella, poroides	Oligo-Miocene	IS
	cuttings	210.3			globiformis	Oligo-Miocene	IS
	cuttings	219.4			Victoriella, Lenticuina	Oligo-Miocene	IS
	cuttings	265.2			Gyroi, Gporoides, Wodella	Oligocene	IS
	cuttings	292.6			Lenticulina	Oligocene	IS
	cuttings	320.0			Lenti, Victoriella, pseudo?, brevoralis	Oligocene	IS
	cuttings	347.4			Victoriella, Lenti, Eporoides	Oligocene	IS
	cuttings	384.0			Lenti, brevoralis, Cibi, bullimina	Oligocene	IS
	cuttings	402.3			Victoriella	Oligocene	IS
	cuttings	411.4					FI?

Results of the biostratigraphic analysis conducted for this study.

WELL	SAMPLE	DEPTH (m)	SPORE/POLLEN	DINOFLAG.	FORAM.	AGE	PALAEOENV.
Northumberland	cuttings	350.9	Proteacidites asperopolus			Early Eocene	
	cuttings	444-447	Proteacidites asperopolus			Early Eocene	
	cuttings	493.2	Proteacidites asperopolus			Early Eocene	
	cuttings	513-516	Proteacidites asperopolus			Early Eocene	
	cuttings	549-552	Proteacidites asperopolus			Early Eocene	
	cuttings	586.0	Proteacidites asperopolus			Early Eocene	
	cuttings	633-636	Lower Malvacipollis diversus			Early Eocene	
	cuttings	700.0	Lower Malvacipollis diversus			Early Eocene	
	cuttings	730.0	Lower Malvacipollis diversus			Early Eocene	
	cuttings	783-786	Lower Malvacipollis diversus			Early Eocene	
	cuttings	807-810	Lower Malvacipollis diversus			Early Eocene	
	cuttings	828-831	Lower Malvacipollis diversus			Early Eocene	
	cuttings	850.0	Lygistepollenites balmei			Late Paleocene	
	cuttings	856.8	Lygistepollenites balmei			Late Paleocene	
	cuttings	861.5	Lygistepollenites balmei			Late Paleocene	
	cuttings	861-864	Lygistepollenites balmei			Late Paleocene	
Reedy Creek 1	cuttings	20.0				< N5	MS
	cuttings	90.0					IS
	cuttings	150.0				P17-P20	MS
	cuttings	160.0				P17-P18	IS
	cuttings	170.0				P17-P18	IS
	cuttings	200.0				P17-P18	IS
	cuttings	376.0	Malvacipollis diversus			Early Eocene	Mm
	cuttings	418.0	Upper Lygistepollenites balmei			Late Palaeocene	Mm

Results of the biostratigraphic analysis conducted for this study

WELL	SAMPLE	DEPTH (m)	SPORE/POLLEN	DINOFLAG.	FORAM.	AGE	PALAEOENV.
Troas 1	cuttings	370-373			dehiscens, Orbulina, conoidea, panda	Late Miocene	MS
	cuttings	376-379			glomerosa, O.sutualis, dehiscens, conoidea, Wodella, wooii, bulloides, S.kochi	Middle Miocene	OS
	cuttings	382-385			glomerosa, O.sutualis, dehiscens, conoidea, Wodella, wooii, bulloides, S.kochi	N10	OS
	cuttings	394-397			trilobus, sicana, glomerosc, mistumida, wooi, connecta, dehiscens	N9	OS
	cuttings	400-403			Dertosubgertina, dehiscens, trilobus, sicana, woodi, glomerosa	Early Miocene	IS
	SWC 57	404.0	Middle Nothofagidites asperus (P16)			Late Eocene	M
	SWC 56	408.0	Middle Nothofagidites asperus (P16)			Late Eocene	M
	cuttings	406-409	Nothofagidites senectus	Nelsoniella aceras zone		Early Campanian	M
	cuttings	412-415	Nothofagidites senectus	Nelsoniella aceras zone		Early Campanian	M
	SWC 54	419.0	Nothing diagnostic, almost barren				
	cuttings	421-424		Nelsoniella aceras zone		Early Campanian	M
	cuttings	427-430	Tricolporites apoxyexinus			Santonian	Mm
	cuttings	442-445	Tricolporites apoxyexinus			Santonian	Mm
	cuttings	448-451	Tricolporites apoxyexinus			Santonian	Mm
	cuttings	505-508	Tricolporites apoxyexinus			Santonian	M
	cuttings	535-538	? Tricolporites apoxyexinus			Santonian	M

WELL	SAMPLE	DEPTH (m)	SPORE/POLLEN	DINOFLAG.	FORAM.	AGE	PALAEOENV.
Trumpet 1	cuttings	187.4			Victoriella, cibi, polymorph, globocassi, Gyroid, Noto	Oligocene	IS
	cuttings	210.3			Victoriella, Lenticulina, Eporoides, Textularina	Oligocene	IS
	cuttings	228.6			Eporoides, Lenti, polymorph	Oligocene	IS
	cuttings	246.9			Eporoides, Lenti, stomatolina, Victoriella	Oligocene	IS
	cuttings	256.0			Wadella, Lenti, Eporoides	Oligocene	IS
	cuttings	265.1			Stomatibina	Oligocene	IS
	cuttings	274.3			Stomatibina, Victoriella, Lenticulina, pseudo?	Oligocene	IS
	cuttings	283.4			Lenticulina, stomatbilina, perforums, Detalina, acanthonucleus	Oligocene	IS
	cuttings	292.6			Lenti, Guthulina	Oligocene	IS

Results of the biostratigraphic analysis conducted for this study.

WELL	LATITUDE S	LONGITUDE E	LST 1.1		HST 1.1		HST 2.1		LST 2.2		HST 2.2	
			thickness (m)	sand %	thickness (m)	sand %	thickness (m)	sand %	thickness (m)	sand %	thickness (m)	sand %
Argonaut 1A	37.971574	140.264700	44.0	25.0	44.0	0.0	44.0	0.0			110.0	10.0
Breaksea Reef 1	38.158576	140.612330	28.0	37.5	49.0	39.0	73.5	9.0	73.5	100.0	38.5	100.0
Burrungule 1	37.771111	140.538330	10.5	0.0	70.0	40.0					42.0	5.0
Caroline 1	37.941667	140.908330	49.0	71.4	35.0	40.0					150.5	18.6
Chama 1A	37.426911	139.543520										
Compton 1	37.795089	140.711920	17.5	0.0	14.0	0.0					108.5	13.0
Copa 1	37.688409	139.756120	38.5	57.0							49.5	44.0
Crayfish 1	37.289444	139.597220										
Douglas Point 1	38.025833	140.595560	14.0	50.0	126.0	22.0	66.5	0.0			105.0	46.7
Kentgrove 1	37.946667	140.623670	27.5	20.0	99.0	22.0	88.0	62.0				
Lake Bonney 1	37.844167	140.472500	11.0	0.0	55.0	80.0	121.0	0.0				
Lake George 1	37.452500	140.043060										
McNamara 1	37.837204	140.629440	17.5	95.0	31.5	5.0					108.5	13.0
McNichol 1	37.832769	140.847930	24.5	100.0	14.0	100.0						
Morum 1	37.502505	139.235490										
Mount Salt 1	37.956944	140.628610										
Neptune 1	37.303608	139.735710										
Normanby 1	38.236542	141.084224	11.0	0.0			49.5	0.0	53.9	61.0	66.0	40.0
Northumberland 1	38.035939	140.666230	10.5	0.0	59.5	0.0	70.0	0.0			91.0	61.5
Rendlesham 1	37.562931	140.231940	22.0	0.0	88.0	20.0						
Troas 1	37.367158	139.389540										
Trumpet 1	37.096472	139.411750										

Total thickness of systems tracts and sequences and the percentage of sand within each unit (calculated from logs).

WELL	LST 2.3		HST 2.3		Sequence 3.1		Sequence 3.2		Sequence 3.3		Sequence 4.1		Sequence 4.2	
	thickness (m)	sand %	thickness (m)	sand %	thickness (m)	sand %	thickness (m)	sand %	thickness (m)	sand %	thickness (m)	sand %	thickness (m)	sand %
Argonaut 1A	22.0	100.0	55.0	0.0	77.0	10.0					93.5	20.0		
Breaksea Reef 1	17.5	0.0	38.5	91.0	17.5	100.0	59.5	41.0	35.0	100.0	56.0	37.5	42.0	50.0
Burrungule 1			56.0	62.5	91.0	69.2					73.5	90.0	203.0	17.0
Caroline 1			42.0	92.0	84.0	79.2					178.5	78.4	259.0	76.0
Chama 1A														
Compton 1			45.8	0.0	105.0	46.7					108.5	100.0	315.0	100.0
Copa 1			110.0	60.0	121.0	100.0								
Crayfish 1														
Douglas Point 1	17.5	0.0	31.5	22.2	70.0	20.0					17.5	80.0	238.0	53.0
Kentgrove 1			137.5	24.0	220.0	40.0					165.0	73.0	203.5	22.0
Lake Bonney 1					93.5	53.0					66.0	25.0	390.5	48.0
Lake George 1														
McNamara 1			84.0	45.8	66.5	79.0					87.5	68.0	140.0	58.0
McNichol 1			63.0	0.0	84.0	54.2					140.0	95.0	287.0	100.0
Morum 1														
Mount Salt 1														
Neptune 1														
Normanby 1	49.5	40.0	55.0	80.0	38.5	100.0	55.6	50.0	39.0	56.0	121.0	73.0	93.5	59.0
Northumberland 1	7.0	0.0	45.5	8.0							10.5	33.3	280.0	50.0
Rendlesham 1			71.5	31.0	121.0	54.0					110.0	30.0	44.0	62.5
Troas 1														
Trumpet 1														

Total thickness of systems tracts and sequences and the percentage of sand within each unit (calculated from logs)

Supersequence 2.0 (interval velocity~Breaksea Reef=2620 m/sec)

LINE	PROGRADATION (m)	AGGRADATION		RATIO
		msec TWT	m	
ua82-43	10,646.9	862-634	298.7	35.6
ua82-41	18,453.4	922-616	400.9	46.0
ua82-35	9,120.8	718-528	248.9	36.6
ua82-31	5,710.2	854-694	209.6	27.2
ua82-27	3,976.7	894-680	280.3	14.2
ua82-23	7,163.3	776-694	107.4	66.7
oh91-411	5,898.4	666-476	248.9	23.7

Supersequence 3.0 (interval velocity~Breaksea Reef=2485 m/sec)

LINE	PROGRADATION (m)	AGGRADATION		RATIO
		msec TWT	m	
ua82-43	5,579.2	736-648	109.3	51.0
ua82-41	*to much erosion*	798-700	121.8	-
ua82-35	7,116.3	596-510	106.9	66.6
ua82-31	5,687.2	710-612	121.8	46.7
ua82-27	8,609.6	710-626	104.4	82.5
ua82-23	4,628.4	696-608	109.3	42.3
oh91-411	3,432.6	450-354	119.3	28.8

Supersequence 4.0 (interval velocity ~ Breaksea Reef=2300 m/sec)

LINE	PROGRADATION (m)	AGGRADATION		RATIO
		msec TWT	m	
ua82-43	-4,065.2	648-544	119.6	-34.0
ua82-41	*to much erosion*	606-502	119.6	-
ua82-35	-3,460.1	508-404	119.6	-28.9
ua82-31	-8,919.9	628-530	112.7	-79.1
ua82-27	-5,465.8	642-512	149.5	-36.6
ua82-23	-4,074.5	656-496	184.0	-22.1
oh91-411	2,094.0	344-226	135.7	15.4

Supersequence 5.0 & 6.0 (interval velocity ~ Breaksea Reef=2300 m/sec)

LINE	PROGRADATION (m)	AGGRADATION		RATIO
		msec TWT	m	
ua82-43	12,672.2	660-154	581.9	21.8
ua82-41	*to much erosion*	618-106	588.8	-
ua82-35	10,945.8	524-112	473.8	23.1
ua82-31	13,045.7	508-78	494.5	26.4
ua82-27	11,381.0	508-84	487.6	23.3
ua82-23	14,087.6	508-108	460.0	30.6
oh91-411	14,356.9	294-152	163.3	87.9

Progradation : Aggradation ratios calculated from seismic data.

Calculations for 2D grid size (m) for offshore extent of supersequences as determined from seismic data.

SUPER SEQUENCE	DURATION of SUPERSEQ (M.y.)	MINIMUM DURATION of SUPERSEQ (M.y.)	MAXIMUM DURATION of SUPERSEQ (M.y.)	VELOCITY of SUPERSEQ (m/sec)	2D GRID SIZE ON SEISMIC (mxm)	GRID SIZE (km^2)
1.0	7.0	0.9	10.9	2,980	29.9x58.8	1.76
2.0	1.167	1.167	2.3	2,620	29.9x51.75	1.55
3.0	1.167	1.167	3.6	2,485	29.9x49.10	1.47
4.0	1.167	1.167	2.8	2,300	29.9x45.43	1.36
5.0	5.0	5.0	5.4	2,300	29.9x45.43	1.36
6.0	16.0	12.0	19.2	2,300	29.9x45.43	1.36

Calculations for sedimentation rates of supersequences in the Gambier Sub-basin.

Calculations for the volume of the preserved sediment and sedimentation rates of sequences present offshore as determined from seismic data.

SUPER SEQUENCE	No. GRIDS PRESERVED on SEISMIC	TOTAL PRESERVED AREA (km^2)	AERIAL EXTENT (NW-SE width, km)	PRESERVED 3D VOLUME (km^3)	SEDIMENT'N RATE (Preserved) (km^3/m.y.)	MINIMUM SEDIMENT'N RATE	MAXIMUM SEDIMENT'N RATE
1.0	87	153.2	110	16,855	2,408	1,546	18,728
2.0	307	475.7	110	52,332	44,843	22,753	44,843
3.0	442	649.9	110	71,486	61,256	19,857	61,256
4.0	194	263.9	110	29,033	24,878	10,369	24,878
5.0	128	174.1	200	34,829	6,966	6,450	6,966
6.0	1,142	1,553.7	200	310,736	19,421	16,184	25,895

Calculations for the estimated volume of original sediment and approximate sedimentation rates of sequences present offshore as determined from seismic data.

SUPER SEQUENCE	No. ORIGINAL GRIDS on SEISMIC	TOTAL ORIGINAL AREA (km^2)	AERIAL EXTENT (NW-SE width, km)	ORIGINAL 3D VOLUME (km^3)	SEDIMENT'N RATE (km^3/m.y.)	MINIMUM SEDIMENT'N RATE	MAXIMUM SEDIMENT'N RATE
1.0	87	153.2	110	16,855	2,408	1,546	18,728
2.0	307	475.7	110	52,332	44,843	22,753	44,843
3.0	464	682.2	110	75,044	64,305	20,846	64,305
4.0	240	326.5	110	35,917	30,777	12,827	30,777
5.0	380	517.0	200	103,397	20,679	19,148	20,679
6.0	1,142	1,553.7	200	310,736	19,421	16,184	25,895

Calculations for sedimentation rates of supersequences in the Gambier Sub-basin.

Calculations of the estimated volume of preserved sediment of sequences across the study area in the Gambier Sub-basin and their approximate sedimentation rates.

SUPER SEQUENCE	AVERAGE THICKNESS IN WELLS (m)	ONSHORE AREA SIZE (km^2)	TOTAL ONSHORE VOLUME (km^3)	TOTAL OFFSHORE SEISMIC VOLUME (km^3)	TOTAL VOLUME (on & offshore) (km^3)	SEDIMENT'N RATE (km^3/m.y.)
1.0	67	5,000	335,000	16,855	351,855	50,265
2.0	176	5,000	880,000	52,332	932,332	798,913
3.0	112	5,000	560,000	71,486	631,486	541,119
4.0	208	5,000	1,040,000	29,033	1,069,033	916,052
5.0	85	5,000	425,000	34,829	459,829	91,966
6.0	99	5,000	495,000	310,736	805,736	50,359

Calculations for sedimentation rates of supersequences in the Gambier Sub-basin

Fault Name	DipDirn	Dip	Strike	Throw SB 1.1	Throw SB 2.1	Throw SB 3.1	Throw SB 4.1	Throw SB 5.1	Throw SB 6.1	Throw Seafloor
R1	208	70.5	298	178.8						
R2	210	60.2	300	110.5						
R3	205	60.2	295	110.5						
R4	212	63.2	302	11.9						
R5	212	35.0	302	110.5						
R6	215	40.5	305	50.9						
R7	212	69.7	302	80.5						
R8	205	77.2	295	137.1						
R9	202	68.2	292	77.5						
R10	28	47.3	298	68.5						
B1	213	56.4	303	95.4		17.4	4.8			
B2	210	52.8	300	83.4	68.1	20.5	4.8			
B3	220	62.5	310	59.6	5.5	5.2				
B4	32	43.3	302	68.5	46.9	5.2				
G1	211	51.8	301	80.5		43.5	9.2	4.8	4.8	
G2	208	52.8	298	166.9		38.3	4.8	32.2		
G3	210	57.1	300	146.0		29.8	4.8	4.8		
G4	205	69.9	295	172.8		22.4	4.8	4.8	4.8	
G5	210	73.8	300	107.3		9.9	4.8	4.8	4.8	
G6	212	47.3	302	137.1		32.3	4.8	4.8	4.8	
G7	220	62.6	310	122.2		5.2	4.8	4.8	4.8	
G8	218	63.2	308	125.2		34.8	11.5	4.8		
G9	215	62.0	305	119.2		42.2	13.8	16.1		
G10	218	73.7	308	160.9		22.4	25.3	6.9		
G11	203	65.3	293	205.6		34.8	23.0	16.1		
G12	203	58.0	293	202.6		27.3	4.8	4.8		
G13	210	56.0	300	187.7	39.5	37.3	20.7	32.2		
G14	210	64.2	300	131.1		32.3	27.6	4.8	4.8	
G15	208	57.6	298	199.7	14.8	37.3	32.2	13.8		

Magnitude of throw at supersequence boundaries in the Gambier Sub-basin.

Fault Name	DipDirn	Dip	Strike	Throw SB 1.1	Throw SB 2.1	Throw SB 3.1	Throw SB 4.1	Throw SB 5.1	Throw SB 6.1	Throw Seafloor
G16	210	53.3	300	169.9	61.7	29.8	4.8	4.8		
G17	217	45.0	307	157.9	5.1	42.2	4.8	4.8		
G18	210	64.4	300	196.7	24.7	19.9	18.4	13.8	4.8	3.2
G19	30	53.8	300	86.4	32.1	5.2	4.8	4.8	4.8	3.2
G20	213	36.0	303	68.5	56.8	24.8	82.8	48.3	20.7	3.2
G21	214	70.2	304	175.8	46.9	57.2	52.9	29.9		
G22	220	58.7	310	259.3	59.3	59.6	23.0	27.6	4.8	
G23	222	51.8	312	80.5	22.2	5.2	9.2	4.8	4.8	
G24	220	52.7	310	122.2	29.6	19.9	4.6	4.8	4.8	
G25	38	62.5	308	54.6		5.2	23.0		4.8	
G26	210	66.5	300	217.5		34.8	89.7	46.0	4.8	
G27	221	53.1	311	119.2			25.3		4.8	
G28	215	59.8	305	375.5		52.2	4.8	4.8		
G29	220	57.5	310	247.3	39.5	34.8	4.8	4.8		
G30	208	68.7	298	324.8				29.9	4.8	
G31	210	64.7	300	262.2				13.8	4.8	
G32	220	48.4	310	134.1	39.5			16.1	18.4	
G33	203	58.0	293	95.4					48.3	36.7
G34	211	56.1	301	92.4					36.8	23.0
O1	215	58.0	305	143.0	54.3	27.3	16.1	4.8	4.8	3.2
O2	225	62.2	315	56.6		5.2	34.5	4.8	4.8	3.2

Fault Name	DipDirn	Dip (°)	Strike	Total Tertiary Throw (m)	Throw SB 1.1	Throw Mid-Late	Throw Early Oligocene	Throw L Oligo-Mid Miocene	Throw Recent
R1	208	70.5	298	144.0	144.0				
R2	210	60.2	300	89.0	89.0				
R3	205	60.2	295	89.0	89.0				
R4	212	63.2	302	9.6	9.6				
R5	212	35.0	302	89.0	89.0				
R6	215	40.5	305	41.0	41.0				
R7	212	69.7	302	64.8	64.8				
R8	205	77.2	295	110.4	110.4				
R9	202	68.2	292	62.4	62.4				
R10	28	47.3	298	55.2	55.2				
B1	213	56.4	303	76.8	60.0	16.8			
B2	210	52.8	300	67.2	4.8	62.4			
B3	220	62.5	310	48.0	43.0	5.0			
B4	32	43.3	302	55.2	9.6	45.6			
G1	211	51.8	301	64.8	24.0	35.8	0.0	5.0	
G2	208	52.8	298	134.4	98.4	2.4	33.6		
G3	210	57.1	300	117.6	88.8	23.8	5.0		
G4	205	69.9	295	139.2	117.6	16.6	0.0	5.0	
G5	210	73.8	300	86.4	76.8	4.6	0.0	5.0	
G6	212	47.3	302	110.4	79.2	26.2	0.0	5.0	
G7	220	62.6	310	98.4	93.4	5.0	0.0	5.0	
G8	218	63.2	308	100.8	67.2	28.6	5.0		
G9	215	62.0	305	96.0	55.2	24.0	16.8		
G10	218	73.7	308	129.6	108.0	14.4	7.2		
G11	203	65.3	293	165.6	132.0	16.8	16.8		
G12	203	58.0	293	163.2	136.8	21.4	5.0		
G13	210	56.0	300	151.2	112.8	4.8	33.6		
G14	210	64.2	300	105.6	74.4	26.2	0.0	5.0	
G15	208	57.6	298	160.8	146.4	0.0	14.4		
G16	210	53.3	300	136.8	76.8	55.0	5.0		
G17	217	45.0	307	127.2	81.4	40.8	5.0		
G18	210	64.4	300	158.4	134.4	9.6	9.4	0.0	5.0
G19	30	53.8	300	69.6	38.4	26.2	0.0	0.0	5.0
G20	213	36.0	303	55.2	0.0	4.8	28.8	16.6	5.0
G21	214	70.2	304	141.6	96.0	14.4	31.2		
G22	220	58.7	310	208.8	151.2	28.8	23.8	5.0	
G23	222	51.8	312	64.8	43.2	16.6	0.0	5.0	
G24	220	52.7	310	98.4	69.6	23.8	0.0	5.0	
G25	38	62.5	308	48.0	19.0	24.0		5.0	
G26	210	66.5	300	175.2	81.6	45.6	43.0	5.0	
G27	221	53.1	311	96.0	69.6	21.4		5.0	
G28	215	59.8	305	302.4	252.2	45.4	5.0		
G29	220	57.5	310	199.2	160.8	33.4	5.0		
G30	208	68.7	298	261.6	230.4		26.2	5.0	
G31	210	64.7	300	211.2	196.8		9.4	5.0	
G32	220	48.4	310	108.0	69.6	19.2	0.0	19.2	
G33	203	58.0	293	76.8	19.2			0.0	57.6
G34	211	56.1	301	74.4	36.0			2.4	36.0
O1	215	58.0	305	115.2	62.4	47.8	0.0	0.0	5.0
O2	225	62.2	315	45.6	9.6	31.0	0.0	0.0	5.0

Summary of the magnitude of throw Gambier Sub-basin faults have experienced during the Cenozoic.

Appendix 2

Methods

APPENDIX 2 METHODS

TABLE OF CONTENTS

LIST OF FIGURES AND TABLES

2.1 SEQUENCE STRATIGRAPHY

Sequence stratigraphy is a powerful tool for the stratigraphic analysis of sedimentary basins and is particularly applicable for hydrocarbon exploration (Kennard et al. 1999). It allows analysis of the sediment fill in basins in terms of sea level changes, tectonism and sediment supply and enables a better understanding of the linkage between sedimentation patterns in different parts of a basin. Ultimately it can be utilised to predict the location of reservoir and seal-prone intervals and zones within a basin (Kennard et al. 1999). Sequence stratigraphy is derived from seismic stratigraphy and with the integration of lithostratigraphy and facies analysis may be considered a special type of event stratigraphy (Miall, 1990).

Many workers have related stratal architecture of sediments to the interplay of three main variables that interact to control sequence development: eustatic sea level changes, subsidence rates and sediment supply (Curray, 1964; Krumbein and Sloss, 1963, Van Wagoner et al. 1988).

Three types of eustacy have been defined within the eustatic component of control on sequence deposition: glacial, tectonic and geoidal (Galloway, 1989). Glacio-eustacy results from the changing volumes of continental ice caps, whilst tectono-eustacy results from changes in ocean volume by large scale plate tectonic interactions (Galloway, 1989). The geoid is the equipotential surface of the combined rotational and gravitational potential fields, which corresponds to mean geodetic sea level. This surface has been shown to vary from an ideal mathematical surface by several tens of metres (Galloway, 1989).

Changes in relative sea level control the space available for sediment deposition, which is termed 'accommodation space' (Figure A2.1) (Jervey, 1988). Hence, the interaction between relative sea level changes and sediment supply controls the geometry of the sequences deposited within the accommodation space (Galloway, 1989). A depositional sequence is divided into different types of facies patterns, which represent different phases within the transgressive-regressive (rising or falling) relative sea level cycle. These phases constitute systems tracts (Posamentier and Vail, 1988), which are defined as a linkage of contemporaneous depositional systems (Brown and Fisher, 1977), while depositional systems are termed 'three-dimensional assemblages of lithofacies' (Fisher and McGowen, 1967).

The systems tracts can be represented by segments of a sinusoidal eustatic curve of third-order frequency and can be characterised by geometry and facies associations (Posamentier et al.

1988). The exact timing of any given systems tract in any given basin will depend on local subsidence and sediment supply (Posamentier and Vail, 1988). Therefore, systems tracts need not be the same age in a basin and thus, systems tract boundaries are not necessarily fixed to a position on the eustatic curve (Wehr, 1993).

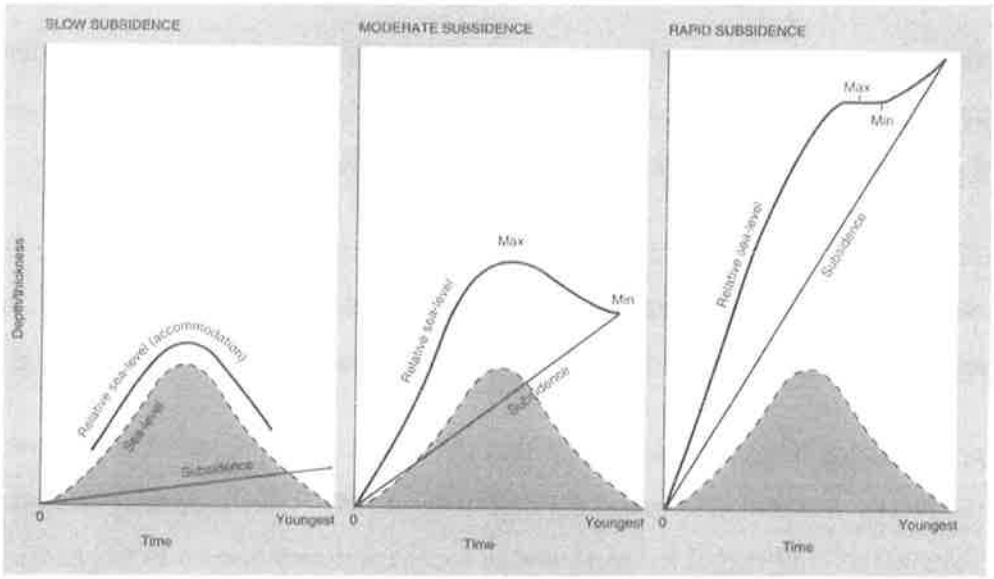

Figure A2.1 Changing accommodation space through time with different rates of subsidence and stable sea level (Jervey, 1988).

2.1.1 Systems Tracts

Each sequence is bounded and punctuated by two key stratigraphic surfaces: (1) the sequence boundary, a basal bounding surface and (2) the maximum flooding surface, a surface formed at the time of maximum transgression. Van Wagoner et al. (1988) characterised two types of sequence boundary. A 'type 1' sequence boundary is characterised by subaerial exposure and erosion, a basinward shift in facies and onlap of overlying strata. A type 1 sequence boundary is interpreted to form when the rate of eustatic sea level fall exceeds the rate of basin subsidence during a relative sea level fall.

A 'type 2' sequence boundary marks the time of minimum rate of sea level rise (i.e. when relative sea level does not actually fall) and maximum regression at the relative sea level curve

inflection point. A type 2 sequence boundary lacks both the subaerial exposure and basinward shift in facies and does not represent an unconformity surface.

Based on the recognition of these key surfaces and the different types of sedimentary stacking patterns that occur between them, a sequence can generally be sub-divided into several systems tracts (Posamentier and Vail, 1988). A model of basin development that links stratigraphic architecture with rates of relative sea level change has been referred to as the Exxon sequence stratigraphic model (Mitchum, 1977). The Exxon model subdivides the sediments into three systems tracts: (1) lowstand; (2) transgressive; and (3) highstand systems tract (Figure A2.2).

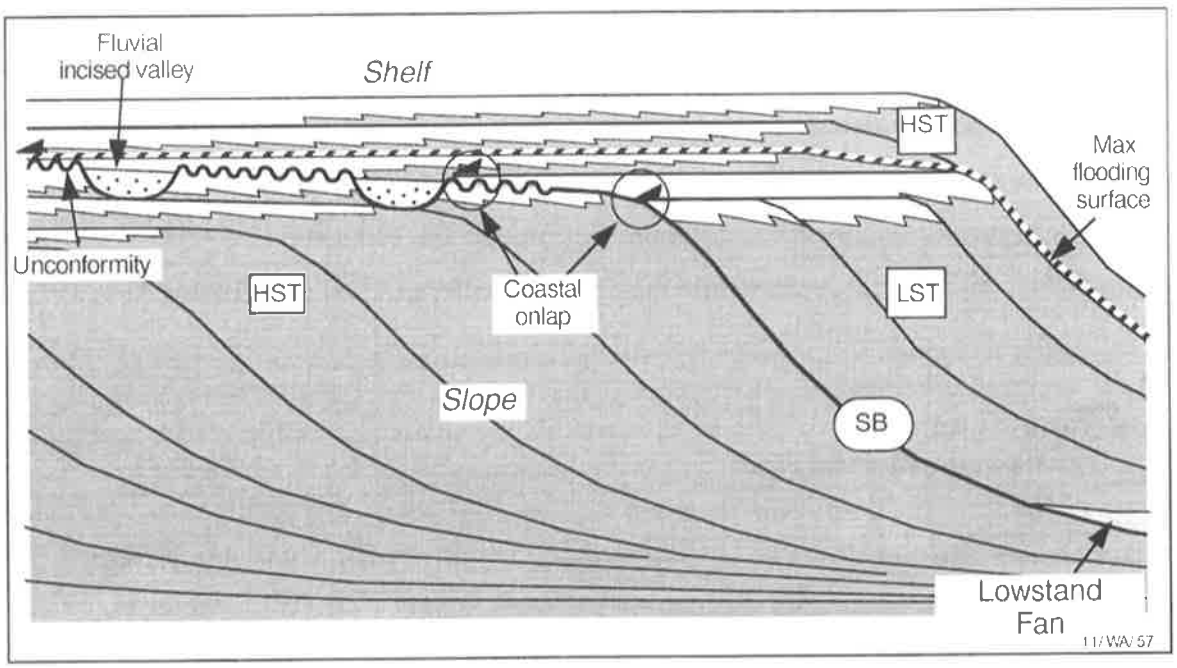

Figure A2.2 Stratal patterns associated with a depositional sequence on the shelf and slope (Allen et al. 1996). The sequence boundary (SB) represents a shelf onlap surface separating highstand deposits of an underlying sequence from overlying lowstand deposits. The SB surface landward of the most distal coastal onlap is an unconformity, while the seaward correlative surface is conformable (Kennard et al. 1999).

2.1.1.1 Lowstand Systems Tract

The lowstand systems tract (LST) (Figure A2.3) forms a regressive succession comprising the sediments deposited during falling relative sea level, the ensuing still stand and the interval of slowly rising relative sea level during which shoreline regression is maintained (Van Wagoner et al. 1988). The LST is composed of two types of deposits: (1) regressive coastal and shelf deposits and (2) aggrading fluvial and shallow marine sediments within incised valleys (Allen and Posamentier, 1993). The LST overlies the sequence boundary, which consists of a stratigraphic unconformity on the exposed shelf surface and a correlative conformity seaward of the lowstand shoreline. The upper limit of the LST is formed by the transgressive surface, which marks the onset of transgression when the rate of relative sea level rise exceeds sediment supply and is overlain by the transgressive systems tract.

The lowstand systems tract is subdivided into an early and late phase. The early lowstand occurs when relative sea level is falling, whereas the late lowstand occurs when relative sea level is stable and slowly rising (Allen and Posamentier, 1993). During early lowstand time, the rivers are incising and the shoreline is subjected to forced regression. The late lowstand is a time of an overall increasing rate of accommodation and the shoreline is subjected to normal regression while the rivers aggrade within their incised valleys (Allen and Posamentier, 1993).

2.1.1.2 Transgressive Systems Tract

The transgressive systems tract (TST) (Figure A2.4) comprises the sediments deposited when relative sea level rises faster than the rate of sediment supply (Van Wagoner et al. 1988). It constitutes an overall transgressive succession characterised by landward stepping parasequences. The upper limit of the TST is marked by the maximum flooding surface (MFS), which marks the uppermost limit of transgression. The TST is generally more shale-prone than the late LST and can contain good source rock and potential seals. It commonly forms an upward-fining and thinning section on well logs.

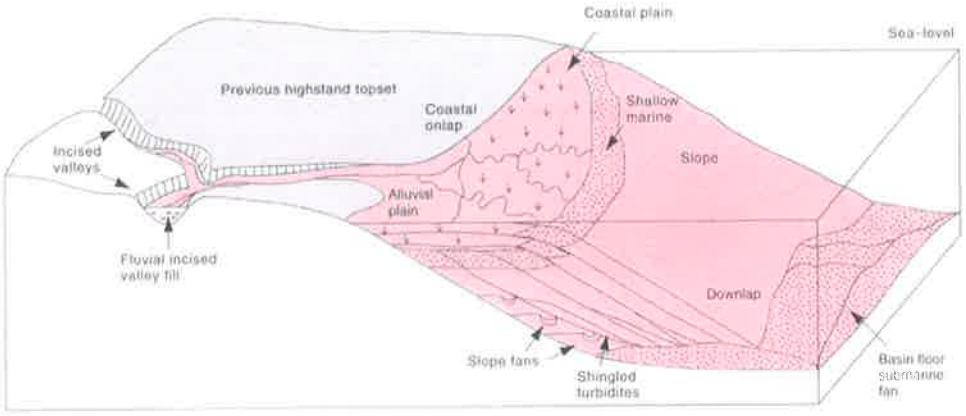

Figure A2.3 Components of the lowstand systems tract on a shelf-break margin. These include a basin-floor fan and a slope fan, but the diagram also shows the active systems of the lowstand wedge; namely valley-fill, alluvial and coastal plain topsets, a shallow marine belt and an active slope system, which in its early stages may contain turbidites (Emery and Myers, 1996).

2.1.1.3 Highstand Systems Tract

The highstand systems tract (HST) (Figure A2.5) constitutes a regressive succession deposited when the rate of relative sea level rise decreases to less than the rate of sediment supply (Van Wagoner et al. 1988). The HST is bounded at its base by the MFS and at the top by the next sequence boundary. During the early phase of the HST, accommodation increases rapidly and deposits are predominantly aggradational, whereas during the late phase of highstand the rate of accommodation decelerates as the rate of relative sea level rise decreases and the succession is predominantly progradational. For this reason, the late highstand is more sand-prone than the early highstand.

The sequence stratigraphic approach is based upon the integration of four basic data sets, each of which is independent but incomplete within itself (Mitchum et al. 1977). These data sets include well-log responses of deposits in each systems tract; seismic facies of each systems tract determined from reflection termination and configuration patterns; high resolution biostratigraphic interpretation of wells penetrating the section; and eustatic cycle charts with correlation of local biostratigraphy for dating physically recognized sequence boundaries and condensed sections (Mitchum et al., 1977).

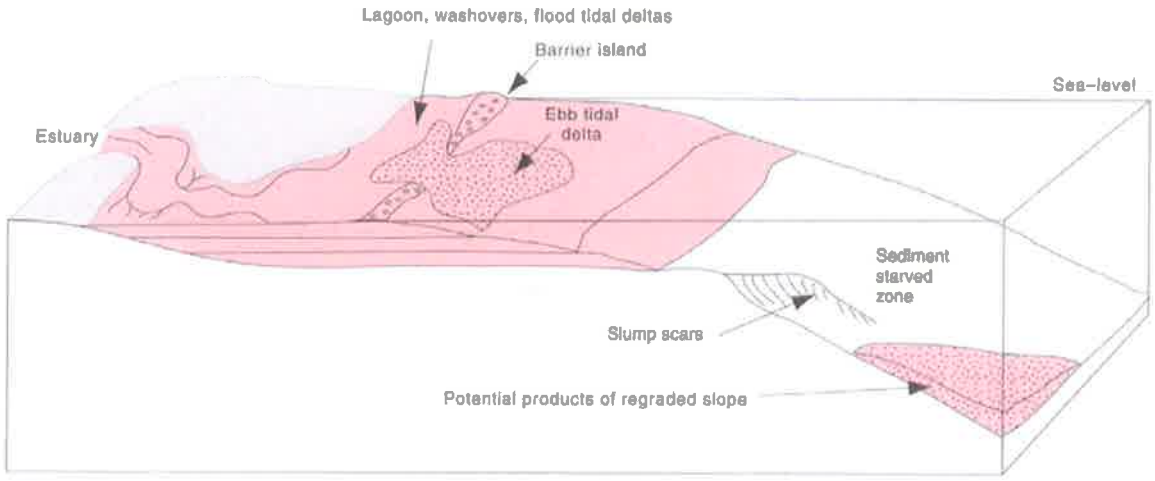

Figure A2.4 Components of the transgressive systems tract. Deposition includes estuarine, lagoonal, barrier and tidal depositional systems, which pass seaward into a shelfal condensed zone (Emery and Myers, 1996).

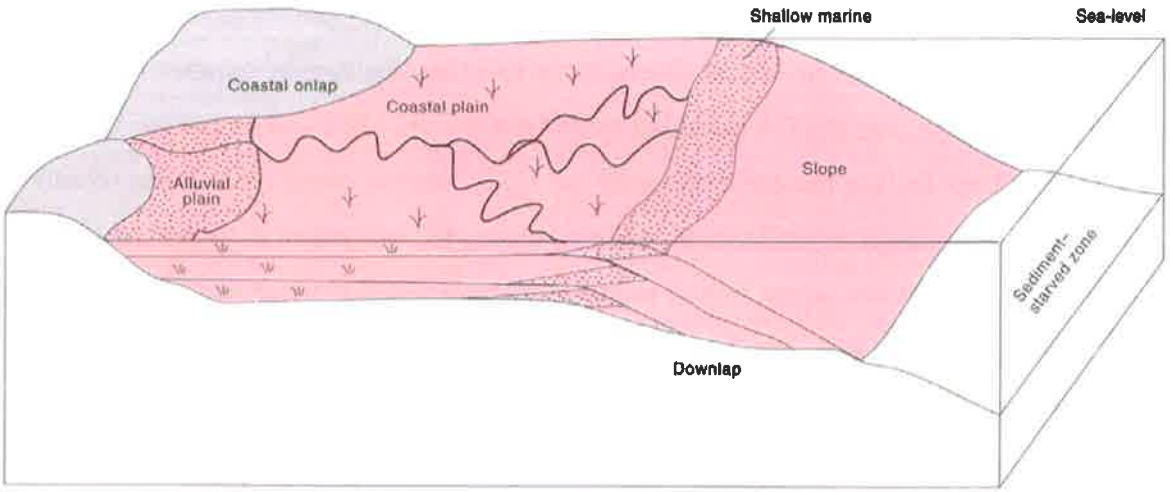

Figure A2.5 Components of the highstand systems tract on a shelf-break margin. These include alluvial, coastal, shallow marine and slope systems (Emery and Myers, 1996).

2.2 CARBONATE SEQUENCE STRATIGRAPHY

Principles of sequence stratigraphy that were initially published in Payton (1977) were developed within the siliciclastic regime. During the 1970's and 1980's a considerable amount of literature was published on the controls on carbonate platform morphology and the close interaction with relative sea level change (Ahr, 1973; Droxler and Schlager, 1985; Kendall and Schlager, 1981; Read, 1982, 1985; Schlager, 1981). However, it was not until Sarg (1988) that that these ideas were combined to form a sequence stratigraphic model for carbonate systems and since then application of sequence stratigraphic principles to the carbonate regime has become more common (e.g. Loucks and Sarg, 1993).

Carbonate sequence stratigraphic studies have adopted a process-based approach in which the response of the various carbonate platform types to changes in relative sea level is discussed.

2.2.1 The Carbonate Factory

Carbonate deposition in the Gambier Sub-basin takes place in an extra-tropical (cool-water), distally steepened ramp setting. Cool-water carbonates differ from tropical carbonates in their reef structure and environmental requirements (Jones and Desrochers, 1992). At higher latitudes reef framework becomes less common and smaller reef complexes that display less aggradation, are dominated by bryozoa and red algae (Figure A2.6) (Emery and Myers, 1996). These organisms do not have a symbiotic relationship with photosynthetic algae and hence are not restricted to the photic zone like their tropical counterparts. When the bryozoa and red algae die, the segments disassociate and form fine to coarse, sand-sized sediment on the ocean floor. This sediment tends to then evolve geometries more akin to siliciclastic systems than tropical reef complexes (Emery and Myers, 1996).

2.2.1.1 Lowstand Systems Tract

During falling relative sea level, landward portions of the carbonate ramp is exposed, during which time karsting and soil profiles may develop (Emery and Myers, 1996). Carbonate deposition may downstep where the onlap point falls below the earlier ramp margin. Erosion

during lowstand takes the form of chemical dissolution and reprecipitation (Emery and Myers, 1996). There is little carbonate sediment eroded from the landward portion of the ramp and re-deposited downslope as a lowstand fan. There may be high siliciclastic input during a lowstand in relative sea level, where a siliciclastic lowstand wedge or fan may develop (Figure A2.7) (Emery and Myers, 1996).

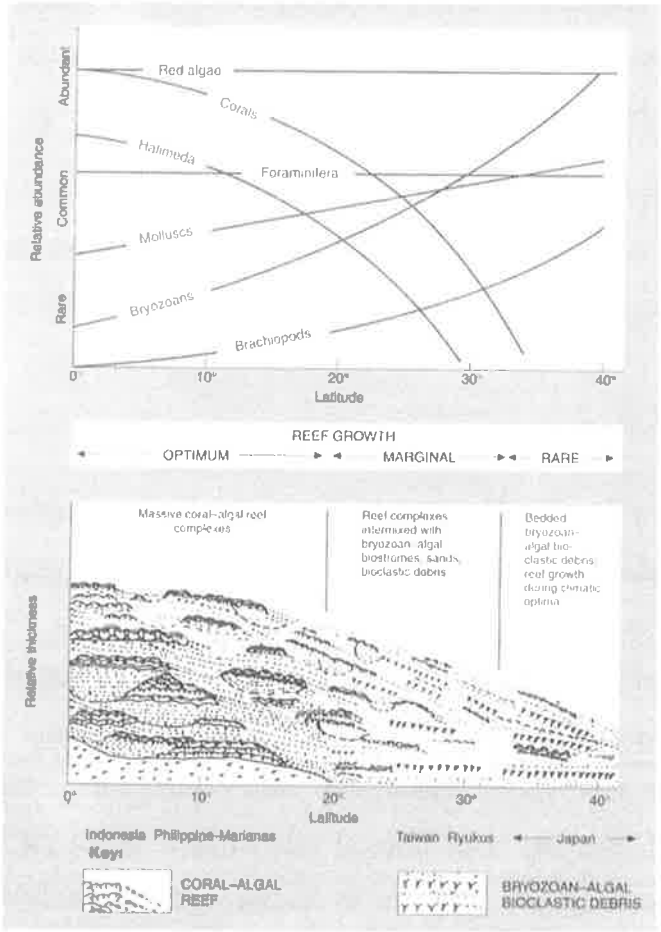

Figure A2.6 Latitudinal change from tropical to temperate carbonate facies in the northern Pacific (Schlager, 1981).

2.2.1.2 Transgressive Systems Tract

During transgression, retrogradation occurs where facies migrate landward and deepwater facies can be observed to overlie shallow water facies. The deepest part of the ramp may be

starved and organic matter may accumulate. One of the key differentiating factors between a siliciclastic and carbonate TST, is the ability of the carbonates to aggrade, rather than backstep during relative sea level rise (Figure A2.7) (Emery and Myers, 1996).

2.2.1.3 Highstand Systems Tract

During the early highstand in relative sea level, the carbonate system continues to aggrade and the HST topsets comprise supra-tidal, inter-tidal and lagoonal facies (Figure A2.7). During late highstand, the system becomes predominantly progradational with little or no topset deposition (Emery and Myers, 1996). Clinoforms appear to have a shingled geometry on seismic, however, the topsets are generally unresolvable.

Highstand shedding may occur on active platforms where the shallow part of the ramp acts as a bypass margin for sediment that is then deposited in deeper water as calciturbidites (Emery and Myers, 1996).

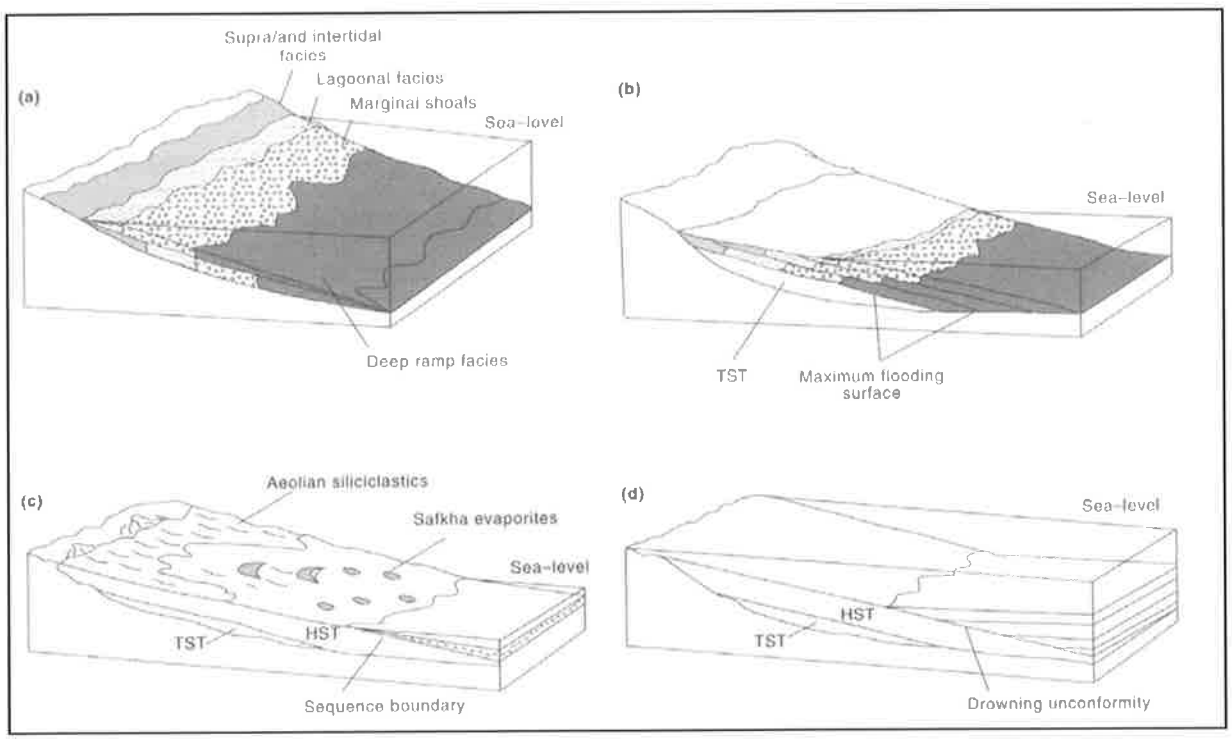

Figure A2.7 Sequence stratigraphic models for ramp systems. (a) Transgressive systems tract shows landward stepping of ramp facies and sediment starvation in the basin, with the

potential for the development of organic-rich mudstones. (b) Highstand systems tract shows seaward progradation of the margin and progressive thinning of topsets. In late highstand, topsets may not be developed and a 'strandplain' system (cf. Calvet et al. 1990) may result. (c) Lowstand systems tract in an arid restricted basin where the basinal facies is developed as a subaqeuous evaporite wedge onlapping deeper ramp facies of the previous highstand systems tract above the sequence boundary. In a humid setting, the exposed ramp may be incised by fluvial channels and karstified, or if the siliciclastic input is relatively low, a new lowstand ramp may nucleate below the margin of the previous ramp system. (d) Drowning of a carbonate ramp followed by siliciclastic progradation over the downed ramp. The ramp and overlying siliciclastic wedge will be separated by a drowning unconformity.

2.3 SEISMIC STRATIGRAPHY

While employing the accepted sequence stratigraphic principals, the following systematic approach was used in the stratigraphic interpretation of seismic.

(1) Identify multiples (water bottom, peg leg) to avoid interpreting the multiple reflection as a real event during the seismic stratigraphic interpretation.

(2) Identify and mark reflection termination.

Reflection terminations are characterised on a 2D section by the geometric relationship between the reflection and the seismic surface against which they terminate (Figure A2.8). They represent the termination of a bedding plane or its thinning below seismic resolution. Thus a change from sedimentation to condensation, non-deposition or erosion can be observed.

By marking where reflections end, and noting the geometrical manner in which they relate to the surface on which they terminate, one can begin to infer:

1. Over what area deposition was occurring at any one time (because of the time significance of seismic reflections).

2. What type of depositional processes might be represented (because certain reflection termination types are more characteristic of certain depositional systems).

3. What type of control was influencing their development.

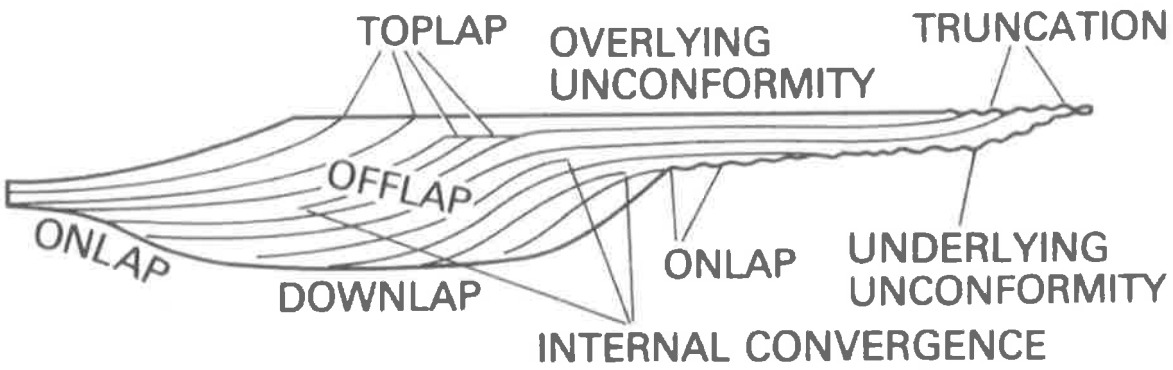

Figure A2.8 Seismic stratigraphic reflection terminations within an idealised seismic sequence (Mitchum et al. 1977).

These relationships described on seismic sections may not represent the original depositional relationships, modification may have occurred through compaction and/or tectonics.

(3) Develop a surface hierarchy.

A terminology convention could be used such that Sequences 2.1, 2.2, 2.3 could occur within Supersequence 2, which in turn could be found in Megasequence 1.

2.3.1 Megasequences

Megasequences represent the sedimentary response to a major phase of basin evolution. They are generally bounded by regional unconformities. Principal controls are interpreted to be tectonic, as reflected by such terms as pre-rift, syn-rift and post-rift (Hubbard, 1988).

Within megasequences, seismic supersequences and sequences may be defined. These are bounded by smaller scale seismic surfaces than the megasequences and are the building blocks to megasequences.

2.3.2 Supersequences

Supersequences are seismic packages bounded by regional unconformities and are influenced by local tectonics and changes in relative sea level. Supersequences comprise smaller scale seismic sequences. They have been labelled in a fashion as Supersequence 1, 2, 3, etc., from oldest to youngest.

2.3.3 Sequences

Seismic sequences are reflector packages bounded by seismic surfaces that are interpreted to represent a characteristic period of deposition. The building blocks of sequences are the systems tracts, which may be identified by characteristic reflector termination patterns (Figure A2.8). Seismic sequences are not necessarily equivalent to depositional sequences, nor are their boundaries necessarily equivalent to depositional sequence boundaries (Mitchum et al. 1977).

(4) Divide seismic into discrete stratigraphic packages:

   (a) Define major seismic surfaces and hence define supersequences.

   (b) Define major seismic surfaces and hence define seismic sequences.

   (c) Define type of seismic sequence and if possible define systems tracts.

(5) Loop interpreted surfaces on seismic grid, consistently rechecking that surfaces tie.

(6) Create time-structure and interval-thickness maps (measured in two way time; TWT) of significant surfaces and sequences.

2.4 Facies Analysis

A facies is a body of rock with specified characteristics (Reading, 1986). Where sedimentary rocks can be handled at outcrop or from boreholes, it is defined on the basis of colour, bedding, composition, texture, fossils and sedimentary structures. A biofacies is commonly used when describing a rock unit based on its biological content. If fossils are absent or of little consequence, then the emphasis is on the physical and chemical characteristics of the rock and the term lithofacies is appropriate (Reading, 1986).

The palaeoenvironmental evolution of the Cenozoic succession was largely interpreted from wireline log character of sequences. Wireline logs are routinely used as an integral part of siliciclastic sequence stratigraphic studies and interpretation of log motifs for depositional facies analysis has been applied in this study in the sense of Van Wagoner et al. (1990) (Figure A2.9a-c).

Depositional facies analysis is also undertaken, in part, by seismic facies analysis. The aim of seismic facies analysis is "the interpretation of depositional facies from seismic reflections" (Lang, 2000). A seismic facies is an areally definable, 3-dimensional unit composed of seismic reflections whose elements, such as reflection configuration, amplitude, continuity, frequency and interval velocity, differ from the elements of adjacent facies units. This is interpreted to express certain lithology, stratification and depositional features that generate the reflections in the units. However, it assumes that seismic facies is the response to a lithofacies (Lang, 2000).

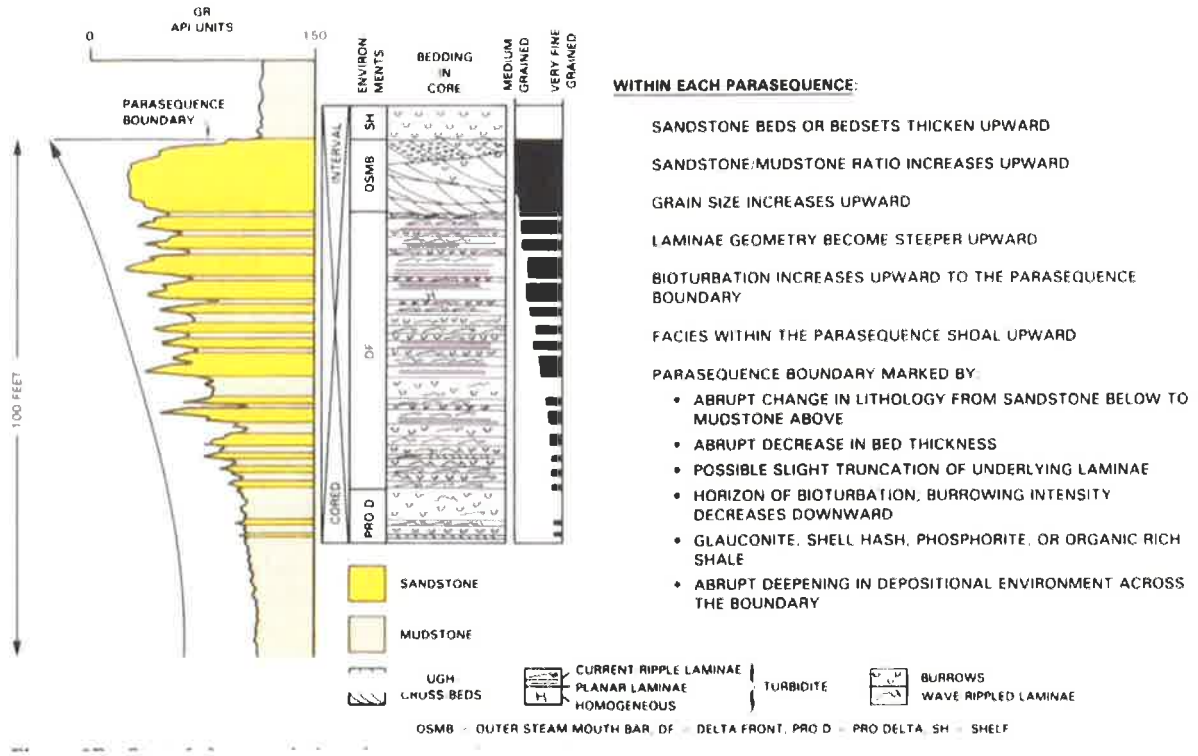

Figure A2.9a Stratal characteristics of an upward-coarsening package interpreted to form in a deltaic environment on a sandy, fluvial or wave-dominated shoreline (Van Wagoner et al. 1990).

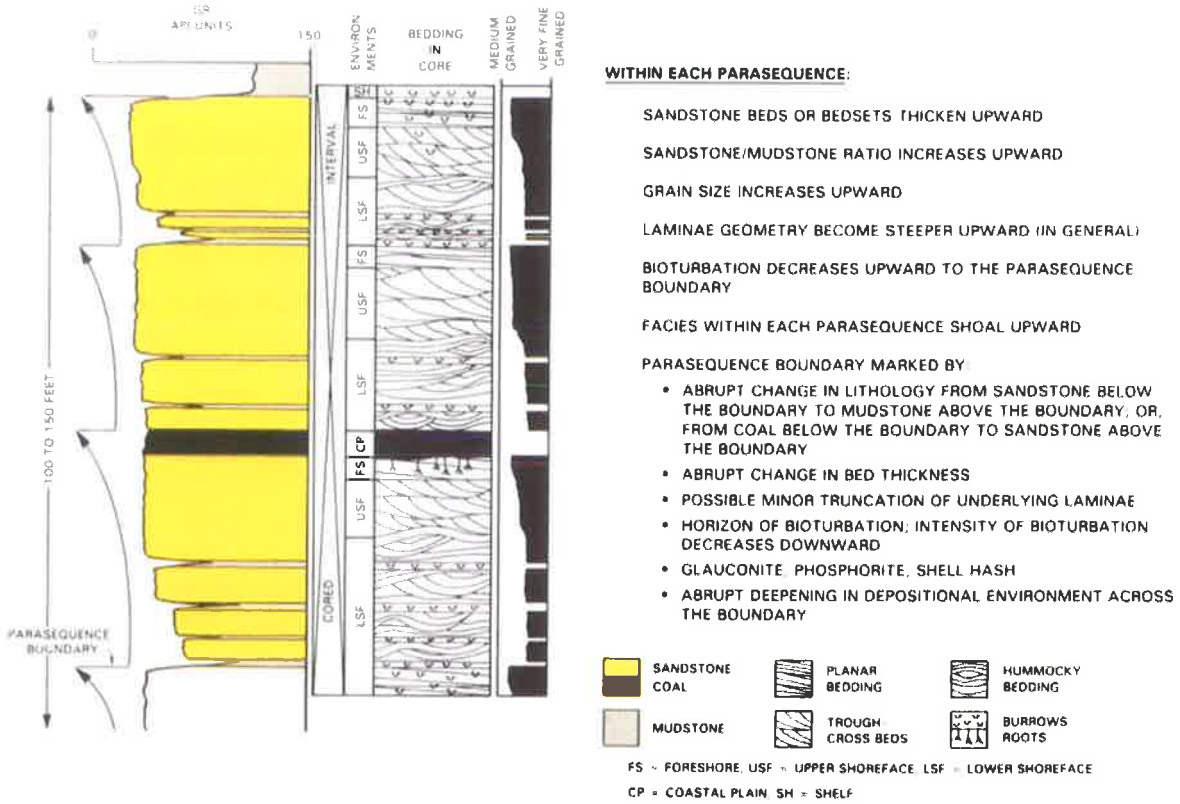

Figure A2.9b Stratal characteristics of stacked upward-coarsening packages interpreted to form in a beach environment on a sandy wave- or fluvial-dominated shoreline (Van Wagoner et al. 1990).

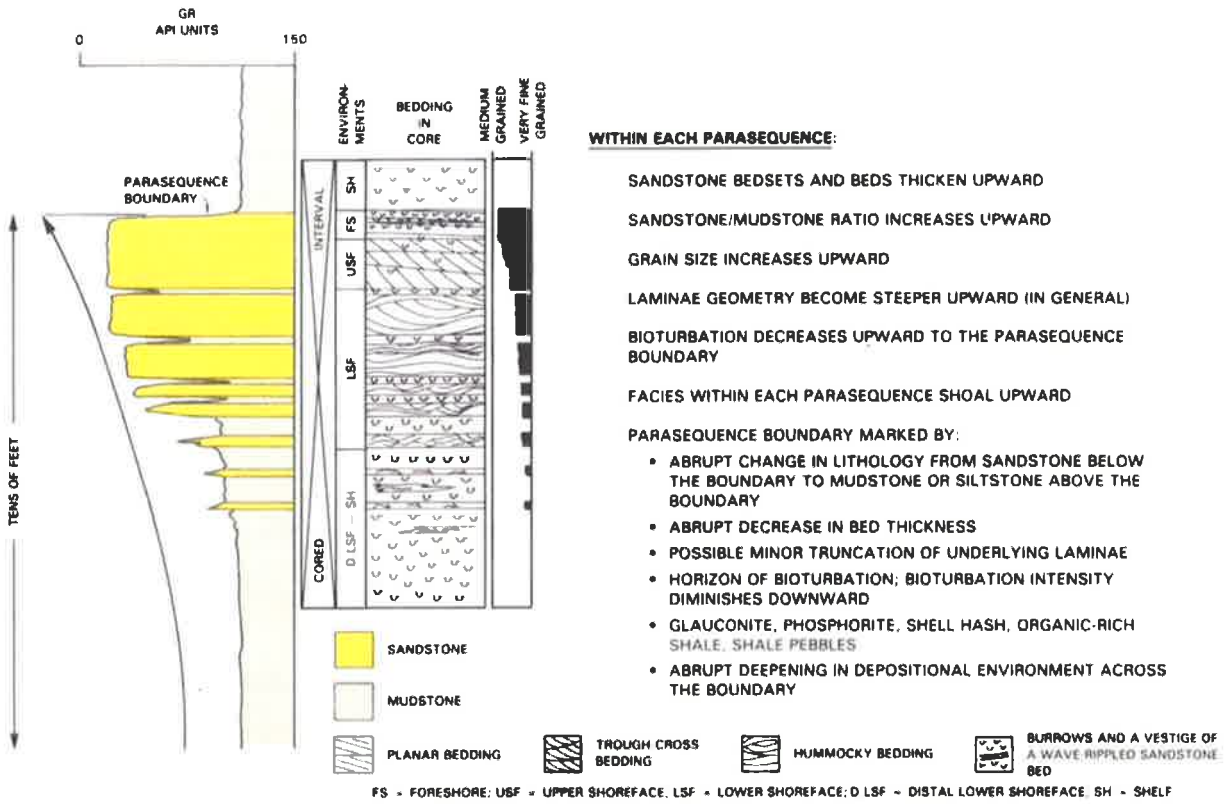

Figure A2.9c Stratal characteristics of an upward-coarsening package interpreted to form in a beach environment on a sandy, wave-dominated shoreline (Van Wagoner et al. 1990).

The following seismic facies notation scheme was employed:

Above ~ Below Internal Configuration

The notations are as follows:

Above (top bounding surface)		**Below (bottom bounding surface)**	
Erosional Truncation	Te	Downlap	Dn
Toplap	Tp	Onlap	On
Concordance	C	Concordance	C

Internal Configuration			
Parallel	P	Prograding Clinoforms	PC
Sub-parallel	Sp	Sigmoid	S
Divergent	D	Oblique	Ob
Chaotic	Ch	Complex sigmoid-oblique	SO
Reflection-free	RF	Shingled	Sh
Mounded	M	Hummocky	HC
Wavy	W		

Figure A2.10 illustrates the types of seismic reflection configurations that can be observed. The observations made on a single line must then be transferred to a map to show the three-dimensional spatial development of the facies. Time-structure maps for the individual seismic intervals are used extensively for they can reveal a characteristic geometry to a depositional system (e.g. submarine fan, reef). They also reveal subtle features that are not seen on

structure maps. Time-structure maps are commonly used to unravel the geological history and make palaeo-structural reconstructions (e.g. remove tilting effects) (Lang, 2000).

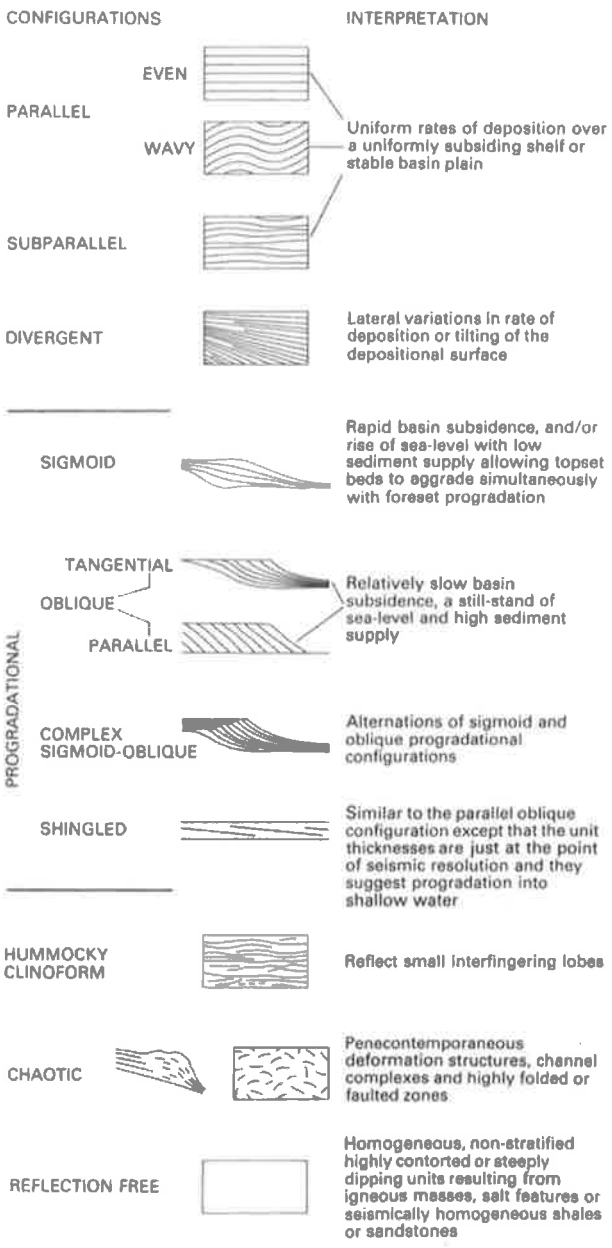

Figure A2.10 Seismic reflection configurations (Mitchum et al. 1977).

2.5 BIOSTRATIGRAPHIC ANALYSIS

In biostratigraphy the fossil contents of the beds are used in interpreting the historical sequence. It is based upon the principle of the irreversibility of evolution. This means that at any one moment in the Earth's history there was living a unique and special assemblage of animals, characteristic of that period and of no other (Clarkson, 1986).

Clarkson (1986) identified the main problems in biostratigraphy as:

a) Many kinds of fossils, especially those of bottom dwelling invertebrates, are facies-controlled. They lived in particular environments only and they were often highly adapted for particular conditions of temperature, salinity or substrate and are not found preserved outside this environment. This means that they can only be used for correlating particular environments and thus are not universally applicable.

b) Some kinds of fossils are very long-ranged. Their rates of evolutionary change were very slow. They can only be used in a broad and general sense for long period correlation and are of very little use for establishing close subdivisions.

c) Such good zone fossils as the graptolites are delicate and only preserved in quiet environments, being destroyed in more turbulent conditions.

d) Since fossil species could migrate following their own environment through time, there is always a possibility of diachronous faunas. The zone as defined in one area may not therefore be exactly time-equivalent to that of another region.

Due to the exploration focus previously being on Cretaceous sediments in the Gambier Sub-basin, palynology and micro-palaeontology sampling was very sparse in the Cenozoic. Hence, analysis of new and existing core and cuttings samples was undertaken in an attempt to achieve higher resolution dating of Cenozoic sediments.

2.5.1 Palynology

Cuttings comprised the dominant sample type, with some cores and sidewall cores used. Wireline logs were consulted and sample depths determined where the lithology was likely to be fine grained (clay or silt). Due to the fine-grained nature of the organic matter that needs to be selected for analysis, well-sorted fine-grained rocks generally have higher yields than well-sorted sandstones or coarser-grained rocks.

Samples were processed according to standard practices (e.g. Traverse, 1988). After cleaning, the crushed sample was dissolved in mineral acids to remove carbonate (HCl) and silicate minerals (HF and HC), followed by heavy liquid treatment ($ZnBr_2$) to remove any remaining minerals. The resultant organic fraction was sieved to concentrate fossils for spore colour measurement, then carefully oxidised (HNO_3 and dilute KOH) to clear the fossils for microscope examination on a slide prepared with glycerine jelly.

All strong mineral acids are harmful and need to be used in a fume cupboard with a scrubber to capture acid fumes before they reach the atmosphere. Hydroflouric acid (HF) is the most dangerous and must be handled with respect according to regulations.

2.5.2 Micropalaeontology

Foraminiferal analysis was undertaken on previously prepared slides. These carbonate samples were broken up and washed with detergent to remove mud and then dried in an oven. The samples were analysed under a binocular microscope and index species assemblage were identified and recorded and related to assemblage charts for age determination.

2.6 CHRONOSTRATIGRAPHIC CHARTS

Sequence stratigraphy involves the interpretation of the relationships of depositional systems in time as well as space. Chronostratigraphic charts are a means of showing the time relationships of these systems and their relationships to surfaces of non-deposition, condensation and erosion. These surfaces have little or no thickness in the rock record and their true significance can be better appreciated by considering them in their time dimension (Emery and Myers, 1996).

Chronostratigraphic diagrams are drawn to summarise the ordering of the deposition of sediment. This highlights any inconsistent geological events and it also enables observations to be made on the time, severity and extent of controlling influences such as sea level rise and fall, which result in deposition, erosion and condensation, or tectonic episodes such as block faulting (Lang, 2000).

A chronostratigraphic chart has a vertical axis in time, with a spatial horizontal axis. On the chart are plotted the distribution of systems tracts, bounded by surfaces of onlap, toplap, downlap, etc. According to the methods for constructing chronostratigraphic charts in Emery and Myers (1996), a representative seismic section was printed out, sequences and surfaces were numbered according to order of deposition, and the extents of each sequence and systems tract was marked directly below the seismic data, noting stratal termination patterns. The constructed chart had a vertical time axis but with a non-linear scale, hence the packages were correlated to biostratigraphic ages known at key surfaces to determine the absolute age of each package.

2.7 DEPTH CONVERSION

Interval velocities of supersequences were determined by averaging checkshot and velocity data from well completion report data. These velocities are represented in Table A2.1 and are used consistently for depth conversion of two way time values derived from seismic data into approximate depths in metres.

SUPERSEQUENCE	INTERVAL VELOCITY (M/SEC)
6	2300
5	2300
4	2300
3	2485
2	2620
1	2980

Table A2.1. Interval velocities used throughout this study for each supersequence.

Appendix 3

Field Trip

Gambier Sub-basin Field Trip

NCPGG

4th - 8th March

Field Trip Leader: Rosalie Pollock (Ph.D. Candidate)
as partial completion of Ph.D. Thesis entitled...

"The influence of Tertiary tectonic movements on the stratal architecture, maturation and migration of hydrocarbons in the Gambier Sub-basin, Otway Basin, southern Australia."

SPONSORS

PIRSA

Boral Energy Resources Ltd.

Lakes Oil Ltd.

TABLE OF CONTENTS

1. ACKNOWLEDGEMENTS

I would like to thank the people who helped to prepare for this field excursion.

I am grateful to Maureen Sutton for helping me organise accommodation and transport, and PIRSA for assisting in preparing this field guide.

I am especially grateful to the Witherstow family for granting us access to the quarries at Compton.

2. HEALTH AND SAFETY

The field excursion will involve visits to roadside outcrops, quarries, and outcrops. All have some risk associated with them but if proper procedures are followed, then the risk of injury is nearly entirely eliminated. As the National Centre for Petroleum Geology and Geophysics takes Health and Safety seriously, all participants must read and sign the H&S Risk Assessment form acknowledging they have read the below mentioned risks and have noted the precautions that must be taken to ensure a safe trip for all participants.

Risks and Precautions

The principal risk at every site will be **vehicular traffic**. Some of the sites visited are on roadside exposures so extreme caution must be taken to remain clear of any passing traffic. This means that attendees must NOT stand on the road itself, but should be on either side of the road when examining outcrops. Cross the road with caution, and in groups of no more than two at a time. Two large caution signs will be placed 100m from either end of the roadside outcrop and support vehicles will be parked at either end with hazard lights flashing. Each attendee must take responsibility for ensuring they check for traffic before crossing the road.

The other main risk is **falling rocks**. This will arise at the quarries and cliff outcrops and rock overhangs along the beach. As a precaution check above before approaching the rock face and if climbing up the face to examine a rock, ensure that no one is directly below. Caution is also required when walking on **wave cut platforms** at the beach because of rogue waves and wave wash making the rock surface slippery.

Hitting rocks presents another risk to eye injury, so you **MUST wear protective glasses** when striking rocks, and ensure others around you are out of range of flying chips.

Other environmental risks include snake and insect bites, stings, allergies etc. It may be hot and snake activity is likely, so make lots of noise when walking in long grass and wear gloves if you get allergies. **Common sense should prevail** at each site regarding health and safety, and any potential risks should be brought to the attention of the field leader or the H&S officer immediately.

First Aid and Emergency Contact

Simon Lang has a current First Aid Certificate and a first aid kit will be carried in the main vehicle. **ALL** injuries however minor should be reported to the **field leader, Rosalie Pollock or the H&S officer**.

- Protective clothing and field equipment
- Boots or other sturdy footwear is essential.
- Long trousers or gaiters and long sleeved shirts are recommended for all stops.
- Sunglasses, sunscreen and a hat are essential (preferable wide brimmed).
- Protective glasses to be worn when using a hammer.
- Raincoat or umbrella is highly recommended as it could rain.
- A hand lens and grain size comparator is strongly recommended.
- Bring your camera or video camera.
- Pack a notebook, pencil, pen or other drawing instruments.

3. ITINERARY

Day 1 Saturday 4th March 2000

13:00 Leave Adelaide for Mt. Gambier (443 km)

A stop to look at Pleistocene aeolian dunes (Bridgewater Formation) and a few stops along the Coorong may be made.

19:00 Arrive at Mt. Gambier where we will stay one night at the Tower Motor Inn, 140 Jubilee Highway West (Phone (08) 87249411).

Day 2 Sunday 5th March 2000

8:00 Visit sites 1&2 (Allan's Sand and Limestone Quarry) and look at the contact between the Dilwyn Formation, Compton Conglomerate and the Gambier Limestone. A thin veneer of the Holocene Molineaux Sand is also visible at these sites. Visit outcrops of the recent volcanics at Mount Schank and Mount Gambier.

14:00 Leave Mt. Gambier for Pt. Campbell (267 km)

Stop at sites 11-13 near the Glenelg River at Dartmoor (~50 km east from Mt. Gambier on the Princess Highway). At these sites the Dilwyn Formation, Narrawaturk Marl and Gambier Limestone equivalent (probably Clifton Formation) are visible.

18:30 Arrive in Pt. Campbell where we will stay one night at the Southern Ocean Motor Inn, Great Ocean Rd., Port Campbell. (Phone (03) 55986231).

Day 3 Monday 6th March 2000

8:00 Leave Port Campbell for Buckley's Point, stopping at Loch Ard Gorge and the Twelve Apostles on the way (where, apart from the spectacular scenery, you can see the contact between the Narrawaturk Marl and the Port Campbell Limestone). There is a 6 km walk along the beach from Point Ronald, at the mouth of the Gellibrand River to Buckley's Point. On this

walk we will see the type section for the Wangerrip Group and the unconformity between the Cretaceous Otway Group and the Tertiary Wangerrip Group.

18:00 Arrive in Apollo Bay (98km) where we will stay for two nights at the Bayside Gardens, 219 Great Ocean Road, Apollo Bay. (Phone (03) 52376248).

Day 4 Tuesday 7th March 2000

8:00 Visit Brown Creek and Castle Cove.

At these locations, the Eocene Nirranda Group outcrops, with the Mepunga Formation, Narrawaturk Formation, Clifton Formation, and Gellibrand Marl visible. Good exposure of Early Cretaceous sediments is also visible at Castle Cove.

18:00 Return to the Bayside Gardens, Apollo Bay

Day 5 Wednesday 8th March 2000

8:00 Leave Apollo Bay for Adelaide (808 km)

Site 10, a road cutting outcrop on the Great Ocean Road, ~6 km east of Princetown will be visited on the way. At this site, the Dilwyn Formation is visible, showing alternating fair and storm weather beds and interesting sedimentary structures.

18:00 Arrive back in Adelaide

4. PROPOSED WORK FLOW FOR VISITING OUTCROPS

Due to the limited time, I have proposed a workflow that will enable us to get the most information out of each outcrop in the short time available.

If we divide into teams that each have a specific purpose, we will be able to obtain all the data required from each outcrop in a relatively short time. The teams may form as follows…

Leader/Director (1 person) - will give a brief description about each outcrop and oversee the team's progress.

Photography (1 person) – photograph the outcrops in both colour and black and white.

Stratigraphic Logging Team (2-4 people) – will log sections at each outcrop.

Palaeo and Sampling Team (2 people) – will observe and record sedimentary structures and fossils present in the outcrop and will take samples.

Sketching team/Occupational Health and Safety Team (2 people) – will sketch the outcrop and ensure all field trip participants are working in a safe manner.

The composition of the teams may change at each outcrop depending on interest and expertise.

5. INTRODUCTION

This field trip is designed to run over five days. The trip will leave Adelaide and travel southeast across the Murray Basin and along the Coorong to Mt. Gambier in the Gambier Sub-basin (Figure 1a). We will stay one night in Mt. Gambier and while there we will look at the recent volcanics and outcrops of the Gambier Limestone and Compton Conglomerate (Sites 1-4). From here we will travel east into Victoria in the Otway Basin, where we will visit some outcrops near Dartmoor on the Glenelg River (Sites 11-13). We will then travel on to Warrnambool and Pt. Campbell (Figure 1b) where we will visit a number of Paleocene-Eocene outcrops (Sites 5-9) over the next two days. We will return to Adelaide on day 5.

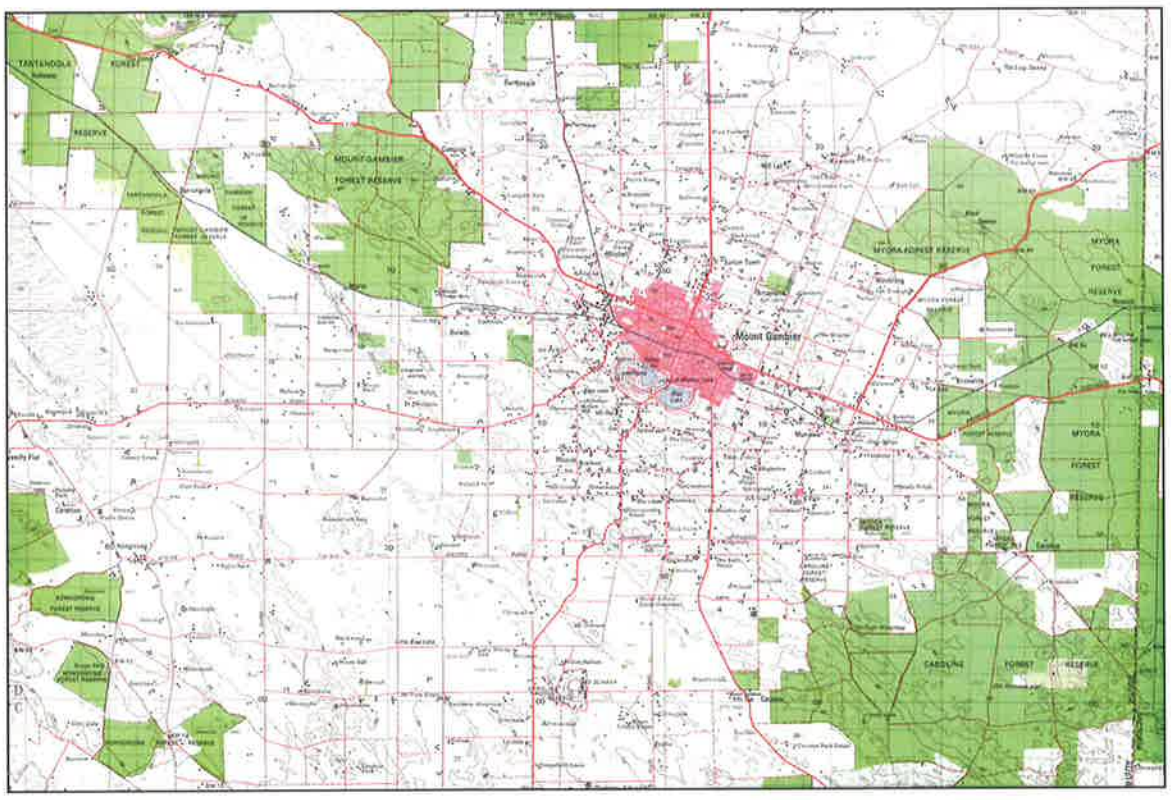

Figure 1a. Topographic map of the Mount Gambier region.

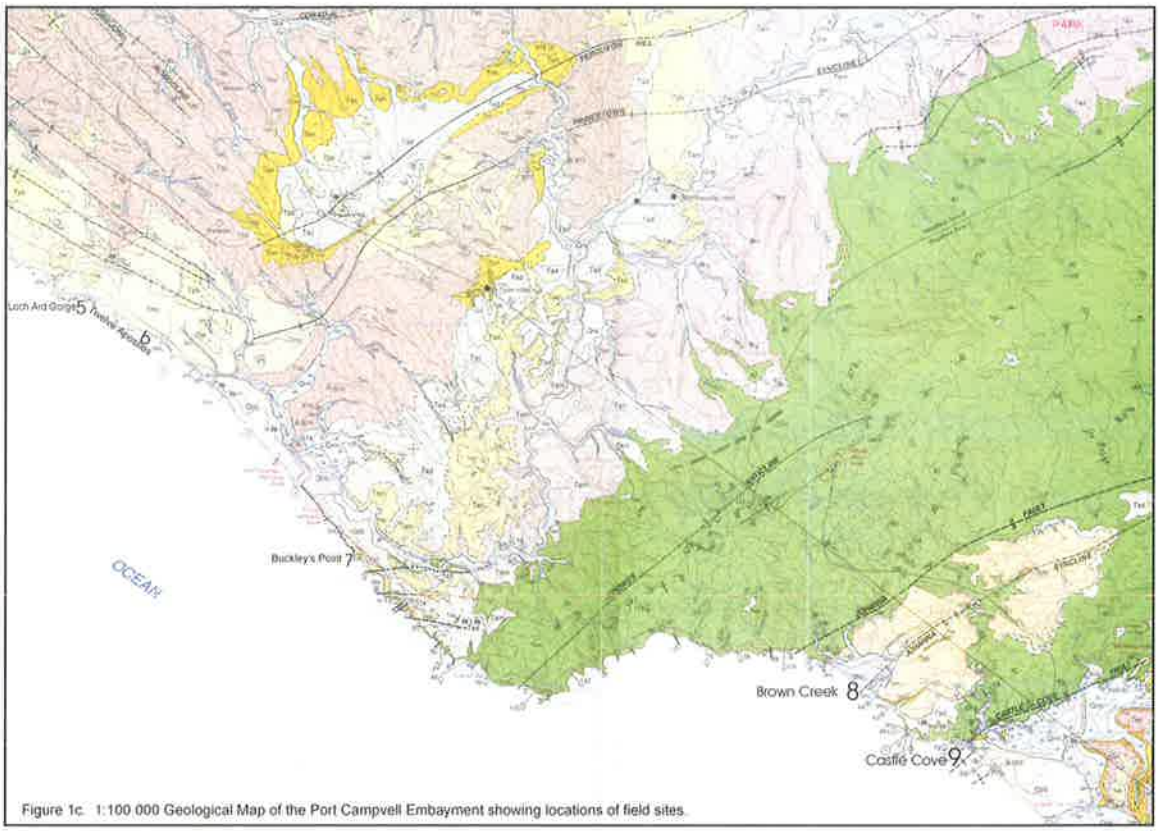

Figure 1b. Geological map of the Port Campbell embayment in the middle part of the Otway Basin.

The Gambier Sub-basin experiences a Mediterranean climate, with hot, humid, dry summers and variably wet winters. Surface expression is minimal within the Gambier Sub-basin with only a handful of outcrops visible. A large part of the basin is expressed as a coastal plain with extinct volcanoes and ridges of sub-parallel northwest trending dunes. These dunes are 15-30 m high and are associated with Pleistocene stranded shorelines (Wopfner and Douglas, 1971). Spectacular karst features have developed throughout the region within the Gambier Limestone and Bridgewater Formation. Overall, this karst region extends as a broad band southwards from Naracoorte towards and beyond the present coastline, reaching a maximum width of more than 60 km (Marker, 1975). Karst in the Gambier Limestone is more spectacular and extensive, and includes large cenotes (e.g. Little Blue Lake and Hell's Hole), complex joint controlled cave systems and dolines (Figure 2). The depth to which karst features have developed increases towards the coast due to an increasing thickness of the Gambier Limestone and lower sea levels and water tables during Pleistocene glacial periods.

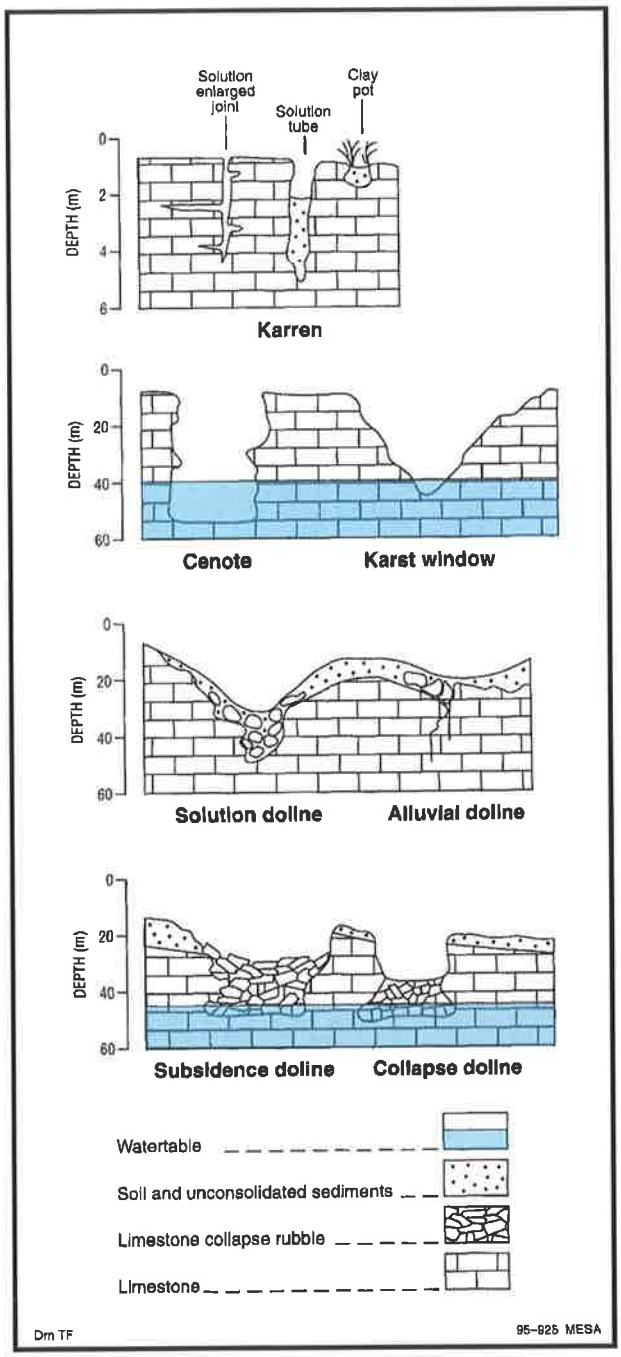

Figure 2. Some common karst forms (Sheard and Smith, 1995 after Bogle, 1980).

The most significant coal resource in the Gambier Basin is the Kingston coal deposit. It comprises 985 Mt of low rank lignite in a northeast-trending depression onlapping the Padthaway Ridge near the northern margin of the basin (Meyer, 1982). Most of the coal is in a single seam up to 12 m thick, with overburden 28-75 m thick.

Gambier Limestone has been quarried and used locally as building stone since 1844. The quarries are located in pale pink to cream or white porous bryozoa calcarenite of the Camelback Member, which outcrops at Marte, 10 km west of Mt. Gambier (Figure 3) (Alley and Lindsay, 1995).

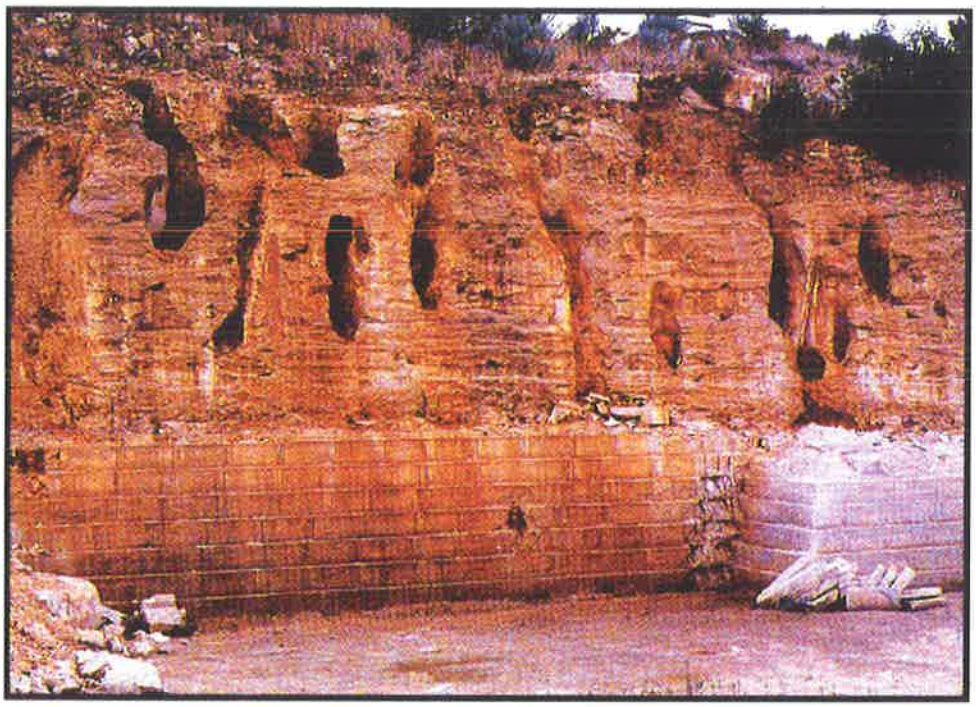

Figure 3. Gambier Limestone with solution pipes at Steetely building stone quarry near Mount Gambier (Smith et al. 1995).

The Gambier Sub-basin comprises several aquifers that are utilised for agricultural and domestic use. The Dilwyn Formation contains the regional confined aquifer, which has been developed for pasture irrigation in the Lucindale-Beachport-Kingston area where artesian conditions exist (Alley and Lindsay, 1995). The Mepunga Formation also forms a confined aquifer, which has been exploited in the Snuggery area and for the Kingston town water supply. In the Mt. Gambier area, the Gambier Limestone is an important high-yielding aquifer.

GEOLOGICAL FRAMEWORK

Extent

The Gambier Sub-basin (previously defined as the Gambier Embayment of the Otway Basin) is located in southern Australia, adjacent to and partially overlying the Otway Basin (Figure 4). The sub-basin straddles the Victorian and South Australian coastline with the western two-thirds located in southeastern South Australia and the eastern third located in southwestern Victoria. The sub-basin covers an area of more than 150,000 km^2, two-thirds of which is located offshore (Yu, 1988).

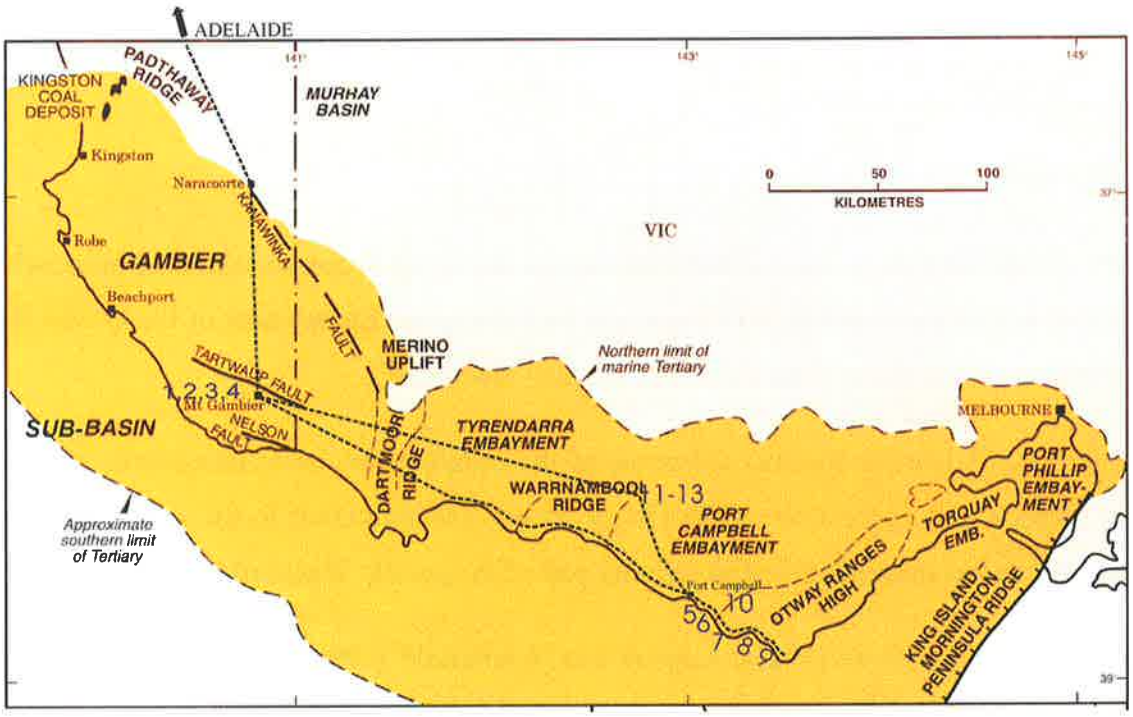

Figure 4. Location map of the Gambier Sub-basin in the western part of the Otway Basin showing basin limits and structural elements. Also illustrated is the path taken on this field trip and locations of field sites (modified from Smith et al. 1995).

The boundary of the Gambier Sub-basin approximately follows the depositional limit of Cenozoic sediments. The northern limit of the basin is the E-W trending Padthaway Ridge (Sprigg, 1952; Morton and Drexel, 1995). This submerged basement high separates the

Gambier Sub-basin from the Murray Basin and is marked by a steep gravity gradient (Wopfner and Douglas, 1971). The Merino Uplift marks the eastern limit of the basin and the southern margin is the present day continental shelf in water depths of 2500 m. This study will concentrate on Cenozoic sediments located to the southwest of the Tartwaup Fault, which trends approximately northwest-southeast through the northern half of the basin (Figure 4).

Geological History

For a detailed discussion on the Geological History of the Gambier Sub-basin please refer to Chapters 2 and 3. The Otway Basin has been defined as consisting of Cambrian to Cretaceous sediments, while the Gambier Sub-basin comprises Cenozoic sediments.

Stratigraphy

Figure 5 (modified from Li et al. 2000) illustrates a stratigraphic column showing nomenclature differences within the Gambier Sub-basin and Port Campbell Embayment of the Otway Basin. The stratigraphic locations of the field sites are also illustrated.

The Cenozoic (Paleocene-Recent) sediments of the Gambier Sub-basin unconformably overlie the Late Cretaceous succession of the Otway Basin. Sedimentation in the Late Paleocene to Middle Eocene has been identified as forming part of the paralic Wangerrip Group.

Authors such as Holdgate (1981), Kopsen and Scholefield (1990); Mehin and Link (1994), White (1995, 1996), Morton and Drexel (1995) and Finlayson et al. (1998) have identified the Wangerrip Group as spanning the Paleocene to Middle Eocene (i.e. from *L. balmei* to *P. asperopolus* palynozone). The basal boundary correlates with being no older than the P4/P5 planktonic foraminiferal zone (White, 1995). The Wangerrip Group comprises sediments partially represented by the Pebble Point Formation, Pember Mudstone, Dilwyn Formation and the Burrungule Member.

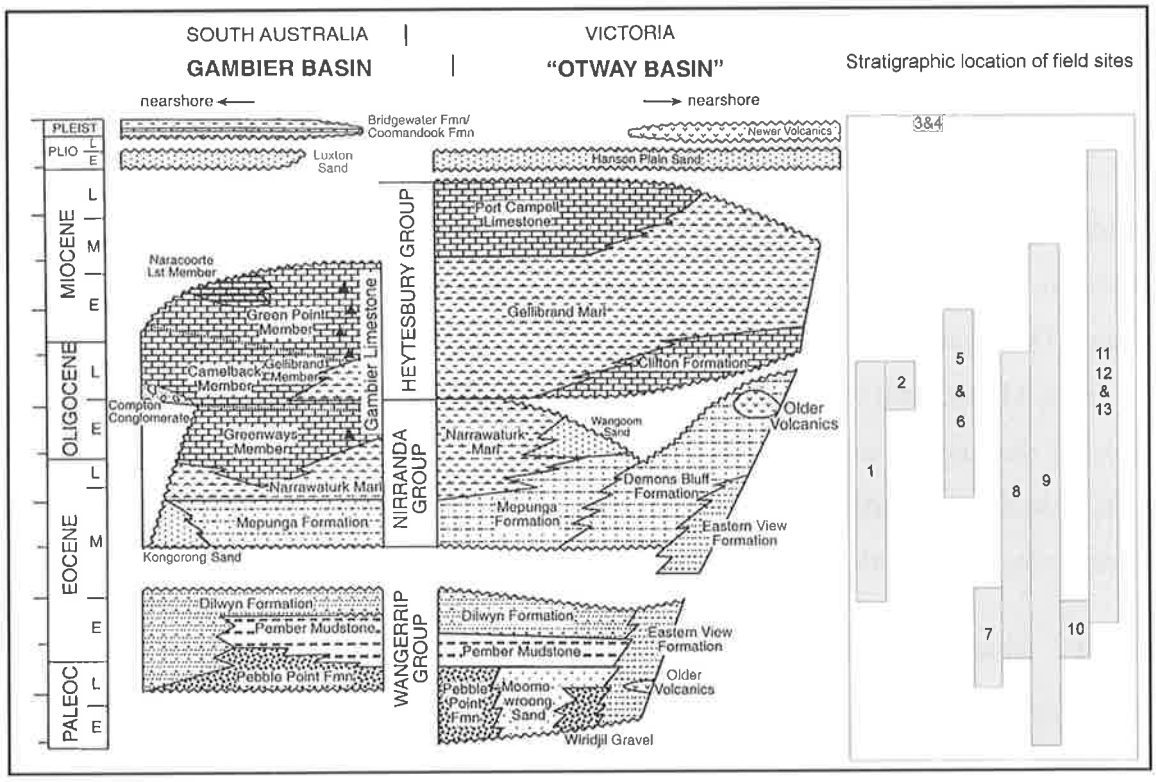

Figure 5. Stratigraphic column (modified from Li et al. 2000) illustrating differences in nomenclature between the Gambier Sub-basin and Otway Basin and the stratigraphic locations of the field sites.

The basal unit of the Wangerrip Group ranges in age from Early Paleocene to Early Eocene (i.e. *L. balmei* to *M. diversus* palynozone) (White, 1995) and is partially represented by the Pebble Point Formation (Holdgate, 1981; Mehin and Link, 1994; White, 1995; Morton and Drexel, 1995; Finlayson *et al.*, 1998). The subsurface type section of this package is located in Caroline 1 between 925-951 m (White, 1996). It comprises a dark green/brown oolitic and chamositic grit, quartz, carbonaceous material and foraminifera. Accessories include bioclasts, glauconite, pyrite, mica, goethite, rock fragments and iron clasts (Morton and Drexel, 1995; White, 1995). These sediments were deposited at a slow rate in a marginal marine environment and the presence of ooids suggests a low energy environment (Morton and Drexel, 1995).

Sediments representing the Pebble Point Formation, may in some places, form an effective seal to underlying upper Cretaceous sandstone reservoirs (Laing et al. 1989). In the southwest of the basin, channel sands identified by Laing and others (1989) may represent valid reservoir targets. In the central part of the basin, the Pebble Point Formation may exist on the southern,

down-thrown side of the Tartwaup Fault, developed as a result of rollover (Laing et al. 1989). Hydrocarbon migration may be along the fault zone from the upper Cretaceous, and if the overlying mudstones form an effective seal, this may be a potential target.

Holdgate (1981) determined three sub-divisions of sediment packages partially represented by the Dilwyn Formation. The oldest unit being sediments depicted in part by the Pember Mudstone (Holdgate, 1981; Kopsen and Scholefield, 1990; Mehin and Link, 1994; White, 1995, 1996; Morton and Drexel, 1995; Finlayson et al. 1998), which is overlain by sediments comprising the undifferentiated Dilwyn Formation. The third unit of the Dilwyn Formation consists of sediments partially represented by the Burrungule Member (Holdgate, 1981), which is mainly recognised south of the Tartwaup Fault, with coaly equivalents north of the fault.

Sediments, which in part constitute the Pember Mudstone, comprise interbedded brown mudstones, sandy mudstones and muddy mudstones (Holdgate, 1981, Morton and Drexel, 1995; White, 1995). Accessory components include bioclasts, glauconite, pyrite, mica and rock fragments (Holdgate, 1981; Morton and Drexel, 1995; White, 1995). The subsurface type section of this unit is in Caroline 1 between 727-925 m (White, 1996).

The Pember Mudstone constitutes a prodelta sequence of marine shales and silty-shales that inter-fingers with a delta-front facies (Holdgate, 1981). These sediments filled the deep east-west trending trough between the Gambier and Tyrendarra Embayments (Holdgate, 1981). The sands have excellent sorting, coarsen upwards and display linear geometries, which suggests they may form palaeo-shorelines with a northward dip indicating the source was from the present-day seaward side (Holdgate, 1981).

Sediments deposited during the Late Paleocene to Middle Eocene (i.e. *L. balmei* to *P. asperopolus* palynozone), partially representing the Dilwyn Formation (Holdgate, 1981; Kopsen and Scholefield, 1990; Mehin and Link, 1994; Morton and Drexel, 1995; White, 1995, 1996; Finlayson et al. 1998), comprise sandstone in the northern part of the basin and approximately 50-50% sand and mud in the southern part of the basin (Morton and Drexel, 1995). The environment of deposition has been interpreted as fluvial in the north, marginal marine and deltaic to the south (Holdgate, 1981; Morton and Drexel, 1995). The subsurface type section of this sediment package is located in Caroline 1 between 195-727 m (White, 1996).

Holdgate (1981) recognised up to seven cycles within the Dilwyn Formation. The cycles commonly commence with a sudden change to a shale or silty-shale from sand, evident on the gamma ray log. These cycles are repetitive and compare favorably with the deltaic cycles described by Galloway (1968), Weber (1971), and Selley (1976).

Cycle A represents a delta front and delta plain sequence, similar to the Pember Mudstone deltaic cycle. The thick channel sands represent delta lobes, akin to the Mississippi Delta (Holdgate 1981). Cycles B to G are thought to represent stacked tidal dominated deltaic cycles, similar to the Niger Delta (Holdgate 1981).

Sediments partially comprising the Burrungule Member (Holdgate, 1981) are represented by well-burrowed grey muddy siltstones with lesser sands, which conformably overlie the undifferentiated Dilwyn Formation (Holdgate, 1981). The sediments also contain calcareous marine fauna of foraminifera and shelly fossils.

Sediments that may partially comprise the Middle to Late Eocene (i.e. *P. pachypolus* to *N. asperus* palynozone, which correlates to latest P14 to ca P17 planktonic foraminiferal zone) (White, 1995) Nirranda Group are not extensively deposited across the Gambier Basin. Sediments representing this group are present in wells north of the Tartwaup Fault, but cannot be identified with any certainty in wells in the southern part of the basin (White, 1995).

During the Early Oligocene starvation of clastic sediment, plate reorganisation and marine transgression lead to deposition of platform carbonates, which are classified by some authors as forming part of the Heytsbury Group (Figure 5) (Morton and Drexel, 1995; Mehin and Link, 1994; White, 1995, 1996, Finlayson et al. 1998; James et al. 1993).

The Gambier Limestone is divided into three members (Figures 6, 7 and 8). Subdivisions of the Gambier Limestone have been made by previous authors (e.g. Lindsay, 1967, 1985; Ludbrook, 1962, 1971; McGowran, 1973), but were based on a limited number of successions and have not been formally defined. A recent examination of 26 petroleum wells by White (1995) confirms the value of a three-fold division of the Gambier Limestone. The type section of the Gambier Limestone is located in the sinkhole in the town centre of Mount Gambier, South Australia (White, 1996).

The basal Greenways Member of the Gambier Limestone (White, 1996) ranges in age from Late Eocene to Early Oligocene (i.e. P15 to no younger than P20 planktonic foraminiferal

zones, correlative with Middle *N. asperus* to *P. tuberculatus* palynozones) (White, 1995) and comprises a basal grey limestone, marly limestone and marl with glauconite, which grades into grey limestone. Accessories include bioclasts, chert, quartz and glauconite (Figure 6).

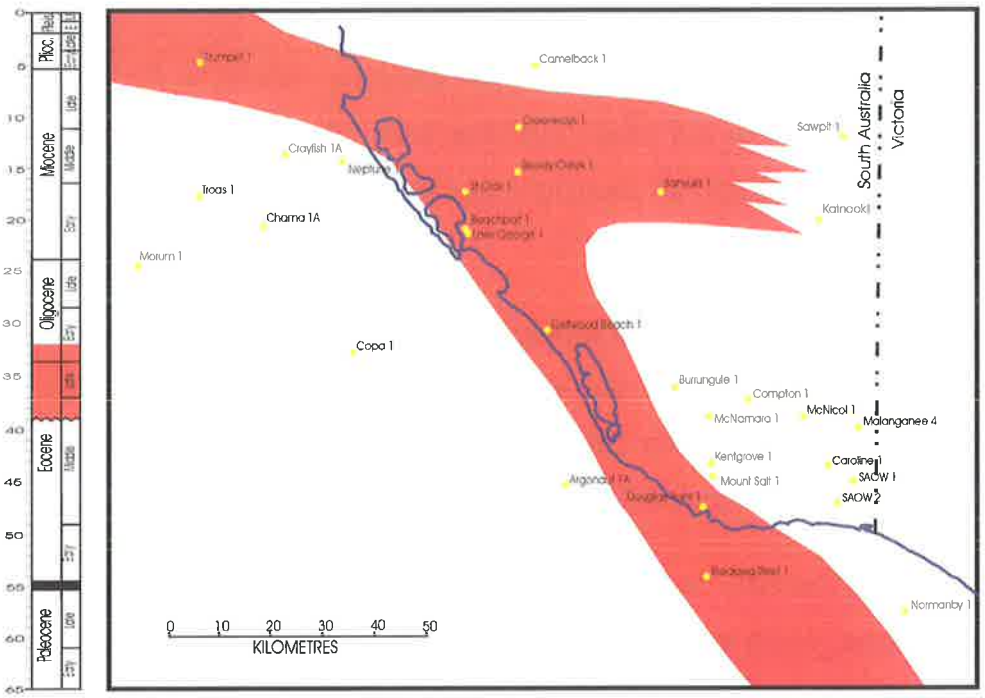

Figure 6. Distribution of the lower Gambier Limestone member, the Greenways Member.

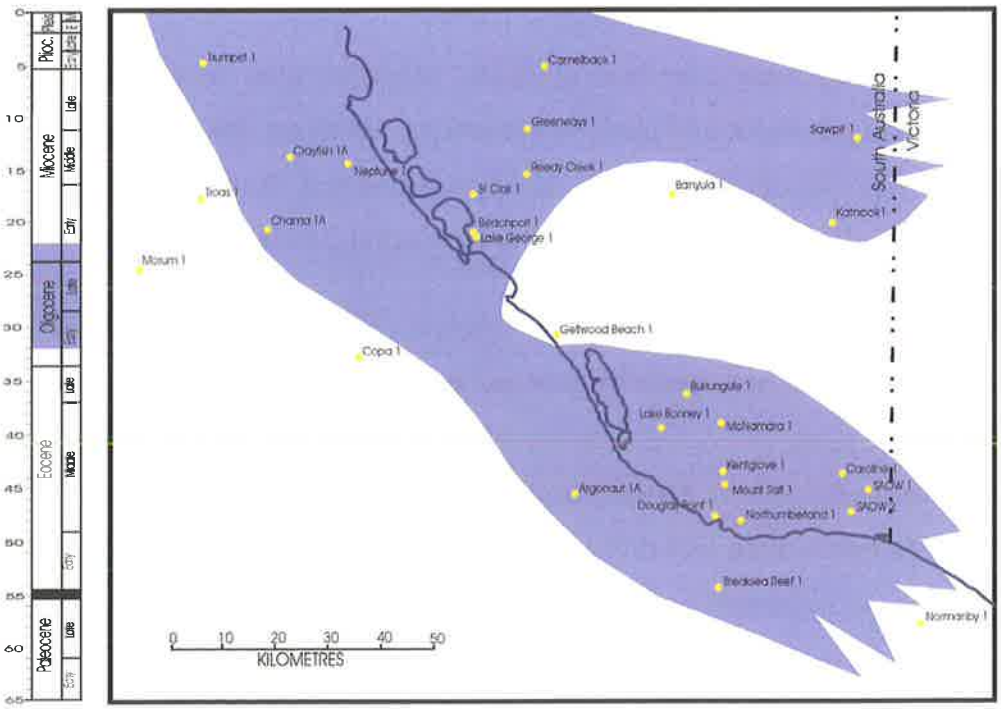

Figure 7. Distribution of the middle Gambier Limestone member, the Camelback Member.

The Camelback Member (White 1996) ranges in age from Early Oligocene too at least Early Miocene (i.e. no younger than top P20 to no older than at least basal N5 planktonic foraminiferal zones, which is correlative with the *P. tuberculatus* palynozone) (White, 1995). It comprises a bryozoa-rich, off-white, white or fawn limestone with macrofossils, forams, rock fragments, quartz, chert and glauconite (White, 1996) (Figure 7). The Camelback Member overlies and grades laterally into the Gellibrand Marl. The boundaries with the Greenways Member and Gellibrand Marl are apparently conformable (White, 1996). The environment of deposition is interpreted to be inner and middle shelf (White, 1995).

The Green Point Member (White, 1996) ranges in age from Early Miocene to at least Middle Miocene (i.e. no younger than N4 to at least N9 planktonic foraminiferal zones, which is correlative with *P. tuberculatus* to at least Lower *T. bellus* palynozones) (White, 1995). It comprises grey limestone with abundant chert as well as macrofossils, forams, quartz, glauconite and pyrite (White, 1996) (Figure 8). The Green Point member conformably overlies the Camelback Member, and is probably partly equivalent to the Naracoorte Member.

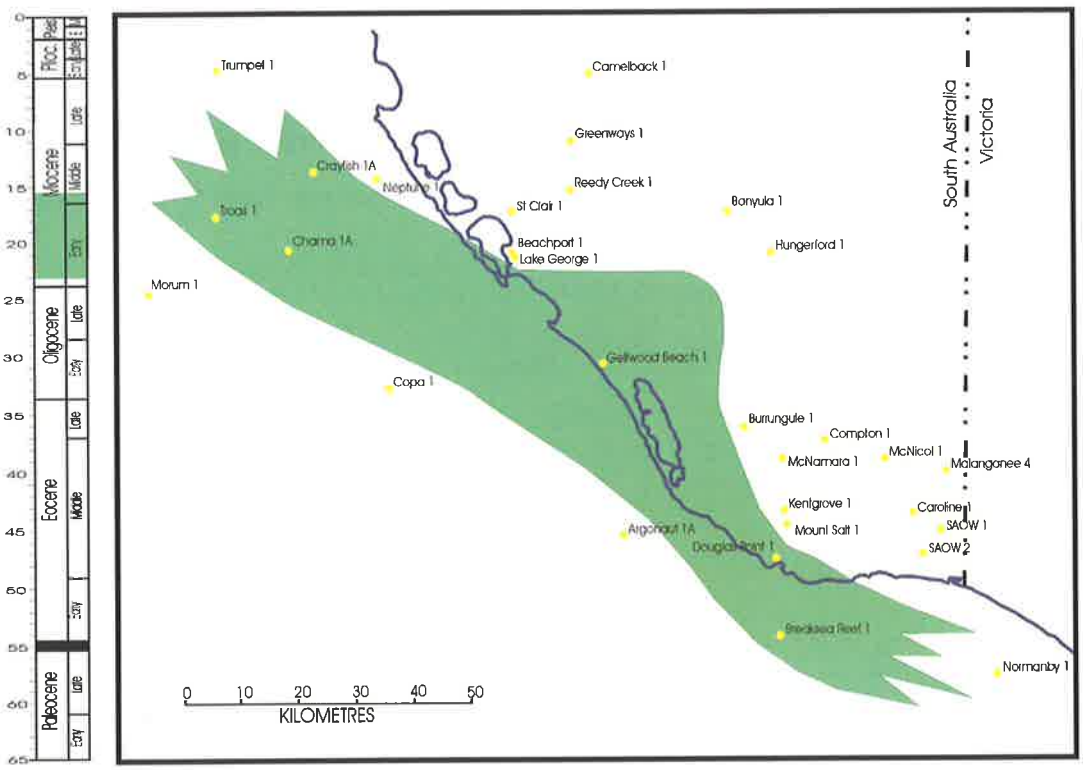

Figure 8. Distribution of the upper member of the Gambier Limestone, the Green Point Member.

In a recent study by Li et al. (2000) the Gambier Limestone has been divided further on the basis of biostratigraphy. Figure 9 shows the sub-divisions of the Gambier Limestone into 7 unconformity-bounded sequences.

James and others (1993) conducted a petrographic and geochemical study on dolomites present within the Gambier Limestone. They drew the conclusion that the dolomites replaced the diagenetically stabilized Gambier Limestone at some time during an uplift event in the Middle-Late Miocene. Geochemistry suggests that dolomitisation was predominantly by seawater, but admixing of continental, possibly fresh groundwater is consistent with the stable isotope and trace element data (James et al. 1993). Fabric selective dissolution of the dolomite crystal core and the Fe-rich zone and later precipitation of calcite within dolomite crystals was also observed in samples of Gambier Limestone (James *et al.*, 1993).

White (1995) states that the overlying Naracoorte Limestone was not recorded in any of the wells examined in that study. Overlying the Naracoorte Limestone is a thin unit called the Gellibrand Marl (White, 1995), which is only present in the northern parts of the basin. The sandy, Pleistocene aged Bridgewater Formation (White, 1995) unconformably overlies the Camelback and Green Point Members of the Gambier Limestone (White, 1995).

Volcanism was active from Pliocene to Recent times. The extrusive volcanics increase the risk for petroleum occurrences by introducing magmatic CO_2 (Morton and Drexel, 1995). The current landscape is a low-relief doline and uvala, multigeneration, karst terrain (Twidale et al. 1983).

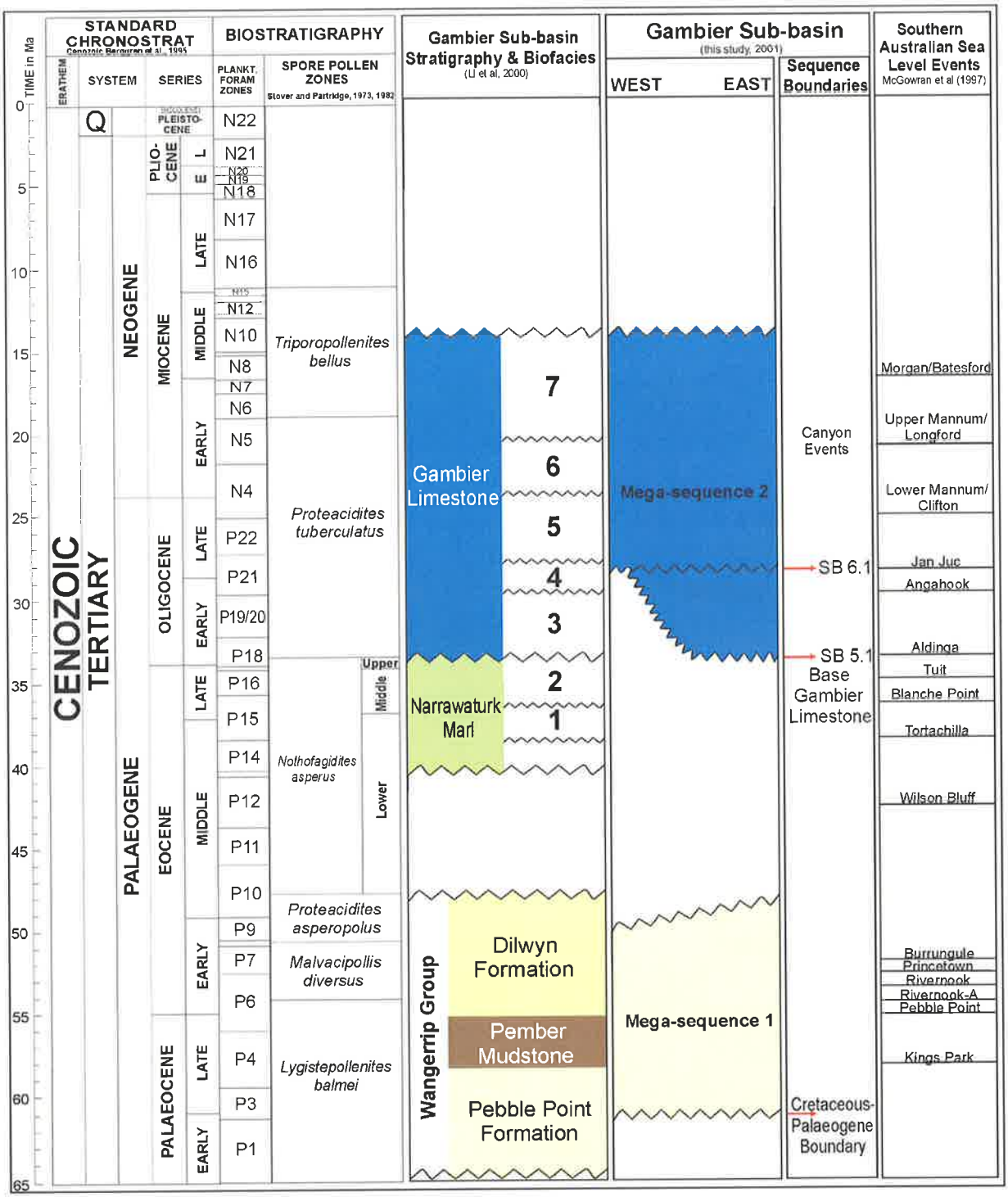

Figure 9. Stratigraphic chart showing the megasequences defined by seismic stratigraphy (Chapters 2 and 3) and the seven unconformity-bounded packages defined by Li et al. (2000).

6. FIELD GUIDE

Day 1 Adelaide to Mount Gambier (traveling only)

Day 2 Mount Gambier to Port Campbell

Sites 1-4 and 11-13

Day 3 Port Campbell to Apollo Bay

Sites 5-7

Day 4 Apollo Bay area

Sites 8 & 9

Day 5 Apollo Bay to Adelaide

Site 10

Map sheets

Topographic Maps 1:100 000

Gambier (7022) (Figure A)

Princetown (7520) (Figure B)

Casterton (7122) (Figure C)

Topographic Maps 1:50 000

Schank III (7022) - Compton area (Figure D)

- Mount Schank area (Figure E)

Geological Maps 1:250 000

Port Campbell (Figure F)

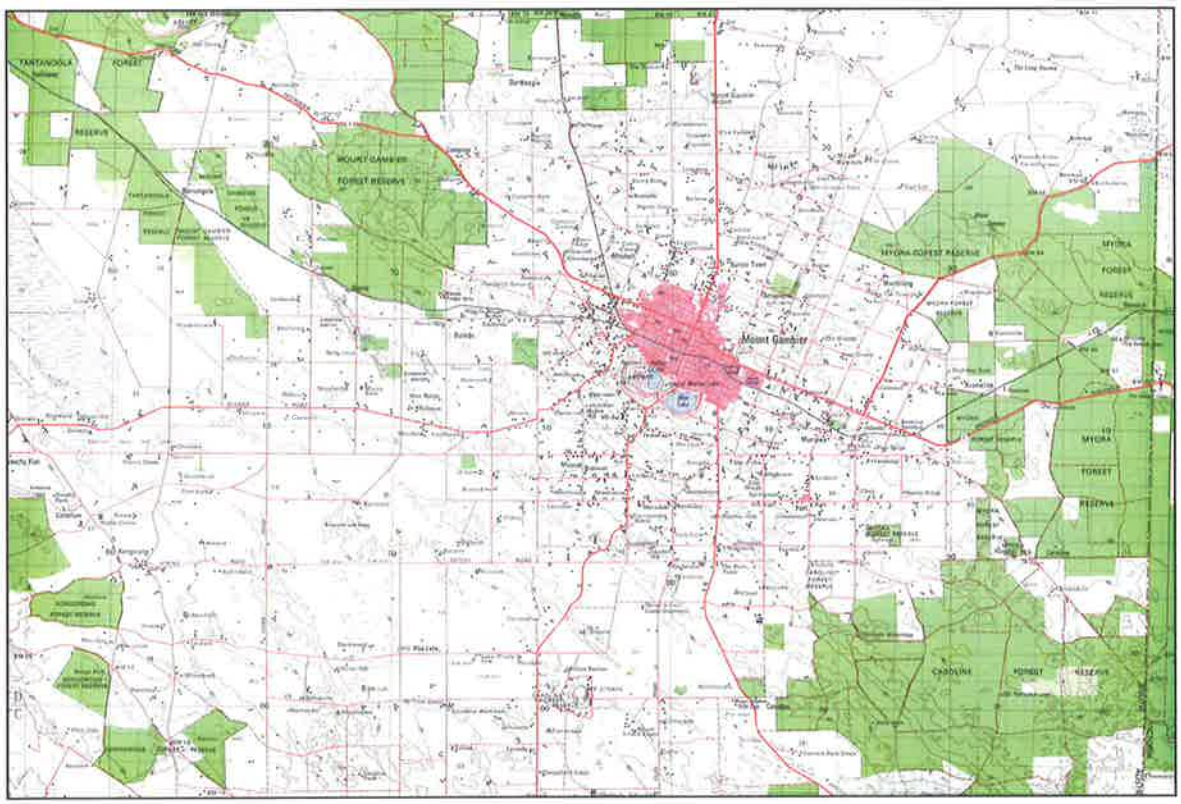

Figure A. Topographic map (7022): Mount Gambier 1:100 000.

Figure B. Topographic map (7520): Princetown 1:100 000.

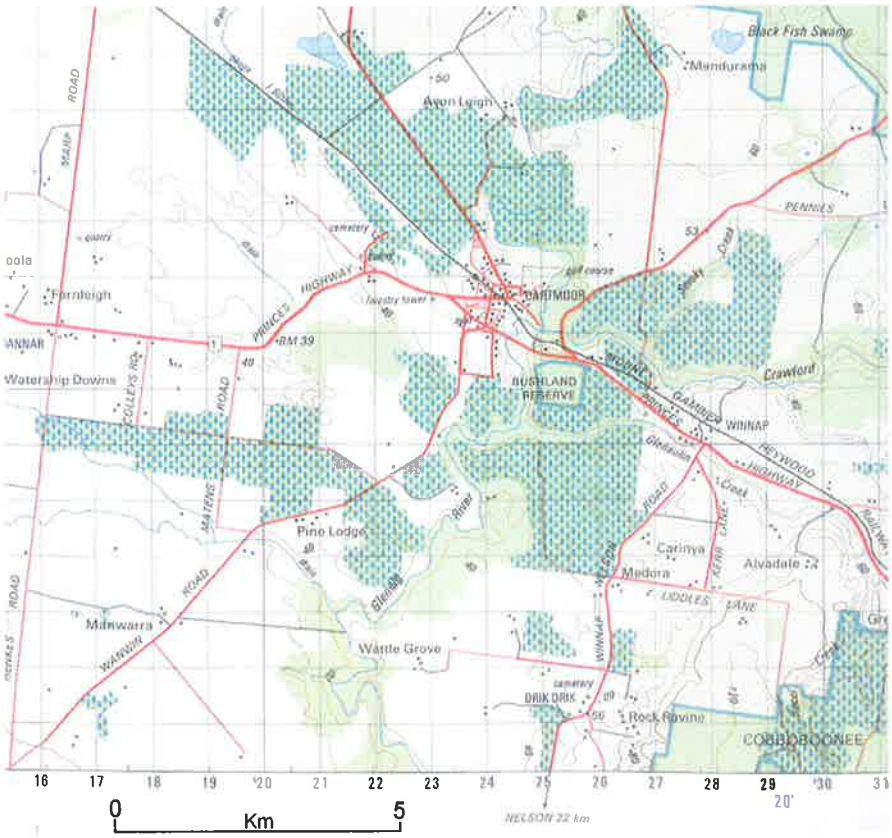

Figure C. Topographic map (7122): Casterton 1:100 000.

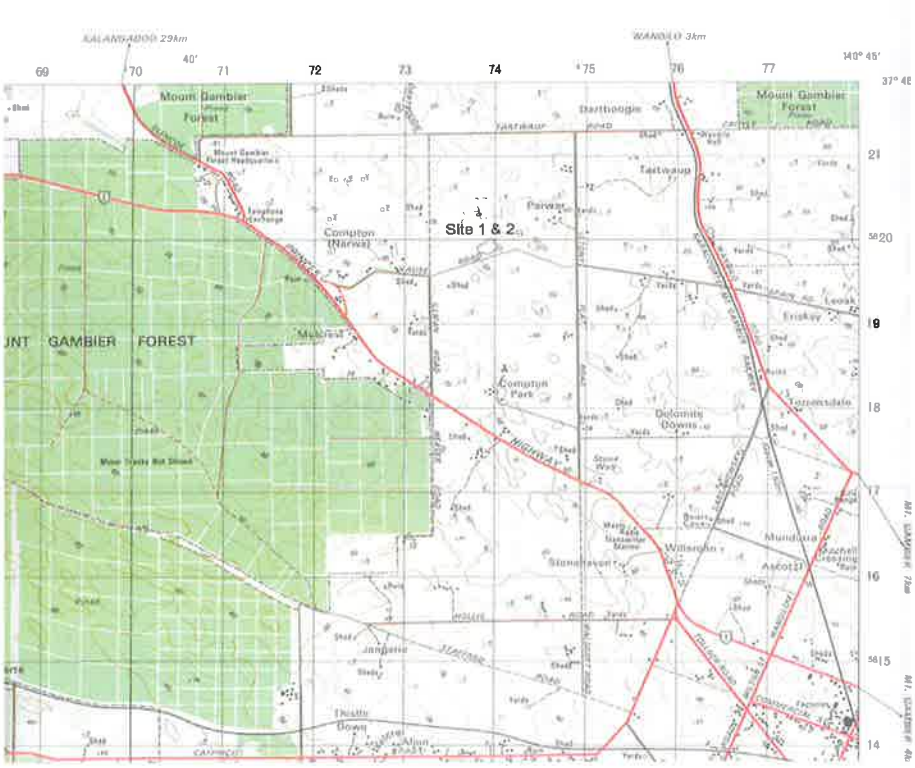

Figure D. Topographic map (7022) Compton area 1:50 000.

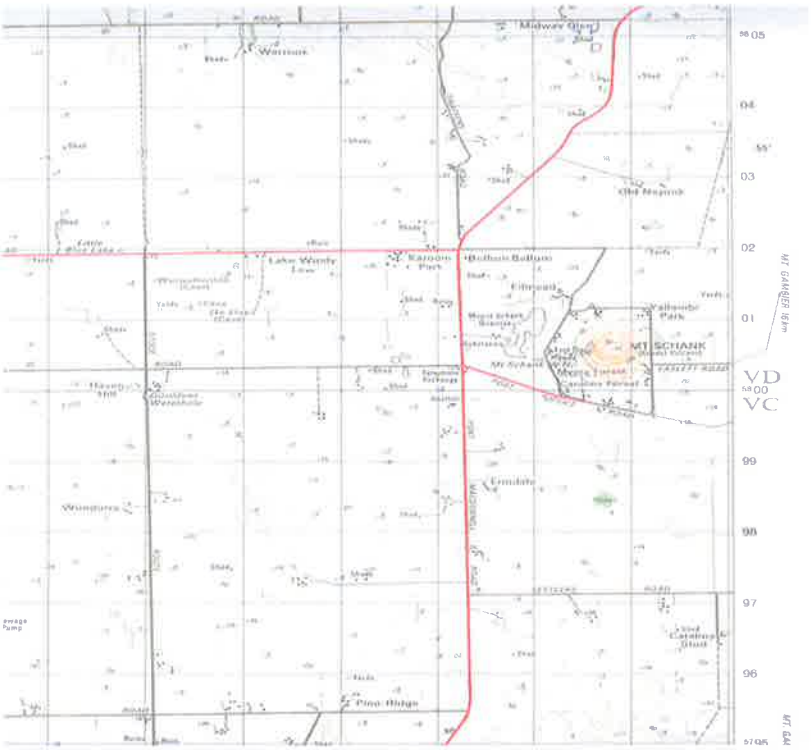

Figure E. Topographic map: Mount Schank area 1:50 000.

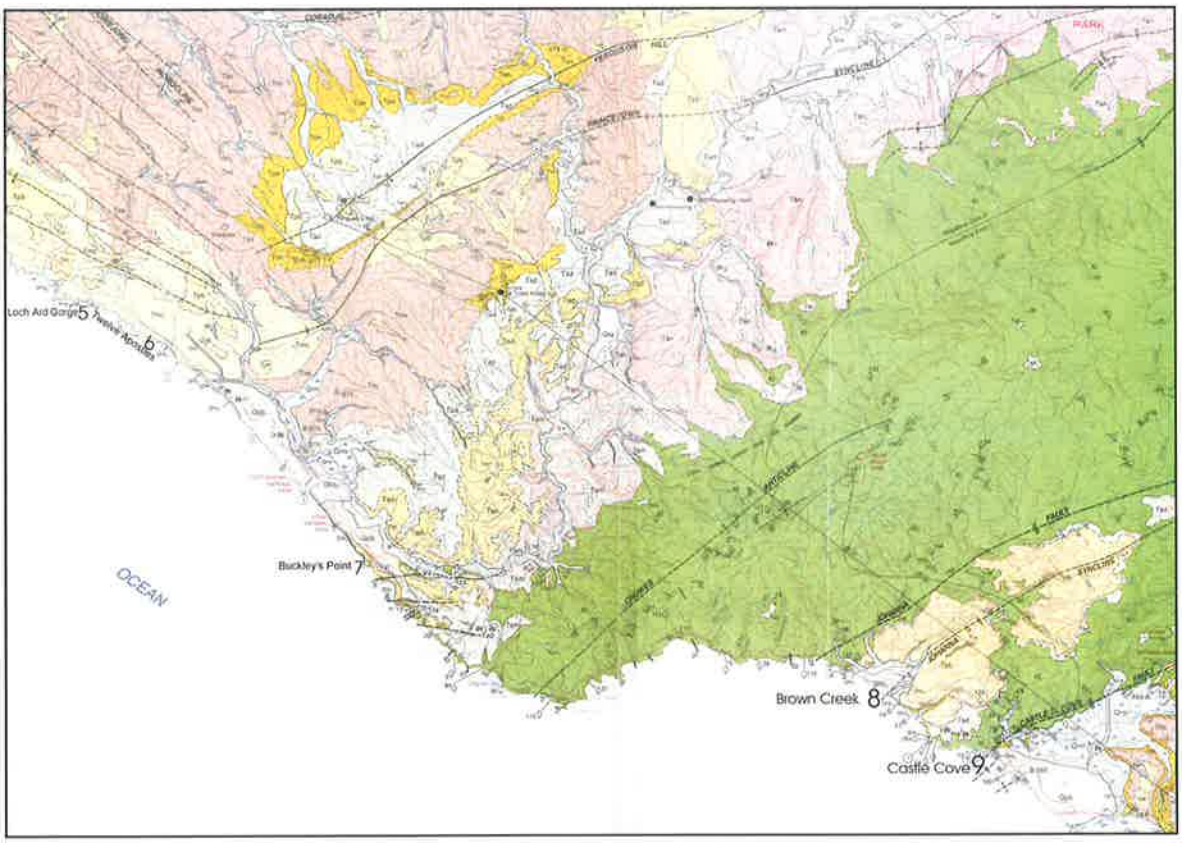

Figure F. Geological map of the Port Campbell area (1:250,000).

DAY 2 MOUNT GAMBIER TO PORT CAMPBELL

Site 1 – Allen's Sand Quarry

Directions:

The quarry is located about 10 km NW of Mt. Gambier. Access is gained from Millicent Rd., north along Stony Flat Road, then west 500 m on Vause Rd (Figure 10).

NOTE: This site is on private land and permission to enter must be sought from the owner, Mr. J. Witherstow.

Health and Safety:

As this is an old quarry, please beware of falling rocks and do not stand under rock overhang.

Objectives:

- To observe and record the nature of the Compton Conglomerate and its contacts with the Dilwyn Formation and the Gambier Limestone.
- To record the location of the outcrop by sketch and photography.
- To log a section through the outcrop and record the composition of the Dilwyn Formation and limestone.
- To run a natural gamma log over one of the outcrops. (At each sample point take three readings, each for 30 seconds, and then average the values.)
- To sample the limestone for fossils and use in isotopic and petrographic analysis.
- To observe the effects of weathering and dolomitisation on the porosity of the limestone.

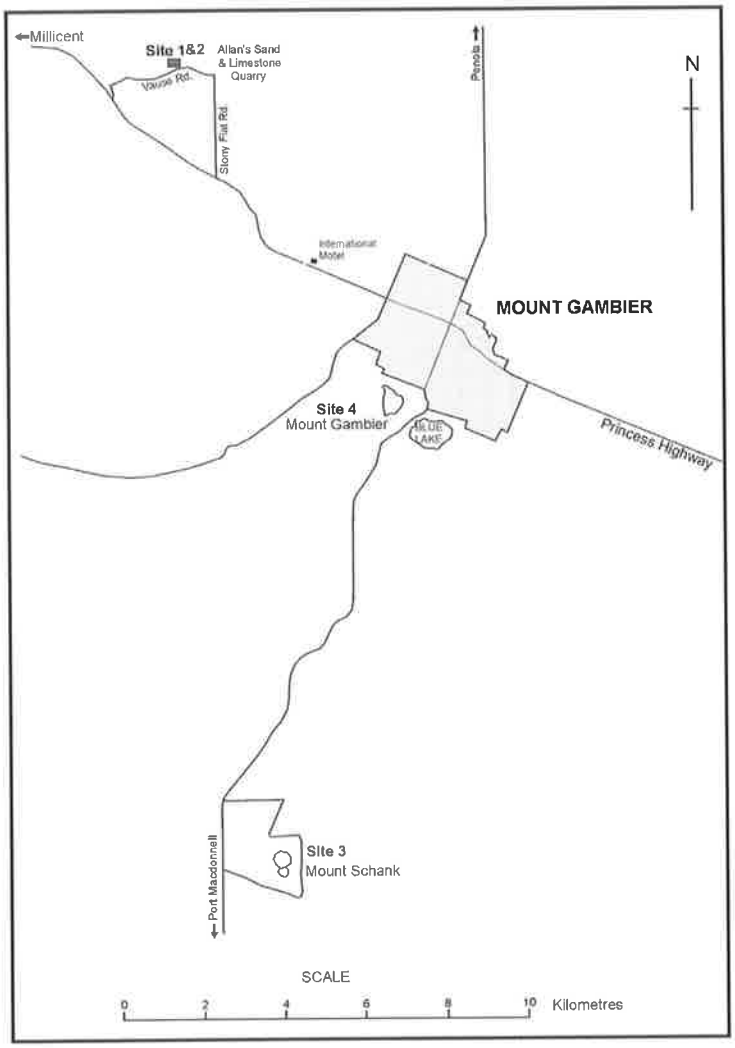

Figure 10. Location of Allen's Quarry, Mount Gambier and Mount Schank in relation to the township of Mount Gambier.

Description:

(Description taken from Smith and Sheard, 1985)

The SE portion of the quarry provides the best exposure and has bee designated as a Geological Monument (McBriar and Mooney, 1976, in Smith and Sheard, 1985). It offers the only outcrop of the contact between the Dilwyn Formation and Gambier Limestone in South Australia.

Figure 11 shows a stratigraphic cross section that runs approximately through Allen's Quarry. The Compton Conglomerate is not seen in wells south of the Tartwaup Fault.

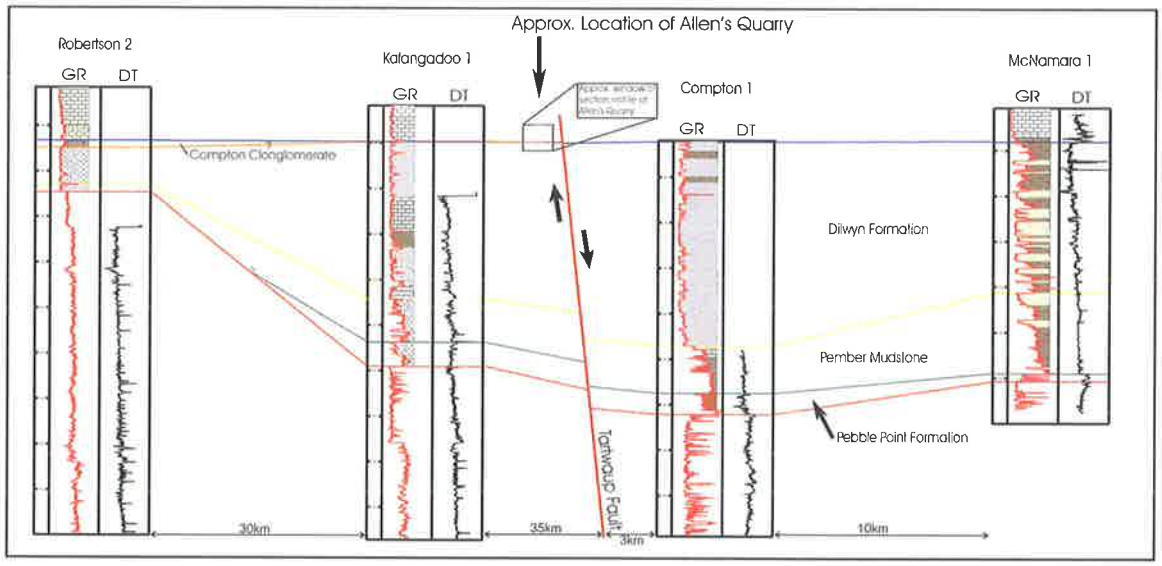

Figure 11. Cross-section through Allen's Quarry.

At the base of the quarry face is 1-2 m of sediments from the Dilwyn Formation, which present as weathered, ferruginised, multi-coloured clays with a variable quartz pebble fraction partially obscured by fill from rehabilitation work. In the sub-surface the clays are highly carbonaceous, dark brown to black and grade into lignite.

Unconformably overlying the Dilwyn Formation is a 0.6 m thick interval of a very well-indurated conglomerate called the Compton Conglomerate. It comprises abundant rounded ironstone pebbles and very coarse-grained sediment in a limonitic matrix.

Overlying the Compton Conglomerate with a gradational contact is the marine Gambier Limestone, which at this site, is less than 1 m thick. It rapidly thickens to the southeast but remains relatively thin to the northwest. Bryozoa fragments and molluscs are weakly cemented to form a permeable material, which is the host to the regional water table aquifer.

The Molineaux Sand (Holocene) unconformably overlies both the Dilwyn Formation and Gambier Limestone erosional surfaces. This blankets much of the region. This sand is a thin veneer of pale yellow, fine-grained quartz of aeolian origin.

The exposure of the Dilwyn Formation in Allen's sand quarry, after some years of controversy, is now interpreted to be a product of its deposition on a structural high followed by erosion before the marine transgression and deposition in the Middle to Late Oligocene. Subsequent erosion of the thin cap of Gambier Limestone has thus exposed the Dilwyn Formation.

Site 2 – Allen's Limestone Quarry

Directions:

The now abandoned limestone quarry is located on private land about 400 m west southwest of Allen's sand quarry. Access is gained from Vause Rd (Figure 10).

Health and Safety:

As this is an old quarry, please beware of falling rocks and do not stand under rock overhang.

Objectives:

- To record the location of the outcrop by sketch and photography.
- To log a section through the outcrop and record the composition of the limestone.
- To sample the limestone for fossils and use in isotopic and petrographic analysis.
- To observe the effects of weathering and dolomitisation on the porosity of the limestone.
- To observe any local structuring (faulting/folding) that has affected the limestone and consider the effect this may have on petroleum development.

Description:

(Description taken from Smith and Sheard, 1985)

The quarry is cut into sub-horizontal Gambier Limestone, which locally is a cream to buff bryozoa calcarenite showing varying degrees of recrystallisation / dolomitisation. The top 3-5 m is rubbly weathered rock underlain by a well-indurated band of calcarenite, which is terminated by a sub-horizontal joint extending throughout the quarry. Below this joint, calcite and friable calcarenite are dominant lithologies. Some reworking of the indurated band is evident where angular to sub-angular fragments of recrystallised limestone are observed in a matrix of friable weathered calcarenite.

Numerous vertical joints striking NNW to NW provide preferential pathways for vadose water and groundwater.

SOUTHEAST VOLCANISM

Background:

Quaternary volcanism is restricted to the lower South-East of South Australia. The volcanoes comprise two distinct groups that constitute a western extension of the late Tertiary to Quaternary 'Newer Volcanics' of western Victoria (Figure 12) (Sheard, 1995).

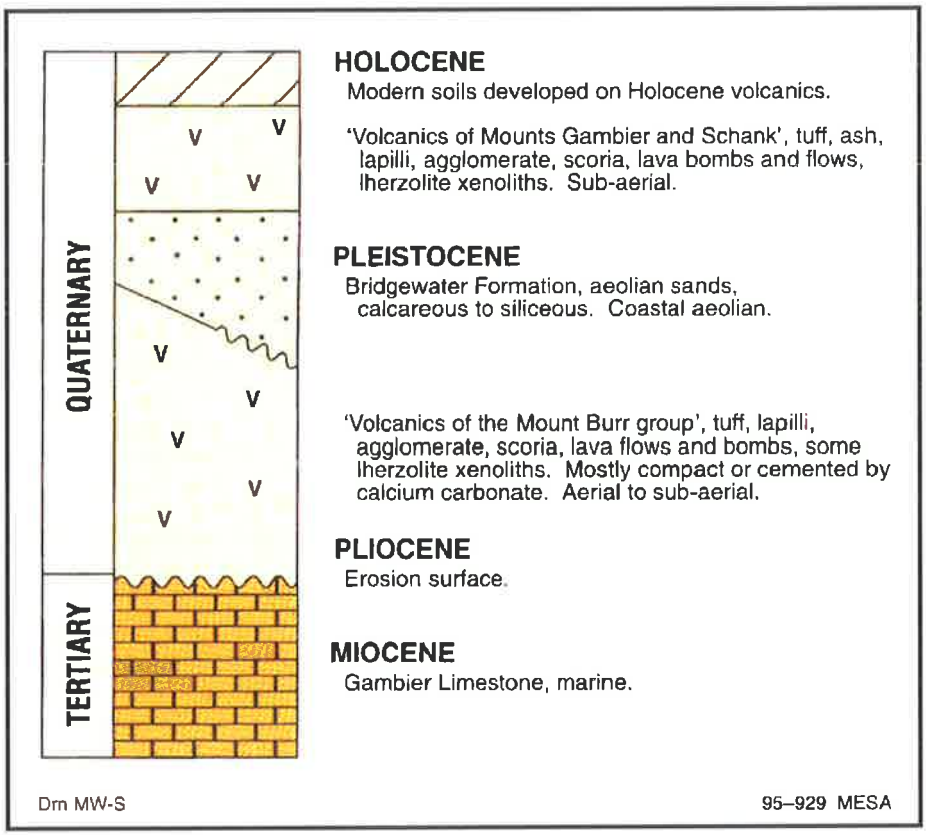

Figure 12. Stratigraphic relationships of Quaternary volcanics in southeast South Australia (Sheard, 1995).

The older Mt. Burr group includes 14 fissure-controlled centres with lava flows, composite domes to cones, and tuff rings or maars (Sheard, 1983). These volcanoes represent alkaline basaltic varieties. Some of the magmas carried mantle-derived xenoliths (usually lherzolite) expressed as green, granular textured inclusions within lava flows or as bombs, blocks and lapilli (20-500 mm diameter) within tephra piles (Sheard, 1995). These xenoliths have been recorded at Mounts Edward, Lyon and Watch (Sheard, 1995). They are considered to represent remnants from partial melting of upper mantle lithotypes. In addition, the tephra piles contain

abundant non-igneous country rock fragments, mostly Cretaceous and Tertiary sedimentary rocks through which the magma conduits passed (Sheard, 1995).

Most of the volcanoes in the Mount Burr group exhibit erosional modification by Pleistocene interglacial high sea levels and mantling to some degree by Bridgewater Formation calcarenites. Radiometric dating of the Mount Burr group has proved unsuccessful due to weathering, however, palynological work by Dodson (1974, 1977) and other geomorphic and stratigraphic evidence suggests volcanic activity from 1,000,000-20,000 years BP.

Southeast of Mount Burr lies the second, younger group of volcanoes consisting of Mount Schank and Mount Gambier. Because both members of this southern group overlie the Bridgewater Formation, they are stratigraphically younger than the Mount Burr group and are considered to be mid-Holocene (Figure 18) (Sheard, 1995). These two volcanoes are thought to have been produced by phreatomagmatic explosive interactions, rather than collapse structures analogous to calderas. Basaltic lithologies determined by Irving and Green (1976) is nepheline hawaiite for Mount Gambier and K-rich nepheline hawaiite or nepheline trachyandesite for Mount Schank. Both magmas have been derived by partial melting of basanite in either deep crustal or upper mantle environments (Sheard, 1995).

Radiocarbon dating by Blackburn et al. (1982) and palaeomagnetic data in Barbetti and Sheard (1981) indicates the Mount Gambier eruptions commenced ~5 000 to 4 300 years BP. Small low maars were quickly formed and lava flowed from a fissure and a vent (Leg of Mutton crater area). A scoria cone developed adjacent to and partly over the lava flow. A section through this cone is visible in the Brownes Lake western crater wall due to subsequent exhumation by volcanic explosions (Sheard, 1995).

Activity ceased for up to 300 years, which was then followed by a second stage of activity that was more dramatic and involved a much larger area (Sheard, 1995). Groundwater interaction with several ascending magma columns resulted in a series of phreatomagmatic explosion vents excavating maar craters (Sheard, 1995). Faulting in the Gambier Basin region controlled the spatial arrangement of these craters in a northwest trending alignment of nested maars (Figure 13). This second stage of volcanism had a moderately high explosive index and a tephra volume of ~1.3 km^3 was ejected (Sheard, 1995).

Mount Schank is located ~9 km south of Mount Gambier and is an order of magnitude smaller in volume than Mount Gambier (Figure 14) (Sheard, 1995). Joyce (1975, 1985) classified this volcano as a hybrid maar-cone structure, formed chiefly by phreatomagmatic explosions. Barbetti and Sheard (1981) demonstrated Mount Schank was not contemporaneous with Mount Gambier with palaeomagnetic data indicating an age of >7 000 to 1 000 years BP. TL dating by Smith and Prescott (1987) yielded an age of 4 930±540 years BP.

Eruptions at Mount Schank commenced from a 1.2 km long fissure in the Gambier Limestone (Sheard, 1995). Ascending magma and ash interacted with groundwater and major vent-clearing phreatomagmatic explosions resulted in a broad cone with both maar and cone crater characteristics (Sheard, 1995).

Figure 13. Southeasterly aerial view of Gambier volcanic complex, a series of fissure controlled nested maars (Sheard, 1995).

Figure 14. Westerly aerial view of Mount Schank, a hybrid maar-cone complex (Sheard, 1995).

Carbon Dioxide in the Gambier Sub-basin

Kalangadoo 1 and Caroline 1 both intersected CO_2 fluid at depths of 2.1 and 2.5 km respectively. Recent isotopic work by Chivas *et al.* (1987), Caffee *et al.* (1988) and Giggenbach *et al.* (1991) has verified a magmatic source for the CO_2. Their analyses of ^{13}C, $^{3}He/^{4}He$ ratios and the concentrations of trace noble gases ^{20}Ne, ^{22}Ne and excess ^{129}Xe from Caroline 1 collectively indicate a distinctly primitive mantle source rather than a crustal or organic source (Sheard, 1995).

Site 3 - Mt. Schank

Directions:

Mt. Schank is located near the Mt. Gambler-Pt. McDonnell road, approximately 9 km south of Mt. Gambier (Figures 15 & 16).

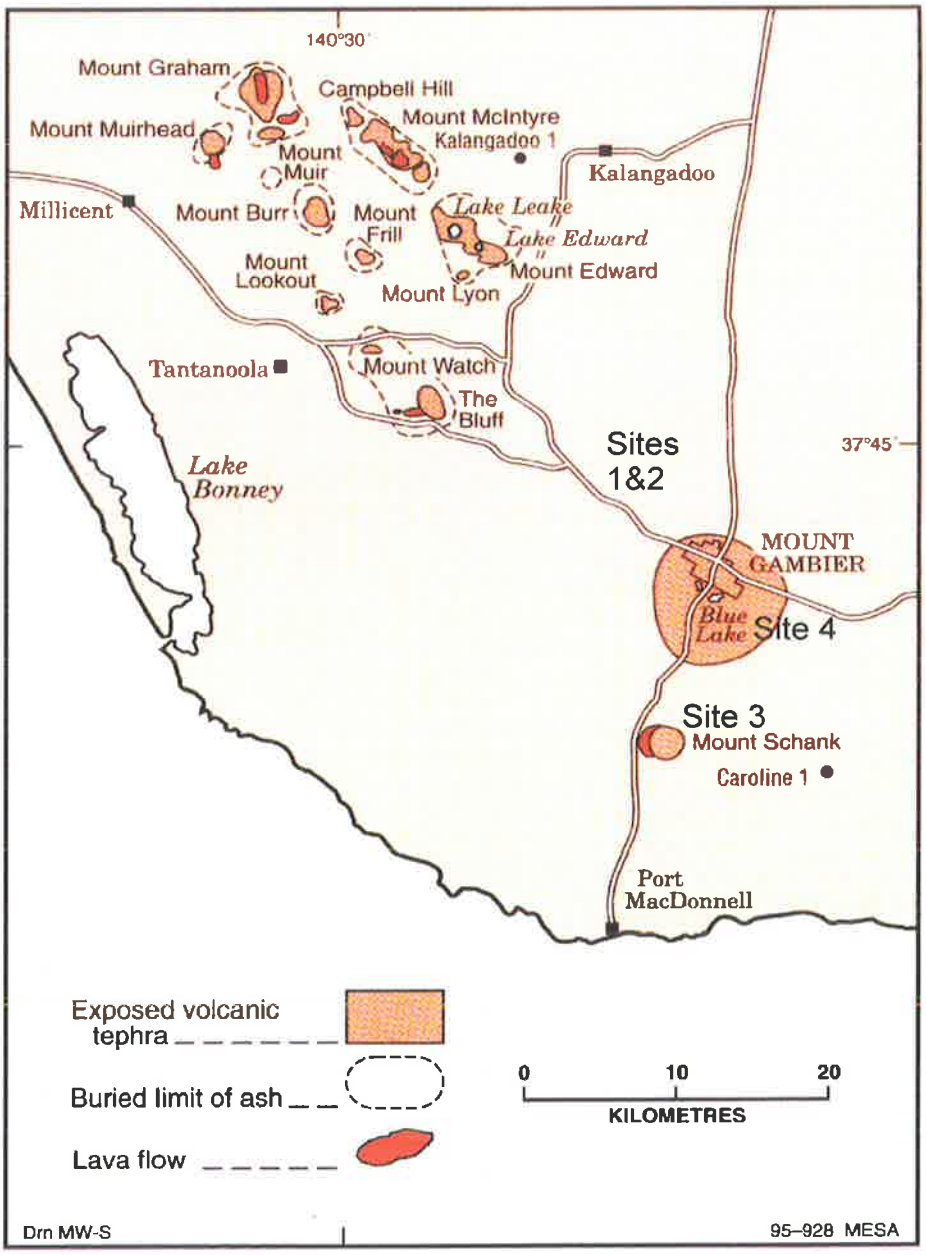

Figure 15. Mount Gambier and Mount Burr groups of volcanic eruption sites (Sheard, 1995).

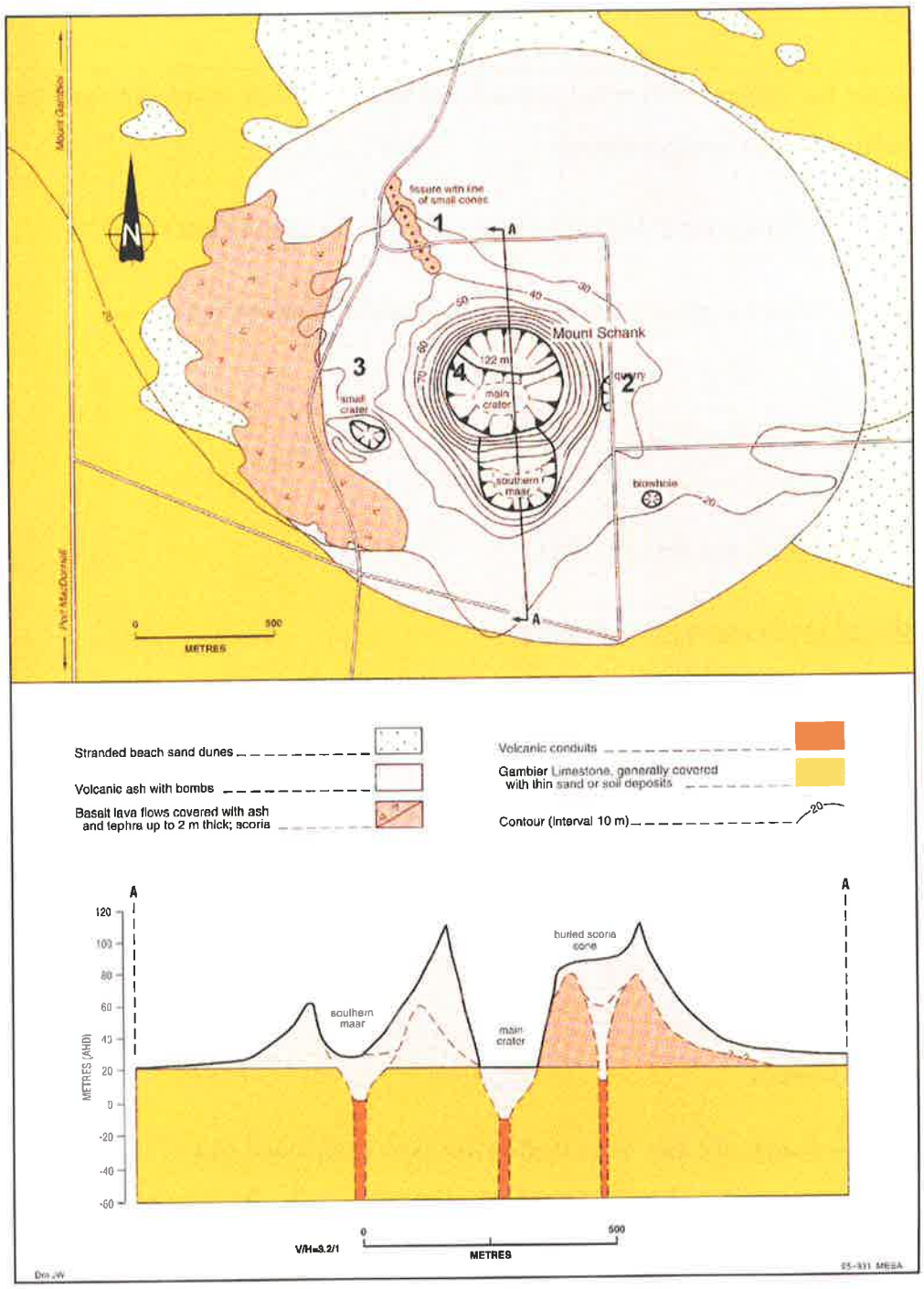

Figure 16. Mount Schank geological map and diagrammatic cross-section (Sheard, 1995). The top map shows the location of Site 3, outcrops 1-4.

Health and Safety:

Beware of falling rocks and do not stand under rock overhang.

Objectives:

- To consider the influence of these volcanoes on the generation, maturation and migration of hydrocarbons in the Gambier Basin.
- Would these volcanics have pushed source rocks into the mature gas zone?
- Would these volcanics act as a lateral or vertical seal to hydrocarbons.

Description:

(description after Smith and Sheard, 1985)

1/ Small line of scoria cones at Mt Schank:

The road cutting through the small cone allows us to see the red and black scoria. It has been quarried here for decorative stone used in gardens. Rare unoxidised samples are jet black and have glassy bubble linings, which often have iridescent colours. The cones represent gas removal (mainly steam) from the main lava mass as it was erupted. Numbering 8 in all, the line of small cones is best seen from the top of Mt. Schank (Figure 16).

2/ Eastern Ash Quarry:

Layering in the volcanic pile can be viewed in this now abandoned quarry. A large size range in ejected fragments is immediately apparent. Country rock fragments such as Gambier Limestone, flint, dolomite, dune sand and clay stones are not uncommon (Figure 16).

3/ Small subsidiary crater, western side of Mt. Schank:

To the southeast of the car park a small explosion crater exposes the various layers making up the Mt. Schank cone. The basal layer (white) is Gambier Limestone and a thin, buff coloured layer of dune sand rests on the limestone. Overlying the sand is a dark lava flow from the initial eruptive phase and on top of this, the tephra of the last active phase. This point is close to the

southern boundary of the lava field, hence its relatively thin exposure here. Much of the lava has been quarried for road aggregate (Figure 16).

4/ Top of Mt. Schank:

To the west, the extensive lava flow can be seen along with the line of scoria cones to the northwest, which are associated with the flow. Across the northern rim of the large crater, a lower less prominent rim appears. This marks the buried remains of an earlier cinder cone. As we walk anti-clockwise around the rim, the partially buried explosion crater on the southern side will come into view. This small maar indicates that groundwater had more influence on eruptive style at this end of the main fissure than elsewhere along its length.

To the southeast a small blowhole exists, marked by a Stobie pole on its northern rim. This vent represents steam emission somewhat away from the main vents. Mt. Schank does not contain a crater lake like Mt. Gambier because its crater floor is only just below ground level of the surrounding plain and above the groundwater table (Figure 16).

Site 4 - Mt. Gambier

Directions:

Mt. Gambier and Blue Lake are located in the town of Mt. Gambier accessed from Bay Road (Figure 17).

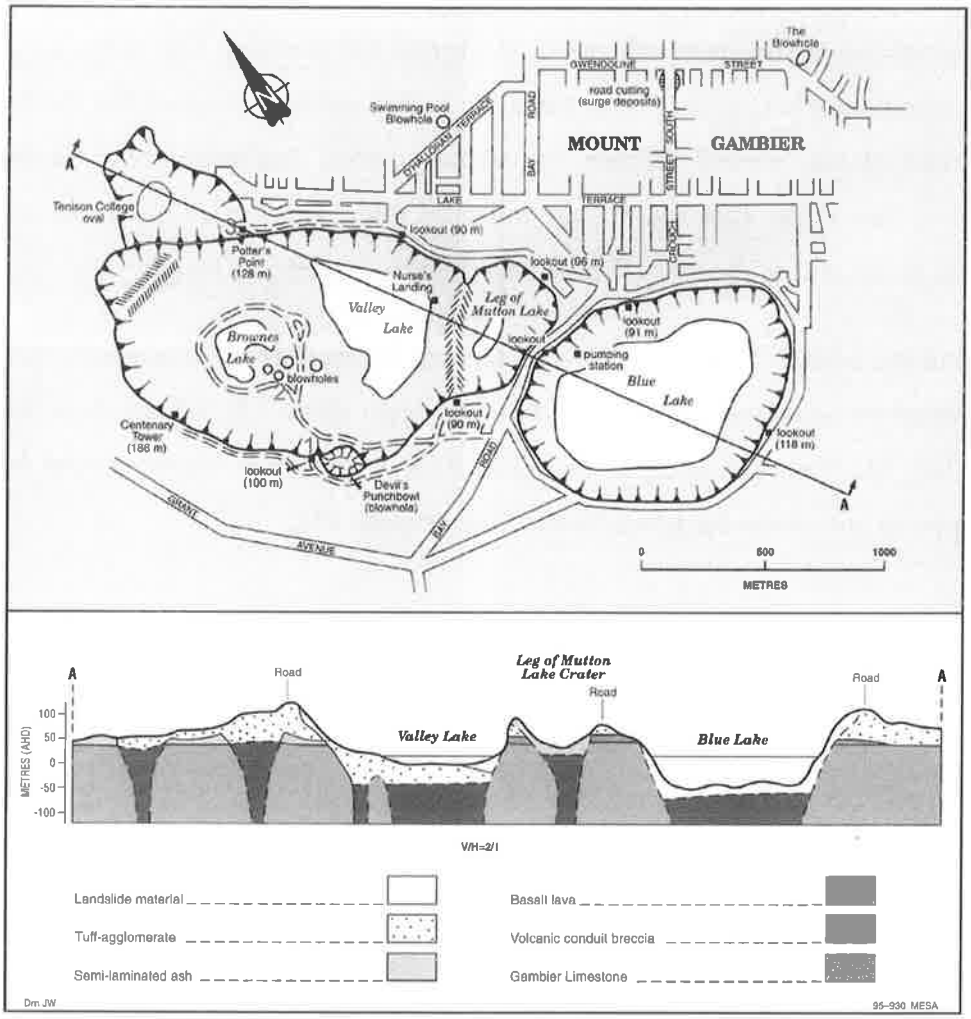

Figure 17. Mount Gambier craters and diagrammatic cross-section (Sheard, 1995, after Sheard, 1983). The top map shows the locations of outcrops 1-3.

Health and Safety:

Beware of falling rocks and do not stand under rock overhang. Take care when near cliff edges.

Objectives:

- To consider the influence of these volcanoes on the generation, maturation and migration of hydrocarbons in the Gambier Basin.
- Would these volcanics have pushed source rocks into the mature gas zone?
- Would these volcanics act as a lateral or vertical seal to hydrocarbons.

Description:

(description after Smith and Sheard, 1985)

1/ Marks Lookout:

Layering in the tuff-agglomerate exposed in the road cutting on the north side of the Devil's Punch Bowl can be closely observed at this location. The full range of volcanic and non-volcanic detritus can be seen and collected here. Olivine bombs (or lherzolite bombs) were once plentiful here, but after years of collection, they are now scarce (Figure 17).

2/ Brownes Lake South:

Lava spatter from the late stage lava fountain activity can be collected and viewed at this site. This type of lava chills rapidly on being thrown into the air, thus preserving forms resembling twisted rope and fresh cow dung! Composed almost entirely of glass, this lava has a metallic ring when struck. Many small spatter piles in this part of the crater give its floor a very irregular appearance (Figure 17).

3/ Potters Point Lookout:

From the lookout (Figure 17), looking east, the dark layer of lava can be seen at the eastern end of the Valley Lake in what is called the Razorback. This lava is part of the same flow exposed in the Blue Lake crater walls. Continuing around the crater wall to the SE, the Devil's Punch

Bowl (a blow hole) can be seen. Directly south of the lookout, the buttressed walls of the Tower ridge exhibit large-scale layering. Large blocks of Gambier Limestone are not uncommon in these layers. To the west, an exposure of the buried scoria cone at Bootlace Cave can be seen as a strange looking outcrop and cuspate break in the crater rim between the Tower ridge and the Sugar Loaf. The scoria, originally black bubbly lava, has been converted to a brick-red colour by steam associated with the eruption, passing up through the scoria pile. Behind the water storage tank from the lookout, to the west, the now partially buried early craters forma distant gully. The floor of one crater forms the Tenison College playing field. This type of volcano called a 'maar' has a naturally flat open crater floor, however, many intersect the water table and thus contain lakes.

DAY 3 PORT CAMPBELL TO APOLLO BAY

Site 5 – Loch Ard Gorge

Directions:

Stop at the sign posted car park on the Great Ocean Road east of Pt Campbell (Figure 18).

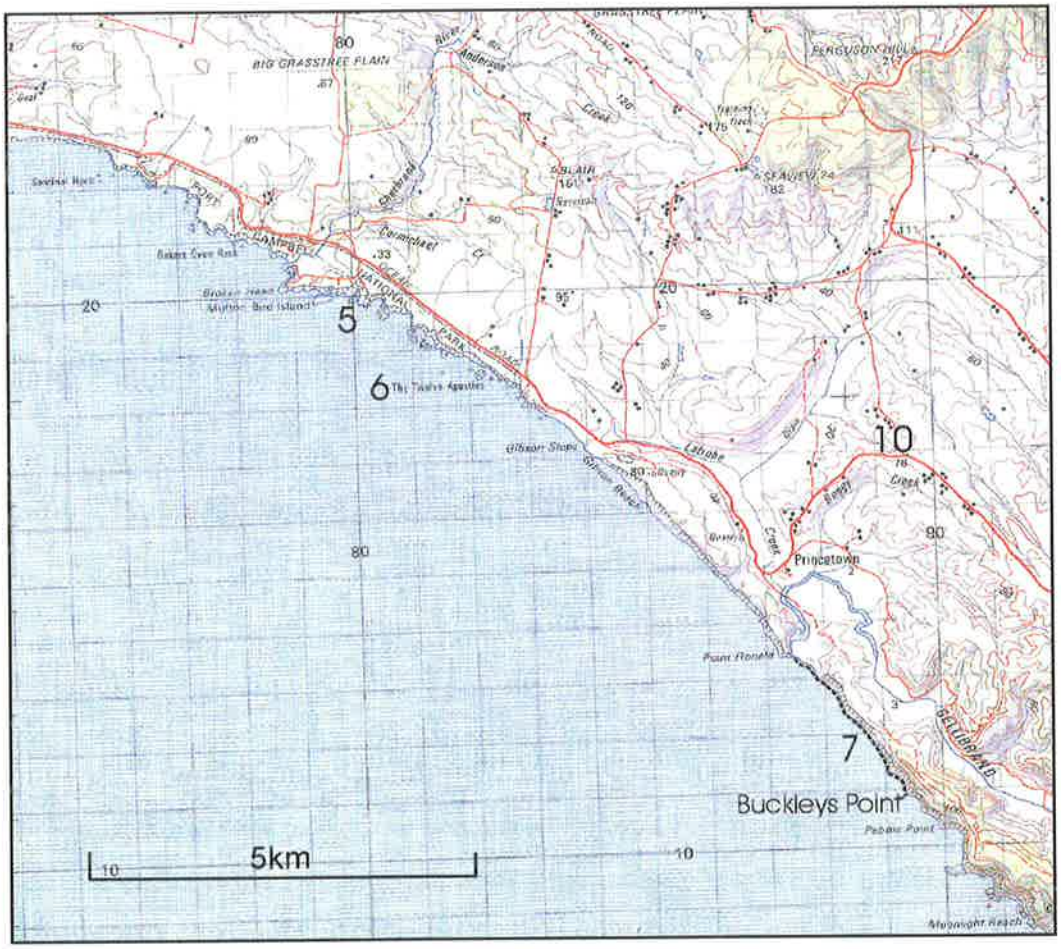

Figure 18. Topographic map of the Princetown area (1:100 000) showing locations of outcrops 5, 6, 7 and 10.

Health and Safety:

Beware of falling rocks and do not stand under rock overhang. Take care when walking near cliff edges and when using the steps that lead down to Carmichael Cave.

Objectives:

- To observe the nature of the contact between the Port Campbell Limestone and Gellibrand Marl in outcrop.
- To record the location of the outcrop by sketching and photography.
- To log a section through the Port Campbell Limestone and Gellibrand Marl.
- To record the composition of the carbonate and marl and reflect on the conditions that might have caused the composition to differ to that of the Gambier Limestone.
- To sample the Port Campbell Limestone for fossils and future isotopic and petrographic analysis.
- To run a natural gamma log down the cliff. At each sample point take three readings, each for 30 seconds, and then average the values.

Description:

This section of coastline consists of steep, often vertical or overhanging cliffs up to 70 m high. The coast is indented by narrow northeasterly trending, joint-controlled gorges and stacks within the Port Campbell Limestone (Edwards et al. 1996). The Haystack, Elephant Rock and The Razorback are stacks with straight, joint-controlled walls. The Island Archway and Mutton Bird Island are elongated stacks penetrated by wide arches. Loch Ard Gorge formed after the roof of a cave collapsed.

The Port Campbell Limestone is a prograding shelf succession deposited in inner neritic water depths of 30-50 m. At Loch Ard Gorge the carbonate succession is approximately 100 m thick and thickens further offshore. The contact between the limestone and the underlying Late Oligocene-Miocene Gellibrand Marl is diachronous. The Gellibrand Marl was deposited in an

outer neritic environment in water depths of more than 100 m. The carbonates rapidly prograded south on the passively subsiding continental margin, producing prograding, clinoformal seismic character. The Port Campbell Limestone dips very shallowly (~1/2°) at the coast and steepens progressively to the south (Arditto, 1999).

Site 6 – Twelve Apostles

Directions:

Stop at the sign posted car park on the Great Ocean Road (Figure 18).

Health and Safety:

Beware of falling rocks and do not stand under rock overhang. Take care when walking near cliff edges.

Objectives:

- To sketch and photograph the outcrop to record the limestone, marl and thrust faulting.
- To observe the thrust faulting that has affected the Port Campbell Limestone.

Description:

This location provides a scenic view along the spectacular coastline in the south east of the Pt Campbell Embayment of the Otway Basin. The Twelve Apostles are a group of tall stacks with joint-controlled walls. Along the coastline the stacks have temporarily protected some headlands, so that there are minor protrusions in their lee. It is possible that several of these protrusions were once linked to the adjacent stacks by arches that have since collapsed.

The Port Campbell Limestone is stratified and coarse grained, suggesting a high-energy depositional environment. The Gellibrand Marl was deposited in deeper, quieter waters and was subjected to bioturbation. The Gellibrand Marl and Port Campbell Limestone dip gently west towards the centre of the embayment. The paler limestone forms the upper portion of the cliffs above the grey coloured marl (Arditto, 1999).

Small north to northwest trending thrusts, usually with only a few centimeters of displacement, cut the limestone and marl and provide evidence of the young tectonic activity in the area. The faulting may have propagated from compression in the Otway Group (Arditto, 1999).

Site 7 – Buckley's Point

Description after Arditto (1999)

Directions:

Turn south off the Great Ocean Road 17.6 km east of Port Campbell just before the Gellibrand River Bridge. Veer left down the gravel road, over the small bridge and 1.4 km to a small roundabout. Take the small foot-track to the mouth of the river. This section starts at the Gellibrand River mouth and entails a 6 km walk. This stop is not tide dependent, but is easier if done at low tide (Figure 18).

Health and Safety:

Beware of falling rocks and do not stand under rock overhang. Take care when walking near cliff edges and do not stand on wave washed platforms on the beach.

Objectives:

- To observe and record the nature of the major surfaces present within the Wangerrip Group.
- To record the location of the outcrops by sketching and photography.
- To examine and log the type section outcrop of the Wangerrip Group.

Description:

The cliffs that form Point Ronald, at the mouth of the Gellibrand River, consist of cemented Pleistocene sand dunes. The rock is composed of sand-sized fragments of calcareous marine organisms such as bryozoans, echinoids and molluscs with lesser amounts of quartz. Note the large-scale dune cross-bedding and the dominantly landward dip of the foreset beds. These deposits were formed as sea levels fell during the ice ages, exposing calcareous sediment on the continental shelf. The sediment was reworked into extensive dunefields, remnants of that are preserved today.

Paleocene and Eocene sediments of the Wangerrip Group are exposed along the coast southeast of the mouth of the Gellibrand River where they rest unconformably on lower Cretaceous

Otway Group sediments. The Otway Group comprises grey-green, fine-medium grained, trough cross-bedded, channel sandstones separated by prominent scour surfaces.

The Pebble Point Formation, at the base of the Wangerrip Group, comprises a series of stacked, upward fining, highly burrowed channel sandstones and minor burrowed mudstones (late LST-early TST). Deposition involved episodes of channeling and channel abandonment followed by biological reworking (inner estuary LST wedge / early TST). Branching dwelling burrows (*Thalassinoides*) are prominent in the sandstone packages. Shelly fauna are rare within the lower half of the Pebble Point Formation at this locality. The upper half, however, contains sparse to common shelly material, associated with thin calcite-cemented glauconitic sandstones. This may represent a change from estuarine conditions to more open marine conditions within the late TST prior to the development of the overlying Pember Mudstone. The contact with the overlying Pember Mudstone is relatively abrupt. The Pember Mudstone is light to medium grey when weathered, heavily bioturbated and largely unstratified. It contains *Chondrites* burrows (distal bay fill to offshore marine TST and early HST). The remaining Pember Mudstone northwest of Buckley's Point is largely covered by vegetation or beach sands and is generally poorly exposed.

The next small beach exposure is within the Dilwyn Formation and contains a succession of medium to coarse grained and sparsely glauconitic muddy sandstone, with common burrows, interpreted as stacked estuarine channel fill units. The base of these units is interpreted to represent a sequence boundary. The uppermost part of this member is exposed in the next small headland where the "Trochocyathus" carbonate-cemented and moderately glauconitic sandstone (greensand) horizon is exposed (Baker, 1950). Besides the solitary corals, commonly in growth positions, this unit also contains sporadic shark's teeth and represents starved sedimentation within the Dilwyn Formation (a condensed interval). The overlying section is made up of the Princetown Member, comprising a series of clean and very fine grained aggradational sand packages, with sparse low angle trough cross bedding and rare dwelling burrows (barrier bar units of the HST?) which pass into an interbedded sand and carbonaceous clay succession (coastal plain back barrier lagoonal HST).

The sediments exposed along this coastal section dip gently northwest towards the Port Campbell Embayment.

DAY 4 –APOLLO BAY - BROWN CREEK & CASTLE COVE

Site 8 – Brown Creek

Description after Arditto (1999)

Direction:

Turn off the Great Ocean Road at Evans Track (35.4 km from Apollo Bay Post Office) and continue for 1.4 km to a gate at a three-way intersection. Beyond the gate the track is narrow and overhanging bushes may scratch cars, so you may wish to walk from here. Follow the track for 1.1 km until the track starts to follow a fence. Park at the locked gate on the left and climb over the gate and head towards the cliffs. There is no easy way down to the beach but the best route is towards the left near Brown Creek. An alternative route is to drive to the Johanna Beach car park via the Red Johanna Road and then walk along the beach for 3.5 km to Rotten Point. This involves crossing the Johanna River at its mouth (Figure 19).

Health and Safety:

Beware of falling rocks and do not stand under rock overhang. Take care when walking near cliff edges and do not stand on wave washed platforms on the beach.

Objectives:

- To observe and record the nature of the major surfaces present within the section.
- To record the location of the outcrops by sketching and photography.
- To examine and log the outcrop section.
- To sketch a structural cross-section of the outcrop in relation to the Johanna Syncline.

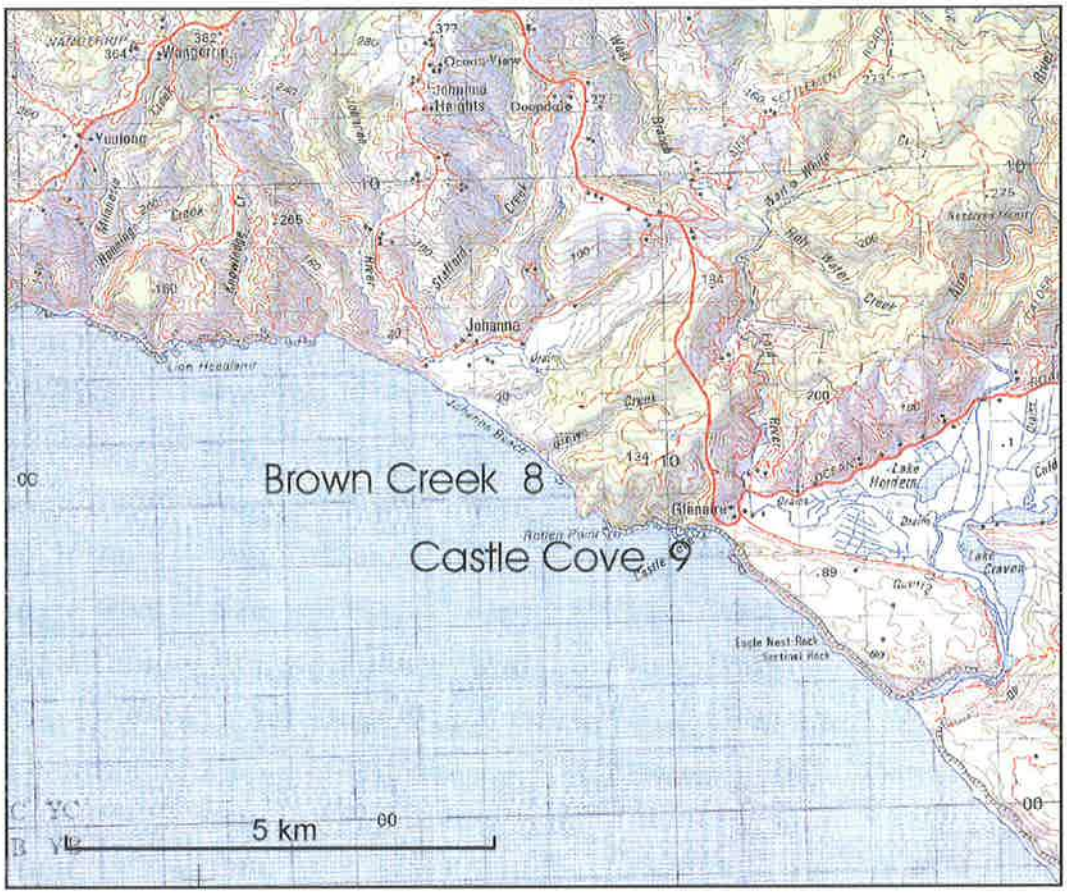

Figure 19. Topographic map of the Princetown area (1:100 000) showing locations of outcrops 8 and 9.

Description:

The Brown Creek section has been a standard section for the Late Eocene since Eocene planktonic foraminifera were identified here in the 1940's. The section is one of the few Eocene sections exposed in Victoria, which contain calcareous nanoplankton, planktonic foraminifera and palynomorphs (Shafik, 1983; Waghorn, 1989). Details of the measured section can be found in Shafik (1983) (in Arditto, 1999). The rocks exposed in the Brown Creek area lie on the eastern limb of the late Tertiary Johanna Syncline and dip gently northwest. A more general section from Johanna River to Rotten Point as well as a more detailed columnar measured section from Tickell et al. (1992).

The Johanna River Sands are exposed at the base of the section and comprise apparently unfossiliferous medium to course sands. The overlying Brown Creek Clays comprise a basal,

dark grey "Turritella" clay, which is silty with quartz sand near the base and glauconitic towards the top (TST). This is overlain by a 2 m "Notostrea" greensand (condensed interval), which is in turn overlain by about 18 m of biogenic marl (early HST) referred to as the Narrawaturk Formation. The uppermost part of the exposed section comprises about 10 m of silty biogenic clay. A short distance along the coast to the west are well-bedded calcarenites, equivalent in age to the Castle Cove Limestone. In nearby offshore seismic data the greensand is represented by a seismic downlap surface (Arditto, 1995) (Figure 19, Arditto, 1999).

Site 9 – Castle Cove

Direction:

Proceed to the car park at Castle Cove off the Great Ocean Road.

Health and Safety:

Beware of falling rocks and do not stand under rock overhang. Take care when walking near cliff edges and do not stand on wave washed platforms on the beach.

Objectives:

- To observe the contacts between all sediment packages and record the composition of each package.
- To sketch a measured section of the outcrop at Castle Cove.
- To sketch a structural cross-section of the outcrop at Castle Cove, observing the faulted anticline.

Description:

Description after Arditto (1999)

The Castle Cove-Aire River area (Figure 19) contains a thin but one of the more complete Tertiary sections in the Otway Basin. The Tertiary formations, which rest unconformably on the Otway Group, in ascending order are: Johanna River Sands (=Dilwyn formation); Brown Creek Clays (=Mepunga Formation); Castle Cove Limestone and Lower Glen Aire Clays (=Narrawaturk Formation); Calder River Limestone (=Clifton Formation); and Upper Glen Aire Clays (=Gellibrand Marl). Note that the Paleocene – early Eocene Pebble Point Formation and Pember Mudstone are absent from this location.

The contact between the Johanna River Sands and the Brown Creek Clays is not exposed. The Brown Creek Clays comprise dark grey sandy clays, glauconitic clays and sands with a general increase in bryozoan grainstone units towards the top. The Castle Cove Limestone comprises predominantly grainstone units with trough and HCS horizons. The overlying section comprises dark grey to grey, burrowed and bioturbated fossiliferous clays with thin bryozoan skeletal grainstones of the Lower Glen Aire Clays. These are capped by the thin Calder River Limestone, which comprises hard, skeletal grainstone with quartz grains. Dark, calcareous clay (Upper Glen Aire Clays = Fishing Point Marls) overlies the limestone.

Castle Cove also provides excellent exposures of early Cretaceous Otway Group continental deposits. The bulk of the outcrop section comprises stacked, low sinuosity fluvial sandstone channel units, with minor overbank sediments preserved. Coaly material in the sandstone has an Rv value of 0.5-0.59% and is dominated by vitrinite (60%0 but contains a relatively high exinite component (25%).

Castle Cove lies on the steep, eastern limb of the anticline that separates the Tertiary inliers of the Johanna and Glenaire Synclines and the local structure is most likely associated with reverse faulting. Small normal faults within the Otway Group are truncated at the base Tertiary unconformity and have been rotated during folding.

DAY 5 – RETURN TO ADELAIDE VIA THE GLENELG RIVER AREA

Site 10 – Road Cutting

Description after Arditto (1999)

Direction:

This site is exposed in a road cutting on the Great Ocean Road, 6.4 km ESE of Princetown (125 m west of Boulevard Road intersection) (Figure 18).

Health and Safety:

Beware of falling rocks. Examination of this outcrop requires crossing of the Great Ocean Road. Be cautious, this can be a very busy road and vehicles travel at high speeds. Be aware that conversations and wind may obscure the sound of approaching vehicles. Drivers will not expect pedestrians near the road.

Objectives:

- To observe fair weather and storm beds and associated sedimentary structures.
- To record the location of the outcrops by sketching and photography.
- To log a section through the outcrop.

Description:

The Dilwyn Formation is exposed in this shallow and relatively fresh road cutting. Here thin, bioturbated (Chondrites), mudstone intervals alternate with HCS sandy siltstone intervals. These are interpreted as alternating fair weather and storm cycle sedimentation within a lower shoreface or storm wave-influenced distal delta front setting. This lithofacies association contrasts with the monotonous light grey bioturbated mudstone lithofacies seen at Buckley's Point that is interpreted as predominantly suspension sediments in an outer bay or offshore

setting. This cutting exposure is 5.3 km NE of the Buckley's Point coastal outcrop and appears to be stratigraphically higher than the Dilwyn Formation exposed at Buckley's Point.

A number of upward coarsening cycles (parasequences) are represented here from offshore to lower shoreface. The HCS lamina geometries indicate both oscillatory flow and combined flow (with unidirectional downlaps indicating palaeoslope dip direction).

Site 11 – Crawford River Valley

Directions:

This site is located on a road that runs off the Princess Highway (Figure 20).

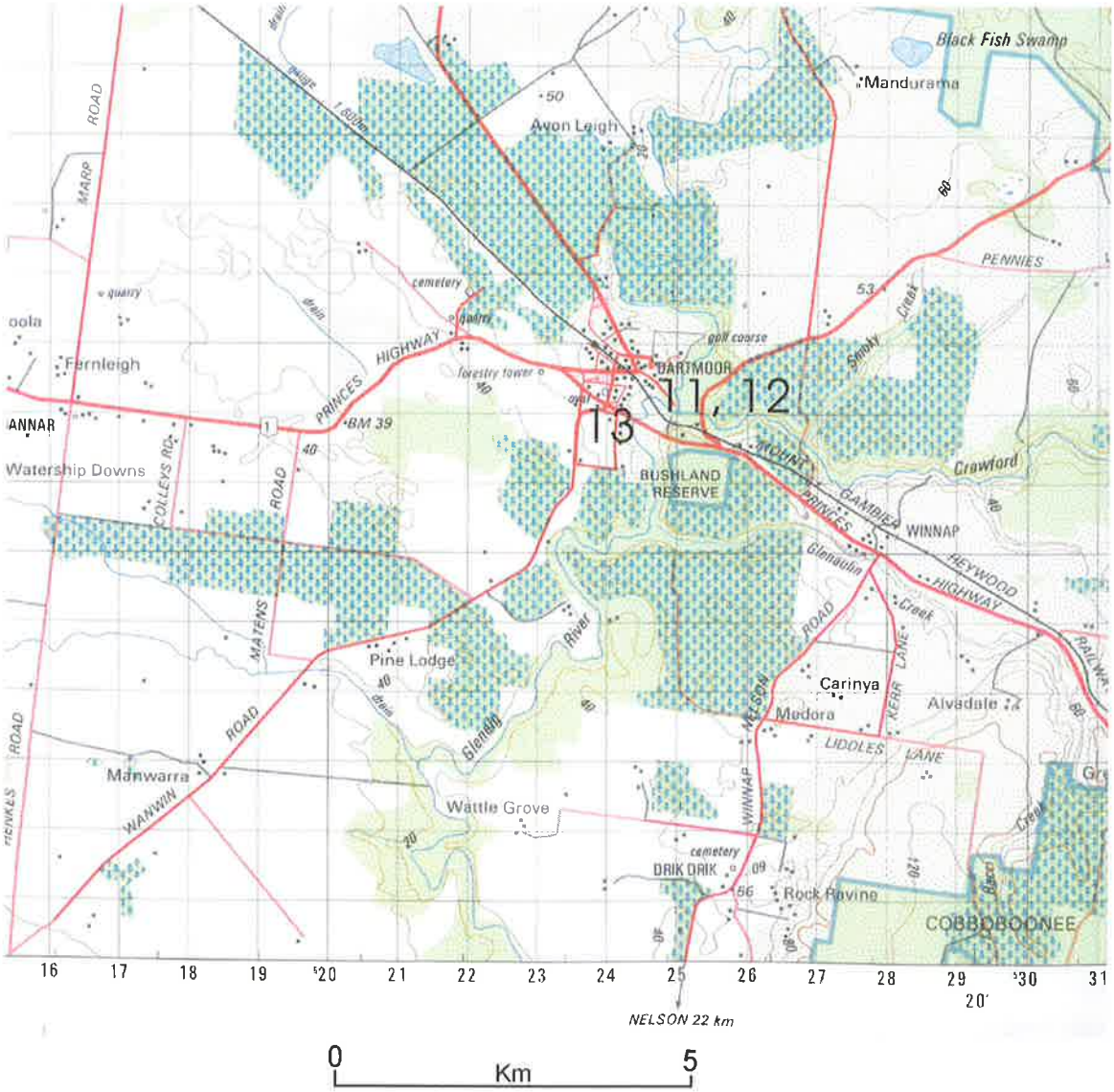

Figure 20. Locations of outcrops 11, 12 and 13 near Dartmoor, Victoria.

Health and Safety:

Beware of falling rocks and do not stand under rock overhang.

Objectives:

- To determine the nature of the boundary between the marls and nodular limestone, and the origin of the "erosional hollows" (could they be submarine canyons or channels?).
- To record the location of the outcrops by sketching and photography.
- To observe and log the Narrawaturk Marl in outcrop.

Description:

Description after Blake and Thompson (1985)

In the southern landslip, the Glenaulin Clay (Narrawaturk Marl) rests with angular discordance of up to 10 degrees on the eroded surface of laminated siltstones of the Dartmoor Formation (Dilwyn Formation). The sequence generally begins with a bed of fairly soft light-grey marly limestone up to 1.10m thick, the basal part of which contains sub-rounded limonite pellets and nodules, and rounded pebbles of quartz and quartzite. Laterally this bed grades to calcareous sand and minor grit or gravel. It is overlain by a deeply weathered, fairly homogeneous sequence of white to yellowish-grey polyzoal clays and marly clays which are characterised by abundant white secondary carbonate concretions throughout the exposed section. A second bed of soft polyzoal marly limestone 1.35m thick, containing brachiopods, echinoid spines and pectinids occurs about 3m from the base.

The top and bottom of the Narrawaturk Marl outcrop is exposed in adjacent landslips, but because of intervening faulting and soil cover, the middle part of the section is not. The member is estimated to be approximately 50m thick.

The basal nodular marly limestone contains a rich but poorly preserved microfauna containing a number of distinctive large fossil species. Fossils present are gastropods, brachiopods, regular and irregular echinoids, polyzoa and the nautiloids *Aturia sp.* This fauna is indicative of shallow, open marine conditions and warm waters. The overlying clays contain abundant foraminifera and occasional thin-shelled pectinids and regular echinoids suggesting an upward transition to deeper, open marine conditions.

In the east landslip the Narrawaturk Marl is overlain by a limestone package. This contact is an angular unconformity with a dip of 2.5-10 degrees. Overlying the limestone package is a distinctive nodular limestone. Thin marls immediately overly the nodular limestone. These marls occur in an "erosional hollow at the top of the Narrawaturk Marl and ranges in thickness from 0-8m over a distance of about 120m".

Site 12 – Crawford River Bridge

Directions:

This site is located in a road cutting on the Princess Highway, west of Dartmoor (Figure 20).

Health and Safety:

Beware of falling rocks and do not stand under rock overhang. Examination of this outcrop requires crossing of the highway. Be cautious, this can be a very busy road and vehicles travel at high speeds. Be aware that conversations and wind may obscure the sound of approaching vehicles. Drivers will not expect pedestrians near the road.

Objectives:

- To observe the nature of the contact between sediments of the Dilwyn Formation and the overlying limestones.
- To record the location of the outcrops by sketching and photography.
- To observe and record the nature of the major surfaces present within the outcrop.

Description:

(description after Blake and Thompson, 1985)

This site shows the typical clean quartz sandstones, which have excellent porosity and permeability in groundwater bores intersecting the Dilwyn Formation in the area.

Overlying the Dilwyn Formation at this site are weathered limestones and marls of the Heytsbury Group, which are in turn overlain by calcarenites of the Pliocene Whalers Bluff Formation.

Site 13 – Whalers Bluff Formation, Glenelg River Valley, Dartmoor

Directions:

This site is located on the Glenelg River where the Princess Highway crosses, near Dartmoor, Victoria (Figure 20).

Health and Safety:

Beware of falling rocks and do not stand under rock overhang. Examination of this outcrop requires crossing of the highway. Be cautious, this can be a very busy road and vehicles travel at high speeds. Be aware that conversations and wind may obscure the sound of approaching vehicles. Drivers will not expect pedestrians near the road.

Objectives:

- To examine and log the Pleistocene section.
- To record the location of the outcrops by sketching and photography.
- To observe and record the nature of the major surfaces present.

Description:

The Whalers Bluff Formation of Plio-Pleistocene age blankets most of the older formations in southwestern Victoria.

A Late Pliocene transgression flooded the karst surface developed on Miocene limestones in the Portland to Glenelg River area. The Whalers Bluff Formation consists predominantly of up to 30 m of calcarenites, resting on fossiliferous clay and limestone.

The Whalers Bluff deposition was initiated over a continental surface, which sank with great speed. The fauna indicates repeated, but slight, movements of the ocean bottom, bringing about small but rapid and recurring changes in bathymetry and geographic environment, such as open sea or closed lagoonal conditions.

Whaler's Bluff deposition began with the invasion of the karst limestone topography by dark, fossiliferous clays and marls. These deposits filled solution channels, caves and every joint open to the surface. Following the smothering of the karst surface by marls deposition of calcarenites and calcareous silts with oyster and shell beds began.

Pleistocene calcareous dune sands of the Bridgewater Formation overlie the calcarenites. This marks the gradual retreat of the sea from the coastal plain and infilling of shallow lagoons by drifting sands.

7. GLOSSARY OF VOLCANIC TERMS[δ]

alkaline basalt [Replacement for *alkali basalt*] Critically silica-undersaturated basalt, containing normative nepheline, diopside and olivine.

basanite (a) A touchstone consisting of flinty jasper or finely crystalline quartzite. (b) A black variety of jasper.

caldera A large, basin-shaped volcanic depression, more or less circular in form, the diameter of which is many times greater than that of the included vent or vents, no matter what the steepness of the walls or form of the floor.

cone [volc] A volcanic cone. A conical hill of lava and/or pyroclastics that is built up around a volcanic vent.

dome [volc] A steep sided, rounded extrusion of highly viscous lava squeezed out from a volcano, and forming a dome-shaped or bulbous mass of congealed lava above and around the volcanic vent. The structure generally develops inside a volcanic crater or on the flank of a large volcano, and is usually much fissured and brecciated.

hawaiite [mineral] A pale green, iron-poor gem variety of olivine from the lavas of Hawaii.

jasper A variety of chert associated with iron ores and containing iron-oxide impurities that give it various colours, characteristically red, although yellow, green, greyish blue, brown and black cherts have also been called jasper.

lapilli Pyroclastics that may be either essential, accessory, or accidental in origin, of a size range that has been variously defined within the limits of 2 and 64mm. The fragments may be either solidified or still viscous when they land, thus there is no characteristic shape. An individual fragment is called a lapillus.

[δ] All terms in the glossary are from Bates, R.L. and Jackson, J.A. (1987) *Glossary of Geology*. 3rd Edition. American Geological Institute. McGraw-Hill.

lherzolite (a) A plutonic rock with 40-90% olivine, and > 5% orthopyroxene and clinopyroxene. (b) Peridotite composed chiefly of olivine, ortho-, and clinopyroxene, in which olivine is the most abundant.

maar A low relief, broad volcanic crater formed by multiple shallow explosive eruptions. It is surrounded by a crater ring and may be filled with water.

nepheline A hexagonal mineral of the feldspathoid group. It occurs as glassy crystals or colourless grains, or as coarse crystals or green to brown masses of greasy lusture without cleavage, in alkalic igneous rocks. It is an essential constituent of some sodium-rich rocks.

phreatomagmatic explosion A volcanic explosion that extrudes both magmatic gases and steam; it is caused by the contact of magma with groundwater or shallow surface water.

tephra A general term for all pyroclastics of a volcano.

trachyandesite An extrusive rock, intermediate in composition between trachyte and andesite, with sodic plagioclase, alkali feldspar and one or more mafic minerals (biotite, amphibole or pyroxene).

tuff A general term for all consolidated pyroclastic rocks.

xenolith A foreign inclusion in an igneous rock.

8. REFERENCES

Alley, N. F. and Lindsay, J.M. (1995). Chapter 10: The Tertiary. *In:* Drexel, J.F. and Preiss, W.V. (**Eds**). *The Phanerozoic. Bulletin 54*: MESA and GSSA, pp 151-157.

Arditto, P.A. (1999) Sequence stratigraphic workshop on the Paleocene-Eocene Wangerrip Group, Eastern Otway Basin, Victoria. *Field Tutorial Guide*.

Arditto, P.A. (1995) The Eastern Otway Basin Wangerrip Group revisited using an integrated sequence stratigraphic methodology. *APEA Journal*, **1995**, pp 372-384.

Baker, G. (1950) Geology and physiography of the Moonlight Head District, Victoria. *Proc. Roy. Soc. Vict.*, **60**, pp 17-44.

Barbetti, M. and Sheard, M.J. (1981). Palaeomagnetic measurements from Mounts Gambier and Schank, South Australia. *Journal of Geological Society of Australia*, **28(4)**, pp 385-394.

Blackburn, G., Allison, G.B. and Leaney, F.W.J. (1982) Further evidence of the age of tuff at Mount Gambier, South Australia. *Royal Society of South Australia, Transactions*, **106**, pp 163-167; erratum, 1984, *ibid*, 108:130.

Blake, R., Thompson, B.R. (1985) Otway 85 Field Excursion Guides. *In* Otway 85 – Earth Resources of the Otway Basin. *Geological Society of Australia*, pp 91-103.

Bourman, R.P. (1987) A review of controversial issues related to the late Paleozoic glaciation of southern South Australia. *In*: Gairdner, V. (**Ed**). *International Geomorphology, 1986. Part II.* John Wiley and Sons Ltd., pp 725-742.

Caffee, M.W., Hudson, G.B., Velsko, C., Alexander, E.C., Huss, G.R. and Chivas, A.R. (1988). Non-atmospheric noble gases from CO_2 well gases. *In: 19th Lunar and Planetary Science Conference, Huston, 1988. Papers* **1**, pp 154-155.

Cande, S.C. and Mutter, J.C. (1982) A revised identification of the oldest seafloor spreading anomalies between Australia and Antarctica. *Earth and Planetary Science Letters*, **58**, pp 151-160.

Chivas, A.R., Barnes, I., Evans, W.C., Lupton, J.E. and Stone, J.O. (1987). Liquid carbon dioxide of magmatic origin and its role in volcanic eruptions. *Nature*, **326**, pp 587-589.

Christ, R. P. A. (1984). The tectonic development of Bass Strait. Proceedings of the Second Australian Petroleum Geophysics Symposium, Melbourne, *Australian Society of Geophysicists.*

Deighton, I., Falvey, D.A. and Taylor, D.J. (1976). Depositional Environments and Geotectonic Framework: Southern Australia Continental Margin. *APEA Journal*, pp 25-36.

Dodson, J.R. (1974) Vegetation history and water fluctuations at Lake Leake, southeastern South Australia. I. 10 000 B.P. to present. *Australian Journal of Botany*, **22**, pp 719-741.

Dodson, J.R. (1977) Late Quaternary palaeoecology of Wyrie Swamp, southeastern South Australia. *Quaternary Research*, **8**, pp 97-114.

Edwards, J., Leonard, J.G., Pettifer, G.R. and McDonald, P.A. (1996) Colac – 1:250 000 map geological report. *Geological Survey of Victoria.* Geological Survey Report **98**.

Finlayson, D. M., Collins, C.D.N., Lukaszyk, I., Chudyk, E.C. (1998). A transect across Australia's southern margin in the Otway Basin region: crustal architecture and the nature of rifting from wide-angle seismic profiling. Tectonophysics **288**, pp 177-189.

Flottmann, T. and Cockshell, C.D. (!995) Paleozoic basins of southern South Australia: new insights to their structural history from regional seismic data. *Australian Journal of Earth Sciences.*

Galloway, W. E. (1968). Depositional systems of the Lower Wilcox Group, North Central Gulf Coast Basin. Trans. Gulf Coast Ass. geol. Socs, **18**, pp 275-289.

Giggenbach, W.F., Sano, Y. and Schmincke, H.U. (1991). CO_2-rich gases from Lakes Nyos and Monoun, Cameroon; Laacher See, Germany; Dieng, Indonesia, and Mt. Gambier, Australia – variations on a common theme. *Journal of Volcanology and Geothermal Research*, **45**, pp 311-323.

Holdgate, G. R. (1981). Stratigraphy, sedimentology and hydrocarbon prospects of the Dilwyn Formation in the central Otway Basin of southeastern Australia. *Proceedings of the Royal Society of Victoria* **93(1-2)**, pp 129-148.

Irving, A.J. and Green, D.H. (1976) Geochemistry and petrogenesis of the Newer Basalts of Victoria and South Australia. *Journal of Geological Society of Australia*, **23**, pp 45-66.

James, N. P., Bone, Y. and Kyser, T.K. (1993). Shallow burial dolomitisation and de-dolomitisation of mid-Cenozoic, cool-water, calcitic, deep-shelf limestones, Southern Australia. *Journal of Sedimentary Petrology*, **63(3)**, pp 528-538.

Joyce, E.B. (1975). Quaternary volcanism and tectonics in southeastern Australia. *In*: Suggate, R.P. and Cresswell, M.M. (**Eds**), *Quaternary Studies*. Royal Society of New Zealand, Wellington, pp 169-176.

Joyce, E.B. (1985). A type of volcano intermediate between the scoria cone and maar of an areal basaltic province. *In:* Otway 85 – Earth Resources of the Otway Basin Conference, Mount Gambier, 1985. Summary papers and excursion guides. *Geological Society of Australia*, pp 55-57.

Kenley, P.R. (1951) Marine Eocene sediments near Casterton, Victoria. Australian Journal of Science, **14**, pp 91-92.

Kopsen, E. and Scholefield, T. (1990). Prospectivity of the Otway Supergroup in the Central and Western Otway Basin. *APEA*, pp 263-278.

Laing, S., Dee, C.N., Best, P.W. (1989). The Otway Basin. APEA Journal, **29**, pp 417-429.

Li, Q., McGowran, B. and White, M.R. (in prep.) Sequences and biofacies packages in the mid-Cainozoic Gambier Limestone, South Australia: reappraisal of foraminiferal evidence.

Lindsay, J. M. (1967). E & WS Department Millicent bores 2 and 5, micropalaeontological examination of Gambier Limestone sections. Adelaide, *South Australia Department Mines*.

Lindsay, J. M. (1985). Aspects of South Australian Tertiary foraminiferal biostratigraphy, with emphasis on studies of *Massilina* and *Subbotina. In*: J. M. Lindsay (**Ed**) *Stratigraphy, palaeontology, malacology: papers in honour of Dr Nell Ludbrook*. Adelaide, South Australia Department of Mines and Energy, Special Publication. **5,** pp 187-232.

Lowry, D. C. (1987). A new play in the Gippsland Basin. *APEA Journal,* **27(1),** pp 164-172.

Ludbrook, N. H. (1962). Mount Salt structure drilling project of Oil Development NL. Adelaide, *South Australia Department of Mines.*

Ludbrook, N. H. (1971). Stratigraphy and correlation of marine sediments in the western part of the Gambier Embayment. *In*: H. Wopfner, and Douglas, J.G. (**Eds**). *The Otway Basin of southeastern Australia.* South Australia and Victoria Geological Survey, Special Bulletin, pp 47-66.

Marker, M.E. (1975) The lower Southeast of South Australia: a karst province. University of Witwatersrand. Department of Geography and Environmental Studies. Occasional Paper, **13**.

McGowran, B. (1973) Observation Bore 2, Gambier Embayment of the Otway Basin: Tertiary Micropalaeontology and stratigraphy. *Mineral Resources Review, South Australia*, **135**, pp 43-55.

McGowran, B., Li, Q. and Moss, G. (1997) The Cenozoic Neritic Record in Southern Australia: the biogeohistorical framework. *In*: James, N.P. and Clarke, J.A. (Eds) Cool-Water Carbonates. *SEPM Special Publication* **56**, pp 185-203.

Mehin, K., Link, A.G. (1994). Source, migration and entrapment of hydrocarbons and carbon dioxide in the Otway Basin, Victoria. *APEA Journal*, pp 439-459.

Meyer, G.M. (1982) Geology of the Kingston lignite deposit. *In*: Mallett, C.W. (**Ed**). Coal Resources – origin, exploration and utilisation in Australia. *Geological Society of Australia. Coal Group Symposium, Melbourne*, 1982. Proceedings, pp 92-100.

Morton, J.G. and Drexel, J.F. (**Eds**) (1995) Petroleum Geology of South Australia. Volume 1: The Otway Basin. *Mines and Energy of South Australia. Report Book* **95/12**.

Pettifer, G., Tabassi, A. and Simons, B. (1991). A new look at the structural trends in the onshore Otway Basin, Victoria, using image processing of geophysical data. *APEA Journal*, pp 213-228.

Prescott, J.R. (1983). TL dating of sands at Roonka, South Australia. *Journal of the European Study Group on Physical, Chemical and Mathematical Techniques applied to Archaeology*, **9**, pp 505-512.

Selley, R. C. (1976). Subsurface environmental analysis of North Sea sediments. *AAPG Bulletin* **60**, pp 184-195.

Shafik, S. (1983) Calcareous nanofossil biostratigraphy: an assessment of foraminiferal and sedimentation events in the Eocene of the Otway Basin of Eastern Australia. *Proc. Roy. Soc. Vict.* **93**, pp 129-148.

Sheard, M.J. (1983) Volcanoes. *In*: Tyler, M.J., Twidale, C.R., Ling, J.K. and Holmes, J.W. (Eds), Natural History of the South-East. *Royal Society of South Australia. Occasional Publications*, **3**, pp 7-14.

Sheard, M.J. (1995). Quaternary Volcanic Activity and Volcanic Hazards. *In:* The Geology of South Australia, Volume 2: the Phanerozoic. *Mines and Energy, South Australia*, Bulletin **54**, pp 264-268.

Sheard, M.J. and Smith, P.C. (1995). Soils, Palaeosoils and Calcretes. *In:* The Geology of South Australia, Volume 2: the Phanerozoic. *Mines and Energy, South Australia*, Bulletin **54**, pp 257-262.

Smith, B.W. and Prescott, J.R. (1987) Thermoluminescence dating of the eruption at Mt. Schank, South Australia. *Australian Journal of Earth Sciences*, **34**, pp 335-342.

Smith, P. C., Rogers, P.A., Lindsay, J.M., White, M.R., Kwitko, G. (1995). Tertiary Gambier Basin. *In*: J. F. Drexel, Preiss, W.V. (**Eds**) *The Phanerozoic, MESA and the Geological Survey of South Australia*, Bulletin 54, vol **2**, pp 151-157.

Smith, P.C. and Sheard, M.J. (1985) Otway 85 Field Excursion Guides. *In* Otway 85 – Earth Resources of the Otway Basin. *Geological Society of Australia*, pp 69-90.

Sprigg, R. G. (1952). The Geology of the southeast province, South Australia, with special reference to Quaternary coastline migrations and modern beach development. *Geological Survey of South Australia*, Bulletin **29,** pp 120.

Sprigg, R. C. (1985). A History of the Search for Commercial Hydrocarbons in the Otway Basin Complex. *Second Southeastern Australia Oil Exploration Symposium, Melbourne*, Petroleum Exploration Society of Australia.

Tickell, S.J., Edwards, J., and Abele, C. (1992) Port Campbell Embayment 1:100,000 Map Geological Report. *Geol. Surv. Vic. Rpt.*, **95**, 1-97.

Twidale, C. R., Campbell, E.M., and Bourner, J.A. (1983). Granite forms, karsts and lunettes. *In:. M. J. Tyler, Twidale, C.R., Ling, J.K. and Holmes, J.W., Royal* (**Eds**) *Natural History of the South East*. Society of South Australia**:** pp 25-39.

Waghorn, D.B. (1989) Middle Tertiary calcareous nanofossils from Aire District, Victoria, a comparison with equivalent assemblages in South Australia and New Zealand. *Marine Micropalaeontology*, **14**, pp 237-255.

Weber, K. J. (1971). Sedimentological aspects of oil fields in the Niger Delta. *Geologie Mijnb,* **50**, pp 559-576.

Weissel, J.K. and Hayes, D.E. (1977) Evolution of the Tasman Sea reappraised. *Earth and Planetary Science Letters*, **36**, pp 77-84.

White, A. H. (1968). Exploration in the Otway Basin. *APEA Journal,* **8(2),** pp 78-87.

White, M. R. (1995). Micropalaeontological analysis of 26 petroleum wells in the Gambier Basin, South Australia. *Adelaide, Department of Mines and Energy South Australia.*

White, M. R. (1996). Subdivision of the Gambier Limestone. *MESA Journal* **1,** pp 35-39.

Wopfner, H. (1980) Development of Permian intracratonic basins in Australia. *In*: Cresswell, M.M. and Vella, P. (**Eds**), *5th International Gondwana Symposium, Wellington, New Zealand, 1980*, pp 185-190.

Wopfner, H. and Douglas, J.G., Ed. (1971). The Otway Basin of Southeastern Australia. Special Bulletin No. **5**. *Adelaide, Geological Surveys of South Australia and Victoria.*

Yu, S. M. (1988). Structure and Development of the Otway Basin. *APEA Journal*, pp 243-254.

Appendix 4

Well Logs
Seismic Maps
Well Correlations

APPENDIX 4

Well Logs, Seismic Maps & Well Correlations

1. **Onshore Strike Cross-Section**: Crayfish 1A, St Clair 1, Reedy Creek 1, Lake George 1, Rendelsham 1, Burrungule 1, Lake Bonney 1, Kentgrove 1, Caroline 1

2. **Offshore Strike Cross-Section**: Troas 1, Morum 1, Crayfish 1A, Copa 1, Argonaut 1A, Breaksea Reef 1, Normanby 1

3. **Dip Cross-Section 1**: Breaksea Reef 1, Northumberland 1, Caroline 1, McNicol 1, Compton 1, Kalangadoo 1.

4. **Dip Cross-Section 2**: Breaksea Reef 1, Northumberland 1, Douglas Point 1, McNamara 1, Compton 1, Burrungule 1, Kalangadoo 1, Hungerford 1.

(NOTE: Wireline logs in Chama 1A did not penetrate the Cenozoic succession and gamma ray log values in Neptune 1 have been clipped, thereby destroying the log character used for correlations).

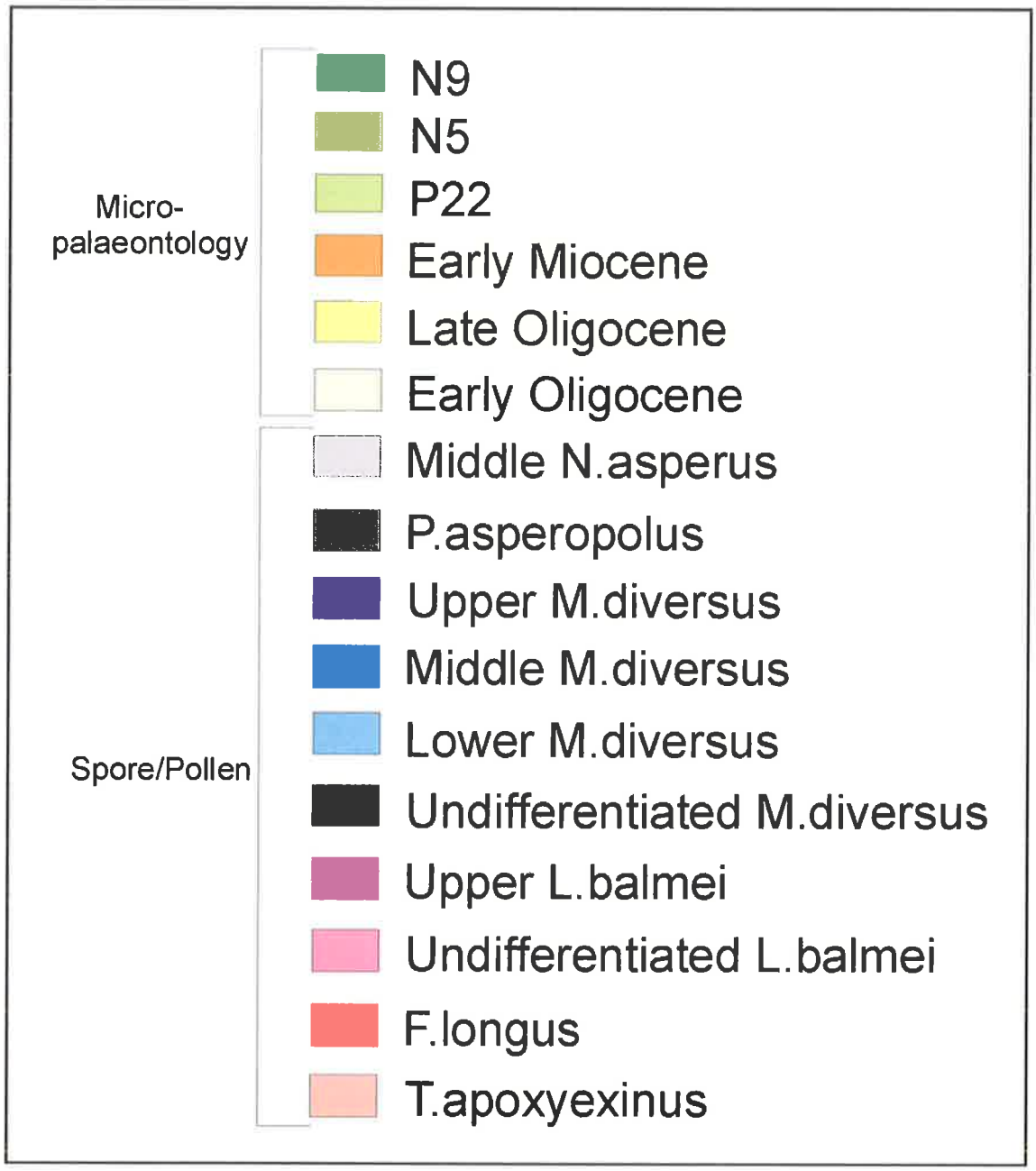

A 4.1 Species key to biostratigraphic zones identified in wells in the Gambier Sub-basin.

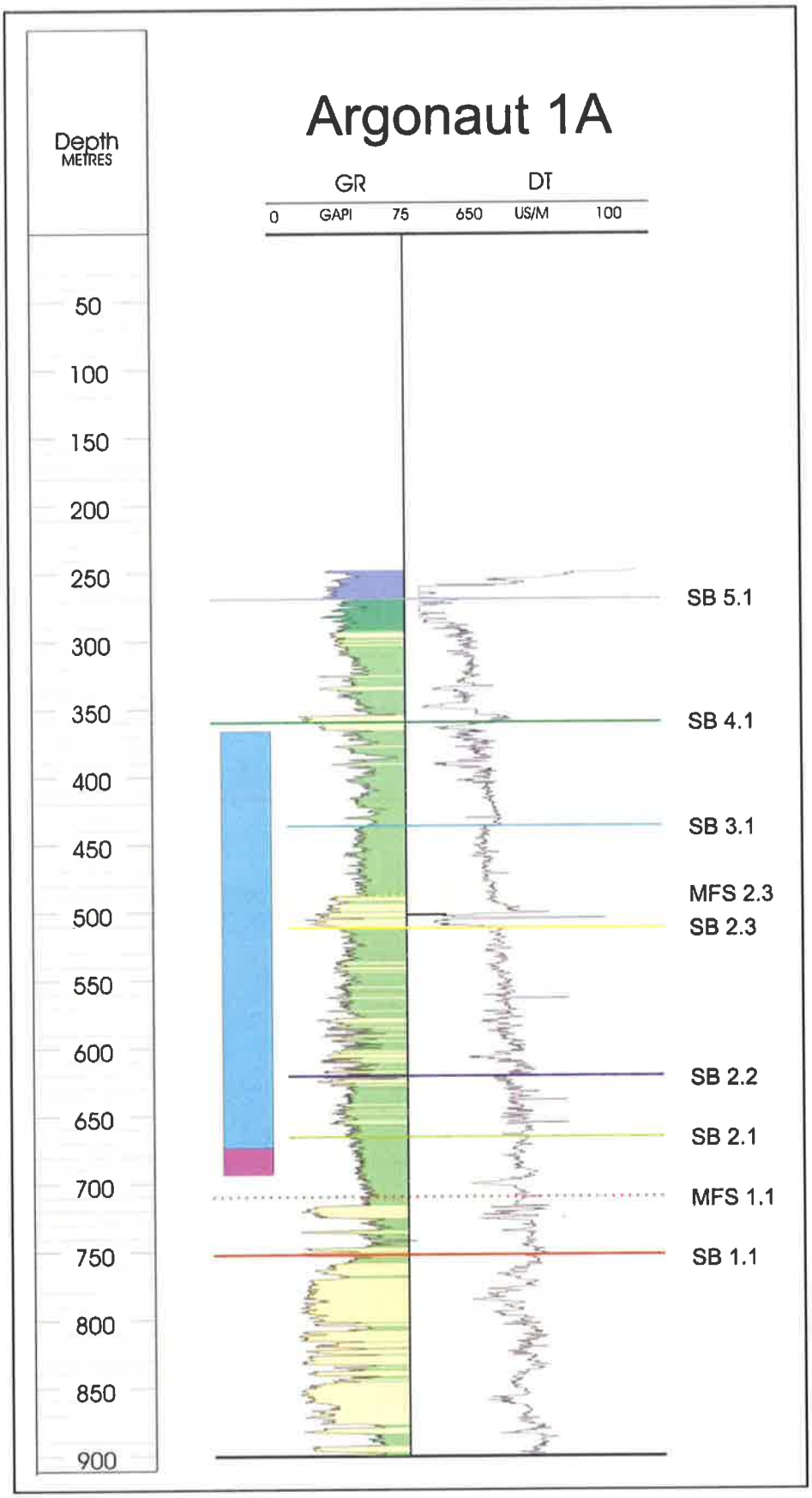

A4.2 Argonaut 1A

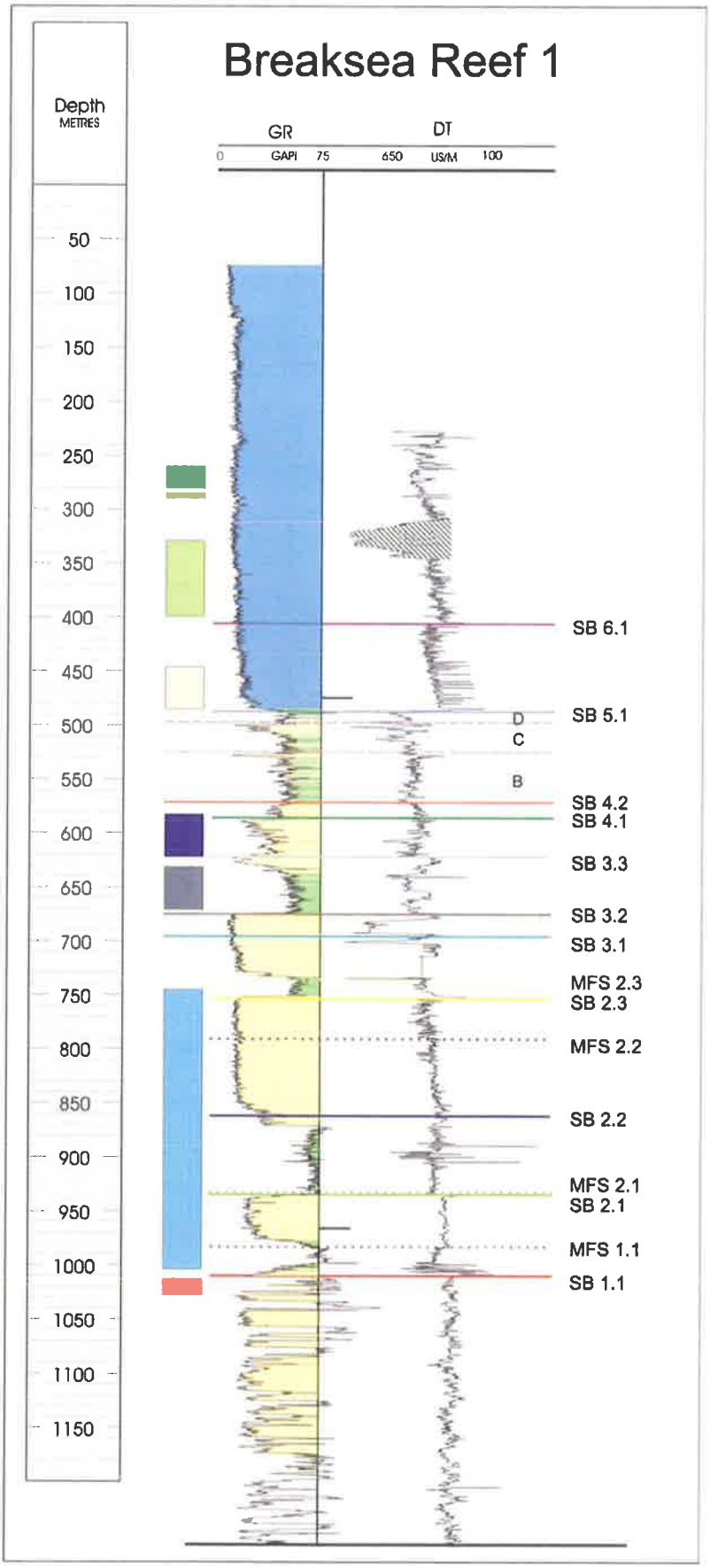

A4.3 Breaksea Reef 1

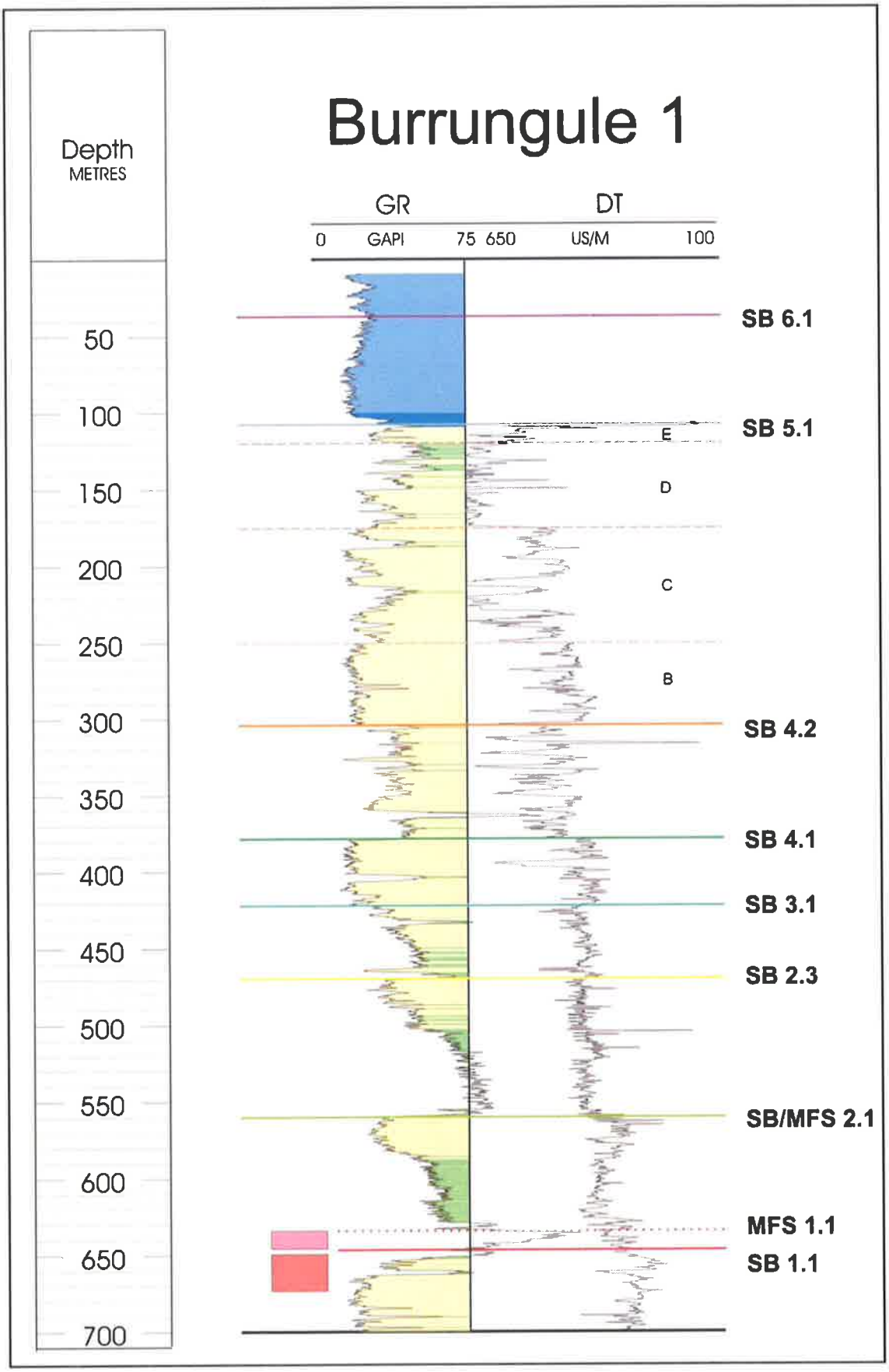

A4.4 Burrungule 1

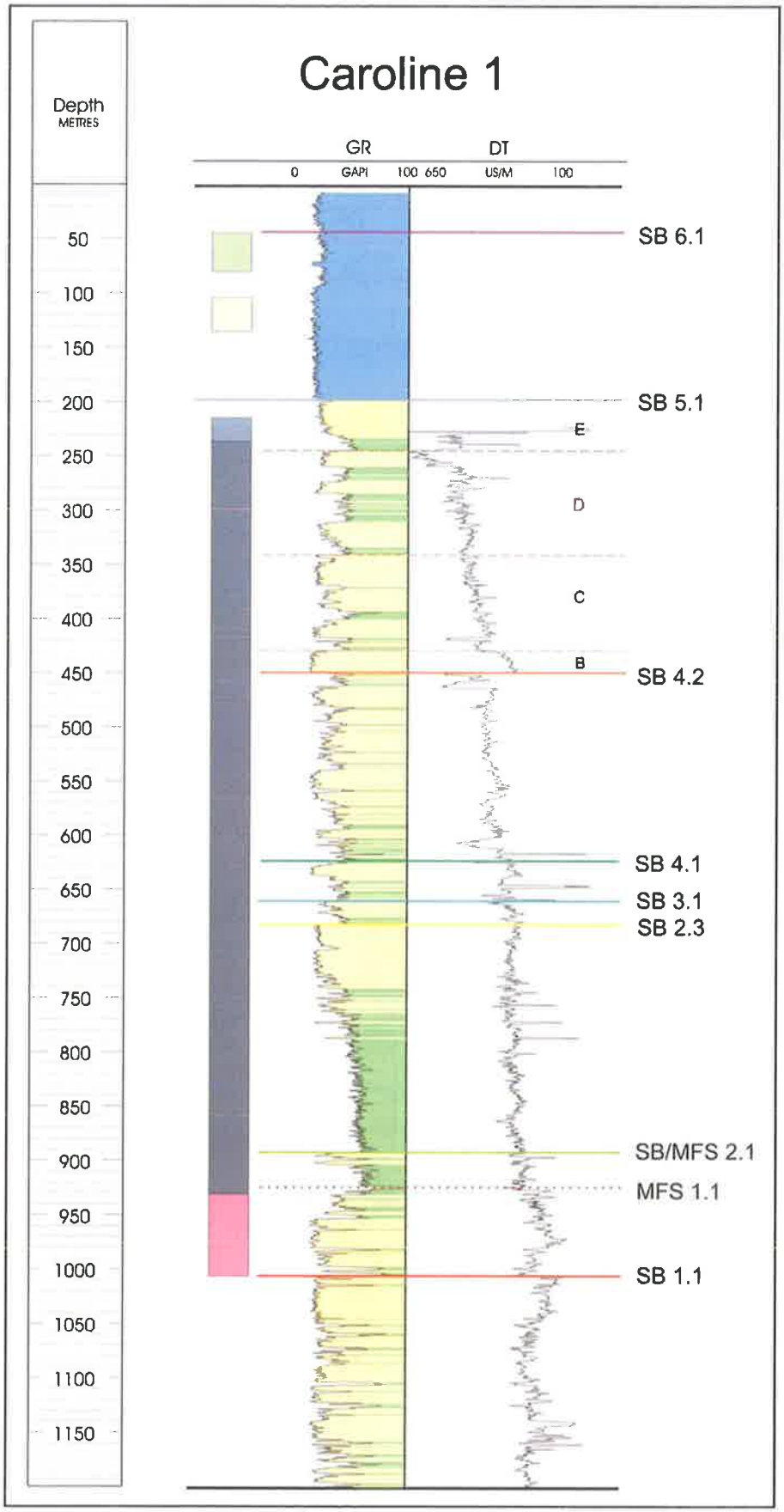

A4.5 Caroline 1

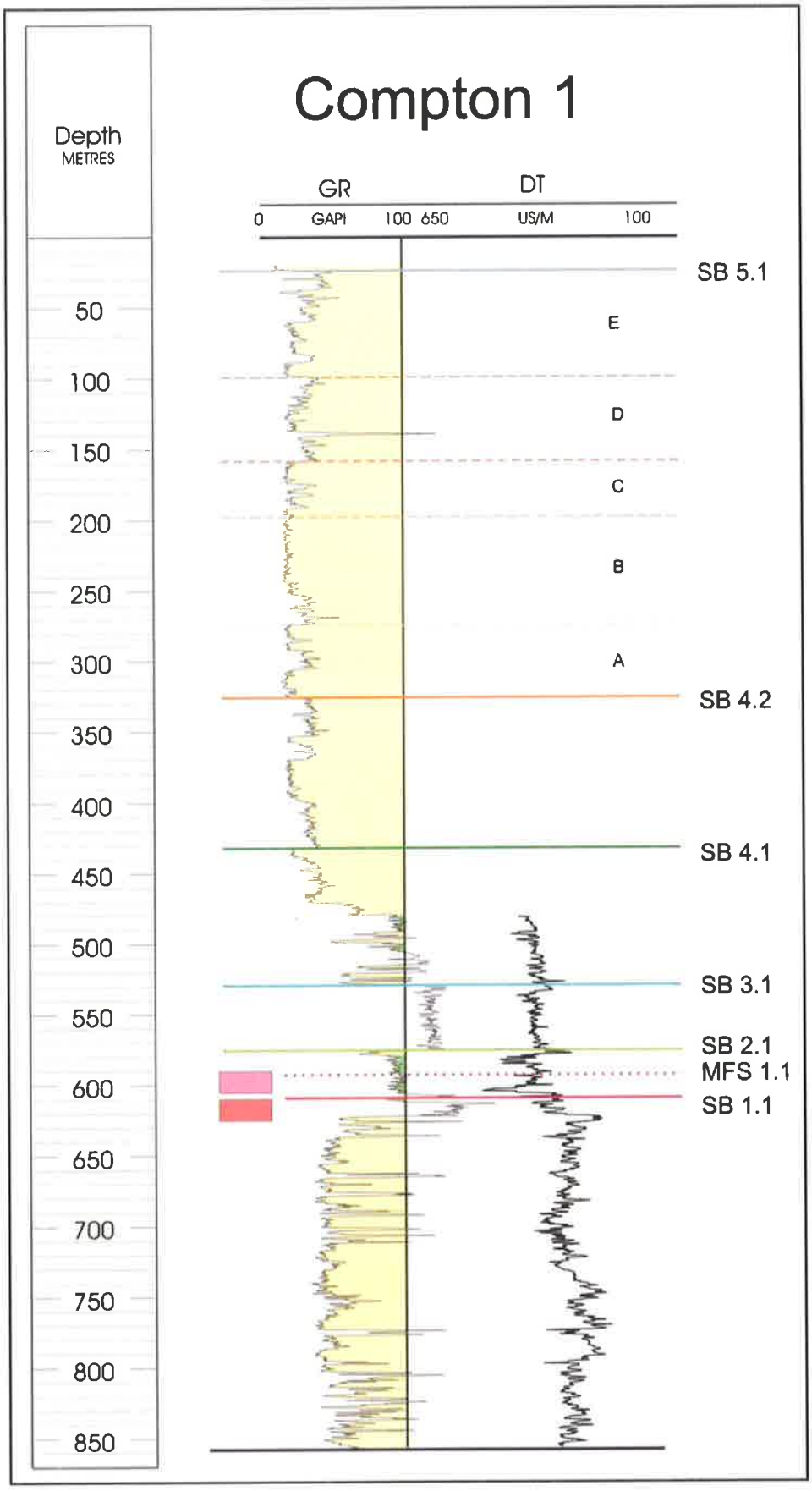

A4.6 Compton 1

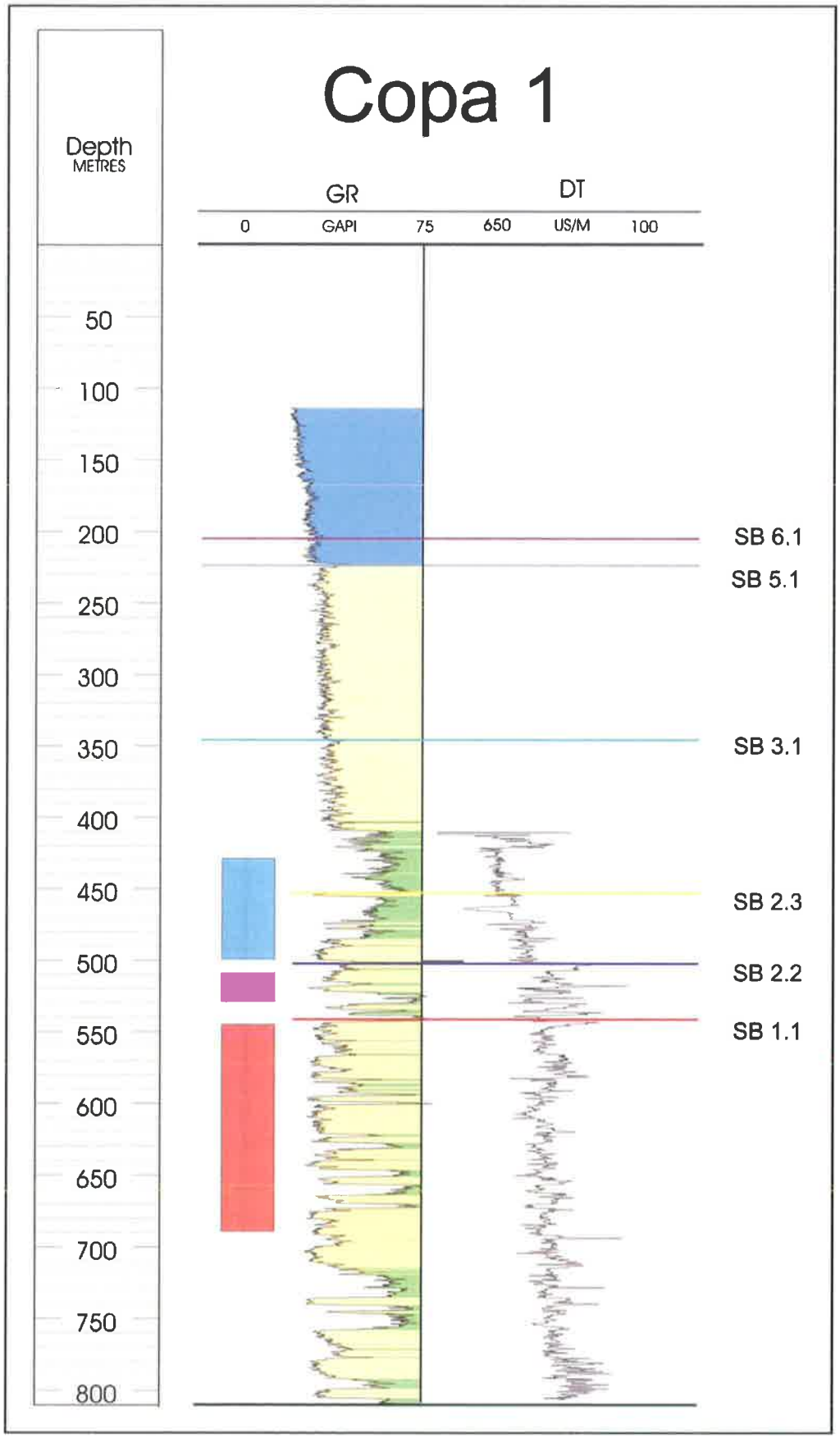
Copa 1
Depth
METRES
GR
DT
0
GAPI
75
650
US/M
100
50
100
150
200
250
300
350
400
450
500
550
600
650
700
750
800
SB 6.1
SB 5.1
SB 3.1
SB 2.3
SB 2.2
SB 1.1

A4.7 Copa 1

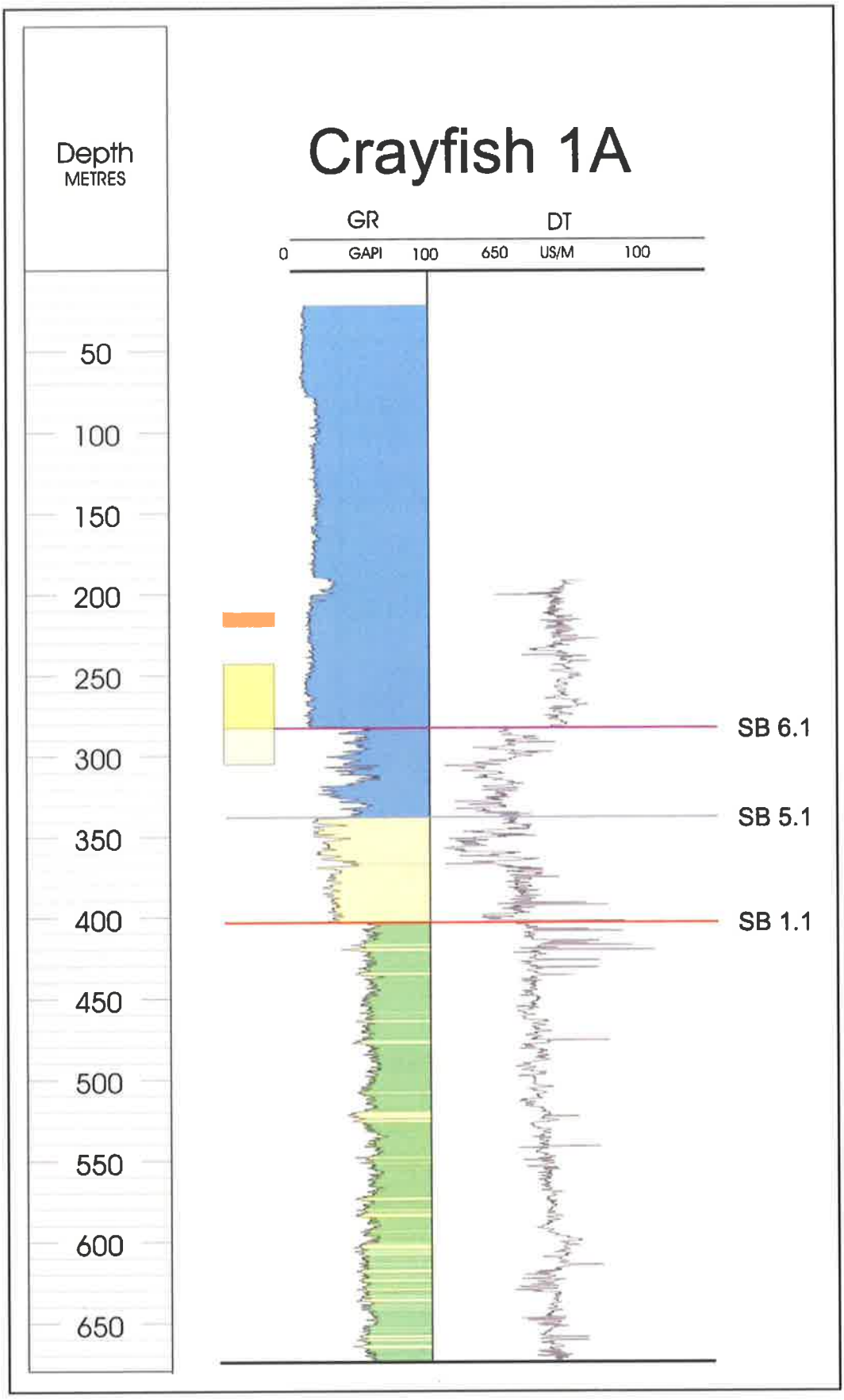

A4.8 Crayfish 1A

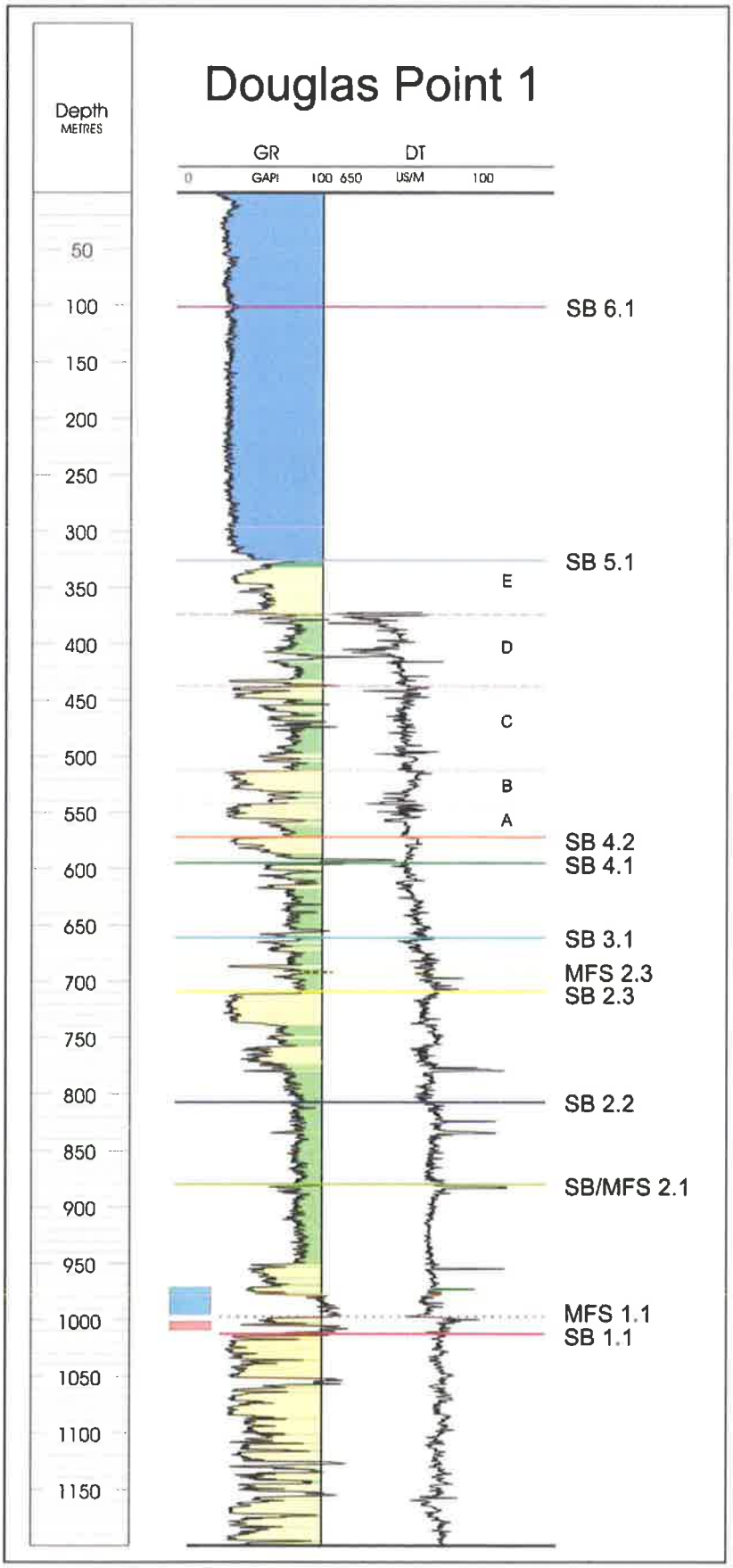

A4.9 Douglas Point 1

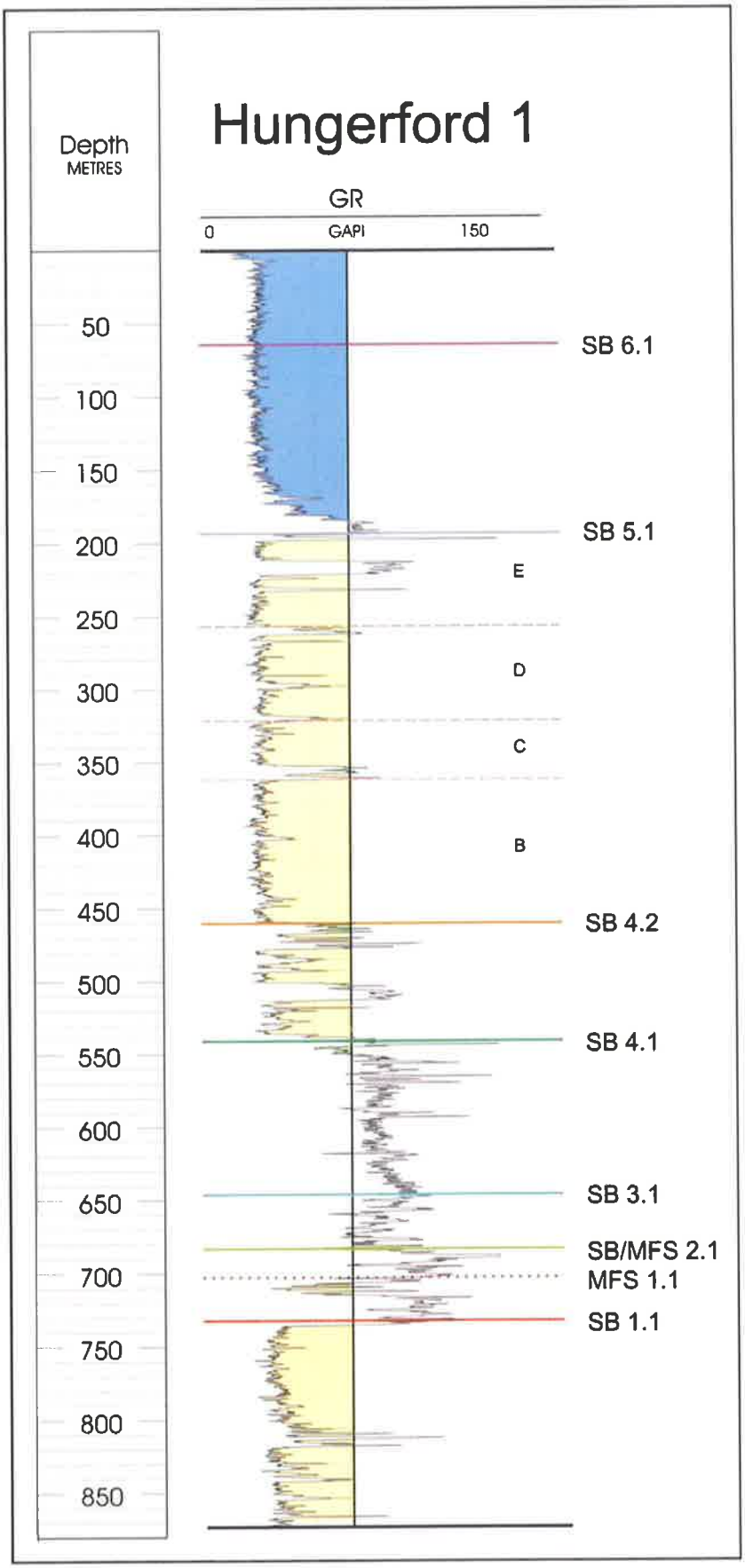

A4.10 Hungerford 1

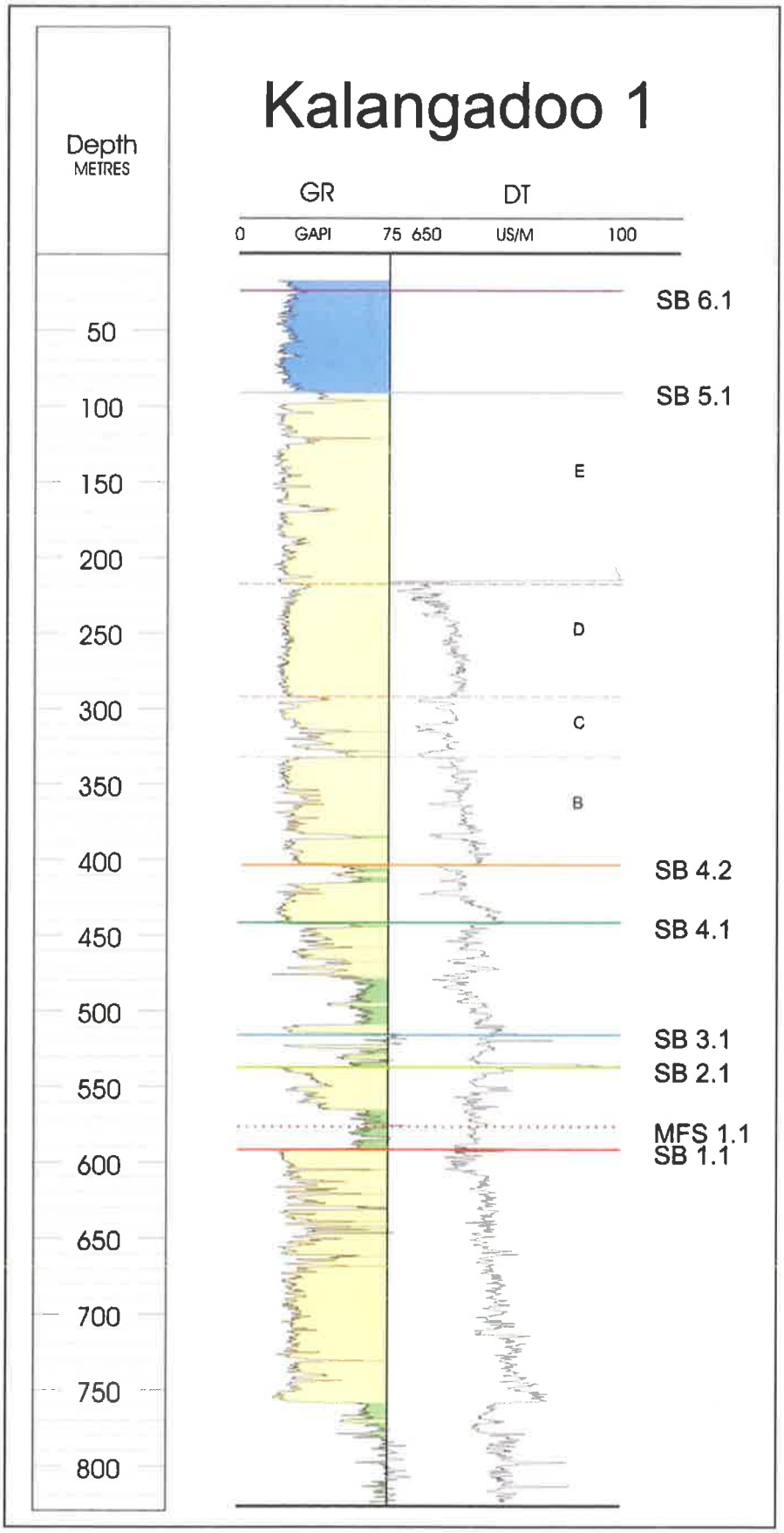

A4.11 Kalangadoo 1

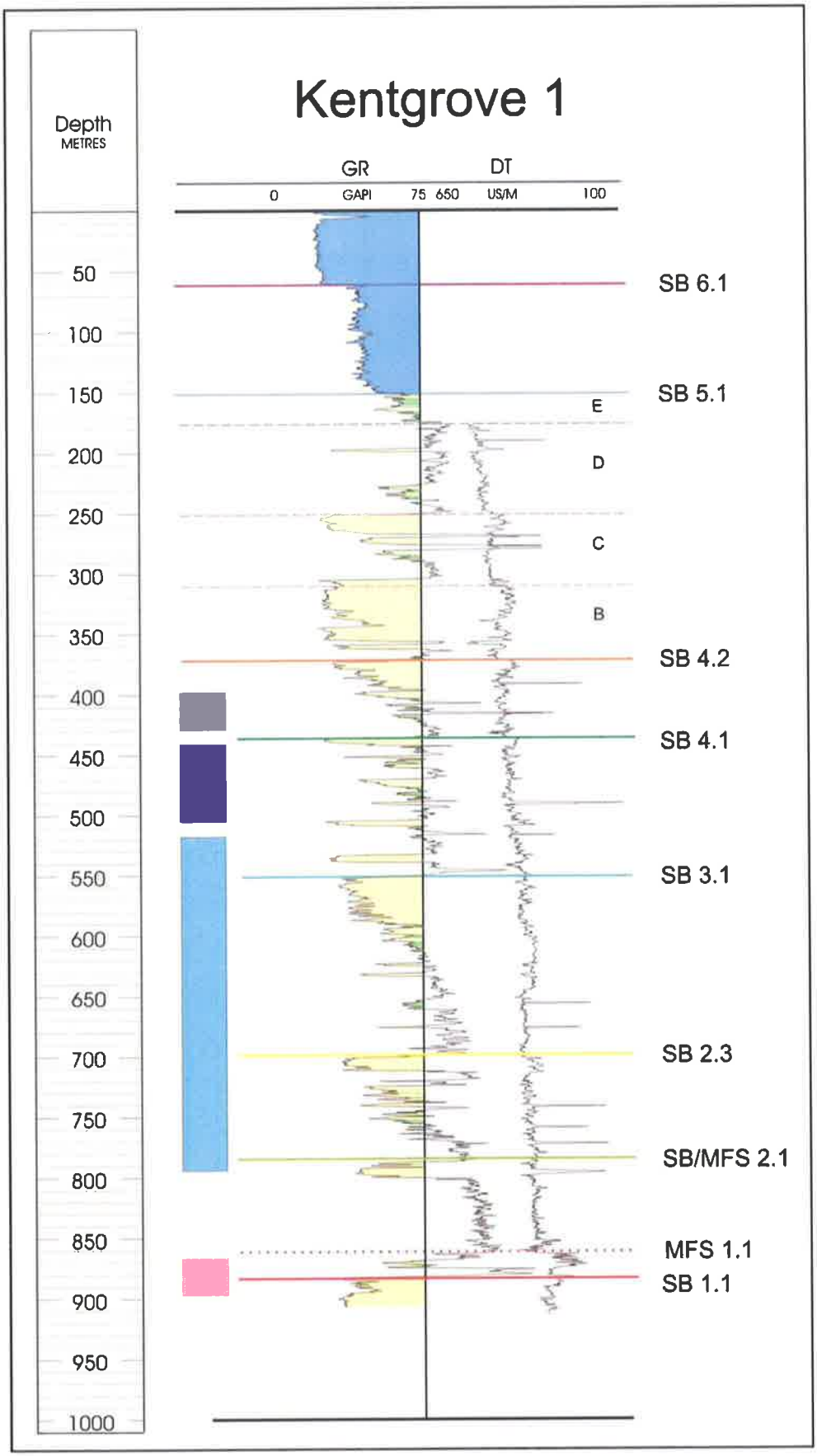

A4.12 Kentgrove 1

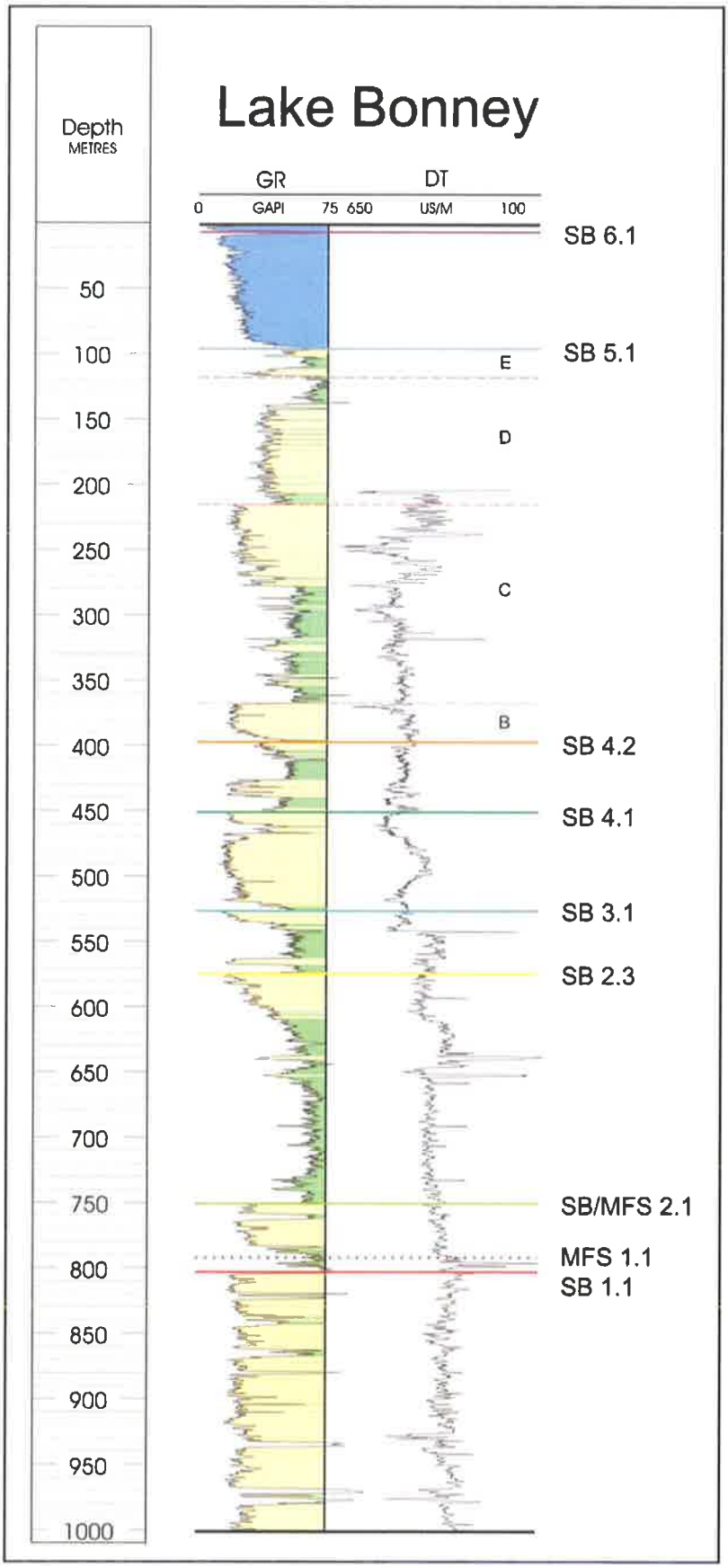

A4.13 Lake Bonney 1

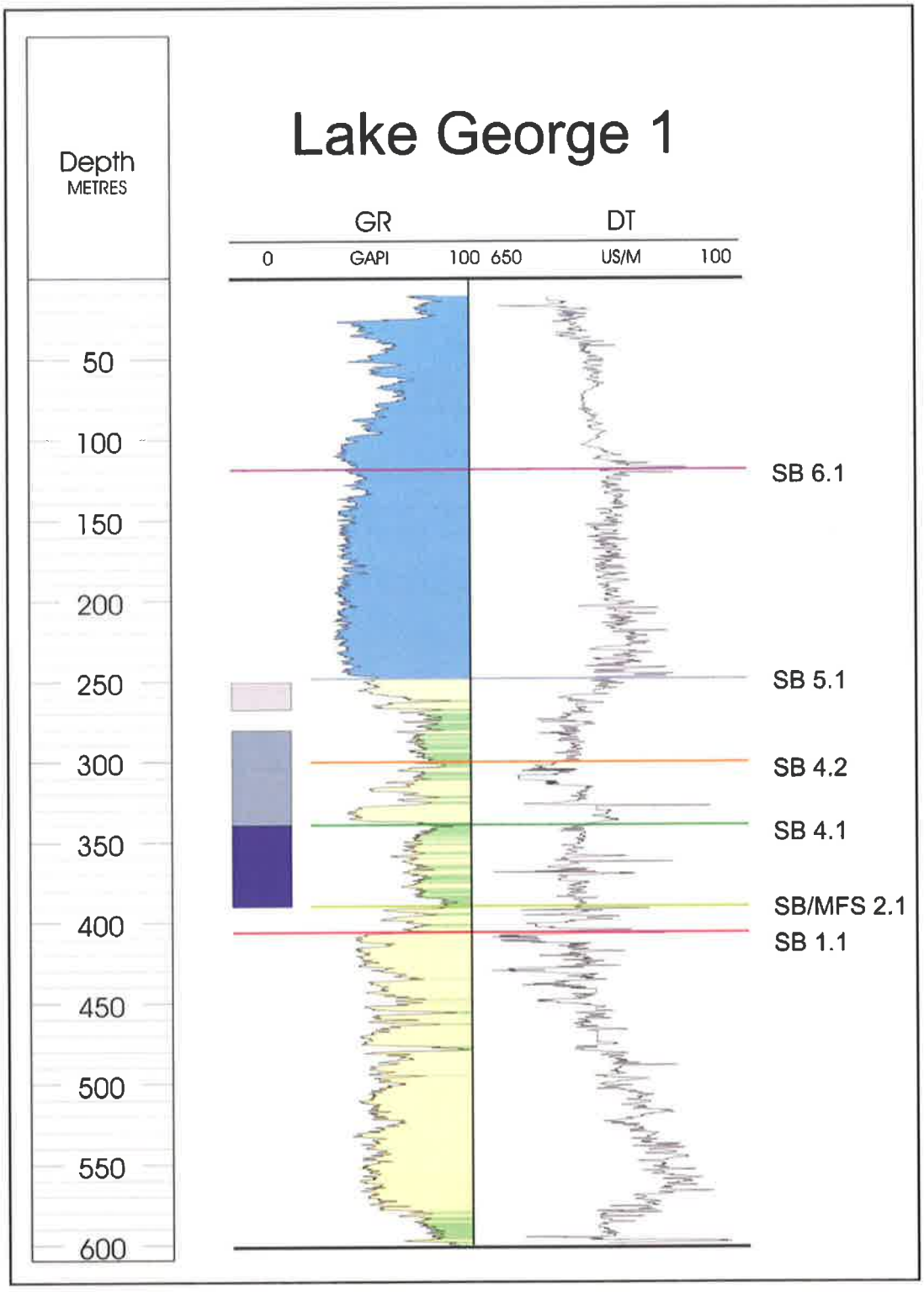

A4.14 Lake George 1

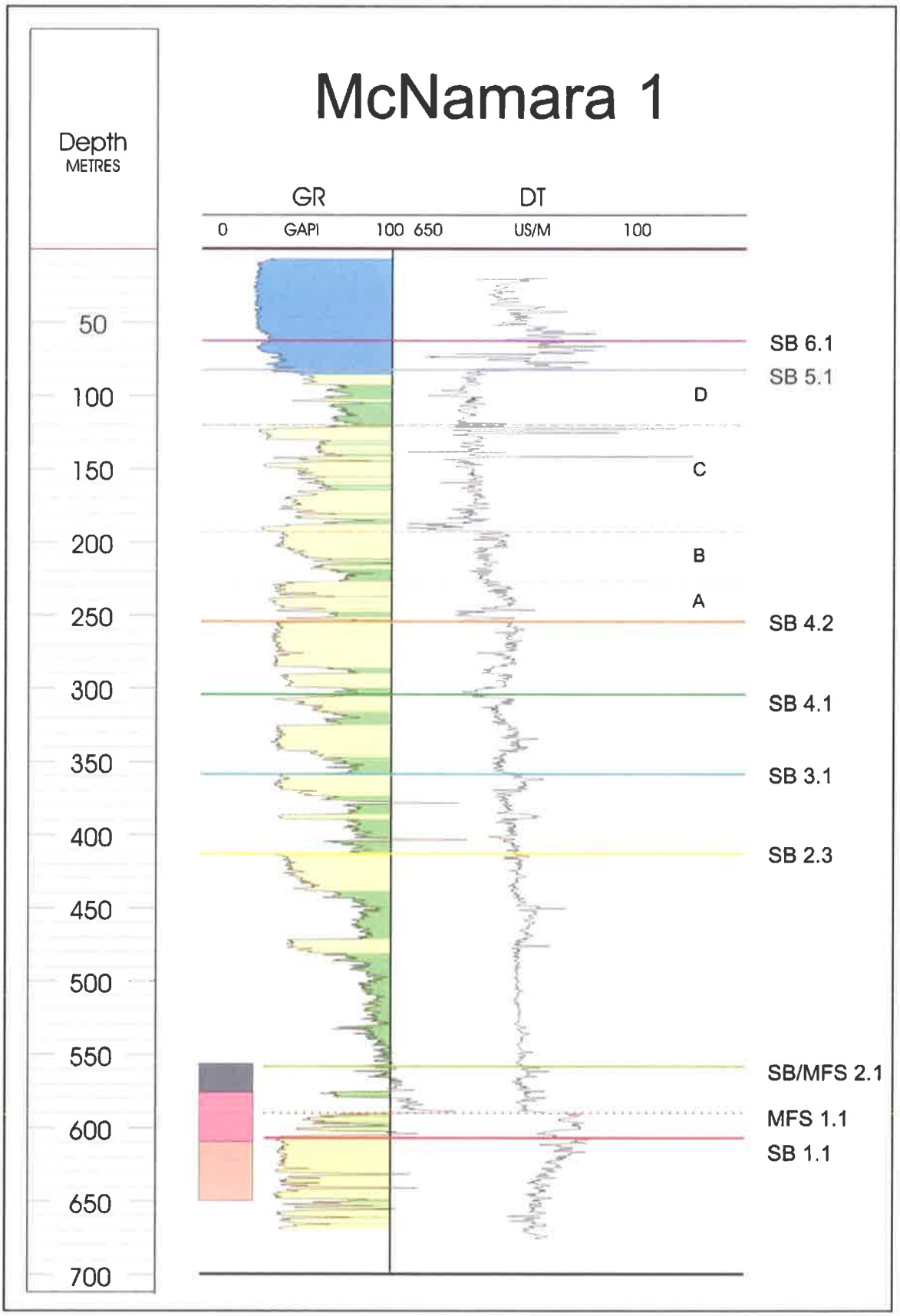

A4.15 McNamara 1

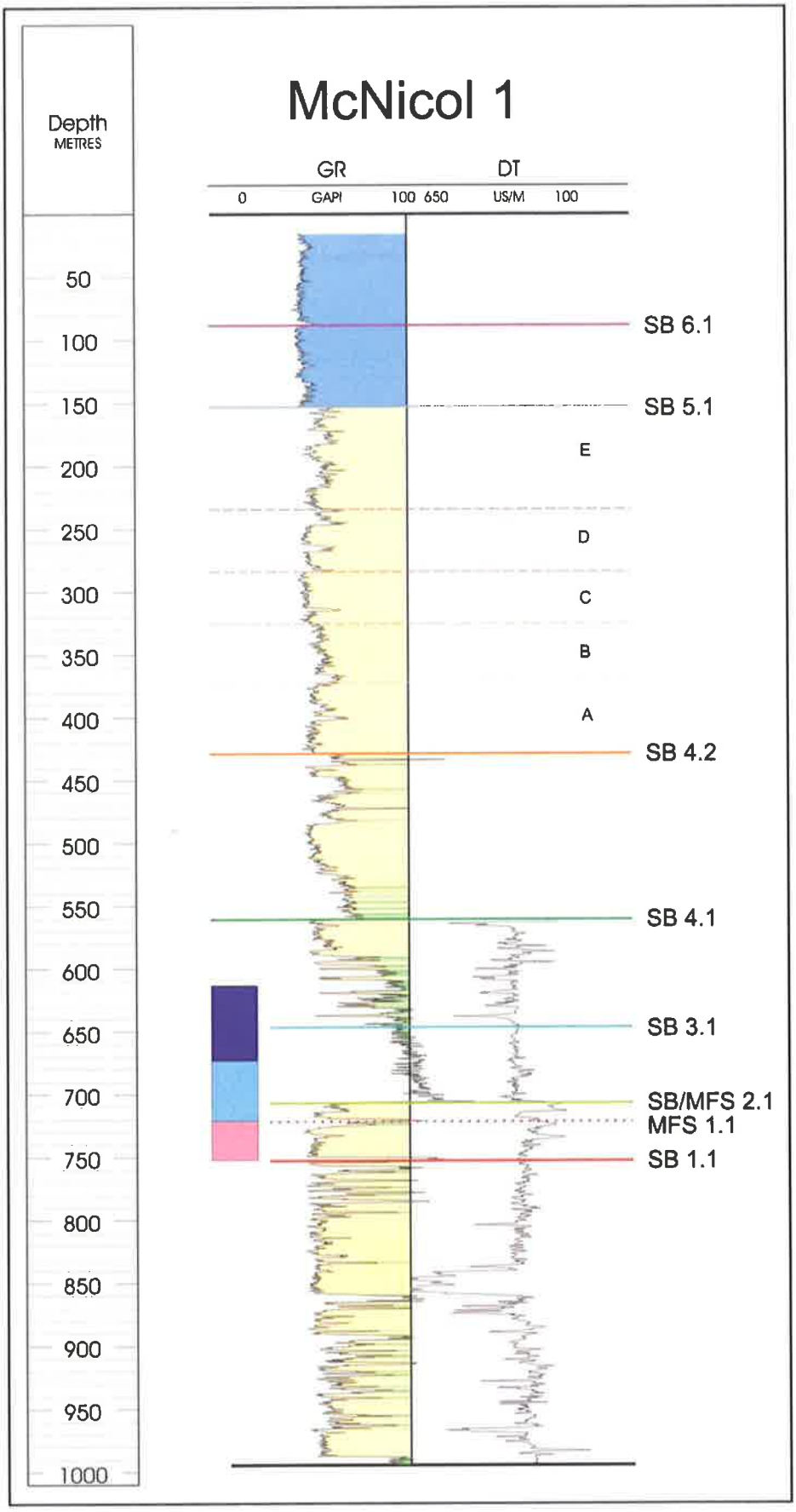

A4.16 McNicol 1

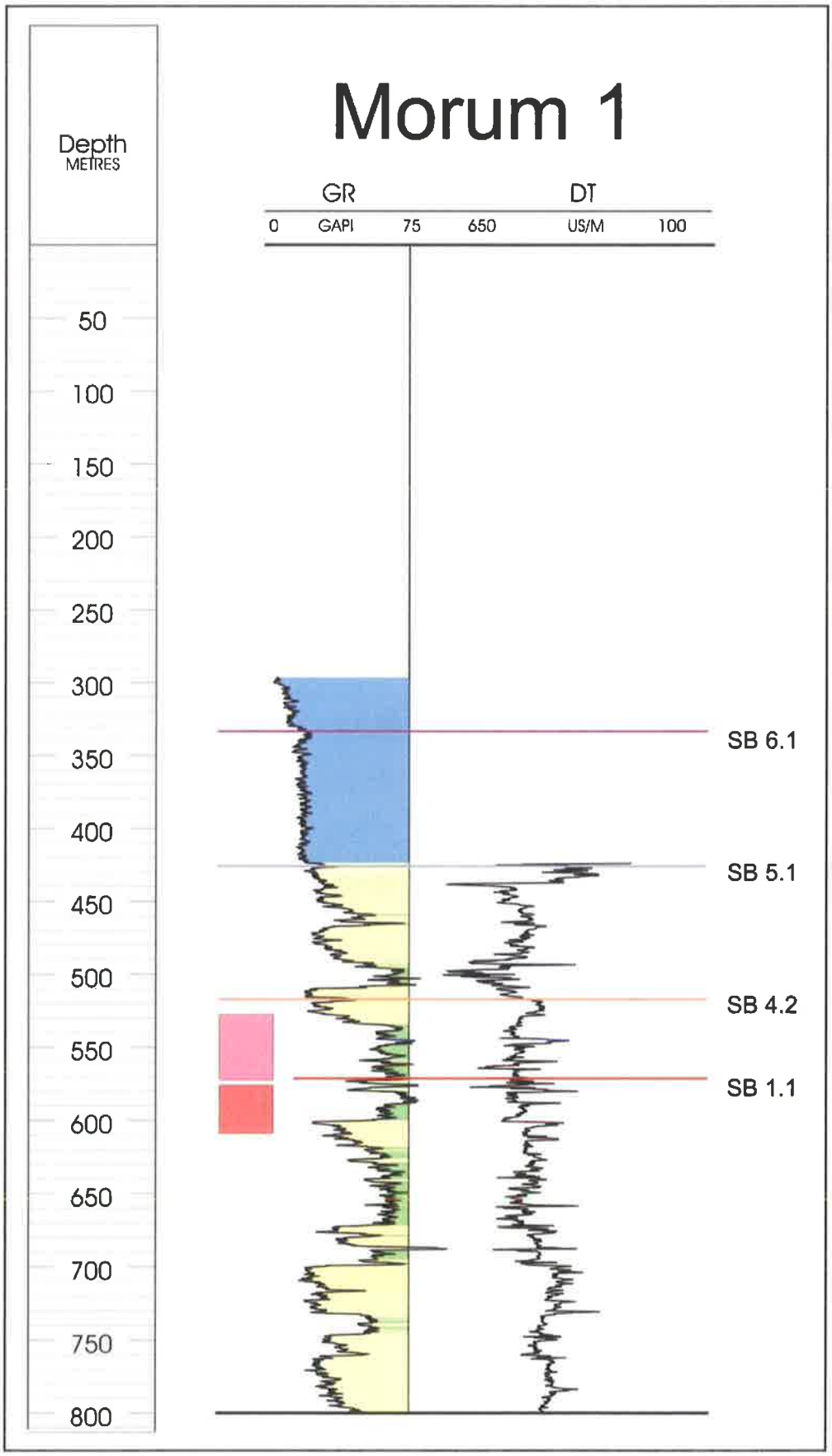
Morum 1
Depth
METRES
GR
DT
0
GAPI
75
650
US/M
100
50
100
150
200
250
300
350
400
450
500
550
600
650
700
750
800
SB 6.1
SB 5.1
SB 4.2
SB 1.1

A4.17 Morum 1

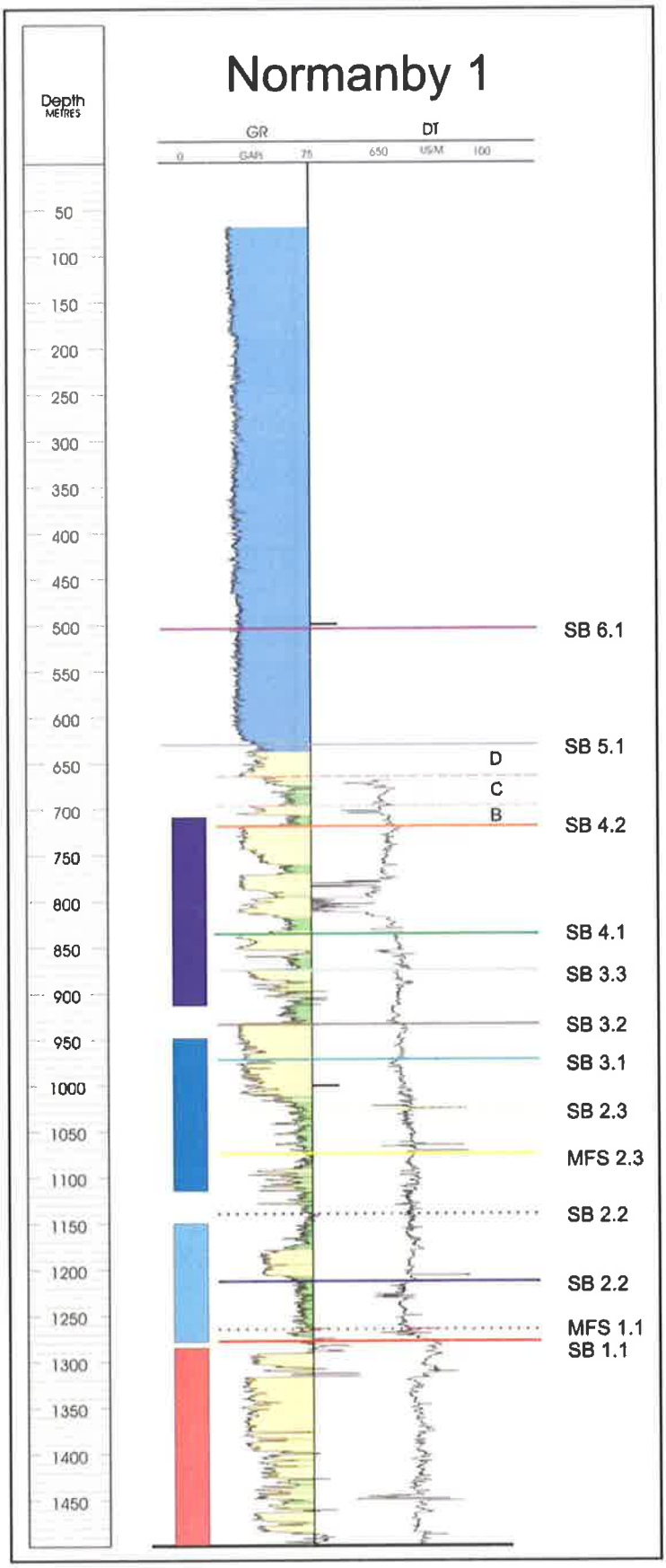

A4.18 Normanby 1

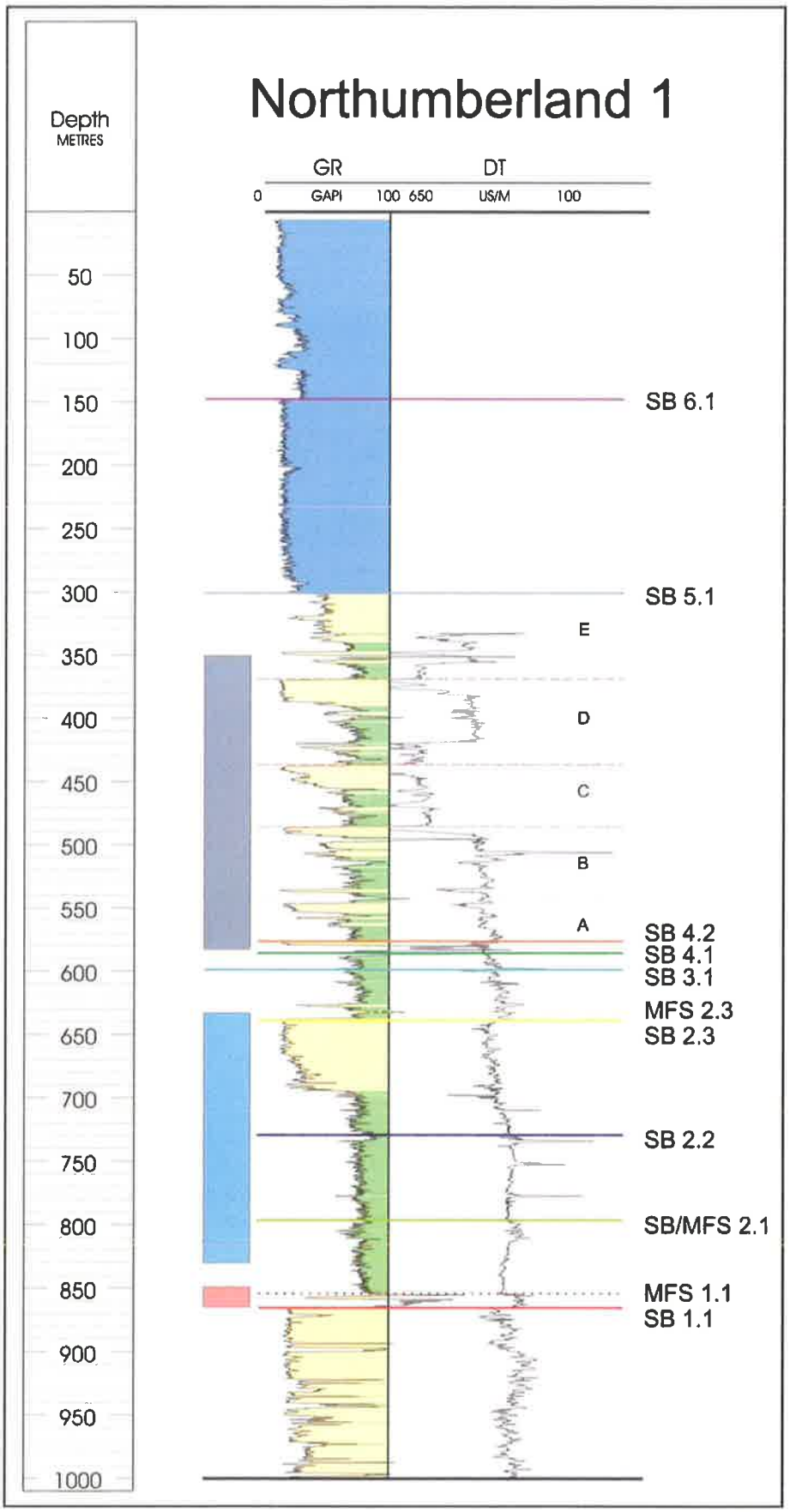

A4.19 Northumberland 1

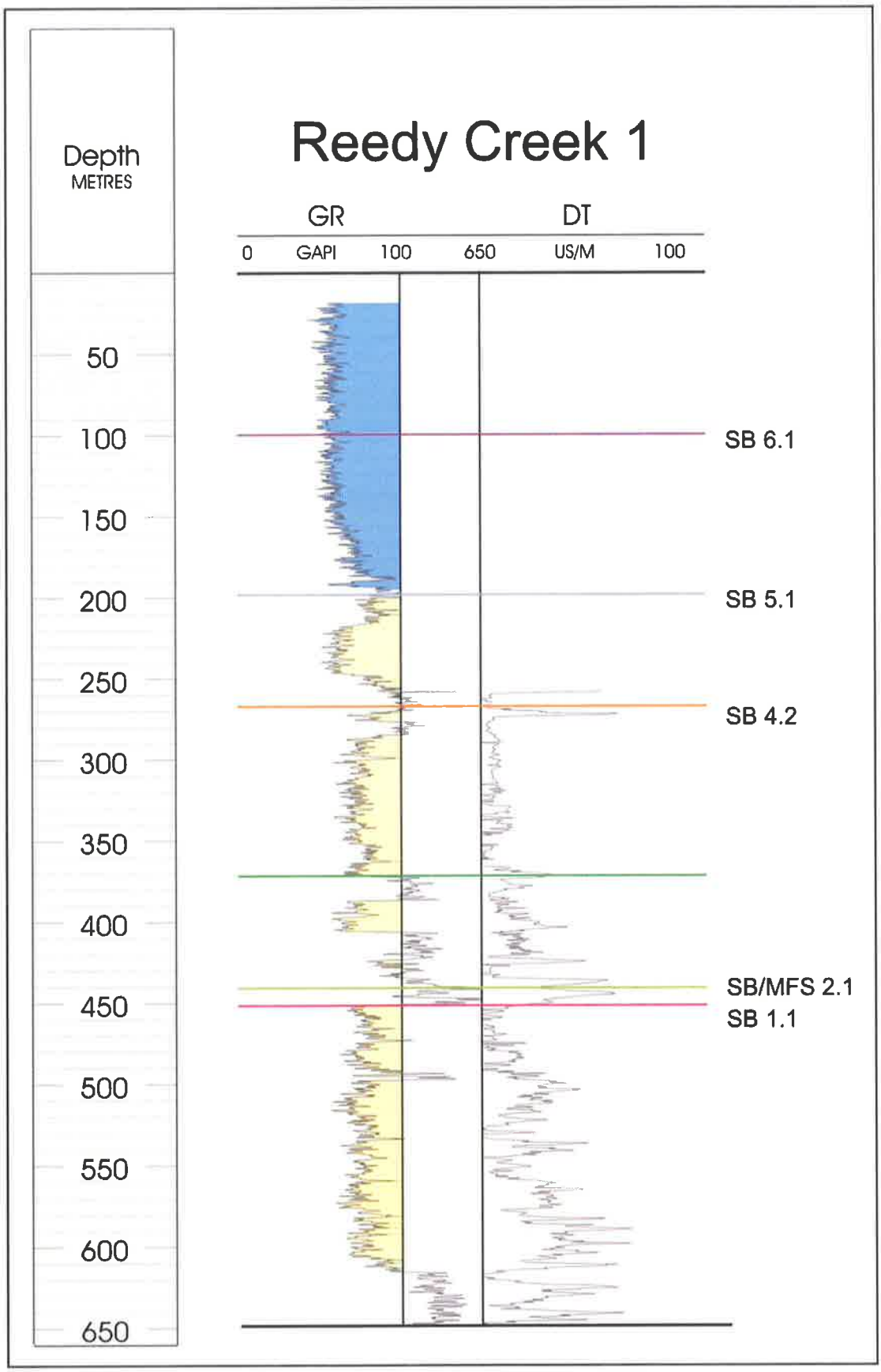

A4.20 Reedy Creek 1

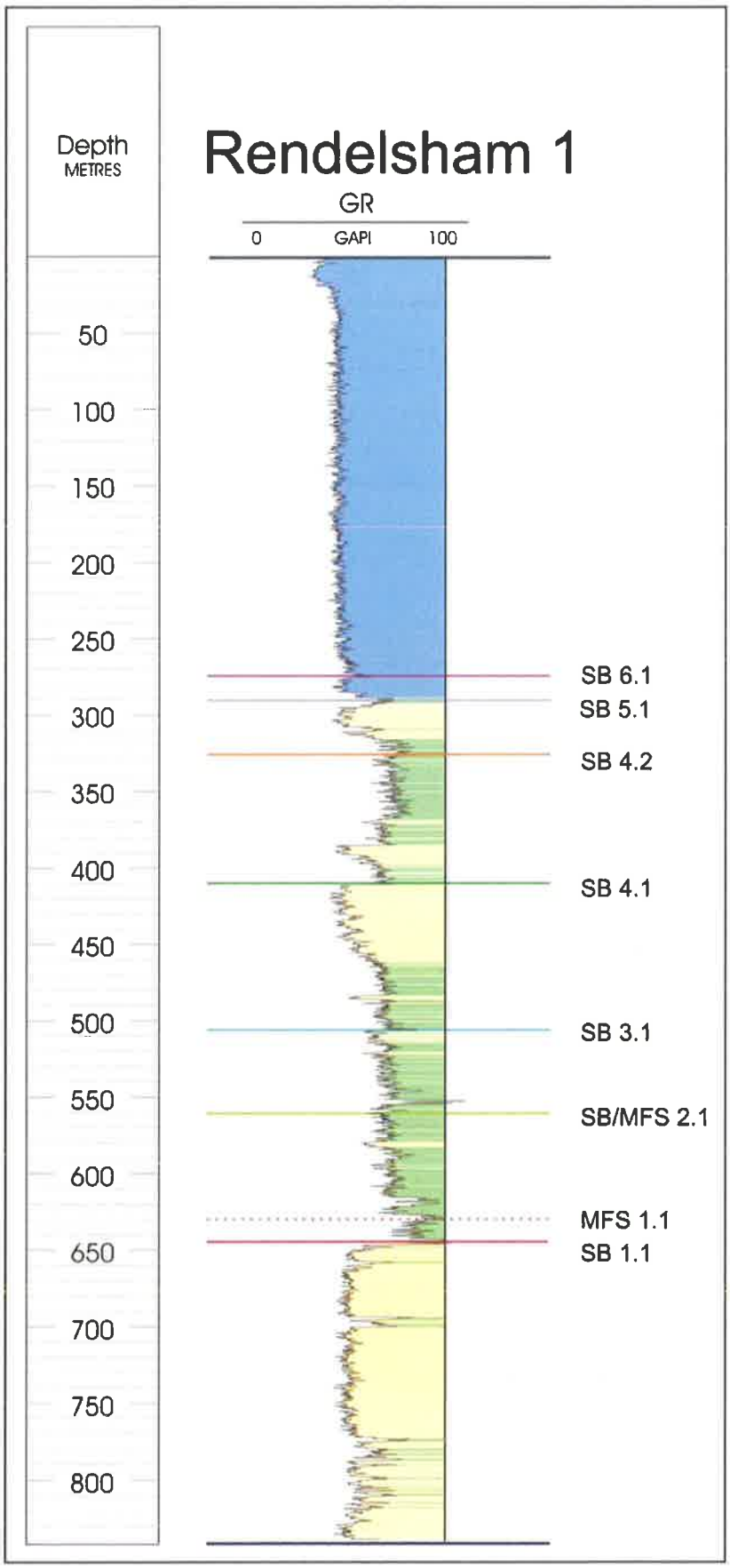

A4.21 Rendelsham 1

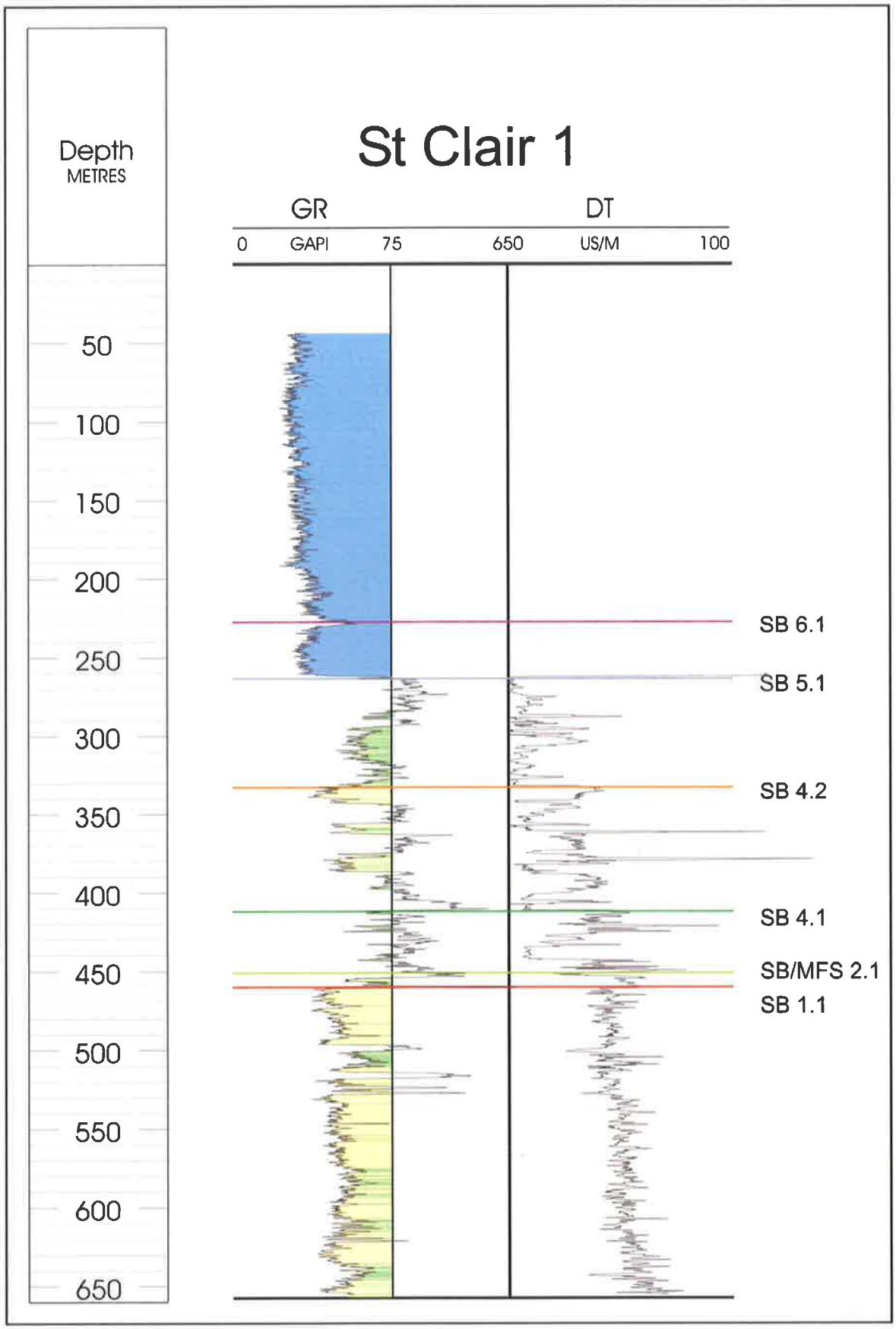

A4.22 St Clair 1

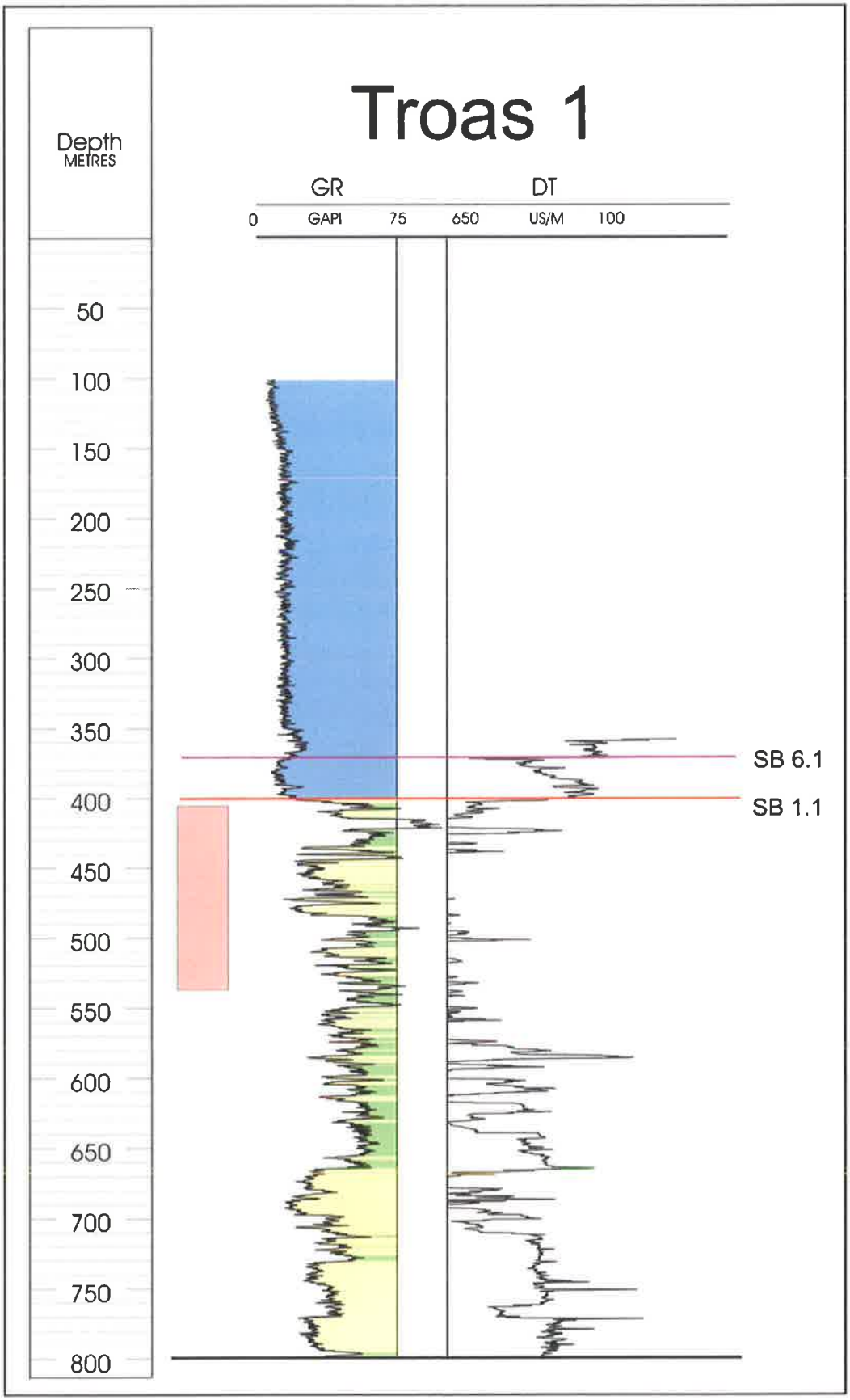
Troas 1
Depth
METRES
GR
DT
0
GAPI
75
650
US/M
100
50
100
150
200
250
300
350
400
450
500
550
600
650
700
750
800
SB 6.1
SB 1.1

A4.23 Troas 1

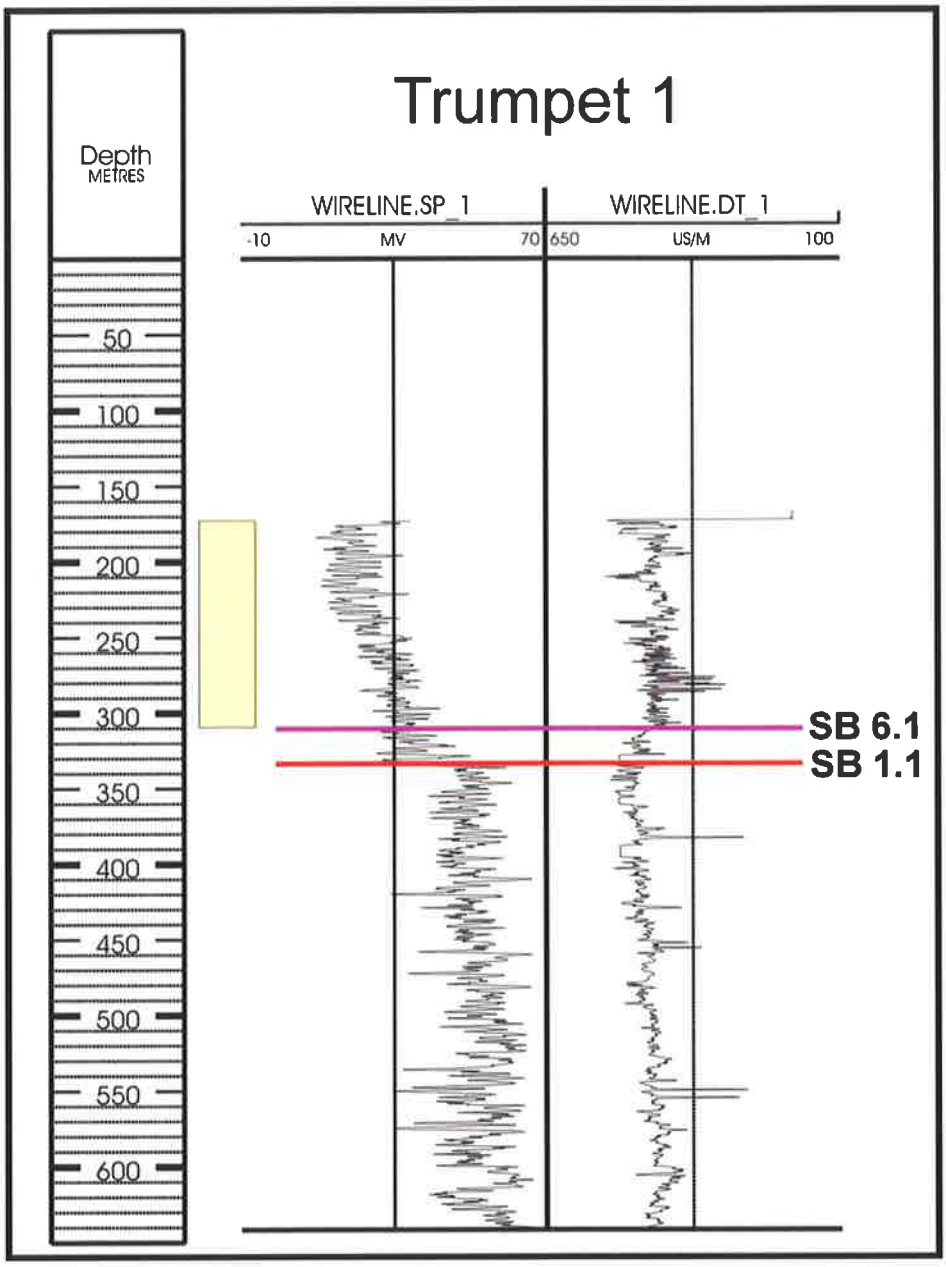

A4.24 Trumpet 1

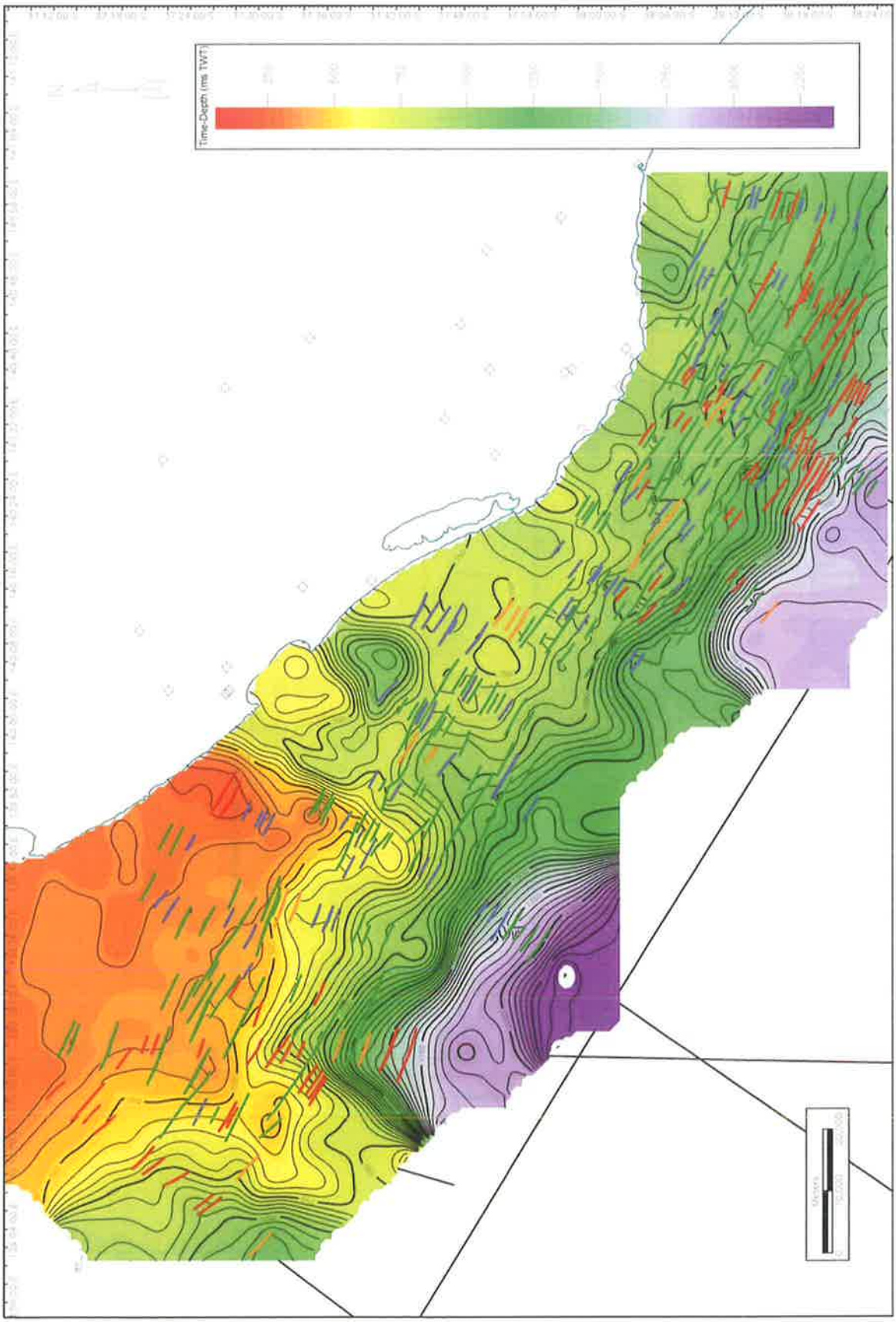

A 4.25 Time-Structure map of SB 1.1 (Cretaceous-Palaeogene boundary)

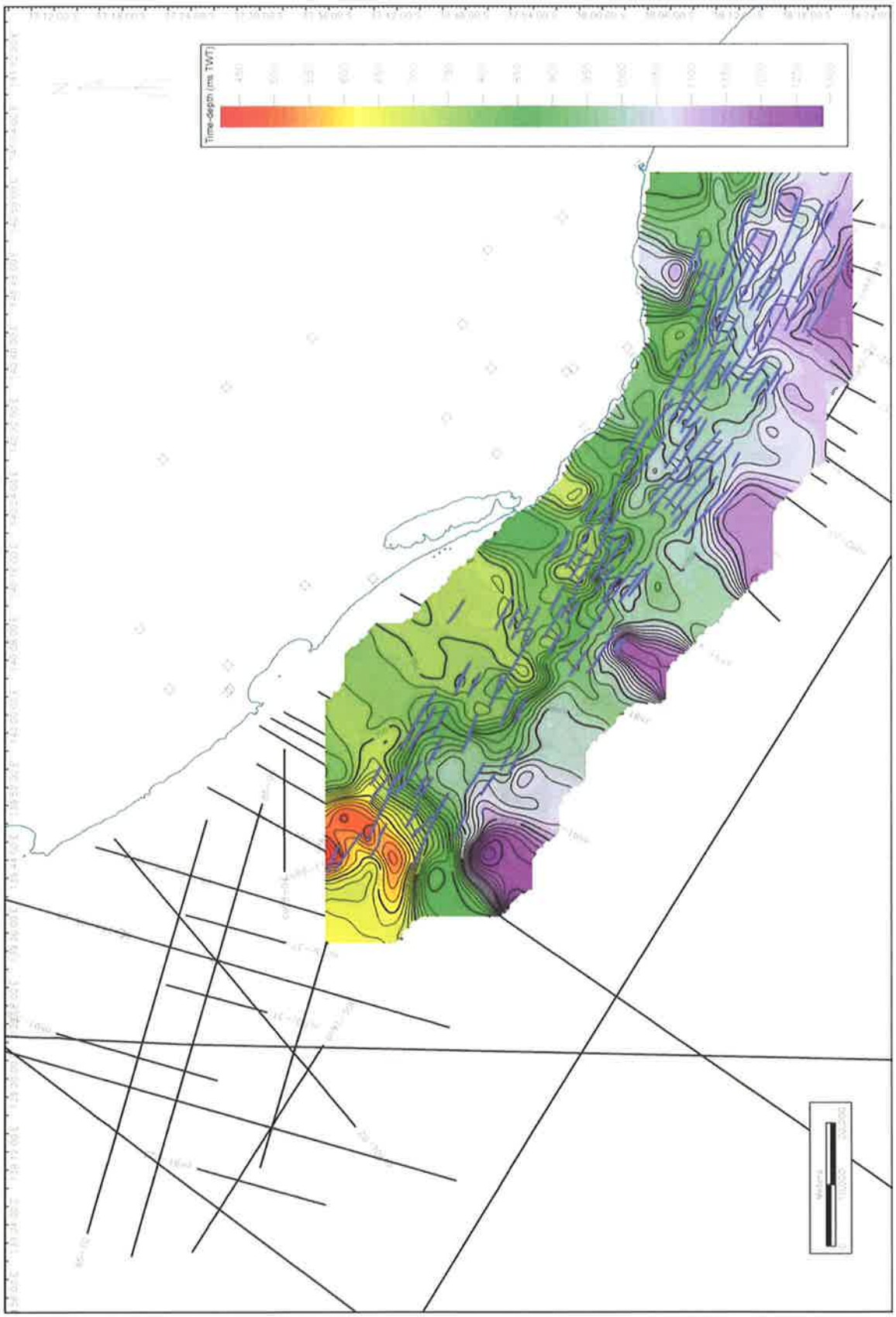

A 4.26 Time-Structure map of MFS 1.1

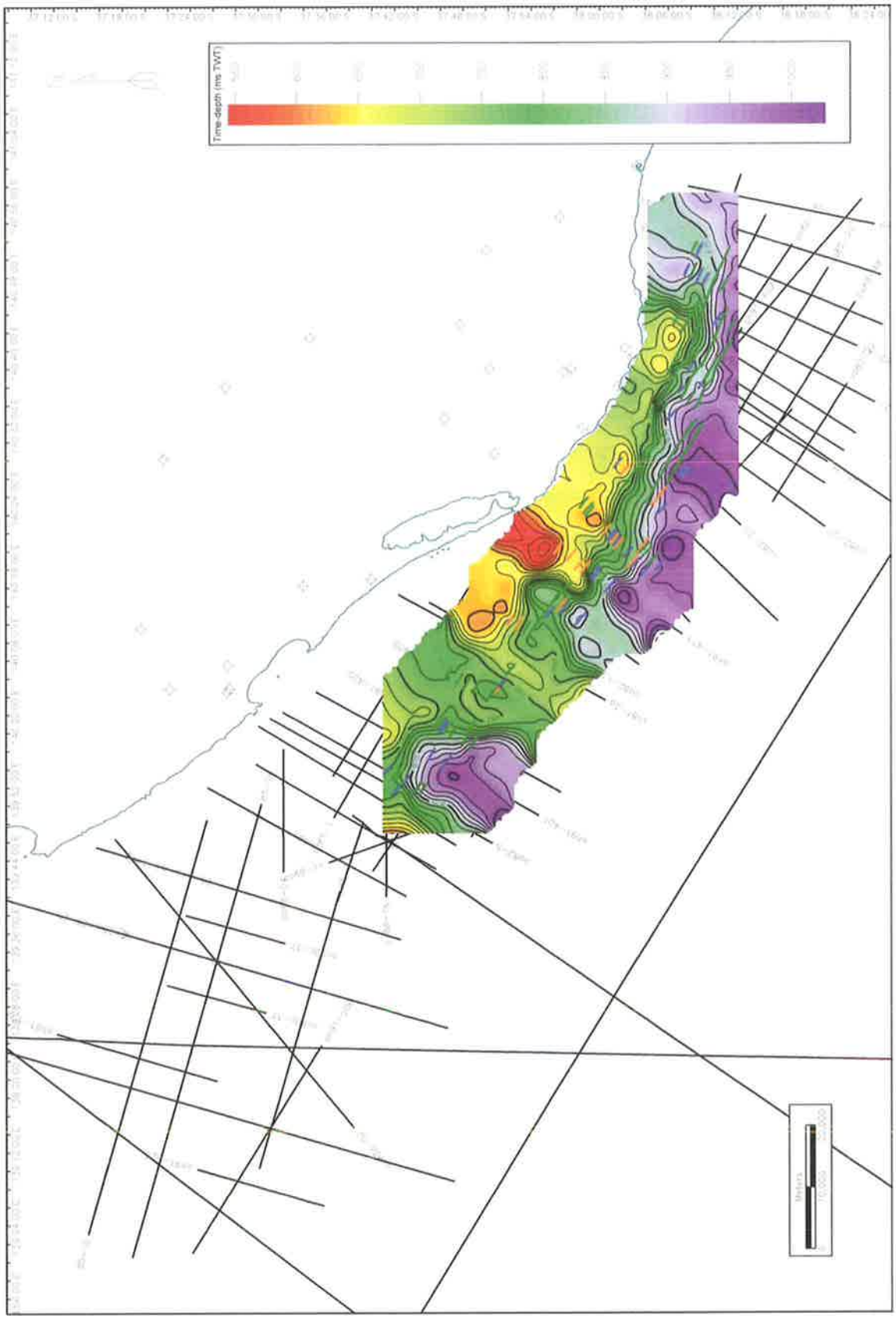

A 4.27 Time-Structure map of SB 2.1

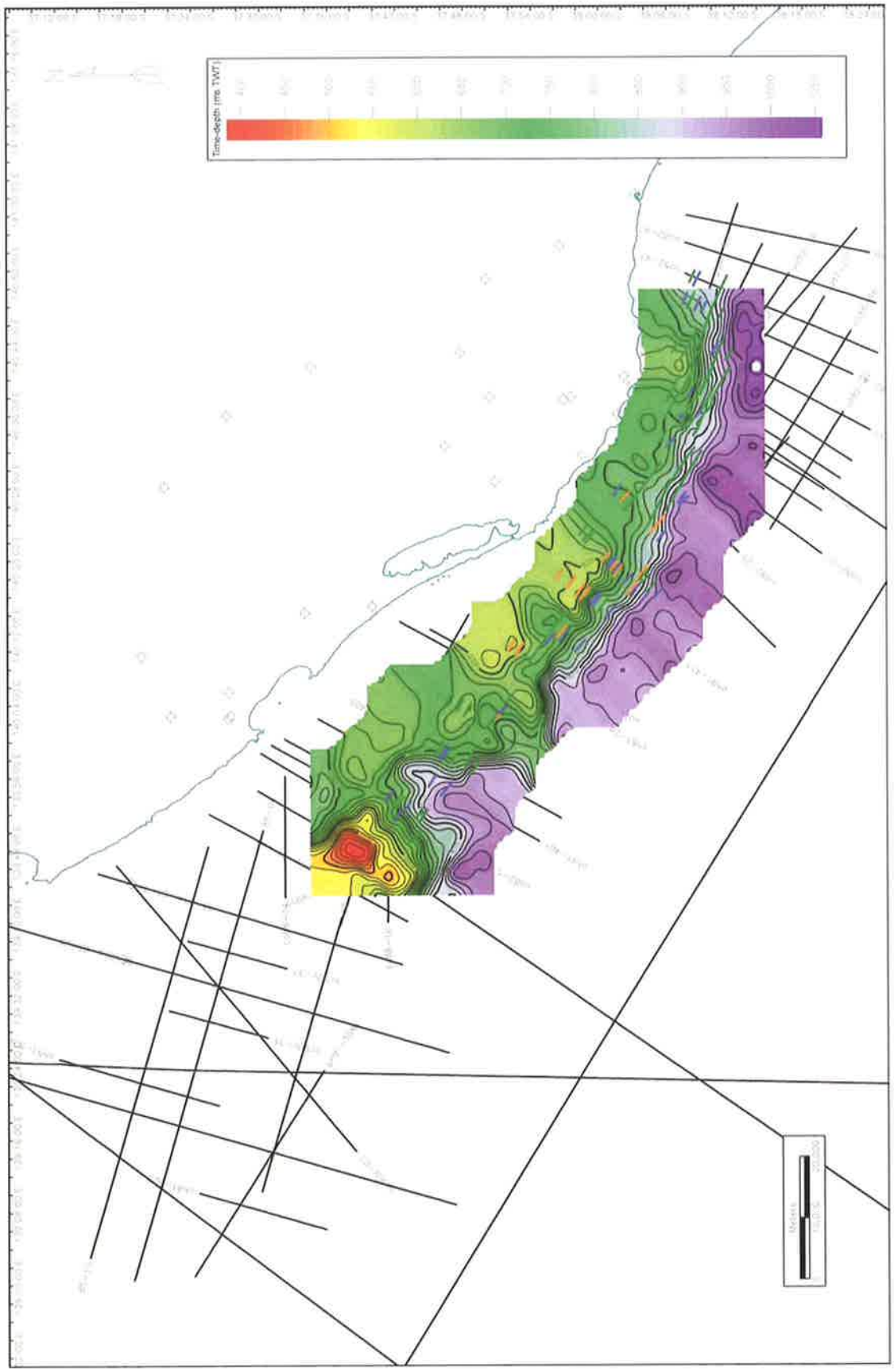

A 4.28 Time-Structure map of SB 2.2

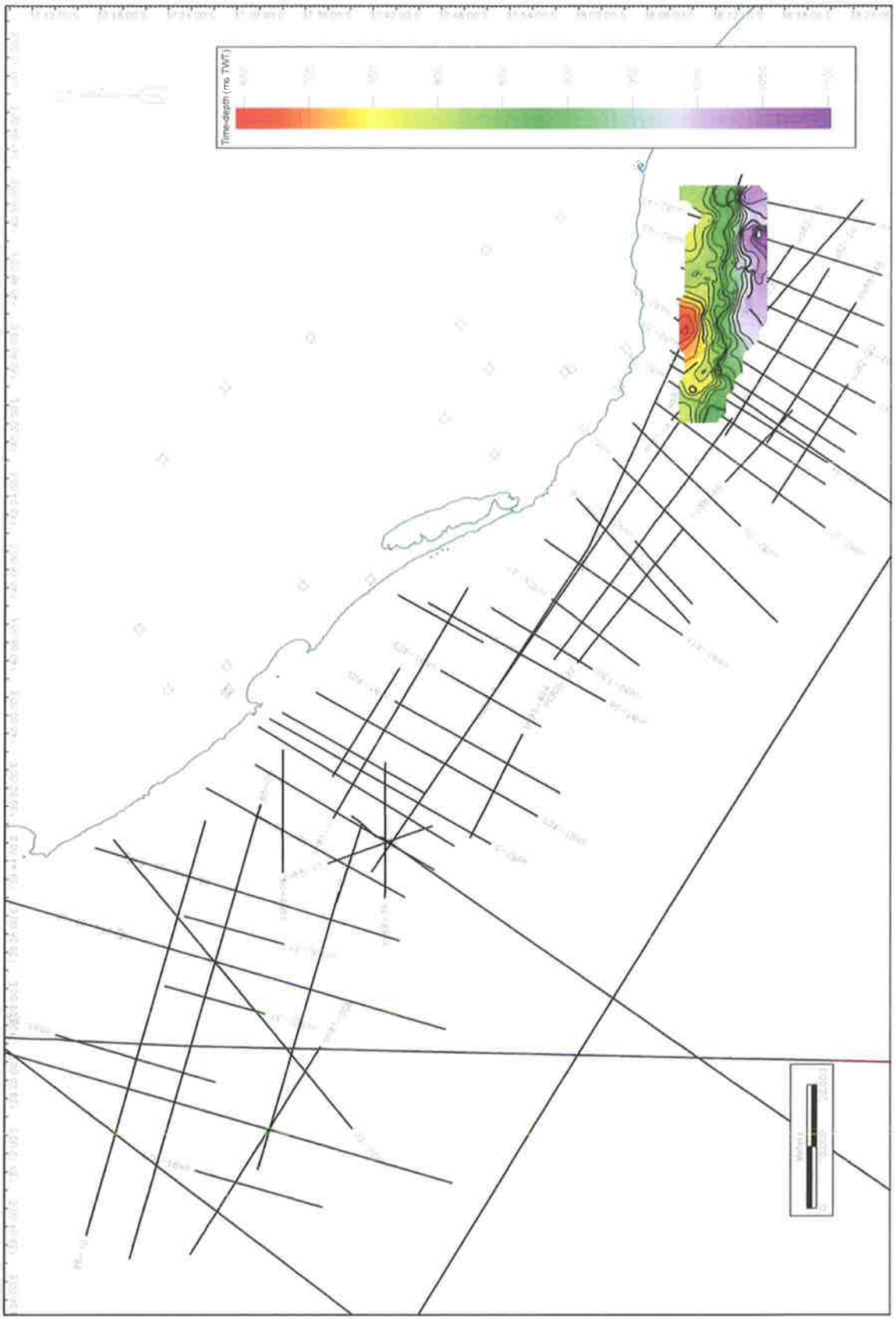

A 4.29 Time-Structure map of MFS 2.2

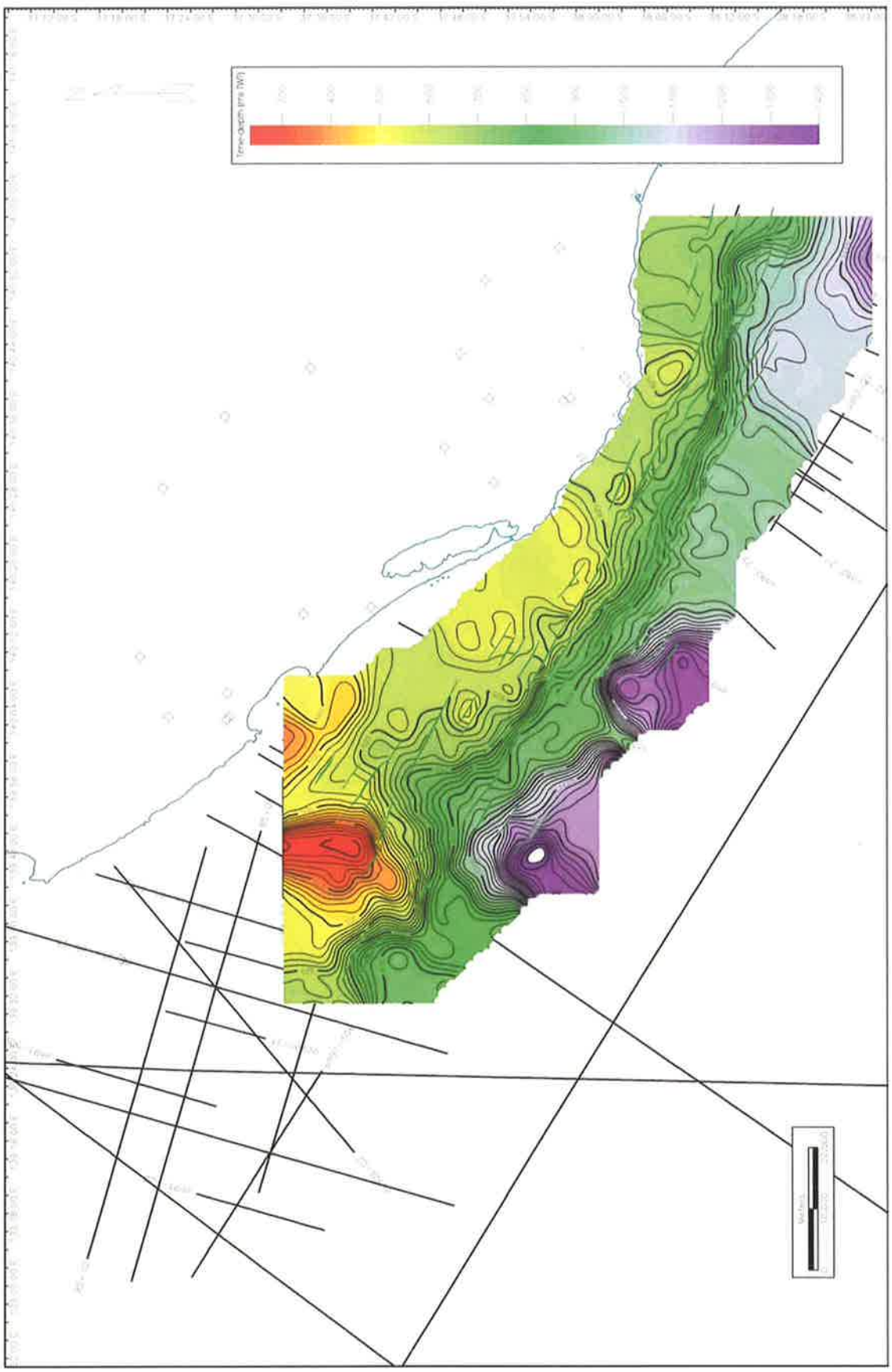

A 4.30 Time-Structure map of SB 2.3

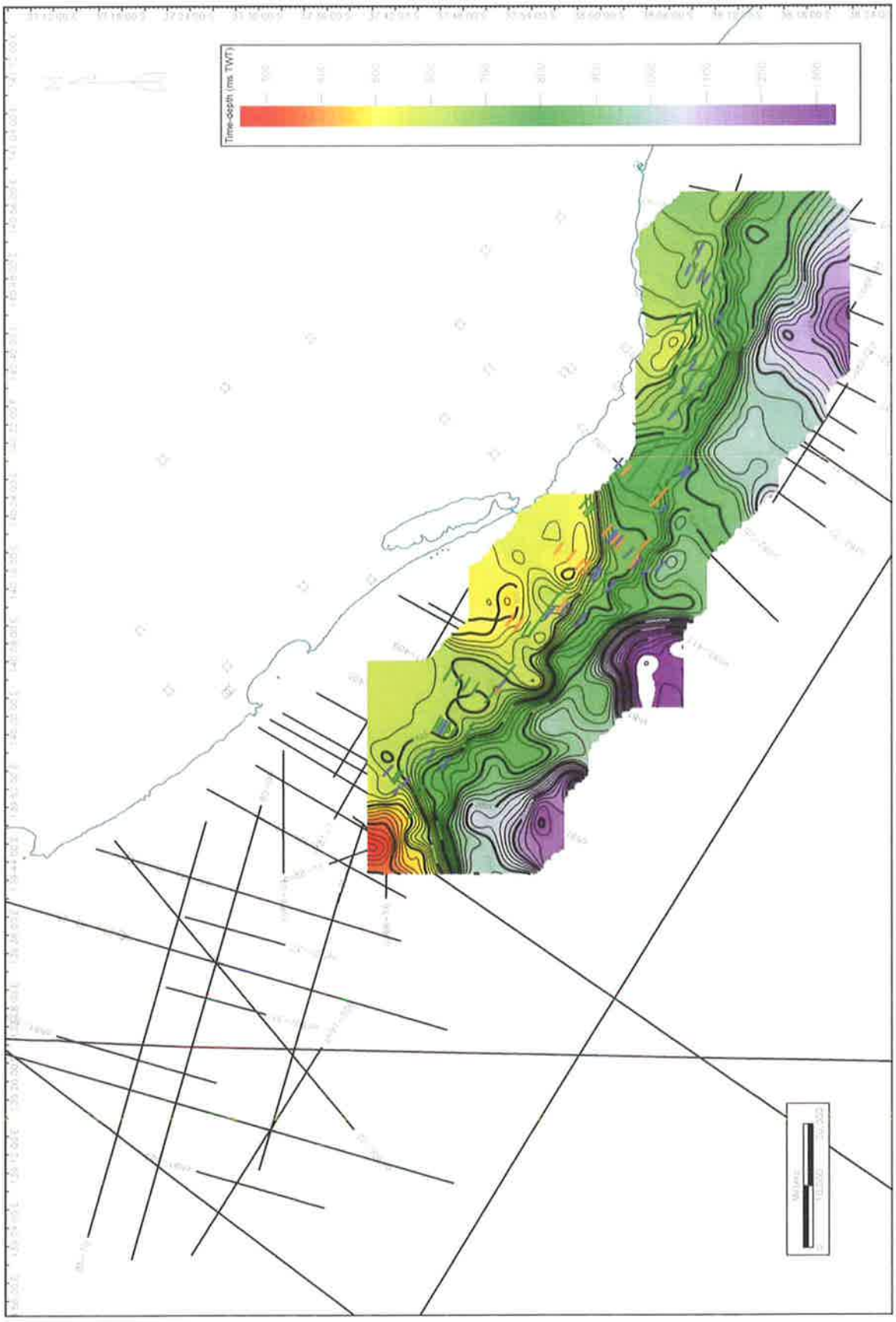

A 4.31 Time-Structure map of MFS 2.3

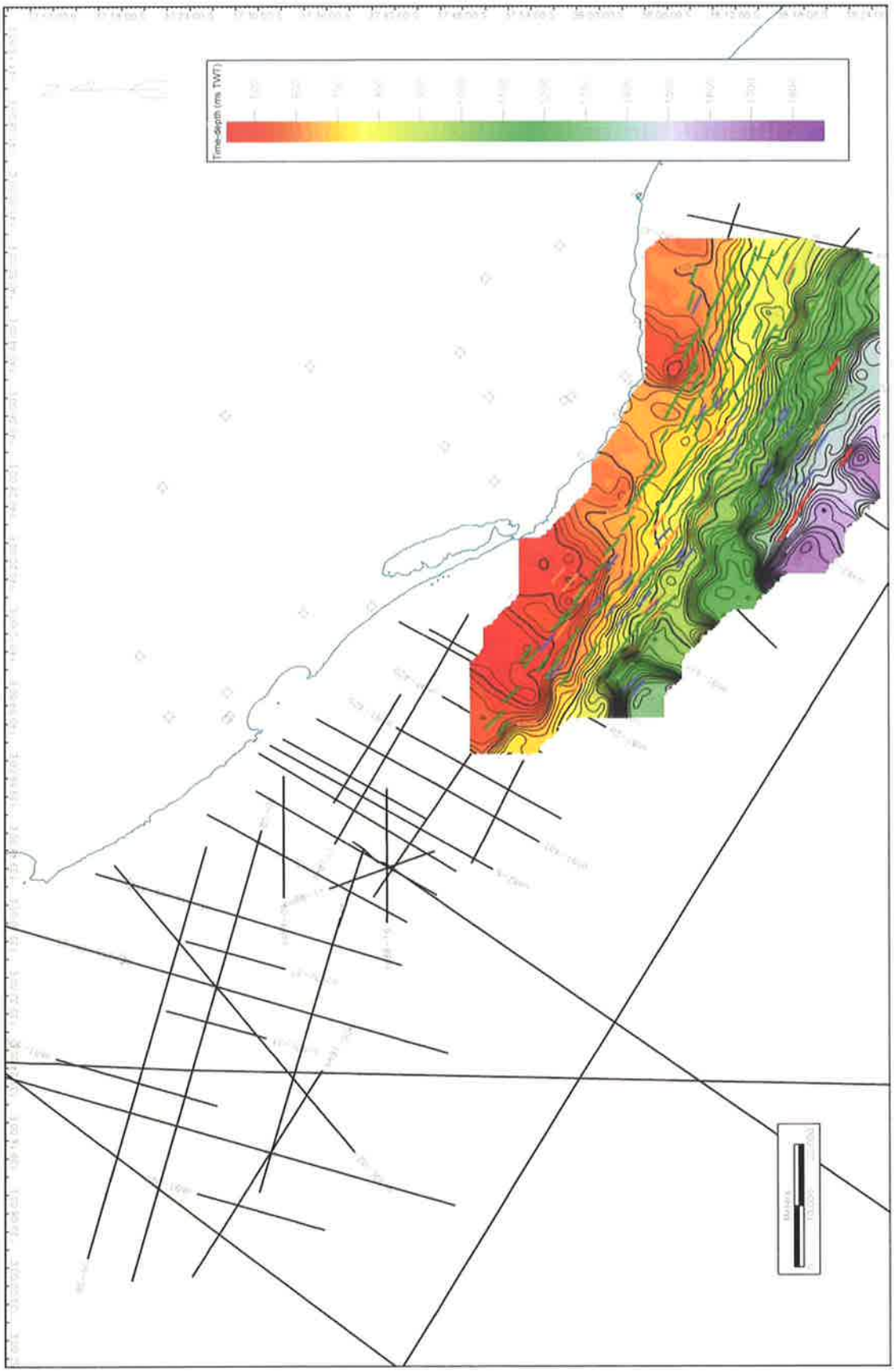

A 4.32 Time-Structure map of SB 3.1

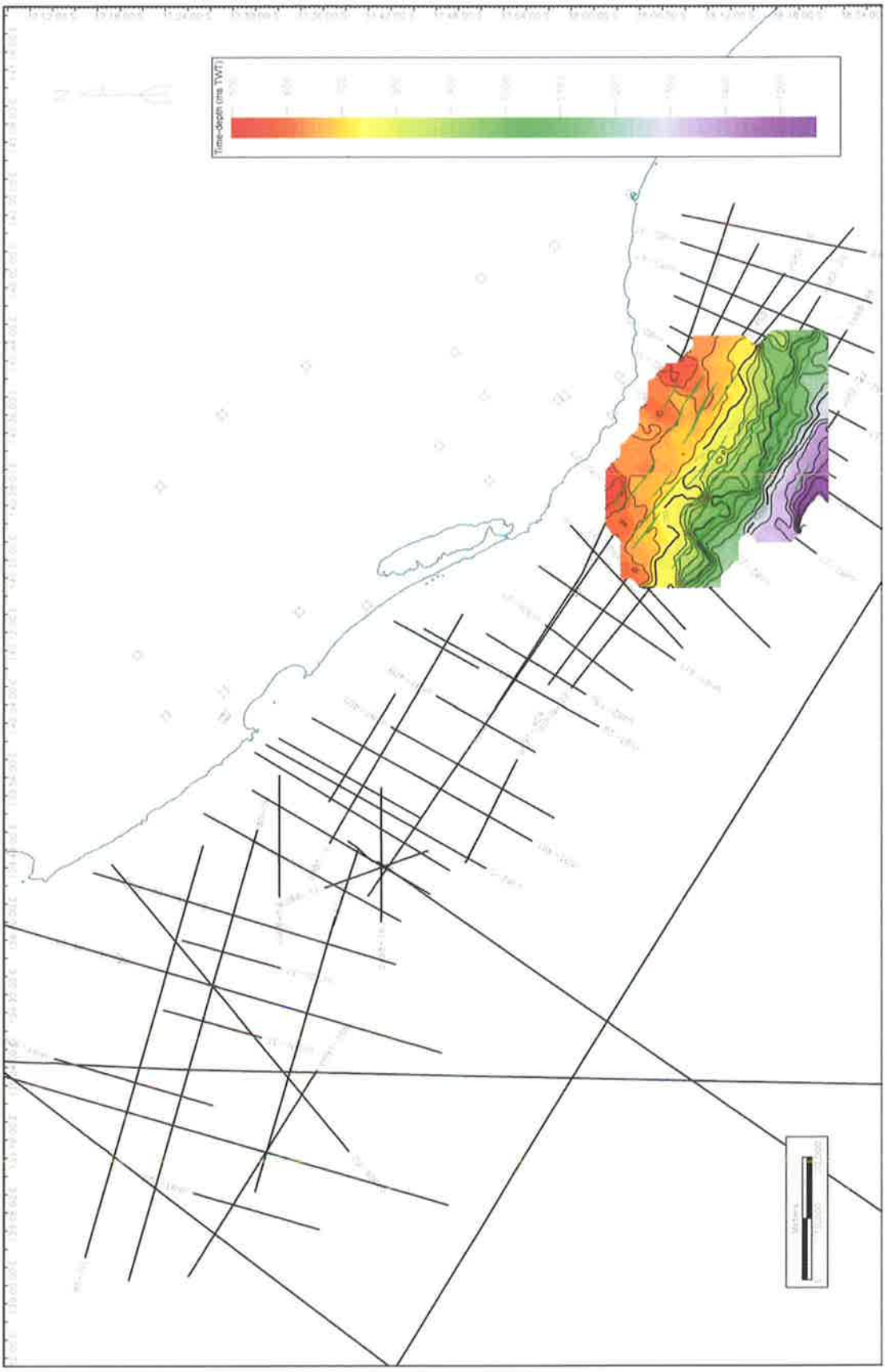

A 4.33 Time-Structure map of SB 3.2

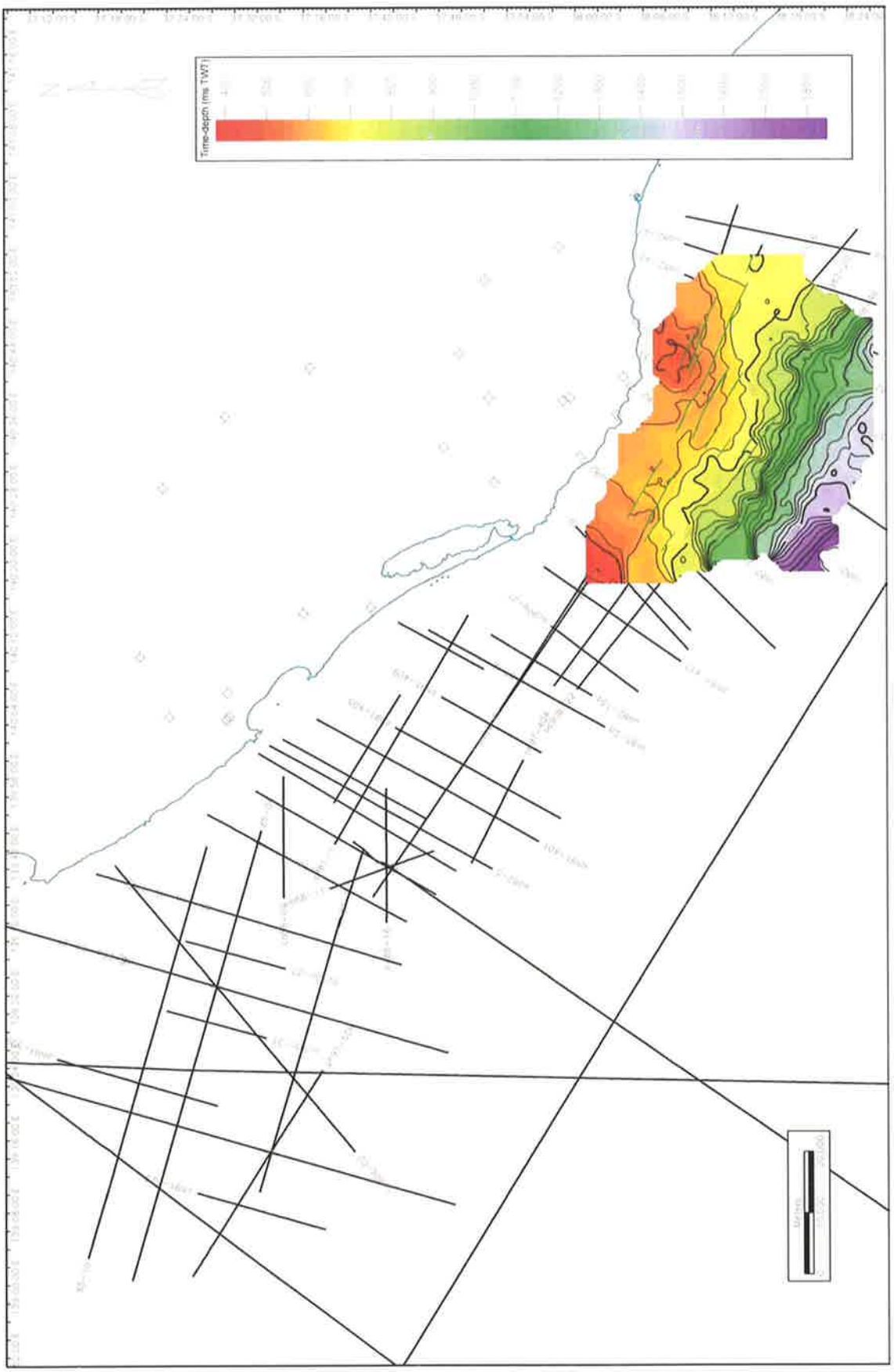

A 4.34 Time-Structure map of SB 3.3

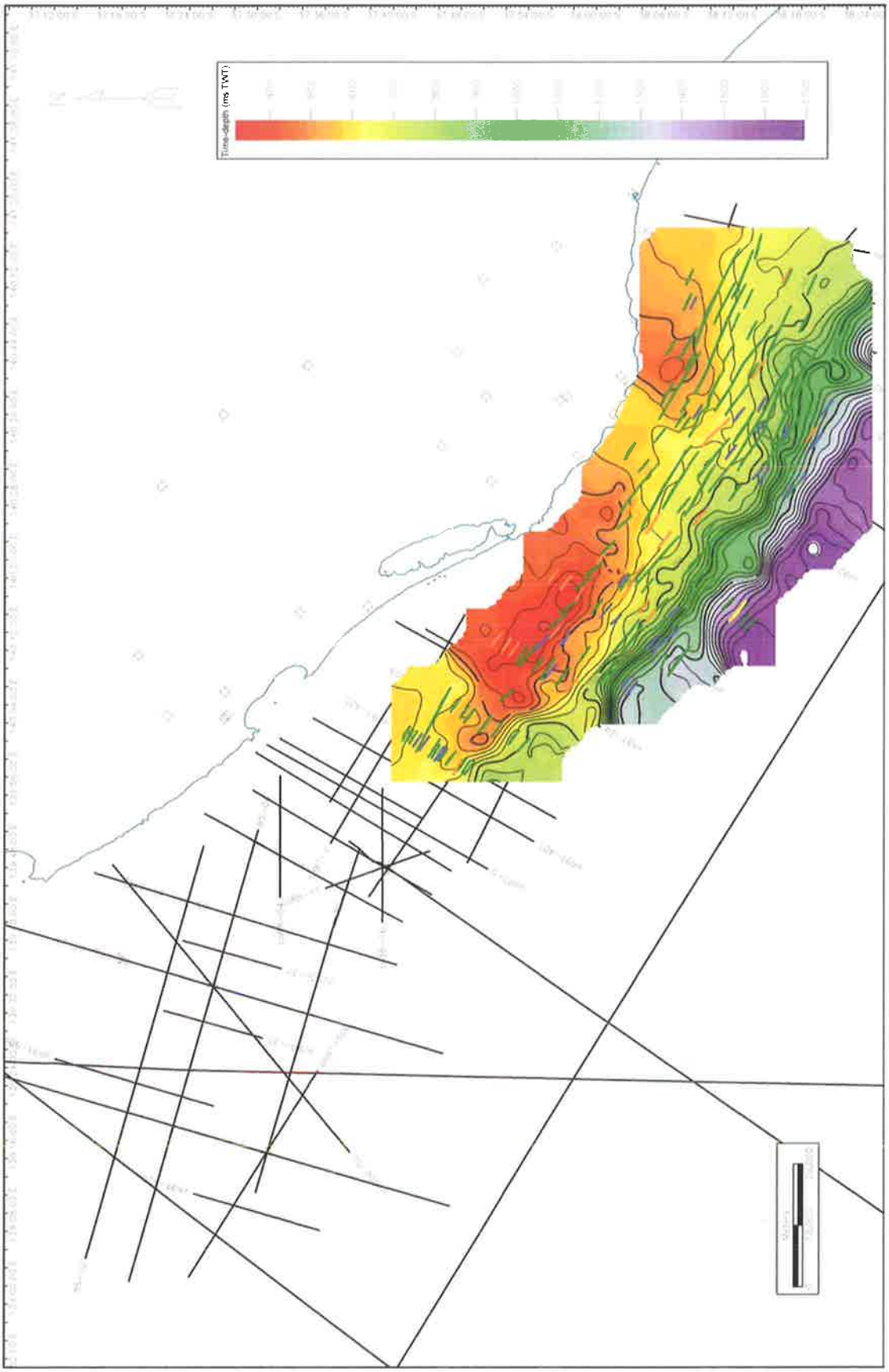

A 4.35 Time-Structure map of SB 4.1

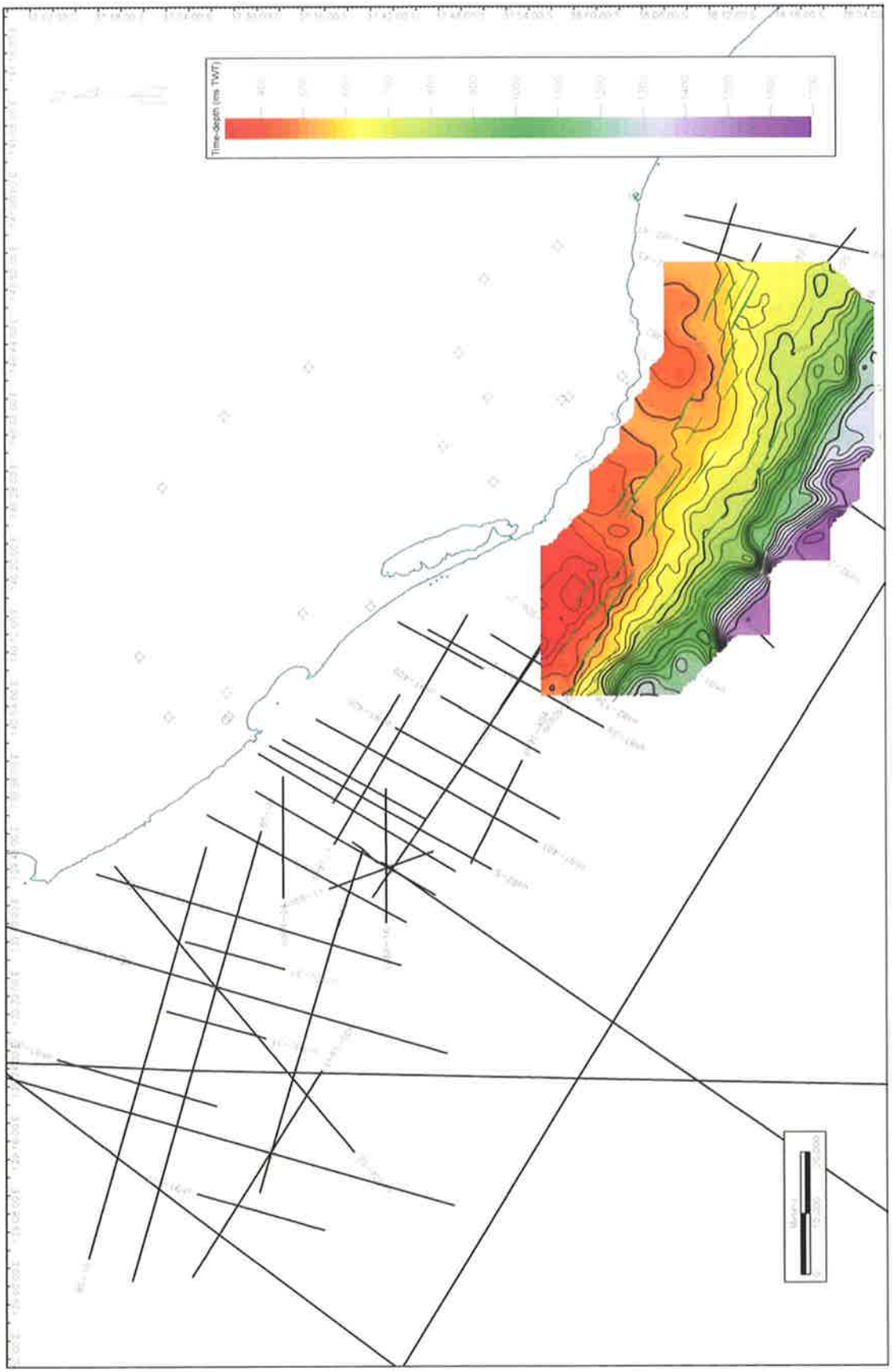

A 4.36 Time Structure map of SB 4.2

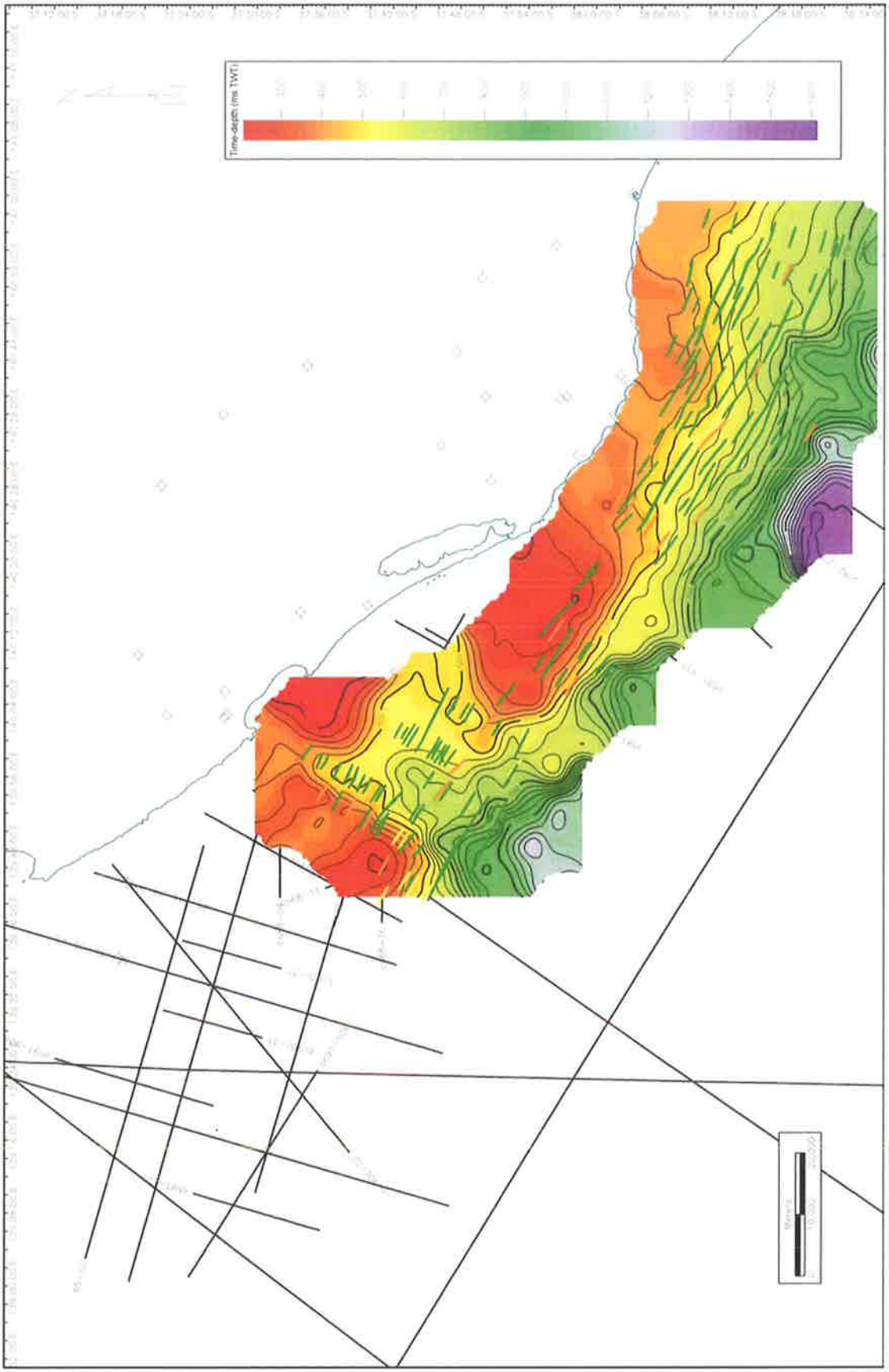

A 4.37 Time-Structure map of SB 5.1

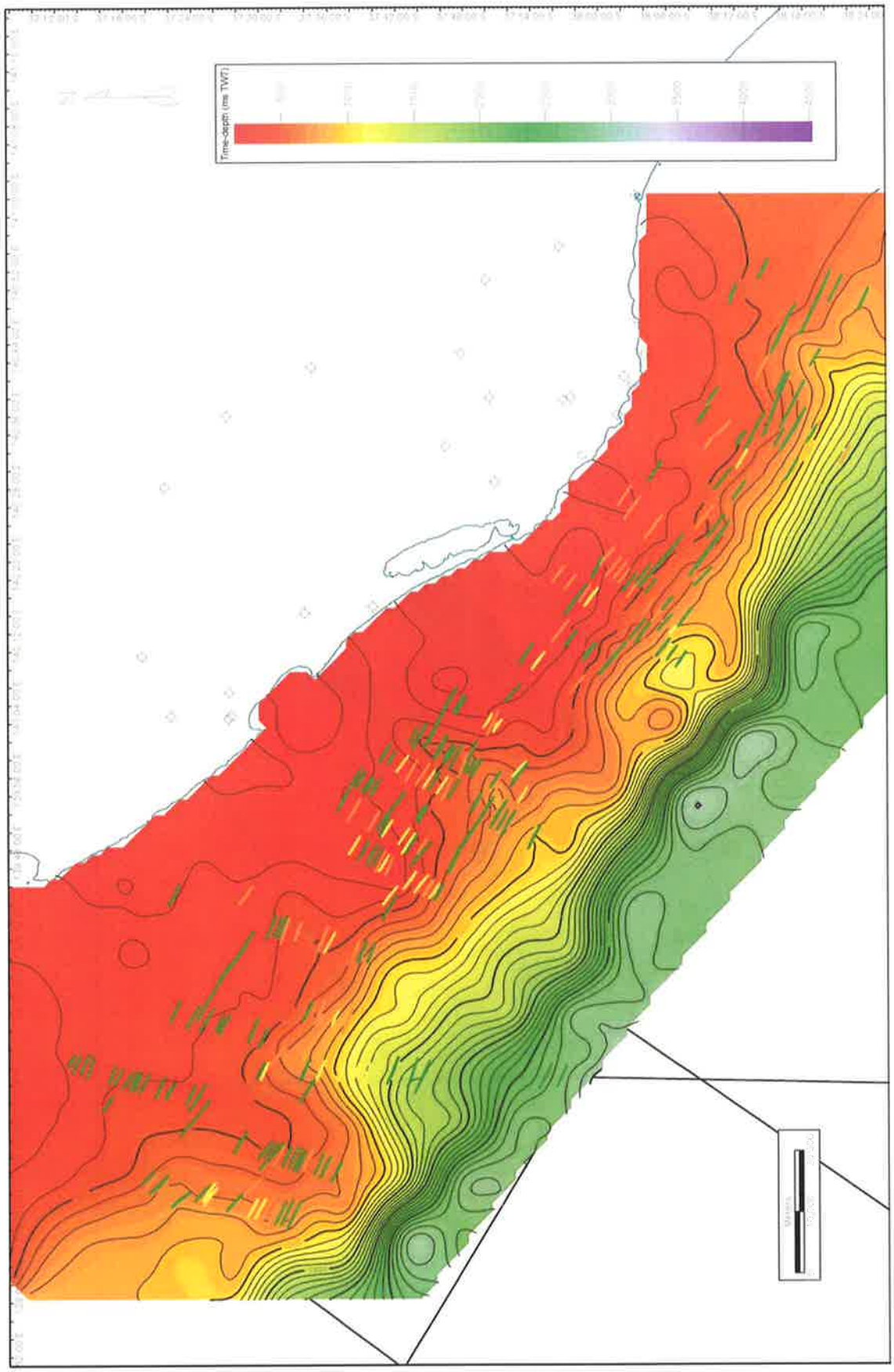

A 4.38 Time-Structure map of SB 6.1

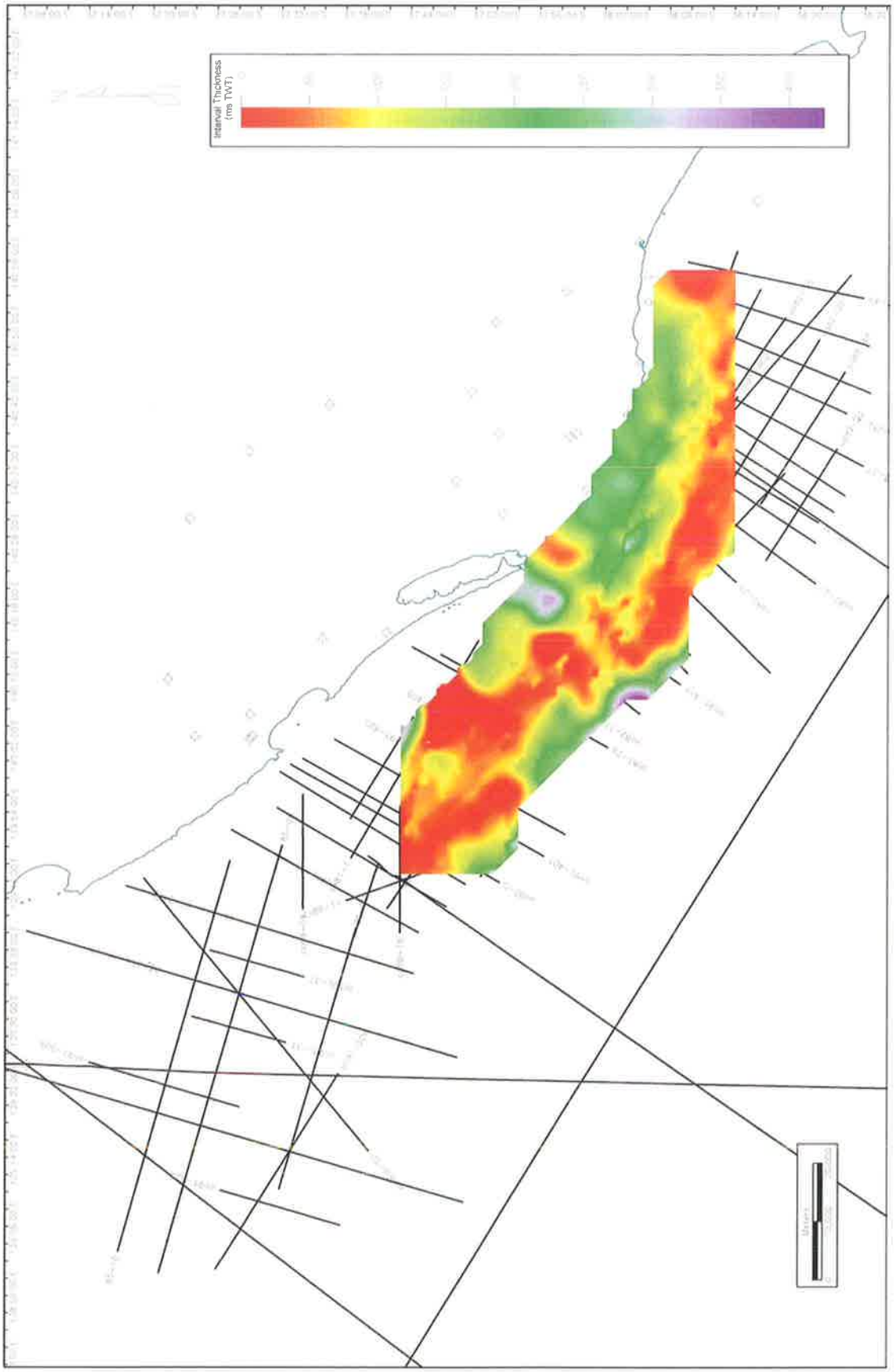

A 4.39 Interval thickness map of Supersequence 1

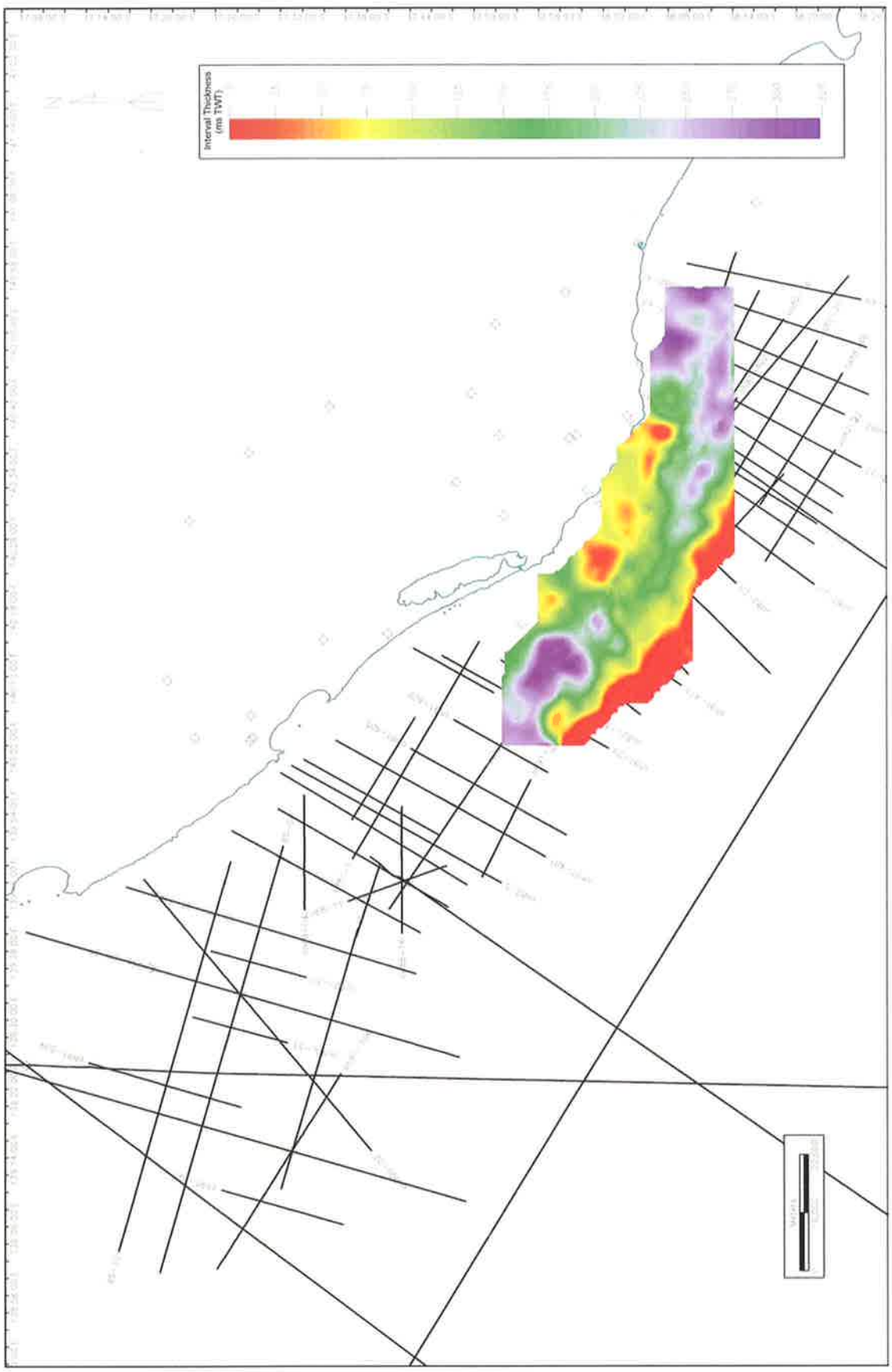

A 4.40 Interval thickness map of Supersequence 2

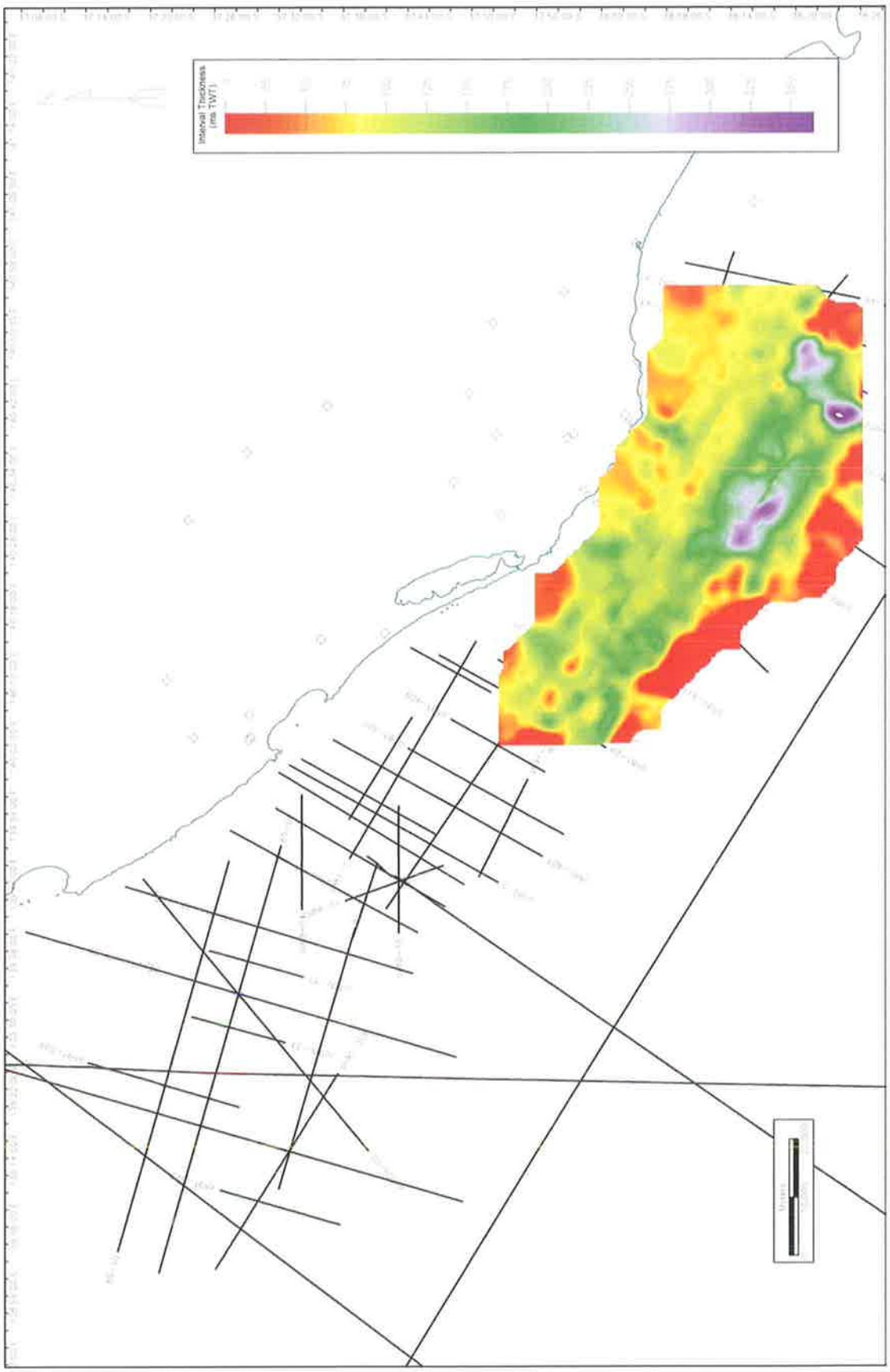

A 4.41 Interval thickness map of Supersequence 3

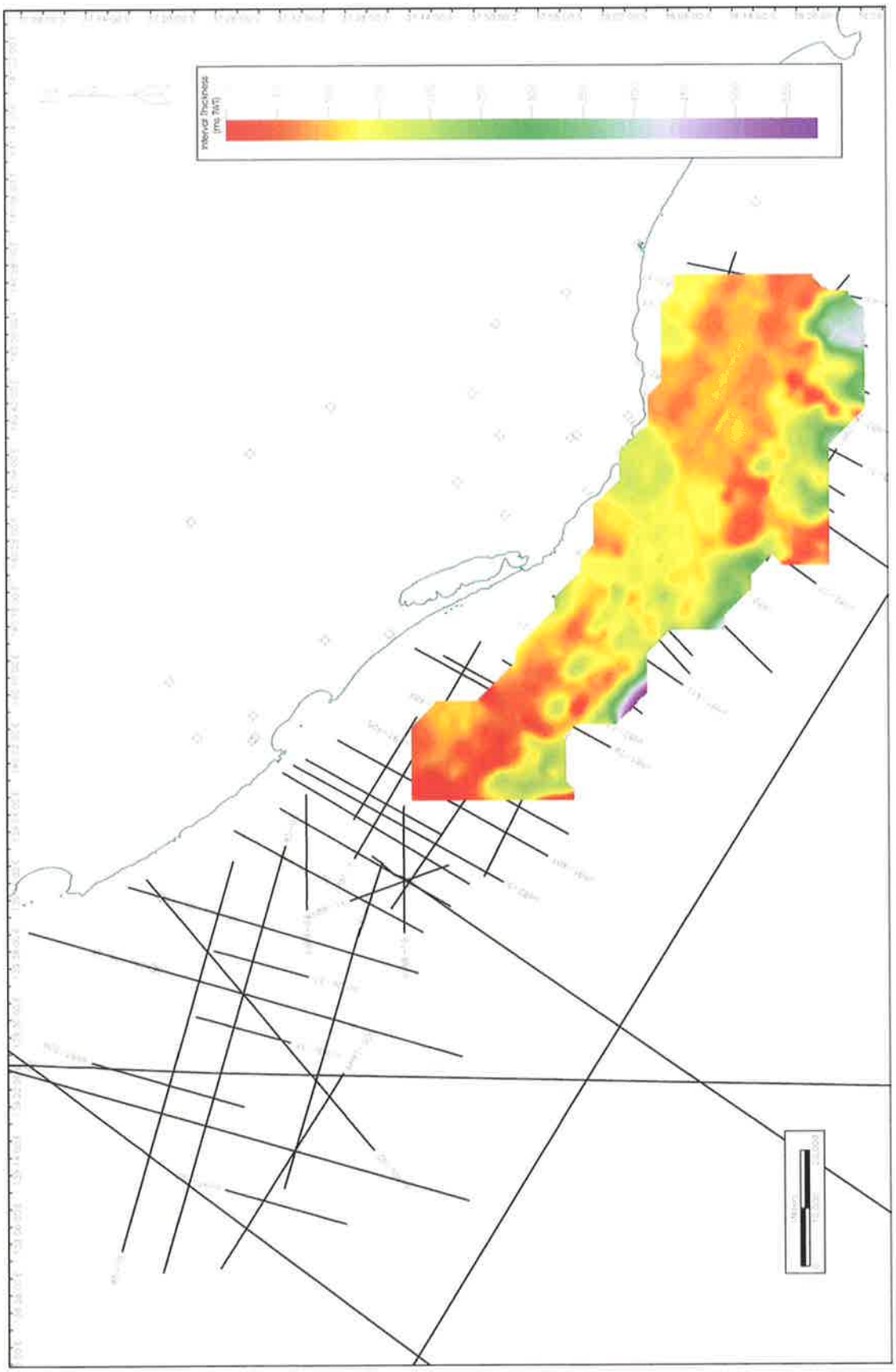

A 4.42 Interval thickness map of Supersequence 4

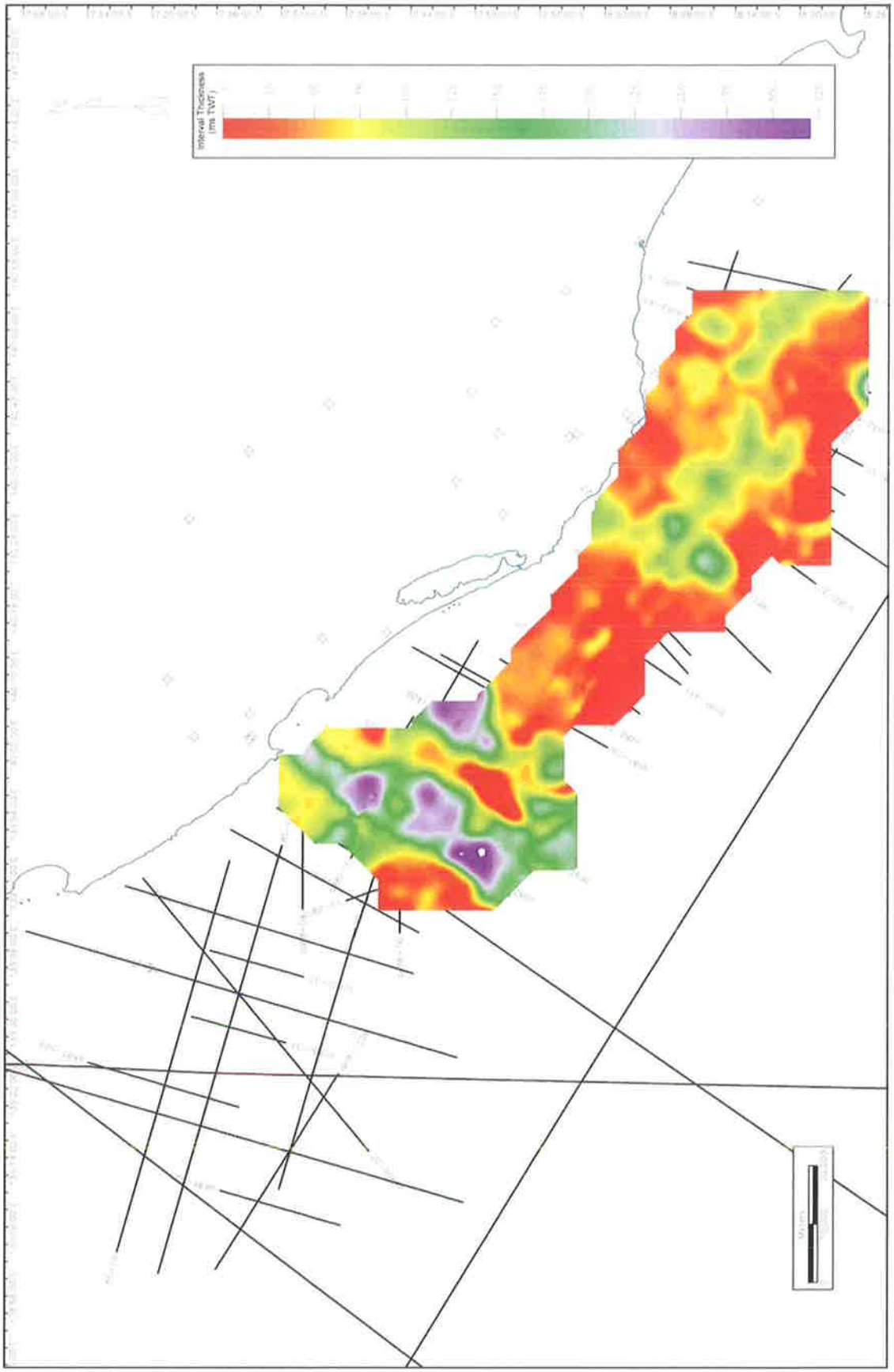

A 4.43 Interval thickness map of Supersequence 5

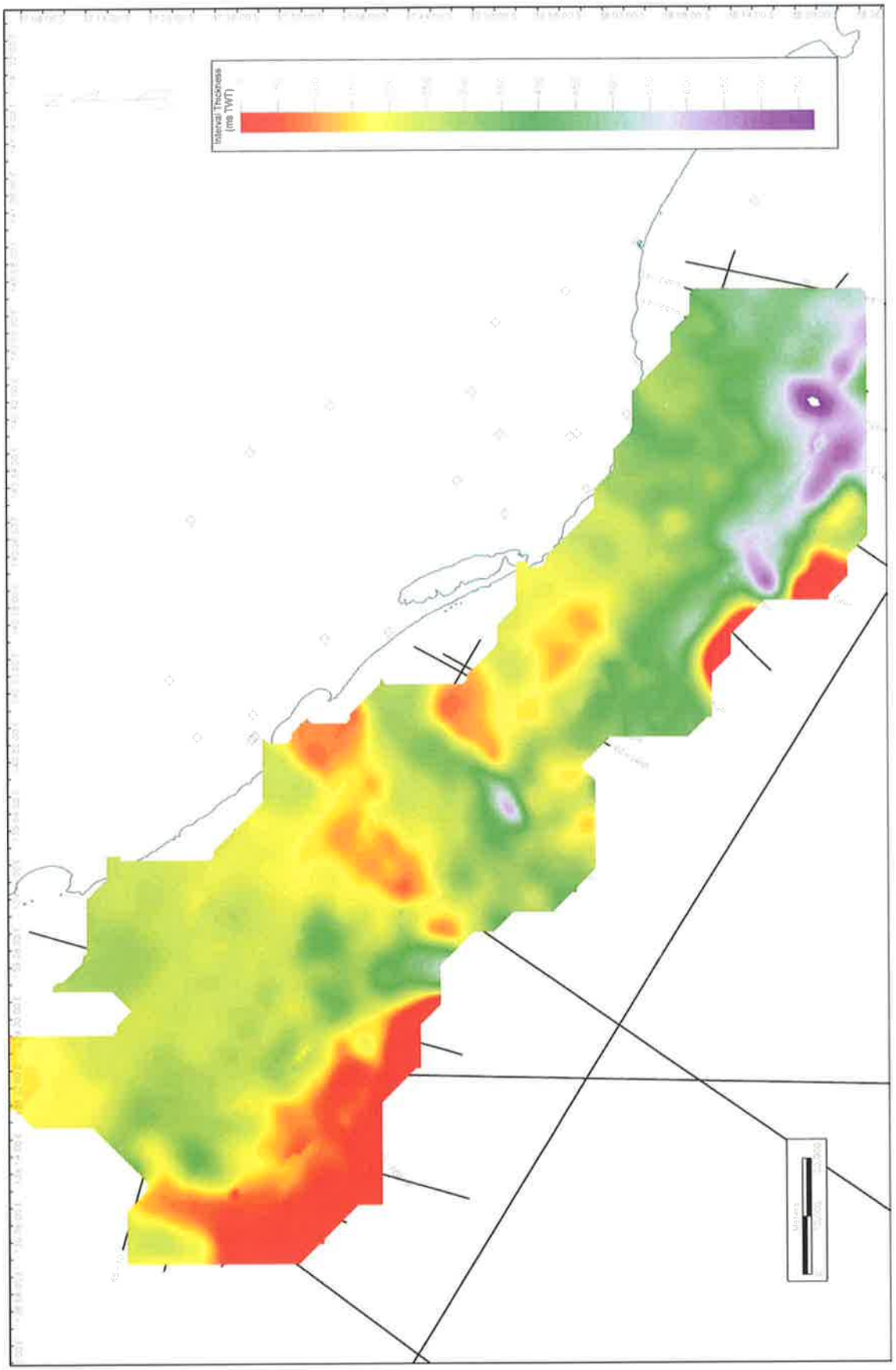

A 4.44 Interval thickness map of Supersequence 6

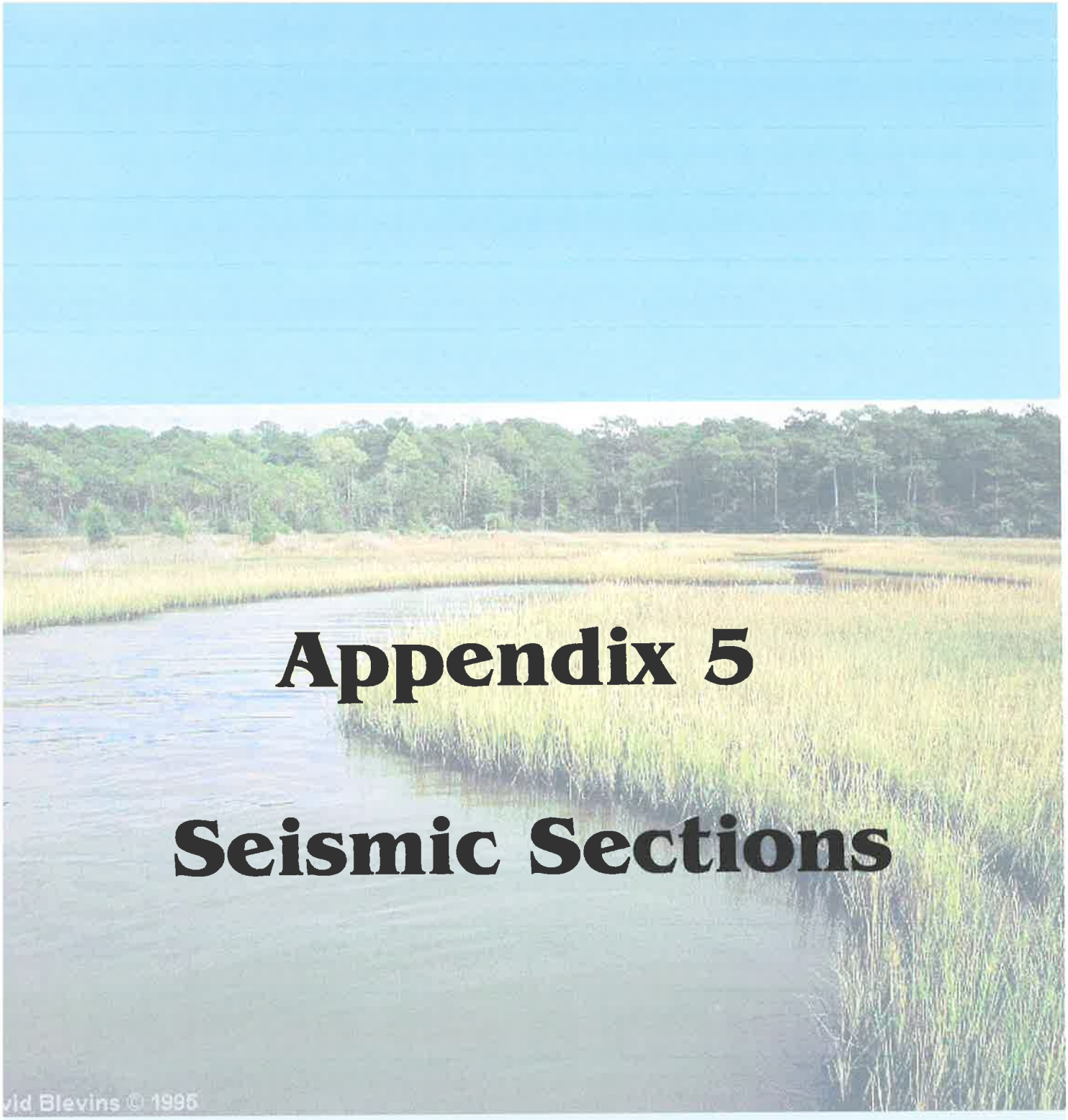

Appendix 5

Seismic Sections

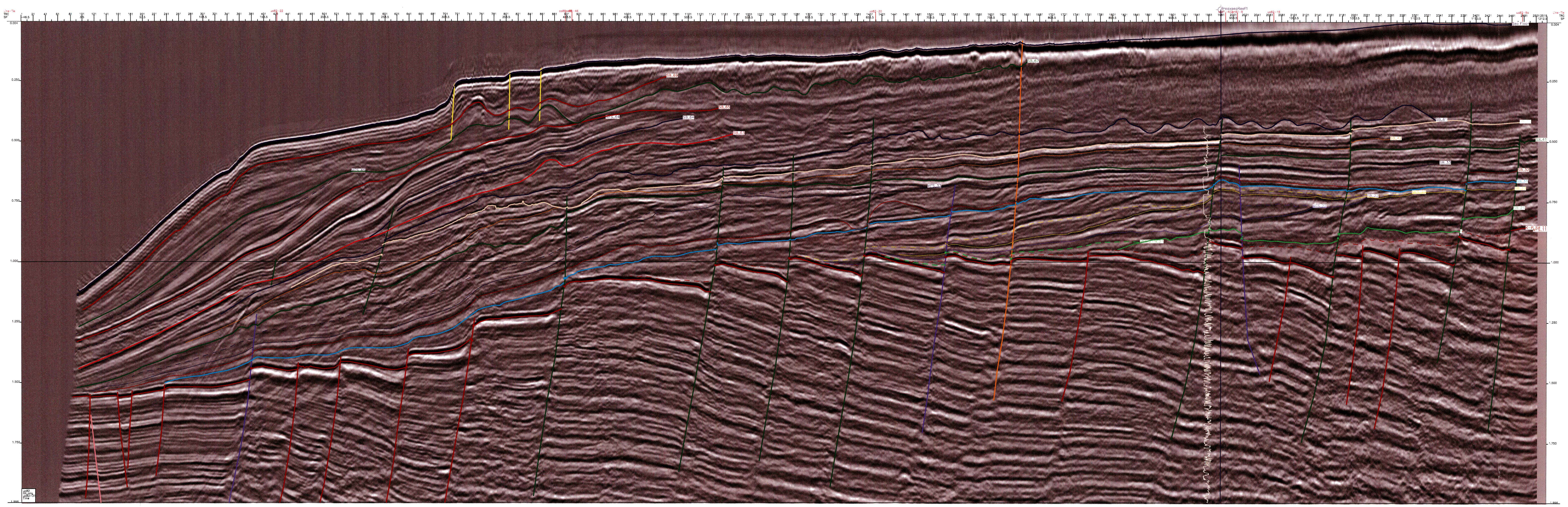

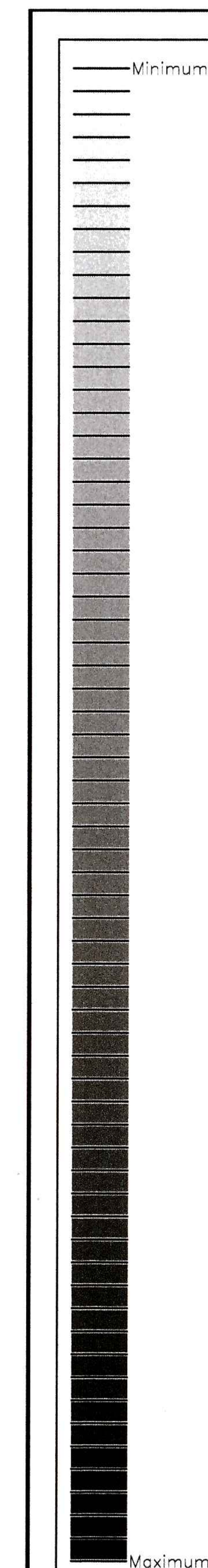

NCPGG & Dept. Geology & Geophysics
University of Adelaide
PhD study area
Offshore, Gambier Sub-basin
Southern Australia

GeoQuest Systems, Inc. Scaled Seismic Hardcopy

Plot title:	Line UA82-31
User:	gambier
Project:	gambier
Plot Creation Date:	November 28, 2003 12:56 PM
Prepared by:	Rosalie M. Pollock

Survey:	ua82
Class:	filt_mig
Line:	ua82-31
Vertical scale:	20.00 cm/sec
Horizontal scale:	9.99 traces/cm
Z:	0.004–1.996 Seconds
Direction displayed on right:	Northeast
Trace spacing:	13. meter
Trace RMS Scaled to 120.00 Trace Deflection	

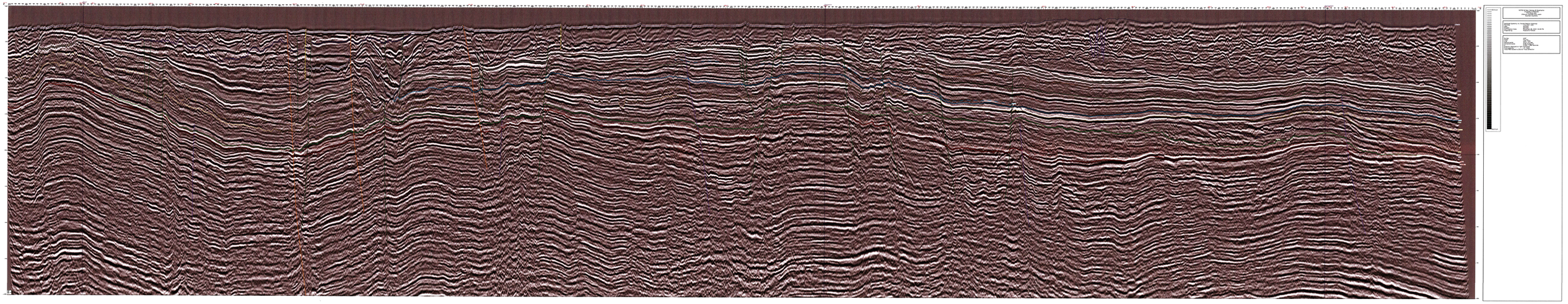

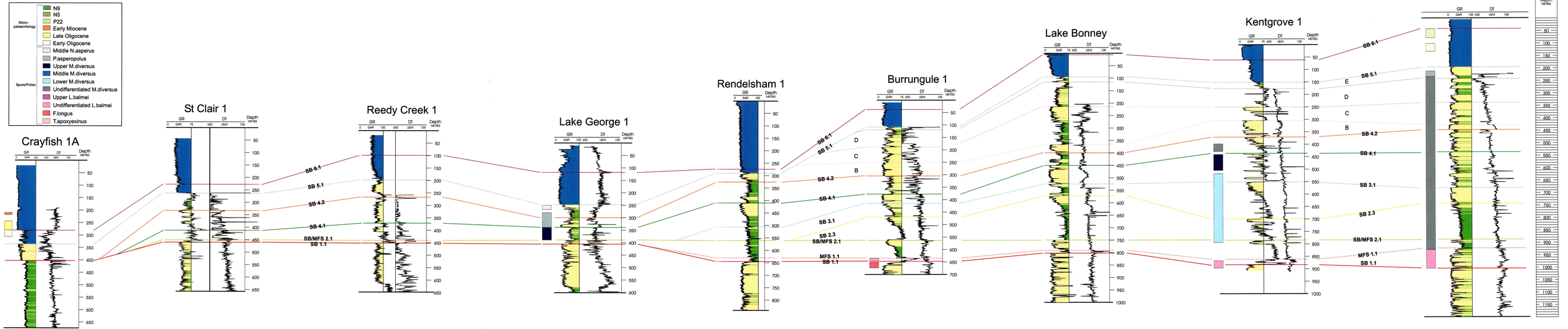
Micro-palaeontology
N9
N5
P22
Early Miocene
Late Oligocene
Early Oligocene
Middle N.asperus
P.asperopolus
Upper M.diversus
Middle M.diversus
Lower M.diversus
Spore/Pollen
Undifferentiated M.diversus
Upper L.balmei
Undifferentiated L.balmei
F.longus
T.apoxyexinus
Crayfish 1A
St Clair 1
Reedy Creek 1
Lake George 1
Rendelsham 1
Burrungule 1
Lake Bonney
Kentgrove 1
Caroline 1
GR
DT
Depth
METRES
SB 6.1
SB 5.1
SB 4.2
SB 4.1
SB 3.1
SB 2.3
SB/MFS 2.1
MFS 1.1
SB 1.1
D
C
B
E

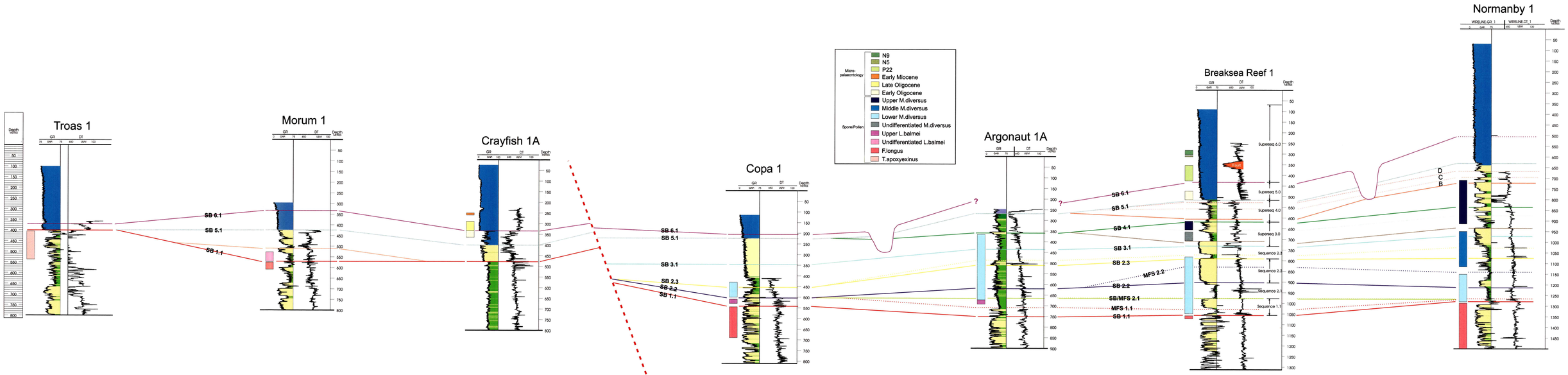
Troas 1
Morum 1
Crayfish 1A
Copa 1
Argonaut 1A
Breaksea Reef 1
Normanby 1
Micro-palaeontology
Spore/Pollen
N9
N5
P22
Early Miocene
Late Oligocene
Early Oligocene
Upper M.diversus
Middle M.diversus
Lower M.diversus
Undifferentiated M.diversus
Upper L.balmei
Undifferentiated L.balmei
F.longus
T.apoxyexinus
SB 6.1
SB 5.1
SB 1.1
SB 3.1
SB 2.3
SB 2.2
SB 1.1
SB 4.1
MFS 2.2
SB/MFS 2.1
MFS 1.1
Superseq 6.0
Superseq 5.0
Superseq 4.0
Superseq 3.0
Sequence 2.2
Sequence 2.3
Sequence 2.1
Sequence 1.1
D
C
B

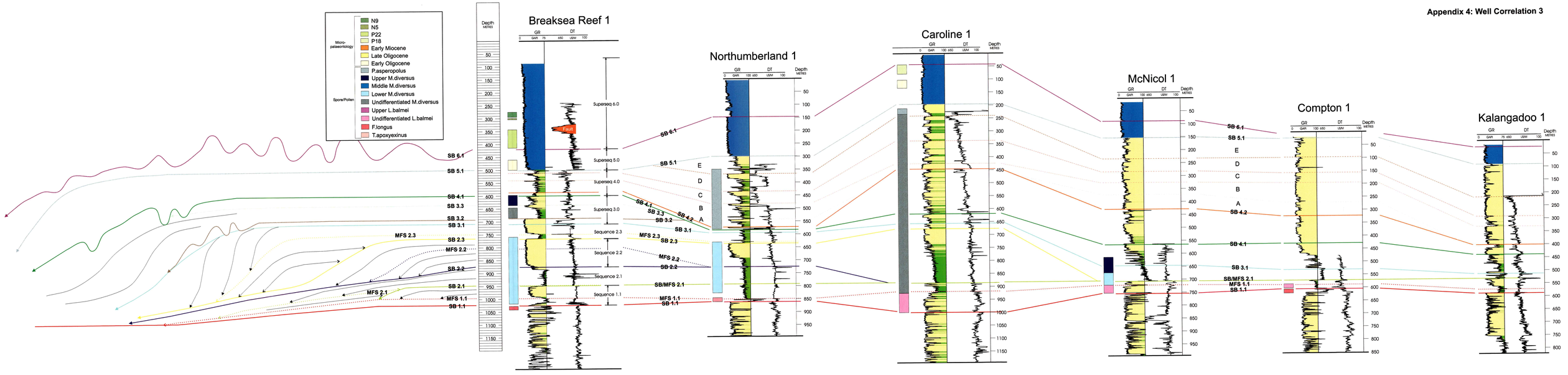
Micro-palaeontology
Spore/Pollen
N9
N5
P22
P18
Early Miocene
Late Oligocene
Early Oligocene
P.asperopolus
Upper M.diversus
Middle M.diversus
Lower M.diversus
Undifferentiated M.diversus
Upper L.balmei
Undifferentiated L.balmei
F.longus
T.apoxyexinus
Depth METRES
SB 6.1
SB 5.1
SB 4.1
SB 3.3
SB 3.2
SB 3.1
MFS 2.3
SB 2.3
MFS 2.2
SB 2.2
SB 2.1
MFS 2.1
MFS 1.1
SB 1.1
Breaksea Reef 1
GR
DT
Fault
Superseq 6.0
Superseq 5.0
Superseq 4.0
Superseq 3.0
Sequence 2.3
Sequence 2.2
Sequence 2.1
Sequence 1.1
Northumberland 1
E
D
C
B
A
SB/MFS 2.1
Caroline 1
McNicol 1
Compton 1
Kalangadoo 1

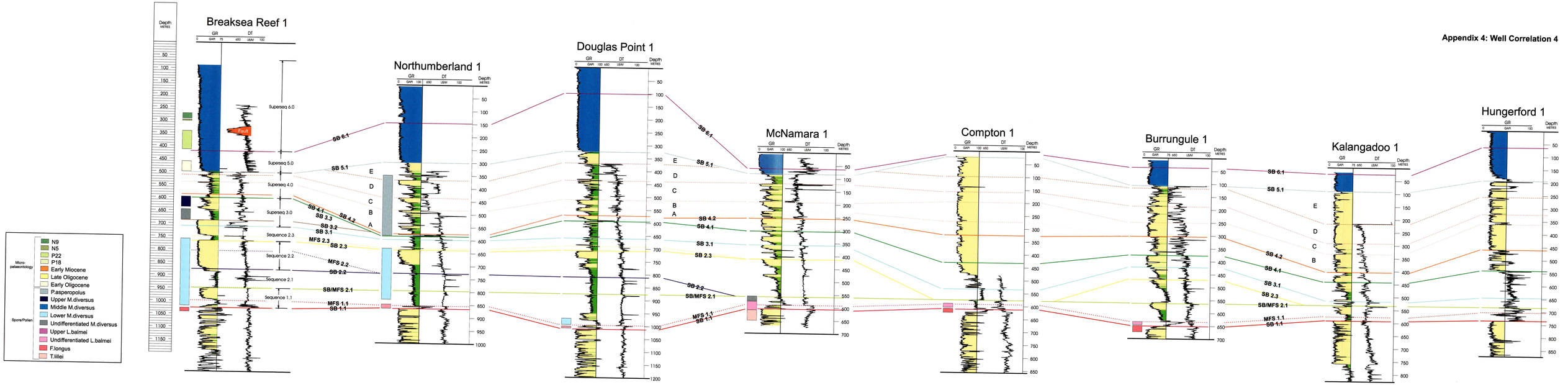
Depth METRES
Breaksea Reef 1
Northumberland 1
Douglas Point 1
McNamara 1
Compton 1
Burrungule 1
Kalangadoo 1
Hungerford 1
GR
DT
GAPI
USM
Superseq 6.0
Superseq 5.0
Superseq 4.0
Superseq 3.0
Sequence 2.3
Sequence 2.2
Sequence 2.1
Sequence 1.1
SB 6.1
SB 5.1
SB 4.1
SB 4.2
SB 3.3
SB 3.2
SB 3.1
MFS 2.3
SB 2.3
MFS 2.2
SB 2.2
SB/MFS 2.1
MFS 1.1
SB 1.1
E
D
C
B
A
N9
N5
P22
P18
Early Miocene
Late Oligocene
Early Oligocene
P.asperopolus
Upper M.diversus
Middle M.diversus
Lower M.diversus
Undifferentiated M.diversus
Upper L.balmei
Undifferentiated L.balmei
F.longus
T.lilliei
Micro-palaeontology
Spore/Polen